

Aanvraagdocumenten
Instemming wijziging opslagplan
Stikstofbuffer Heiligerlee A-438

Inhoudsopgave

Aanvraagdocumenten instemming wijziging opslagplan stikstofbuffer Heiligerlee
A-438

1. Aanbiedingsbrief aanvraag instemming wijziging opslagplan
2. Wijziging Opslagplan Heiligerlee
3. Brief SodM; Reactie SodM op inzetprofiel van de stikstofopslag
4. Feasibility Proof HL-K Injection Capacity Increase
5. Rock mechanical program en enclosures
6. Permeabilitatuntersuchungen an Steinsalz
7. Mapping Winschoten Saltdome
8. Actualisering bestaande geologische kaarten
9. History matching of surface subsidence due to solution mining
10. HL WP1 Report Subsidence Documentation
11. HL WP2 Report Subsidence Modelling
12. HL WP3 Report Subsidence Prediction
13. Seismic Network Specifications

Tab: Aanbiedingsbrief aanvraag instemming wijziging
opslagplan

Ministerie van Economische Zaken en
Klimaat
T.a.v. [REDACTED]
Postbus 20401
2500 EK Den Haag

Gasunie Transport Services B.V.
Postbus 181
9700 AD Groningen
Concourslaan 17
T (050) 521 22 55
E info@gastransport.nl
Handelsregister Groningen 02084889
www.gasunietransportservices.com

Datum 10 januari 2020 Doorkiesnummer +31 6 1100 5731

Ons kenmerk OI 19.854 Uw kenmerk

Onderwerp
Aanvraag goedkeuring gewijzigd opslagplan Stikstofbuffer
Heiligerlee A-438 nabij Winschoten (gemeente Oldambt)

Geachte [REDACTED]

Het vigerende opslagplan kent een injectiecapaciteit van 16.000 M3 stikstof per uur, de uitzendcapaciteit is 190.000 M3 stikstof per uur. Als gevolg van de uitbreiding van de stikstofcapaciteit te Zuidbroek, wordt het aanbod stikstof voor tijdelijke opslag in de stikstofbuffer te Heiligerlee groter. GTS wil daarom de injectiecapaciteit in het opslagplan wijzigen van 16.000 M3 stikstof per uur naar 190.000 M3 stikstof per uur. Hiervoor zijn geen technische aanpassingen voor de caverne nodig, omdat de aanwezige verbuizing (tubing) reeds geschikt is voor deze capaciteit.

Wij verzoeken de minister om goedkeuring te geven aan het bijgevoegde gewijzigde opslagplan.

T.a.v. het besluit op dit opslagplan is ingevolge paragraaf 3.6.3 Wro de Rijkscoördinatieregeling van toepassing. Hierbij is de minister van Economische Zaken en Klimaat de aangewezen minister voor de coördinatie. Op grond van art. 3.35 lid 4 van de Wro wordt de uitgebreide voorbereidingsprocedure zoals beschreven in paragraaf 3.3 van de Wabo gevolgd. U bent hierover reeds geïnformeerd door de projectleider voor de rijkscoördinatieregeling van uw ministerie, [REDACTED] en/of Bureau Energieprojecten, de [REDACTED]. U kunt bij haar of hem nadere informatie over de voorbereidingsprocedure verkrijgen.

1: O.g.v. de Wro dient u als bevoegd gezag een afschrift van deze aanvraag aan de minister van Economische Zaken en Klimaat te versturen. Gasunie Transport Services BV (hierna Gasunie) zal er echter voor zorgen dat de minister van Economische Zaken en Klimaat een exemplaar van deze aanvraag ontvangt. U hoeft dus geen exemplaar door te sturen.

2: In reactie op deze kopie van de aanvraag zal de minister u per brief melden wanneer van u verwacht wordt het ontwerpbesluit (ontwerp-goedkeuringsbesluit gewijzigd opslagplan) gereed te hebben.

Gasunie Transport Services B.V.

Datum: 10 januari 2020

Ons kenmerk: OI 19.854

Onderwerp: Aanvraag goedkeuring gewijzigd opslagplan Stikstofbuffer Heiligerlee A-438 nabij Winschoten (gemeente Oldambt)

3: Het ontwerpbesluit en later ook het besluit, stuurt u niet aan Gasunie, maar aan de minister van Economische Zaken en Klimaat, t.a.v. Bureau Energie Projecten, postbus 93144, 2509 AC Den Haag. De minister stuurt het besluit door aan Gasunie. Dit is juridisch gezien de bekendmaking.

Wij vertrouwen er op u hiermee voldoende geïnformeerd te hebben. In geval van inhoudelijke vragen of onduidelijkheden verzoeken wij u op korte termijn contact op te nemen met [REDACTED]. Voor procedurele vragen verzoeken wij u contact op te nemen met Bureau Energieprojecten, tel 070-379 8979.

Met vriendelijke groet,

[REDACTED]

Petroleum Engineer

Tab: Wijziging opslagplan Heiligerlee

Gasunie Transport Services (GTS)



A Gasunie Company

**Aanvraag Instemming Wijziging Opslagplan
stikstofbuffer Heiligerlee**

OI 19.854

Versie 1.0- Final

3/6/2019

Inhoud

Inhoud.....	2
Formulier aanvraag instemming wijziging opslagplan.....	4
1 Inleiding.....	7
1.1 Doel van het Opslagplan.....	7
1.2 Leeswijzer	7
1.3 Overige vergunningen.....	8
2 Plaats van Opslag	9
2.1 Voorkomen(s) in dit opslagplan	9
2.2 Overzicht ligging voorkomens.....	9
2.3 Situering van het mijnbouwwerk	10
2.4 Beknopte beschrijving van de opslag.....	12
2.5 Beknopte beschrijving van de wijze van opslag	12
2.6 Wijze van terugwinning en opslag (procesbeschrijving).....	12
2.7 Injectieproces.....	13
2.8 Productieproces.....	13
2.9 Operationele filosofie.....	14
3 Boring.....	16
3.1 Inleiding: Algemene beschrijving van de Heiligerlee K boring.....	16
3.2 Overzicht boringen in voorkomen(s)	19
3.3 Schematische voorstelling putverbuizing(en).....	21
3.4 Plaats en wijze waarop stikstof in de verbuizing treedt.....	22
4 Ondergrond.....	23
4.1 Inleiding: hoe worden de ondergrond-eigenschappen gemeten	23
4.2 Geologie en gesteente-eigenschappen van het voorkomen.....	24
5 Ontwikkelingsvooruitzichten.....	25
5.1 Inleiding.....	25
5.2 Achtergrond Project Wijzigingen naar Status 2018.....	26
5.3 Vooruitzichten gebruik stikstofcaverne	27
5.4 Caverne als strategische reserve.....	27
5.5 Historische inzet huidige stikstof caverne.....	27
5.6 Onzekerheden.....	29
5.7 Inzetstrategie stikstofcaverne.....	29
5.8 maximale drukvariatie in de caverne.....	29

5.9	Duur van de opslag wijze waarop voorkomen wordt achtergelaten na beëindiging activiteiten.....	29
5.10	Afblazen stikstof bij normaal bedrijf.....	29
5.11	Stoffen die jaarlijks worden mee geproduceerd.....	29
6	Bodemdaling/beweging.....	30
6.1	Inleiding hoe komt bodemdaling tot stand	30
6.2	Bodemdalingsmodel & kalibratie	31
6.3	Bodemdalingsvooruitzichten	32
6.4	Onzekerheid in verwachte bodemdaling	33
6.5	Monitoring van bodemdaling.....	34
6.6	Mogelijke gevolgen van de verwachte bodemdaling	35
6.7	Maatregelen om (gevolgen van) bodemdaling te voorkomen of te beperken	35
7	Bodemtrilling.....	36
7.1	Inleiding: hoe komen bevingen ten gevolge van gaswinning tot stand.....	36
7.2	Historische bevingen in de voorkomens van dit winningsplan.....	36
7.3	Seismische Risico Analyse.....	36
7.4	Seismische Risico Analyse voor het voorkomen in dit opslagplan	37
7.5	Mogelijke gevolgen van bevingen ten gevolge van stikstofopslag in de caverne HL-K.....	37
7.6	Monitoring van bodemtrillingen	37
7.7	Maatregelen die gevolgen van bodemtrillingen beperken of voorkomen	37
8	Overige veiligheidsaspecten.....	39
8.1	Inleiding.....	39
8.2	Bodem- / grondwaterverontreiniging.....	39
8.3	Luchtverontreiniging.....	39
8.4	Oppervlaktewaterverontreiniging	40
8.5	Externe veiligheid	40
8.6	Natuur	40
8.7	Schade aan landbouw	40
9	Verklarende woordenlijst.....	41
10	Referenties.....	43
11	Bijlage 1: Grote foto's van de opslaglocatie	44

Formulier aanvraag instemming wijziging opslagplan

ex artikel 34 lid 1 Mijnbouwwet (Mw) juncto artikel 24 Mijnbouwbesluit (Mb)

Elektronisch in te dienen bij:

De Minister van Economische Zaken

Directoraat-Generaal voor Energie, Telecom en Mededinging

Directie Energie en Omgeving

mijnbouwaanvragen@minez.nl

<u>Artikel</u>	<u>Onderwerp</u>	<u>Beschrijving</u>
Mw 34 lid 1 Mw 39	Verzoek om instemming voor een wijziging / actualisatie van het opslagplan	<input type="checkbox"/> een opslagplan voor voorkomens in het continentaal plat vanaf de 3 zeemijlszone <input checked="" type="checkbox"/> een opslagplan voor voorkomens in Nederlands territorium tot 3 zeemijl De wijziging/actualisatie bestaat uit het verhogen van de injectiecapaciteit in caveerne HL-K van stikstofbuffer Heiligerlee in verband met de constructie van Zuidbroek II (van 16.000 m ³ per uur naar 190.000 m ³ per uur)
	Algemene gegevens	
	Naam indiener	Gasunie Transport Services (GTS)
	Adres	Concourslaan 17 9727 KC Groningen
	postadres	(postbus 181 9700 AD Groningen)
	Contactpersoon	Patrick Roordink / Michel Timmermans
	E-mail	P.J.P.Roordink@gasunie.nl M.M.J.Timmermans@gasunie.nl
	Telefoon	+31 61100 5731 / +31611005460
Mw 34 lid 2	Indiener	<input type="checkbox"/> is houder van de vergunning <input checked="" type="checkbox"/> is uitvoerder cf artikel 22 Mw
	Opslagvergunninggebied(en)	<input checked="" type="checkbox"/> Opslagvergunning Winschoten II; (ref.: DGETM-EO / 16117710)
Mw 34 lid 1 Mb 24 lid 1a	Voorkomens cavernes	Opslagvergunning Winschoten II Vergunninghouders: 1) Gasunie Transport Services GTS
Mb 24 lid 1a	Soort stof die wordt opgeslagen	<input type="checkbox"/> olie <input type="checkbox"/> hoog calorisch gas <input checked="" type="checkbox"/> stikstof gas <input type="checkbox"/> Groningen kwaliteit gas <input type="checkbox"/> laag calorisch gas <input type="checkbox"/> zwavelhoudend gas <input type="checkbox"/> aardgascondensaat Uit alle voorkomens wordt hoogcalorisch gas gewonnen.
Mr 1.2.1 lid 3	Bestaande of nieuwe opslag	<input checked="" type="checkbox"/> opslagplan voor reeds bestaande opslag <input type="checkbox"/> opslagplan voor nieuwe winning
Mw 34 lid 7	Samenloop vergunningen	<input type="checkbox"/> nee <input checked="" type="checkbox"/> ja: te weten: <input checked="" type="checkbox"/> Omgevingsvergunning <input type="checkbox"/> Watervergunning <input type="checkbox"/> Vergunning Natuurbescheringswet <input type="checkbox"/> Anders, namelijk:

	Bedrijfs- en productiegegevens	Paragraaf
Mw 35 lid 1	Beknopte beschrijving van het opslagplan	1.2
Mw 35 lid 1c Mb 24 lid 1c,d	Beknopte beschrijving van wijze van opslag door middel van (een) mijnbouwwerk(en)	2.4
Mb 24 lid 1a	Geologische beschrijving van voorkomen(s)	4.1, 4.2
Mb 24 lid 1a Mb 24 lid 1b	Geologische doorsnede van voorkomen(s)	4 (figuur 9)
Mw 35 lid 1a Mb 24 lid 1d,e	Overzicht ligging voorkomens, gasputten	3.2 (Figuur 7)
Mb 24 lid 1d,e,g	Situering mijnbouwwerken situatietekening /eventueel foto	2.2 (figuur 3), 2.3
Mb 24 lid 1e,f	Overzicht boringen in voorkomen(s)	3.2 (Tabel 5/6)
Mb 24 lid 1g	Schematische voorstelling putverbuizing(en)	3.3 (Figuur 8)
Mb 24 lid 1h	Plaats en wijze waarop stikstof in verbuizing treedt	3.4
Mb 24 lid 2	Productieontwikkeling strategie	5.1
Mb 24 lid 2	Productie filosofie	2.7, 5.4
Mb 24 lid 2	Caverne management	5.5
Mw 35 lid 1a,d Mb 24 lid 1a	Omvang opslag	2.7
Mw 35 lid 1b	Duur van de opslag (per voorkomen)	5.9
Mb 24 lid 1i	Stoffen die jaarlijks worden mee geproduceerd	5.11
Mb 24 lid 1j	Jaarlijks eigengebruik bij opslag	n.v.t.
Mb 24 lid 1j	Jaarlijks bij opslag afgeblazen/afgefakkelde stikstof	5.10
Mb 24 lid 1k	Jaarlijks bij opslag in de ondergrond terug te brengen delfstoffen en andere stoffen	n.v.t.
Mw 36 lid 1 sub b	Planmatig gebruik of beheer van delfstoffen, aardwarmte, andere natuurlijke rijkdommen, waaronder grondwater met het oog op de winning van drinkwater, of mogelijkheden tot het opslaan van stoffen	n.v.t.
	Gegevens inzake bodemdaling als gevolg van de opslag van stikstof.	Paragraaf
Mw 35 lid 1f	Aard van de bodemdaling alsmede de daarmee verband houdende activiteiten	6.1
Mb 24 lid 1m Mb 24 lid 1n Mb 24 lid 1o	Gekalibreerde bodemdaling en bodemdalingprognoses (uiteindelijk verwachte mate van bodemdaling)	6.2
Mb 24 lid 1 m	Bodemdalingsvooruitzichten	6.3
Mb 24 lid 1q	Omvang en aard van de schade	6.6
Mb 24 lid 1r	Maatregelen om bodemdaling te voorkomen / te beperken	6.7
Mb 24 lid 1s Mw 35 lid 1f	Maatregelen die gevolgen van schade door bodemdaling beperken of voorkomen	6.7
	Gegevens inzake bodemtrilling als gevolg van opslag van koolwaterstoffen.	Paragraaf
Mw 35 lid 1f	Aard van de bodemtrilling alsmede de daarmee verband houdende activiteiten	7.1
Mb 24 lid 1p	Risicoanalyse bodemtrilling	7.3
Mb 24 lid 1q	Omvang en aard van de schade	7.5
Mb 24 lid 1r	Maatregelen om bodemtrillingen te voorkomen / te beperken	7.7
Mb 24 lid 1s Mw 35 lid 1f	Maatregelen die gevolgen van schade door bodemtrillingen beperken of voorkomen	7.7
	Overige veiligheidsaspecten	Paragraaf
Mw 35 lid 1g	De risico's voor omwonenden, gebouwen of infrastructurele werken of de functionaliteit daarvan met een risicobeoordeling, voor zover het winnen van delfstoffen niet geschiedt in het continentaal plat	8.1-8.7

<p>Ondertekening</p> <p><i>P.J.P. Roordink</i></p> <p>Naam: Patrick Roordink Functie: Petroleum Engineer</p>	<p><i>Datum: 3/6/2019</i> <i>Plaats: Groningen</i></p>
<p>Ondertekening</p> <p><i>M.M.J. Timmermans</i></p> <p>Naam: Michel Timmermans Functie: Projectcoördinator Mijnbouw/conversie</p>	<p><i>Datum: 3/6/2019</i> <i>Plaats: Groningen</i></p>

1 Inleiding

Dit opslagplan is een actualisatie van het Opslagplan Heiligerlee d.d. 25 februari 2010 (ref. ET/EM/10007048) en overgedragen van Akzo Nobel aan GTS d.d. 12 augustus 2016 (ref. DGETM-EO / 16117710). De reden voor de actualisatie is het feit dat er meer stikstof beschikbaar komt door een forse uitbreiding van de stikstofproductie-capaciteit van GTS. GTS bouwt namelijk een nieuwe stikstofinstallatie met een maximale capaciteit van 180.000 m³ per uur naast de bestaande stikstofinstallatie in de Tussenklappenpolder, gemeente Midden-Groningen. De bestaande installatie heeft een maximale uur-capaciteit van 16.000 m³ per uur. Door een groter aanbod van stikstof is een verhoogde injectiecapaciteit naar de caveerne mogelijk. Door een groter aanbod van stikstof is een verhoogde injectie naar de caveerne mogelijk. GTS heeft het voornemen om de stikstofinjectiecapaciteit te vergroten van 16.000 m³ per uur naar 190.000 m³ per uur, 190.000 m³ per uur injectie is worst case aangehouden i.v.m. de thermodynamische en rock mechanische studies. Hiermee wordt de maximale injectiecapaciteit en de uitzendcapaciteit gelijk.

1.1 Doel van het Opslagplan

- (i) *artikel 34 en 35 Mw, artikel 24 en 26 Mb*

GTS (100% dochter van N.V. Nederlandse Gasunie) is houder van de Opslagvergunning voor de concessie Winschoten II. Conform artikel 34 Mijnbouwwet (Mw) dient de opslag van stikstof te gebeuren overeenkomstig een opslagplan. In het Mijnbouwbesluit (Mb) is in artikel 24 aangegeven welke informatie het opslagplan moet bevatten. Overeenkomstig artikel 35, lid 1c van de mijnbouwwet dient een beschrijving van de wijze van de opslag als mede de daarmee verband houdende activiteiten te worden gegeven.

De reden voor de actualisatie van het vigerend opslagplan is het voorgenomen besluit om na de bouw van de stikstoffabriek een hogere injectiecapaciteit te kunnen realiseren van 190.000 m³ per uur.

Tabel 1 Geschiedenis Instemming Opslagplan Heiligerlee

Datum	Referentie	Benaming
15-02-2010	ET/EM/10007048	Instemmingsbesluit opslagplan stikstofbuffer Heiligerlee.
15-11-2010	ETM/EM /10155497	Besluit Splitsing opslagvergunning Winschoten en toestemming overdracht opslagvergunning Winschoten II.
12-08-2016	DGETM-EO / 16117710	Toestemming overdracht opslagvergunning Winschoten II; uittreding N.V. Nederlandse Gasunie; toetreding Gasunie Transport Services B.V.
23-01-2017	Brief SodM ref. [1]: 17013267	Brief SodM; Reactie SodM op inzetprofiel van de stikstofopslag Heiligerlee.

1.2 Leeswijzer

Nabij Heiligerlee wordt stikstof tijdelijk opgeslagen in een ondergrondse caveerne die geconstrueerd is en de Heiligerlee zoutdome. GTS heeft hier momenteel één caveerne in gebruik. De stikstofcaveerne is verbonden met de bestaande stikstofinstallatie te Zuidbroek en zal eveneens worden gebruikt in combinatie met de nieuwe stikstofinstallatie die naast de bestaande installatie zal worden gebouwd. De "tijdelijke opgeslagen" stikstof uit de caveerne wordt op het mengstation te Zuidbroek gemengd met hoog calorisch gas om zo gas te verkrijgen met dezelfde kwaliteit als het Groningen-gas. (G-gas). Dit "pseudo" G-gas vervangt het echte G-gas omdat de productie hiervan zo spoedig mogelijk wordt gereduceerd naar 12 miljard m³ per jaar en in 2030 naar nul.

In dit document wordt ingegaan op de manier waarop stikstof wordt opgeslagen in de ondergrondse zoutcaveerne van Heiligerlee, de geologie en de eigenschappen van het zoutgesteente, de verwachte operationele inzet, en de mate van bodemdaling en het risico op aardbevingen.

Per onderdeel in dit document wordt daar waar relevant een verwijzing gemaakt naar wet- en regelgeving (i). De betekenis van de gebruikte afkortingen is als volgt:

- Mw = Mijnbouwwet
- Mb = Mijnbouwbesluit
- Mr = Mijnbouwreglement

De verwachte bodemdaling als gevolg van de stikstofopslag in de caveerne in de periode 2010 - 2050 is ca. 15 mm. In hoofdstuk 6 staan nadere aspecten van bodemdaling beschreven. De bodemdaling wordt regelmatig gemonitord volgens een meetplan (art. 30, 1e lid Mb) conform de geldende normen, onder toezicht van Staatstoezicht op de Mijnen (SodM).

De seismische risicoanalyse laat zien dat op grond van het viscoplastisch (kruip) gedrag van zout er geen bodemtrillingen te verwachten zijn, ook in de literatuur zijn geen aanwijzingen te vinden over het optreden van bodemtrilling in relatie tot de opslag van gas in zoutcavernes. Hiermee is aannemelijk gemaakt dat stikstofopslag in zoutcavernes in de laagste seismische risicocategorie valt (categorie I). Hoofdstuk 7 gaat verder in op de seismische risico analyse.

Het opslagplan zal aangepast worden als de gemeten bodemdaling en de prognose, zoals in dit opslagplan beschreven, overschrijdt. Als nieuwe inzichten tot een wijziging van de dalingsvoorspelling of seismische risicoanalyse leiden zal er eveneens een wijziging van het opslagplan worden ingediend. Een dergelijke actualisatie vereist opnieuw de instemming van de minister van Economische Zaken en Klimaat, waarvoor weer de uniforme openbare voorbereidingsprocedure wordt gevolgd.

1.3 Overige vergunningen

GTS is voornemens om op de locatie Heiligerlee tussen 2020 en 2022 bovengronds een slug catcher (vochtvanger) en een diesel-noodstroomvoorziening te installeren. Beide items kunnen worden gerealiseerd binnen de regels van het vigerende bestemmingsplan. De bovengenoemde aspecten "milieu" en "bouw" (ten behoeve van de vochtvanger en mogelijk de diesel-noodstroomvoorziening) zullen met één revisie omgevingsvergunning worden gereguleerd. Het bevoegd gezag is de minister van Economische Zaken en Klimaat.

Dit betekent dat tegelijk met deze aanvraag tot instemming van de wijziging van het opslagplan een aanvraag ingediend zal worden tot revisie van de bestaande milieuvergunning. Deze milieuvergunning, met kenmerk ET/EM / 10008147, is op 22 februari 2010 verleend aan AkzoNobel Salt te Delfzijl. Inmiddels is GTS al weer een aantal jaren drijver van deze inrichting. Omdat er sprake is van een wijziging van het opslagplan en een omgevingsvergunning, is op deze besluiten de Rijkscoördinatierегeling (RCR) van toepassing (artikel 141a Mijnbouwwet).

De aanpassingen op de locatie Heiligerlee hangen samen met het project "aanvullende stikstofproductiefaciliteit Zuidbroek". Dit project valt onder de Rijkcoördinatierегeling (RCR). De ontwerpbesluiten voor het inpassingsplan en een aantal vergunningen heeft ter inzage gelegen van 18 januari 2019 tot en met 28 februari 2019. Vanaf eind mei 2019 liggen de definitieve besluiten ter inzage. De caveerne HL-K is niet opgenomen in het inpassingsplan omdat de voorziene wijzigingen niet noodzakelijk zijn voor de bouw van de aanvullende stikstofproductiefaciliteit. Wel is in het inpassingsplan in de toelichting een paragraaf opgenomen waarin uitgebreid wordt ingegaan op de gewenste activiteiten met betrekking tot de stikstofcaveerne. Aan de caveerne hoeft technisch niets gewijzigd te worden.

Deze aanvraag tot instemming wijziging opslagplan kent een eigen coördinatie-procedure op grond van de Mijnbouwwet. Het bevoegde gezag voor zowel de revisie omgevingsvergunning als deze aanvraag is de minister van Economische Zaken en Klimaat (EZK). In verband met de samenhang tussen de bouw van de aanvullende stikstofproductiefaciliteit en de wijzigingen op de opslagcaveerne bij Heiligerlee worden de procedures gedeeltelijk parallel uitgevoerd.

2 Plaats van Opslag

(i) *artikel 34 lid 1c Mw, artikel 24 lid 1a en 26 Mb*

2.1 Voorkomen(s) in dit opslagplan


Dit opslagplan beschrijft de opslag van stikstof in de Heiligerlee caveerne. In bijlage 1 is een grote foto van de opslaglocatie weergegeven.

2.2 Overzicht ligging voorkomens

(i) *artikel 35 lid 1a Mw, artikel 24 lid 1d,e en artikel 26 lid 1b Mb*

Voor de concessie Adolf van Nassau zijn drie opslagvergunningen verleend en weergegeven in onderstaande figuur 1.

Opslagvergunningen Adolf van Nassau

<p>Winschoten II (stikstofbuffer) Vergunninghouder: Gasunie Transport Services Operator: N.V. Nederlandse Gasunie Voorkomen: Zoutdome Heiligerlee</p>	
<p>Winschoten III Vergunninghouder: Akzo Nobel Salt B.V. Operator: Akzo Nobel Salt B.V. (Nouryon) Voorkomen: Zoutdome Heiligerlee</p>	
<p>Zuidw ending (Aardgas) Vergunningshouders: EnergyStock B.V. Akzo Nobel Salt B.V. Operator: N.V. Nederlandse Gasunie Voorkomen: Zuidw ending zoutdome</p>	

Figuur 1 Opslagvergunningen Adolf van Nassau

In onderstaande figuur 2 is een luchtfoto weergegeven van de stikstofcaverne Heiligerlee en omgeving.



Figuur 2 Luchtfoto stikstof opslag Heiligerlee

2.3 *Situering van het mijnbouwwerk*

(i) *artikel 24 lid 1d,e,g en artikel 26 lid 1b Mb*

Volgens artikel 24, lid 1d dient de ligging van het mijnbouwwerk gegeven te worden. In figuur 3 is een totaal overzicht gegeven. Het terrein bevindt zich zuidwestelijk van Winschoten en wordt ingesloten door de Tranendallaan, Meidoornlaan en de Ontsluitingsweg.

2.4 **Beknopte beschrijving van de opslag**

(i) *artikel 35 lid 1c Mw, artikel 24 lid 1,c en artikel 26 Mb*

De stikstofopslag te Heiligerlee bestaat uit een caveerne, gelegen op ruim 1000 meter diepte. De in de caveerne opgeslagen stikstof vormt een buffervoorraad stikstof, die aangesproken kan worden in geval van toenemende vraag naar stikstof. Deze stikstof wordt gebruikt om hoogcalorische gassen te mengen tot G-gas kwaliteit. Het mengproces vindt plaats op Zuidbroek.

De stikstof wordt in gasvormige toestand opgeslagen in een zoutcaveerne, die speciaal voor dit doel is omgebouwd in het zoutvoorkomen bij Heiligerlee binnen de zoutwinningsvergunning "Adolf van Nassau ". De stikstof wordt opgeslagen onder hoge druk. Deze druk kan variëren van 70/90 bar tot 147 bar aan de casingschoen (CS).

2.5 **Beknopte beschrijving van de wijze van opslag**

(i) *artikel 35 lid 1c Mw, artikel 24 lid 1c,d*

De toevoer van stikstof naar de caveerne vindt plaats door middel van een 10 kilometer hoge druk leiding vanuit de locatie Zuidbroek. Het mijnbouwwerk bestaat uit de locatie Heiligerlee, caveerne HL-K en de 10 kilometer hoge druk leiding (16" ontwerpdruk 171 bar) tot aan de eerste isolatieafsluiter op locatie Zuidbroek. De injectiecapaciteit betreft 16.000 m³ stikstof per uur en wordt vergroot naar 190.000 m³ stikstof per uur.

Na de bouw van de aanvullende stikstofinstallatie in Zuidbroek (operationeel eerste kwartaal 2022) is het mogelijk om 190.000 m³ stikstof per uur te injecteren in de caveerne. De uitzendcapaciteit van de caveerne is gedimensioneerd op 190.000 m³ stikstof per uur. Dat betekent dat er voor de hogere injectiecapaciteit technisch niets gewijzigd hoeft te worden aan de caveerne en onderdelen daarvan zoals de verbuizing. Bij de injectiefase wordt in Zuidbroek met elektrisch aangedreven compressoren stikstof gecompriëerd. Vervolgens wordt de stikstof met luchtkoelers afgekoeld naar max 45 graden Celsius. Door een 10 km lange leiding wordt de stikstof, via een bovengronds te plaatsen slug catcher, naar de caveerne gezonden. Bij het produceren van de stikstof uit de caveerne naar Zuidbroek wordt de stikstof geleid door een slug catcher en een filter die opgesteld staan in Zuidbroek. De gefilterde stikstof wordt vervolgens verwarmd tot ca. 25 graden Celsius. Het verwarmingssysteem heeft een totaalvermogen van ca. 1.4 MW. Via smookkleppen wordt de druk van de stikstof gereduceerd tot het de vereiste druk heeft bereikt voor de droogkolom. Daar wordt de laatste aanwezige waterdamp met gebruikmaking van glycol verwijderd tot beneden het vereiste dauwpunt. Vervolgens wordt de stikstof ingevoerd in het mengstation.

2.6 **Wijze van terugwinning en opslag (procesbeschrijving)**

(i) *artikel 35 lid 1c Mw*

Volgens artikel 35, lid 1c van de mijnbouwwet en artikel 24, lid c van het mijnbouwbesluit dient een beschrijving van de wijze van terugwinning en opslag alsmede de daarmee verband houdende activiteiten gegeven te worden.

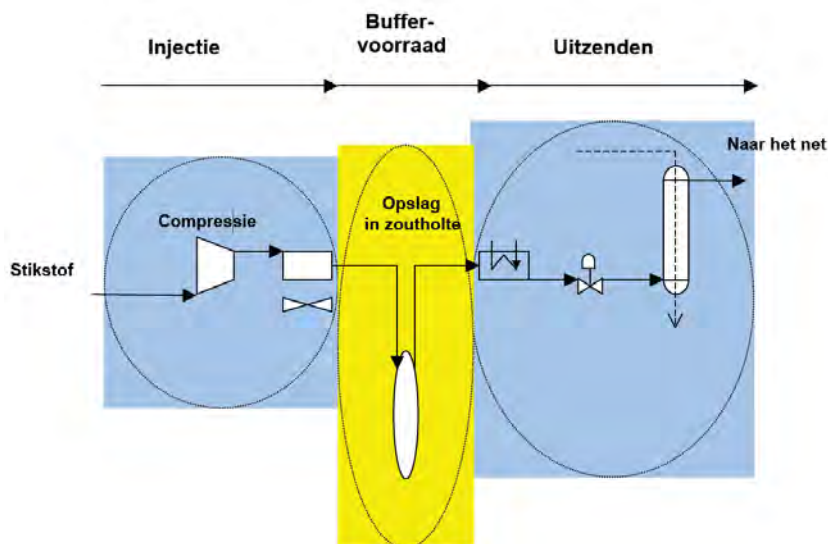
De belangrijkste gegevens van de gasopslag zijn weergegeven in tabel 3.

Grootheid eenheid		Eenheid
aantal cavernes	1 stuks	Stuks
totaal geometrisch volume	<0,81	miljoen m ³
totaal werkgas volume	36,6	miljoen m ³ (n) (bij 147 bar @ CS)
Kussengasvolume	63,7	miljoen m ³
totale injectie capaciteit	190.000	m ³ (n) /h
totale productie capaciteit	190.000	m ³ (n) /h
maximale druk in de caveerne	ca. 147	Bar @ CS
minimale druk in de caveerne	ca. 70/90	Bar @ CS

Tabel 2 Kerngegevens van Stikstofbuffer Heiligerlee

2.7 Injectieproces

De stikstof wordt geproduceerd door een luchtscheidingsinstallatie met een druk van 9 bar, hierna zal de stikstof worden gecomprimeerd in twee stappen tot een maximaal druk van 131 bar aan de wellhead. De stikstof wordt vanaf Zuidbroek met een 10 km lange leiding naar de caveerne gestuurd/geïnjecteerd. Bij productie zal de stikstof met dezelfde leiding vanuit de caveerne richting Zuidbroek gaan en wordt hier behandeld voordat het wordt geïnjecteerd in het mengstation. In figuur 4 is het opslag- en terugwinningproces schematisch weergegeven.



Figuur 4 Schematische voorstelling stikstofopslag proces

De geproduceerde stikstof wordt eerst verwarmd. Via smoorkleppen wordt de druk gereduceerd tot de stikstof de vereiste druk heeft voor het droogproces. Hierna wordt het gebruikt in het mengstation om hoogcalorische gasen te mengen tot pseudo G-gas.

2.8 Productieproces

Bij uitzenden wordt de stikstof verwarmd voordat de druk wordt gereduceerd tot de vereiste druk voor de droogkolommen. Nadat de stikstof de vereiste specificaties (druk, temperatuur, dauwpunt) heeft bereikt kan de stikstof worden geleverd aan het leidingnet.

Opslagproces

(i) *artikel 24 lid 2 Mb*

Het injectie- en productieproces vindt plaats binnen de op basis van thermodynamische en gesteente mechanische studies geadviseerde grenzen voor stabiliteit en integriteit van de caveerne en beperking van de convergentie. Dit wordt de bedrijfsvoeringenveloppe genoemd. De grenzen zijn bepaald op basis van de geldende inzichten en zijn afhankelijk van de diepteligging, grootte en vorm van de caveerne, maar ook van de locatie specifieke zouteigenschappen.

De bedrijfsvoeringenveloppe is vastgesteld door ESK en IfG en wordt beschreven in het volgende documenten:

1. Feasibility Proof HL-K Injection Capacity Increase_signed, zie ref. [2]
2. Rock mechanical report B IfG - 47_2018_Report_HLK _final_2", zie ref. [3].

In de rapporten is rekening gehouden met caveerne specifieke convergentiesnelheden, voor de caveerne HL-K is dit 2 %/per jaar.

De bedrijfsvoeringenveloppe wordt aan de bovenkant begrensd door de maximaal toegestane cavernedruk, welke afhankelijk is van de diepteligging van de Last Cemented Casing Shoe (LCCS) (zie tabel 3). Hierbij is een drukgradiënt van 0.15 bar per meter gehanteerd.

Aan de onderkant wordt de bedrijfsvoeringenveloppe begrensd door de minimum cavernedruk. De minimum cavernedruk is afhankelijk van de diepteligging van de bodem (de sump) van de caveerne maar ook van tijdsduur waarop de caveerne op deze minimumdruk wordt bedreven.

De cavernedruk waaronder een caveerne maximaal 90 dagen per jaar bedreven mag worden, wordt gedefinieerd als $P_{min,0}$. De druk waarop een caveerne zich maximaal 30 dagen per jaar mag bevinden wordt P_{min} genoemd. In tabel 3 zijn de minimum en maximum caveerne drukken ter hoogte van de LCCS opgenomen.

Druk	Caverne HL-K
P_{max} [in barg]	147
$P_{min,0}$ [in barg]	90
P_{min} [in barg]	70
$P_{max}-P_{min}$ [in barg]	77

Tabel 3 Minimum en maximum caveerne druk @ LCCS

De maximale hoeveelheid stikstof die per dag aan de caveerne wordt onttrokken, wordt gelimiteerd door gesteente-mechanische grenzen en wordt uitgedrukt in een maximum drukverandering per dag. De maximum drukverandering per dag is afhankelijk van de caveerne druk, zie tabel 4.

Caverne druk	Maximale drukwijziging [bar per dag]
$P_{min,0} < P_{cav} < P_{max}$	$-10 \leq dp/dt \leq 10$
$P_{min} < P_{cav} < P_{min,0}$ (maximaal 90 dagen per jaar)	$-3 \leq dp/dt \leq 3$

Tabel 4 Maximum drukwijzigingen per dag

2.9 Operationele filosofie

(i) *artikel 24 lid 2 Mb*

Inleiding

De Nederlandse markt is op dit moment voornamelijk geschikt voor het G-gas. G-gas bevat 14 procent stikstof en heeft daardoor een lagere calorische waarde dan het meeste buitenlandse gas afkomstig uit bijvoorbeeld Rusland en Noorwegen. Omdat dit buitenlands gas steeds belangrijker wordt voor de Nederlandse energievoorziening door afname van de binnenlandse G-gas productie is de stikstofbehoefte van GTS door de jaren heen toegenomen, zowel in de basis als op piekmomenten. Daarom is in 2012 nabij Heiligerlee een stikstofpiekinstallatie in gebruik genomen met een werkvolume van circa 37 mln. m³, een injectiecapaciteit van 16.000 m³/h en een uitzendcapaciteit van 190.000 m³/h.

Groningen dossier

Als direct gevolg van het besluit in maart 2018 van de minister van Economische Zaken en Klimaat om de winning van aardgas uit het Groningenveld te beperken tot strikt noodzakelijk met ingang van het komend gasjaar en zelfs helemaal te stoppen in 2030 (of eerder indien mogelijk), neemt de stikstofbehoefte van GTS fors toe. Deze behoefte zal grotendeels worden ingevuld door het bouwen van een extra stikstofinstallatie in Zuidbroek met een capaciteit van 180.000 m³/h (3 productie units van

elk 60.000 m³/h). Met deze installatie kan vanaf Q1 2022 op jaarbasis 7-10 bcm pseudo-G-gas worden geproduceerd, aardgas dat dus niet meer uit het Groningenveld wordt onttrokken.

Relatie stikstofcaverne Heiligerlee en stikstofinstallatie Zuidbroek

De rol van de caverne blijft met de uitbreiding van de stikstofinstallatie nabij Zuidbroek hetzelfde: het kunnen opvangen van pieken in de G-gas markt en het hebben van een strategische voorraad stikstof voor uitval van stikstof-beschikbaarheid elders in het land. GTS verwacht de caverne flexibeler in te zetten nu de nieuwe stikstofinstallatie het mogelijk maakt de caverne sneller te kunnen vullen. De toegevoegde waarde van de caverne neemt daardoor toe ook omdat de beschikbaarheid van het nieuwe mengstation er door wordt verhoogd. Daarnaast wordt ook de inzet van de installatie efficiënter omdat een kortdurende extra behoefte aan stikstof opgevangen kan worden door de caverne in plaats van extra baseload capaciteit op te starten en kan bij een eventueel overschot aan geproduceerde stikstof dit snel in de caverne worden geïnjecteerd voor later gebruik. In het geval dat de stikstoffabriek op Zuidbroek om wat voor reden dan ook uitvalt, kan de productie van stikstof uit de caverne gewoon doorgaan.

Injectiecapaciteit stikstofcaverne Heiligerlee

Gelet op bovenstaande is de huidige injectiecapaciteit ontoereikend, de caverne moet namelijk in beperkte tijd snel kunnen worden gevuld met stikstof afkomstig uit Zuidbroek. De injectiecapaciteit moet daarom worden verhoogd van 16.000 m³/h naar van 190.000 m³/h, in lijn met de huidige uitzendcapaciteit. De infrastructuur (stikstofleiding en installatie Heiligerlee) hoeft voor de verhoogde injectiecapaciteit niet te worden aangepast. Uiteraard wil GTS zeker weten dat een flexibelere inzet van de caverne niet ten koste gaat van de veiligheid en betrouwbaarheid. Recente studies (zie ref. [2] en ref. [3]) door onafhankelijke instituten hebben uitgewezen dat het intensiever bedrijven van de caverne geen additioneel risico vormt voor de omgeving en dat binnen de vergunningsvoorwaarden wordt geopereerd.

In 8 dagen kan met een capaciteit van 190.000 m³ per uur deze 36,6 miljoen m³ worden uitgezonden. Het hele opslag- en productieproces beweegt zich binnen de door de rock mechanische en thermodynamische gestelde grenzen.

Omvang van de opslag

- (i) *artikel 35 lid 1a,d Mw, artikel 26 lid 1a en artikel 24 lid 1a Mb*

Volgens artikel 26, lid a van het mijnbouwbesluit dient een beschrijving van de hoeveelheid en de samenstelling van de stoffen die worden opgeslagen gegeven te worden. De omvang van het geometrisch volume is 0,81 * 10e6 m³ en er wordt 100% stikstof opgeslagen. De hoeveelheid jaarlijks opgeslagen stikstof is afhankelijk van het aantal cycli (vullen en weer legen) dat in een jaar wordt gerealiseerd. In 2018 is er ca. 65 miljoen m³ stikstof geïnjecteerd en 56 miljoen m³ stikstof geproduceerd uit caverne HLK.

3 Boring

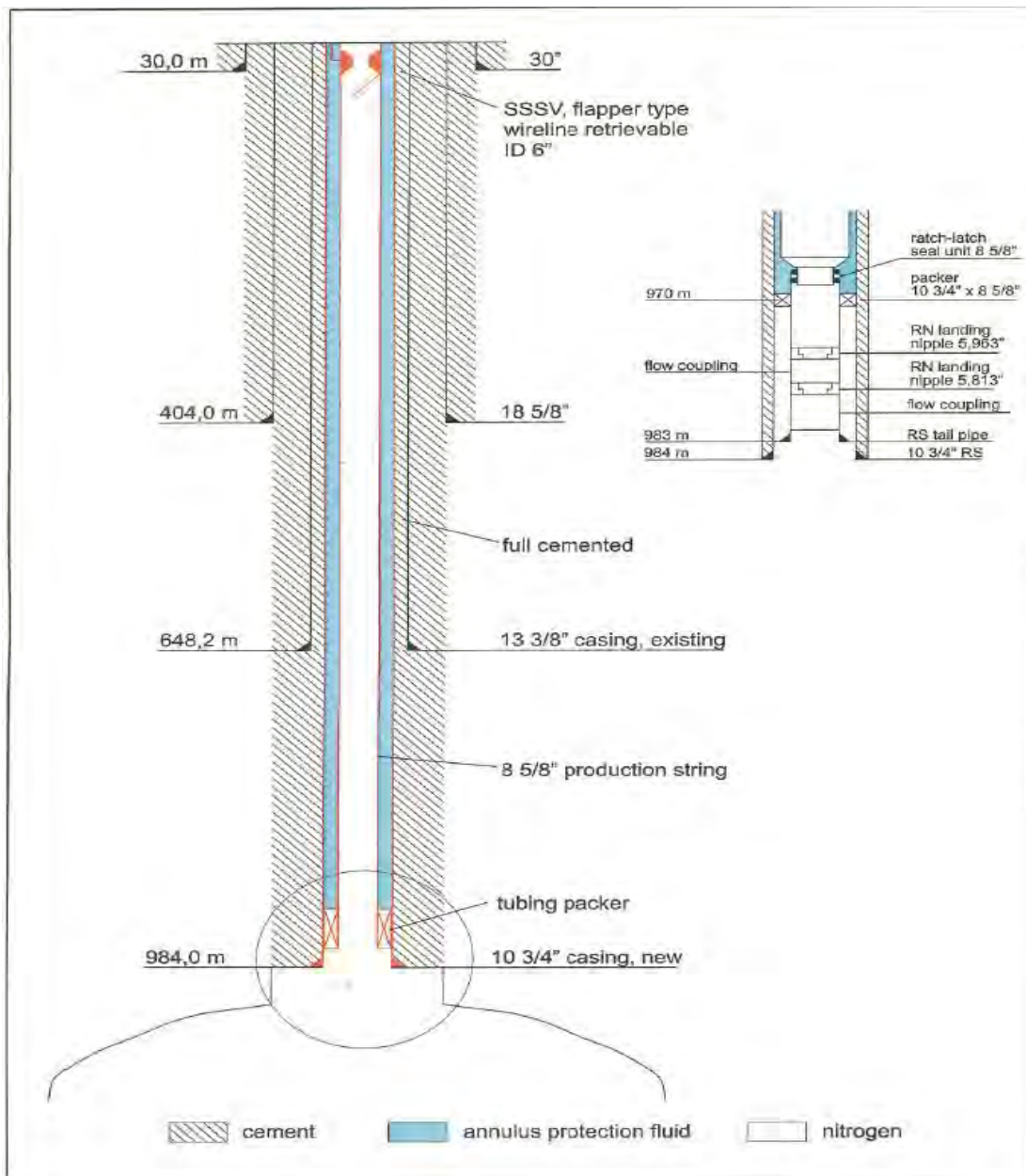
(i) artikel 24 lid 1e,f,g Mb

Voordat de caveerne in gebruik is genomen als stikstofopslag is de caveerne in de eerste fase gebruikt voor zout winning door Akzo Nobel. Later is de put van Heiligerlee K gereconstrueerd en omgebouwd naar een opslag put voor de opslag van stikstof.

Volgens artikel 24, lid g van het mijnbouwbesluit dient een opgaaf van de ligging, lengte en diameter van de verbuizing van het boorgat te worden gegeven. Eerst zal een inleiding worden gegeven hoe de boring is uitgevoerd waarbij de caveerne is ontwikkeld. Vervolgens zal aangegeven worden hoe de put van de caveerne is gereconstrueerd voor de ombouw naar een stikstofcaveerne.

3.1 Inleiding: Algemene beschrijving van de Heiligerlee K boring

In figuur 5 is een schematische weergave van de huidige Heiligerlee K boring weergegeven. De belangrijkste onderdelen van het constructieproces worden hier besproken.



Figuur 5 Schematische weergave van de Heiligerlee K put

Ter bescherming van de directe oppervlakte en de grondwatervoerende lagen is bij aanleg van de locatie d.m.v. heien een gelaste conductor (diameter 32"wanddikte 11 mm) tot op een diepte van 30 m aangebracht.

De boring is verdeeld over drie secties te weten:

1. Van 0 – 408 meter. Deze sectie tot net boven de caprock werd uitgevoerd met een zoete bentoniet spoeling. Normaal "Rotary drilling" zonder Measuring While Drilling systeem (MWD) werd toegepast. Het boorgat is met een boordiameter van 23" geboord. Hierin is een 18 5/8" K55, 87,6 # BTC casing gecementeerd met een lead en tailslurry van Pozmix 8000.
2. Van 404 – 653 m. Deze sectie werd met een zoute bentoniet spoeling uitgevoerd. In deze sectie werd gebruik gemaakt van een downhole mudmotor en een MWD-systeem. Het boorgat is met een boordiameter van 16" geboord. Hierin is een 13 3/8" J55, 45,5 # BTC casing gecementeerd met een zout verzadigde lead en tailslurry van Pozmix 8000.
3. Van 648 – 1650 m, Ook hier werd gebruik gemaakt van een downhole mudmotor en een MWD-systeem. Boordiameter 12 1/4".

Vanuit deze boring is middels 2 loogstringen, een 10 3/4" en een 7" de huidige caveerne HL-K gecreëerd middels oplossing mijnbouw. Dat wil zeggen, fris water injecteren en pekewater produceren.

Om de caveerne HL-K te gebruiken voor stikstofopslag, moest de put worden geconverteerd van een leaching completion naar een gasopslag completion. Tevens moest het casing design aangepast worden. De laatste gecementeerd casing tijdens de uitlogperiode was een 13 3/8" casing met een schoendiepte op 648,2m. De connecties van de 13 3/8" casing zijn niet gasdicht. Omdat deze 13 3/8" casing niet geschikt is voor gasopslag is er een nieuwe gasdichte laatst gecementeerde casing geplaatst waarbij de casingschoen op een diepte van 981m is gezet. De LCCS betreft een 10 3/4" N80 51 # casing met gelaste verbinding.

De hoogte van de cementkolom en de kwaliteit van de cementatie bepaalt in grote mate de gasdichtheid van de caveerne. Daarom wordt nadat de 10 3/4" gecementeerde casing is aangebracht de put getest op gasdichtheid (zogenaamde MIT; mechanical integrity test). De eerste MIT is uitgevoerd op 27 juni tot 30 juni, 2010, om de integriteit van het de laatst gecementeerde casing te bewijzen.

Vóór de installatie van de productie-tubing hebben er cement loggingen plaatsgevonden (USIT- en CBL-meting). Deze zijn uitgevoerd om de condities van de cementatie en corrosie van de laatst gecementeerde casing vast te leggen. Tevens worden deze metingen gebruikt om het exacte gebied te bepalen waar de productie packer gezet moet worden.

De maximum mogelijke diameter van een extra nieuw, gecementeerde casing in de 13 3/8" casing was 11 3/4". Echter vanwege de kleine annulaire ruimte was de beslissing alleen het bovenste te bouwen deel tot ~ 78 m in 11 3/4" uitgevoerd om een grote binnendiameter van de ondergrondse SC-SSSV (Surface Controlled Sub-Surface Safety Valve) te krijgen en het onderste deel tot 981 m in 10 3/4" uitgevoerd. Afhankelijk van de dimensie van de laatste gecementeerde casing was een 9 5/8" x 8 5/8" productie-tubing mogelijk.

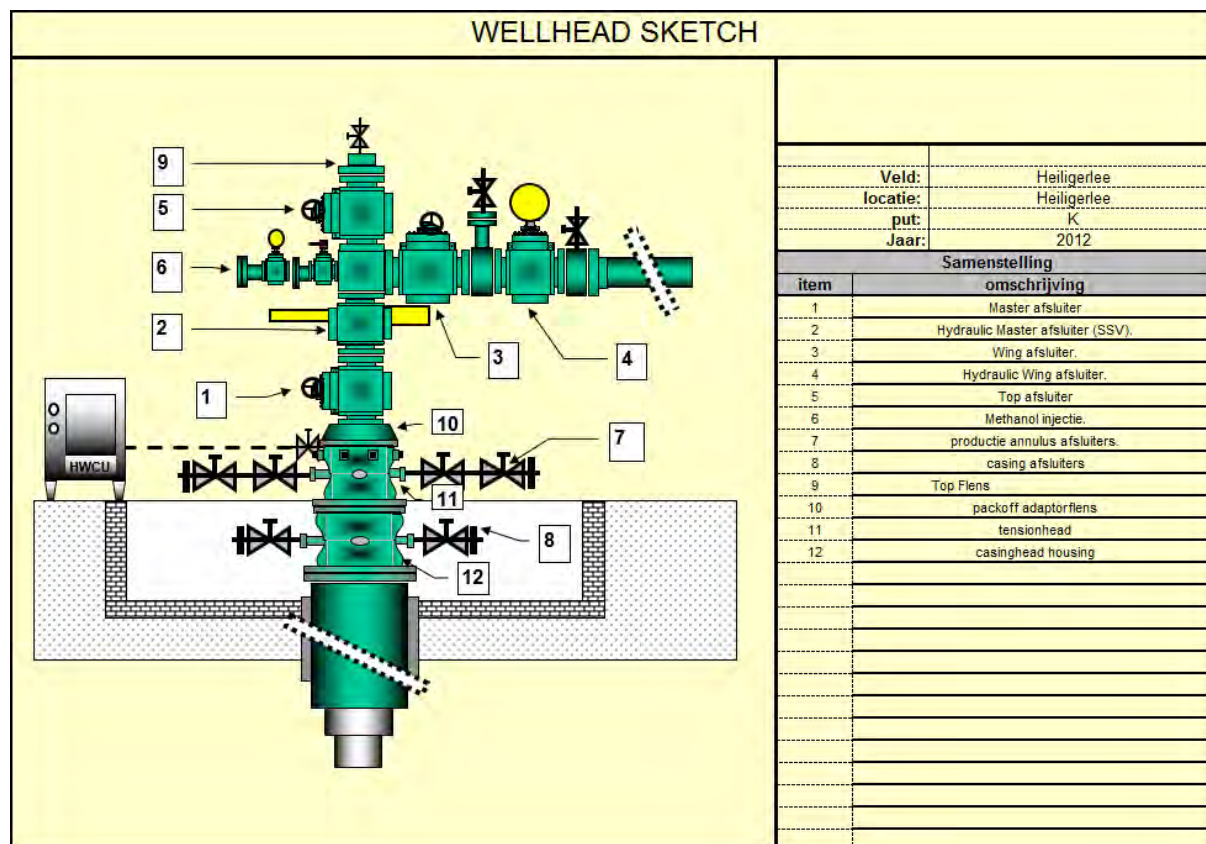
De ruimte tussen de productie-tubing en de casing wordt A-annulus genoemd. Voor het afdichten van de annulus is tussen laatste gecementeerde casing en productie-tubing een packer met tailpipe geïnstalleerd op 962 m. De tailpipe bevat landing nipples en profielen om pluggen en tools in af te kunnen hangen. De A-annulus is gevuld met een vloeistof inclusief corrosie inhibitor. Bovenop deze vloeistofkolom staat een stickstofkolom van ca. 15 meter met een pre-charge van ca. 15 bar.

De druk in deze A-annulus wordt continu gemonitord om de goede staat, de integriteit, van de put te kunnen waarborgen. Tevens wordt de B-annulus (annulaire ruimte van de laatst gecementeerde casing en 13 3/8" casing) continue gemonitord met hetzelfde doel.

Een belangrijk onderdeel van de productie-tubing is een ondergrondse veiligheidsafsluiter SC-SSSV die boven het maaiveld bedienbaar is. Deze ondergrondse veiligheidsafsluiter bevindt zich op een diepte van ca. 50 meter en is fail-safe uitgevoerd, dit betekent dat bij het wegvallen van de hydraulische stuurdruk de veiligheidsafsluiter automatisch wordt gesloten.

De putkop van de Heiligerlee HL-K put is gedimensioneerd op basis van de te verwachte druk van ongeveer 131 bar (statisch) aan de wellhead. De drukklasse van de wellhead en X-mass tree

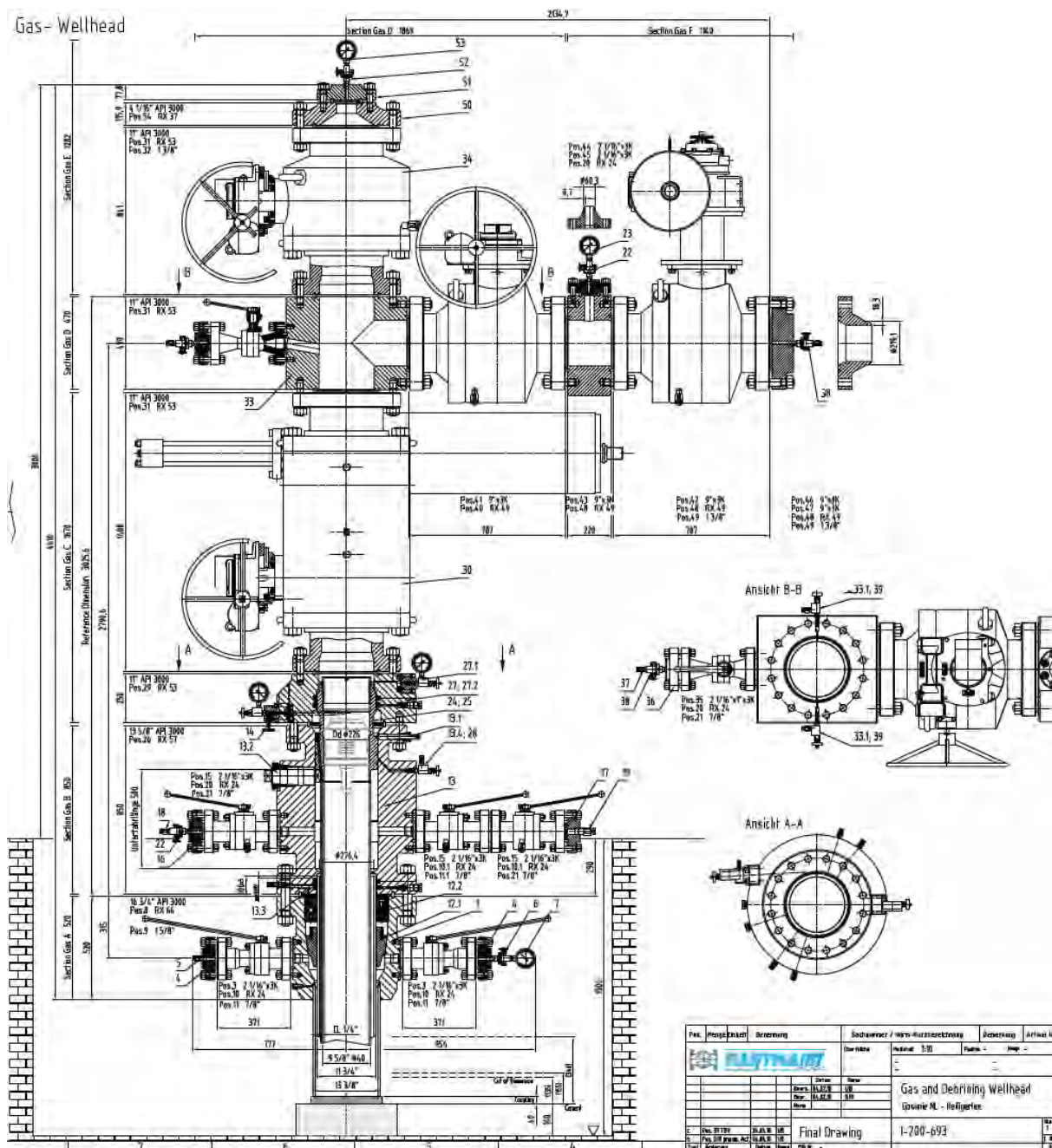
(spuitkruis) is API 3000 (206,8 bar). De X-mass tree bevat de diverse kleppen die nodig zijn om de put te bedienen. In Hieronder in figuur 6 staat schematisch weergegeven welke onderdelen deze X-mass tree bevat. In figuur 7 is voor Heiligerlee de uitvoering van de X-mass tree weergegeven.



Figuur 6 schematische weergave X-mass tree Heiligerlee K

Na het inbouwen van de productietubing is een tweede MIT uitgevoerd om de put inclusief de productietubing met haar componenten te testen op gasdichtheid.

Na het completeren van de put inclusief X-mass tree is er een zgn. debrining pijp ingebouwd om het brine uit de caveerne te drukken met het opslagmedium stikstof. De debrining pijp is ingebouwd tot de bodem van de caveerne. Na een aantal maanden was het pekelwater volledig uit de caveerne gedrukt. Vervolgens werd de debrining pijp uit de caveerne gebouwd door middel van een zgn. snubbing operatie. Met een snubbing unit, een soort workover unit, kunnen er werktuigen of verbuizingen veilig in of uit een op druk staande put worden ingebracht of uitgehaald.



Figuur 7 Uitvoering spuitkruis Heiligerlee

3.2 Overzicht boringen in voorkomen(s)

(i) artikel 24 lid 1e,f en artikel 26 lid 1b Mb

Volgens artikel 24, lid 1 e en lid 1 f van het mijnbouwbesluit dient een opgaaf van het aantal boorgaten, de volgorde en het tijdsbestek van het maken de boorgaten te worden gegeven.

De Heiligerlee K put is geboord door Akzo Nobel in juli 1996 t/m oktober 1996. De put is gebruikt door Akzo Nobel voor de pekels winning waardoor er een caveerne is gecreëerd. De ombouw naar een stikstofopslag heeft plaats gevonden in de periode van maart 2010 t/m juni 2010. De start van de stikstof injectie vond plaats in 2011. De debrining pijp is in augustus 2012 uit de put gehaald middels een snubbing operatie.

In tabel 5 staan de put coördinaten en put diepte weergegeven.

Tabel 5 Overzicht putcoördinaten en putdieptes

Caverne put	Spud-in X-as	Spud-in Y-as	LCCS X-as	LCCS Y-as	Diepte LCCS [m TVD]	Diepte put [m TVD]
HL-K	263 573.89	574 318.32	263 573.89	574 318.32	981	1650

In onderstaande tabel 6 is een overzicht gegeven van het boorgat en specifieke gegevens van de toegepaste verbuizingen.

Tabel 6 Lengte en diameter boorgat verbuizing

Caverne put	32" [m MD]	18 ⁵ / ₈ [m MD]	13 ³ / ₈ [m MD]	10 ³ / ₄ " [m MD]
HL-K	0 - 30	0 - 404	0 - 648	0 - 981

3.3 Schematische voorstelling putverbuizing(en)

(i) artikel 24 lid 1g

In figuur 8 is een schematische voorstelling gegeven van de put verbuizing van Heiligerlee K.

WELL SKETCH							
Heiligerlee			Veld:		Heiligerlee		
			locatie:		K		
			put:		HL-K		
			datum:		19-5-2016		
coordinates		X=263573.891 Y=574318.32					
schema	diepte MD (mtr)	diepte TVD (mtr)	onderdeel	ID (mm)	drift (mm)	opmerking	
	0,00		9 5/8" Hanger, hartmann, 9 5/8"BTC, BPV profile			profile for Hartmann BPV, niet gebruiken ivm shearwaarde hangerbolts	
	57,30		tubing from 9 5/8" - 47# N80 to 8 5/8" #36 J55				
	60,00		FRP savety valve landing nipple, 8.250" sealbore, Halliburton				
			WR - TRSV 9 5/8", Halliburton flapper				
			tubing 8 5/8 - 36# J55				
	962,00		Halliburton Packer				
			Landing Nipple 5,963" RNT No-go landing nipple (min ID 5,843 inch) integretd in packer assy				
			no-go				
			flow coupling,				
	970,20		Landing Nipple 5,813" RNT No-go landing nipple (min ID 5,655 inch)				
			no-go				
		flow coupling,					
972,30		tailend				deviatie uit Final drilling reports	
						ESD waarde WHP 168,86 bar(g)	
						ESD Maasp A Annulus 21,5 bar(g) HH	
		caverne				ESD Maasp B Annulus 20,0 bar(g) HH	
		sum p				ESD MAASP Clamp 4,0 bar(g) HH	
Casing schema				deviatie			
maat	diepte MD (mtr)	diepte TVD (mtr)	omschrijving	ID (mm)	drift (mm)	diepte MD (mtr)	max grad
32 - 162 # K55	30,0		Conductor			nvt	
18 5/8" - 87,5# K55	404		Anchor casing, cemented				
13 3/8" - 61 # - K55	648,2		Oils last cemented				
11 3/4" 60 # J55	78,5		New last cemented casing				
	78,5 -		New last cemented casing				
10 3/4" 51 # N80	981						
opmerking : annulus 9 5/8"x11 3/4", inhibited NaCl brine sm 1205 kg/m3, 10 mtr nitrogen cap, precharge 12 bar.							

Figuur 8 Schematisch Voorstelling put verbuizing Heiligerlee K

Doordat Zuidbroek II met een hogere injectieflow de caveerne kan vullen dient de put daarvoor bestand te zijn tegen turbulentie, erosie/corrosie. De put was al bi directioneel ontworpen en kan 190.000 m3/uur produceren en injecteren. Met Zuidbroek I was dat 16.000 m3/uur injectie. Om turbulentie, erosie en corrosie door stikstofflow op te vangen zijn er flow koppelingen geplaatst. Flow koppelingen zijn verbuizingen met een grotere wanddikte die b.v. boven en onder de flapper en landing nippels zitten. Hiermee zijn er voldoende mitigerende maatregelen genomen om erosie en fracs te voorkomen.

3.4 ***Plaats en wijze waarop stikstof in de verbuizing treedt***

(i) *artikel 24 lid 1h Mb*

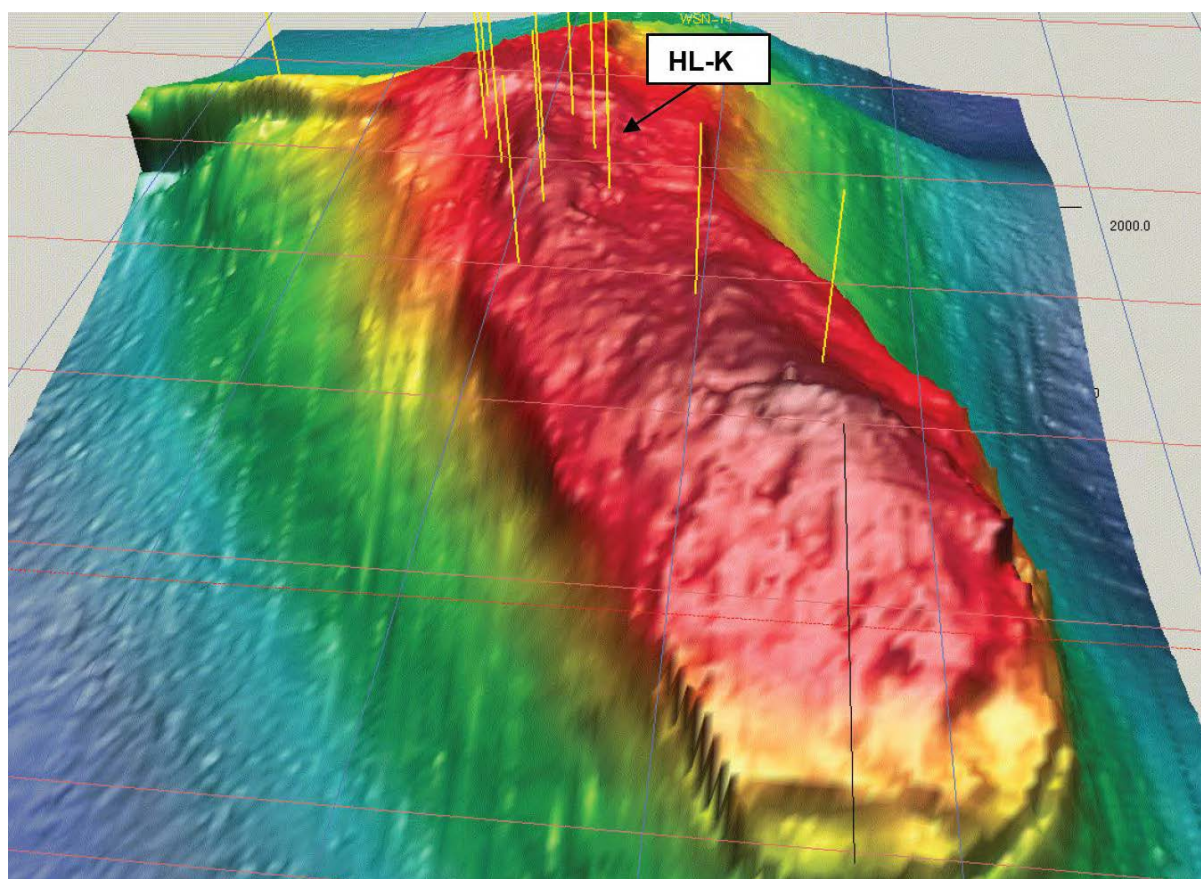
Bij injectie (vullen van de caveerne) komt de stikstof via het spuitkruis in de gasproductie-stijgbuis (tubing) en bij productie rechtstreeks vanuit de caveerne.

4 Ondergrond

(i) artikel 26 lid 1b Mb

Volgens artikel 26, lid b van het mijnbouwbesluit dient een beschrijving gegeven te worden van de structuur van het voorkomen en de ligging van het voorkomen ten opzichte van andere aardlagen, met bijbehorende geologische, geofysische en petro fysische studies en de daarbij gehanteerde onzekerheidsanalyses.

In figuur 9 is een schematische geologische doorsnede van het zoutvoorkomen weergegeven, evenals de locaties van de cavernes.



Figuur 9 Geologische doorsnede van het zoutvoorkomen met gasopslag cavernes gezien vanuit het noordoosten

4.1 Inleiding: hoe worden de ondergrond-eigenschappen gemeten

(i) artikel 25 lid 1a

Conform artikel 25, lid a van het mijnbouwbesluit zijn de ondergrondeigenschappen en de rheomorfolologische eigenschappen van het Zechsteinzout vastgesteld aan de hand van laboratoriumanalyses van zoutmonsters, zie ref [4] "Permeabilitatuntersuchungen an Steinsalz". Om vast te kunnen stellen of stikstof veilig en betrouwbaar opgeslagen kan worden in steenzout is het bijzonder belangrijk om belangrijke details, niet alleen van het steenzout zelf maar ook van alle geologische lagen die daarboven liggen, goed te kennen. Het vakgebied dat zich hiermee bezighoudt is stratigrafie en is een vakgebied binnen de aardwetenschappen.

4.2 **Geologie en gesteente-eigenschappen van het voorkomen**

De opslag van stikstof vindt plaats in steenzout van de Zechsteinformatie, in de zoutdome van Winschoten [Heiligerlee]. De opslagcaverne wordt met name in de Stassfurt (Z2) serie geconstrueerd, jongere Zechsteinformaties komen aan de flanken van de zoutdome voor.

De geologische opbouw van het gebied bestaat globaal uit quartair zand en klei tot een diepte van circa 150 meter, tertiaire klei tussen 150 en 440 meter. Top zout bevindt zich op een diepte van ca. 450 m. Top Zechstein rondom de zoutdome bevindt zich op een diepte van ca. 2.500 m, de basis van het Zechstein bevindt zich op een diepte van ca. 2.800 m. De zoutdome is ontwikkeld in N – Z richting en heeft relatief steile flanken. De zuiverheid van het zout is zeer groot (> 96 % NaCl); er worden slechts geringe (< 1 %) bijmengingen van andere mineralen (anhydriet ('onoplosbaar materiaal'), polyhaliet, kieseriet, sylviet) gevonden. Kalium- en magnesiumlagen worden niet aangetroffen. Hetzelfde geldt voor 'floaters' of gaspockets. Meer informatie over de structuur en de ligging van de formatie is opgenomen in het TNO-report "Mapping of the Winschoten Salt Dome" uit 2000, zie ref. [5], en de actualisatie van de geologische kaarten uit 2002, zie ref. [6].

5 Ontwikkelingsvooruitzichten

(i) Artikel 24 lid 2 Mb

5.1 Inleiding

De komende decennia blijft aardgas een belangrijke rol vervullen in onze energievoorziening. Vrijwel alle huishoudens zullen nog geruime tijd gas gebruiken om hun woningen te verwarmen en te koken, ook zal een aanzienlijk deel van onze elektriciteit worden opgewekt met gas. Veel bedrijven gebruiken bovendien gas, naast verwarming en verhitting, als grondstof in chemische processen. Op weg naar een volledig duurzame energievoorziening in 2050 blijven fossiele energiebronnen nog decennia een belangrijke rol spelen, waarbij gas niet alleen de schoonste bron is, maar ook voor de benodigde flexibiliteit kan zorgdragen.

Gasbeleid

Uitgangspunt van het gasbeleid was oorspronkelijk het optimaal benutten van de aanwezige gasvoorraad. In 2005 is onderkend dat deze positie aan verandering onderhevig is, omdat de Nederlandse gasvoorraden langzaam maar zeker afnemen en heeft de Rijksoverheid de ambitie uitgesproken om Nederland "gasronde" van Noordwest-Europa te laten worden. Dit hield in dat Nederland een knooppunt moest worden waar gas naartoe wordt getransporteerd, waar gas wordt opgeslagen en van waaruit gas wordt geëxporteerd. Met deze gasrondestrategie wil de overheid de energievoorziening veiligstellen. Dit omdat tijdig moet worden ingespeeld op veranderingen in onze gasvoorziening, maar tevens omdat Nederland ook zonder grootschalige eigen productie een spilfunctie in de Noordwest-Europese gasvoorziening kan vervullen.

De acties die gekoppeld zijn aan de gasronde-ambitie zijn inmiddels nagenoeg afgerond. Hierdoor functioneert de gasmarkt goed, zijn de voor de lange termijn leveringszekerheid noodzakelijke gasbuffers (ondergrondse opslagen, LNG-installatie) aanwezig en beschikken we over goede verbindingen met gasbronnen elders in de wereld. De aanwezige infrastructuur kan Nederland van gas voorzien, ook als de eigen winning sterk is terug gelopen. Nederland is hiermee de beoogde, belangrijke, schakel in de gasstromen die Noordwest-Europa van gas voorzien.

Kwaliteitsconversie

Het gas (G-gas) dat uit het Groningenveld wordt gewonnen heeft als unieke eigenschap dat het een lagere verbrandingswaarde heeft dan vrijwel alle andere voorkomens van gas wereldwijd, zo ook gas uit de Nederlandse kleine velden. Dit betekent dat het G-gas in het gebruik niet zonder meer uitwisselbaar is voor gas uit andere bronnen. Het Nederlandse gastransportnet kent dan ook gescheiden netwerken voor hoog- en laagcalorisch gas. Hierbij spelen tientallen mengstations verspreid over heel Nederland een cruciale rol. Deze twee netwerken zijn via kwaliteitsconversie met elkaar verbonden, waardoor het mogelijk is om hoogcalorisch gas te leveren aan gebruikers van laagcalorisch gas. Met kwaliteitsconversie wordt stikstof toegevoegd aan hoogcalorisch gas, waardoor de verbrandingswaarde afneemt tot binnen de bandbreedte voor laagcalorisch gas. Met verrijking wordt zeer laagcalorisch gas aangevuld met hoogcalorisch gas om de verbrandingswaarde te verhogen.

Het toepassen van kwaliteitsconversie is een wettelijke taak van GTS, (Gaswet, artikel 10a, lid 1 onder c). Door de landelijke netwerkbeheerder verantwoordelijk te maken voor het converteren van kwaliteit krijgen ook aanbieders van hoogcalorisch gas toegang tot de markt voor laagcalorisch gas, zonder dat zij zelf over conversiemiddelen hoeven te beschikken. Om deze taak uit te voeren moet GTS de beschikking hebben over voldoende infrastructurele middelen, zoals stikstofinstallaties en mengstations. Mocht GTS toch tegen de grenzen van de maximaal mogelijke kwaliteitsconversie aanlopen dan zal GTS, bij gebrek aan ander gasaanbod, moeten overgaan tot het "afschakelen" van afnemers.

In het netontwikkelingsplan 2017 concludeerde GTS reeds dat er door de afnemende productie van Groningengas er in de toekomst een tekort ontstaat aan capaciteit om op momenten dat het gasverbruik het hoogst is voldoende hoogcalorisch gas te converteren om aan de vraag naar laagcalorisch gas te voldoen. Alternatieve maatregelen om het verbruik van laagcalorisch gas te beperken, zoals het ombouwen van installaties en het verduurzamen van de energievoorziening, kennen een langere doorlooptijd dan de bouw van een additionele stikstoffabriek.

Ontwikkeling van de vraag naar laagcalorisch gas

Sinds de start van de exploitatie van het Groningenveld is Nederland een belangrijke leverancier van gas aan omringende landen. Nederland heeft op het gebied van laagcalorisch gas een bijzondere verantwoordelijkheid. Als gevolg van het Nederlandse exportbeleid, dat stamt uit de jaren zestig van de vorige eeuw, zijn ook gebruikers in België, Duitsland en Frankrijk afhankelijk van laagcalorisch gas. De gehele laagcalorisch markt bedraagt circa 70 miljard m³ per jaar. Deze markt wordt voor een groot deel beleverd uit het Groningenveld. In de dan nog resterende vraag naar laagcalorisch gas wordt voorzien door de Duitse productie, het bijmengen van hoogcalorisch gas bij Groningengas ("verrijken") en het converteren van hoogcalorisch gas.

Een overstap naar hoogcalorisch gas vergt een lange voorbereidingstijd omdat alle toestellen die nu zijn ingesteld op laagcalorisch gas moeten worden omgebouwd dan wel moeten worden vervangen alvorens de overstap kan worden gemaakt.

Uiterlijk 2030 wordt de volledige export van laagcalorisch gas naar het buitenland gestaakt. Gasunie heeft hiertoe inmiddels de nodige voorbereidingen getroffen. In Duitsland wordt vanaf 2020 de jaarlijkse import van laagcalorisch gas uit Nederland verminderd met 10%, waardoor in 2030 geen export naar Duitsland meer plaatsvindt. De apparatuur in de Duitse huishoudens zal daartoe omgeschakeld worden naar hoogcalorisch gas. In België en Frankrijk worden vergelijkbare voorbereidingen en zal de ombouw ook in 2030 zijn afgerond.

Laagcalorisch gas wordt in Nederland vooral gebruikt door kleinverbruikers (huishoudens en de klein zakelijke markt), de kleine industrie en WKK installaties die warmte produceren voor de industrie, de tuinbouw of voor stadsverwarming. Grote industrieën en elektriciteitscentrales maken, mede met het oog op de toekomst, vooral gebruik van hoogcalorisch gas. Ook bij kleinverbruikers in Nederland worden, met het oog op de toekomst, voorbereidende maatregelen getroffen. Vanaf 2017 mogen in Nederland alleen nog cv-ketels en gasfornuizen verkocht worden die, met een simpele ingreep, ook op hoogcalorisch gas aangesloten kunnen worden.

5.2 Achtergrond Project Wijzigingen naar Status 2018

Ten gevolge van de aardbevingenproblematiek in de provincie Groningen heeft toenmalige minister Kamp van EZ beleid gevoerd op het naar beneden bijstellen van het winningsplan van de NAM. Om dit te kunnen realiseren was het uitbreiden van de bestaande installatie op Zuidbroek een effectief middel om jaarlijks voldoende pseudo G-gas (7 bcm) te produceren zodat de leveringszekerheid gewaarborgd zou blijven. Uit een advies van het SodM in 2016 kwam naar voren dat de jaarlijkse productie van 24 bcm uit het Groningen veld als veilig werd beschouwd. Hierdoor werd de noodzakelijke inzet van de stikstofinstallatie beperkt tot een periode van enkele jaren en heeft GTS de minister geadviseerd om de uitbreiding om bedrijfseconomische redenen op hold te zetten. Halverwege september 2016 is het project daadwerkelijk op hold gezet.

Na de zware beving bij Zeerijp begin januari 2018 adviseerde het SodM op 1 februari 2018 om de gaswinning uit het Groningen veld zo snel als mogelijk naar 12 bcm per jaar terug te brengen.

De minister van EZK heeft ook duidelijk gemaakt dat de gaswinning in Groningen niet alleen naar 12 bcm per jaar moet maar uiterlijk in 2030 zelfs naar 0 bcm. Daarvoor heeft de minister inmiddels een aantal maatregelen in gang gezet, hiertoe behoort de bouw van de stikstofinstallatie in Zuidbroek. Om zo snel mogelijk tot het niveau van 12 bcm per jaar te komen, is de bouw van de stikstofinstallatie de meest effectieve maatregel. Het kabinet heeft daarom op 29 maart 2018 de Tweede Kamer geïnformeerd dat de stikstofinstallatie er zo snel als mogelijk moet komen.

Op basis van de gepresenteerde afbouwscenario's, het herstel van de veiligheid van Groningen en het kunnen blijven garanderen van leveringszekerheid aan G-gas klanten is het van groot belang dat de installatie er snel komt en begin 2022 operationeel is.

Eind april 2018 heeft de minister van Economische Zaken en Klimaat de betrokken overheden op de hoogte gebracht van het hervatten van de procedure voor de ruimtelijke inpassing en vergunningverlening voor de bouw van de stikstofinstallatie bij Zuidbroek. Deze procedure valt onder de Rijkscoördinatie-regeling (RCR) en is hervat op basis van de eerder gekozen voorkeurslocatie en resultaten van reeds uitgevoerde onderzoeken. De planning is dat definitieve besluitvorming over de ruimtelijke inpassing en de vergunningen plaatsvindt voor de zomer van 2019, waarna GTS met de bouw van de stikstofinstallatie kan beginnen. De voorbereidende werkzaamheden zoals het aanleggen van een toegangsweg vanaf de rotonde Duurkenakker – Spoorhavenweg gemeente Midden-Groningen en het bouwrijp maken van de bouwlocatie zijn in volle gang. Deze werkzaamheden worden eind juni 2019 afgerond, zodat een goede bereikbaarheid en een bouwklaar terrein is gewaarborgd. De stikstofinstallatie zal operationeel zijn in het eerste kwartaal van 2022.

5.3 **Vooruitzichten gebruik stikstofcaverne**

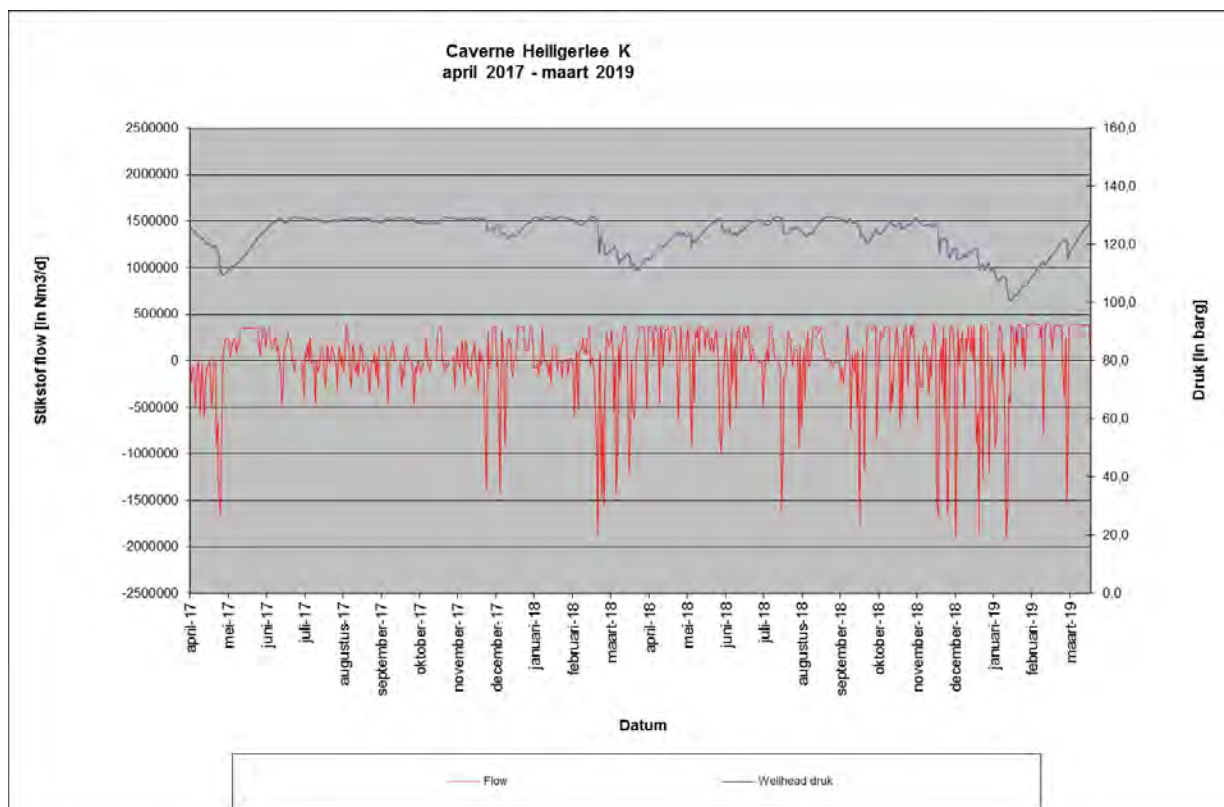
Het ontwikkelen van een caverne voor de opslag van stikstof is een kostbare aangelegenheid en moet financieel- en bedrijfseconomisch verantwoord zijn. De markt voor opslag van stikstof (t.b.v. conversie van hoog calorisch gas na G-gas kwaliteit) is afhankelijk van vele nationale en internationale factoren waaronder de ontwikkeling van duurzame energie en de afbouw van fossiele brandstoffen (ombouw buitenland G-gas → H-gas).

5.4 **Caverne als strategische reserve**

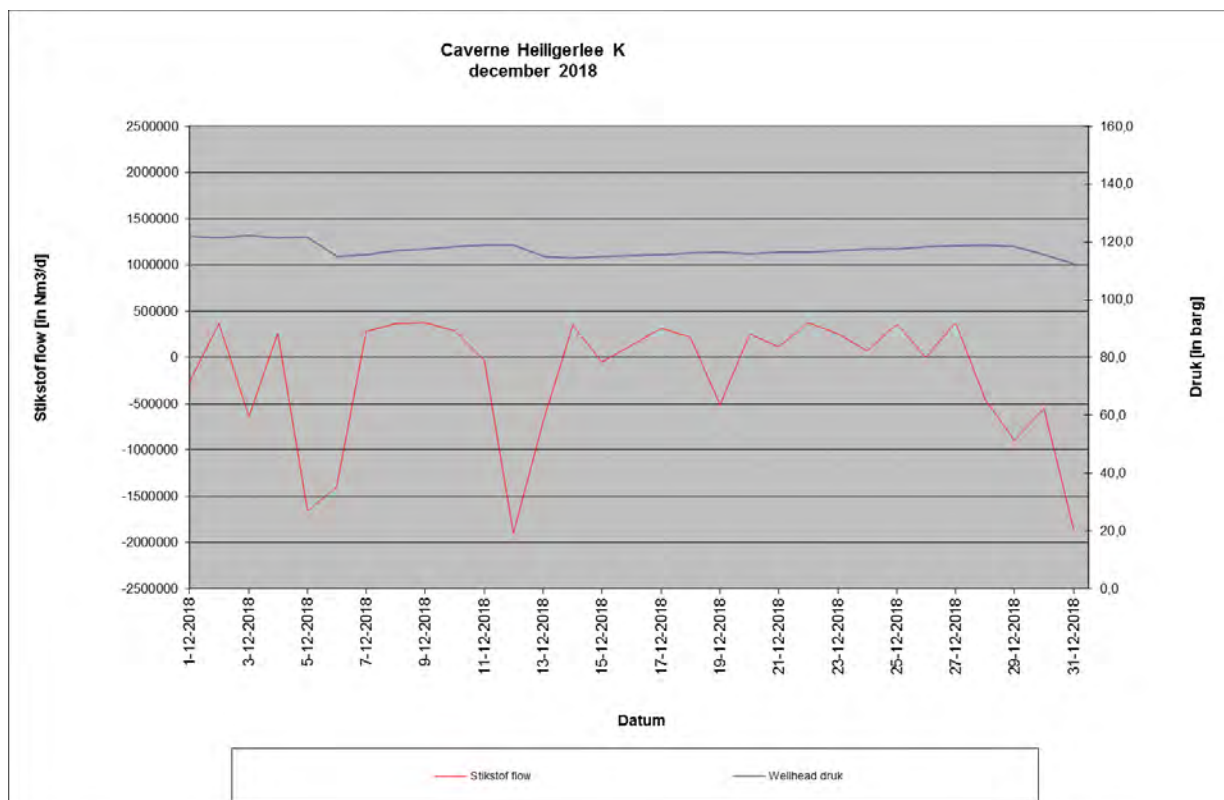
Voor de toekomst zal de caverne ook worden ingezet als strategische reserve om bij een calamiteit in combinatie met het mengstation grote hoeveelheden gas van Groningen kwaliteit te kunnen produceren.

5.5 **Historische inzet huidige stikstof caverne**

In onderstaande figuren 10 en 11 is de historische inzet van Heiligerlee Stikstofcaverne weergegeven over de periode van april 2017 t/m maart 2019. Ook is de periode over december 2018 weergegeven. De caverne wordt vooral gebruikt voor zogenaamde back-up dienst.



Figuur 10 Historische inzet caverne Heiligerlee K april 2017 – maart 2019



Figuur 11 Historische inzet caverne Heiligerlee K december 2018

5.6 **Onzekerheden**

De inzet van de caveerne is afhankelijk van het gedrag van shippers (de markt). De markt mag zowel G-gas als H-gas in het GTS netwerk invoeden. GTS is verantwoordelijk voor de juiste balans tussen het H en G-gas. Het middel om deze balans te regelen is gebruik te maken van conversie. Bij hoge vraag naar conversie en ongeplande onbeschikbaarheid van conversiemiddelen zal de caveerne ingezet worden. De stikstofcaveerne zal te allen tijde bedreven worden binnen het toegestane veilige werkgebied van de caveerne, de zogenaamde "Operating Envelope".

5.7 **Inzetstrategie stikstofcaveerne**

De inzetstrategie van GTS is er op gericht om te voldoen aan de voor de markt beschikbare conversieruimte en hierbij de caveerne zo efficiënt mogelijk binnen te bedrijven. Gestreefd zal worden de stikstofcaveerne, gezien de strategische functie, zo vol mogelijk te houden.

5.8 **maximale drukvariatie in de caveerne**

Voor de stikstofcaveerne te Heiligerlee wordt een internationaal geaccepteerde maximale druk variatie van 10 bar per dag aangehouden. Met een maximale injectie/uitzend capaciteit van 190.000 m³/hr. zal de 10 bar per dag niet gehaald worden.

Een en ander is uitvoerig beschreven in het IfG rapport "B IfG - 47_2018_Report_HLK _final_2". Zie ref. [3]

5.9 **Duur van de opslag wijze waarop voorkomen wordt achtergelaten na beëindiging activiteiten**

(i) *Artikel 35 lid 1b Mw, artikel 26 lid 1f Mb*

De opslagvergunning is afgegeven op 31 maart 2009 en geldt tot 70 jaren na afgifte, 31 maart 2079. Na beëindiging van de stikstofopslag wordt de caveerne met water/pekkel gewuld. Aansluitend kan de boring eventueel na ombouw voor reguliere pekkelproductie worden gebruikt. Een en ander wordt op dat tijdstip beschreven in overleg met het (openbare) sluitingsplan als bedoeld in de wet en ter instemming voorgelegd aan de Minister van Economische Zaken en Klimaat.

5.10 **Afblazen stikstof bij normaal bedrijf**

(i) *Artikel 24 lid 1j Mb*

De installatie is zodanig ingericht dat bij normaal bedrijf geen stikstof wordt afgeblazen. Alleen bij gepland onderhoud en een noodstop wordt op een veilige locatie stikstof afgeblazen.

5.11 **Stoffen die jaarlijks worden mee geproduceerd**

(i) *Artikel 24 lid 1i Mb*

Alle stikstof wordt schoon en droog geproduceerd, eventuele door condensatie ontstane vloeistof wordt voor de caveerne in de vochtvanger opgevangen voordat de stikstof in de caveerne wordt geïnjecteerd. Bij het uitzenden van stikstof uit de caveerne wordt het eventuele vloeistof op Zuidbroek in een vochtvanger opgevangen en wordt de stikstof vervolgens in een glycol contactor gedroogd. De volgende stoffen zijn tijdens het proces vereist en zijn als zodanig op Heiligerlee aanwezig:

Stof	Wijze van opslag	Maximale hoeveelheid (m ³)	Functie/herkomst
Hydraulische olie	Stalen tank in well control unit	0,2	Voorraadvat t.b.v. het bedienen van afsluiters
Blusmiddelen	Nader te bepalen	Nader te bepalen	Blussen

GTS rapporteert jaarlijks over haar milieu-impact (footprint gastransport) .

6 Bodemdaling/beweging

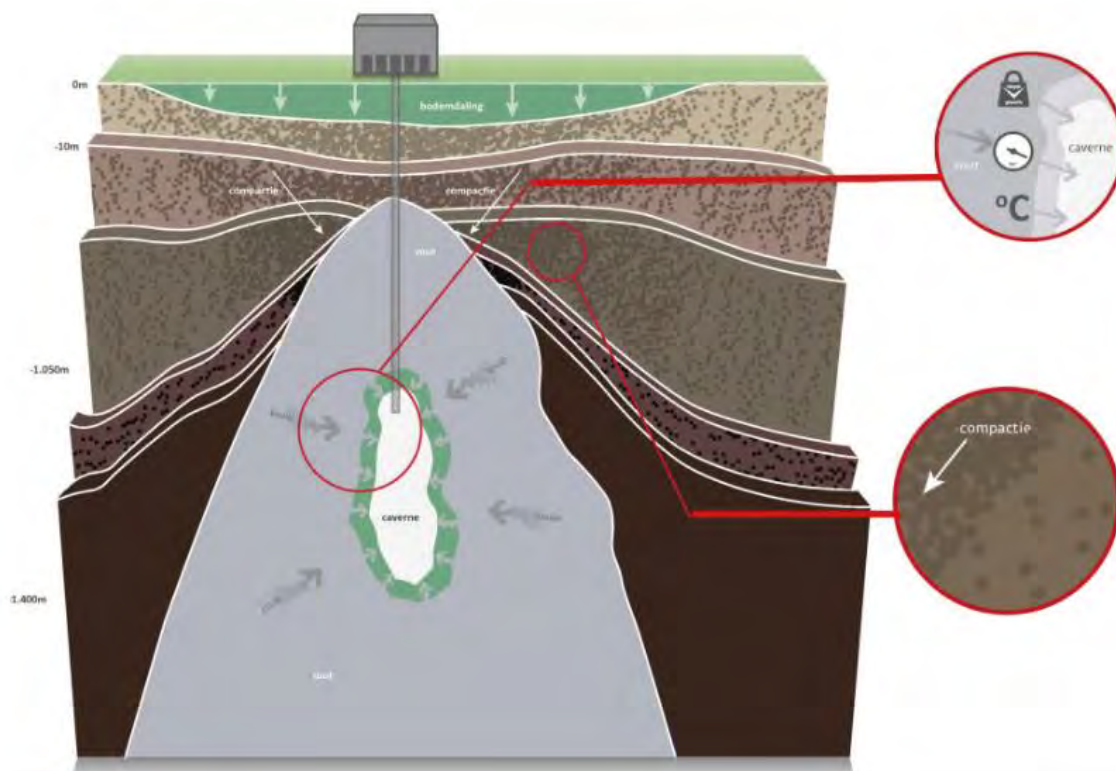
(i) Artikel 35 lid 1f Mw

Volgens artikel 35, lid 1f van de mijnbouwwet dient een beschrijving gegeven te worden van de bodembeweging ten gevolge van de opslag en van de maatregelen ter voorkoming van schade door beweging.

6.1 Inleiding hoe komt bodemdaling tot stand

De zoutcavernes zorgen voor een lichte bodemdaling. Dit komt door het gewicht van de aardlagen boven de cavernes en een hoge temperatuur op deze diepte. Hierdoor gedraagt het zout zich als een stroperige vloeistof. Dit effect heet 'kruip'. De snelheid van de kruip hangt met name af van de druk van de aardlagen, de diepte en de temperatuur. Het gevolg van kruip is dat de caveerne langzaam steeds iets kleiner wordt. De opslag van stikstof onder druk zorgt voor een tegendruk en vermindering van het 'kruipeffect'. Bewegingen zoals kruip en compactie (het samendrukken van aardlagen) kunnen aan de oppervlakte voor bodemdaling zorgen. Hoeveel de bodem daalt, hangt af van een aantal factoren: de mate van kruip, de diepte en het volume van de caveerne en eventueel andere cavernes in de buurt.

Naast bodemdaling door mijnbouwactiviteiten, vindt er ook zogenaamde autonome bodemdaling plaats. Die is onafhankelijk van de stikstofopslag. Dat gebeurt door verschillende mechanismes, waar veen- en klei-inklinking er een van is. Ook door veranderde grondwaterstanden kan de bodemdaling worden beïnvloed. De verwachte bodemdaling als gevolg van de stikstofopslag bedraagt enkele millimeters per jaar. In figuur 12 is een schematisch overzicht gegeven van de verschillende factoren die bodemdaling veroorzaken.

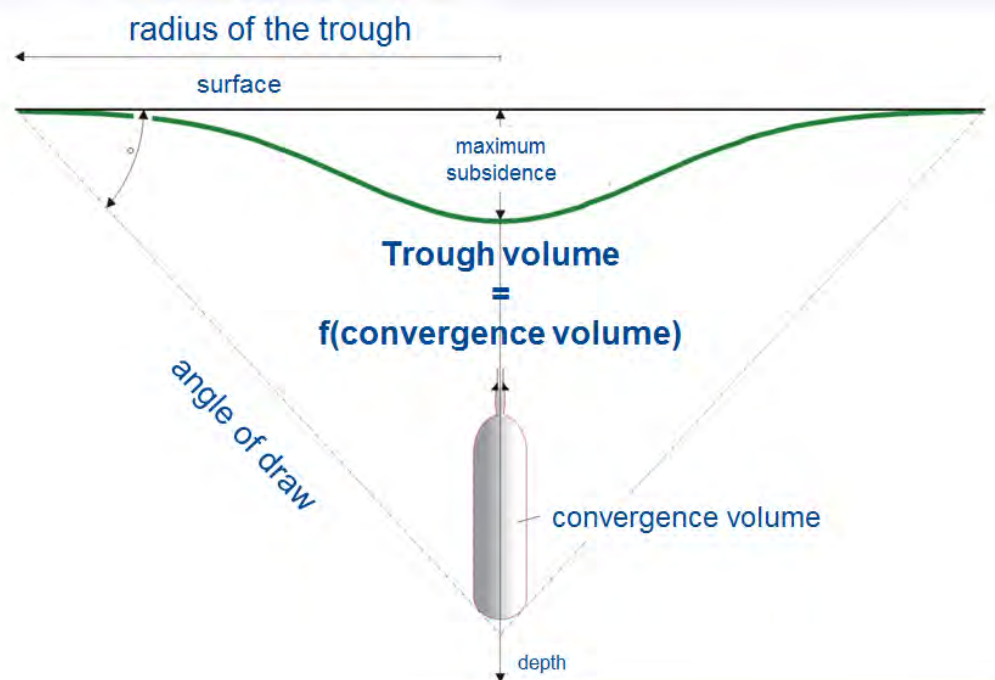


Figuur 12 Bodemdaling bij cavernes

6.2 Bodemdalingsmodel & kalibratie

(i) artikel 24 lid 1m,n,o Mb

Zoals eerder genoemd gedraagt zout zich op grote diepte en dus ook bij hoge temperatuur als een stroperige massa, ook wel het viscoplastisch (kruip) gedrag genoemd. Een caveerne in een zoutgesteente is eigenlijk niets anders dan een gat en vanwege het viscoplastisch gedrag van zout en de druk van ongeveer 1200 meter 'grond' zal dit gat heel langzaam dichtgedrukt worden. Dit verschijnsel noemen we de convergentie en de snelheid waarmee de caveerne kleiner wordt (krimpen) noemen we de convergentie snelheid (% per jaar). Het kleiner worden van de caveerne zal zich vertalen in een bodemdaling boven de caveerne. De bodemdalingsmodellen gaan ervan uit dat de convergentievolumen van de caveerne gelijk is aan het volume van de bodemdaling, zie figuur 13.



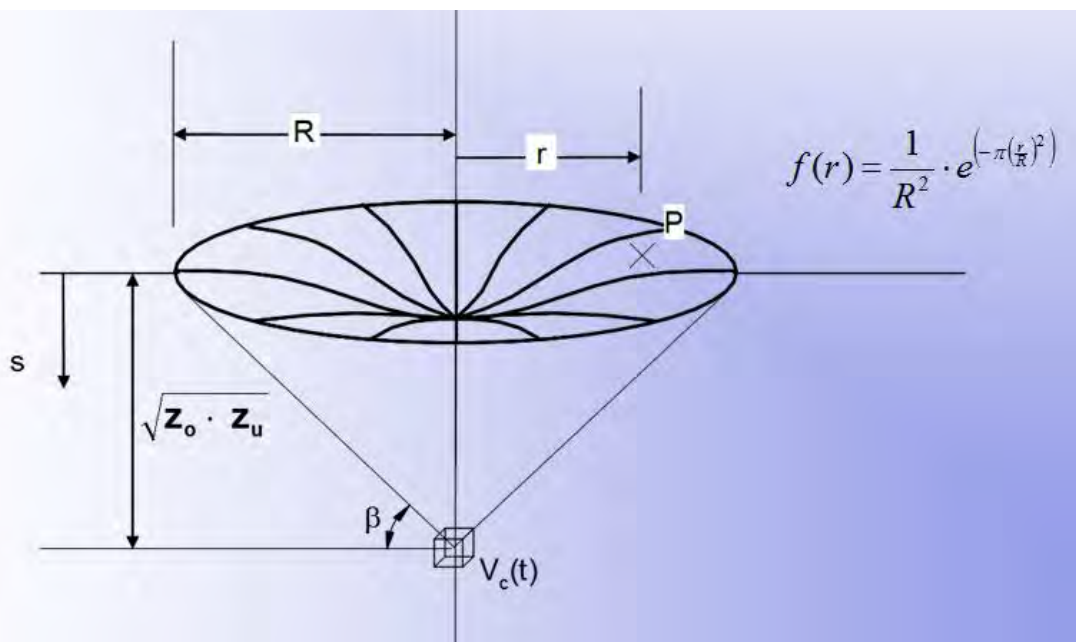
Figuur 13 Principe bodemdalingsmodellen

De mate van bodemdaling en de snelheid waarmee dit gebeurt is sterk afhankelijk van de diepte van de caveerne, de plaats in de zoutdome, de temperatuur van het zout en de tegenwerkende druk in de caveerne zelf. De jaarlijkse toename van het volume van de bodemdalingkom boven een caveerne is gelijk aan de volumeconvergentie van de caveerne in dat jaar (convergentie in % per jaar x caveernevolume in m³). Het totale volume van de bodemdalingkom over de levensduur van een caveerne is gelijk aan de som van de jaarlijkse volumeconvergenties.

Omdat de convergentiesnelheid zeer laag is, orde van grootte is 0,4% per jaar, zal de bodemdaling voor caveerne die gebruikt wordt voor stikstofopslag ook zeer gering zijn. Het bodemdalingsmodel dat GTS hanteert is specifiek ontwikkeld voor de stikstofopslag in de caveerne van Heiligerlee en gefinetuned aan de hand van beschikbare historische gegevens, een zogenaamde "history match subsidence".

Ref. [7] History matching of surface subsidence due to solution mining operations in the Zuidwending and Heiligerlee brinefields geeft deze history match weer.

De rekenkern van het model voor het bepalen van de bodemdalingkom is gebaseerd op een internationaal geaccepteerd model ontwikkeld door Sroka, Schber en Eckemeier en is vereenvoudigd weergegeven in onderstaand figuur 14.



Figuur 14 Rekenkern bodemdalingsmodel

Het model zelf is uiteindelijk gevalideerd door de “Bundesanstalt für Geowissenschaften und Rohstoffe” (BGR), uit Hannover. Ook is dit specifiek bodemdalingsmodel besproken met SodM.

Omdat het bodemdalingsmodel een prognose geeft van de bodemdaling over de tijd is de bodemdaling berekend voor de tijdstippen waarop we nauwkeurige meetgegevens hebben zoals de waterpasmetingen en de sonar caveerne volume metingen. De berekende en gemeten waarden vertonen geen significante afwijkingen.

6.3 Bodemdalingsvooruitzichten

(i) artikel 24 lid 1m Mb

Volgens artikel 24, lid m van het mijnbouwbesluit dient een kaart met daarop de contouren van de verwachte uiteindelijke mate van bodemdaling gegeven te worden.

KBB Underground Technologies GmbH, Hannover, Duitsland, heeft in opdracht van AkzoNobel en GTS een model ontwikkeld dat in staat is om de tot nu toe bestaande bodemdaling te modelleren. Dit model maakt betrouwbare voorspellingen van de bodemdaling voor de toekomst mogelijk veroorzaakt door pekelpductie en stikstofopslag in de cavernes van Heiligerlee.

De volgende 3 rapporten over deze studies zijn:

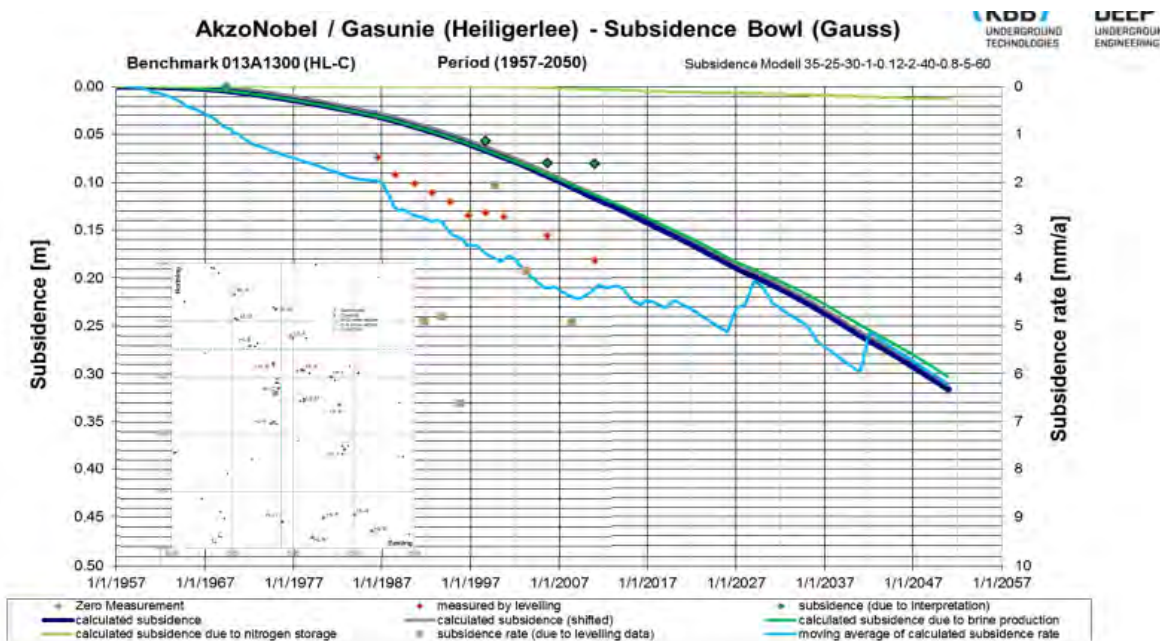
1. Ref. [8] 150331 HL WP1 Report Subsidence Documentation-rev00
2. Ref. [9] 150831 HL WP2 Report Subsidence Modelling-rev01
3. Ref. [10] 160413 HL WP3 Report Subsidence Prediction-rev00c

WP1 bevat een samenvatting van de relevante documentatie over bodemdaling als gevolg van pekelpductie en stikstofopslag in Heiligerlee. Op basis van de informatie uit WP1 kan het simulatiemodel worden vastgesteld.

WP2 beschrijft de belangrijkste stappen van dit simulatiemodel. In de daaropvolgende WP3 is dit model toegepast voor de voorspelling van de bodemdaling.

Met behulp van het eerder beschreven bodemdalingsmodel is de verwachte bodemdaling tot het jaar 2050 uitgerekend voor stikstofopslag en zoutwinning. Als voorbeeld voor het verloop van de bodemdaling in de tijd is dit voor HL-K weergegeven in onderstaand figuur 15.

De lichtgroene lijn laat de bodemdaling zien veroorzaakt door stikstofopslag en de donkergroene veroorzaakt door zoutproductie. De paarse lijn geeft de gezamenlijke bodemdaling weer. De te verwachte bodemdaling als gevolg van de stikstofopslag tot 2050 bedraagt ca. 15 mm.



Enclosure 22

Heiligerlee – Benchmark 013A1300 – Comparison of observed subsidence with measured values

Figuur 15 verloop bodemdaling als gevolg van stikstofopslag en zoutwinning

6.4 Onzekerheid in verwachte bodemdaling

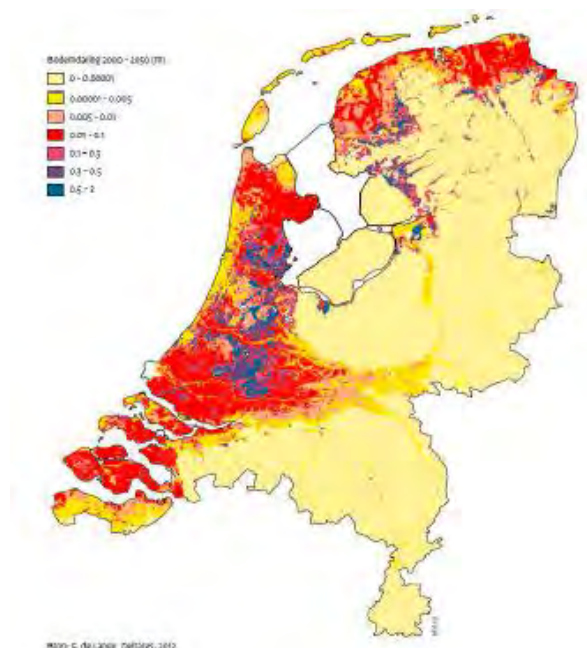
Stikstofopslag is niet de enige oorzaak van bodemdaling. In een groot deel van Nederland daalt de bodem door o.a. inklinking en oxidatie van klei- en veenlagen. Deze processen spelen zich af in de bovenste meters van de bodem. Door verschillen in de ondiepe bodemopbouw ontstaan vaak op korte afstand, grote verschillen in bodemdaling hetgeen kan leiden tot schade aan gebouwen en infrastructuur.

De volgende oorzaken voor diepe en ondiepe bodemdaling kunnen worden onderscheiden (zie figuur 16):

Diepte in m-mv	Natuurlijke oorzaken	Antropogene oorzaken
Diep: >400	Tektonische beweging Isostasie	Mijnbouw: gas- en zoutwinning, gasopslag
Middeldiep: 20 20-400	Compactie	Bemaling van een bouwput Grondwaterwinning
Ondiep: 0 0-1 0-1 0-1 1 1 1-5		Ophoging Irreversibele krimp Oxidatie Ophoging en zetting Droogte Polderpeilverlaging Begroeiing / bomen

Figuur 16 Oorzaken bodemdaling

In figuur 17 is een kaart opgenomen met een prognose van de bodemdaling in Nederland als gevolg van diepe en ondiepe oorzaken.



Figuur 17 Bodemdaling 2000-2050 voor ondiepe oorzaken

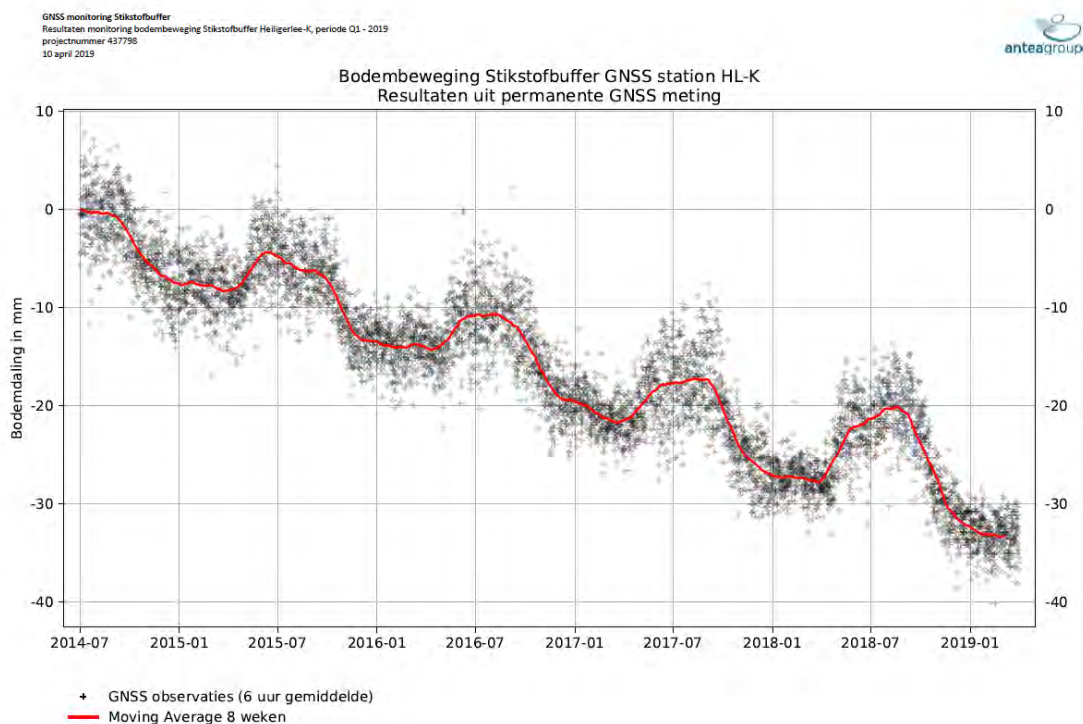
De invloed van bodemdaling, anders dan die veroorzaakt door stikstofopslag en zoutwinning, is niet in de modellering meegenomen. De invloed van de overige oorzaken zijn beschreven in een rapport van de Commissie Bodemdaling (zie <http://www.commissiebodemdeling.nl/bodemdeling/diepe-en-ondiepe-bodemdeling/>).

6.5 Monitoring van bodemdaling

Er worden regelmatig metingen uitgevoerd. Met het Staatstoezicht op de Mijnen (SodM) is afgesproken dat GTS elke vijf jaar een optische waterpasmeting zal uitvoeren. Dat is een veelgebruikte methode, waarbij gebruik gemaakt wordt van waterpastaostellen. Deze metingen zijn zeer betrouwbaar en reproduceerbaar. De laatste meting is geweest in 2015/2016.

Daarnaast is in overleg met SodM gekozen om ook een GPS-meetsysteem te installeren waarmee continu de bodembeweging wordt gemeten en geregistreerd. Eind 2013 is de caveerne uitgerust met een dergelijk systeem. Start van de meting vond plaats op 1 juli 2014. Elk kwartaal worden gegevens van dit systeem (meetrapport) verkregen en worden deze beoordeeld. Het meetrapport wordt tevens doorgestuurd naar SodM. In figuur 18 zijn de resultaten weergegeven voor de GPS-antenne op caveerne HL-K. Seizoensinvloeden zijn hierop goed terug te zien.

Aangezien de GPS antennes continu meten en de gegevens opgeslagen worden bij Antea (specialist op het gebied van dit soort metingen) wordt elke storing aan het GPS-systeem direct gemeld door Antea en wordt door GTS plus eventueel Antea actie ondernomen om de storing te verhelpen.



Figuur 18 Overzicht van GPS meetresultaten Heiligerlee

Indien er afwijkende waarden worden geconstateerd die wijzen op een onacceptabel versnelde bodemdaling wordt direct onderzoek gedaan naar de oorzaak ervan. Mogelijke nadere onderzoeken kunnen zijn inwendige caveerne inspectie met behulp van een camera of een aanvullende sonar meting.

6.6 **Mogelijke gevolgen van de verwachte bodemdaling**

(i) *artikel 24 lid 1q Mb*

Bodemdaling door stikstofopslag manifesteert zich aan de oppervlakte in de vorm van een platte, zeer gelijkmatige schotel, die met het oog niet te zien is. Die schotel heeft een zeer geringe helling, daarom worden geen nadelige gevolgen verwacht voor gebouwen, infrastructuur, en voor natuur en milieu. Bij de geringe dalingen die hier verwacht worden, wordt ook niet verwacht dat de bodemdaling significante gevolgen heeft voor het normale beheer en het onderhoud van waterkeringen en waterlopen, en van het waterpeil.

6.7 **Maatregelen om (gevolgen van) bodemdaling te voorkomen of te beperken**

(i) *artikel 35 lid 1f Mw, artikel 24 lid 1s Mb*

Vanwege de geringe maximale bodemdaling, worden er geen nadelige gevolgen voorzien, en wordt er niet voorzien in (extra) maatregelen om (gevolgen van) bodemdaling te voorkomen of te beperken, anders dan het periodiek monitoren van de bodemdaling volgens het meetplan. Mochten de dalingsmetingen die volgens het meetplan uitgevoerd worden, afwijken van de voorspelde waarden, dan zal gehandeld worden als hierboven beschreven. Indien als gevolg van bodemdaling door gasopslag toch schade ontstaat, dan zal deze worden vergoed overeenkomstig de regels van het burgerlijk recht.

7 Bodemtrilling

(i) artikel 35 lid 1f Mw

De seismische risicoanalyse laat zien dat de zoutdome Heiligerlee in de laagste seismische risicocategorie valt.

7.1 **Inleiding: hoe komen bevingen ten gevolge van gaswinning tot stand**

Op grond van het viscoplastisch (kruip) gedrag van zout zijn geen bodemtrillingen te verwachten. Ook in de literatuur zijn geen aanwijzingen te vinden over het optreden van bodemtrilling in relatie tot de opslag van gas en stikstof in zoutcavernes.

Het overzicht van de seismische stations in Nederland laat zien dat er in de provincies Groningen en Drenthe oppervlakte-seismometers zijn geïnstalleerd. Geïnduceerde bodemtrillingen zullen door het bestaande net van permanente seismometers van het KNMI geregistreerd worden.

7.2 **Historische bevingen in de voorkomens van dit winningsplan**

Er waren geen aanwijzingen dat in de periode tot november 2017 bodemtrillingen binnen de vergunning Winschoten II opgetreden zijn als gevolg van de winning van zout door middel van oplosmijnbouw. Ook informatie van de website van het KNMI (<http://www.knmi.nl>) laat zien dat er gedurende de zoutwinningactiviteiten geen door de winning van zout geïnduceerde aardbevingen in die periode zijn opgetreden. De opslagactiviteiten worden zo uitgevoerd dat het uiterst onwaarschijnlijk is dat door stikstofopslag in cavernes bodemtrillingen geïnduceerd zullen worden.

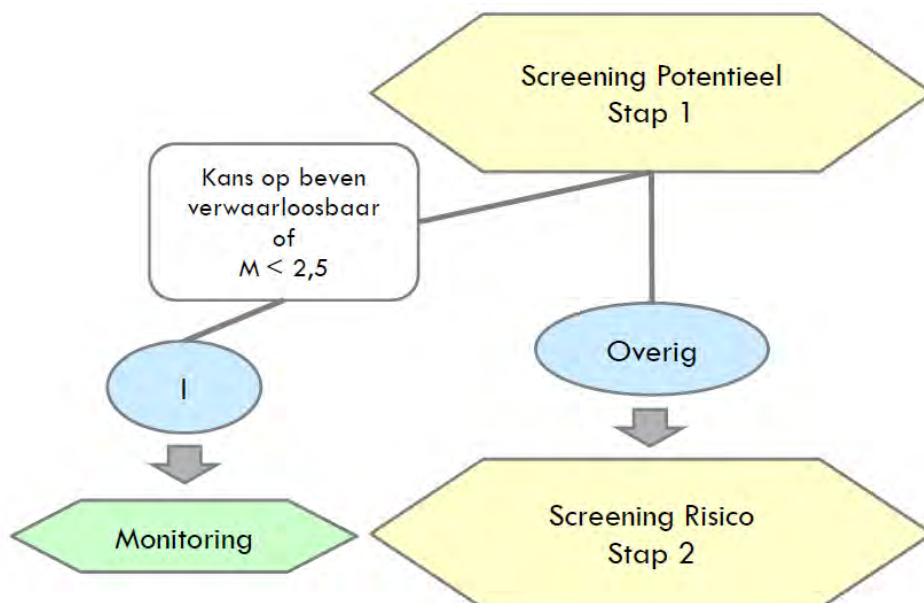
Op 19 november 2017 zijn ten oosten van Groningen bij Winschoten vier kleine bevingen gemeten bij de Heiligerlee zoutdome, ref. KNMI website. GTS heeft direct actie ondernomen aan de hand van deze trilling door nauwlettend operationeel de caveerne te monitoren en een volledige sonar uit te voeren. Hierop zijn geen aanwijzing gevonden dat de trilling werd veroorzaakt door HL-K. AkzoNobel heeft aan haar zijde ook dergelijke activiteiten ontplooit.

Veruit de meeste bevingen in Groningen vinden plaats in of nabij het Groningen-gasveld. Analyse van deze aardbevingssignalen duiden op een bron ondieper dan het gasreservoir. Nabij het epicentrum bevindt zich de Heiligerlee zoutcavernes bij Winschoten. Er is onderzoek gedaan naar deze bevingen. De grootste beving had een magnitude 1,3, ervan uitgaande dat de beving zich net in het krijtkalk bevond en niet in het zoutgesteente van de cavernes. De andere drie bevingen waren veel kleiner. Gezien de geringe diepte zou deze grootste beving gevoeld kunnen zijn. De bevingen hebben waarschijnlijk plaatsgevonden op ongeveer 400 meter diepte. Rond deze diepte is er een overgang van slappe sedimenten naar het iets vastere krijtkalk.

7.3 **Seismische Risico Analyse**

(i) artikel 24 lid 1p Mb, artikel 26 lid 1g Mb

Het kader en de hier beschreven methodiek is gebaseerd op: Methodiek Voor Risicoanalyse Omtrent Geïnduceerde Bevingen Door Gaswinning; Tijdelijke Leidraad Voor Adressering Mbb. 24.1.p, Versie 1.2, 1 februari 2016, Staatstoezicht op de Mijnen (SodM).



Figuur 19 Weergave van de verschillende stappen in de seismische risico analyse (SRA)

Screening Potentieel

In de eerste stap (Niveau 1) wordt primair gekeken naar de kans op een trilling (met een magnitude groter dan 1.5 op de schaal van Richter). Daarbij wordt gekeken naar de breuk-configuratie in het veld, en naar de stijfheidsverhouding tussen de reservoir-lagen en het afdekkende gesteente. Als er meer breuken zijn, neemt de kans toe op trilling. Hetzelfde geldt als het afdekkende gesteente stijver is ten opzichte van het reservoir. Aangezien de kans op trilling verwaarloosbaar klein is (zie paragraaf 7.1) zijn geen aanvullende onderzoekstappen noodzakelijk en volstaat monitoring d.m.v. het bestaande KNMI netwerk.

7.4 Seismische Risico Analyse voor het voorkomen in dit opslagplan

In paragraaf 7.3 is reeds geconcludeerd dat de kans op trilling verwaarloosbaar klein is en hierdoor valt het risiconiveau voor de Heiligerlee zoutdome onder categorie I. De implicatie hiervan is dat de monitoring met het huidige geofon en accelerometer netwerk van het KNMI uitgevoerd zal worden. Tevens heeft GTS op de stikstofcaverne zelf ook een accelerometer geplaatst en worden de waarden geregistreerd en gemonitord.

7.5 Mogelijke gevolgen van bevingen ten gevolge van stikstofopslag in de caverne HL-K.

- (i) *artikel 24 lid 1q Mb*

Omdat de maximale sterkte van de bevingen verwaarloosbaar klein is, wordt er geen schade aan infrastructuur verwacht.

7.6 Monitoring van bodemtrillingen

AkzoNobel heeft vanwege de trilling een Micro Seismic Monitoring MSM netwerk aangelegd waarbij GTS haar accelerometer heeft laten aansluiten welke daarvoor al geplaatst was op de caverne pad HL-K. AkzoNobel heeft door bedrijf Arup een specificatie laten opstellen voor dit netwerk, zie ref. [11] "20180320_Seismic_Network_Specifications". Het bedrijf Magnitude heeft de geofoons/hydrofoons en accelerometers geïnstalleerd. Magnitude registreert de MSM data en slaat deze data op en verspreid dit vervolgens naar AkzoNobel en het KNMI. Magnitude analyseert tevens de data en wanneer er zich een event voordoet wordt dit direct gemeld aan AkzoNobel (AkzoNobel meldt dit vervolgens direct aan GTS, dit is een onderlinge afspraak). Ook op bij de pekelwinningscavernes en gasopslag van Zuidwending zal een dergelijk netwerk worden geïmplementeerd.

7.7 Maatregelen die gevolgen van bodemtrillingen beperken of voorkomen

- (i) *artikel 35 lid 1f Mw, artikel 24 lid 1r,s Mb*

Gezien de indeling in categorie I, door de lage maximaal realistische bevingsmagnitude, wordt er geen schade van betekenis verwacht, en voorziet het productieproces niet in maatregelen om trillingen te voorkomen of te beperken. Indien als gevolg van bodemtrillingen door de opslag van stikstof toch schade ontstaat, dan zal deze worden vergoed overeenkomstig de regels van het burgerlijk recht.

8 Overige veiligheidsaspecten

(i) *artikel 35 lid 1g Mw*

8.1 Inleiding

De opslag van stikstof kan mogelijke gevolgen, anders dan bodemdaling en trillingen met zich meebrengen voor de omgeving. Deze mogelijke gevolgen worden beoordeeld door het bevoegd gezag in andere vergunningen dan het winningsplan.

Een overzicht van de mogelijke gevolgen en in welke vergunningen deze worden behandeld, staat in de volgende tabel.

Gevolgen m.b.t.:	Besluit:
Bodemverontreiniging	MER Omgevingsvergunning milieu
Luchtverontreiniging (emissies)	MER Omgevingsvergunning milieu
Grondwaterverontreiniging	MER Omgevingsvergunning milieu
Oppervlaktewaterverontreiniging	MER Omgevingsvergunning milieu Evt. Watervergunning
Externe veiligheid	MER Omgevingsvergunning milieu BRZO
Natuur	MER Wet Natuurbescherming

Tabel 7 Gevolgen versus vergunningen

De Minister van Economische Zaken en Klimaat bevordert op grond van artikel 34 lid 7 Mijnbouwwet een doelmatige en samenhangende besluitvorming ten aanzien van het besluit omtrent instemming met het winningsplan en een aantal overige besluiten, waaronder de besluiten zoals genoemd in bovenstaande tabel (coördinatieregeling).

Met betrekking tot bovenstaande tabel zal hieronder worden aangegeven wat door mijnbouwondernemingen wordt gedaan om genoemde gevolgen te voorkomen, dan wel de effecten hiervan te beperken.

8.2 Bodem- / grondwaterverontreiniging

(i) *artikel 26 lid 1d Mb*

De mijnbouwonderneming dient zich in te spannen om installaties zo te bouwen, onderhouden en beheren dat het risico op bodem/grondwaterverontreiniging verwaarloosbaar klein is. De wijze waarop dit dient te gebeuren is vastgelegd in onder andere de Nederlandse Richtlijn Bodembescherming (NRB) en de Publicatiereeks Gevaarlijke Stoffen (PGS). Hierdoor worden de risico's tot een minimum beperkt en blijven de eventuele gevolgen beheersbaar. De NRB en de PGS worden voorgeschreven in het Activiteitenbesluit en de Omgevingsvergunning. Toezicht vindt plaats door Staatstoezicht op de Mijnen (SodM). Indien toch door een incident bodem/grondwaterverontreiniging is ontstaan, dan dient de mijnbouwonderneming deze verontreiniging te saneren in het kader van de Wet bodembescherming. De desbetreffende provincie is hiervoor bevoegd gezag. De mijnbouwonderneming en toezichthouders hanteren een strikt controlebeleid waardoor de kans op bodemverontreiniging zeer gering is. Gevaar voor de volksgezondheid door het optreden van incidenten is niet te verwachten.

8.3 Luchtverontreiniging

De maximale uitstoot van stoffen die vrijkomen bij de activiteiten ten behoeve van stikstofopslag (zoals NO_x, SO₂, etc.) naar de lucht (emissies), de wijze van meten en rapporteren is vastgelegd in het Activiteitenbesluit en de omgevingsvergunning. SodM controleert of wordt voldaan aan de voorschriften. Mijnbouwondernemers streven altijd naar een zo laag als redelijkerwijs mogelijke emissie. Verder hanteren de mijnbouwonderneming en toezichthouders een strikt controlebeleid op emissies. Gevaar voor de volksgezondheid door het optreden van incidenten is niet te verwachten.

8.4 **Oppervlaktewaterverontreiniging**

De mijnbouwonderneming dient zich in te spannen om installaties zo te bouwen, onderhouden en beheren dat het risico op oppervlaktewaterverontreiniging verwaarloosbaar klein is. De wijze waarop dit dient te gebeuren is vastgelegd in onder andere de Nederlandse Richtlijn Bodembescherming (NRB) en de Publicatierreeks Gevaarlijke Stoffen (PGS). Hierdoor worden de risico's tot een minimum beperkt en blijven de eventuele gevolgen beheersbaar. De NRB en de PGS worden voorgeschreven in het Activiteitenbesluit en de Omgevingsvergunning. Toezicht vindt plaats door Staatstoezicht op de Mijnen (SodM). Indien toch door een incident het oppervlaktewater verontreinigd is, dan dient de mijnbouwonderneming deze verontreiniging te saneren in het kader van de Waterwet en eventueel de Wet bodembescherming. De desbetreffende waterbeheerder en provincie zijn hiervoor bevoegd gezag. De mijnbouwonderneming en toezichthouders hanteren een strikt controlebeleid waardoor de kans op verontreiniging van het oppervlaktewater zeer gering is. Gevaar voor de volksgezondheid door het optreden van incidenten is niet te verwachten.

8.5 **Externe veiligheid**

De beoordeling van het risico voor personen buiten de mijnbouwlocatie (kwantitatieve risicoanalyse) vindt plaats in het kader van de omgevingsvergunning (Wabo)

8.6 **Natuur**

Voor natuur geldt een rechtstreekse zorgplicht van beschermde flora en fauna. Als mijnbouwactiviteiten negatieve effecten zouden kunnen hebben op de aanwezige flora en fauna dan dient er een ecologisch onderzoek uitgevoerd te worden. Indien effecten niet uitgesloten kunnen worden dan dient een ontheffing aangevraagd te worden.

Indien mijnbouwactiviteiten of de gevolgen hiervan invloed kunnen hebben op de instandhoudingdoelstellingen van aangewezen Natura 2000-gebieden dan dienen de effecten en gevolgen onderzocht worden en eventueel een passende beoordeling opgesteld te worden. Indien hieruit blijkt dat er negatieve effecten kunnen optreden, dan is een vergunning nodig. Een en ander wordt geregeld in de Wet Natuurbescherming.

8.7 **Schade aan landbouw**

De bodemdaling uit zich door een gelijkmatige daling van het maaiveld, waardoor ook objecten en drainagebuizen gelijkmatig mee dalen. Zetting schade is doorgaans geen gevolg van die gelijkmatige daling, zo ook de werking van drainage daarvan in beginsel geen hinder ondervindt. Uit onderzoeken van onder meer de Commissie Bodemdaling wordt verder geconcludeerd, dat het waterpeil door de bodemdaling ten gevolge van de gaswinning/gasopslag in absolute zin niet wordt beïnvloed. Dit zal voor stikstofopslag niet anders zijn. Wel is er een verband gelegd tussen de invloed van deze bodemdaling op het waterpeil in relatieve zin (ten opzichte van het maaiveld). In algemene zin is vernatting tot een grondwaterstand van 120 cm beneden het maaiveld positief voor agrarische productie (vermindering van droogte-schade).

Bij een vernatting waarbij de grondwaterstand stijgt tot minder dan 120 cm beneden het maaiveld kan sprake zijn van agrarisch productieverlies. De bereikbaarheid van het land vermindert, het groeiseizoen verkort, oogstbaarheid neemt af en kans op bepaalde ziekten neemt toe. Indien vernatting van de bodem dergelijke effecten sorteert kan het waterpeil worden aangepast. Het aanpassen van het waterpeil bij bodemdaling of om andere redenen is een verantwoordelijkheid van het Waterschap. Aangezien de verwachte bodemdaling door gasopslag in cavernes zeer gering is, is het niet te verwachten dat hierdoor vernatting of verdroging optreedt met mogelijk nadelige gevolgen voor de landbouw.

9 Verklarende woordenlijst

Accelerometer	Een meetapparaat waarmee versnellingen van objecten gemeten en geregistreerd kan worden
Adolf van Nassau	Concessiegebied voor zoutwinning/aardgasopslag en stikstofopslag
Adolf van Nassau II	Winningsvergunning m.b.t. concessiegebied voor stikstofopslag
Adolf van Nassau III	Winningsvergunning m.b.t. concessiegebied voor zoutwinning
Akzo Nobel Salt b.v.	Mede vergunninghouder en bedrijf die de cavernes maakt c.q. gemaakt heeft
Anchor-pipe	Eerst gecementeerde casing die het fundament biedt voor de wellhead en X-mass tree
Annulus	Ruimte tussen twee verbuizingen
barg	De gemeten druk beschouwd ten opzichte van de atmosferische druk
bcm	billion cubic metres
BGR	Bundesanstalt für Geowissenschaften und Rohstoffe
BRZO	Besluit Risico Zware Ongevallen
Casing	Stalen buis die de afdichting vormt met het omliggend steenzout
Caverne	Ruimte gemaakt in steenzout door oplossen van het zout
Compactie	Het samendrukken van de aardlagen
dp/dt	Drukverandering per tijdseenheid
GTS	100% Gasunie dochter en eigenaar van de stikstofopslag caverne Heiligerlee HL-K
EZK	Ministerie van Economische Zaken en Klimaat
Gasunie	Gasunie is een Europees gasinfrastructuurbedrijf.
Geofoon	Sensor waarmee seismische trillingen kunnen worden gemeten
G-gas	Gas met een kwaliteit van het Groningen gasveld
GPS	Global Positioning System: systeem voor plaats- en hoogtebepaling met behulp van satellieten
Heiligerlee	Plaats waar de stikstof caverne zich bevind
Hydraat	Vaste stof in de vorm van kristallen gevormd bij vocht onder hoge druk
IfG	Institut für Gebirgsmechanik GmbH (Onafhankelijk onderzoeksinstituut voor rock mechanische analyses)
InSAR	Interferometric synthetic-aperture radar is een radar techniek met satellieten om o.a. bodembeweging te meten en te registreren
Kern	Gesteentemonster uit de ondergrond verkregen bij het boren van een put
KNMI	Koninklijk Nederlands Meteorologisch Instituut
Kruip	Het bewegen van steenzout (kleiner worden van de caverne) doordat druk in de caverne lager is dan het gewicht van bovenliggende gesteente en aardlagen
LCCS	Last Cemented Casing Shoe; afdichtende overgang van verbuizing naar steenzout
m ³ (n)	m ³ bij 0 °C en 1.01325 bara

Mb	Mijnbouwbesluit
MER	Milieu-Effect-Rapportage
MIT	Mechanical Integrity Test; gasdichtheidstest
Mw	Mijnbouwwet
NRB	Nederlandse Richtlijn Bodembescherming
Packer	Is een afdichting welke geproduceerde gassen en drukken in de caveerne isoleren van de LCC.
PBZO	Preventie Beleid Zware Ongevallen
PGS	Publicatiereeks Gevaarlijke Stoffen
PSinSAR	Verbeterd InSAR techniek
SCSSV	Surface Controlled Sub-Surface Safety Valve; ondergrondse automatisch sluitende veiligheidsklep
SEVESO II-richtlijn	Europese regelgeving m.b.t. het voorkomen van zware ongevallen
SodM	Staatstoezicht op de Mijnen
Spud-in	Exacte plaats van de boring
SRA	Seismische Risico Analyse
Stove-pipe	Geheide 1 ^e metalen casing die dient voor stabiliteit van de bodem in de beginfase van de boring en om grondwater en bodem contaminatie te voorkomen
TCBB	Technische Commissie Bodembeweging
TNO	Nederlandse Organisatie voor Toegepast-Natuurwetenschappelijk Onderzoek
Tubing	Stalen buis waardoor het gas in de caveerne geïnjecteerd wordt of waardoor geproduceerd wordt uit de caveerne
Uitbreiding Adolf van Nassau II	Winningsvergunning m.b.t. concessiegebied voor aardgasopslag
Uitbreiding Adolf van Nassau III	Winningsvergunning m.b.t. concessiegebied voor zoutwinning
VBS	Veiligheidsbeheerssysteem m.b.t. BRZO
Vertical seismic processing survey	Seismische techniek om verticale correlaties te leggen met seismische metingen aan het oppervlak
Viscoplastisch	Zie kruip
VR	Veiligheidsrapport m.b.t. BRZO
Wabo	Wet algemene bepalingen omgevingsrecht
Winschoten II	Opslagvergunning Gasunie Transport Services m.b.t. gebied voor opslag van stikstof
Winschoten III	Opslagvergunning Akzo Nobel Salt b.v. m.b.t. gebied voor opslag van stikstof
Zuidbroek	Plaats waar stikstof wordt gewonnen uit de buitenlucht met een stikstofinstallatie.

10 Referenties

1. 17013267 Brief SodM; Reactie SodM op inzetprofiel van de stikstofopslag, Den Haag 23-01-2017.
2. Heiligerlee Feasibility Proof HL-K Injection Capacity Increase_signed, Freiberg 26-11-2018.
3. Rock mechanical report B IfG - 47_2018_Report_HLK_final_2, Leibzig 08-03-2019.
4. Permeabilitatuntersuchungen an Steinsalz, Leibzig 11-06-2010.
5. Mapping of the Winschoten Saltdome, TNO 01-09-2000.
6. Actualisering bestaande geologische kaarten, Utrecht 18-12-2002.
7. Subsidence Prognosis for N2-storage HL-K, Hengelo 05-11-1999.
8. 150331 HL WP1 Report Subsidence Documentation-rev00, Hannover 31-03-2015.
9. 150831 HL WP2 Report Subsidence Modelling-rev01, Hannover 31-08-2015.
10. Ref. [10] 160413 HL WP3 Report Subsidence Prediction-rev00c, Hannover 13-04-2016.
11. 20180320_Seismic_Network_Specifications, London 20-03-2018.

11 Bijlage 1: Grote foto's van de opslaglocatie

Foto van opslaglocatie



Figuur 20 foto opslaglocatie



Figuur 21 Foto Wellhead/X-mass tree

Tab: Brief Sodem: Reactie Sodem op inzetprofiel van de
stikstofopslag



> Retouradres Postbus 24037 2490 AA Den Haag

N.V. Nederlandse Gasunie
t.a.v. dhr. P.J.P. Roordink
postbus 19
9700 MA Groningen

Staatstoezicht op de Mijnen

Bezoekadres

Henri Faasdreef 312
2492 JP Den Haag

Postadres

Postbus 24037
2490 AA Den Haag

T 070 379 8400 (algemeen)

F 070 379 8455 (algemeen)

sodm@minez.nl

www.sodm.nl

Behandeld door

dr. A.G. Muntendam-Bos

T 070 379 8494

Ons kenmerk

17013267

Uw kenmerk

Bijlage(n)

Datum 23 januari 2017


Betreft Reactie SodM op inzetprofiel van de stikstofopslag Heiligerlee

Geachte heer Roordink,

Met deze brief breng ik u op de hoogte van de evaluatie van Staatstoezicht op de Mijnen (SodM) naar aanleiding van uw mail dd. 23-12-2016, met het voorgenomen inzetprofiel voor de put HL-K bij de stikstofopslag Heiligerlee.

SodM heeft het profiel bestudeerd en is van mening dat, zo lang de druk bij de schoen van de put (BHP) onder de 147 bar(g) blijft, de stikstofopslag met dit profiel veilig ingezet kan worden. SodM staat inzet van de gasopslag toe onder de voorwaarde dat de BHP niet hoger wordt dan deze 147 bar, waarbij tenminste 1x per jaar een cyclus met een drukdaling van minimaal 10 bar wordt toegepast.

Met vriendelijke groet,


drs. H.A.J.M. van der Meijden, MBA
Inspecteur-generaal der Mijnen.

Tab: Feasibility Proof HL-K Injection Capacity Increase

Feasibility Proof on Injection Capacity Increase at HL-K Nitrogen Buffer

For: **N.V. Nederlandse Gasunie**
Mining & Operations
Postbus 19
9700 MA Groningen
Concourslaan 17

Freiberg, 26.11.2018


ppa. Wagler


i. V. Bannach

List of Content

- 1 INTRODUCTION 3**
- 2 CHARACTERISTICS OF CAVERN HL-K..... 3**
- 3 OPERATIONAL PARAMETERS & LIMITS 4**
- 4 OPERATIONAL HISTORY 4**
- 5 SONAR SURVEYS 5**
- 6 THERMODYNAMIC MODELING 6**
 - 6.1 SET UP OF THERMODYNAMIC MODEL 7
 - 6.2 MODEL QUALIFICATION 7
 - 6.3 PREDICTION RUNS..... 8
- 7 FEASIBILITY PROOF 10**
- 8 SUMMARY 11**
- LIST OF REFERENCES AND SOURCE DATA 12**
- LIST OF APPENDICES..... 12**

1 Introduction

Gasunie operates a nitrogen cavern at Heiligerlee salt diapir. The large scale storage of nitrogen became necessary when the domestic production from the Groningen gas field began to decline. The stored nitrogen is used to blend imported high calorific gas to fulfil the requirements of the Dutch gas grid. Due to the recent earthquakes (increased in number and severity) in the Groningen area, the Loppersum cluster production capacity from the Groningen gas field has been further reduced significantly. This will result in a considerably higher demand of flexibility of the nitrogen storage operation. Currently the injection capacity is substantially lower than the withdrawal capacity. It is intended to upgrade the existing air separation plant in order to reach equal injection and withdrawal capacities. The objective of the study is to proof the feasibility of safe cavern storage operations applying equally high injection rates as per withdrawal rates.

A thermodynamic model is generated to predict cavern pressure and temperature responses based on different realistic yearly nitrogen injection and withdrawal scenarios including the targeted maximum injection figures. The thermodynamic model is qualified against historical data as operational pressure and temperature measurements as well as available sonar surveys.

Once the model is qualified the developed injection and withdrawal scenarios are simulated. The calculated pressure and temperature responses will be evaluated under consideration of set operational constraints as a basis for feasibility proof from a thermodynamic perspective.

Additionally, the calculated cavern pressure and temperature responses will be used as input data for subsequent rock mechanic modeling work.

2 Characteristics of Cavern HL-K

Cavern HL-K is part of a set of brine production caverns located at the Heiligerlee salt dome. The cavern has been selected to be converted into a nitrogen buffer to fulfill the increased demand of nitrogen in the Dutch gas grid. In year 2010 the cavern was equipped with an appropriate gas completion consisting of the following components (appendix 2.1):

- 9 ⁵/₈" x 8 ⁵/₈" production string
- 10 ³/₄" permanent packer
- 8 ¹/₄" x 7 ³/₄" tailpipe with landing nipples and flow couplings
- Wireline retrievable surface controlled subsurface safety valve

The installed wellhead equipment includes (appendix 2.2):

- 13 ⁵/₈" API 3000 tubing hanger spool
- 11" API 3000 pack off adapter flange
- 11" API 3000 master valve, hydraulically (fail safe) operated
- 11" API 3000 production tee
- 11" API 3000 top valve, hand operated
- 9" API 3000 wing valves, hand operated
- 9" API 3000 wing valves, hydraulically (fail safe) operated

For the gas first fill of the cavern a 5" debrining string was temporarily installed. The debrining process was operated from April 2011 to July 2012. After completion of the debrining process the debrining

string was snubbed out and the cavern has been echometrically surveyed providing the following characteristic data:

- Depth of last cemented casing shoe: 981 m
- Depth of cavern roof: 1,013 m
- Depth of cavern sump: 1,502 m
- Free cavern volume: 824,651 m³
- Max cavern diameter (average): 60 m @ 1,450 m

The overall cavern shape is quite regular. Representative sections (horizontal & vertical) are shown in appendix 2.3.

3 Operational Parameters & Limits

The cavern HL-K was subject of an intensive rock mechanic assessment. Based on a realistic-conservative rock mechanical model nitrogen storage cycles have been simulated. As a result from this modeling work a set of operational constraints were defined for flow rates, cavern pressures as well as for particular cycle instructions.

The set of operational constraints are listed in table 3.1.

Operational Parameter	Constraint
Max. Injection Rate	16,000 m ³ /h → 190,000 m ³ /h
Max. Production Rate	190,000 m ³ /h
Max. Pressure	147 bar @ Casing Shoe
Min. Pressure	70/90 bar @ Casing Shoe
Max. Pressure Change	10 bar/day
Cycle Instructions:	Max. 90 days/year @ 90 bars Max. 30 days/year @ 70 bars Min. 10 bars pressure change per year

Table 3.1: operational constraints for cavern HL-K

As the air separation plant was originally designed for a maximum capacity of 16,000 m³/h, the maximum nitrogen injection rate considered in former assessment studies was of this magnitude. As it is planned to increase the capacity of the plant in order to reach equal injection and withdrawal capacities a maximum injection rate of 190,000 m³/h is now considered.

4 Operational History

Nitrogen storage operation started in summer 2012. The operational history in terms of operated flow rates, measured wellhead pressures and temperatures is shown in appendix 4.1. According to this picture it is obvious that operational activities were rather poor in the period from 2011 to 2014. During this period the nitrogen buffer is nearly at its maximum filling level represented by a relatively con-

stant and high wellhead pressure. Contrary to this, the measured wellhead temperature corresponds with the ambient air temperature and shows clearly night and day as well as seasonal fluctuations, as it is commonly the case for shut in wells.

At the beginning of year 2015 the cavern pressure was substantially decreased as a consequence of the identified pressure responses in the B annulus. Subsequently, the shut in cavern has been monitored until November 2015 showing a wellhead pressure of about 125 bars. From December 2015 a bit more frequent storage operation started with some considerable pressure reductions down to approximately 110 bar (wellhead pressure) in spring 2017 and spring 2018. The operated flow rates reached up to 100,000 m³/h during nitrogen withdrawal out of the cavern and nearly the plant capacity of 16,000 m³/h while injecting nitrogen into the cavern.

Overall, it can be noted that the nitrogen buffer at Heiligerlee has not experienced an extensive storage operation so far. Nevertheless, the available operational data can be used to conclude on the thermodynamic behavior of the subsurface system (cavern & well) applying a thermodynamic modeling approach.

5 Sonar Surveys

For the time period from 2010 to 2018 in total 4 sonar surveys have been run at cavern HL-K.

- Last sonar in brine: 16/02/2010
- First sonar in gas: 15/08/2012
- 1. Repeat sonar in gas: 19/05/2014
- 2. Repeat sonar in gas: 20/12/2017

Table 5.1 shows the measured free cavern volume and the measured average cavern fluid temperature for each individual sonar survey.

Date of Sonar Survey	Free Cavern Volume	Cavern Fluid Temperature
16/02/2010	829,292 m ³	31.5 °C
15/08/2012	824,651 m ³	41.5 °C
19/05/2014	821,479 m ³	44.5 °C
20/12/2017	802,854 m ³	47.0 °C

Table 5.1: Results from Sonar Surveys

From a thermodynamic analysis perspective the free cavern volume and the measured fluid temperature in the cavern are the most important results from a sonar survey. The measured free cavern volume at different points of time allows to evaluate the cavern shrinkage over time. As the free cavern volume is part of the applied thermodynamic equation of state, its variation over time might become essential in the course of thermodynamic analyses.

Appendix 5.1 illustrates the cavern shrinkage over a period of time from 2010 to 2017. It is obvious from this illustration that cavern convergence was very limited during the first five years of the observation period. Due to the intensified storage operation from year 2015 onwards the induced cavern shrinkage is increased but is still limited to cavern convergence rates of clearly less than 1% per year.

In total the measured cavern shrinkage is merely 3% over a period of 8 years and will therefore have very limited impact on the thermodynamic analysis.

Measurements of the cavern fluid temperature are of high importance in association with thermodynamic analysis of gas storage operations in solution mined salt caverns. While measured wellhead pressures can be reliably used to conclude on the pressure inside of the cavern, measured wellhead temperatures are not even comparatively suitable to state on the actual fluid temperature inside the cavern. On one hand this is due to the already mentioned impact of the ambient air temperature when the cavern is shut off. On the other hand the heat exchange processes along the cavern well are much more complex compared to those with the cavern surroundings. This is mainly attributed to the complex well configuration – casing, cement, annular fluids – as well as to the usually wide range of different geological sequences encountered by the cavern well for which there are no reliable thermal properties available.

For cavern HL-K there are in total 4 measurements providing direct information about the temperature of the fluid inside of the cavern within the observation period. The first measurement (16/02/2010) represents the temperature of the brine at the end of the leaching process. For all other measurements the cavern was completely filled up with nitrogen. Appendix 5.2 shows measured cavern fluid temperature over time. The measurements show a regular increase of the fluid temperature with elapsed time which is commonly the case for solution mined salt caverns after conversion from brine production to gas storage caverns.

6 Thermodynamic Modeling

For thermodynamic modeling the gas cavern simulator KAVPOOL is applied. KAVPOOL is a software tool developed in-house by ESK to support gas cavern storage operators in their day-to-day business and assist subsurface engineers in planning and designing storage facilities.

The model incorporates all thermodynamic processes associated with gas storage operations in salt caverns. This includes:

- Pressure-volume-temperature relationship of the gas in flow zones
- Heat transfer between storage medium and surrounding rock
- Friction losses due to fluid flows along production tubing and connection pipelines

Appendix 6.1 illustrates the modeling principle of the KAVPOOL software.

Parallel to thermodynamic calculations, the rock mechanics option that was implemented provides information about the operationally induced shrinkage of each individual cavern at storage facilities. The model can be run as a forecasting tool or can be used for back analyses for purposes of investigating actual cavern behavior by applying common history match procedures. The history match procedure allows initially selected parameters to be adjusted to real storage conditions and the model to be subsequently used to predict specific operational conditions.

KAVPOOL takes a wide range of pure gaseous components into account, meaning it can not only be used for natural gas storage but also in compressed air energy storage (CAES) and hydrogen storage in solution-mined salt caverns.

KAVPOOL is in use for more than two decades. Since then, numerous applications for different gas cavern storage facilities across Europe have been performed.

6.1 Set up of thermodynamic model

The thermodynamic model includes all relevant components of the subsurface system which can be mainly subdivided into the cavern section and the well section. As the cavern is in direct contact with the salt rock no other components need to be considered in this model region. For the well section a series of casing strings are implemented in the model as well as the respective cement and annular fluid intervals.

As the heat conductivity of rock salt is certainly different to those of other rock materials (e.g. sands, clays, marls, etc.) the top of salt is additionally considered in the model.

A schematic overview of the model set up is given in appendix 6.2. Table 6.1 sets out a list of relevant properties for each material component incorporated in the model.

Material component	Heat conductivity W/(m*K)	Heat capacity kJ/(kg*K)	Density kg/m ³
Rock salt	5.0	0.9	2,200
Overburden rock	2.0	0.9	2,000
Casing (carbon steel)	44.0	0.46	7,850
Cementation	0.8	0.8	2,000
Annular fluid	0.6	4.8	1,200

Table 6.1: Model Properties

6.2 Model qualification

Prior to using thermodynamic models for the prediction of pressure and temperature responses due to gas injection and withdrawal processes such models need to be qualified based on available historical data.

The model qualification process for the HL-K cavern was subdivided in two steps. The first step covers the cavern debrining period as well as the relatively quiet gas storage period until the beginning of year 2014. During this period there are nearly no dynamic effects which influence the whole thermodynamic system significantly. The occurring heat exchange process is mainly driven by the heat flow from rock mass zones further away from the cavern as the cavern surroundings have been essentially cooled down during the leaching phase. This process is mainly controlled by the heat conductivity of the rock salt. During the debrining process the cavern fluid is changing from brine to nitrogen. As the heat capacity of these fluids is substantially different the increase of the cavern fluid temperature is significantly accelerated when nitrogen dominates the cavern fluid content. In the course of thermodynamic modeling the actually gradually running process of the brine displacement is modeled by an instantaneous exchange of the cavern fluid after 50% fill. Appendix 6.3 shows the measured and calculated cavern fluid temperature over a period of time from year 2010 to year 2018. The measured regular increase of the cavern fluid temperature is more than satisfactorily reflected by the model results.

The same is for the calculated wellhead pressures. Appendix 6.4 shows a comparison between the measured and calculated wellhead pressures (time period from 2014 to 2018). There is an excellent match of measured and modeled data over the whole simulation period.

Even though the overall cavern convergence within the observation period is very limited the model has been tuned to reflect the measured cavern shrinkage adequately. Appendix 6.5 illustrates the calculated cavern shrinkage over the simulated operational period (2014-2018).

As discussed in section 4 the nitrogen buffer at Heiligerlee has not experienced an extensive storage operation so far. For that reason it is investigated how strong the calculated pressure and temperature respond to variations of relevant model parameters. One of the most complex parameter to control the heat exchange between the cavern fluid and the cavern surroundings is the heat transfer coefficient. The heat transfer coefficient is a function of various dimensionless numbers as Nusselt number, Prandtl number and Grasshof number. For an exact determination of the heat transfer coefficient in real caverns very excessive CFD-modeling is necessary to characterize actual flow conditions. From a comparison of all storages simulated by ESK so far, in practice effective heat transfer coefficients in the range from 10 to 30 W/m²*K are able to yield a realistic modeling of the heat exchange between the fluid inside of a cavern and the cavern surroundings.

The nitrogen storage operation has been simulated for both heat transfer coefficient of 10 W/m²*K and 30 W/m²*K. Appendix 6.6 shows the comparison of the calculated cavern fluid temperatures versus time. It is obvious that the effects of different heat transfer coefficients are very limited over the entire operational lifetime. Even for the more intensive storage dynamics the differences in the calculated cavern fluid temperatures are less than 2.5 Kelvin. In less intensive operational periods the results differs certainly less (< 1.0 Kelvin). Focusing on the measured cavern fluid temperature on 20 December 2017 it appears that the higher heat exchange coefficient (30 W/m²*K) represents the actual thermodynamic processes slightly better. Therefore this parameter is chosen for the subsequent prediction runs. The shown differences in calculated cavern fluid temperatures do not have a considerable impact on the calculated wellhead pressure responses (< 1.0 bar) and can therefore be considered negligible for the intended prediction runs.

6.3 Prediction runs

Future storage operation of the nitrogen buffer is subject of numerous influencing factors (e.g. overall gas supply situation, outside air temperature, etc.) each of them is difficult to predict. Nevertheless, there are particular expectations how the demand on nitrogen withdrawal out of the buffer as well as nitrogen injection into the buffer may look like. As a result of these expectations two different import/export schedules for a yearly operational period have been developed. The two operational profiles A and B are shown in the appendices 6.7 and 6.8. Each profile includes maximum injection and withdrawal rates up to 190,000 m³/h with some single larger withdrawal rates up to 300 m³/h (scenario A only). The nitrogen turnover is approximately 40 Mill. m³ for each profile. Both scenarios are based on historical data and differ mainly by the point of time of maximum cavern depletion (scenario A in January/February, scenario B in late April) and by their total standstill duration.

Based on the qualified thermodynamic model the rate schedules for profile A & B have been simulated. At the beginning the model state represents approximately 95% of maximum GIP to account for the expected cavern temperature increase during continuous injection periods which may lead to considerably higher cavern pressures at similar filling levels. Appendices 6.9 and 6.10 show the calculated casing shoe pressures for a yearly cycle according to the operational profiles A and B. It is obvious that the maximum as well as the minimum allowable casing shoe pressures (max: 147 bar, min: 70 bar) are not exceeded. The corresponding wellhead pressures ranges from 40 bars at minimum filling levels to 140 bars at maximum filling levels (appendices 6.11 & 6.12).

Appendices 6.13 and 6.14 show the development of the cavern fluid temperatures of both scenarios. The calculated temperatures do not fall below 35 °C in both scenarios. It is interesting to note that the calculated minimum cavern temperatures do not coincide with calculated minimum pressures. This is in particular true for the operational profile B. Operating this profile the minimum cavern temperature is reached after the first significant withdrawal period. The subsequent injection period leads to sufficient temperature rise preventing the cavern fluid temperature to drop to lower values when lowering the cavern pressure to its minimum level. After the nitrogen reinjection periods the cavern fluid temperature is continuously increasing but is not reaching temperature levels of 55 °C. Therefore, the overall temperature spread inside of the cavern is limited to less than 20 °C although the total working gas volume is nearly turned over within a limited period of time (6 weeks in case of scenario B).

A further operational constraint is set out in terms of limited change of cavern pressure within a certain period of time. This criterion is associated with the particular rheological behavior of rock salt (ability to creep). Rapid pressure changes will lead to higher loads intensities in the surrounding rock mass as there is less time available to compensate the applied deviatoric stresses by creep mechanisms. The resulting daily changes in cavern pressure from running scenarios A & B is given in appendices 6.15 and 6.16. As the operational profiles include frequent intraday changes of injection and withdrawal rates the simulation results must be adequately processed. This is done for every time step (hour) by representing the difference between calculated casing shoe pressures of the past 24 hours. The approach allows to state about the daily pressure change but prevents peak shaving.

The processed simulation results showed in appendices 6.15 and 6.16 clearly state limited daily changes in cavern pressures of less than 10 bars/day.

High injection and withdrawal rates are always linked to increased gas flow velocities. This is in particular true when high flow rates are operated in lower pressure levels. Appendices 6.17 and 6.18 illustrate the calculated gas flow velocities at the wellhead of cavern HL-K for scenario A and B, respectively. It is obvious that for both scenarios the flow velocities are predominantly limited to less than 25 m/s, which is a common design criterion for gas production and gas storage wells. However, for certain operational conditions the calculated gas flow velocity clearly exceeds the limit of 25 m/s. But this is only the case when high withdrawal rates ($Q > 150,000 \text{ m}^3/\text{h}$) coincide with low well head pressures ($p_{\text{head}} < 70 \text{ bars}$).

It is recommended to pay particular attention on withdrawal rates when the wellhead pressure drops below 70 bars to avoid frequent occurrence of excessive flow velocities.

7 Feasibility Proof

The storage operation of the nitrogen buffer at Heiligerlee is subject to certain operational constraints which are set out in section 3. These constraints are mainly related to the adherence of minimum and maximum permissible cavern pressures as well as the limitation of the daily change in cavern pressure. Further constraints are related the yearly storage cycle as the cavern is allowed to be operated under lower pressure for a limited period of time only. Furthermore, in order to stimulate creep in the depth of the last cemented casing shoe some change of cavern pressure throughout the year is requested. Table 7.1 lists the operational constraints to be adhered at cavern HL-K.

Operational Parameter	Constraint
Max. Pressure	147 bar @ Casing Shoe
Min. Pressure	70/90 bar @ Casing Shoe
Max. Pressure Change	10 bar/day
Cycle Instructions:	Max. 90 days/year @ 90 bars Max. 30 days/year @ 70 bars Min. 10 bars pressure change per year

Table 7.1 Operational constraints at cavern HL-K

Based on the qualified thermodynamic model realistic future operational scenarios has been simulated. The simulation results are used to state if the expected yearly storage operation cycles comply with the defined operational constraints. Table 7.2 shows the comparison between the defined operational constraints and the respective simulation results for the operational profiles A & B. Storage operations according to profile A & B will not exceed any limit set out in rock mechanic cavern design. The feasibility of such storage operating scenarios including nitrogen injection rates up to 190,000 m³/h is therefore proven.

Operational Parameter	Constraint	Actual Profile A	Actual Profile B
Max. Casing Shoe Pressure	147 bar	143.6 bar	144.2 bar
Min. Casing Shoe Pressure	70/90 bar	80.5 bar	76.9 bar
Casing Shoe Pressure in the range from 90 bar to 70 bar	30 days	19 days	8 days
Max. Pressure Change	10 bar/day	7.6 bar/day	7.6 bar/day
Min. pressure change per year	> 10 bar	63.1 bar	67.3 bar

Table 7.2: Comparison of operational constraints and simulation results

8 Summary

Currently, the injection capacity into the nitrogen buffer at Heiligerlee is substantially lower than the withdrawal capacity. It is intended to upgrade the existing air separation plant in order to reach equal injection and withdrawal capacities. Based on a thermodynamic modeling approach the feasibility of safe cavern storage operations shall be proven considering equally high injection rates as per withdrawal rates. As it is common practice for gas storage operations in solution mined salt caverns there are certain operational limits set out in the rock mechanic design phase to be adhered in the storage operational phase. For the nitrogen buffer HL-K the following constraints are defined:

- Maximum casing shoe pressure: 147 bar
- Minimum casing shoe pressure: 90 bar for a period of 90 days
- Minimum casing shoe pressure: 70 bar for a period of 30 days
- Maximum daily pressure change: 10 bar/day
- Minimum yearly pressure change: 10 bar/year

A thermodynamic model has been generated which represents the entire subsurface system of the existing nitrogen buffer (cavern HL-K and the corresponding cavern well). In a first step the thermodynamic model was qualified against historical data as operational pressure and temperature measurements as well as available sonar surveys. The calculated model responses show a quite good coincidence with the available measuring data including both the historical wellhead pressures as well as cavern shrinkage and cavern fluid temperature evolution coming from available sonar surveys.

For future nitrogen storage operations two different import/export schedules for a yearly operational period have been developed each of them includes withdrawal and injection rates of 190,000 m³/h and turn over nitrogen volume of approximately 40 Mill. m³. Both scenarios were simulated applying the qualified thermodynamic model.

The simulation results were used to state if the defined operational constraints are adhered for the entire yearly storage operation cycle. The results clearly show that storage operations according to profile A & B will not exceed any limit set out in rock mechanic cavern design.

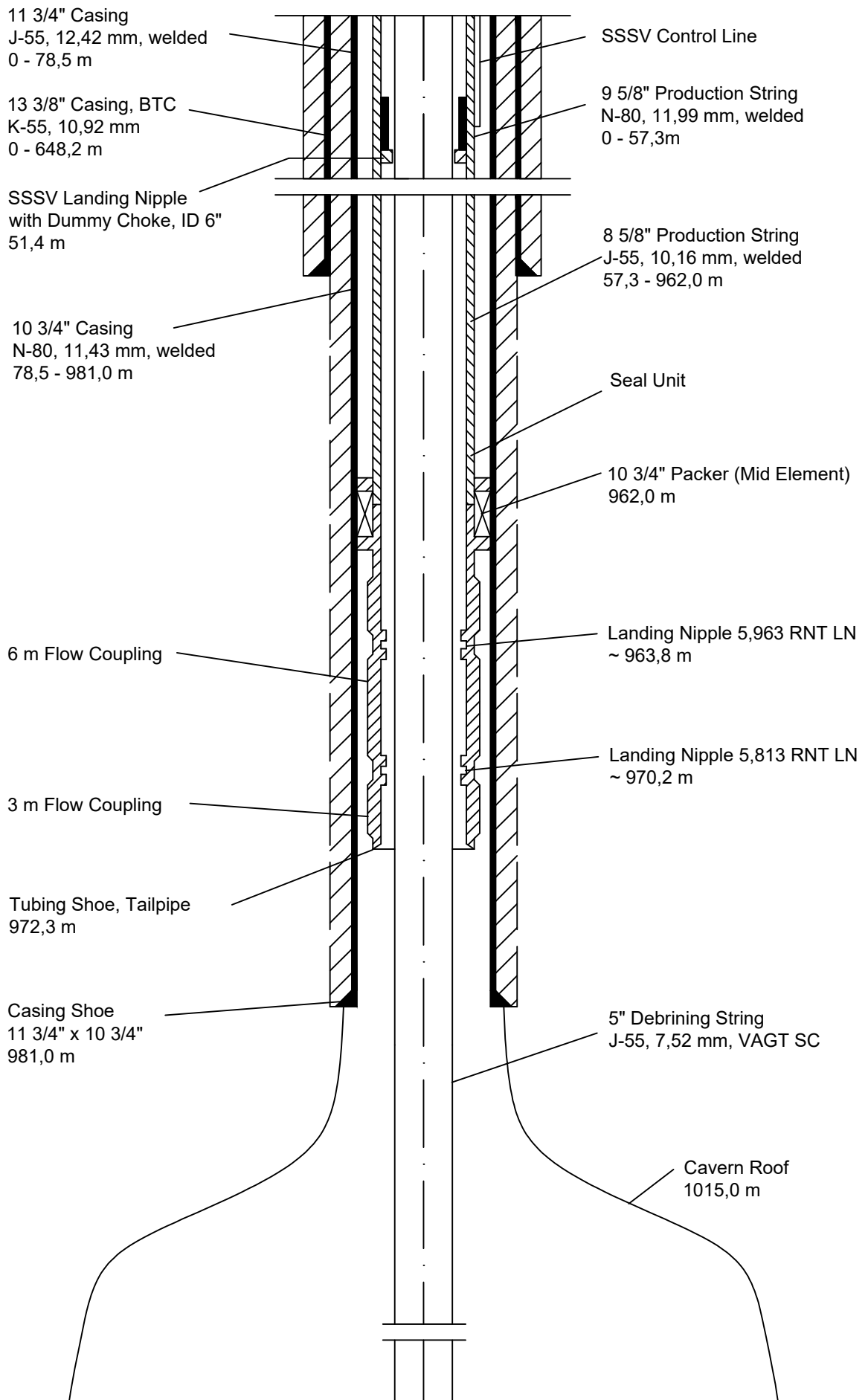
The feasibility of such storage operating scenarios including nitrogen injection rates up to 190,000 m³/h is therefore proven.

List of References and Source Data

- /1/ Rock mechanical assessment of the conversion of the Heiligerlee HL-K cavern to a nitrogen storage cavern, IfG GmbH, 2008
- /2/ Numerical stability verification concerning the conversion of the cavern Heiligerlee HL-K into a nitrogen buffer, IfG GmbH, 2010
- /3/ Cavern pass Heiligerlee HL-K, ESK GmbH, 2010
- /4/ Cavern HL-K, 4th sonar survey, Socon GmbH, 2010
- /5/ Cavern HL-K, 5th sonar survey, Socon GmbH, 2012
- /6/ Cavern HL-K, 6th sonar survey, Socon GmbH, 2014
- /7/ Cavern HL-K, 8th sonar survey, Socon GmbH, 2017
- /8/ Operational data (flow rates, wellhead pressures & temperatures) for the period from 2012 to 2108

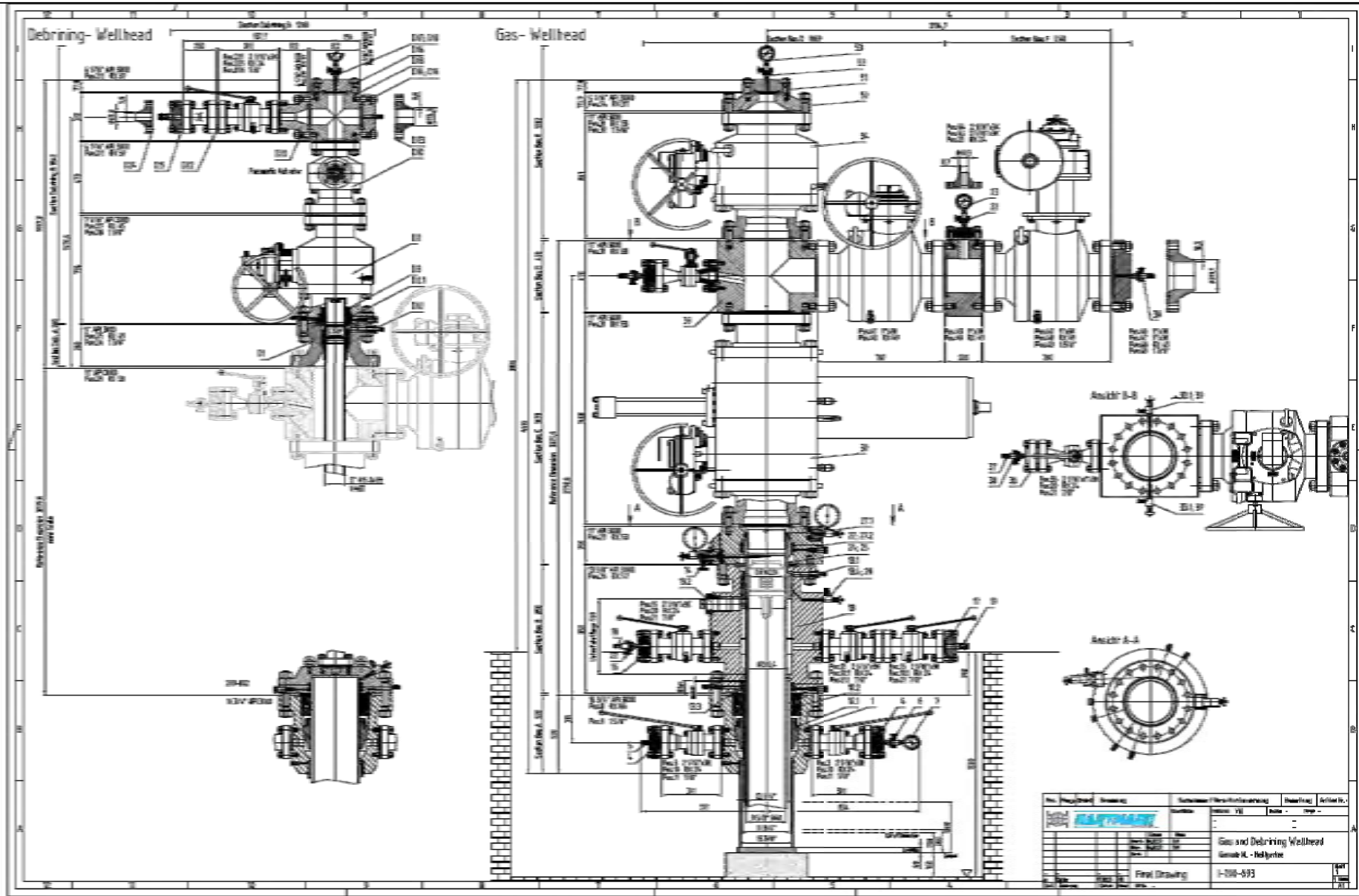
List of Appendices

- Appendix 2.1: Cavern HL-K – well completion schematics
- Appendix 2.2: Cavern HL-K – wellhead assembly
- Appendix 2.3: Cavern HL-K – representative cavern sections
- Appendix 4.1: Cavern HL-K – operational history
- Appendix 5.1: Cavern HL-K – cavern shrinkage from year 2010 to 2017
- Appendix 5.2: Cavern HL-K – measured cavern fluid temperature over time
- Appendix 6.1: Gas cavern simulator KAVPOOL – modeling principle
- Appendix 6.2: Schematic overview of model set up
- Appendix 6.3: Measured and calculated cavern fluid temperature over time
- Appendix 6.4: Measured and calculated wellhead pressures over time
- Appendix 6.5: Calculated cavern shrinkage during operational period from 2014 to 2018
- Appendix 6.6: Calculated cavern fluid temperatures for different heat transfer coefficients
- Appendix 6.7: Operational profile A
- Appendix 6.8: Operational profile B
- Appendix 6.9: Calculated casing shoe pressures for a yearly cycle according to scenario A
- Appendix 6.10: Calculated casing shoe pressures for a yearly cycle according to scenario B
- Appendix 6.11: Calculated wellhead pressures for a yearly cycle according to scenario A
- Appendix 6.12: Calculated wellhead pressures for a yearly cycle according to scenario B
- Appendix 6.13: Calculated cavern fluid temperatures for a yearly cycle according to scenario A
- Appendix 6.14: Calculated cavern fluid temperatures for a yearly cycle according to scenario B
- Appendix 6.15: Daily changes of cavern pressure for a yearly cycle according to scenario A
- Appendix 6.16: Daily changes of cavern pressure for a yearly cycle according to scenario B
- Appendix 6.17: Calculated gas flow velocities for a yearly cycle according to scenario A
- Appendix 6.18: Calculated gas flow velocities for a yearly cycle according to scenario B



Nitrogen Buffer HL-K
Injection Capacity
Increase

Cavern HL-K - well completion schematics

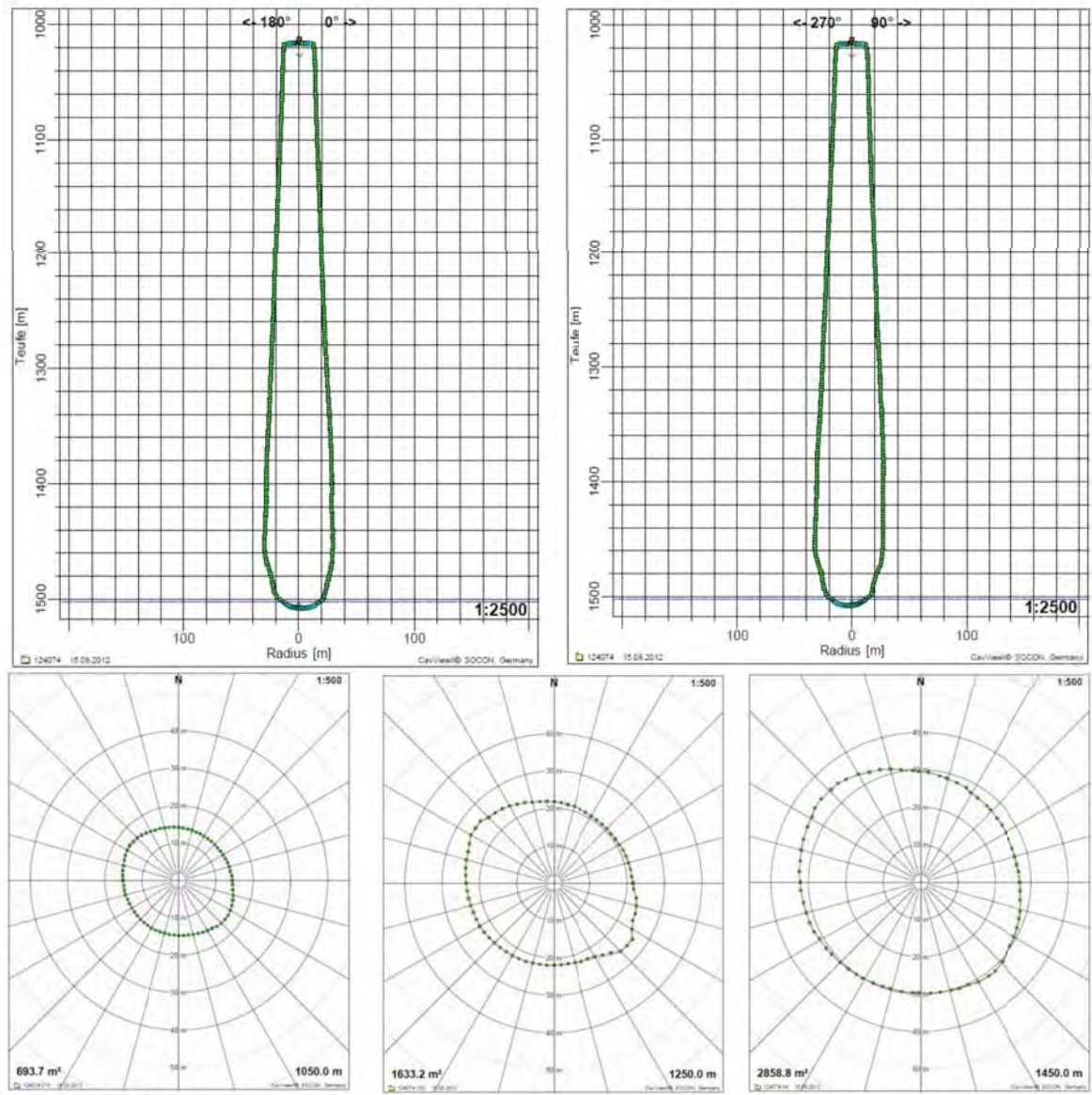


Nitrogen Buffer HL-K
Injection Capacity
Increase

Cavern HL-K - wellhead assembly

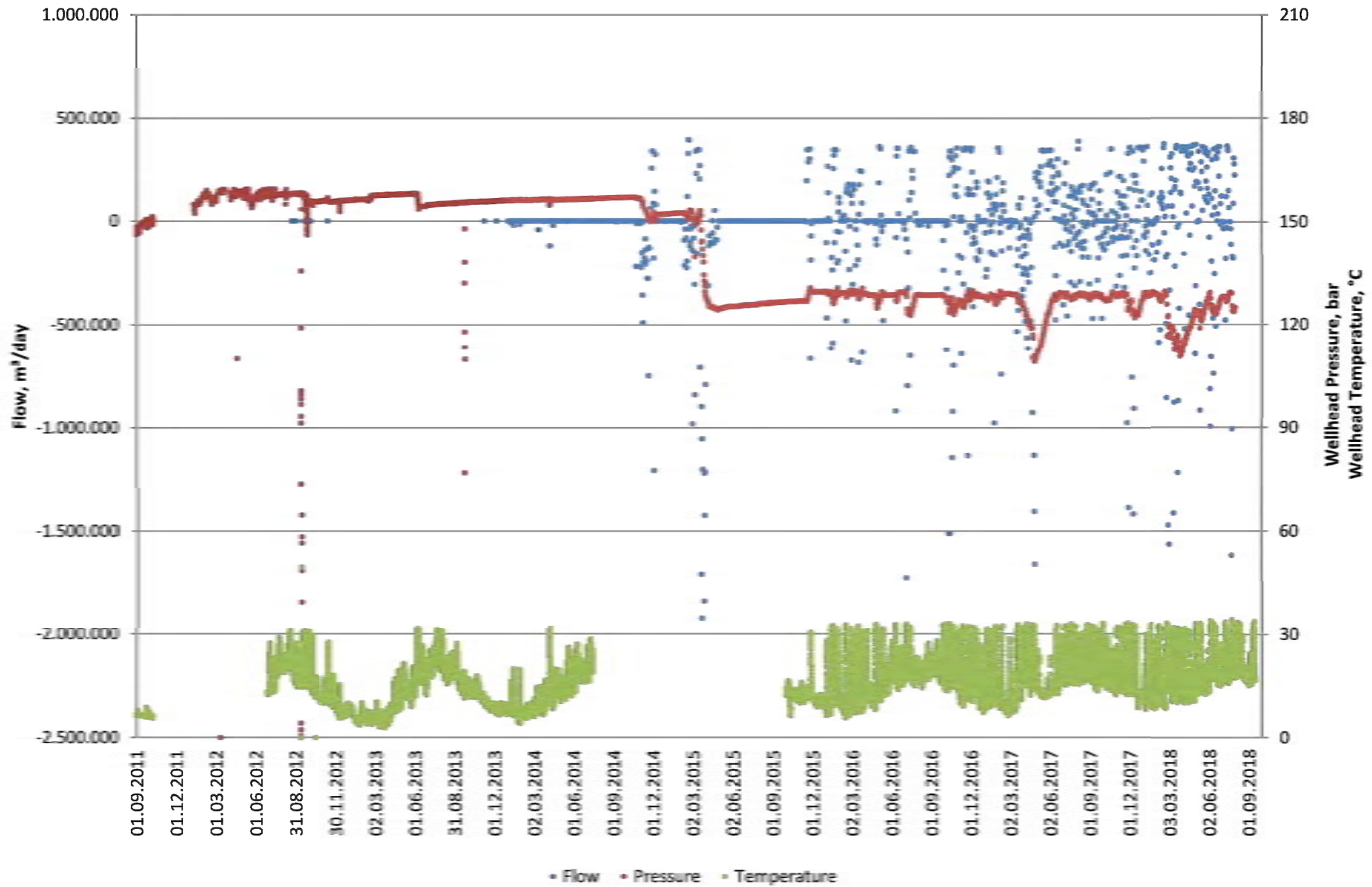


Part of innogy



Nitrogen Buffer HL-K
Injection Capacity
Increase

Cavern HL-K - representative cavern sections

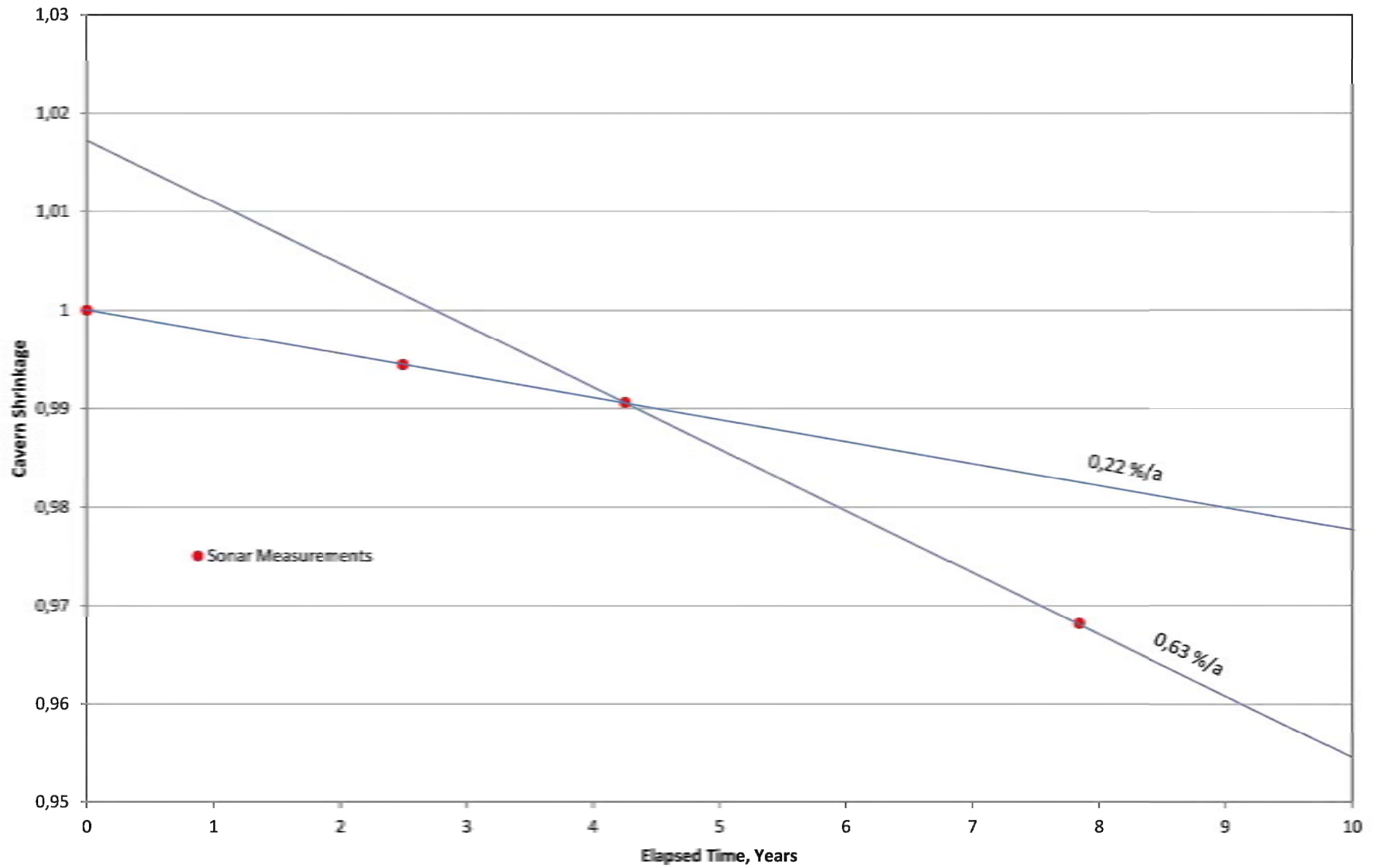


Nitrogen Buffer HL-K
Injection Capacity
Increase

Cavern HL-K - operational history

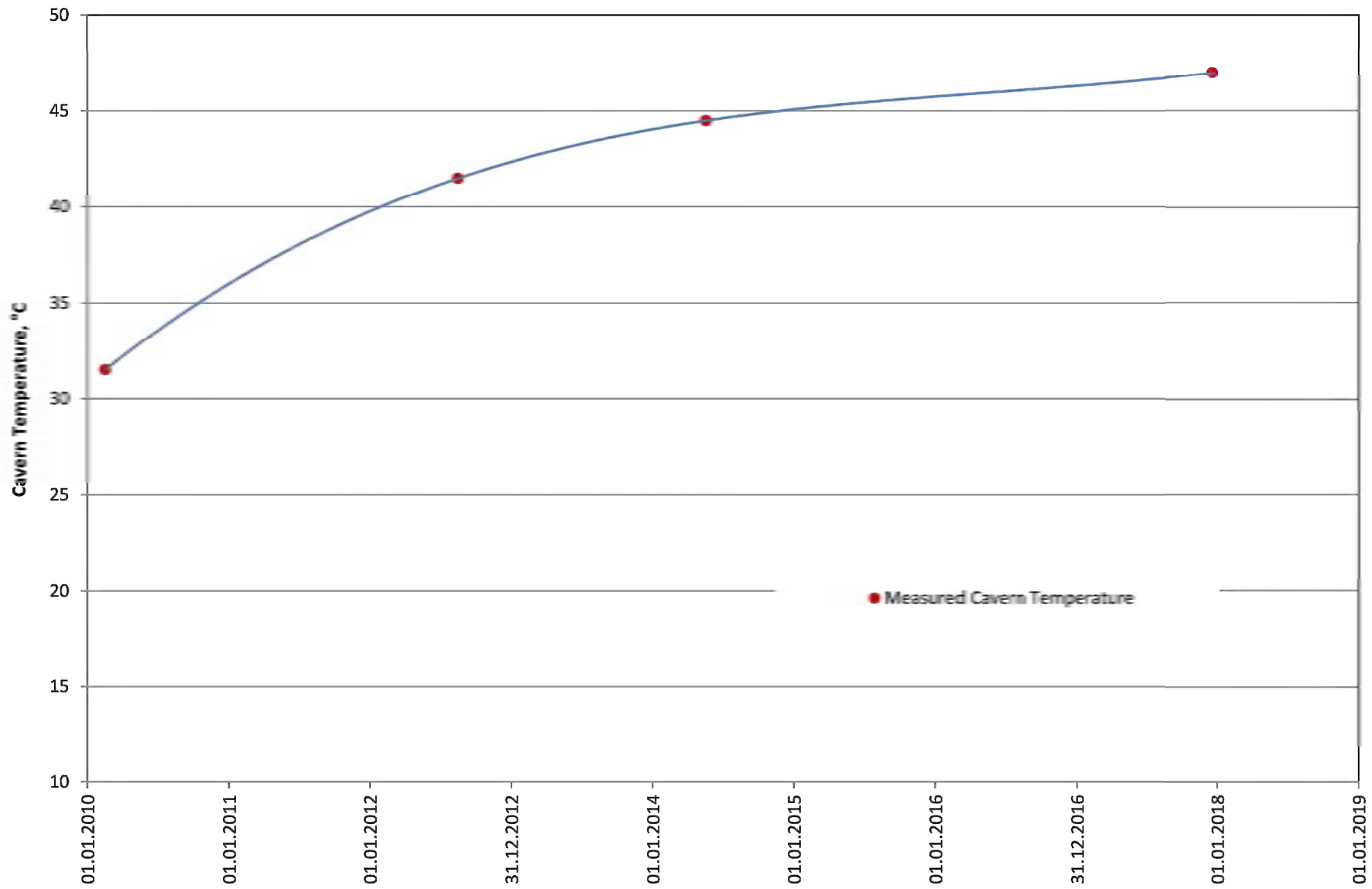


Part of innogy



Nitrogen Buffer HL-K
Injection Capacity
Increase

Cavern HL-K - cavern shrinkage from year 2010 to 2017



Nitrogen Buffer HL-K
Injection Capacity
Increase

Cavern HL-K - measured cavern fluid temperature over time

1

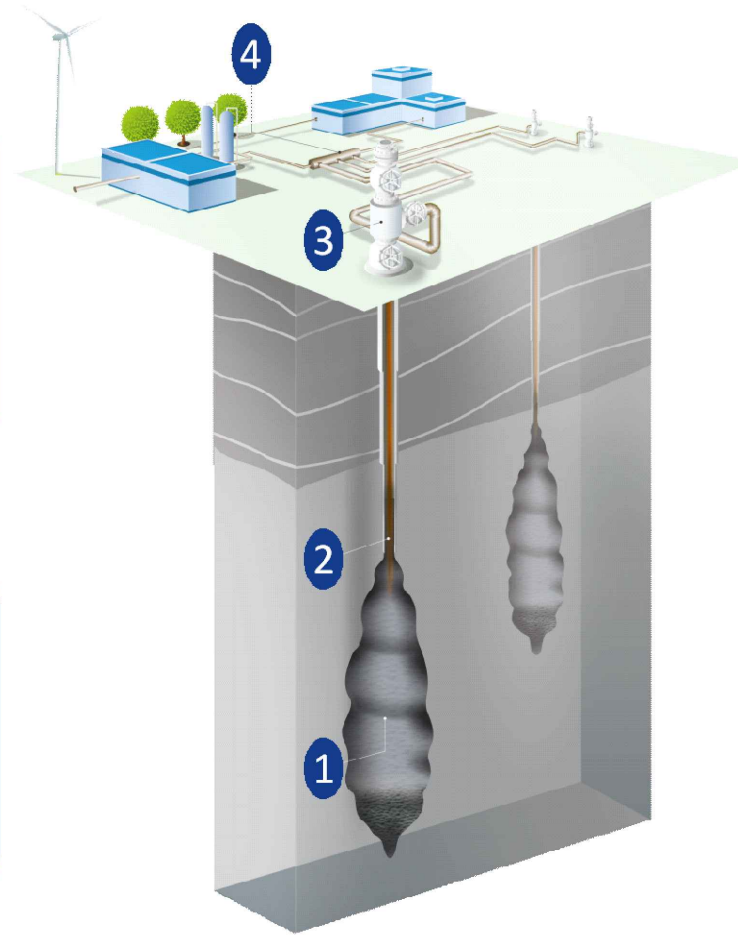
Thermodynamic processes inside of the cavern and through the surroundings

Cavern pressure/temperature versus volume/time

2

Resulting thermodynamic states at casing shoe of the last cemented casing

Casing shoe pressure/temperature versus volume/time



3

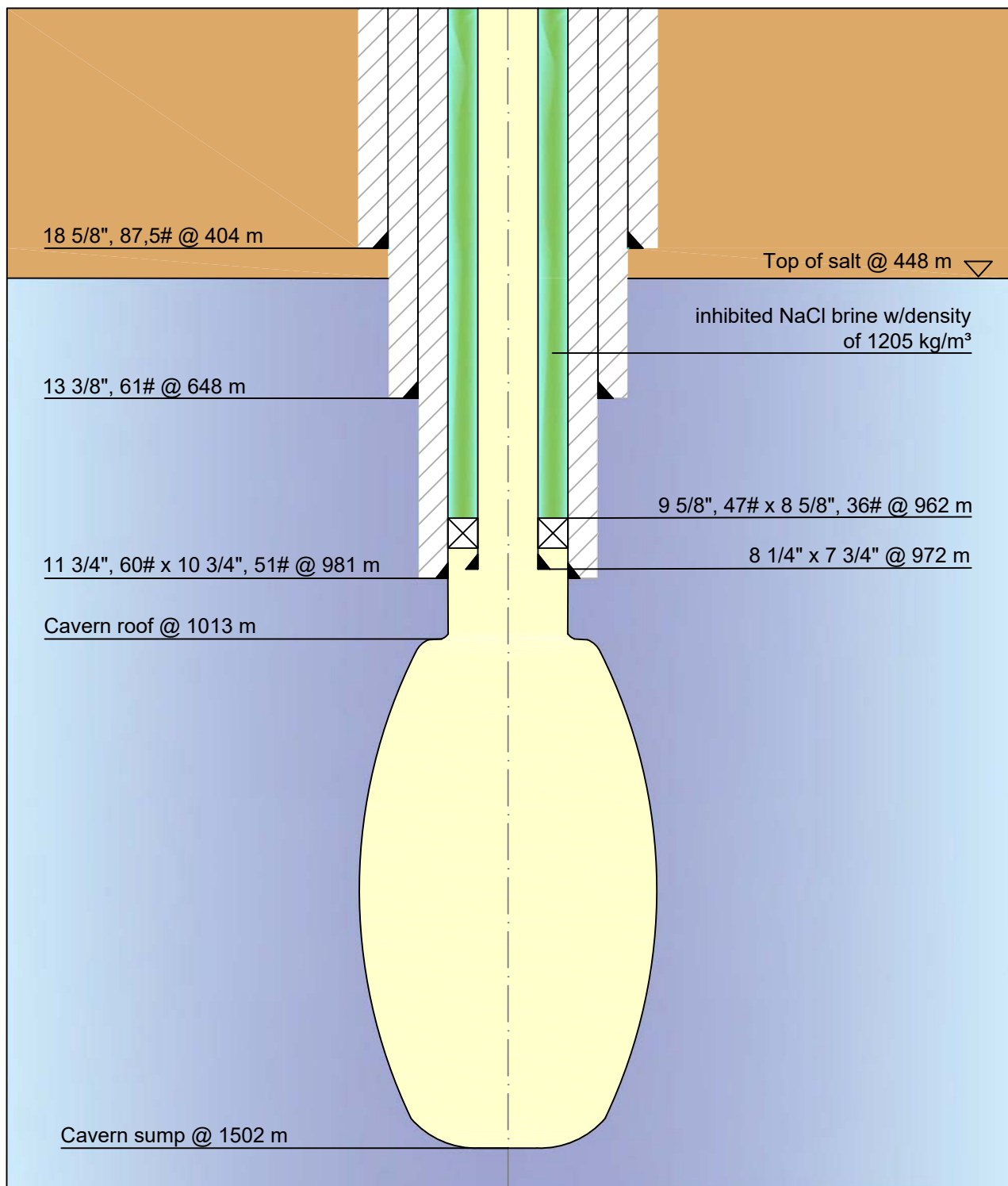
Thermodynamic processes along the wellbore including heat exchange with the surrounding rock

Wellhead pressure/temperature versus volume/time

4

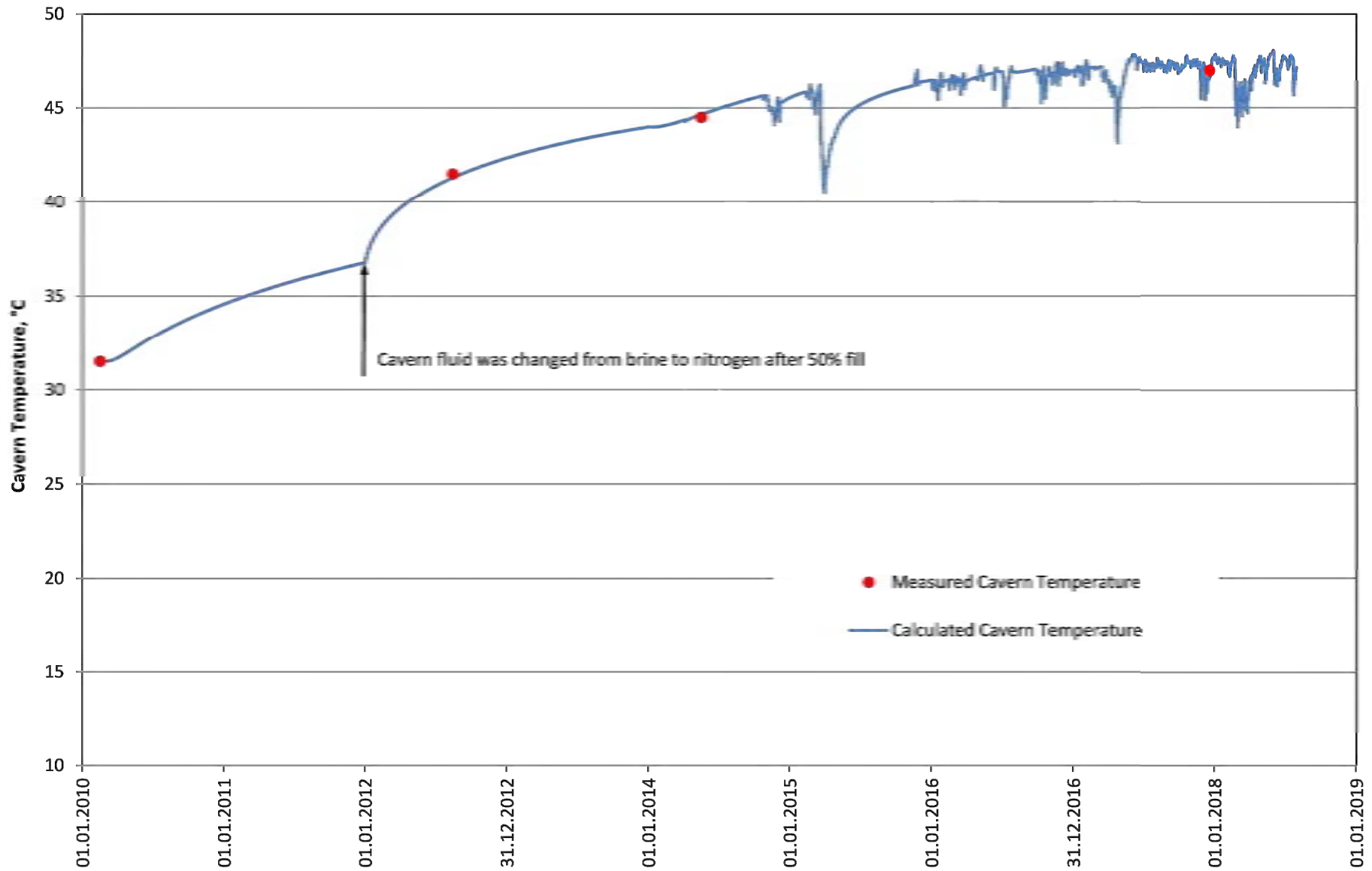
Friction losses along the connecting lines between wellheads and manifold

Wellhead pressure versus time



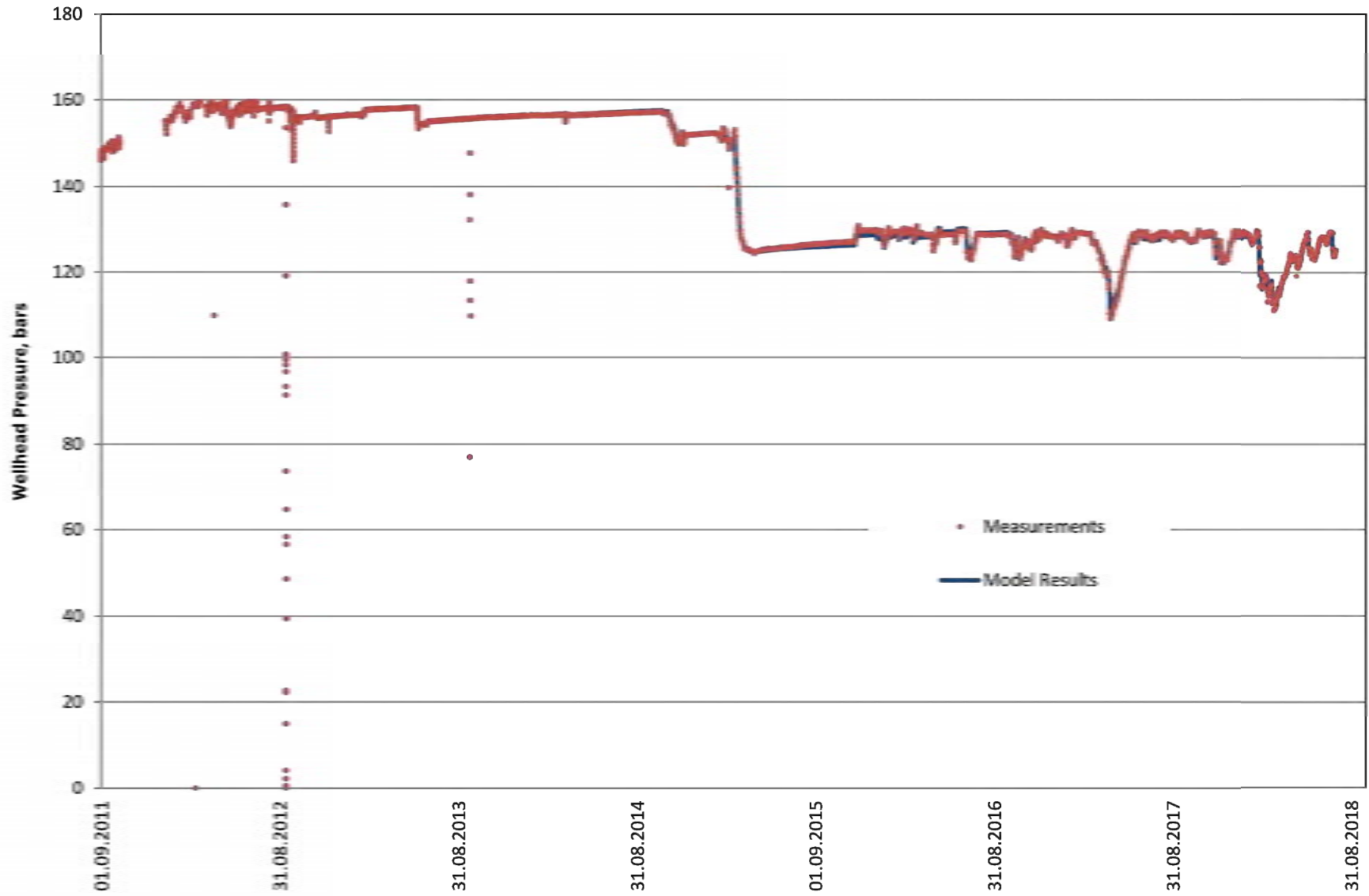
Nitrogen Buffer HL-K
Injection Capacity
Increase

Schematic overview of model set up



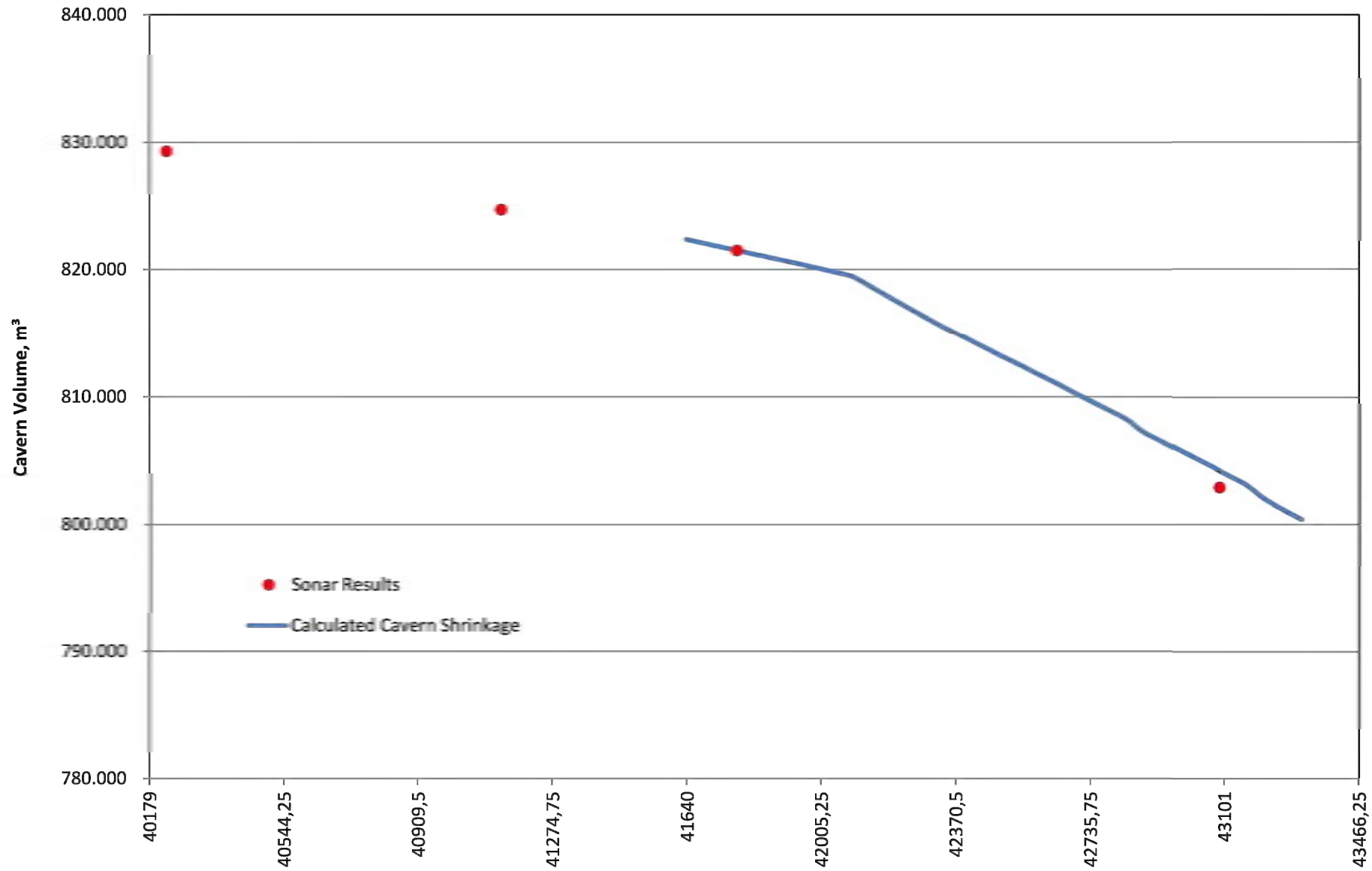
Nitrogen Buffer HL-K
Injection Capacity
Increase

Measured and calculated cavern fluid temperature over time



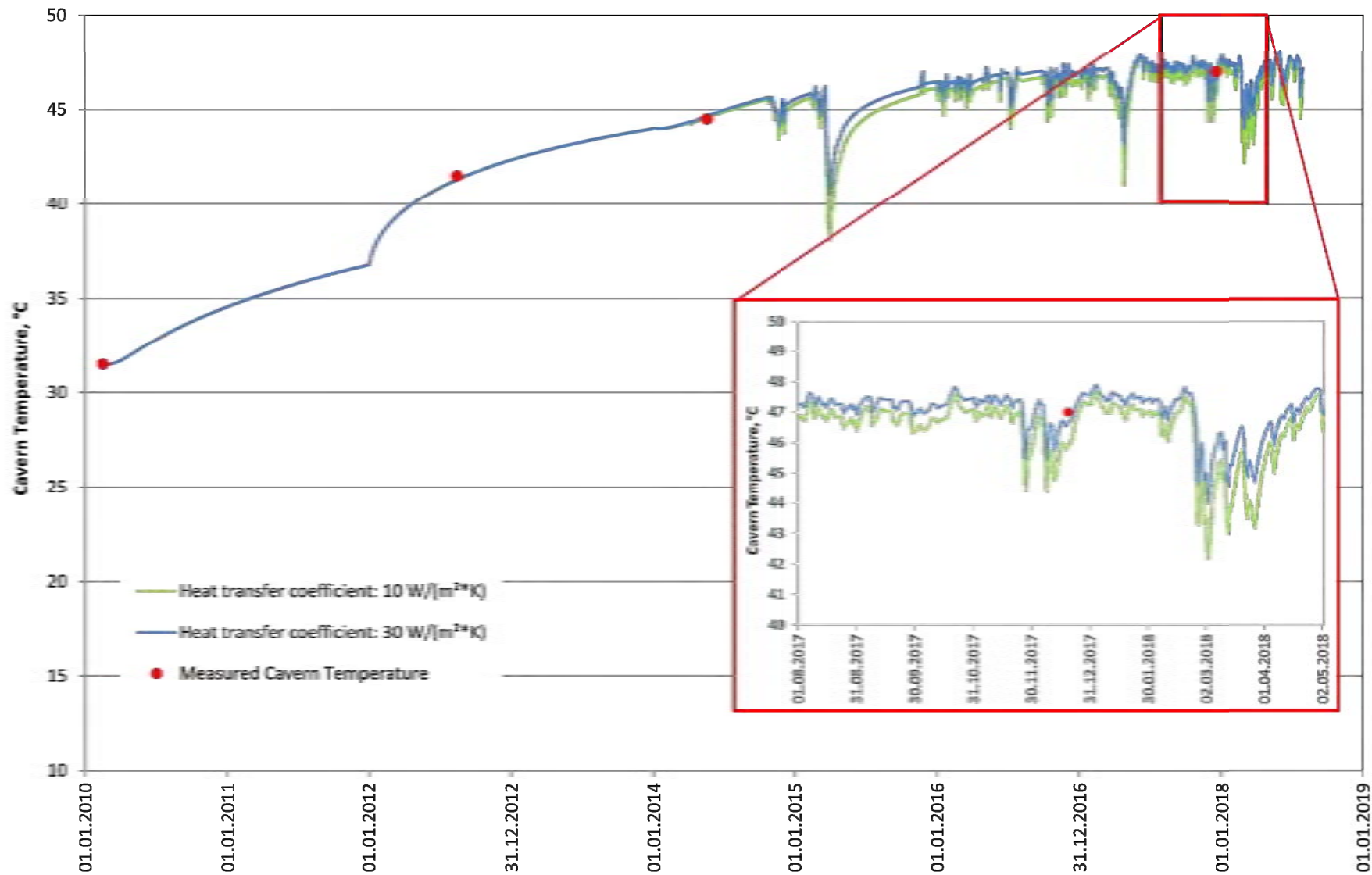
Nitrogen Buffer HL-K
Injection Capacity
Increase

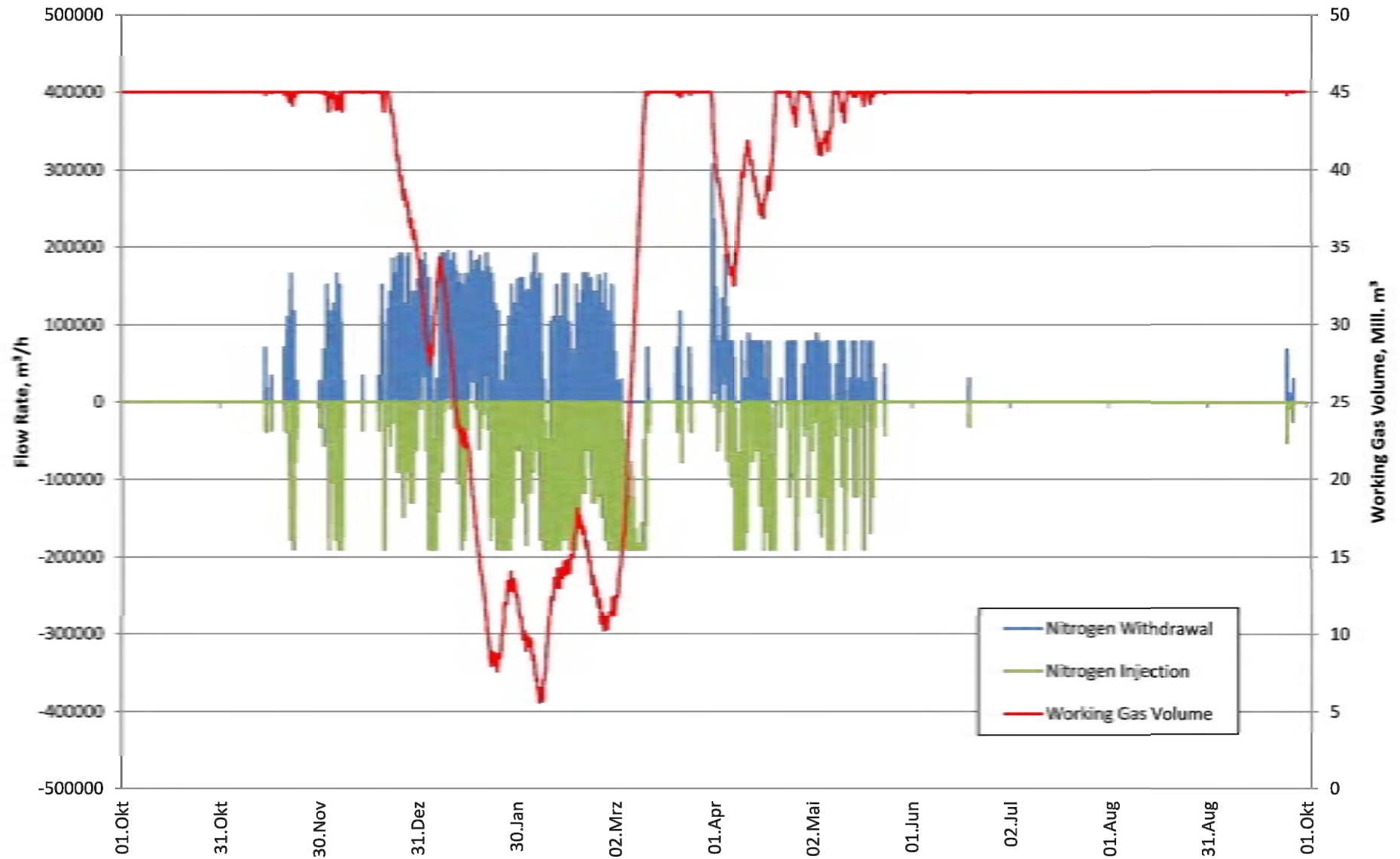
Measured and calculated wellhead pressures over time



Nitrogen Buffer HL-K
Injection Capacity
Increase

Calculated cavern shrinkage during operational period from 2014 to 2018

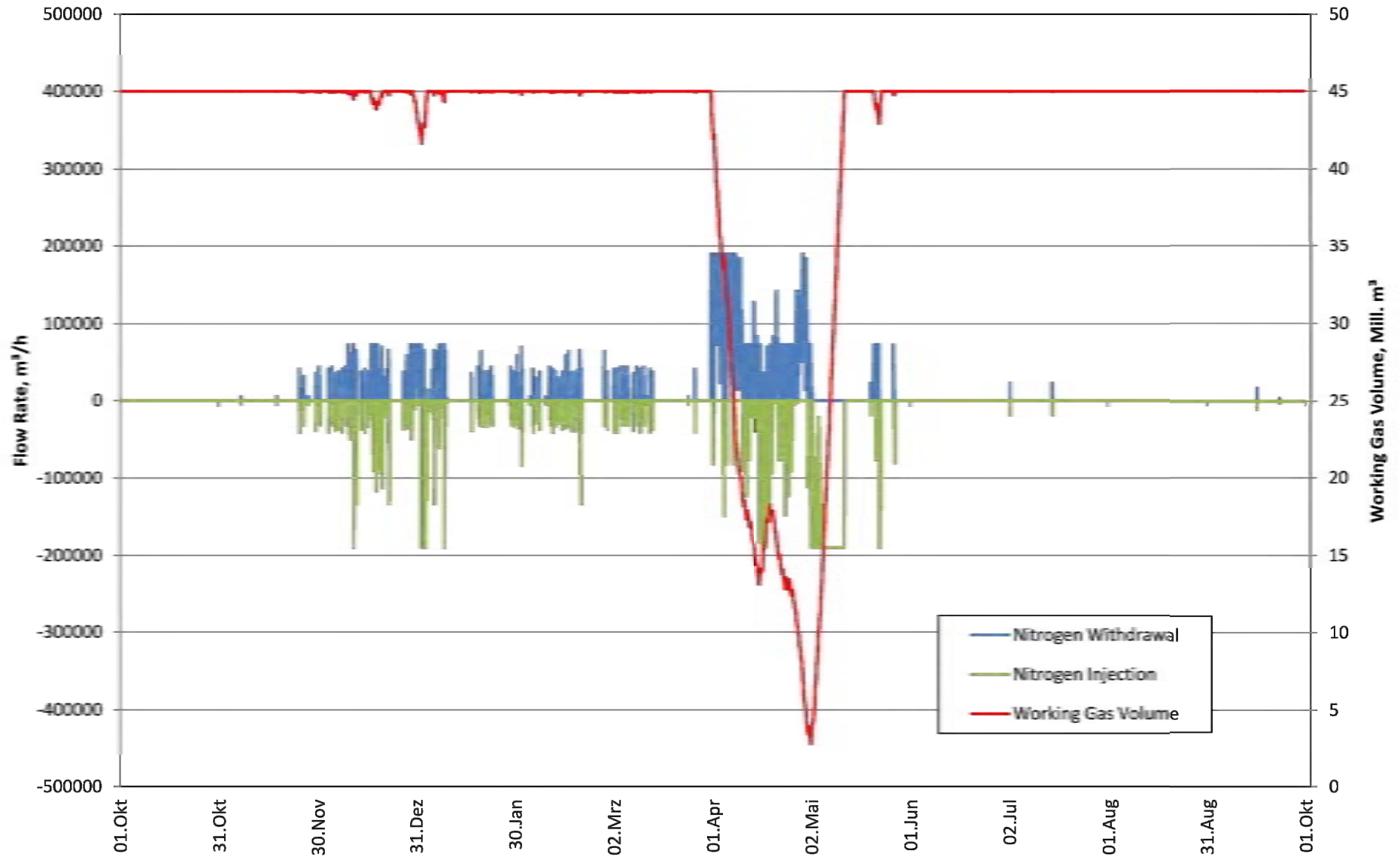




Nitrogen Buffer HL-K
Injection Capacity
Increase

Operational profile A

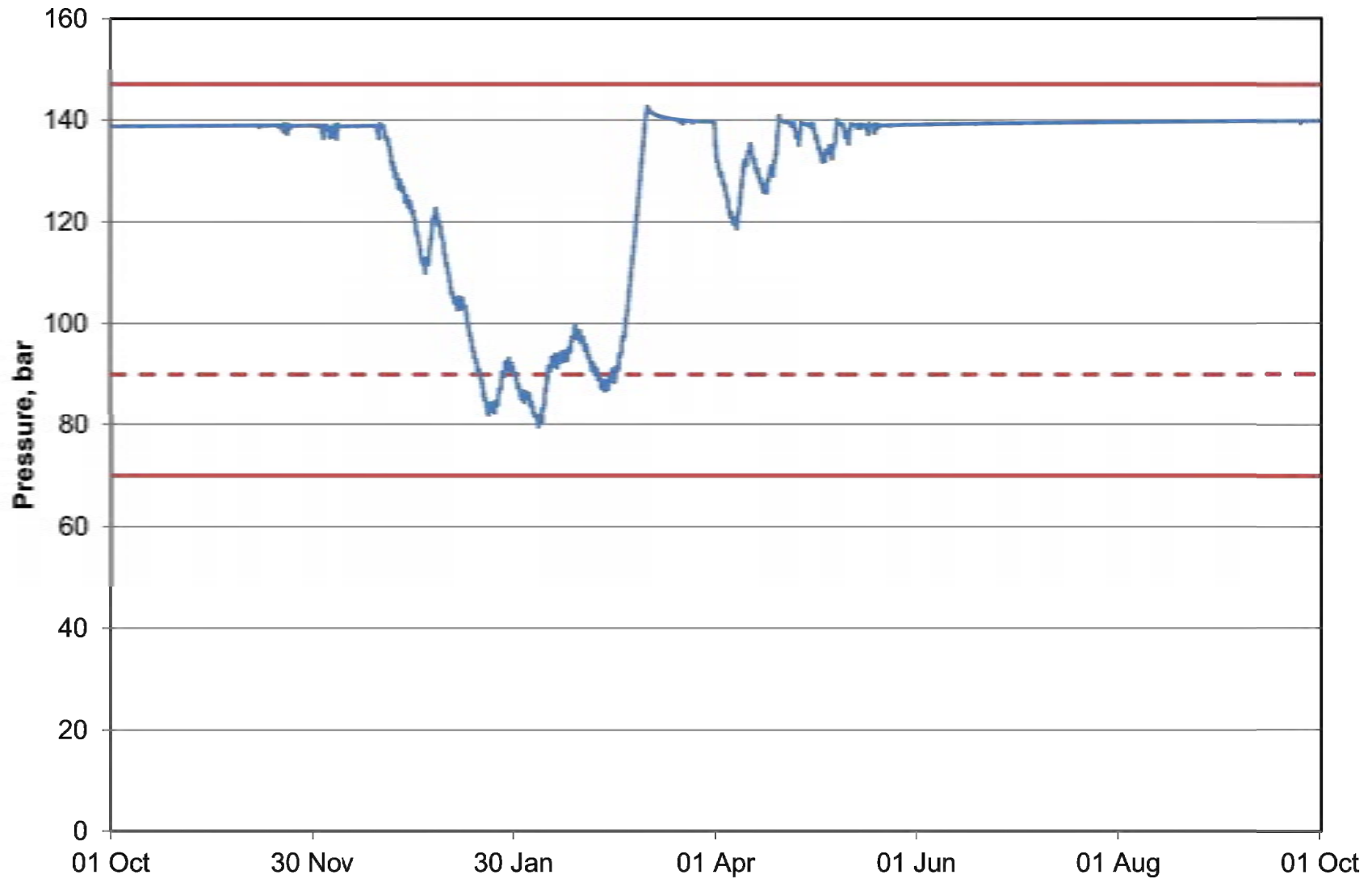




Nitrogen Buffer HL-K
Injection Capacity
Increase

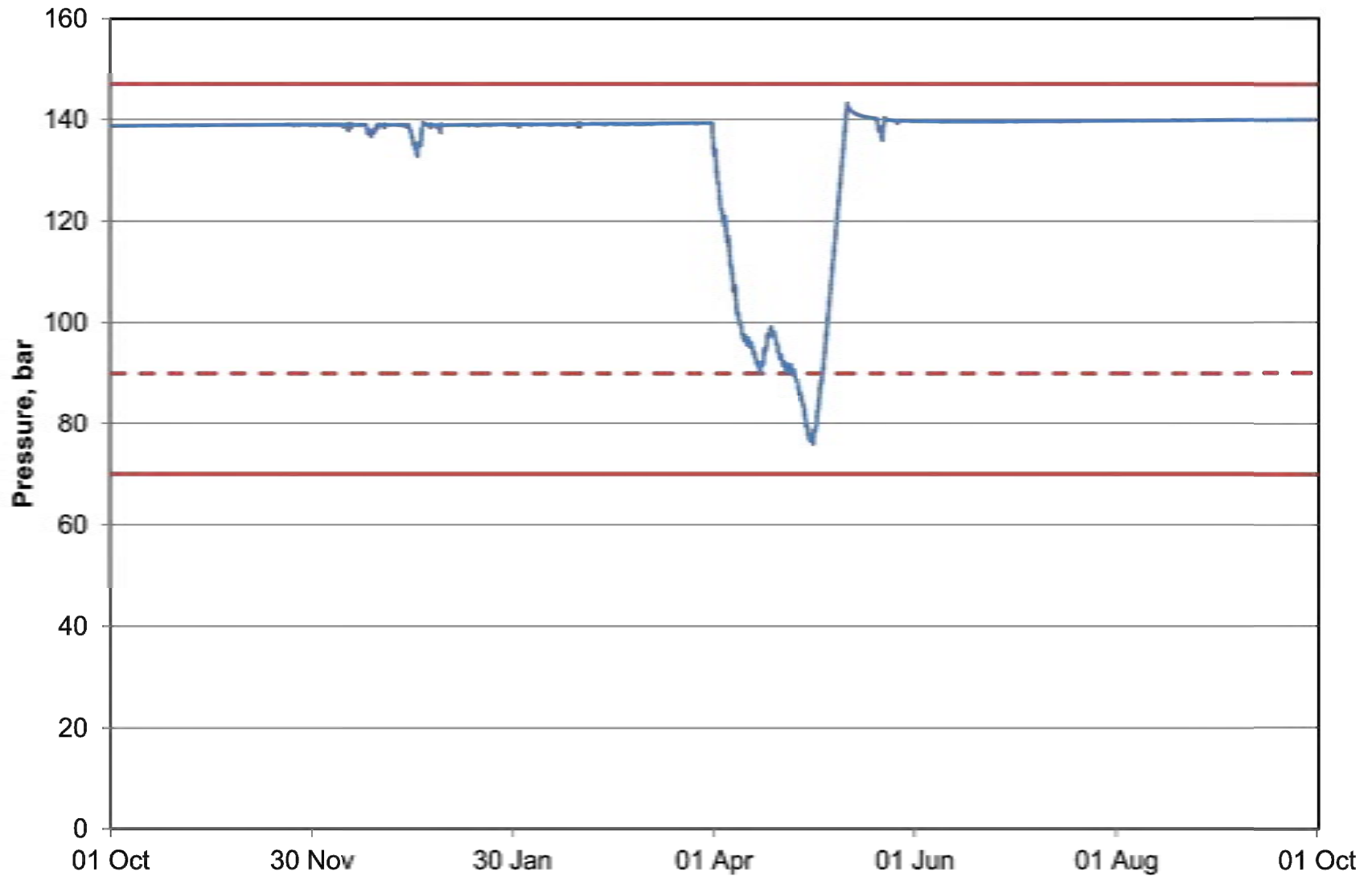
Operational profile B





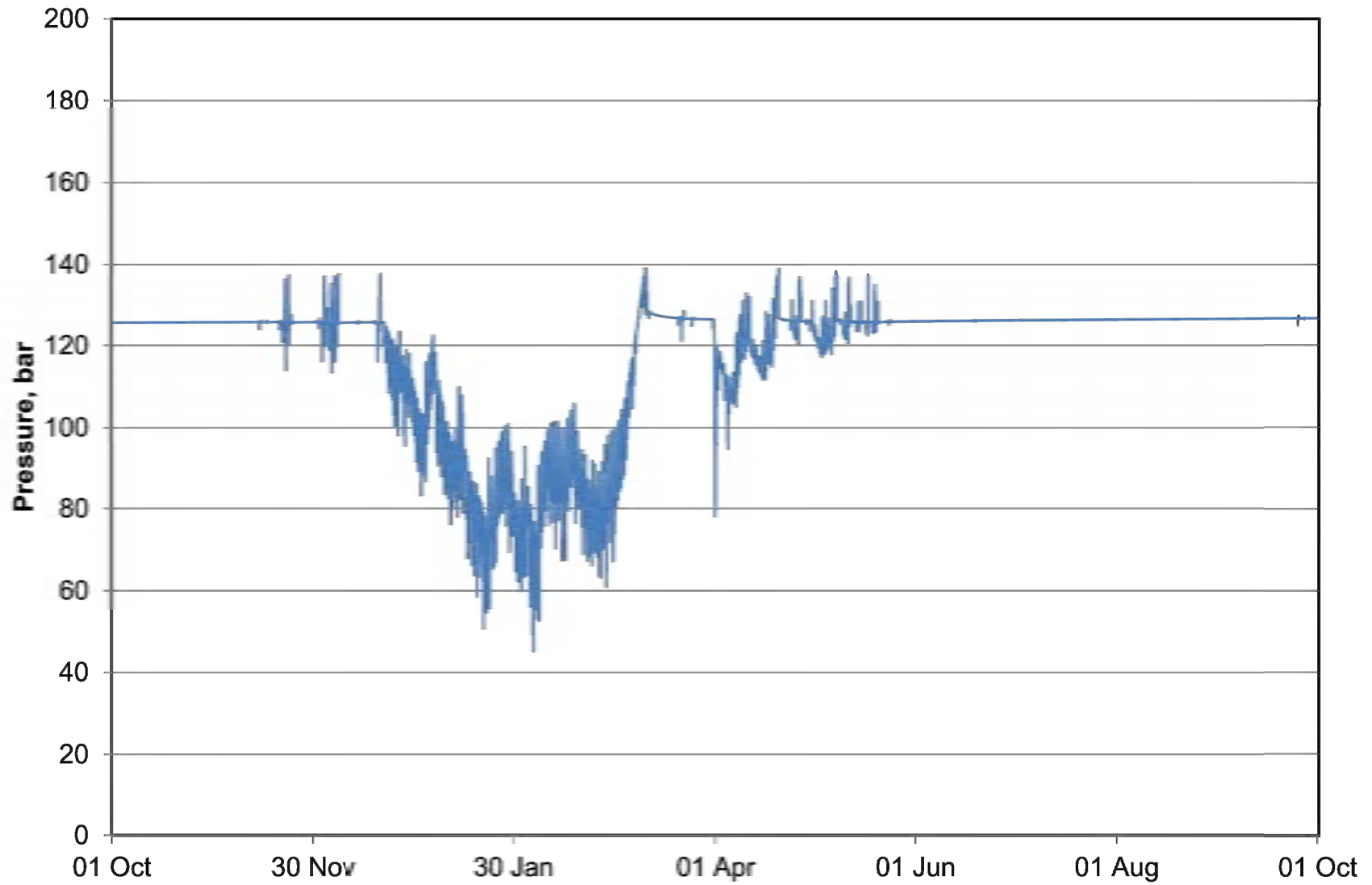
Nitrogen Buffer HL-K
Injection Capacity
Increase

Calculated casing shoe pressures for a yearly cycle according to scenario A



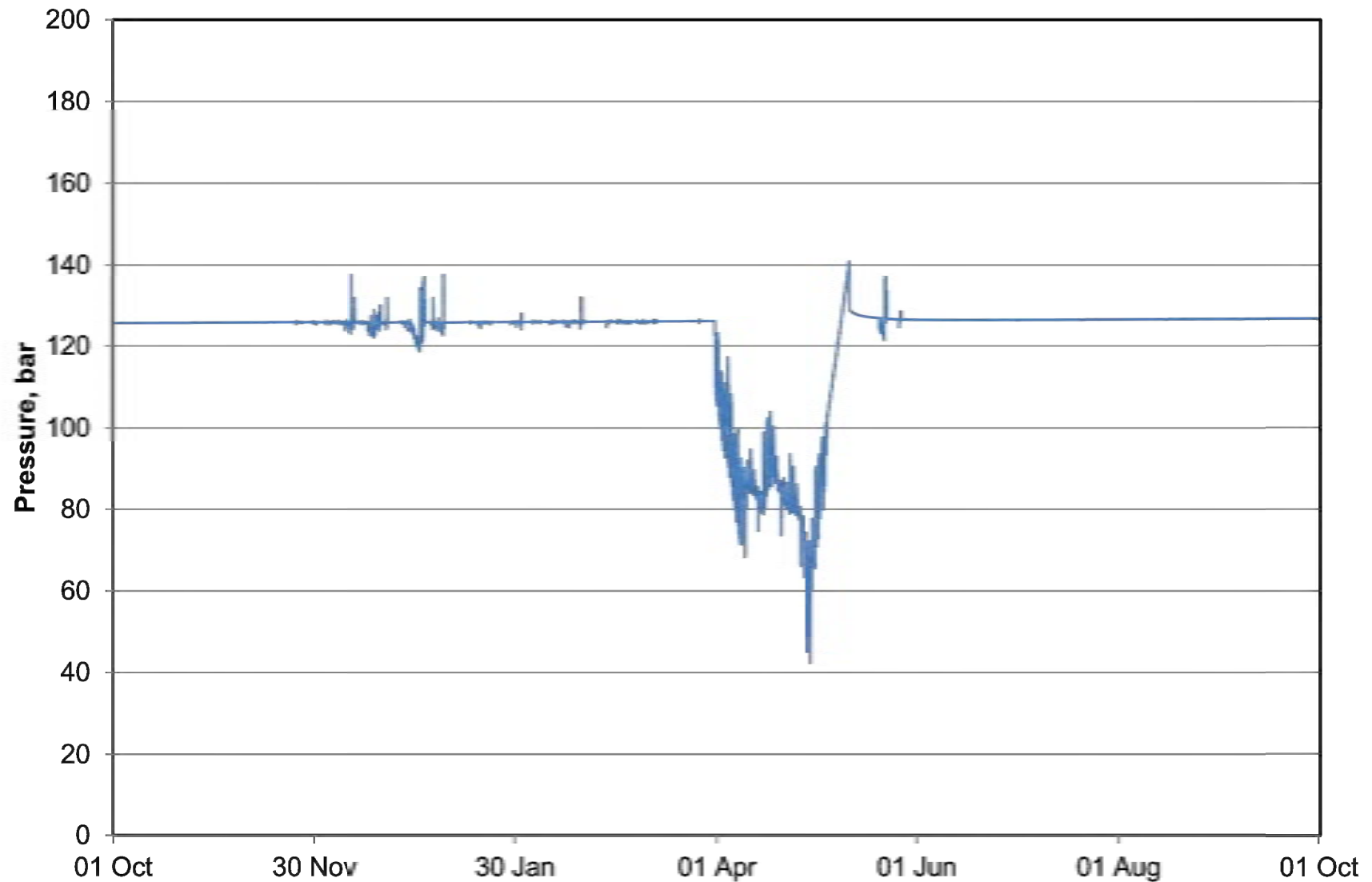
Nitrogen Buffer HL-K
Injection Capacity
Increase

Calculated casing shoe pressures for a yearly cycle according to scenario B



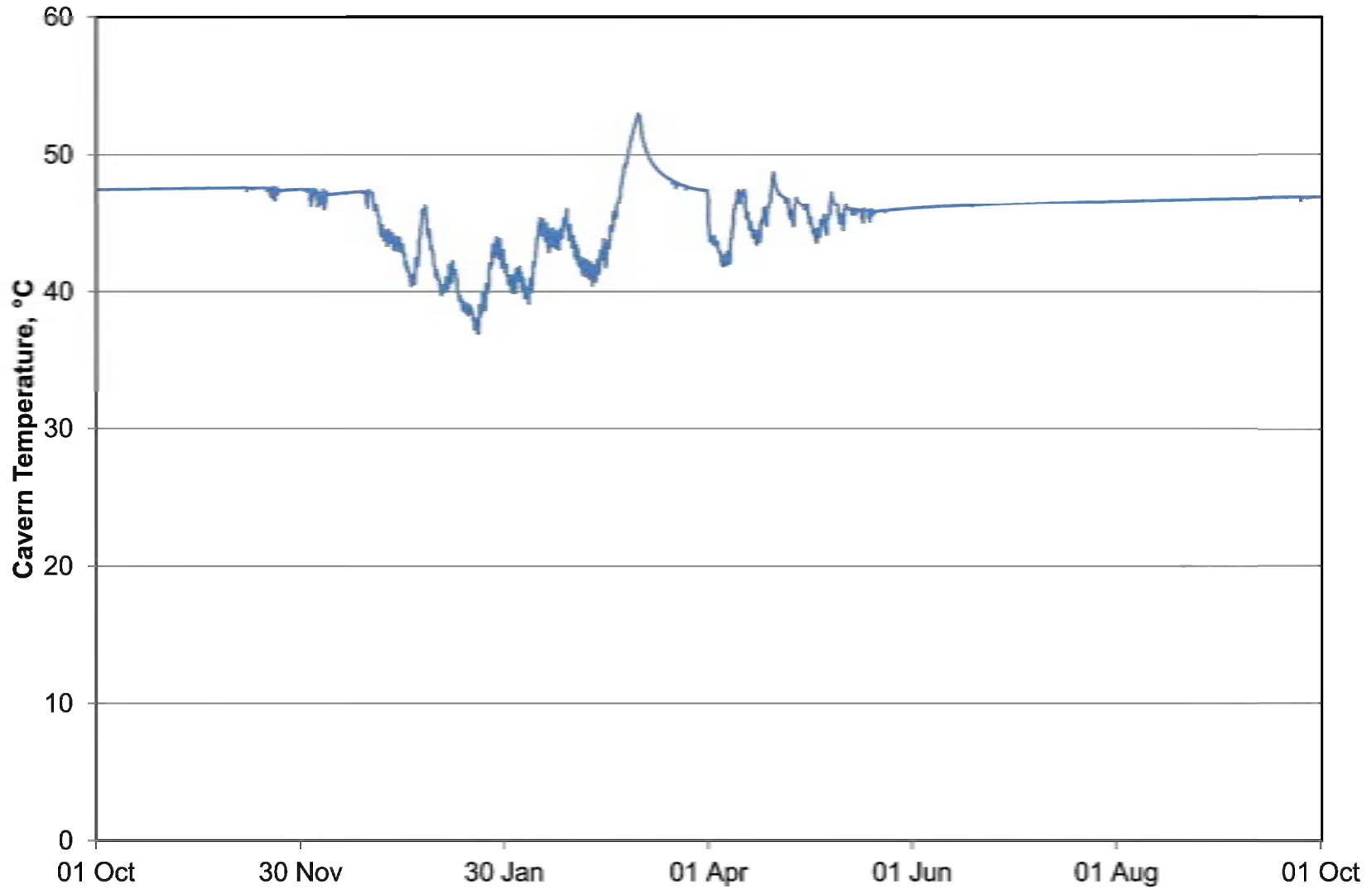
Nitrogen Buffer HL-K
Injection Capacity
Increase

Calculated wellhead pressures for a yearly cycle according to scenario A



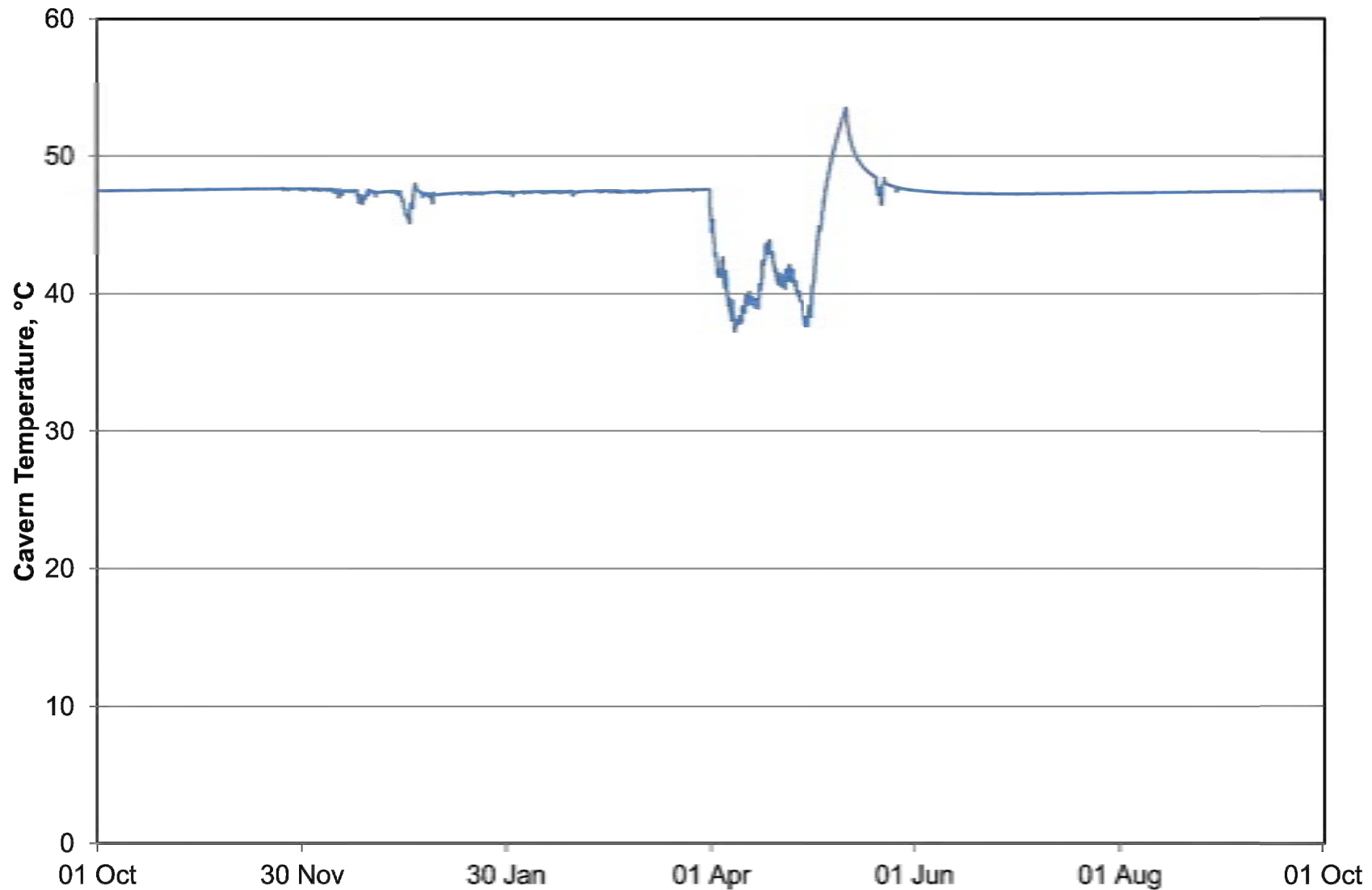
Nitrogen Buffer HL-K
Injection Capacity
Increase

Calculated wellhead pressures for a yearly cycle according to scenario B



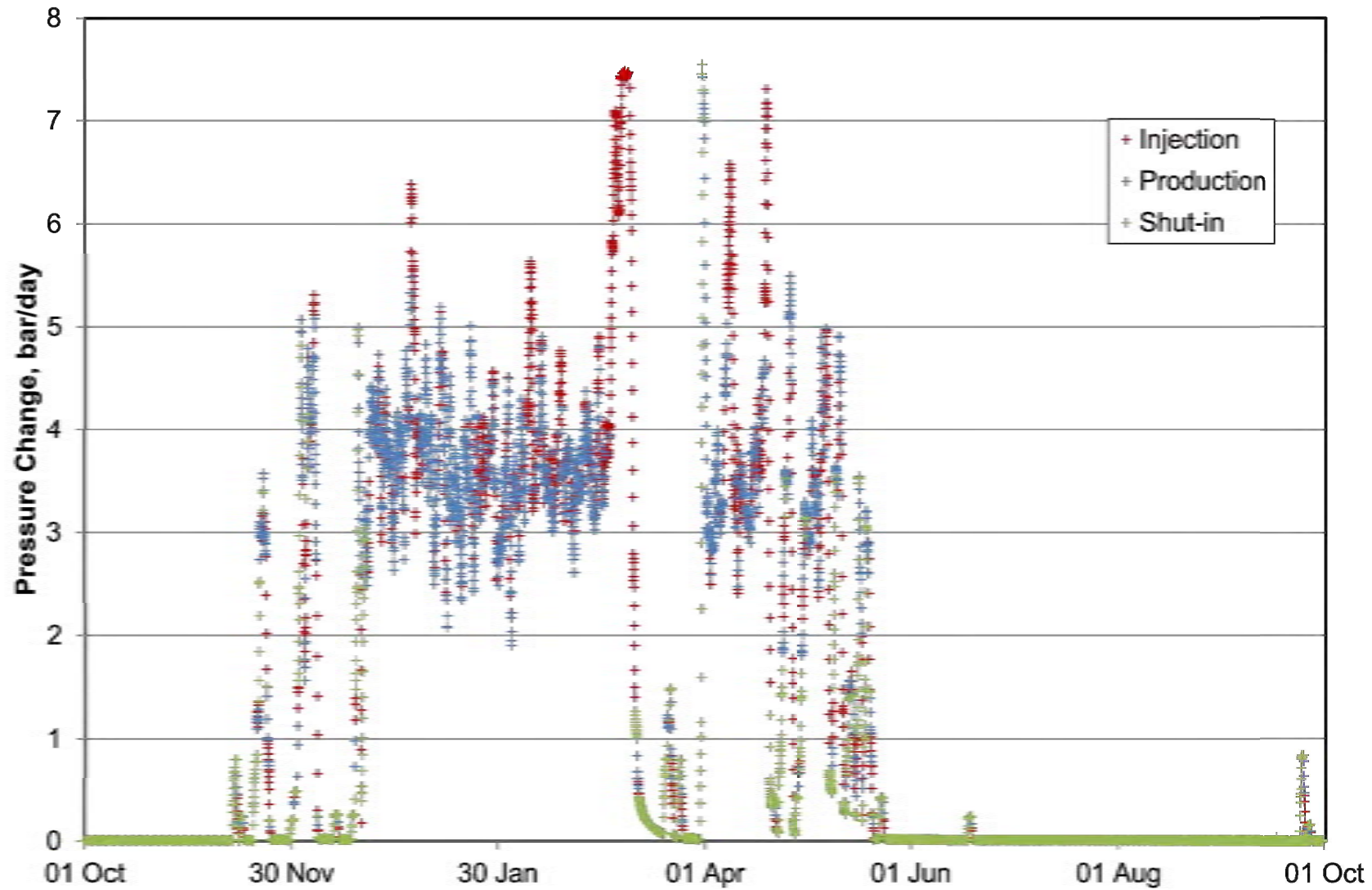
Nitrogen Buffer HL-K
Injection Capacity
Increase

Calculated cavern fluid temperatures for a yearly cycle according to scenario A



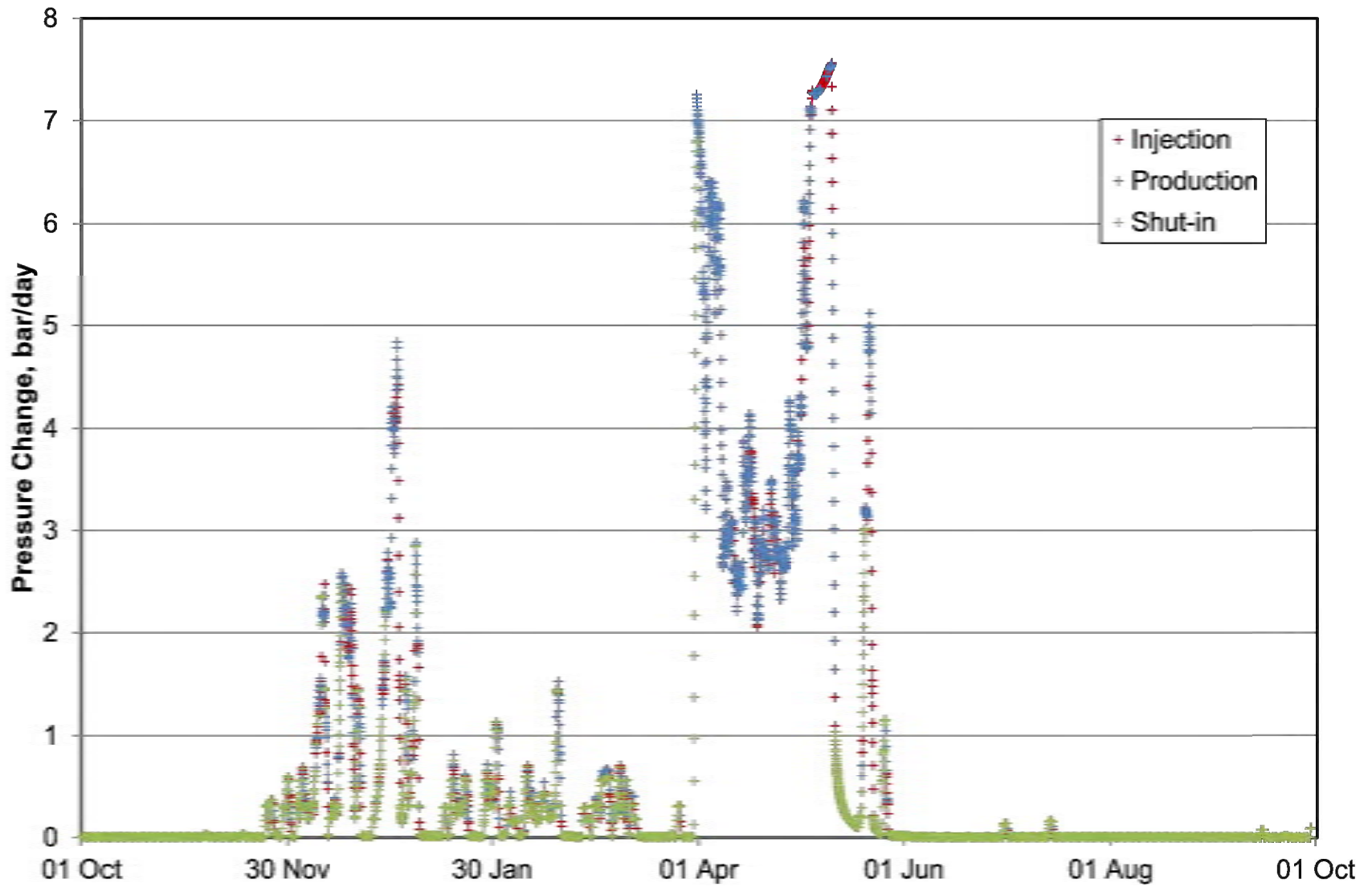
Nitrogen Buffer HL-K
Injection Capacity
Increase

Calculated cavern fluid temperatures for a yearly cycle according to scenario B



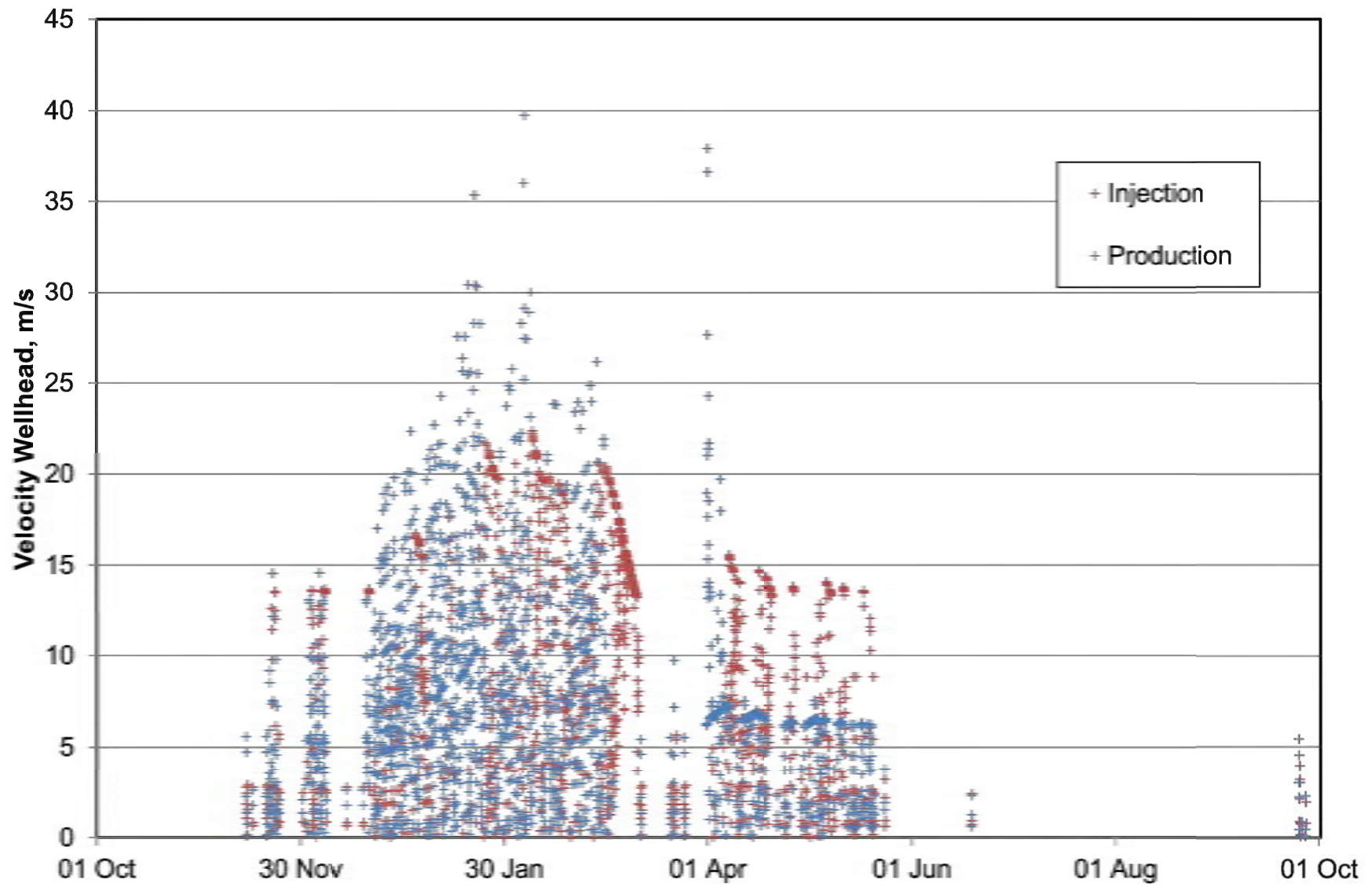
Nitrogen Buffer HL-K
Injection Capacity
Increase

Daily changes of cavern pressure for a yearly cycle according to scenario A



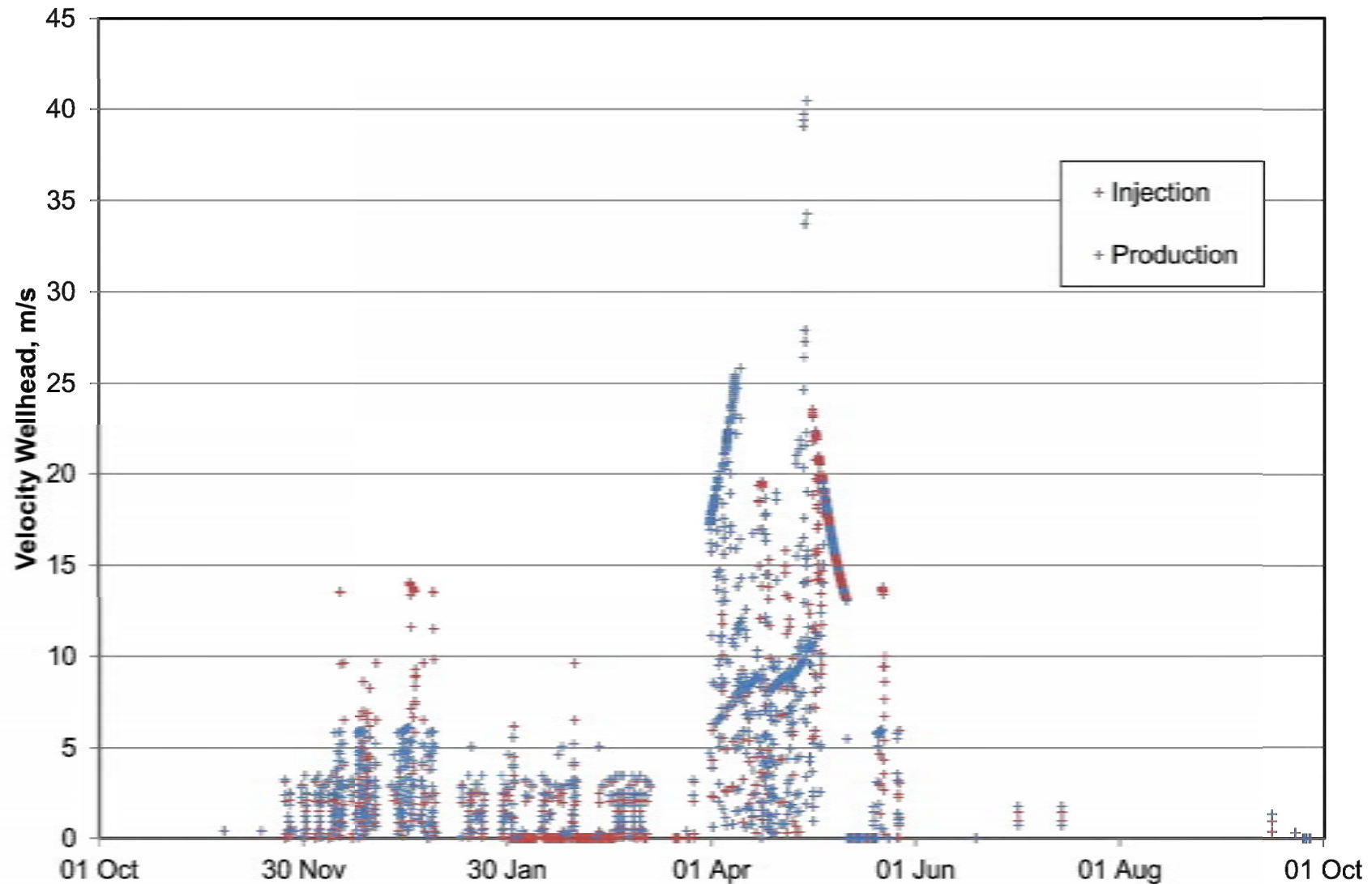
Nitrogen Buffer HL-K
Injection Capacity
Increase

Daily changes of cavern pressure for a yearly cycle according to scenario B



Nitrogen Buffer HL-K
Injection Capacity
Increase

Calculated gas flow velocities for a yearly cycle according to scenario A



Nitrogen Buffer HL-K
Injection Capacity
Increase

Calculated gas flow velocities for a yearly cycle according to scenario B

Tab: Rock mechanical program en enclosures

**Rock Mechanical Modelling Program for the
Nitrogen Storage Cavern Heiligerlee HL-K**

- Flow rate optimization -



Institut für Gebirgsmechanik GmbH
Untersuchung · Prüfung · Beratung · Begutachtung



Institut für Gebirgsmechanik GmbH
Untersuchung · Prüfung · Beratung · Begutachtung

**Rock Mechanical Modelling Program for the
Nitrogen Storage Cavern Heiligerlee HL-K**

- Flow rate optimization -

Customer: N.V. Nederland's Gasunie
Concourslaan 17; 9727 Groningen, The Netherlands

Contractor: Institute für Gebirgsmechanik GmbH
Friederikenstraße 60
04279 Leipzig

Purchase Order No.: 5200106405

IfG-Order No.: B-IfG 47/2018

Authors: Dipl.-Phys. Dieter Brückner
Dipl.-Geol. Tobias Fabig

Date: Leipzig, 08.03.2019

Dr.-Ing. habil. Wolfgang Minkley
— Managing Director —

Dipl.-Phys. Dieter Brückner
— Project Manager —

Table of Content

1	General Remark	6
2	Facts about Cavern HL-K	7
2.1	Characteristics of Cavern HL-K	7
2.2	Operational History	8
2.3	Sonar Survey	9
3	Thermodynamics	11
3.1	Setup of thermodynamic model	13
3.2	Model qualification	14
3.3	Feasibility Proof.....	17
4	Geomechanical modelling of the cavern HL-K	18
4.1	Geomechanical Model.....	19
4.2	Simulation Tool and used material law	21
4.3	Assessment criteria	21
4.4	Evaluation and Assessment	23
4.4.1	Assessment of tightness at maximum cavern pressure	24
4.4.2	Assessment of contour stability and tightness at minimum cavern pressure....	25
4.4.3	Assessment of volume convergence and displacements.....	26
5	Conclusion and Recommendations	27
6	List of Literature	30

Table directory

Table 2-1: Operational constraints for cavern HL-K	8
Table 2-2: Results from Sonar Surveys	10
Table 3-1: Thermodynamic model Properties	13
Table 3-2: Comparison of operational constraints and simulation	17
Table 4-1: Summary of the geomechanical model conditions.	20
Table 4-2: Assessment Criteria for caverns.	23
Table 4-3: List of selected enclosures of the coupled rock mechanical simulations for cavern HL-K representing the nitrogen storage operation.	23
Table 4-4: Overview of rock mechanical recommendations for cavern HL-K.	29

Table of figures

Figure 2-1: Cavern HL-K - operational history	9
Figure 2-2: Cavern HL-K - cavern shrinkage from year 2010 to 2017	10
Figure 2-3: Cavern HL-K - measured cavern fluid temperature over time	11
Figure 3-1: Cavern HL-K - measured cavern fluid temperature over time	12
Figure 3-2: Schematic overview of thermodynamic model setup (after ESK, 2018)	13

Table of Enclosures

Enclosure 1.1	Measured and calculated cavern fluid temperature over time
Enclosure 1.2	Measured and calculated wellhead pressure over time
Enclosure 1.3	Calculated cavern shrinkage during operational period from 2014 to 2018
Enclosure 1.4	Calculated cavern fluid temperature for different heat transfer coefficients
Enclosure 1.5	Operational profile A
Enclosure 1.6	Operational profile B
Enclosure 1.7	Calculated casing shoe pressure for a yearly cycle according to scenario A
Enclosure 1.8	Calculated casing shoe pressure for a yearly cycle according to scenario B
Enclosure 1.9	Calculated wellhead pressure for a yearly cycle according to scenario A
Enclosure 1.10	Calculated wellhead pressure for a yearly cycle according to scenario B
Enclosure 1.11	Calculated cavern fluid temperature for a yearly cycle according to scenario A
Enclosure 1.12	Calculated cavern fluid temperature for a yearly cycle according to scenario B
Enclosure 1.13	Daily changes of cavern pressure for a yearly cycle according to scenario A
Enclosure 1.14	Daily changes of cavern pressure for a yearly cycle according to scenario B
Enclosure 1.15	Calculated gas flow velocities for a yearly cycle according to scenario A
Enclosure 1.16	Calculated gas flow velocities for a yearly cycle according to scenario A
Enclosure 2.1	Generation of the model from SOCON US-measurements
Enclosure 2.2	Primary stress state and leaching phases of the model
Enclosure 2.3	Simulation Case A - Temperature Calculation performed by ESK
Enclosure 2.4	Simulation Case B - Temperature Calculation performed by ESK
Enclosure 2.5	Simulation Case C - Temperature Calculation performed by IfG
Enclosure 2.6	Assessment of p_{MAX} after immediately reaching the pressure after the first year – Case A
Enclosure 2.7	Assessment of p_{MAX} after immediately reaching the pressure after the 5 th year – Case A

-
- Enclosure 2.8 Assessment of p_{MAX} after immediately reaching the pressure after the first year – Case B
 - Enclosure 2.9 Assessment of p_{MAX} after immediately reaching the pressure after the 5th year – Case B
 - Enclosure 2.10 Assessment of p_{MAX} after immediately reaching the pressure after the first year – Case C
 - Enclosure 2.11 Assessment of p_{MAX} after immediately reaching the pressure after the 5th year – Case C
 - Enclosure 2.12 Development of stress at Casing shoe of HL-K after 5 years storage operation – Case A
 - Enclosure 2.13 Development of stress at Casing shoe of HL-K after 5 years storage operation – Case B
 - Enclosure 2.14 Development of stress at Casing shoe of HL-K after 5 years storage operation – Case C
 - Enclosure 2.15 Confining pressure (technical tightness) at maximum storage pressure
 - Enclosure 2.16 Vertical displacement and compression/extension in a profile above the cavern HL-K
 - Enclosure 2.17 Stress situation at minimum stress – Case A (84 bar)
 - Enclosure 2.18 Stress situation at minimum stress – Case B (81 bar)
 - Enclosure 2.19 Stress situation at minimum stress – Case C (70 bar)
 - Enclosure 2.20 Utilization of dilatancy boundary at p_{MIN}
 - Enclosure 2.21 Development of stresses at cavern contour and assessment of p_{MIN} regarding stability – Case A
 - Enclosure 2.22 Development of stresses at cavern contour and assessment of p_{MIN} regarding stability – Case A
 - Enclosure 2.23 Development of stresses at cavern contour and assessment of p_{MIN} regarding stability – Case A
 - Enclosure 2.24 Volume convergence

1 General Remark

The Dutch gas supply company GASUNIE operates the former AKZO NOBEL NaCl-brine production cavern, Heiligerlee HL-K, as a nitrogen storage cavern since 2012. The reason for a high-pressure storage of nitrogen is to mix large amounts of nitrogen with H-gas (e.g. North Sea gas) into L-gas-quality (Groningen gas) supporting the L-gas distribution system in the Netherlands. According to corresponding demand situations main withdrawal cycles are in Spring and Autumn.

The argumentation for the selection of this cavern and for its special suitability is explained from a geomechanical point of view in the IfG-report “Rock mechanical assessment of the repurpose of the cavern Heiligerlee HL-K into a nitrogen gas storage cavern” (IfG, 2008) in detail.

The rock mechanical effects resulting from the repurposing of cavern HL-K into a storage cavern and the associated injection and withdrawal cycles are analyzed and verified in the report “Numerical stability verification concerning the repurpose of the cavern Heiligerlee HL-K into a nitrogen buffer” (IfG, 2010) on the results of a state-of-the-art computational modeling.

In the authorized pressure range the cavern HL-K was operated with flow rates of more or less than 16.000 m³(n)/hour (pressure change is about 0.5 bar/day). Temperature influence on the cavern surrounding stress state is of minor importance. Nevertheless, in this case temperature change in a slow process, and former numerical modelling took into account the temperature as boundary condition, i.e. the cooling process from the brine production phase and the re-warming when cavern HL-K was converted to a gas storage cavern

In 2018 the conditions changed, and the question arise if higher send in and send out capacity will be possible. In the specific case IfG was asked to assess a maximum production and injection rate of 190.000 m³(n)/hour operate in a range between p_{MAX} (147 bar) and p_{MIN} (70 bar) within a special operation plan and under maximum cyclic conditions. In this context, thermodynamic aspects of cavern operation became more important.

So far, case studies suggested by ESK, Freiberg have been investigated which includes the proposed withdrawal and injection rate in a special operation plan.

2 Facts about Cavern HL-K

In the following chapters the cavern HL-K will be described regarding her characteristics, US-measurements and her operation history.

2.1 Characteristics of Cavern HL-K

Cavern HL-K is part of a set of brine production caverns located at the Heiligerlee salt dome. The cavern has been selected to be converted into a nitrogen buffer to fulfill the increased demand of nitrogen in the Dutch gas grid. In year 2010 the cavern was equipped with an appropriate gas completion consisting of the following components:

- 9 5/8" x 8 5/8" production string
- 10 3/4" permanent packer
- 8 1/4" x 7 3/4" tailpipe with landing nipples and flow couplings
- Wireline retrievable surface controlled subsurface safety valve

The installed wellhead equipment includes:

- 13 5/8" API 3000 tubing hanger spool
- 11" API 3000 pack off adapter flange
- 11" API 3000 master valve, hydraulically (fail safe) operated
- 11" API 3000 production tee
- 11" API 3000 top valve, hand operated
- 9" API 3000 wing valves, hand operated
- 9" API 3000 wing valves, hydraulically (fail safe) operated

The cavern has been echometrically surveyed providing the following characteristic data:

- Depth of last cemented casing shoe: 981 m
- Depth of cavern roof: 1,013 m
- Depth of cavern sump: 1,502 m
- Free cavern volume: 824,651 m³
- Max cavern diameter (average): 60 m @ 1,450 m

The overall cavern shape is quite regular. The cavern HL-K was subject of an intensive rock mechanic assessment. Based on a realistic conservative rock mechanical model nitrogen stor-

age cycles have been simulated. As a result from this modeling work a set of operational constraints were defined for flow rates, cavern pressures as well as for particular cycle instructions. The set of operational constraints are listed in Table 2-1.

Table 2-1: Operational constraints for cavern HL-K

Operational Parameter Constraint	
Max. Injection Rate	16,000 m ³ (n)/h → 190,000 m ³ (n)/h
Max. Production Rate	190,000 m ³ (n)/h
Max. Pressure	147 bar @ Casing Shoe
Min. Pressure	70/90 bar @ Casing Shoe
Max. Pressure Change	10 bar/day
Cycle Instructions:	Max. 90 days/year below 90 bars
	Max. 30 days/year @ 70 bars

As the air separation plant was originally designed for a maximum capacity of 16,000 m³(n)/h, the maximum nitrogen injection rate considered in former assessment studies was of this magnitude. As it is planned to increase the capacity of the plant in order to reach equal injection and withdrawal capacities a maximum injection rate of 190,000 m³(n)/h is now considered.

2.2 Operational History

Nitrogen storage operation started in summer 2012. The operational history in terms of operated flow rates, measured wellhead pressures and temperatures is shown in appendix 4.1. According to this picture it is obvious that operational activities were rather poor in the period from 2011 to 2015. From December 2015 a bit more frequent storage operation started with some considerable pressure reductions down to approximately 110 bar (wellhead pressure) in spring 2017 and spring 2018. The operated flow rates reached up to 100,000 m³/h during nitrogen withdrawal out of the cavern and nearly the plant capacity of 16,000 m³/h while injecting nitrogen into the cavern.

Overall, it can be noted that the nitrogen buffer at Heiligerlee has not experienced an extensive storage operation so far. Nevertheless, the available operational data can be used to conclude on the thermodynamic behavior of the subsurface system (cavern & well) applying a thermodynamic modeling approach.



Figure 2-1: Cavern HL-K - operational history

Overall, it can be noted that the nitrogen buffer at Heiligerlee has not experienced an extensive storage operation so far. Nevertheless, the available operational data can be used to conclude on the thermodynamic behavior of the subsurface system (cavern & well) applying a thermodynamic modeling approach.

2.3 Sonar Survey

For the time period from 2010 to 2018 in total 4 sonar surveys have been run at HL-K. Table 2-2 shows the measured free cavern volume and the measured average cavern fluid temperature

From a thermodynamic analysis perspective, the free cavern volume and the measured fluid temperature in the cavern are the most important results from a sonar survey. The measured free cavern volume at different points of time allows the cavern shrinkage to evaluate over time. As the free cavern volume is part of the applied thermodynamic equation of state, its variation over time might become essential in the course of thermodynamic analyses.

Table 2-2: Results from Sonar Surveys

Last sonar in brine:	16/02/2010	829,292 m ³	31.5 °C
First sonar in gas:	15/08/2012	824,651 m ³	41.5 °C
1. Repeat sonar in gas:	19/05/2014	821,479 m ³	44.5 °C
2. Repeat sonar in gas:	20/12/2017	802,854 m ³	47.0 °C

Figure 2-2 illustrates the cavern shrinkage over a period of time from 2010 to 2017. It is obvious from this illustration that cavern convergence was very limited during the first five years of the observation period. Due to the intensified storage operation from year 2015 onwards the induced cavern shrinkage is increased but is still limited to cavern convergence rates of clearly less than 1% per year. In total the measured cavern shrinkage is merely 3% over a period of 8 years and will therefore have very limited impact on the thermodynamic analysis.

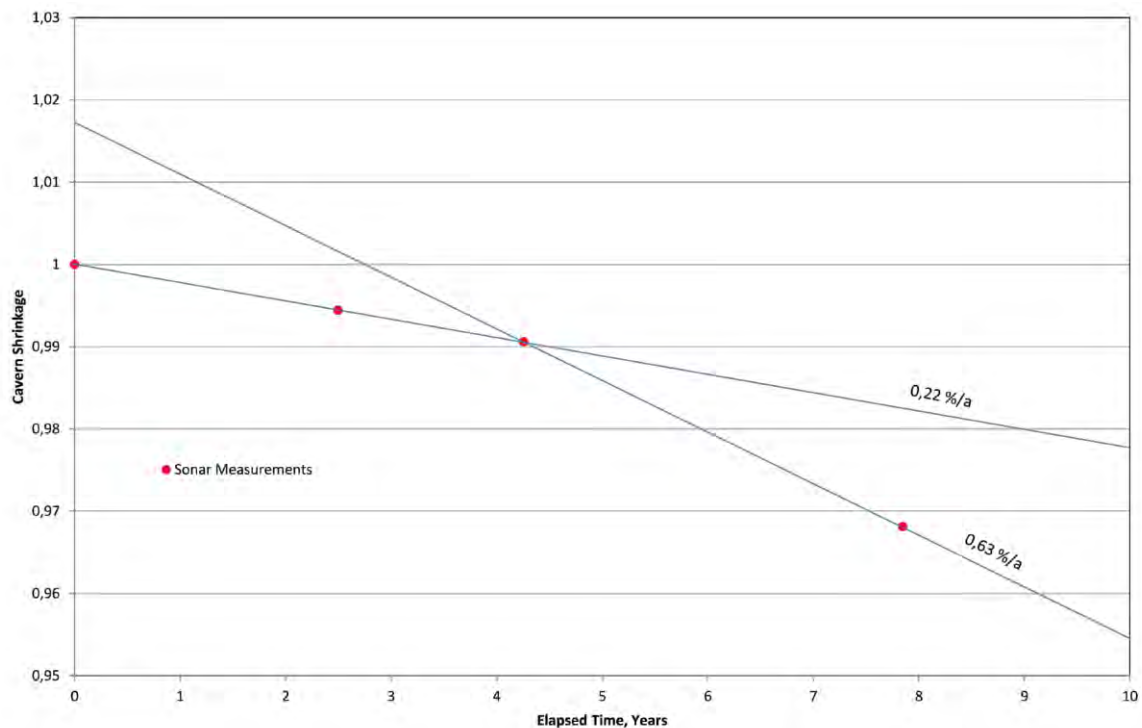


Figure 2-2: Cavern HL-K - cavern shrinkage from year 2010 to 2017

Measurements of the cavern fluid temperature are of high importance in association with thermodynamic analysis of gas storage operations in solution mined salt caverns. While measured wellhead pressures can be reliably used to conclude on the pressure inside of the cavern, measured wellhead temperatures are not even comparatively suitable to state on the actual fluid temperature inside the cavern. On one hand this is due to the already mentioned impact

of the ambient air temperature when the cavern is shut off. On the other hand the heat exchange processes along the cavern well are much more complex compared to those with the cavern surroundings. This is mainly attributed to the complex well configuration – casing, cement, annular fluids – as well as to the usually wide range of different geological sequences encountered by the cavern well for which there are no reliable thermal properties available.

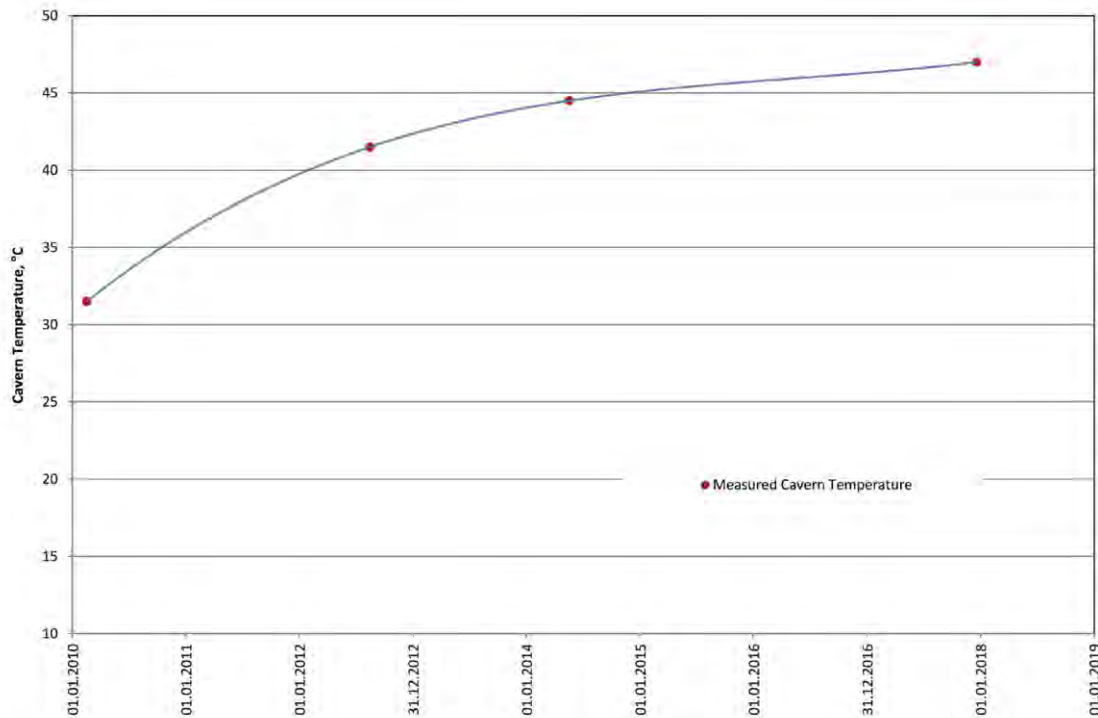


Figure 2-3: Cavern HL-K - measured cavern fluid temperature over time

For cavern HL-K there are in total 4 measurements providing direct information about the temperature of the fluid inside of the cavern within the observation period. The first measurement (16/02/2010) represents the temperature of the brine at the end of the leaching process. For all other measurements the cavern was filled up with nitrogen. Figure 2-3 shows measured cavern fluid temperature over time. The measurements show a regular increase of the fluid temperature with elapsed time which is commonly the case for solution mined salt caverns after conversion from brine production to gas storage caverns.

3 Thermodynamics

For thermodynamic modeling the gas cavern simulator KAVPOOL is applied. KAVPOOL is a software tool developed in-house by ESK to support gas cavern storage operators in their day-to-day business and assist subsurface engineers in planning and designing storage facilities.

The model incorporates all thermodynamic processes associated with gas storage operations in salt caverns. This includes:

- Pressure-volume-temperature relationship of the gas in flow zones
- Heat transfer between storage medium and surrounding rock
- Friction losses due to fluid flows along production tubing and connection pipelines

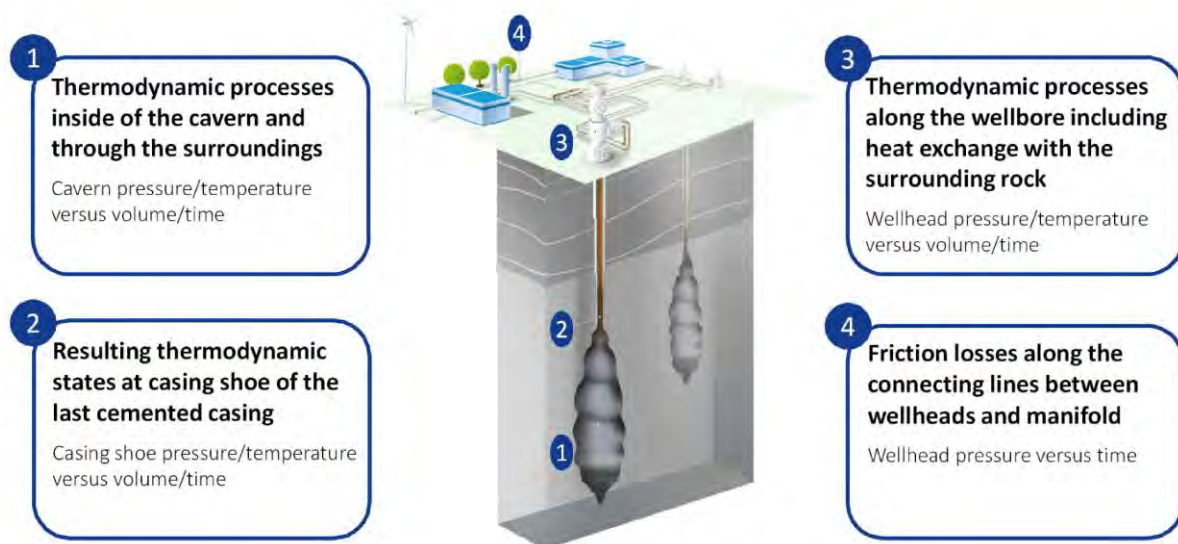


Figure 3-1: Cavern HL-K - measured cavern fluid temperature over time

Figure 3-1 illustrates the modeling principle of the KAVPOOL software. Parallel to thermodynamic calculations, the rock mechanics option that was implemented provides information about the operationally induced shrinkage of each individual cavern at storage facilities. The model can be run as a forecasting tool or can be used for back analyses for purposes of investigating actual cavern behavior by applying common history match procedures. The history match procedure allows initially selected parameters to be adjusted to real storage conditions and the model to be subsequently used to predict specific operational conditions. KAVPOOL takes a wide range of pure gaseous components into account, meaning it can not only be used for natural gas storage but also in compressed air energy storage (CAES) and hydrogen storage in solution-mined salt caverns. KAVPOOL is in use for more than two decades. Since then, numerous applications for different gas cavern storage facilities across Europe have been performed.

The thermodynamic simulations and the following results which are written in chapter 3.1 to 3.3 and describe Case A and B were done and provided by ESK.

3.1 Setup of thermodynamic model

The thermodynamic model includes all relevant components of the subsurface system which can be mainly subdivided into the cavern section and the well section. As the cavern is in direct contact with the salt rock no other components need to be considered in this model region. For the well section a series of casing strings are implemented in the model as well as the respective cement and annular fluid intervals.

As the heat conductivity of rock salt is certainly different to those of other rock materials (e.g. sands, clays, marls, etc.) the top of salt is additionally considered in the model.

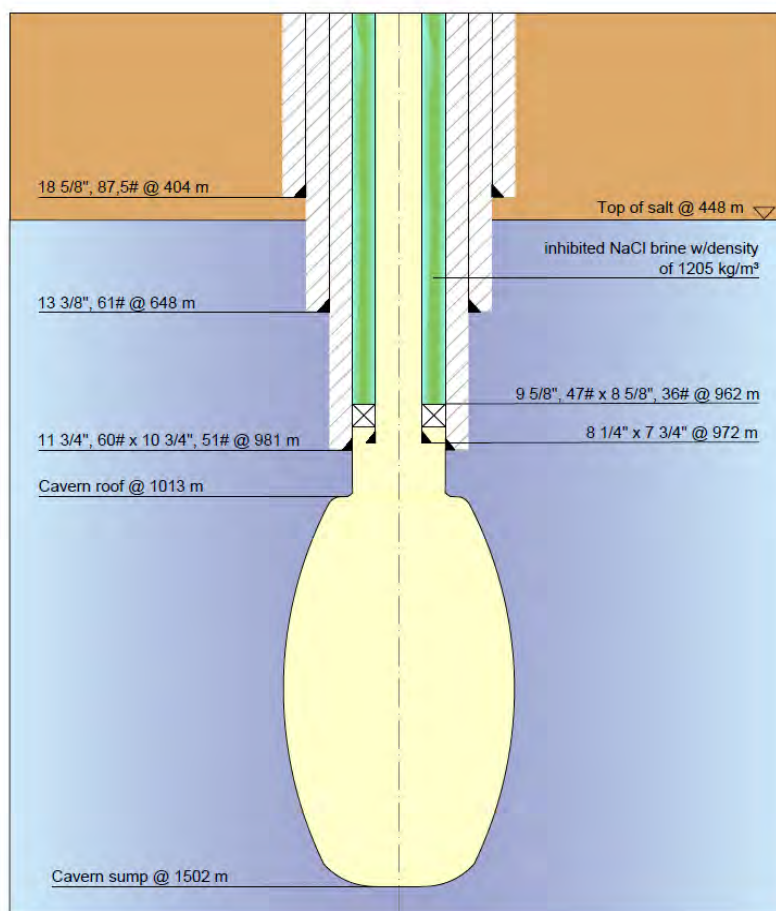


Figure 3-2: Schematic overview of thermodynamic model setup (after ESK, 2018)

A schematic overview of the model set up is given in Figure 3-2 while Table 3-1 sets out a list of relevant properties for each material component incorporated in the model.

Table 3-1: Thermodynamic model Properties

Material component	Heat conductivity	Heat capacity	Density
--------------------	-------------------	---------------	---------

	W/(m*K)	kJ/(kg*K)	kg/m ³
Rock salt	5.0	0.9	2,200
Overburden rock	2.0	0.9	2,000
Casing (carbon steel)	44.0	0.46	7,850
Cementation	0.8	0.8	2,000
Annular fluid	0.6	4.8	1,200

3.2 Model qualification

Prior to using thermodynamic models for the prediction of pressure and temperature responses due to gas injection and withdrawal processes such models need to be qualified based on available historical data. The model qualification process for the HL-K cavern was subdivided in two steps. The first step covers the cavern debrining period as well as the relatively quiet gas storage period until the beginning of year 2014. During this period there are nearly no dynamic effects which influence the whole thermodynamic system significantly. The occurring heat exchange process is mainly driven by the heat flow from rock mass zones further away from the cavern as the cavern surroundings have been essentially cooled down during the leaching phase. This process is mainly controlled by the heat conductivity of the rock salt. During the debrining process the cavern fluid is changing from brine to nitrogen. As the heat capacity of these fluids is substantially different the increase of the cavern fluid temperature is significantly accelerated when nitrogen dominates the cavern fluid content. In the course of thermodynamic modeling the actually gradually running process of the brine displacement is modeled by an instantaneous exchange of the cavern fluid after 50% fill.

Enclosure 1.1 shows the measured and calculated cavern fluid temperature over a period of time from year 2010 to year 2018. The measured regular increase of the cavern fluid temperature is more than satisfactorily reflected by the model results. The same is for the calculated wellhead pressures. Enclosure 1.2 shows a comparison between the measured and calculated wellhead pressures (time period from 2014 to 2018). There is an excellent match of measured and modeled data over the whole simulation period. Even though the overall cavern convergence within the observation period is very limited the model has been tuned to reflect the measured cavern shrinkage adequately. Enclosure 1.3 illustrates the calculated cavern shrinkage over the simulated operational period (2014-2018).

As discussed in chapter 2.2 the nitrogen buffer at Heiligerlee has not experienced an extensive storage operation so far. For that reason, it is investigated how strong the calculated pressure and temperature respond to variations of relevant model parameters. One of the most complex parameters to control the heat exchange between the cavern fluid and the cavern surroundings is the heat transfer coefficient. The heat transfer coefficient is a function of various dimensionless numbers as Nusselt number, Prandtl number and Grashof number. For an exact determination of the heat transfer coefficient in real caverns very excessive CFD-modeling is necessary to characterize actual flow conditions. From a comparison of all storages simulated by ESK so far, in practice effective heat transfer coefficients in the range from 10 to 30 W/m²*K are able to yield a realistic modeling of the heat exchange between the fluid inside of a cavern and the cavern surroundings. The nitrogen storage operation has been simulated for both heat transfer coefficient of 10 W/m²*K and 30 W/m²*K.

Enclosure 1.4 shows the comparison of the calculated cavern fluid temperatures versus time. It is obvious that the effects of different heat transfer coefficients are very limited over the entire operational lifetime. Even for the more intensive storage dynamics the differences in the calculated cavern fluid temperatures are less than 2.5 Kelvin. In less intensive operational periods the results differs certainly less (< 1.0 Kelvin). Focusing on the measured cavern fluid temperature on 20 December 2017 it appears that the higher heat exchange coefficient (30 W/m²*K) represents the actual thermodynamic processes slightly better. Therefore, this parameter is chosen for the subsequent prediction runs. The shown differences in calculated cavern fluid temperatures do not have a considerable impact on the calculated wellhead pressure responses (< 1.0 bar) and can therefore be considered negligible for the intended prediction runs.

Future storage operation of the nitrogen buffer is subject of numerous influencing factors (e.g. overall gas supply situation, outside air temperature, etc.) each of them is difficult to predict. Nevertheless, there are particular expectations how the demand on nitrogen withdrawal out of the buffer as well as nitrogen injection into the buffer may look like. As a result of these expectations two different import/ export schedules for a yearly operational period have been developed.

Three operational profiles A, B are shown in the Enclosures 1.5 and 1.6. Each profile includes maximum injection and withdrawal rates up to 190,000 m³(n)/h. The nitrogen turnover is approximately 40 Mill. m³ for each profile. The scenarios A and B are based on historical data and differ mainly by the point of time of maximum cavern depletion (scenario A in January/February, scenario B in late April) and by their total standstill duration.

An additional run was performed by IfG with SCGS-Toolbox (RESPEC). The so-called Scenario C has been assumed as a “worst” case scenario with limited operation in the range of minimum pressure but a maximum injection and withdrawal rate between p_{MAX} and p_{MIN} . Boundary input parameters were used are the same as for Case A and B. Enclosure 2.5 show the pressure profile and calculated temperature for Case C.

At the beginning the model state represents approximately 95% of maximum GIP to account for the expected cavern temperature increase during continuous injection periods which may lead to considerably higher cavern pressures at similar filling levels. Enclosure 1.7 and 1.8 show the calculated casing shoe pressures for a yearly cycle according to the operational profiles A and B. It is obvious that the maximum as well as the minimum allowable casing shoe pressures (max: 147 bar, min: 70 bar) are not exceeded. The corresponding wellhead pressures ranges from 40 bars at minimum filling levels to 140 bars at maximum filling levels (Enclosure 1.9 & 1.10). Enclosure 1.11 and 1.12 show the development of the cavern fluid temperatures of both scenarios. The calculated temperatures do not fall below 35 °C in both scenarios. It is interesting to note that the calculated minimum cavern temperatures do not coincide with calculated minimum pressures. This is in particular true for the operational profile B. Operating this profile the minimum cavern temperature is reached after the first significant withdrawal period.

The subsequent injection period leads to sufficient temperature rise preventing the cavern fluid temperature to drop to lower values when lowering the cavern pressure to its minimum level. After the nitrogen reinjection periods the cavern fluid temperature is continuously increasing but is not reaching temperature levels of 55 °C. Therefore, the overall temperature spread inside of the cavern is limited to less than 20 °C although the total working gas volume is nearly turned over within a limited period of time (6 weeks in case of scenario B).

A further operational constraint is set out in terms of limited change of cavern pressure within a certain period of time. This criterion is associated with the particular rheological behavior of rock salt (ability to creep). Rapid pressure changes will lead to higher loads intensities in the surrounding rock mass as there is less time available to compensate the applied deviatoric stresses by creep mechanisms. The resulting daily changes in cavern pressure from running scenarios A & B is given in Enclosures 1.13 and 1.14. As the operational profiles include frequent intraday changes of injection and withdrawal rates the simulation results must be adequately processed. This is done for every time step (hour) by representing the difference between calculated casing shoe pressures of the past 24 hours. The approach allows to state about the daily pressure change but prevents peak shaving. The processed simulation results showed in Enclosures 1.13 and 1.14 clearly state limited daily changes in cavern pressures of

less than 10 bars/day. High injection and withdrawal rates are always linked to increased gas flow velocities. This is in particular true when high flow rates are operated in lower pressure levels.

Enclosures 1.15 and 1.16 illustrate the calculated gas flow velocities at the wellhead of cavern HL-K for scenario A and B, respectively. It is obvious that for both scenarios the flow velocities are predominantly limited to less than 25 m/s, which is a common design criterion for gas production and gas storage wells. However, for certain operational conditions the calculated gas flow velocity clearly exceeds the limit of 25 m/s. But this is only the case when high withdrawal rates ($Q > 150,000 \text{ m}^3(\text{n})/\text{h}$) coincide with low well head pressures ($p_{\text{head}} < 70 \text{ bars}$). It is recommended to pay particular attention on withdrawal rates when the wellhead pressure drops below 70 bars to avoid frequent occurrence of excessive flow velocities.

3.3 Feasibility Proof

The storage operation of the nitrogen buffer at Heiligerlee is subject to certain operational constraints which are set out in chapter 2.1. These constraints are mainly related to the adherence of minimum and maximum permissible cavern pressures as well as the limitation of the daily change in cavern pressure. Further constraints are related the yearly storage cycle as the cavern is allowed to be operated under lower pressure for a limited period of time only. Based on the qualified thermodynamic model realistic future operational scenarios has been simulated. The simulation results are used to state if the expected yearly storage operation cycles comply with the defined operational constraints. Table 3.2 shows the comparison between the defined operational constraints and the respective simulation results for the operational profiles A, B and C. Storage operations according to profile A, B and C will not exceed any limit set out in rock mechanic cavern design.

Table 3-2: Comparison of operational constraints and simulation

Operational Parameter	Constraint	Profile A	Profile B	Profile C
Max. Casing Shoe Pressure	147 bar	143.6 bar	144.2 bar	147 bar
Min. Casing Shoe Pressure	70/90 bar	80.5 bar	76.9 bar	70.4 bar

Casing Shoe Pressure in the range from 90 bar to 70 bar	30 days	19 days	8 days	30 days
Max. Pressure Change	10 bar/day	7.6 bar/day	7.6 bar/day	9,1 bar/day
Min. pressure change per year	> 10 bar	63.1 bar	63.7 bar	76.6 bar

4 Geomechanical modelling of the cavern HL-K

The generation of the geomechanical model and the results of the simulation are described and presented in the following chapters. The results from the thermodynamic simulations were implemented in the geomechanical calculations.

The cavern HL-K was repurposed into nitrogen storage cavern since 2012. The rock mechanical effects resulting from the conversion of cavern HL-K into a storage cavern and the associated injection and withdrawal cycles are analyzed and verified in the report “Numerical Stability Verification concerning the Conversion of the cavern Heiligerlee HL-K into a Nitrogen Buffer” (IfG, 2010) on the results of a state of the art computational modeling.

The currently performed investigations for the nitrogen storage cavern HL-K had the aim to determine a new range for the operation mode regarding maximum and minimum cavern pressure as well as possible gas flow rates. Thus, investigations performed within the scope of this study the simulation was carried out as a thermodynamic and rock mechanic calculation which represents the current standard.

The applied combined thermodynamic/geomechanical model represents a functional model, i.e. the actual deposit and mining situation has been simplified in an acceptable manner and the rock mechanical behavior occurring during the phases of withdrawal with an intended gas flow is generalized.

4.1 Geomechanical Model

By 3D-numerical simulation of the cavern HL-K as part of the storage field Heiligerlee the proof of the cavern stability, integrity and tightness during long-term storage operation shall be verified. The storage operation parameters have to be re-defined.

This 3D-model of the cavern HL-K includes a cuboid-shaped segment of the cavern field (Enclosure 2.1) includes the neighbouring brine filled cavern HL-E. Because of its shape, depth situation and distance to the nitrogen storage cavern HL-E is the most significant influence factor acting on cavern HL-K. The influences of the other adjacent brine-caverns (HL-F, HL-C) are also considered and can be explained by the axial-symmetry of the model.

The extension of the model is 250 m in width, while is it 500 m long and 1200 m high. It is located in a depth range of 500 to 1,700 m below surface. The modelled segment of the cavern field contains the complete caverns. For the assessment of the pillar between the caverns only the vertical section in N-W direction were considered for interpretation. The shape of the cavern was generated using the US-measurements presented by SOCON 2014 for HL-K and for HL-E in 2004.

Vertical boundaries of the model were fixed with regard to horizontal and to vertical deformations respectively at the basis of the model. At the top of the model in a depth of 500 m an initial load of 9.79 MPa (according to a gradient of the specific weight of $\gamma = 19.7$ kPa/m for the overburden and $\gamma = 21.8$ kPa/m for the rock salt) is applied. According to this approach a stress of 31.6 MPa is acting at the base of the cavern HL-K representing the overburden load and the weight of the model, when a mean pressure gradient of $\gamma = 21.1$ kPa/m is assumed for the considered rock mass section in the model, which can be deduced from rock mass densities. The primary stress at the last cemented casing shoe is calculated to 20.3 MPa (depth 981 m) assuming these figures.

The distance between the boreholes of the caverns HL-K and HL-E are 250 m. The cavity of the HL-K was modelled between 1,015 and 1,506 m. The cavity of the HL-E was modelled between 711 and 1,325 m. The volume of the rock mechanical model of the HL-K amounts to about 773,000 m³. The volume of the neighbouring cavern HL-E amounts 2.904 million m³. The extent of the developed volume of the model is conservative enough, in terms of the modelled and real volume of both caverns. In summary Table 4-1 shows the boundary conditions of the geomechanical model.

Table 4-1: Summary of the geomechanical model conditions.

	3D-Modell HL-K and HL-E	
Horizontal extension of the model	500 x 250 m	
Vertical extension of the model	1,200 m	
Borehole distance HL-K to HL-E	250 m	
Depth of the model	500 – 1,700 m	
Initial load top of the model	9.79 MPa	
	HL-K	HL-E
Cavern heights	491 m	614 m
Max. cavern radius	35 m	60 m
Depth of caverns	1,015 – 1,506 m	711 – 1,325 m
Cavern volume	773,000 m ³	2.904,000 m ³

After model generation the primary load condition for the rock mass is calculated assuming the pressure gradients for rock salt $\gamma_{\text{Salt}} = 21.8 \text{ kPa/m}$ and the overburden $\gamma_{\text{overb}} = 19.7 \text{ kPa/m}$.

Considering of the viscous behaviour of salt rock it is common to assume an isotropic stress state on the basis of the mentioned overburden gradients. This is confirmed by the 3D-model calculations demonstrating stress equilibrium with nearly isotropic pressure conditions (see Enclosure 2.2).

After initiation of the primary stress state cavity leaching were simulated. The process of leaching the caverns has been simulated by deleting relevant mesh elements. In several leaching steps with continuous depressurising from primary stress state to a hydrostatic pressure of the brine column was applied. The time- and pressure-dependent divisions of leaching steps are shown in Enclosure 2.2.

By finalising the leaching process, the initially stress and strain state has been established which is going to be the basis for further prognosis calculations. With the prognosis calculation pressure and temperature profiles from thermodynamic analysis (chapter 3) will be applied as boundary conditions (see Enclosure 2.3, 2.4 and 2.5). The prognosis has been done as coupled thermodynamic / rock mechanical simulation.

4.2 Simulation Tool and used material law

The calculation program FLAC^{3D} (ITASCA, 2009) was used for the numerical modelling. The program has been developed particularly for solving geotechnical problems. This tool represents the current state of the art on an international level. A lot of practical experience exists with this code in the modelling of various rock mechanical problems. By the option of applying user defined modules, specific material laws can be implemented in the calculation procedure, thus the program developed by adapting to practical needs and considering latest research work. A specially developed visco-elasto-plastic constitutive law was applied for modelling the time-dependent stress, deformation, and softening behaviour as well as the associated dilatancy processes of salt rocks (MINKLEY, W., 2004).

The parameters used for the numerical modelling represent the stress and strain behaviour of the rock salt from Heiligerlee bases on site specific rock mechanical investigations. The material parameters that were mentioned had already been used in the previous studies (IfG, 2010 and 2016).

4.3 Assessment criteria

The simulation results had to be assessed with regard to long-term integrity of the rock mass which surrounds the cavern. Thereby, integrity is interpreted as stability and tightness of the salt rock mass around the cavern. The following criteria have been applied in order to assess the rock mass stability beginning from the cavern contour (MINKLEY et al. 2011):

- *Dilatancy Criterion (2 in Table 4-2)*

It has to be proven that structural damage is limited to restricted areas close to the cavern wall and does not propagate into the main load-bearing elements of the rock mass. Zones of structural damage of the rock mass can be identified through the violation of the dilatancy criterion according to $\varepsilon_{vol}^p > 0$ and the amount of plastic shear strain ε^p .

Zones, where plastic shear stains and dilatant deformation occur, have to be restricted to the rock mass zone directly behind the cavern wall and thereby remain within limiting values as observed in laboratory tests performed on rock salt samples from the specific location.

If no dilatancy is calculated from the model the acting stress distribution is below the dilatancy boundary. In this case the utilization of the boundary can be shown according to $\eta_{Dil} = \sigma_{eff} / \sigma_{eff(Dil)}$. The degree of utilization is an indicator how far away from exceeding the dilatancy boundary is the actual load

- *Minimum Stress Criterion (1 in Table 4-2)*

The acting minimum principal rock mass stress must be higher than the gas pressure in the cavern in a zone surrounding the cavern, which has to be sufficiently wide in extent, ($\sigma_{MIN} - p_{GAS} > 0$). So far, no effective tensile stresses are permitted in this zone. However, in a restricted area directly behind the cavern contour effective tensile stresses occur and a fluid pressure-driven generation of flow paths with percolation is possible. η

With respect to the safety demands at maximum cavern pressure it has to be proven that the tightness of the cavern surrounding rock salt mass is fulfilled. This is of special interest for the assessment of high-frequently cycling hydrogen storage operations with temporarily relatively high flow rates and intercalated standstill phases (Case B; Peak Storage Operation), because creep processes, which are acting in the salt behind the cavern wall, are time dependent and therefore stress states differ from those which develop due to slow cycling operations. Criteria which have been applied for the assessment of the rock mass state at maximum storage pressure with regard to long-term tightness are given below:

- *Geological tightness criterion (4 in Table 4-2)*

The geological tightness of a cavern is guaranteed, if the cavern under the maximum pressure p_{MAX} is enclosed by a sufficiently extended zone, where the minimum principal stress is higher by 10% than the maximum cavern pressure ($1.1 * p_{MAX} \leq \sigma_{MIN}$ in a zone of 30 m).

- *Technical tightness criterion (5 in Table 4-2)*

The technical tightness of a cavern is guaranteed, when a sufficient thickness of salt above the last cemented casing shoe – is existing, where the acting horizontal compressive stress on the contact interfaces between salt, cement and casing is higher by 15% of the cavern pressure ($\sigma_{MIN} \leq 1.15 * p_{MAX}$).

In order to ensure the integrity of the rock mass surrounding the caverns a set of assessment criteria as compiled in Table 4-2 were applied to the results of numerical simulations. These

assessment criteria cover the required proofs against loss of tightness and stability of the rock mass.

Table 4-2: Assessment Criteria for caverns.

Criterion	Name	Assessment of
1	Minimum Stress Criterion	potential percolation zones
2	Dilatancy Criterion	damage at micro scale
3	Tensile Stress Criterion	tensile cracks
4	Geological Tightness Criterion	tightness conditions of the salt surrounding the cavern
5	Technical Tightness Criterion at Casing Shoe	horizontal confinement at casing shoe
6	Integrity Criterion at Casing Shoe	deformation at casing shoe

4.4 Evaluation and Assessment

Essential results of the coupled thermodynamic / rock mechanical simulations are shown in the enclosures as listed in Table 4-3.

Table 4-3: List of selected enclosures of the coupled rock mechanical simulations for cavern HL-K representing the nitrogen storage operation.

Representation	Enclosure
Generetaion of the model from SOCON US-measurements	Enclosure 2.1
Primary stress state and leaching phases of the model	Enclosure 2.2
Simulation Case A – Temperature Calculation performed by ESK	Enclosure 2.3
Simulation Case B – Temperature Calculation performed by ESK	Enclosure 2.4
Simulation Case C – Temperature Calculation performed by IfG	Enclosure 2.5
Assessment of p_{MAX} after immediately reaching the pressure after the first year – Case A	Enclosure 2.6
Assessment of p_{MAX} after immediately reaching the pressure after the 5th year – Case A	Enclosure 2.7
Assessment of p_{MAX} after immediately reaching the pressure after the first year – Case B	Enclosure 2.8
Assessment of p_{MAX} after immediately reaching the pressure after the 5th year – Case B	Enclosure 2.9
Assessment of p_{MAX} after immediately reaching the pressure after the first year – Case C	Enclosure 2.10

Assessment of p_{MAX} after immediately reaching the pressure after the 5th year – Case C	Enclosure 2.11
Development of the stress at Casing shoe of HL-K after 5 years storage operation – Case A	Enclosure 2.12
Development of the stress at Casing shoe of HL-K after 5 years storage operation – Case B	Enclosure 2.13
Development of the stress at Casing shoe of HL-K after 5 years storage operation – Case C	Enclosure 2.14
Confining pressure (technical tightness) at maximum storage pressure	Enclosure 2.15
Vertical displacement and compression/extension in a profile above the cavern HL-K	Enclosure 2.16
Stress situation at minimum stress – Case A (84 bar)	Enclosure 2.17
Stress situation at minimum stress – Case B (81 bar)	Enclosure 2.18
Stress situation at minimum stress – Case C (70 bar)	Enclosure 2.19
Utilization of dilatancy boundary at p_{MIN}	Enclosure 2.20
Development of stresses at cavern contour and assessment of p_{MIN} regarding stability – Case A	Enclosure 2.21
Development of stresses at cavern contour and assessment of p_{MIN} regarding stability – Case B	Enclosure 2.22
Development of stresses at cavern contour and assessment of p_{MIN} regarding stability – Case C	Enclosure 2.23
Volume convergence	Enclosure 2.24

The simulation results will be assessed in the next Chapters with the aim to prove long-term integrity (stability and tightness) of the salt rock mass enclosing the cavern. For this purpose, relevant representations showing the stress and tightness conditions of the rock mass, have been selected. These presentations are described below.

4.4.1 Assessment of tightness at maximum cavern pressure

The evaluation of the limiting conditions regarding geological and technical tightness is of great importance, when the cavern pressure approaches the maximum pressure after a certain operation phase at minimum pressure. The assessment of the geological tightness applies the “Minimum principle stress Criterion” The criterion demands at maximum pressure p_{MAX} that the

cavern must be enclosed by a sufficiently extended zone, where the minimum principal stress is higher than the maximum cavern pressure by a certain amount.

Enclosure 2.6 to 2.11 show that the cavern is adequately surrounded by such kind of safety zone against loss of tightness at p_{MAX} for the storage operations of all three cases. The minimum extension of the safety zones above the roof is not less than 140 m over the years of the assumed operation history. In the pillar section there is almost no change of the zone extent over time. It could be proven that a sufficient stress difference between cavern pressure and minimum principal stress at casing shoe exist over long lasting period of nitrogen storage (Enclosure 2.12 to 2.14).

In order to assess the tightness conditions, Enclosure 2.15 is presented. The so called safety zones against loss of geological tightness, where minimum stresses of the rock mass must be higher than the internal cavern pressure at maximum level in a sufficient range. The results are depicted in the shown diagram. For all studied load cases the calculated values of the minimum extent of the tightness zone above the cavern roof are close together. By means of Enclosure 2.15 the technical tightness at casing shoe can be evaluated. Lateral (horizontal) stresses are compared with the internal cavern pressure at maximum state. Concerning technical tightness requirements at the last cemented casing shoe, the results of the simulated cases are nearly identical. The safety factor for technical tightness with a sufficient extension is than demanded 15%. The technical tightness criterion is fulfilled for the maximum cavern pressure of $p_{MAX} = 147$ bar for all cases which were calculated.

4.4.2 Assessment of contour stability and tightness at minimum cavern pressure

The simulation results show that for all investigated storage modes – (Case A, B and C) with nitrogen as storage fluid – the safety requirements for contour stability and tightness of the cavern are guaranteed during minimum cavern operations.

The dilatancy strength is never exceeded and therefore it can be concluded that no specific zone behind the cavern wall will be created, where plastic shear strains as wells as the volumetric deformation cumulate (see Enclosure 2.21 Case A, Enclosure 2.22 Case B an Enclosure 2.23 Case C). The maximum utilization of the dilatancy boundary is between 50 – 60 % in all three cases (see Enclosure 2.17 Case A, Enclosure 2.18 Case B an Enclosure 2.19 Case C). The zones with the highest degree of utilization are concentrated close to the cavern contour. Inside the pillar the utilization is reduced below 25 %. In conclusion, due to the dilatancy

criterion the stability of the cavern HL-K and the cavern surrounding pillar can be assessed as long-term stable.

There are also no zones where the minimum principal stress criterion (or effective tension stress criterion) is violated at the cavern contour. Enclosure 2.21 (Case A), Enclosure 2.23 (Case B) and Enclosure 2.24 (Case C) show the development of the principal stresses against the time during the assumed storage operation mode in a point at the cavern contour. At each time all stress components are above the cavern pressure. In Case C where 6 full cycles between p_{MAX} and p_{MIN} with a constant flow rate of 190,000 m³(n)/h were realized also the minimum stress close to the cavern contour remained above the cavern pressure. In conclusion no additional thermodynamic induced tensile stresses ($p_{MIN} < p_{CAV}$) and resulting deformation will occur.

The modelling results show that for each model configuration tensile failures ($\varepsilon_{ten}^p > 0$) of contour elements are excluded with respect to the modelled storage regime. Therefore, the long-term tightness during minimum pressure operations can be considered as guaranteed. However, the cavern is completely enveloped by the salt rock mass, which remains in perfect stability and tightness conditions when the pressure is at p_{MIN} . In relation to Case C it is possible to operate the cavern HL-K with a minimum cavern pressure of $p_{MIN} = 70$ bar.

4.4.3 Assessment of volume convergence and displacements

Based on the calculated displacement rates the resulting subsidence of the cavern roof and the top of the model as well as the uplift of the cavern bottom can be predicted. An average convergence rate (see Enclosure 2.24) for each case has been estimated by means of the numerical simulation results. These results show that the convergence rate in case of the multi-cyclic operation (Case C) is slightly higher than in the other both cases. From the simulation a value of 2 ‰/year can be predicted. Regarding to the stability of the cavern and the influence of the surface the calculated convergence rates can be assumed as are permissible.

For the casing shoe and the hanging wall it is important to limit extension deformation because of the tensile properties of the casing, the rock mass and the cementation. In the case of cavern HL-K slightly compression deformations are observed in the hanging wall and at the position of the last cemented casing shoe. As shown in Enclosure 2.16 down to the last cemented

casing shoe compression occurs while the uncased cavern neck is characterised by little extension. It has to be mentioned that it is uncommon to have compression in the hanging wall, but in this case the secondary stress field as induced by the brine and storage caverns interacting in a very special manner. Vertical strain will occur in the vicinity of the last cemented casing shoe as a consequence of cavern convergence. The maximum allowable strain at the last cemented casing shoe is requested to be less than 1% (10 mm/m). Calculation results show no significant differences in relative vertical displacements for all cases in a long term cyclic operation mode. A value below approx. 0.1% can be predicted in the depth of the casing shoe after the storage operation of 5 years (see Enclosure 24), i.e. there is no risk of tightness loss for a long-term nitrogen storage operation under the assumed operation pressures (p_{MAX} , p_{MIN}).

5 Conclusion and Recommendations

As known from a lot of numerical case studies carried out for natural gas storage as well as for hydrogen storage high flow rate will cause temperature differences during and between gas withdrawal and injection. And, high temperature changes cause additional thermodynamically induced stress interacting with the mechanically induced stresses from the pressure change. Based on this knowledge the nitrogen storage must be assessed in the case of envisaged high flow rates in the range of 190.00 m³(n) per hour.

For thermodynamic-rock mechanical coupled processes during storage operation stability and integrity of the salt cavern is guaranteed

- @ p_{Min} the cavern contour is free of tension stresses
- @ p_{Min} the additional damage induced by dilatancy is limited
- @ p_{Min} the zone where the effective stresses are in a tension range is limited
- @ p_{Max} sufficient confinement acts at the last cemented casing shoe
- @ p_{Max} the geological tightness is guaranteed

Mark two means that the combined stresses (thermodynamic and mechanical) may lead to overcome the dilatancy boundary where damage is induced like additional porosity and increased grain boundaries all summarized as possible additional flow paths for the storage medium. In a zone where the gas can penetrate, effective stresses ($\sigma_{Rock} - p_{Fluid}$) occur under special circumstances, i.e. hydraulic tension stresses will be induced if the fluid pressure is larger than the stress in the rock close to the contour.

For cavern HL-K three cases as suggested by ESK, Freiberg (A and B) and the hypothetical case C suggested by IfG have been modelled. In all cases the maximum flow rate of 190.000 m³(n)/h was implemented in a general annual (Case A and B) respective high-cyclic (Case C) operation mode.

Without restriction of generality the numerical models show that all demands for stability and integrity of the nitrogen storage cavern HL-K are fulfilled. The performed simulation Case C within the pressure range of 147 and 70 bar show that long-term high cyclic nitrogen operations of cavern HL-K with flow rates of 190,000 m³(n)/h compared with an annual operation mode (Case A and B) do not generate significant differences of the stress distribution in the rock mass state during withdrawal and injection over the prospected lifetime of the cavern. This becomes evident when comparing the assessment of deformations (by means of strain) and effective tensile stresses as well as the stress situation at maximum cavern pressure.

No tension stresses at the cavern contour, no damage caused by dilatante deformation, no effective stresses in the tension range could be proven. At maximum pressure a sufficient confinement at the casing shoe is proven to guarantee the technical tightness as well.

These outcomes confirm that:

1. The operated maximum pressure/gradient is very conservative. The gradient of 0.15 bar/m creates more than enough differences between the stresses in the rock mass and those acting from cavern pressure and the thermodynamic stress component.
2. The operated minimum pressure of 70 bar is high enough to ensure that the combined, rock mechanical and thermodynamically, stresses at p_{MIN} are far away from the tension region.
3. The intended maximum flow rate causes just stress changes of less than 10 bar/day, which is a normal older limitation in the case of an annual operated cavern.

Caused by the data base it can be expected that even in the case of an even more cyclical driving style with flow rates of 190,000 m³(n)/h with maximum life time of 30 day in the storage year at minimum storage pressure the above-mentioned requirements will be met.

From the rock mechanical point of view geological and technical tightness will be guaranteed in a long-term gas storage operation also under the far field influence of the brine production caverns (HL-E) if the HL-K is used with a maximum pressure of $p_{\text{MAX}} = 147$ bar.

The simulations have proven a safe storage operation regarding the permissible minimum cavern pressure. The outcomes have shown that the cavern HL-K can be used with $p_{\text{MIN}} = 70$ bar within the lower pressure range. Stability and integrity of cavern are guaranteed. The cavern convergence depends from storage operation regime and remains limited to less 2‰/year.

The lifetime at p_{MIN} should be less equal 30 day during a storage year. The upper limit of the minimum pressure range is $p_{\text{MIN},0} = 90$ bar. The whole lifetime per storage year for $p \leq p_{\text{MIN},0}$ is limited to 90 day for convergence and cavern lifetime reasons.

The cavern HL-K can be operated up to six full cycles per year, i.e. also partial cycles are possible if the lifetime at p_{MIN} is not exceeded. It could be proven by the previous study from IfG (2016) that if the cavern is in a standstill mode at $p_{\text{MAX}} = 147$ bar a sufficient stress difference between cavern pressure and minimum principal stress at casing shoe exist over long-lasting period.

Based on the assessment of the results of the coupled thermodynamic-mechanic simulations the following in Table 5-1 is recommended for the operation of cavern HL-K as nitrogen storage.

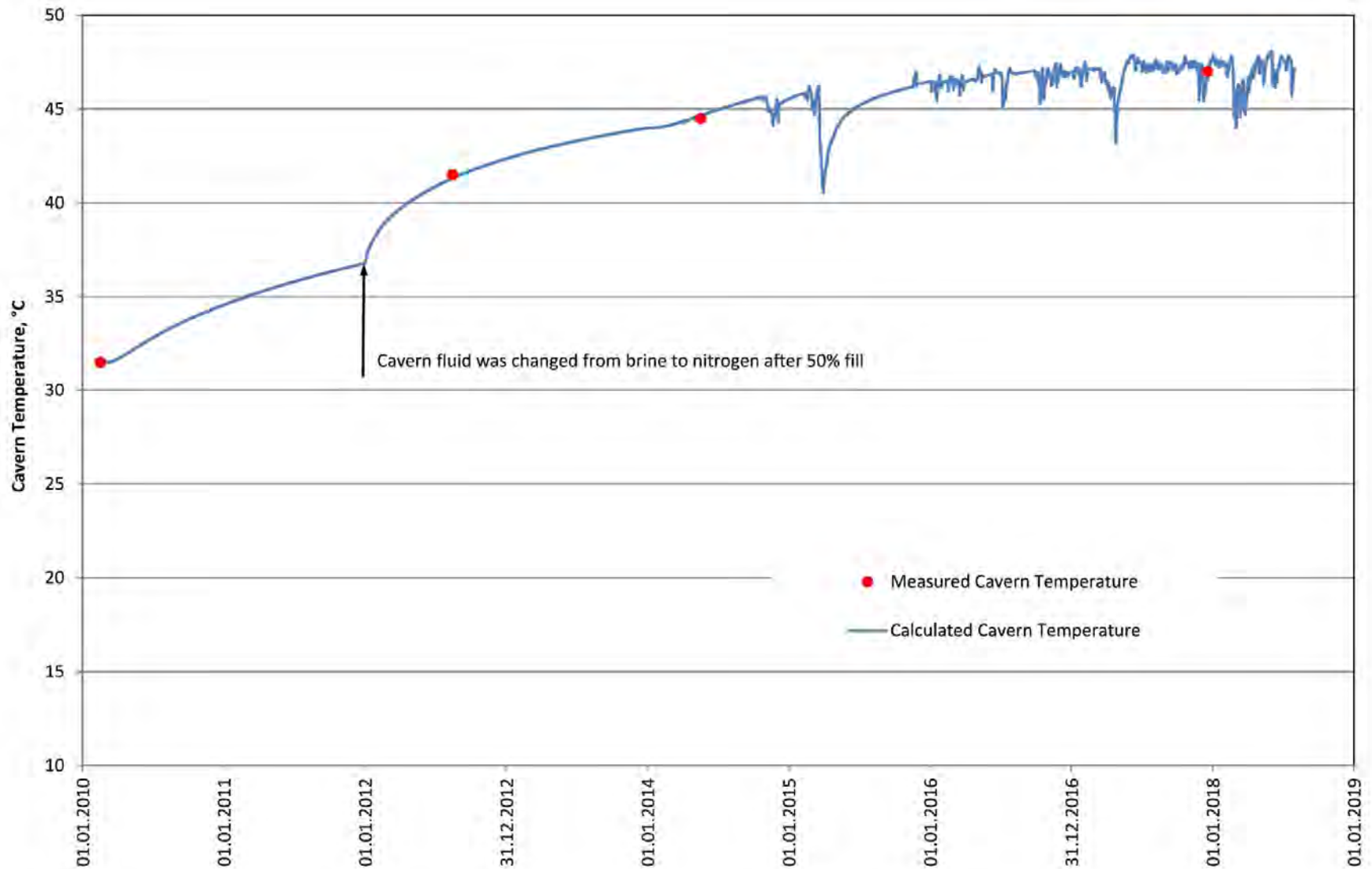
Table 5-1: Overview of rock mechanical recommendations for cavern HL-K.

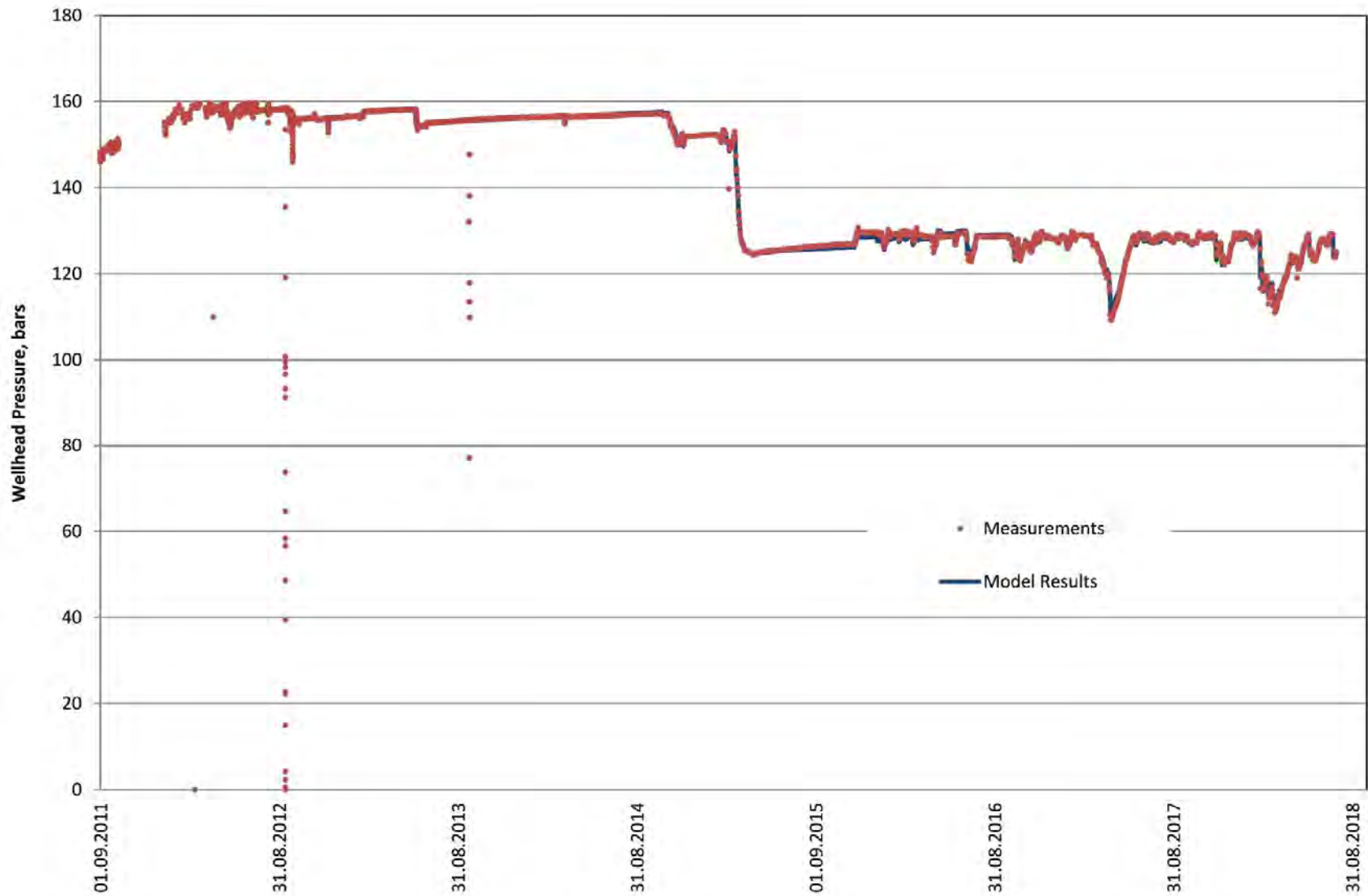
Item	Unit	HL-K
depth reference of last cemented casing shoe	[m TVD]	981
maximum cavern pressure p_{MAX} at casing shoe depth	[barg]	147
minimum cavern pressure $p_{\text{MIN},0}$ at casing shoe depth	[barg]	90
minimum cavern pressure p_{MIN} at casing shoe depth	[barg]	70
maximum permissible flow rate	[m ³ (n)/h]	190,000
Lifetime for $p \leq 90$ bar	days	Max. 90 days/year
lifetime at $p_{\text{MIN}} = 70$ bar	days	Max. 30 days/year

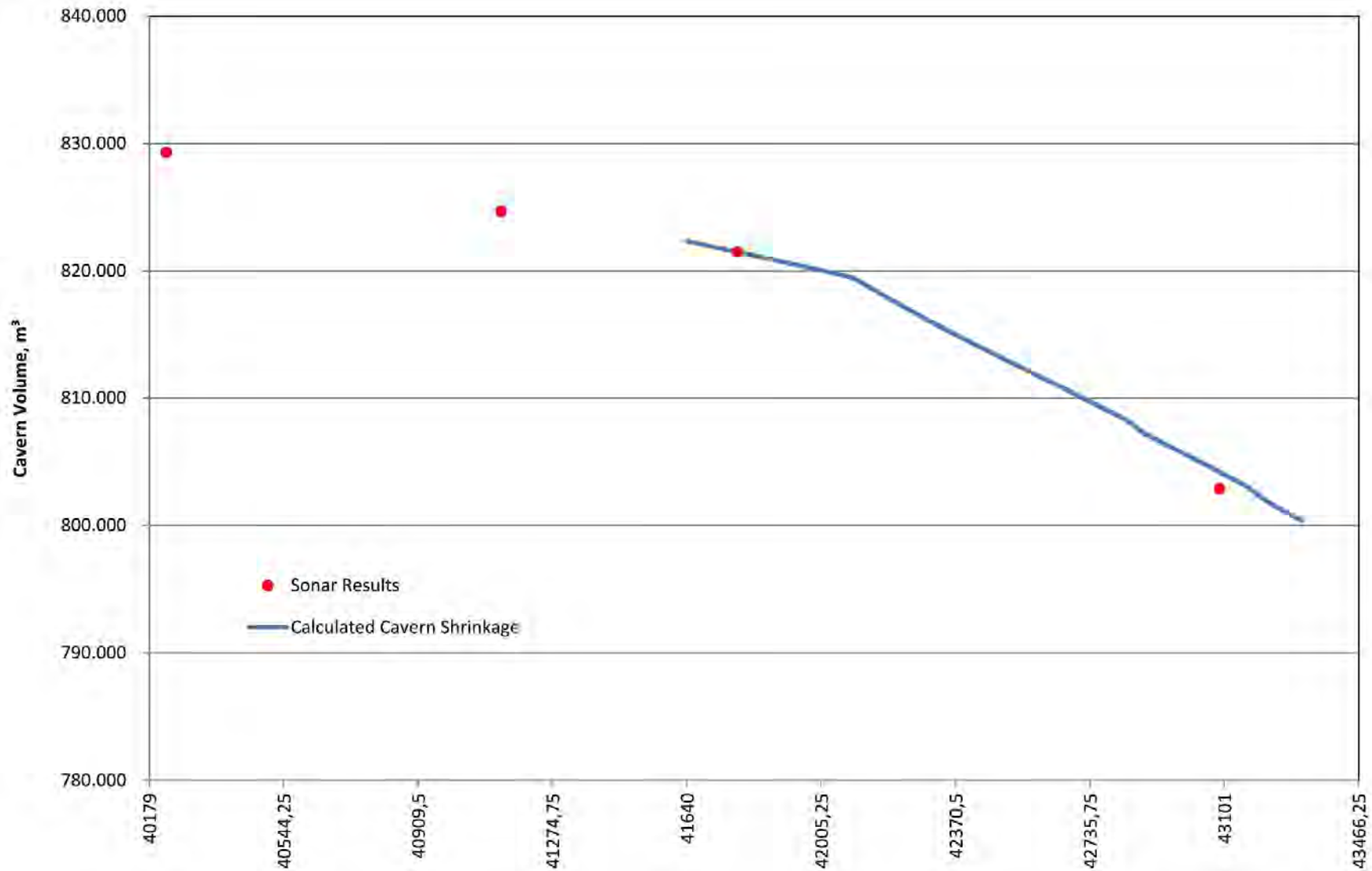
In the present study the integrity of the cavern surrounding salt rock mass has been investigated for two annual and one multi-cycling nitrogen storage operation mode. It could be proven and suggested from the rock mechanical point of view to operate cavern HL-K in a manner that is described in this report as permissible.

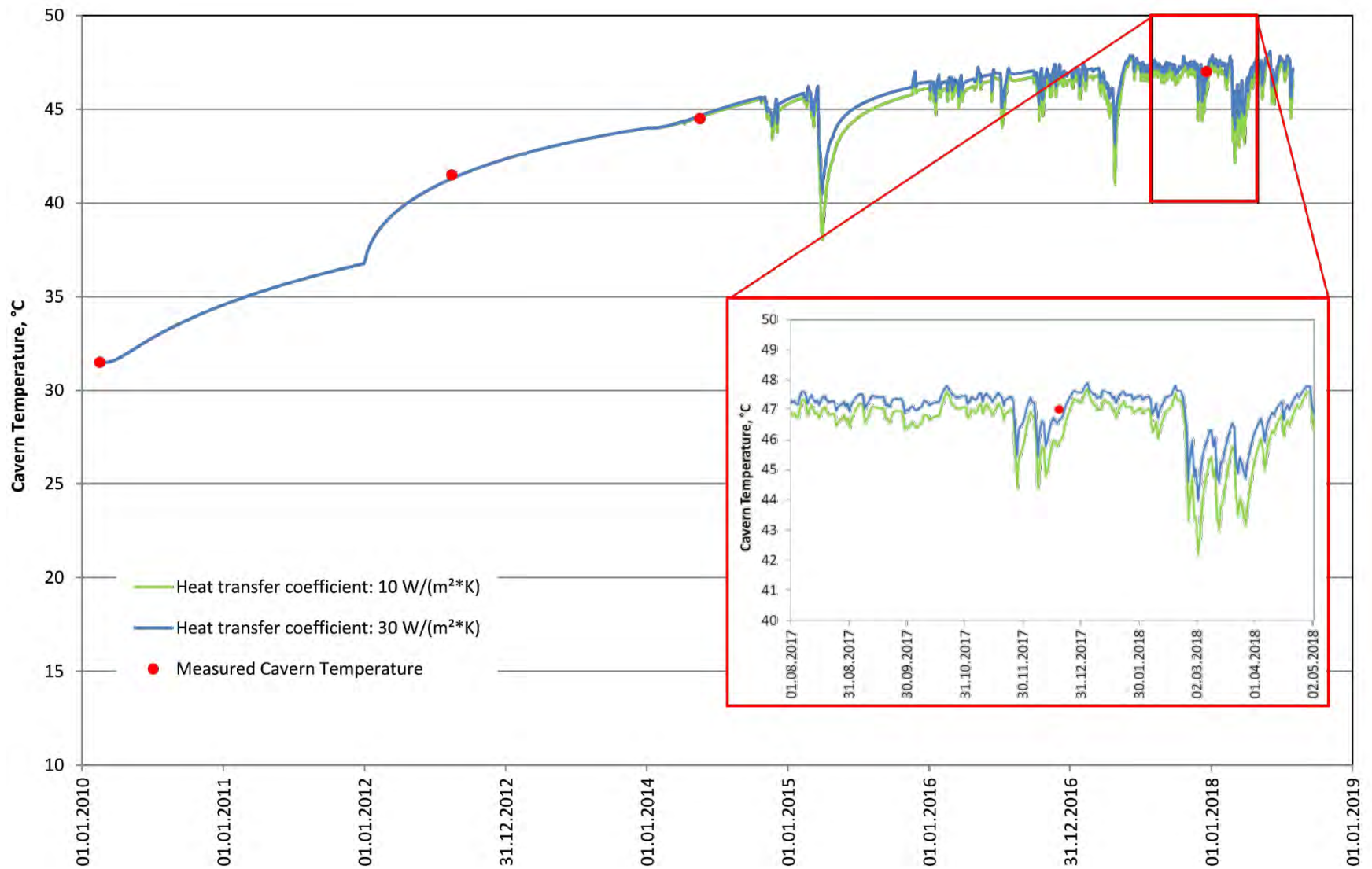
6 List of Literature

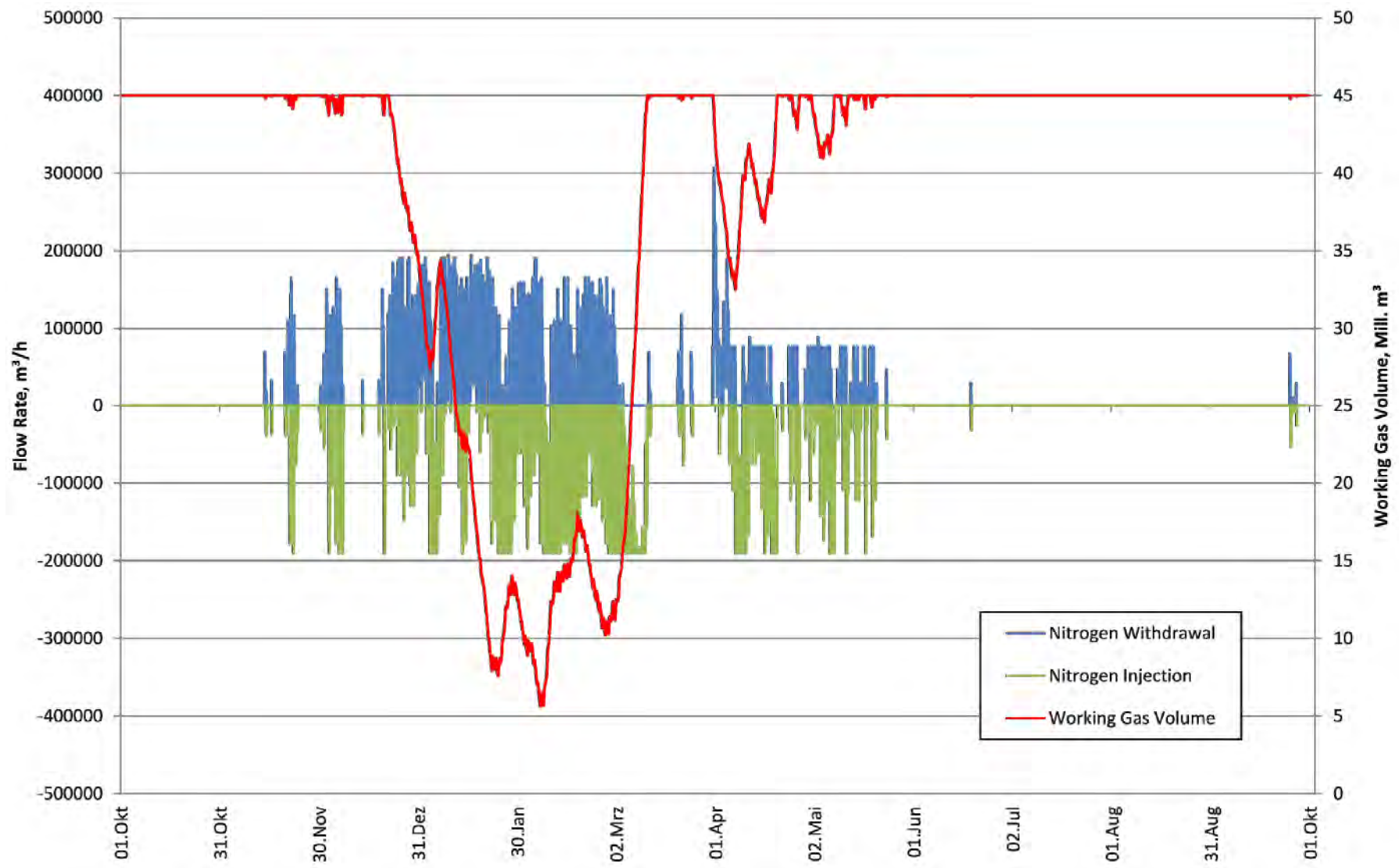
- ESK (2018): Feasibility Proof on Injection Capacity Increase at HL-K Nitrogen Buffer
26.11.2018
- IfG (2008): Rock Mechanical Assessment of the Conversion of the Heiligerlee HL-K Cavern to
a Nitrogen Storage Cavern. 01.07.2008
- IfG (2010): Numerical Stability Verification Concerning the Repurpose of the Cavern
Heiligerlee HL-K into a Nitrogen Buffer. 01.10.2010
- Itasca (2013): Fast Lagrangian Analysis of Continua in 3 Dimensions, Version 5.01. ITASCA
Consulting Group Inc. Minneapolis, Minnesota USA
- MINKLEY, W. (2004): Gebirgsmechanische Beschreibung von Entfestigung und Sprödbrech-
erscheinungen im Carnallitit. Schriftenreihe des Institutes für Gebirgsmechanik - Band
1, Shaker Verlag
- MINKLEY, W.; LINDERT, A.; BRÜCKNER, D. (2011): The improved IfG Storage Cavern Design
Concept. SMRI Fall 2011 Technical Conference. York, United Kingdom, 3-4 Oct. 2011
- SOCON (2004): ECHO-LOG Heiligerlee E 8. Messung. Bericht über die Ergebnisse der echo-
metrischen Hohlraumvermessung in der Kaverne Heiligerlee E. 24.06.2004
- SOCON (2010): ECHO-LOG Heiligerlee K 4. Messung. Bericht über die Ergebnisse der echo-
metrischen Hohlraumvermessung in der Kaverne Heiligerlee K. 16.02.2010
- SOCON (2012): ECHO-LOG Heiligerlee K 5. Messung. Bericht über die Ergebnisse der echo-
metrischen Hohlraumvermessung in der Kaverne Heiligerlee K. 15.08.2012
- SOCON (2014): ECHO-LOG Heiligerlee K 6. Messung. Bericht über die Ergebnisse der echo-
metrischen Hohlraumvermessung in der Kaverne Heiligerlee K. 19.05.2014
- SOCON (2017): ECHO-LOG Heiligerlee K 7. Messung. Bericht über die Ergebnisse der echo-
metrischen Hohlraumvermessung in der Kaverne Heiligerlee K. 20.12.2017

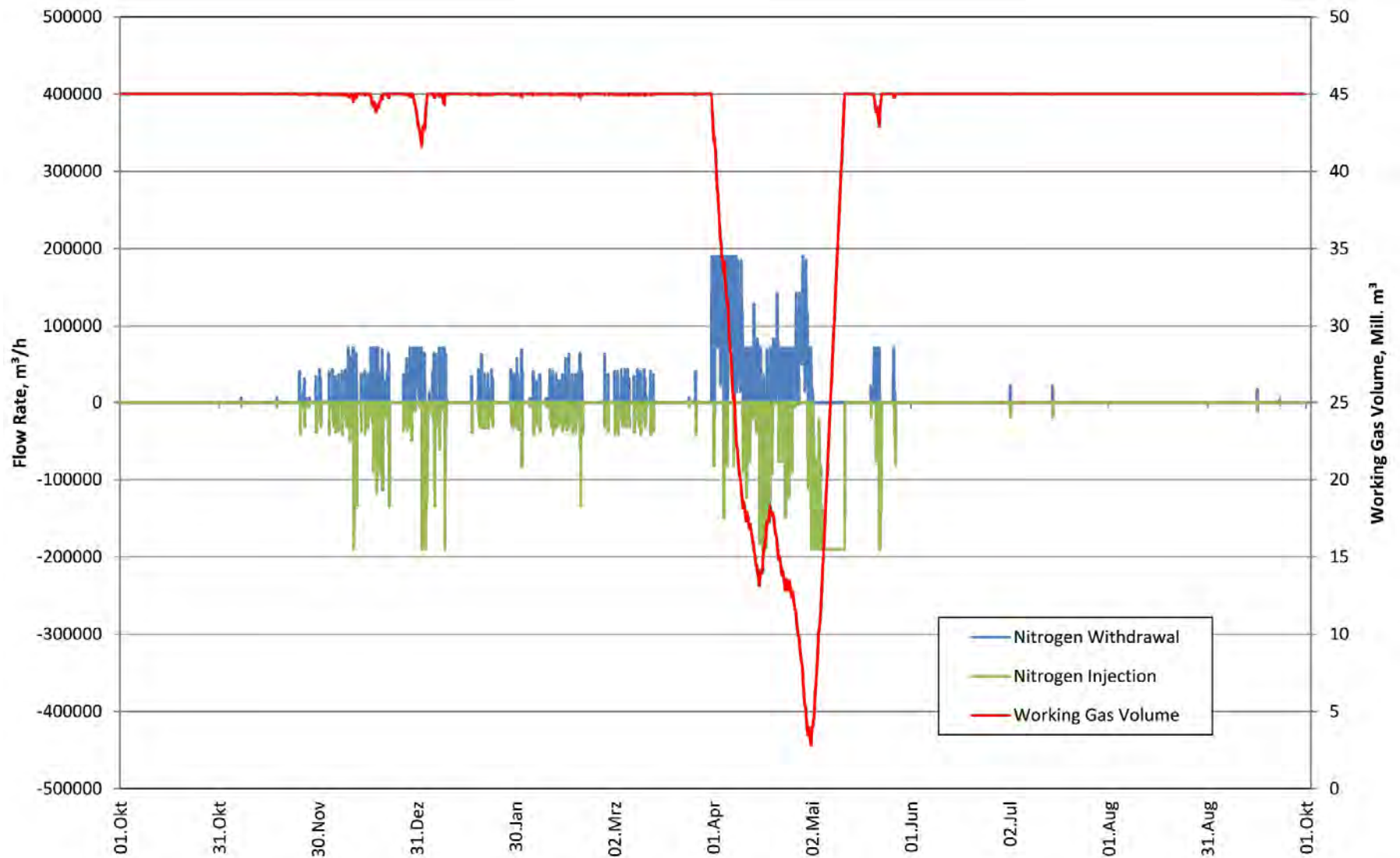






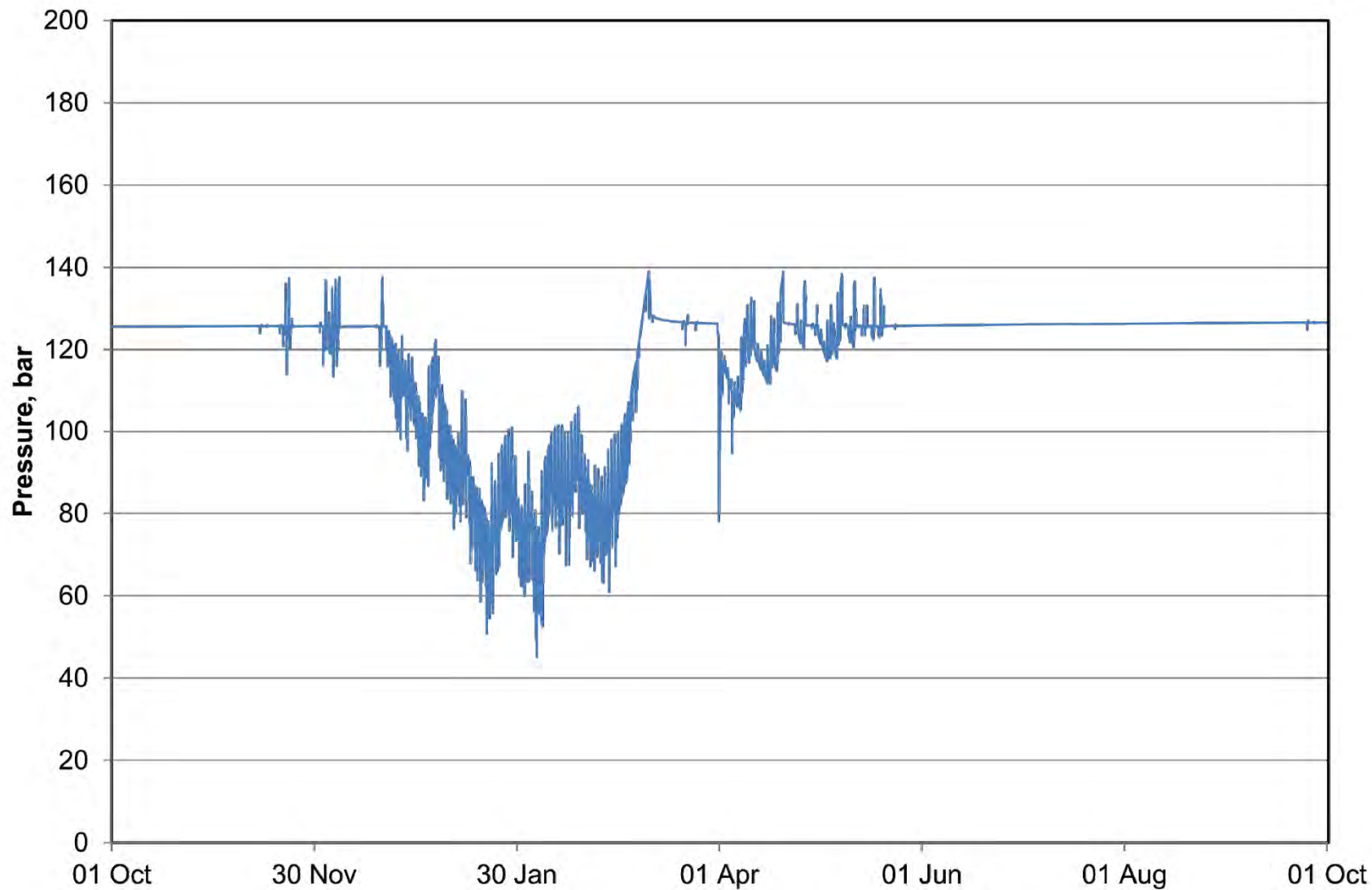










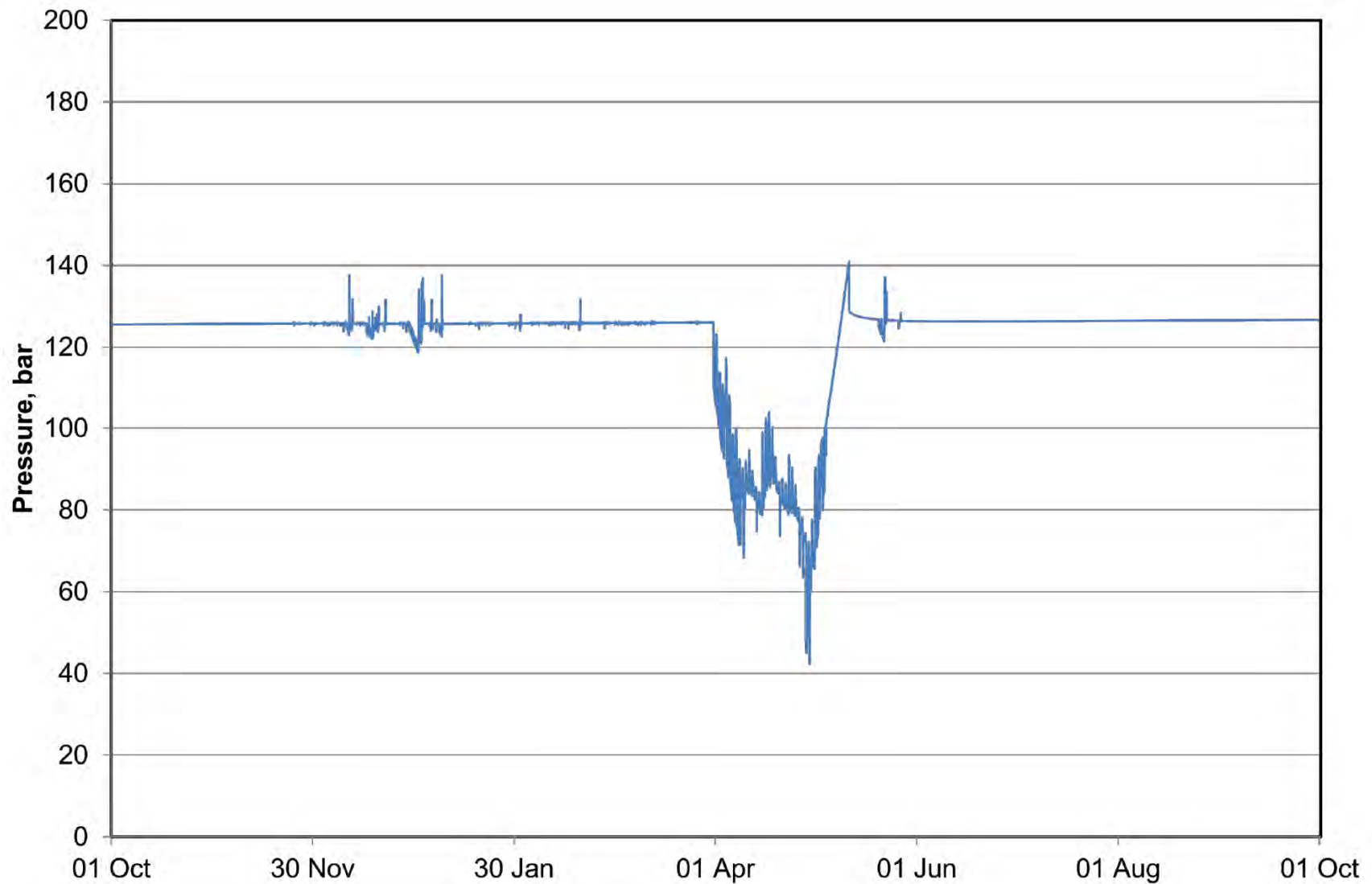


Institut für
Gebirgsmechanik GmbH
2019



Calculated wellhead pressure for a yearly cycle according to
scenario A

Enclosure 1.9

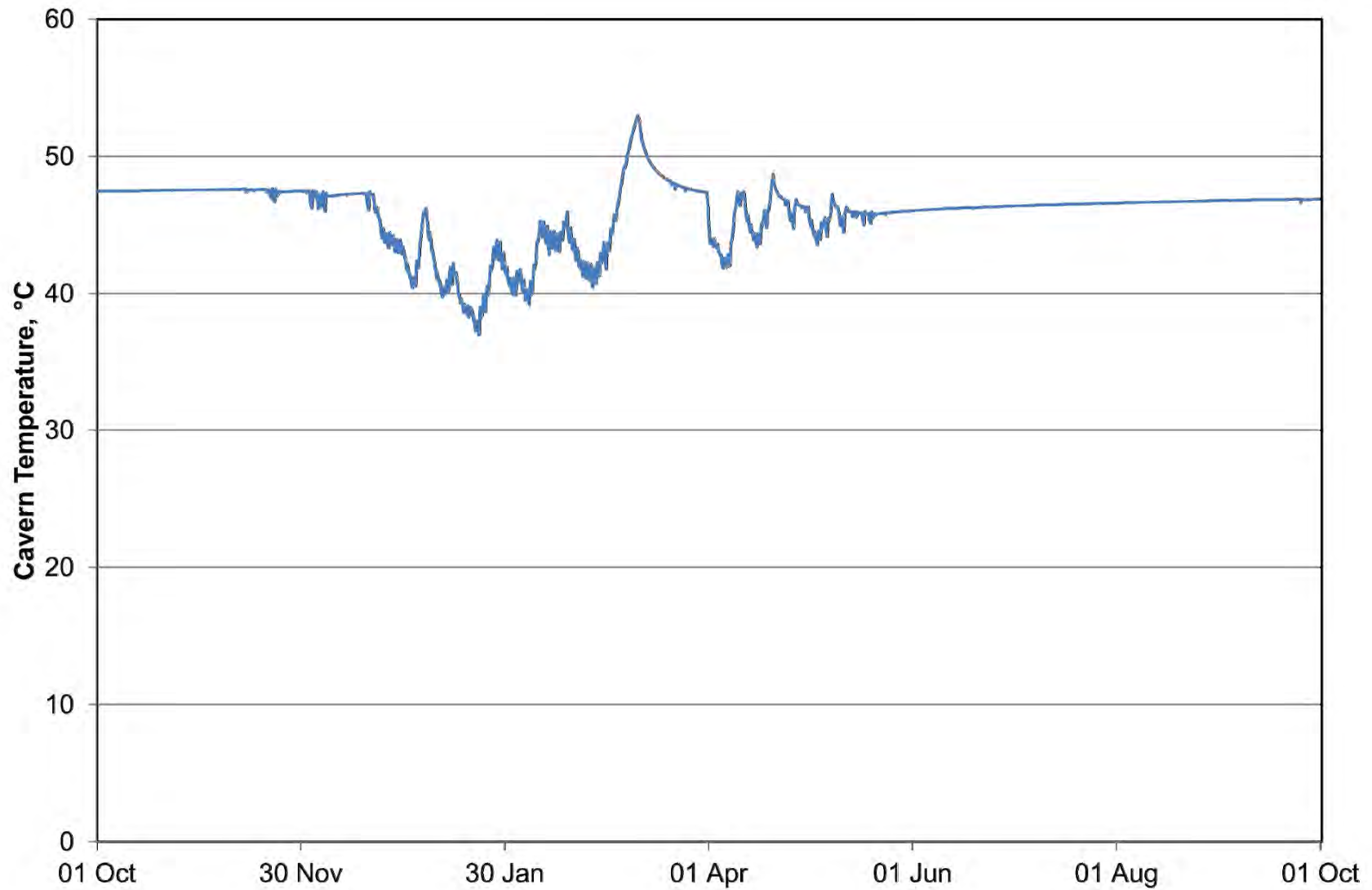


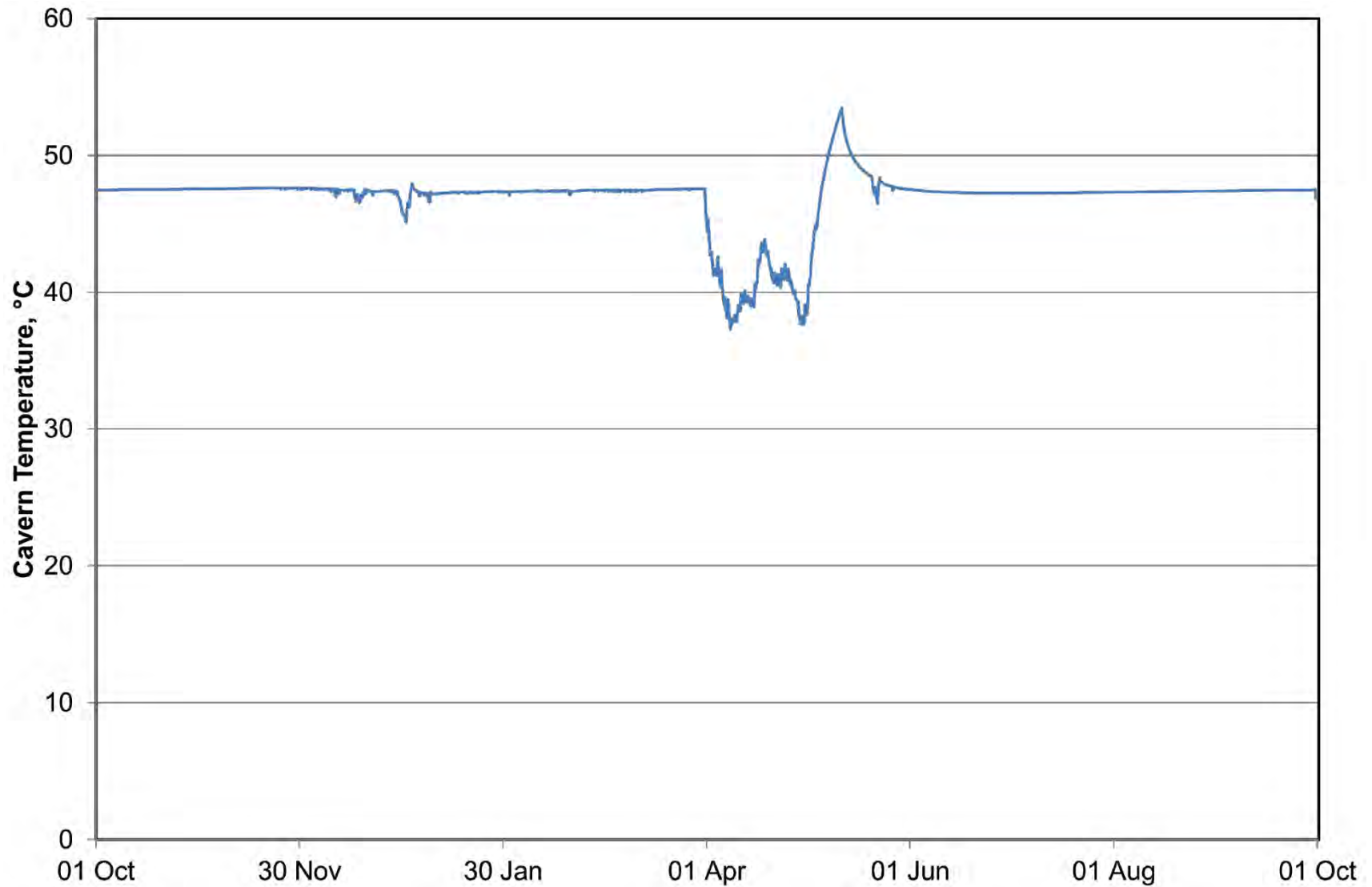
Institut für
Gebirgsmechanik GmbH
2019

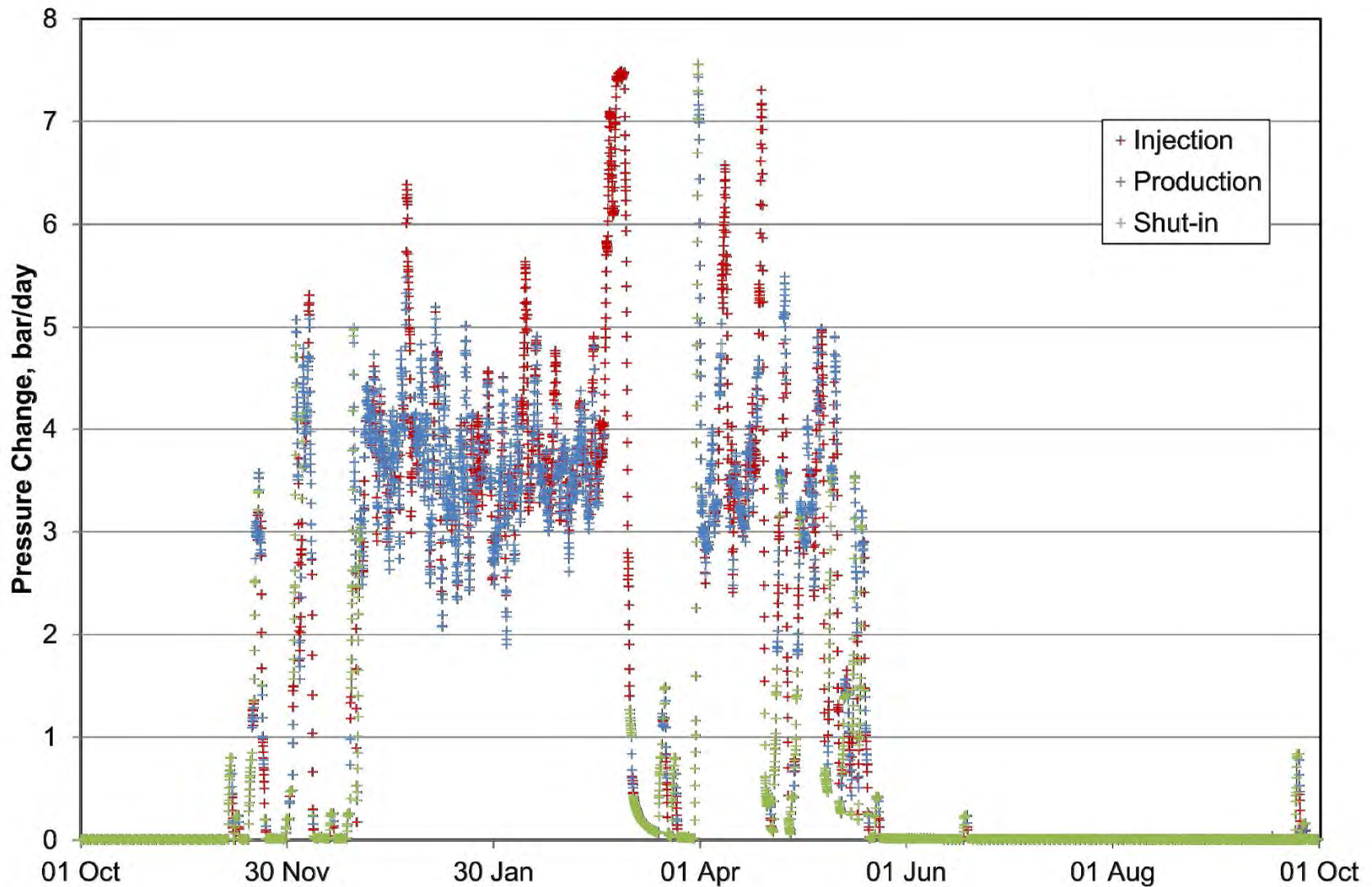


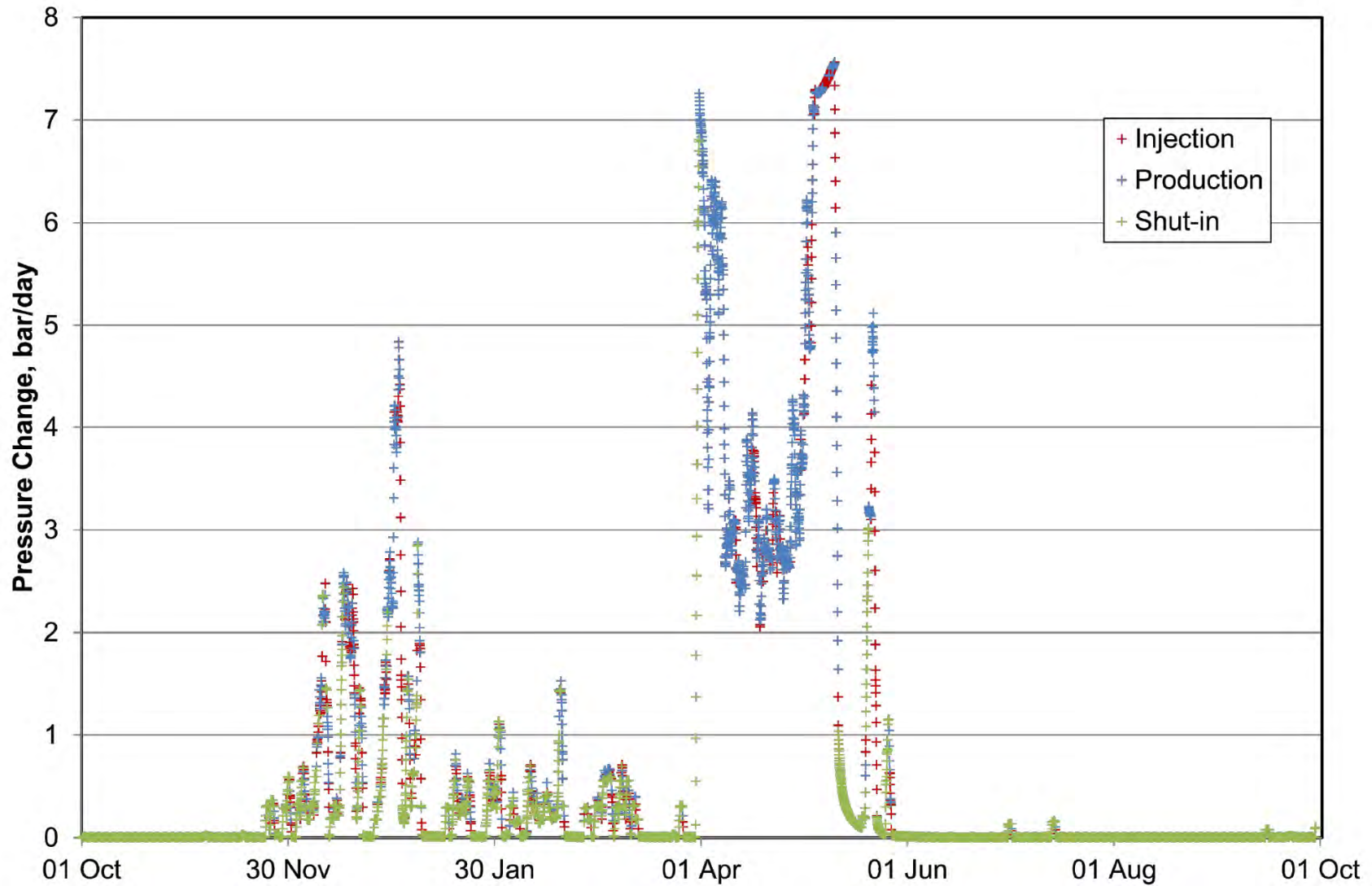
Calculated wellhead pressure for a yearly cycle according to
scenario B

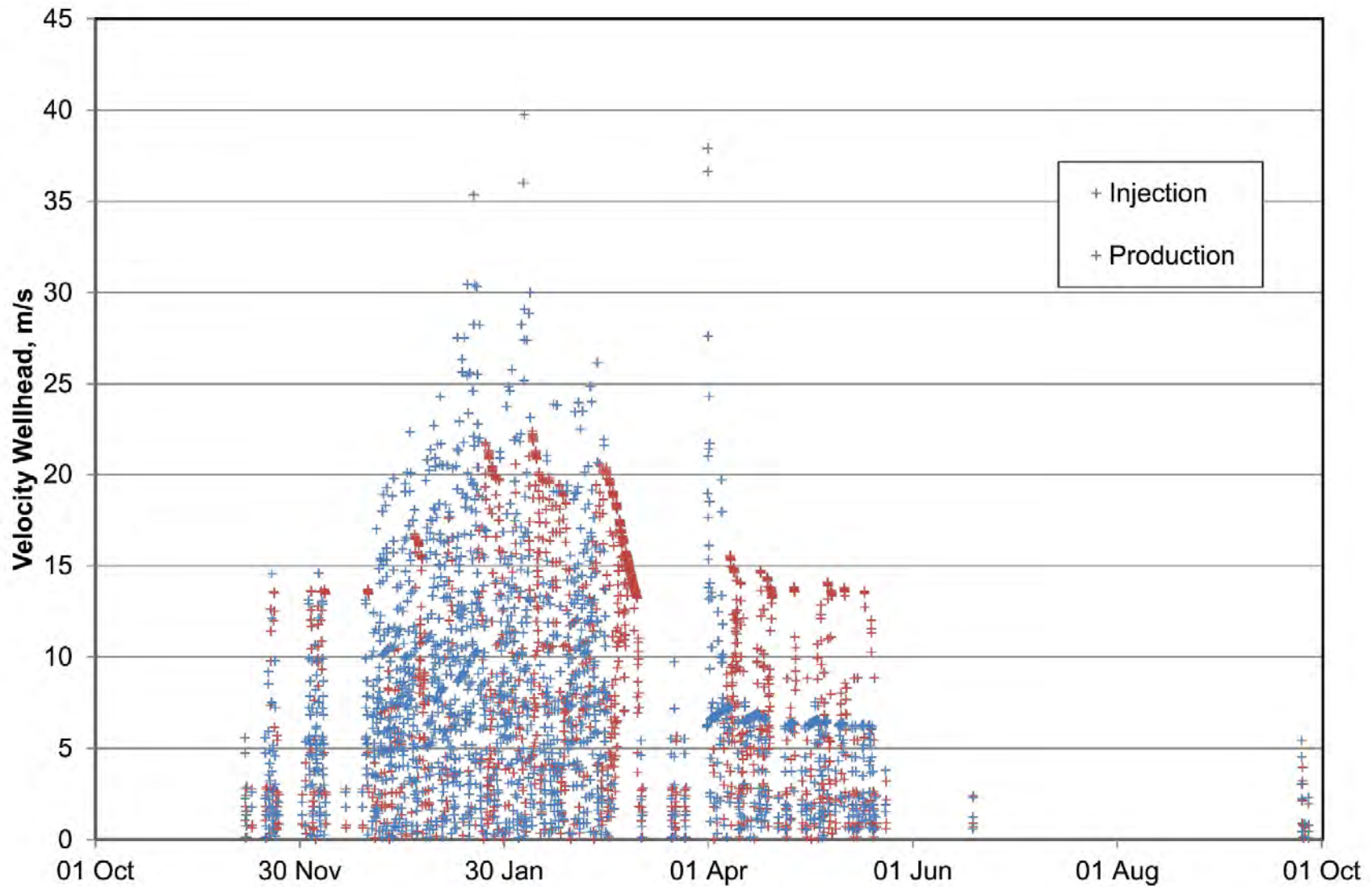
Enclosure 1.10

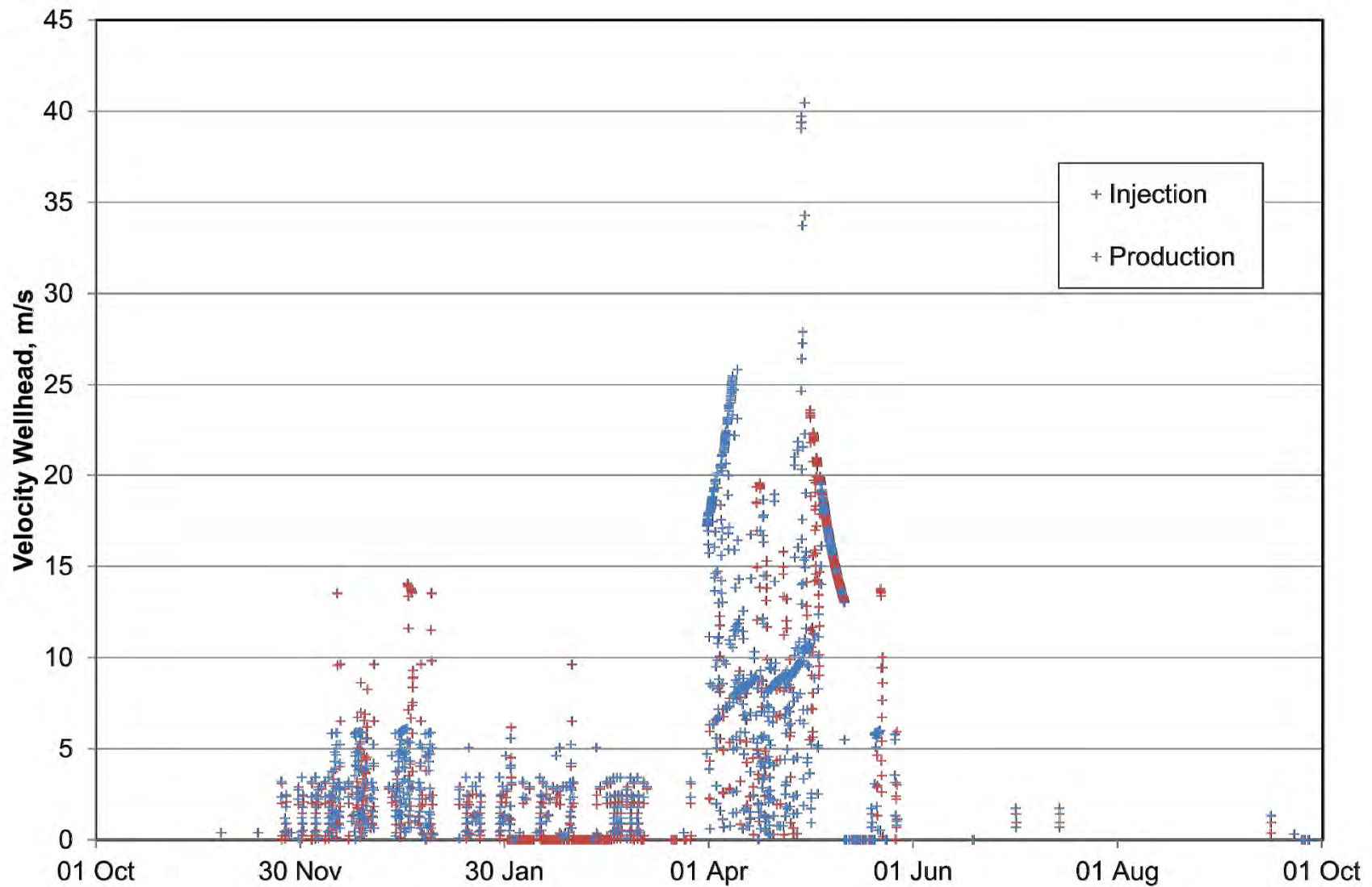


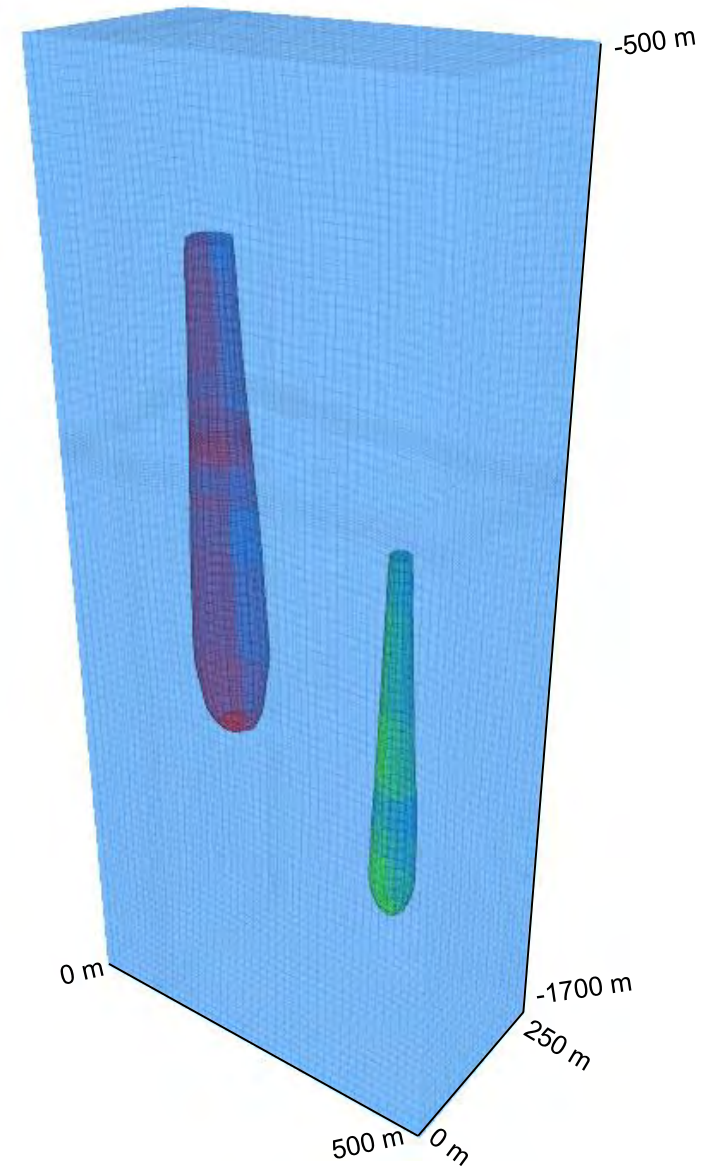
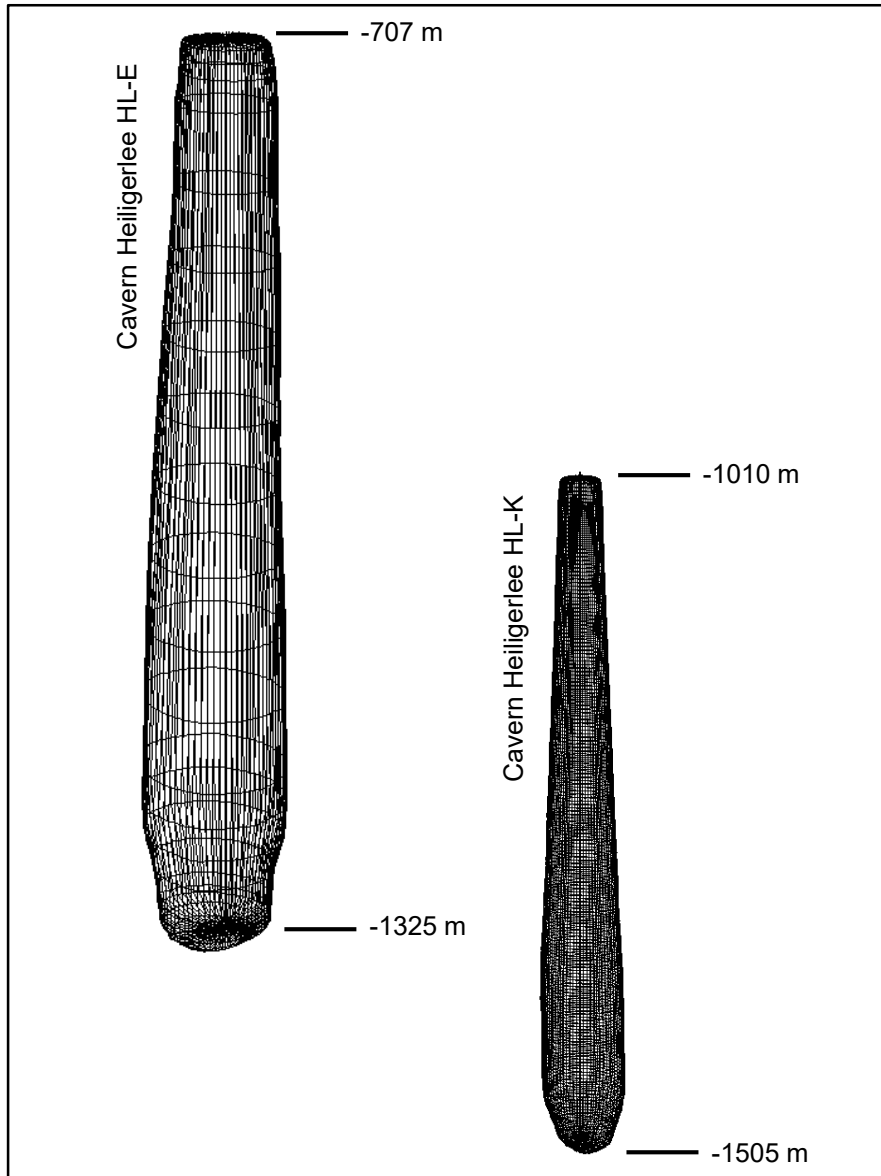




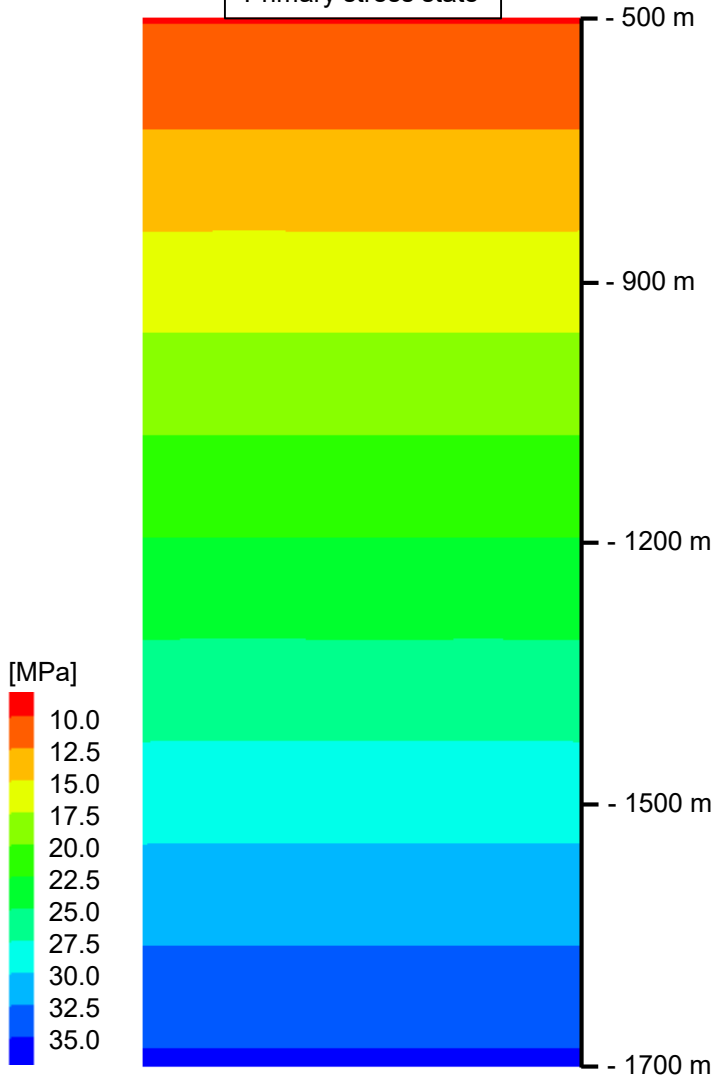






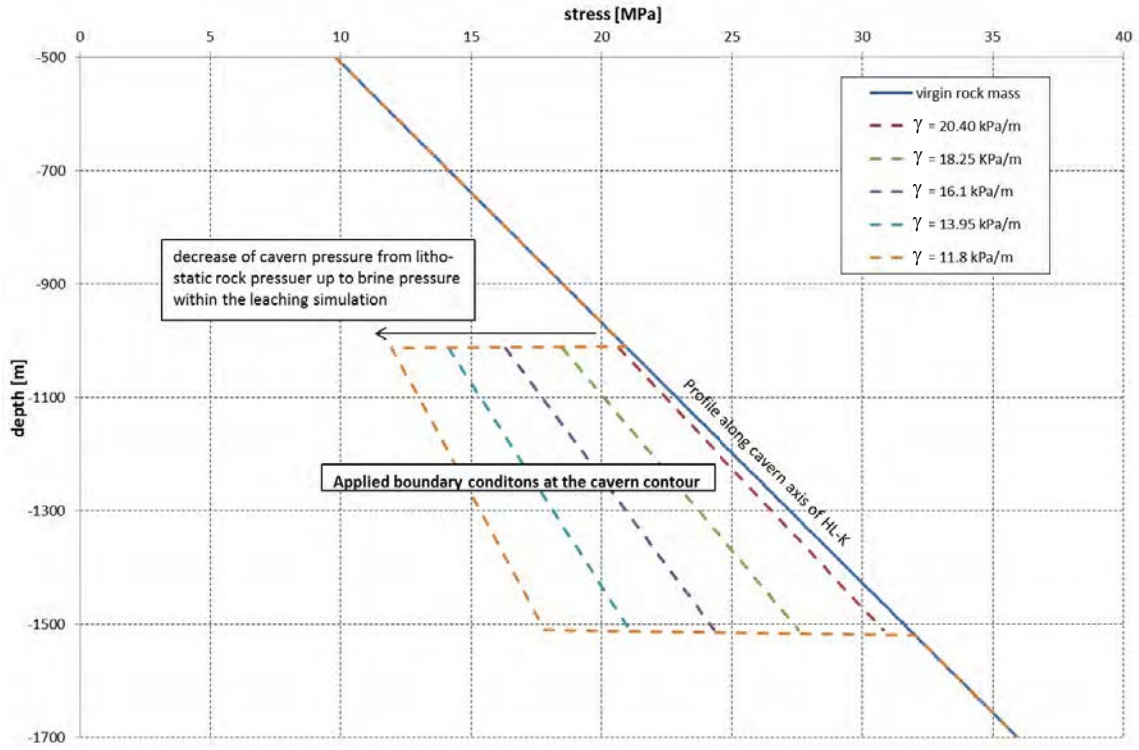


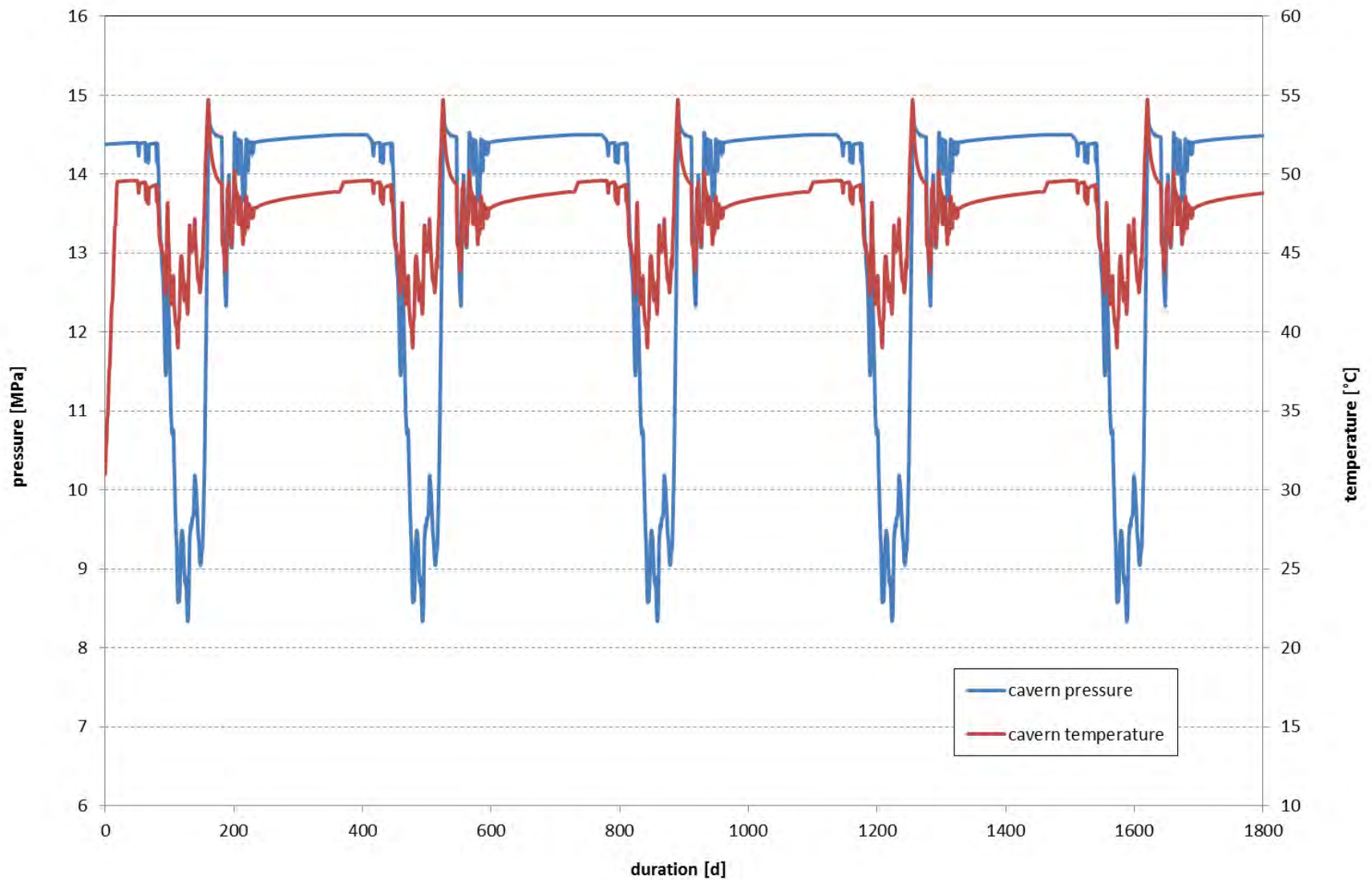
Primary stress state

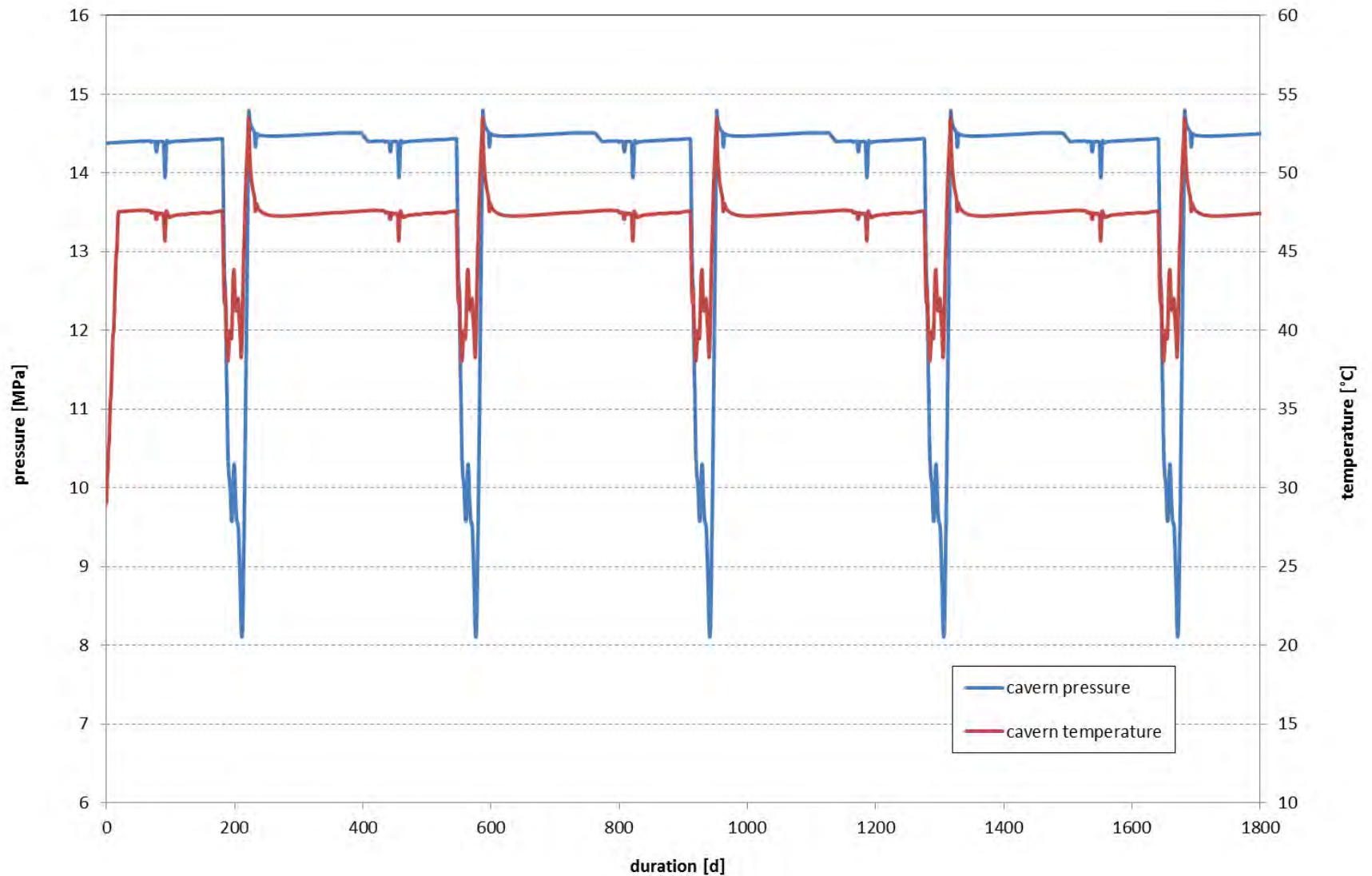


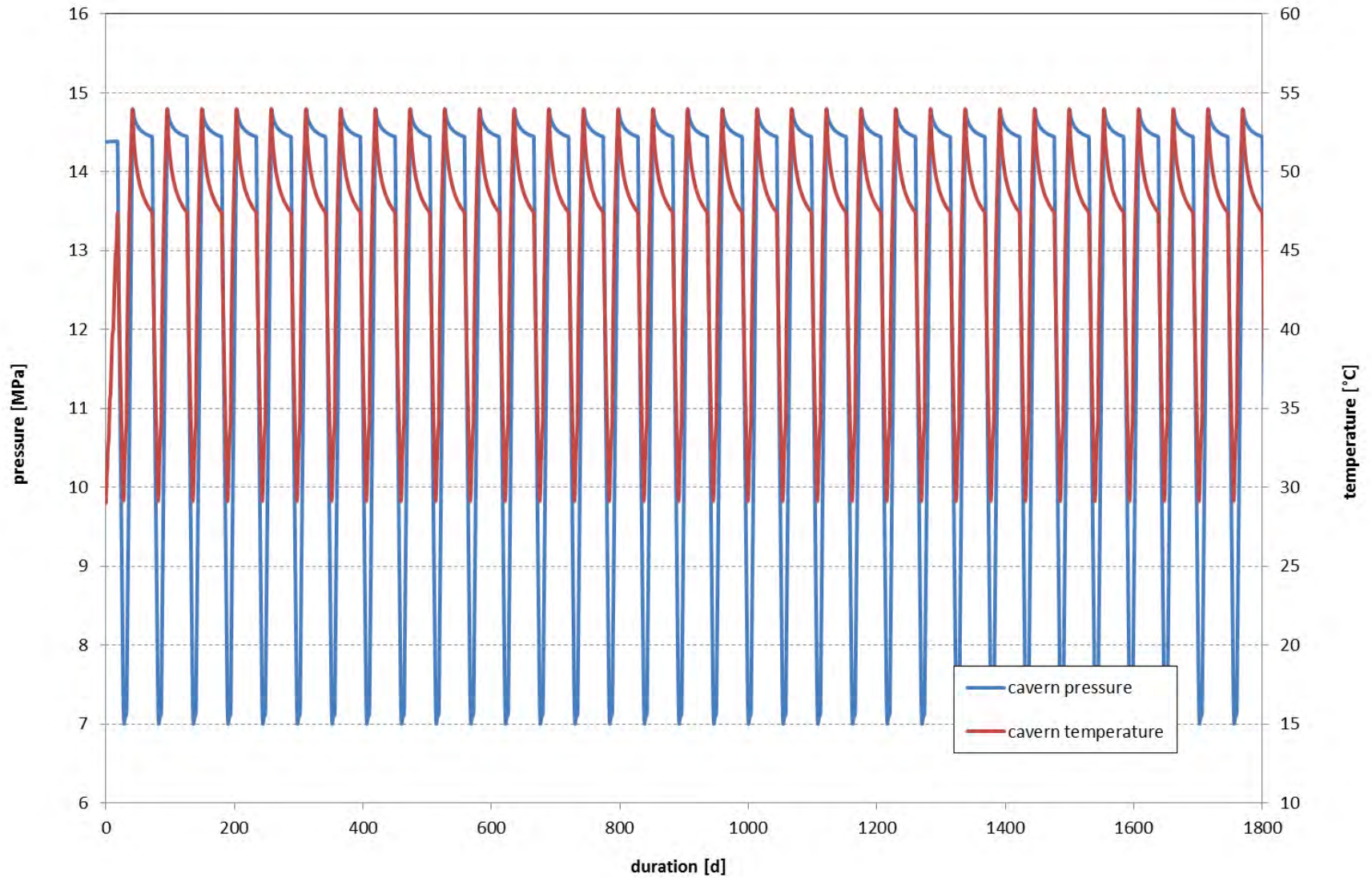
Boundary conditions of HL-K during leaching simulation

At the beginning of the leaching period the mesh elements of the whole cavern were excavated!!

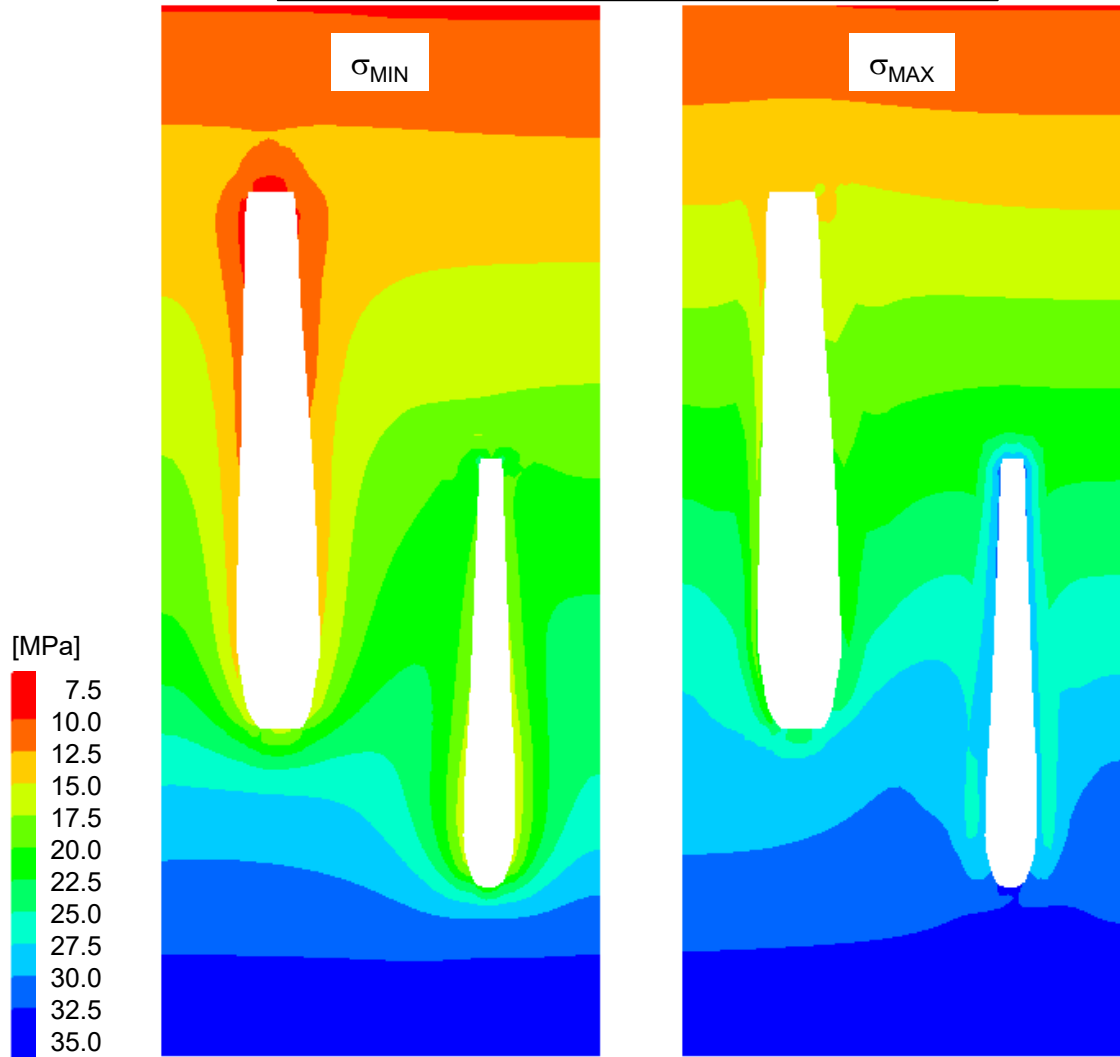




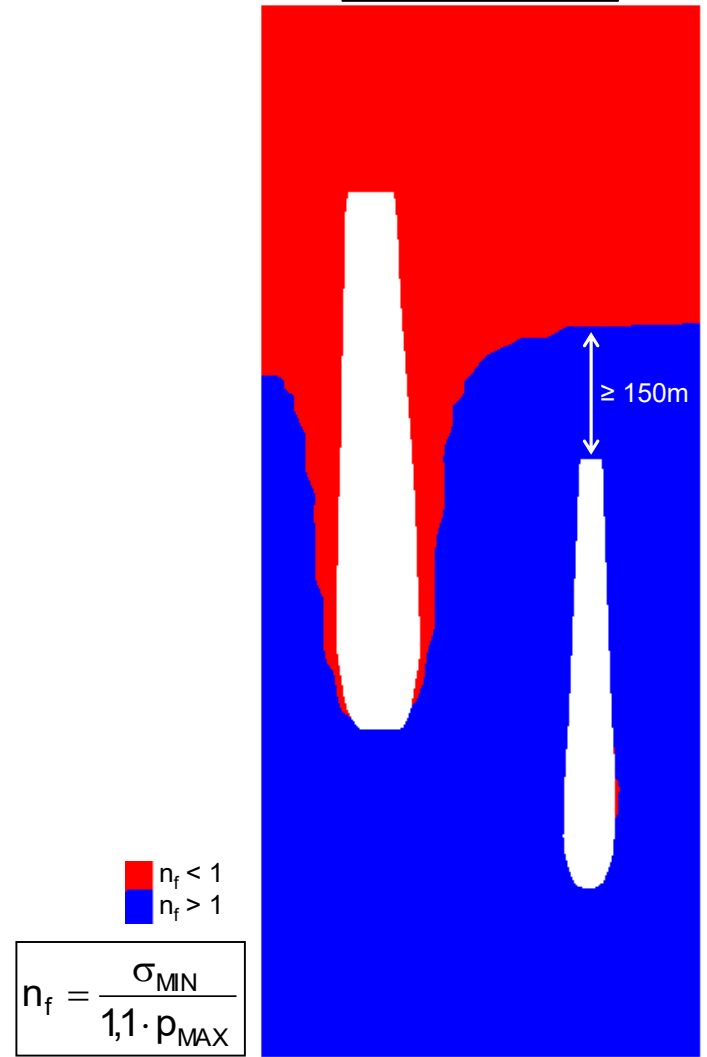




Principal stress distribution at maximum storage pressure

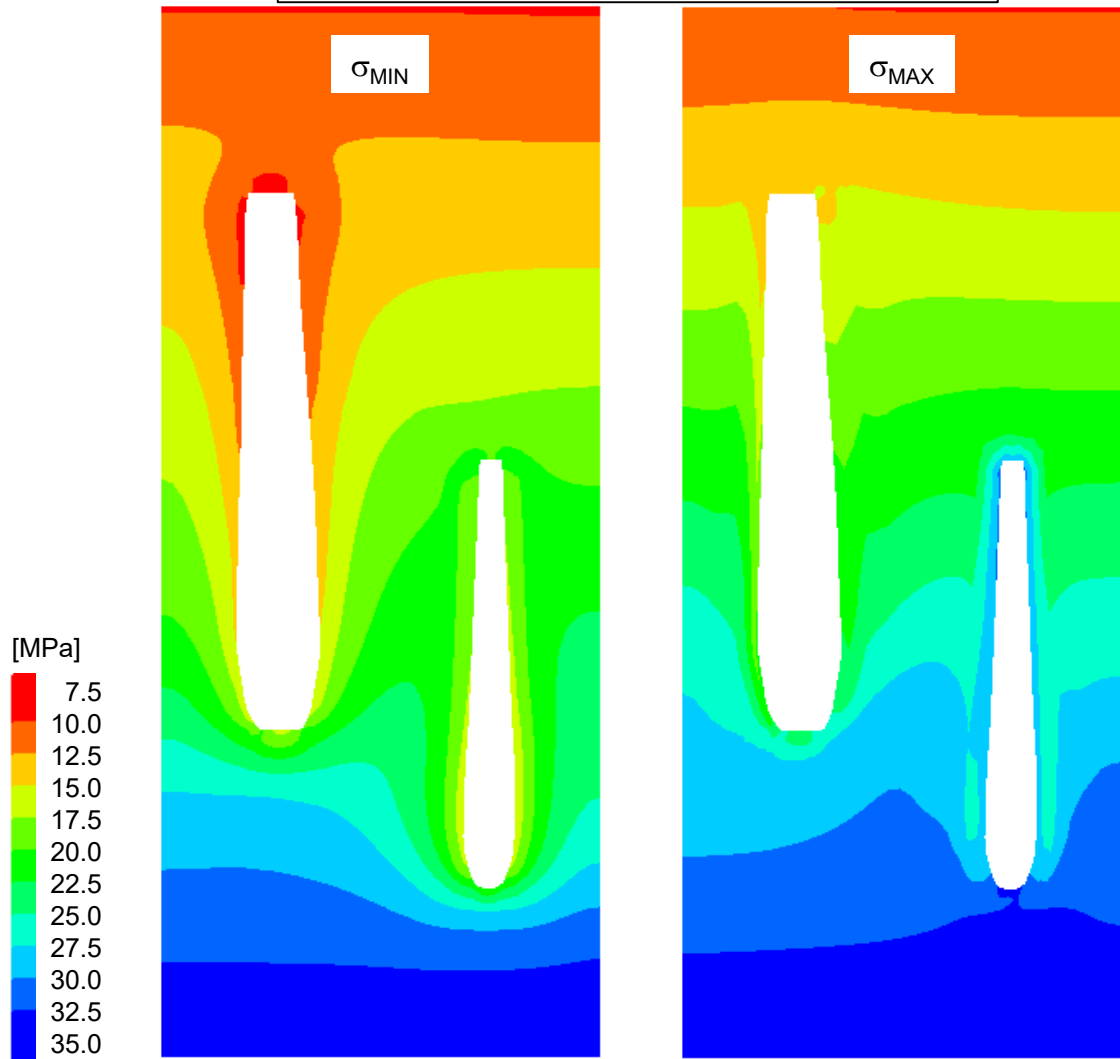


Assessment of p_{MAX}

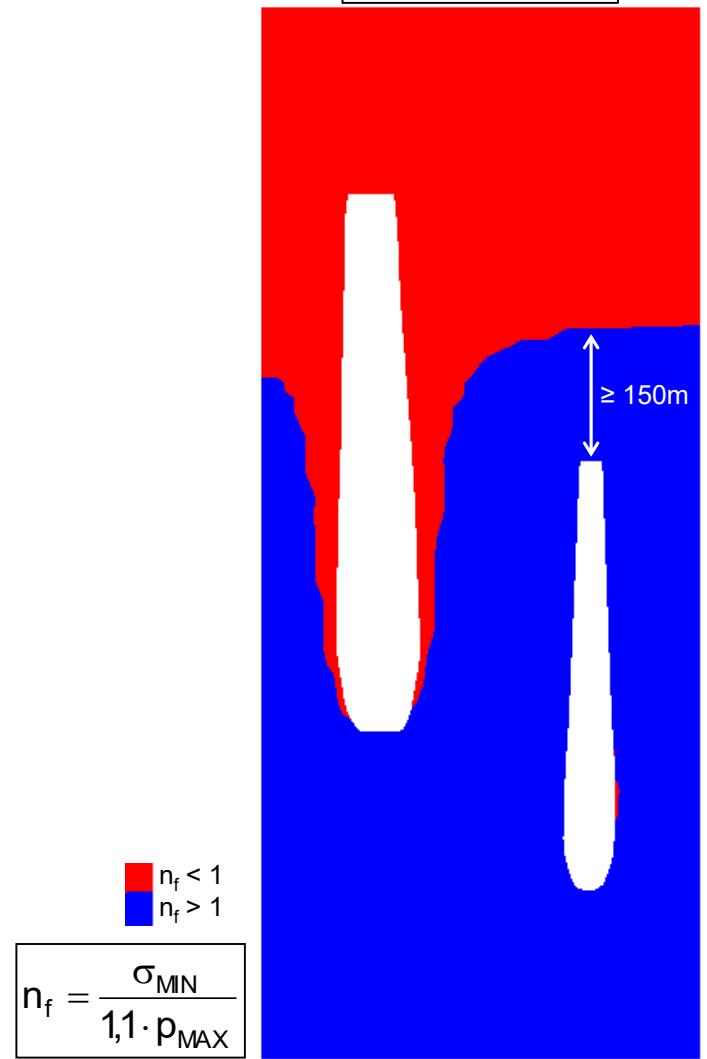


$$n_f = \frac{\sigma_{MIN}}{1,1 \cdot p_{MAX}}$$

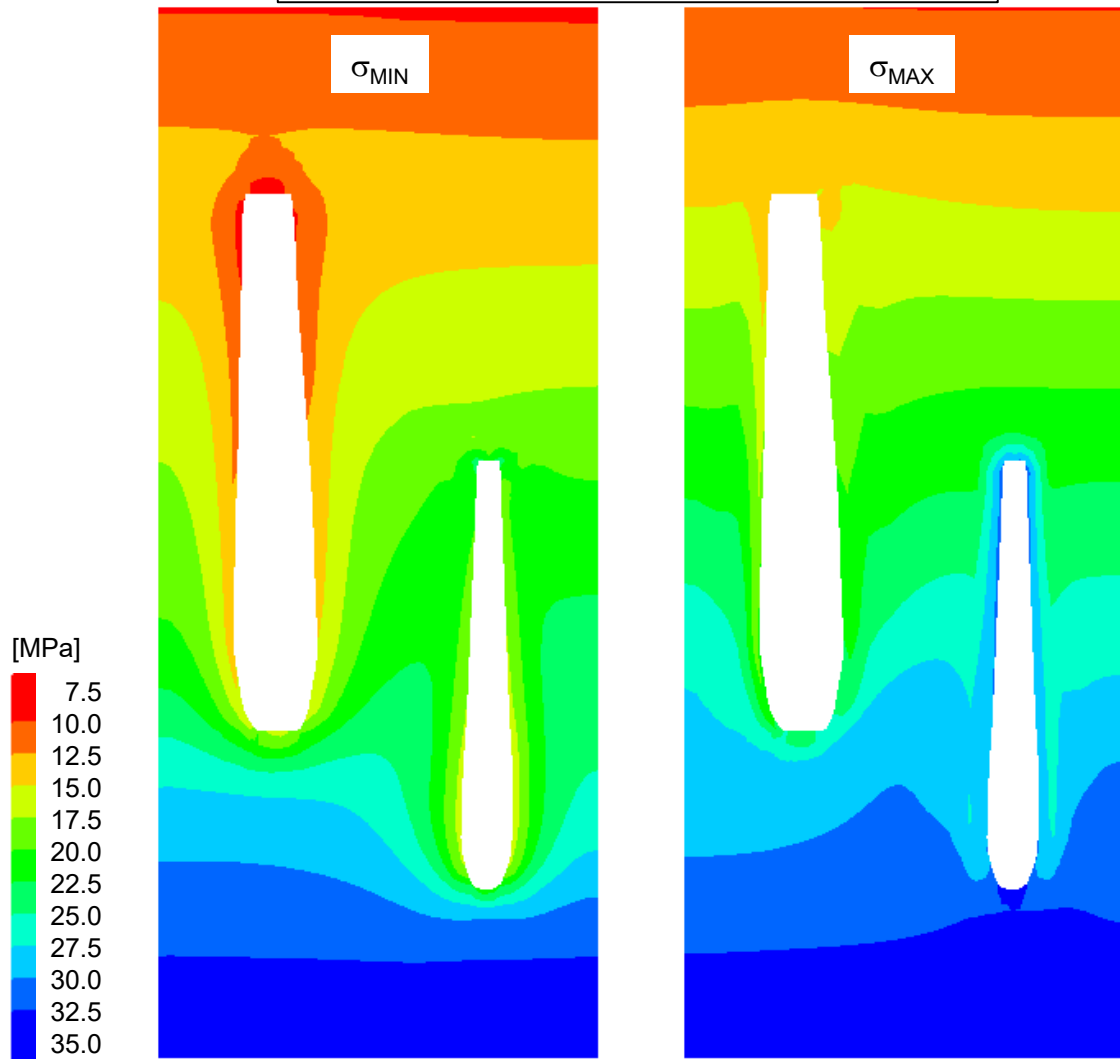
Principal stress distribution at maximum storage pressure



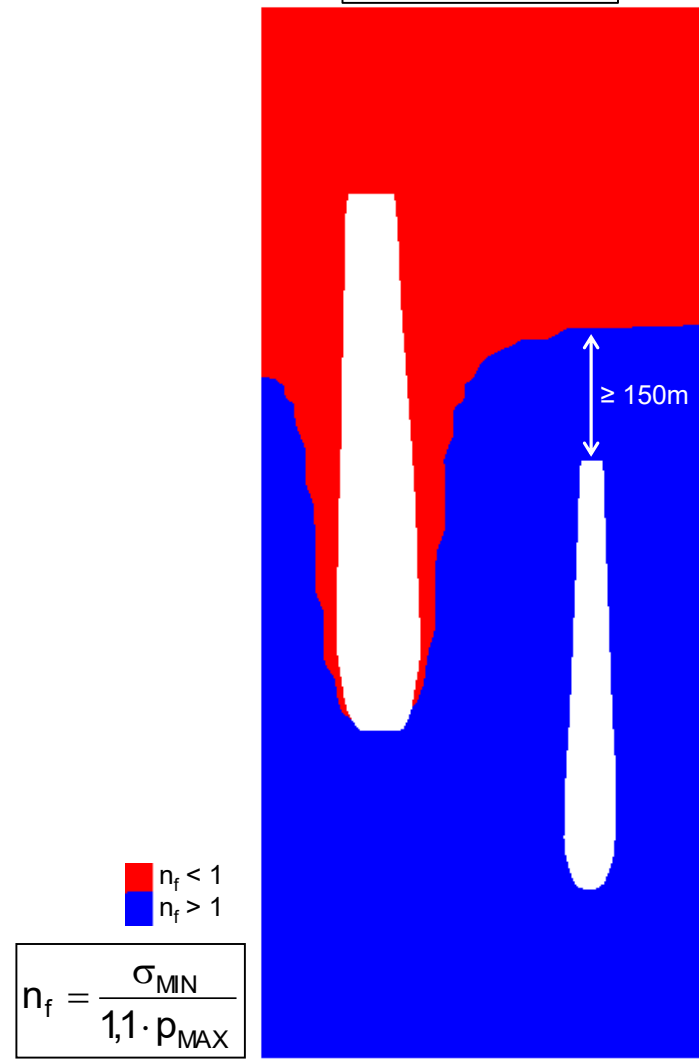
Assessment of p_{MAX}



Principal stress distribution at maximum storage pressure

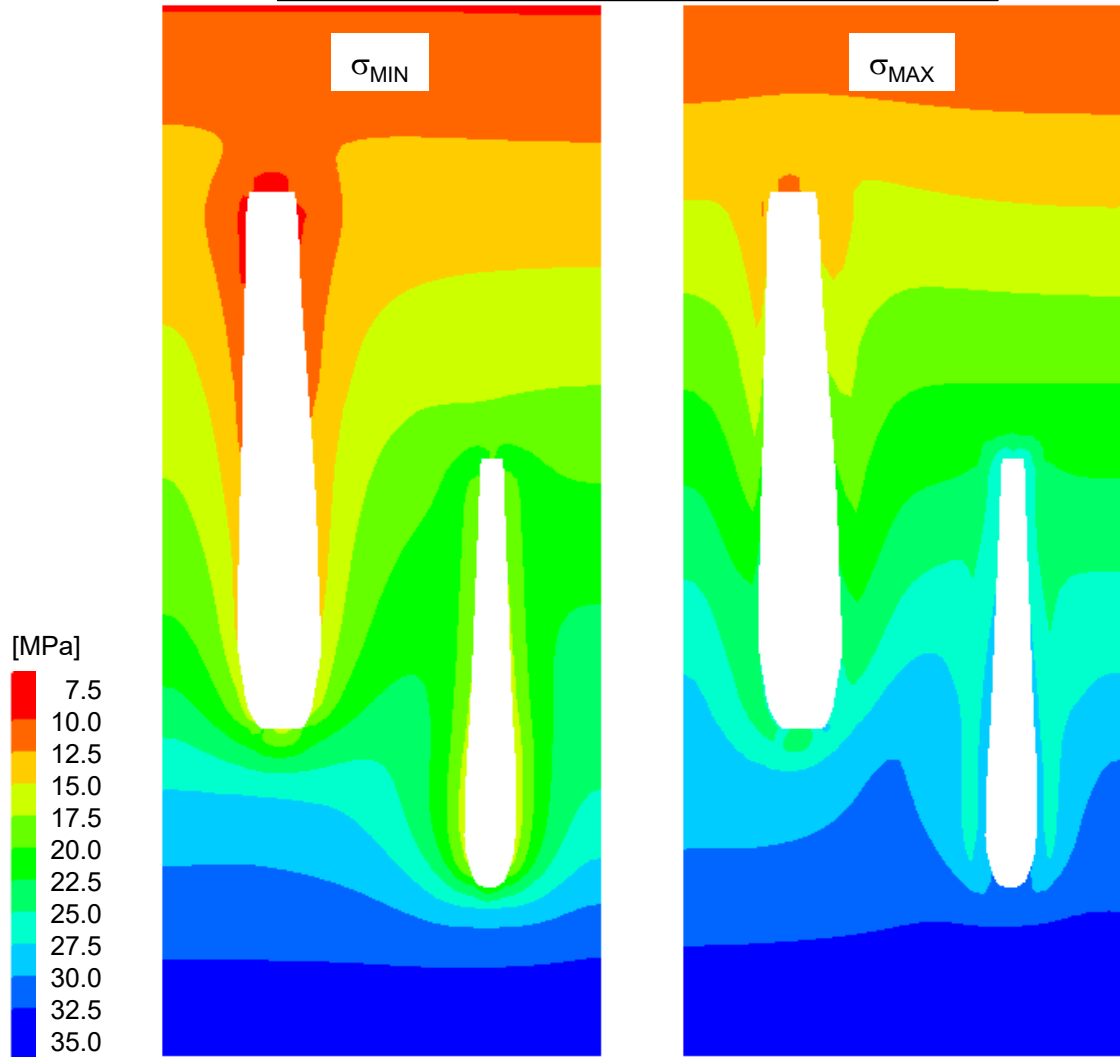


Assessment of p_{MAX}

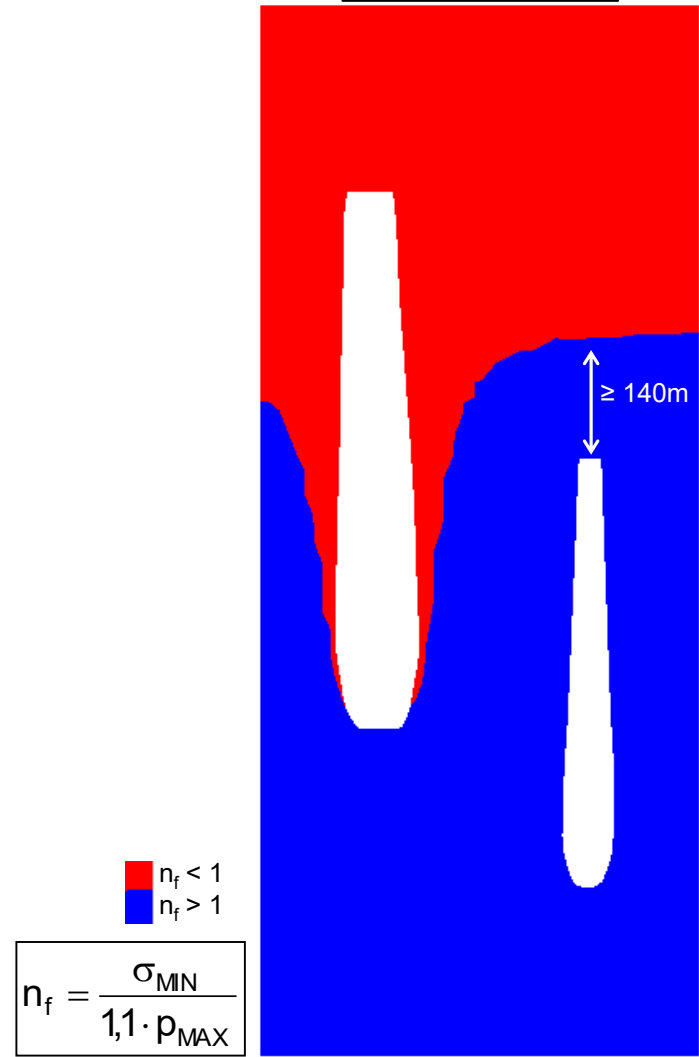


$$n_f = \frac{\sigma_{MIN}}{1,1 \cdot p_{MAX}}$$

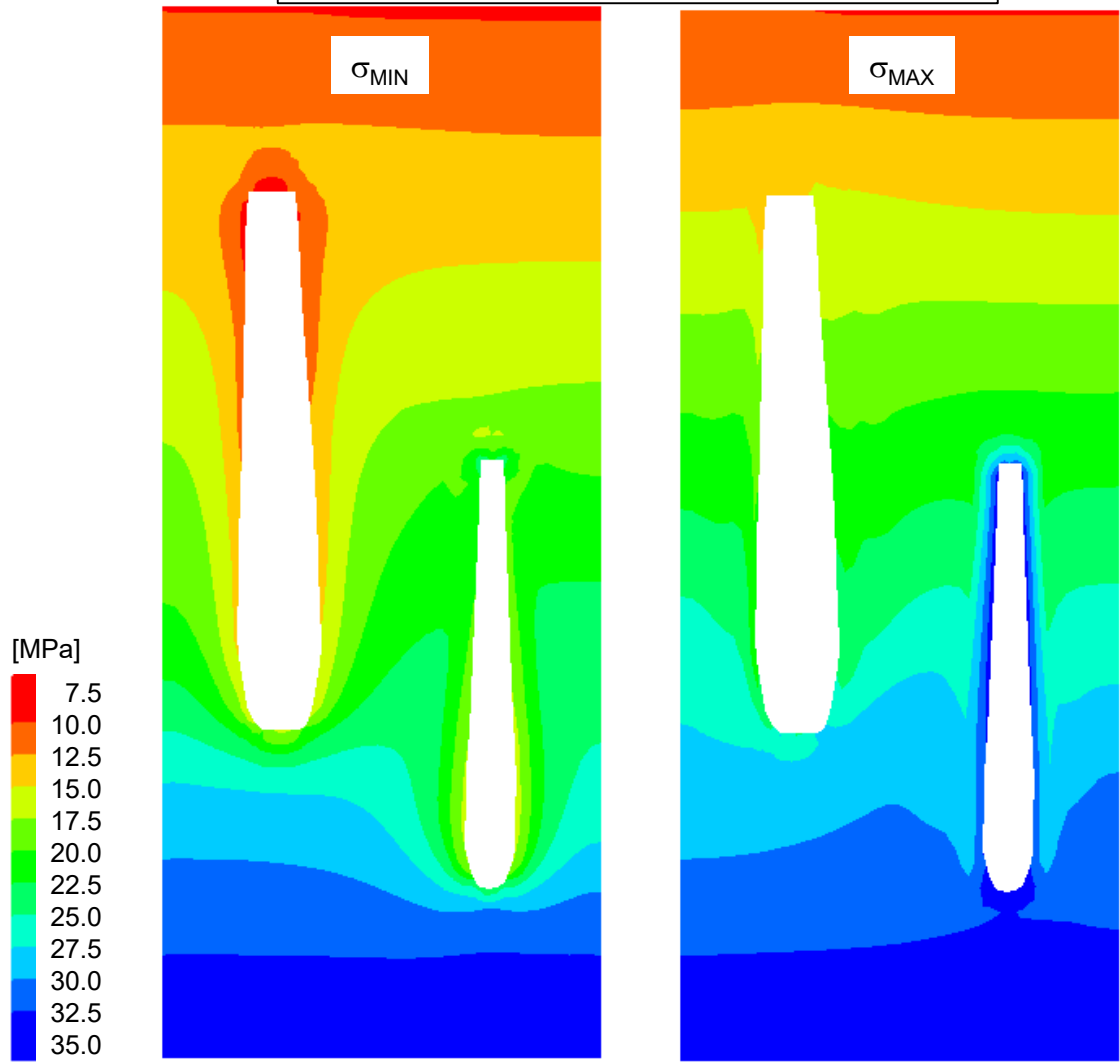
Principal stress distribution at maximum storage pressure



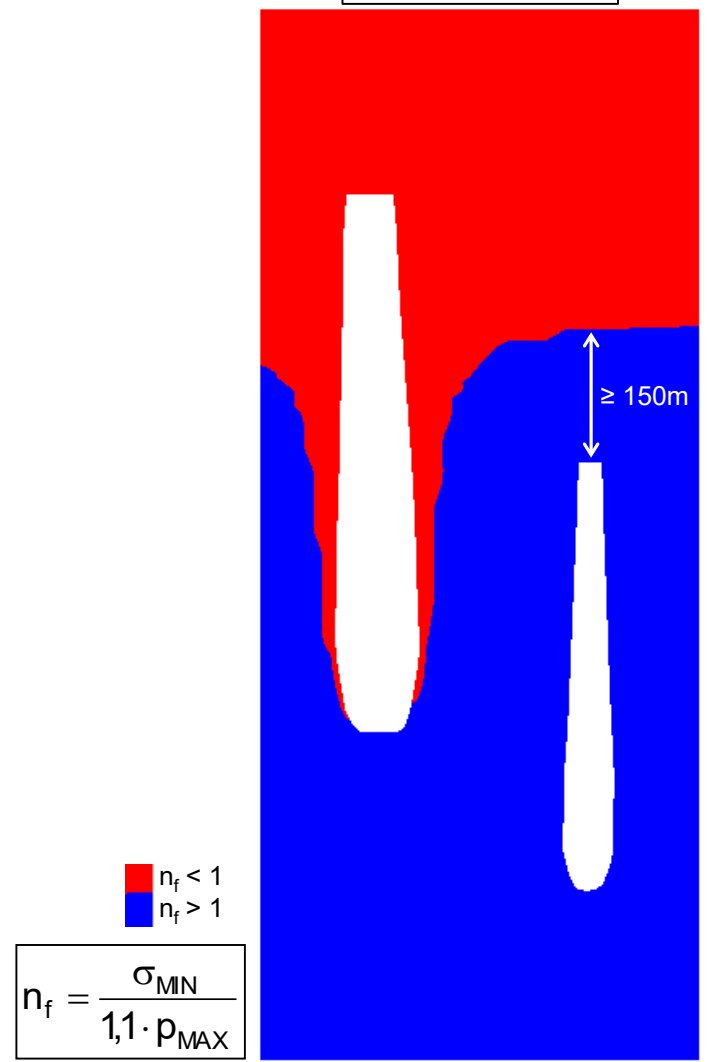
Assessment of p_{MAX}



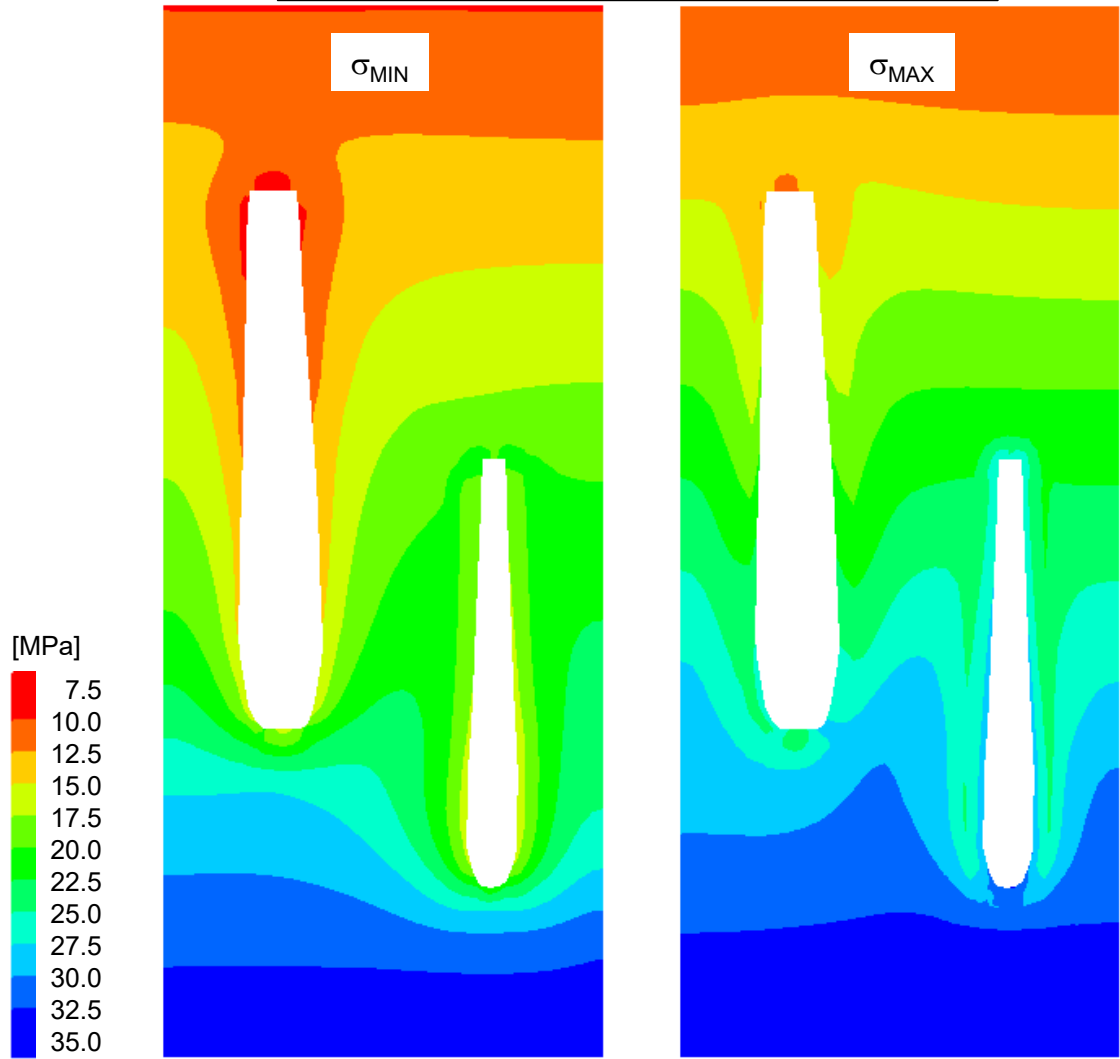
Principal stress distribution at maximum storage pressure



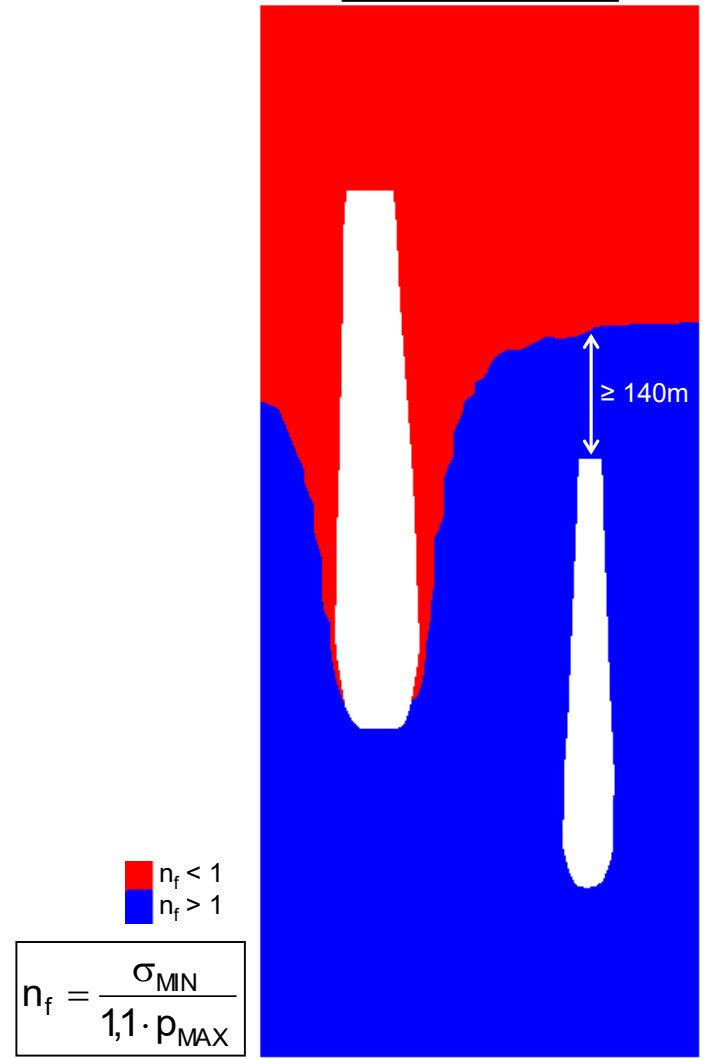
Assessment of p_{MAX}

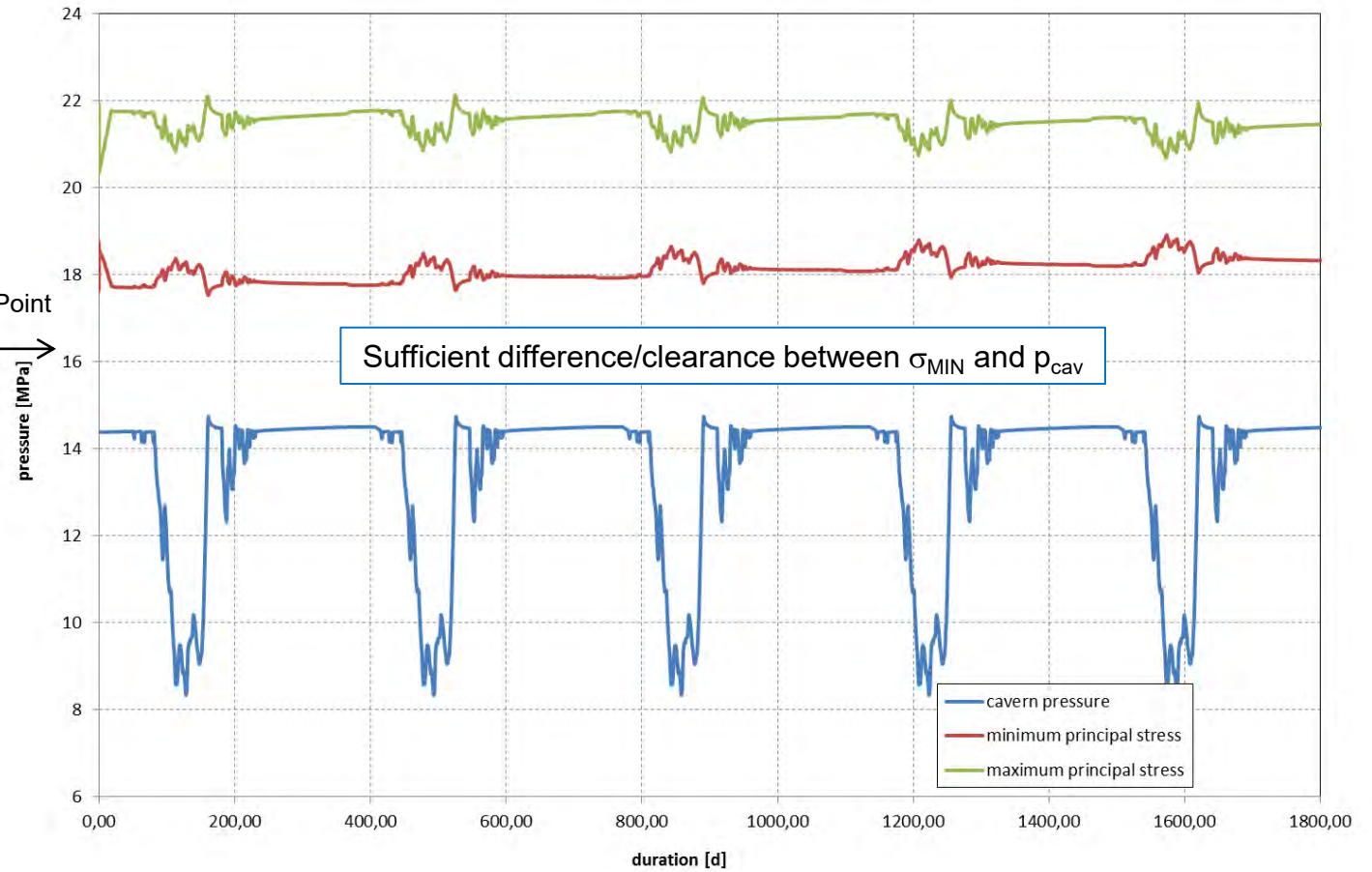
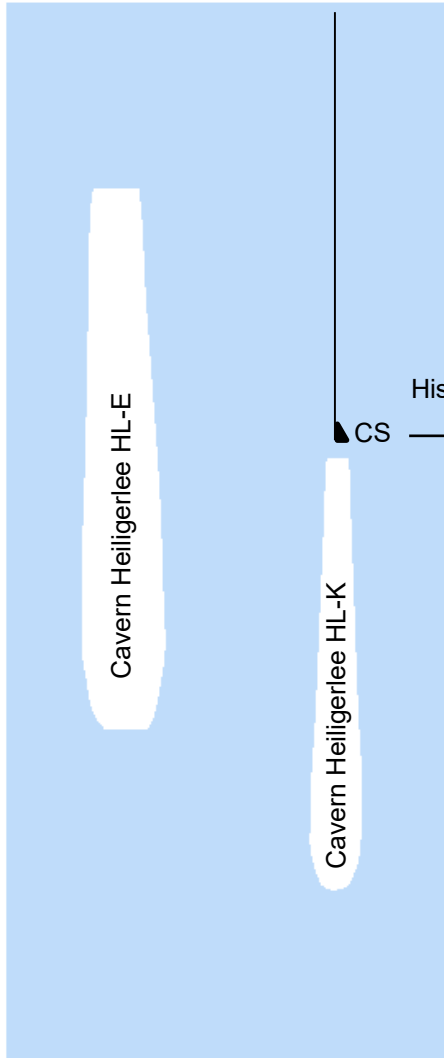


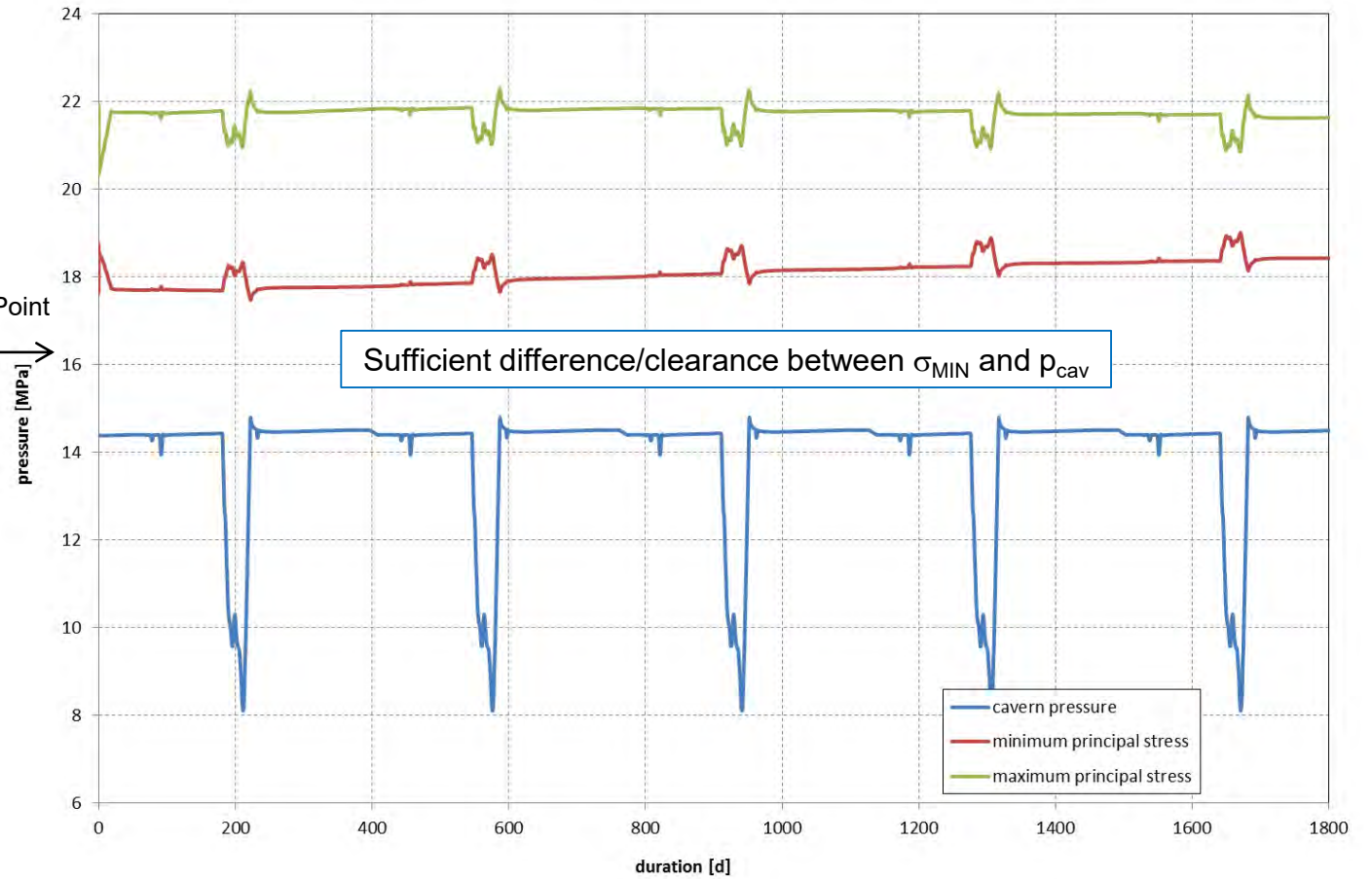
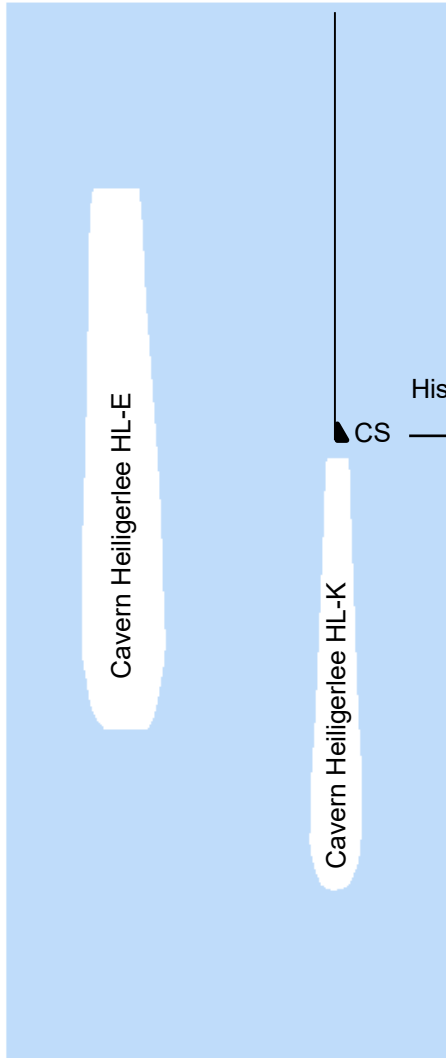
Principal stress distribution at maximum storage pressure

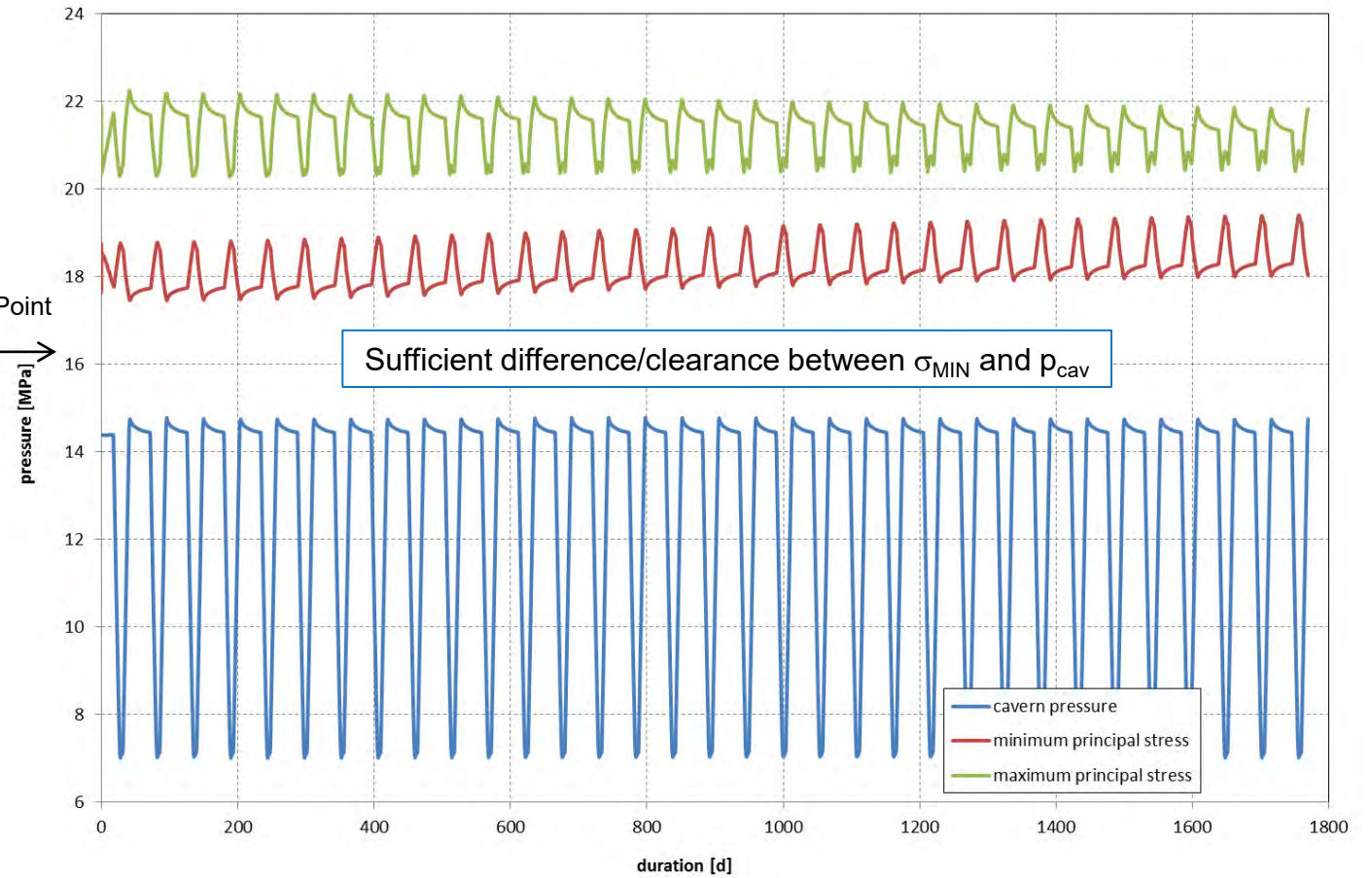
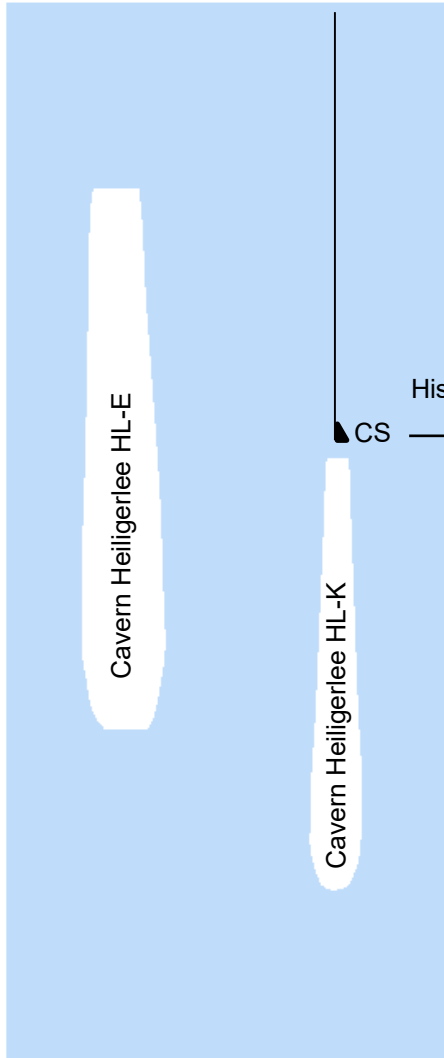


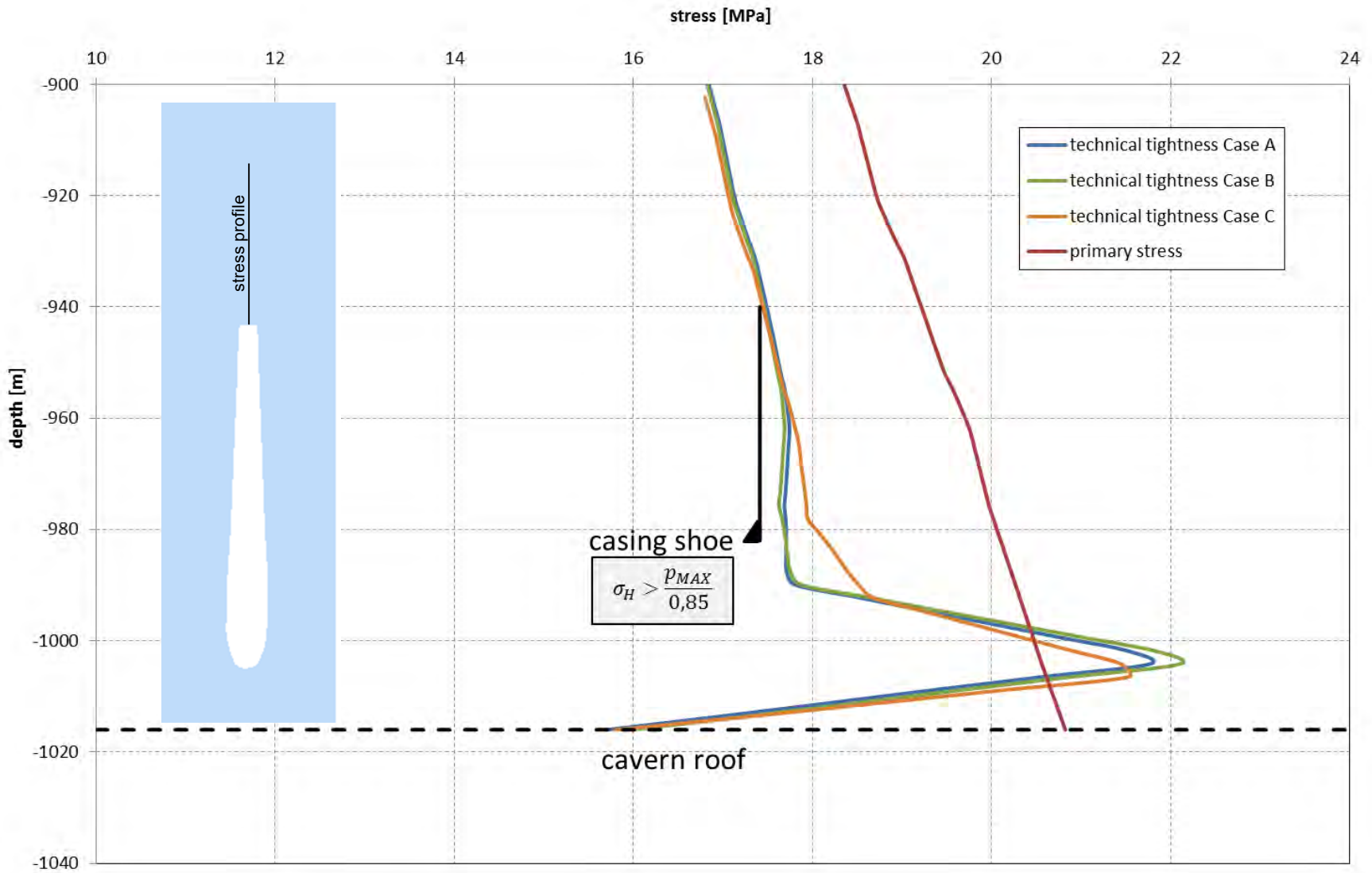
Assessment of p_{MAX}

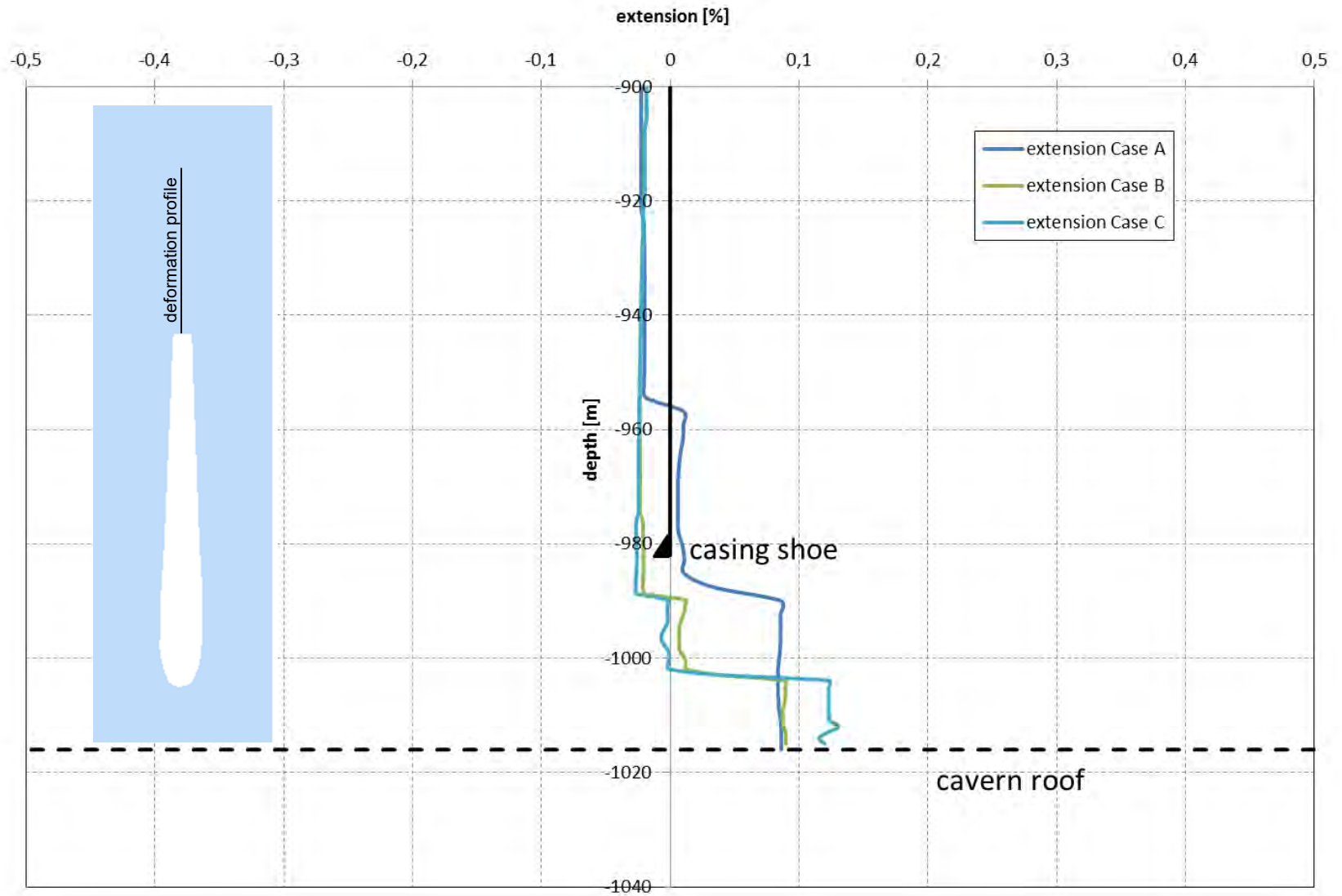


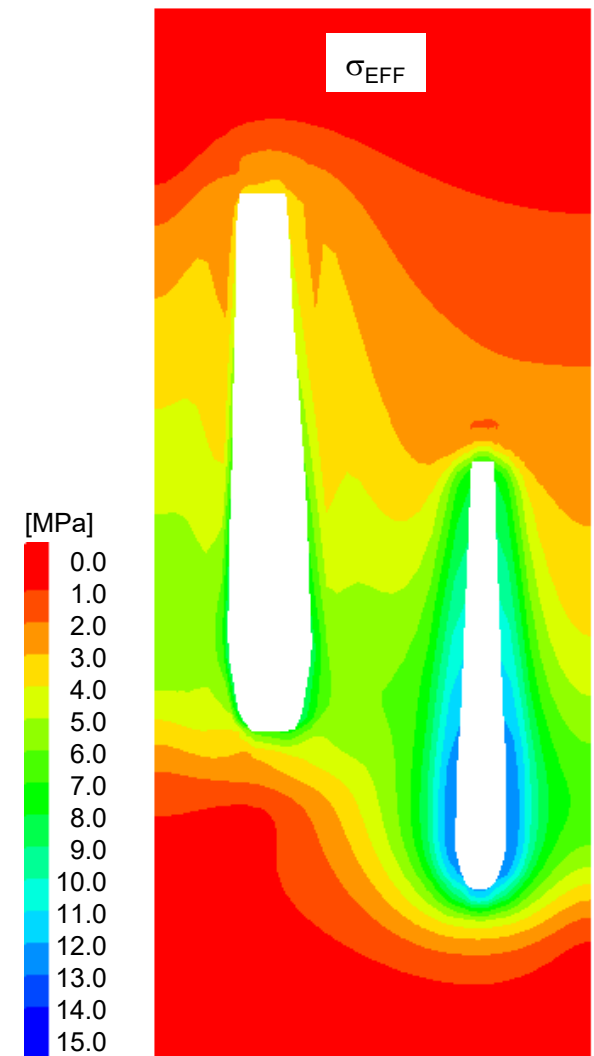
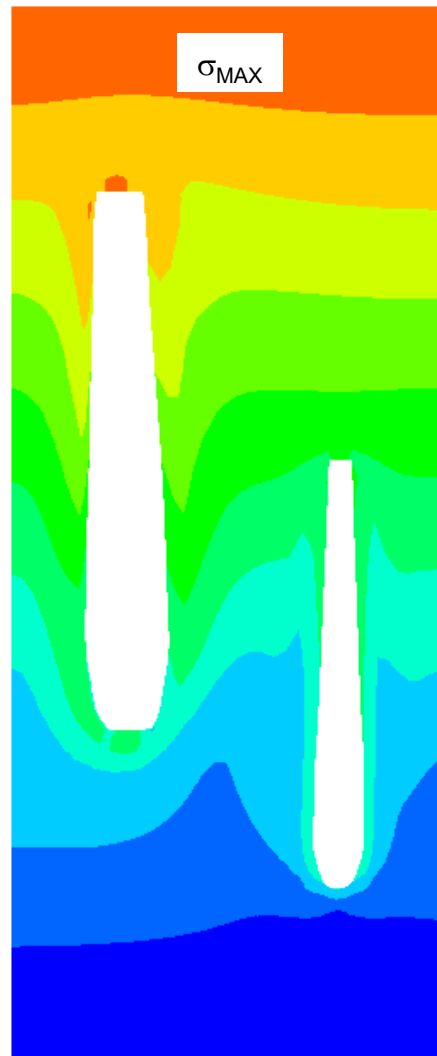
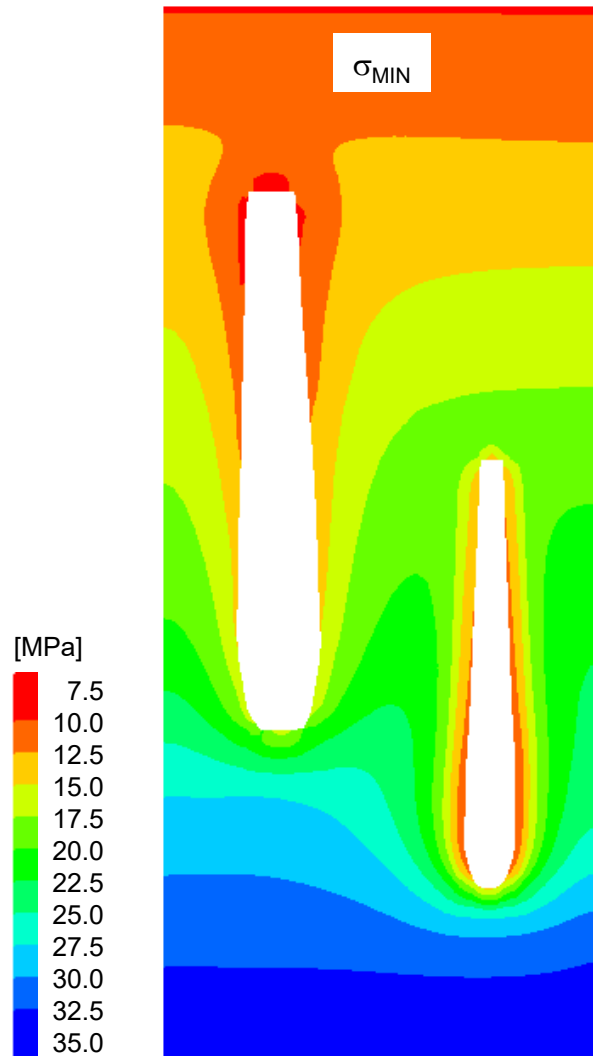


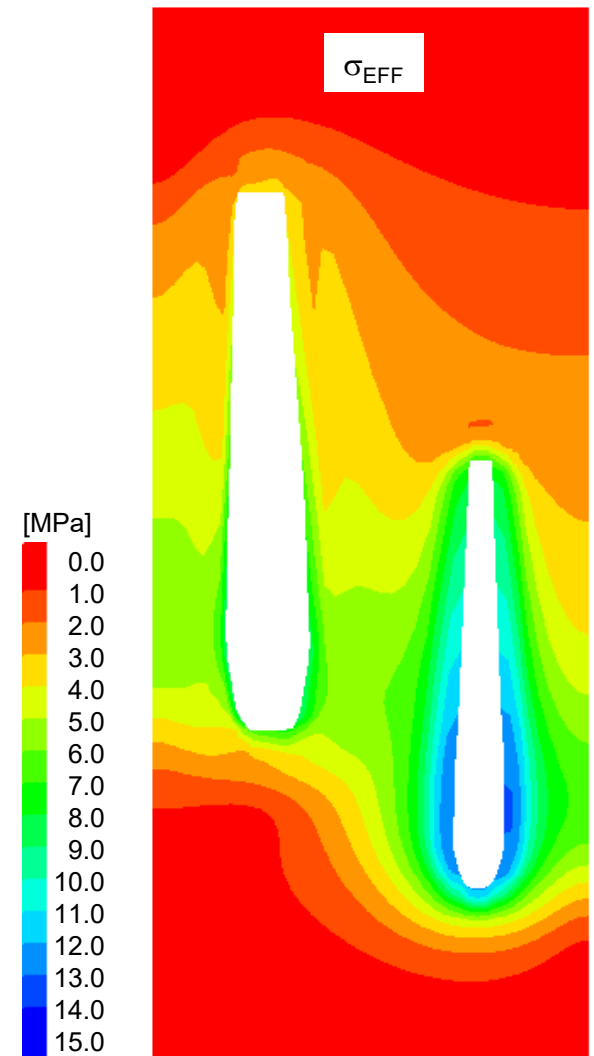
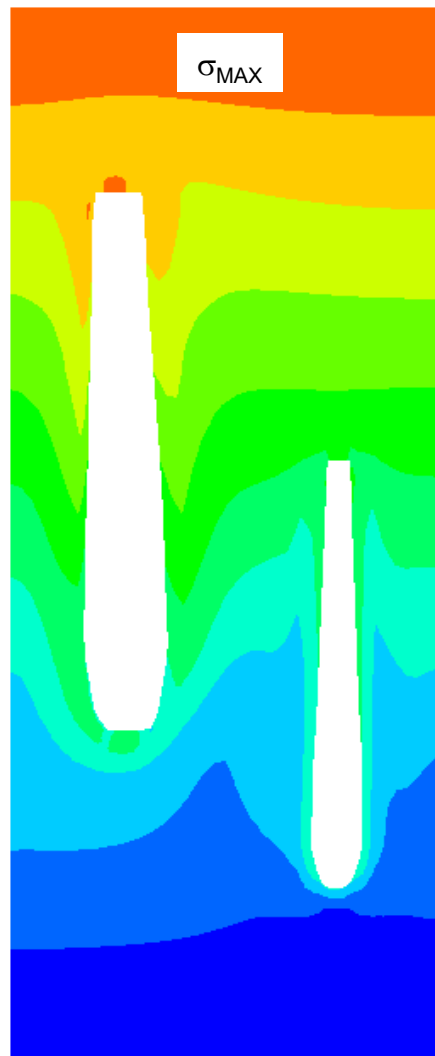
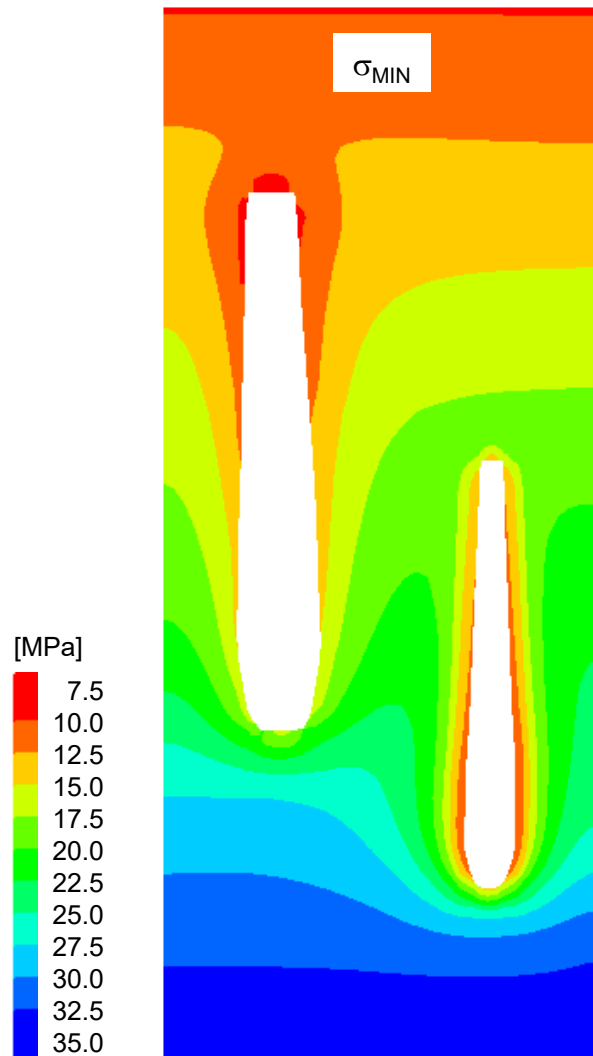


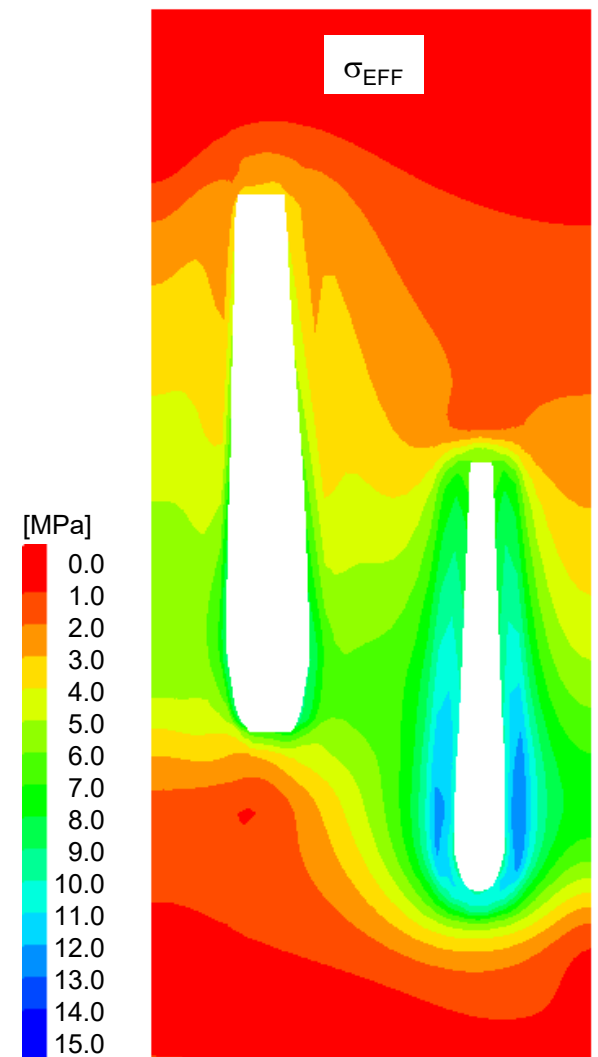
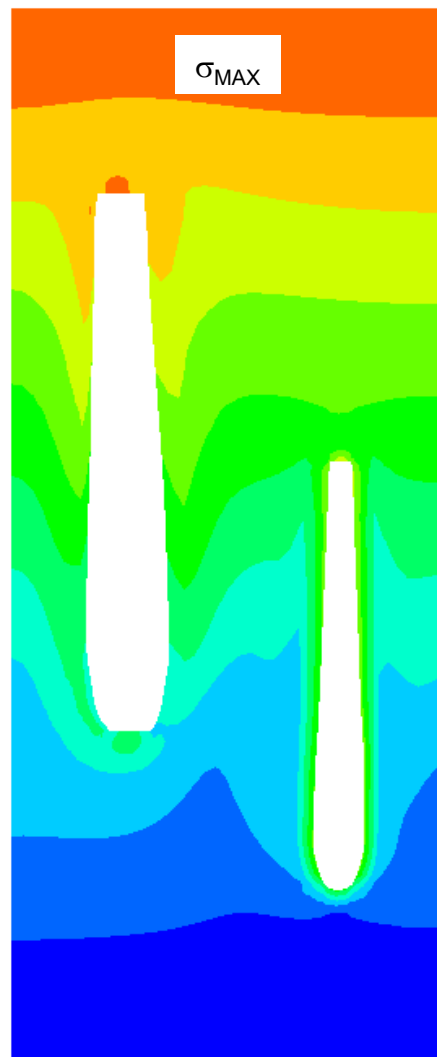
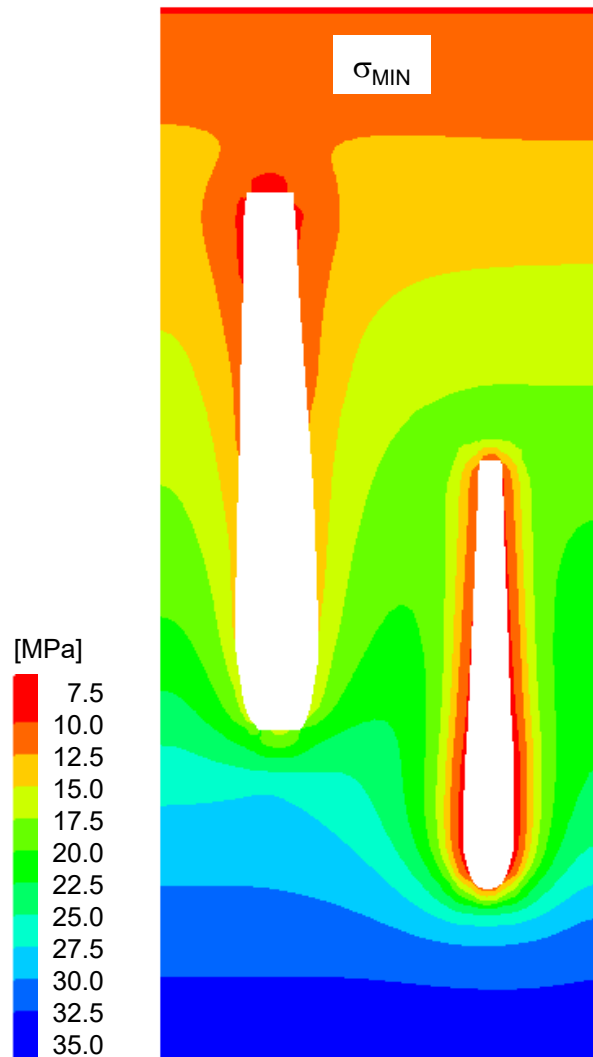


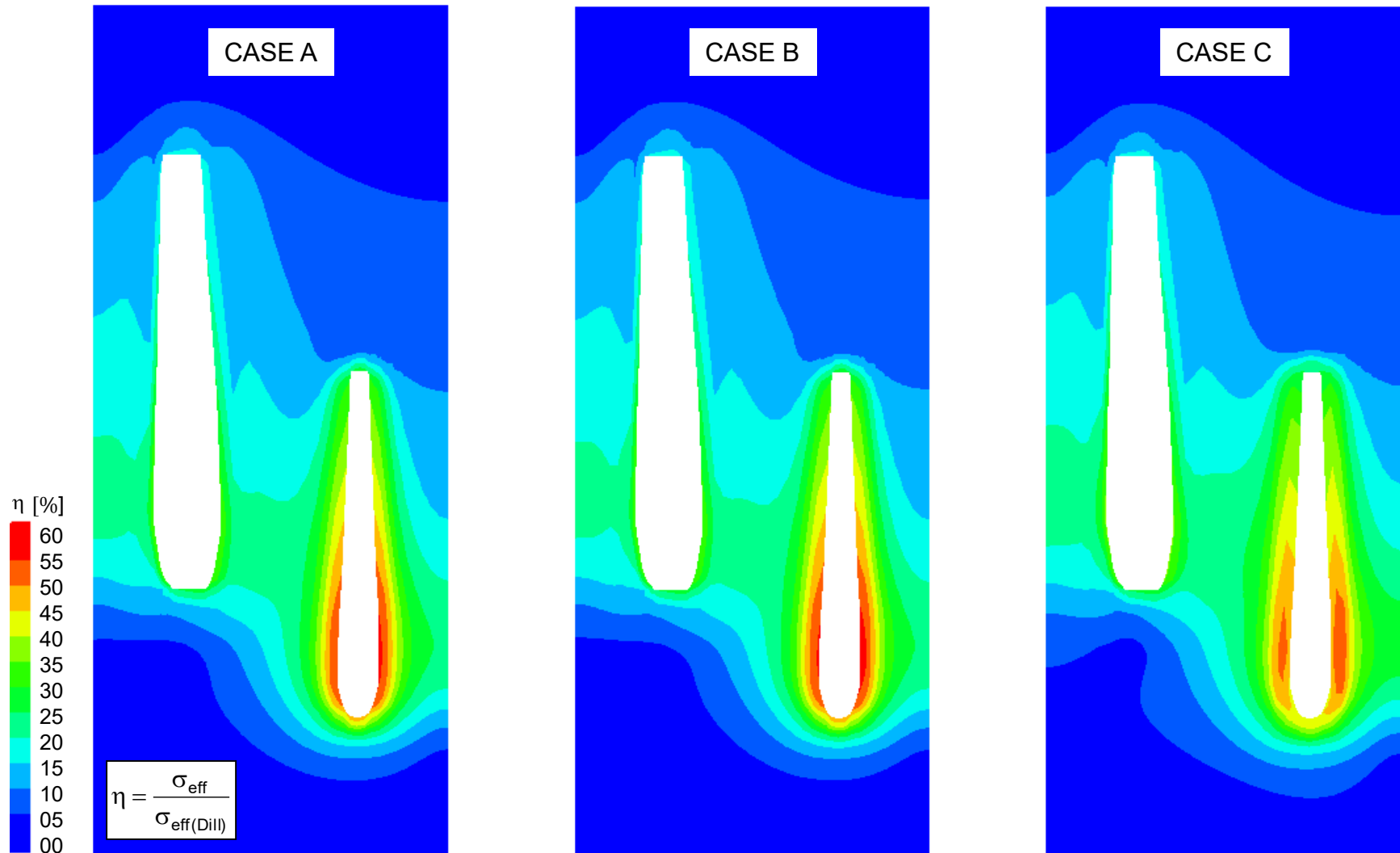












Plastic-volumetric-deformation

$$\varepsilon_{Vol}^P(MAX) = 0\%$$

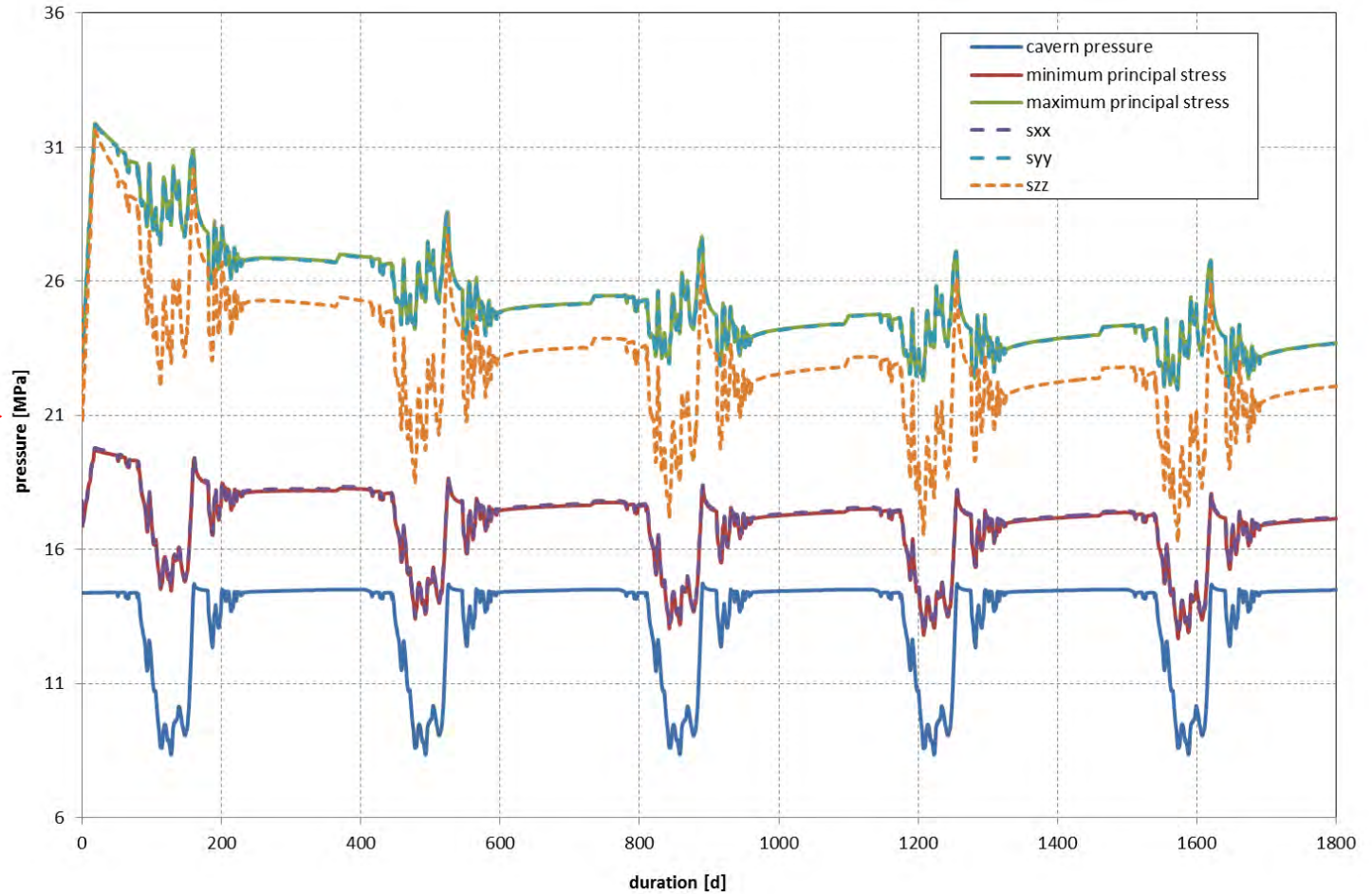
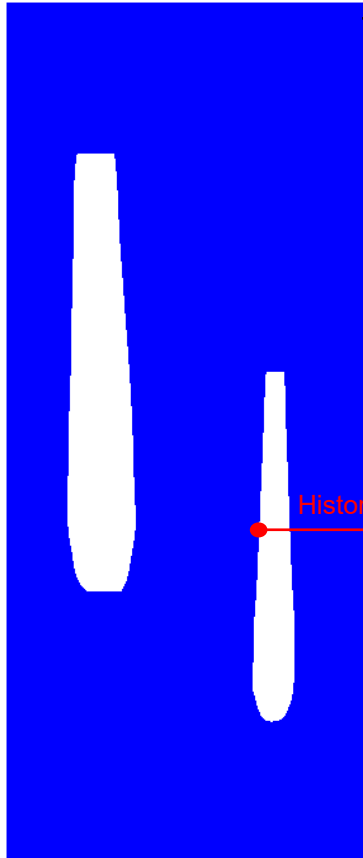
Plastic-shear-deformation

$$\varepsilon^P(MAX) = 0\%$$

Effective tensile stress

$$\sigma_{ten}^{eff} = 0$$

Concerning p_{MIN} the realized gas flow rates neither deformation infiltration of nitrogen arise at cavern contour



Plastic-volumetric-deformation

$$\varepsilon_{Vol}^P(MAX) = 0\%$$

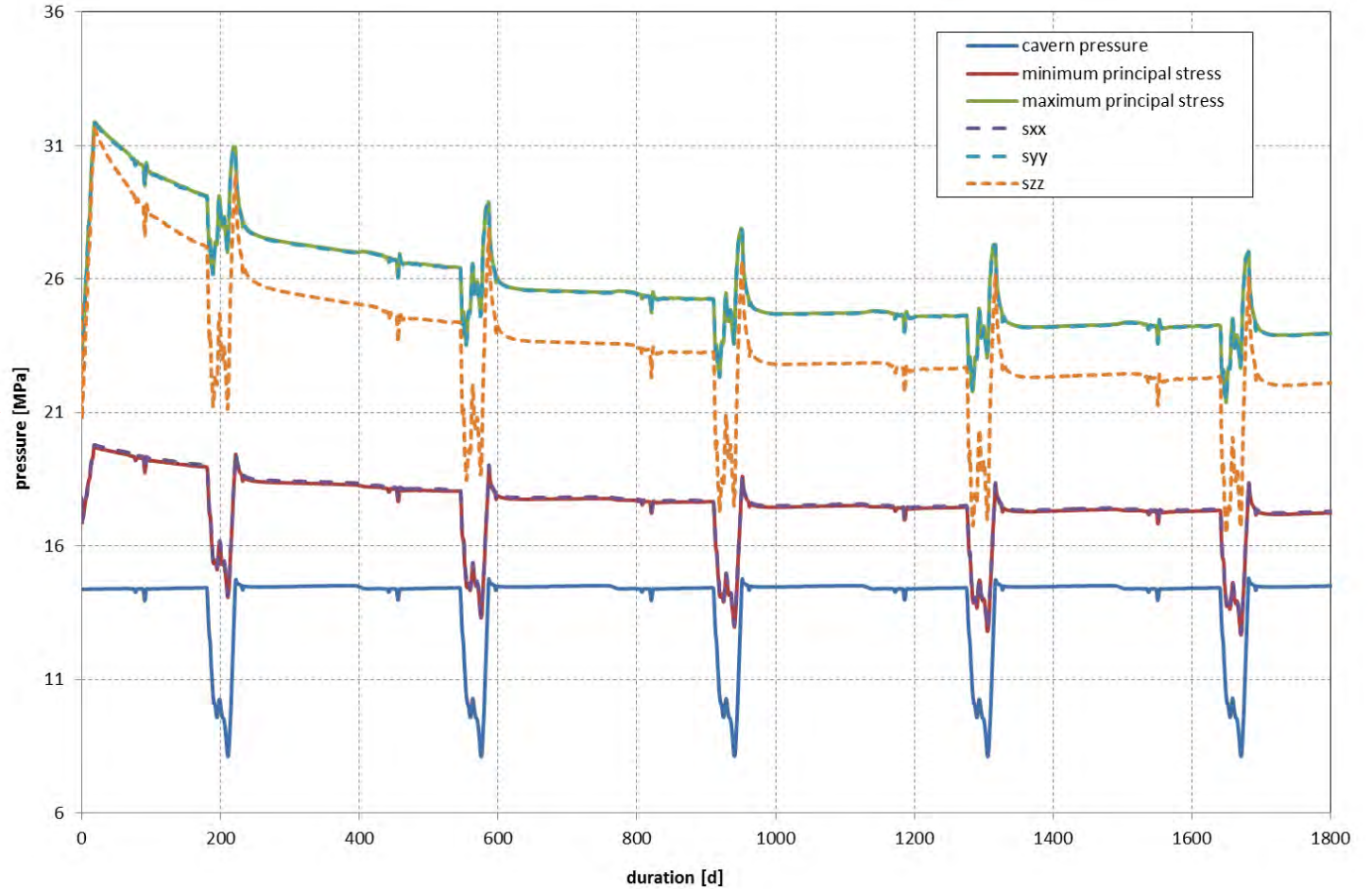
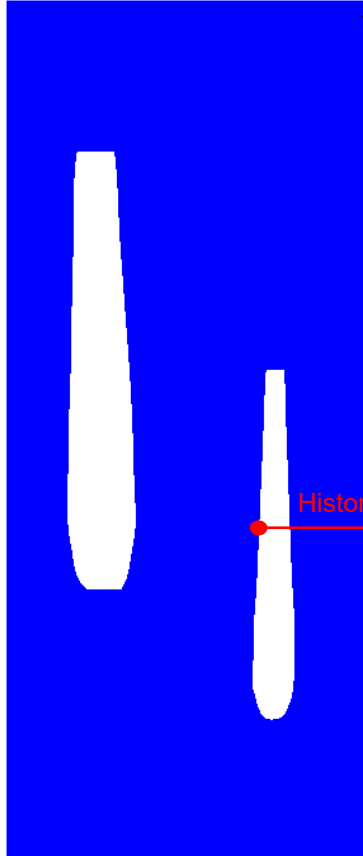
Plastic-shear-deformation

$$\varepsilon^P(MAX) = 0\%$$

Effective tensile stress

$$\sigma_{ten}^{eff} = 0$$

Concerning p_{MIN} the realized gas flow rates neither deformation infiltration of nitrogen arise at cavern contour



Plastic-volumetric-deformation

$$\varepsilon_{Vol}^P(MAX) = 0\%$$

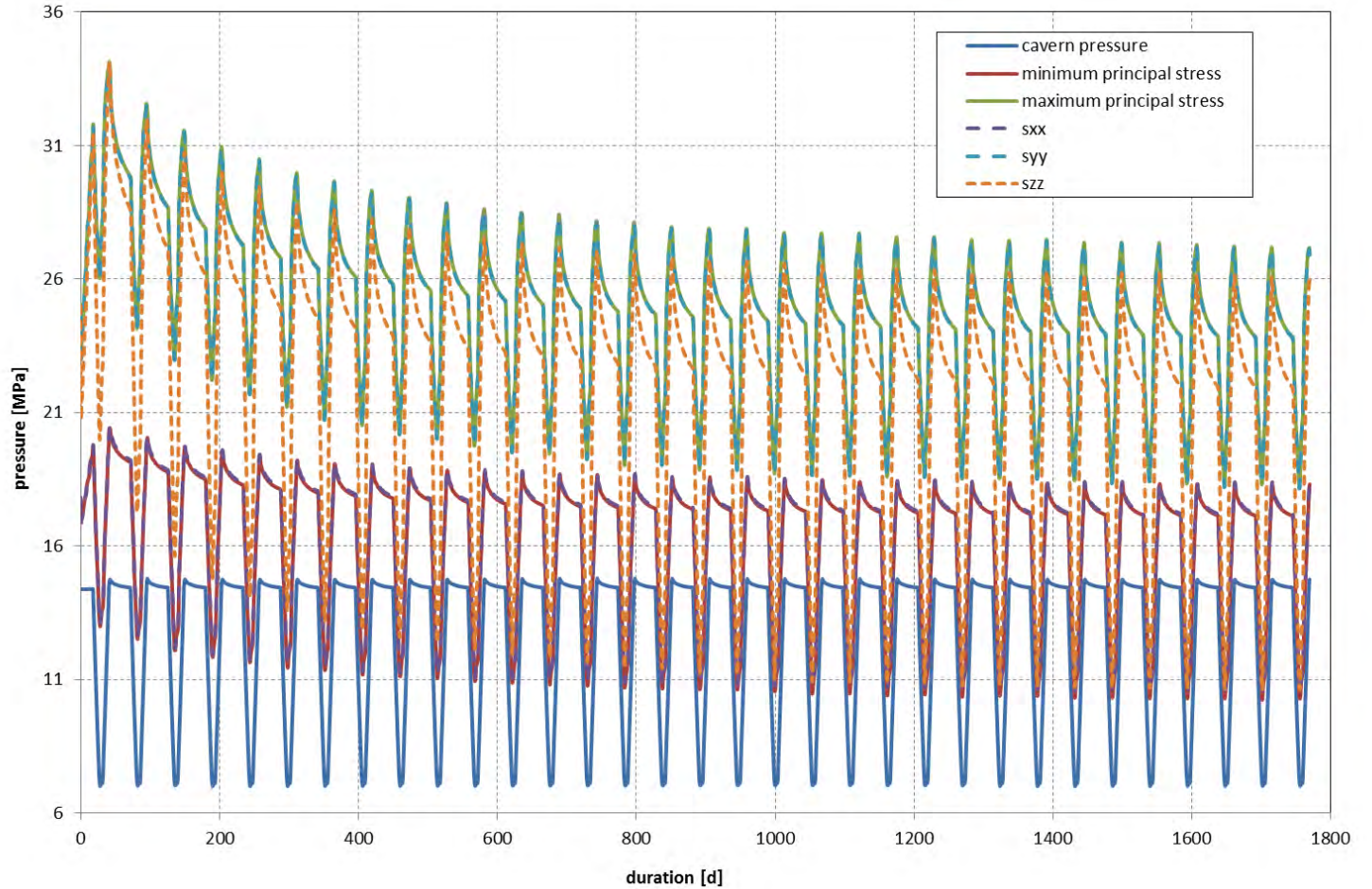
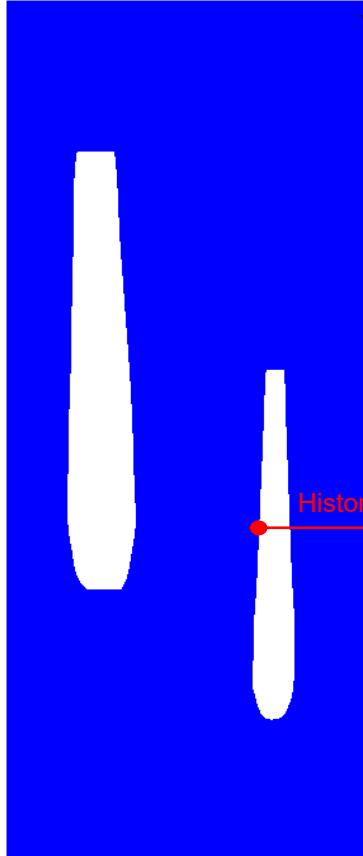
Plastic-shear-deformation

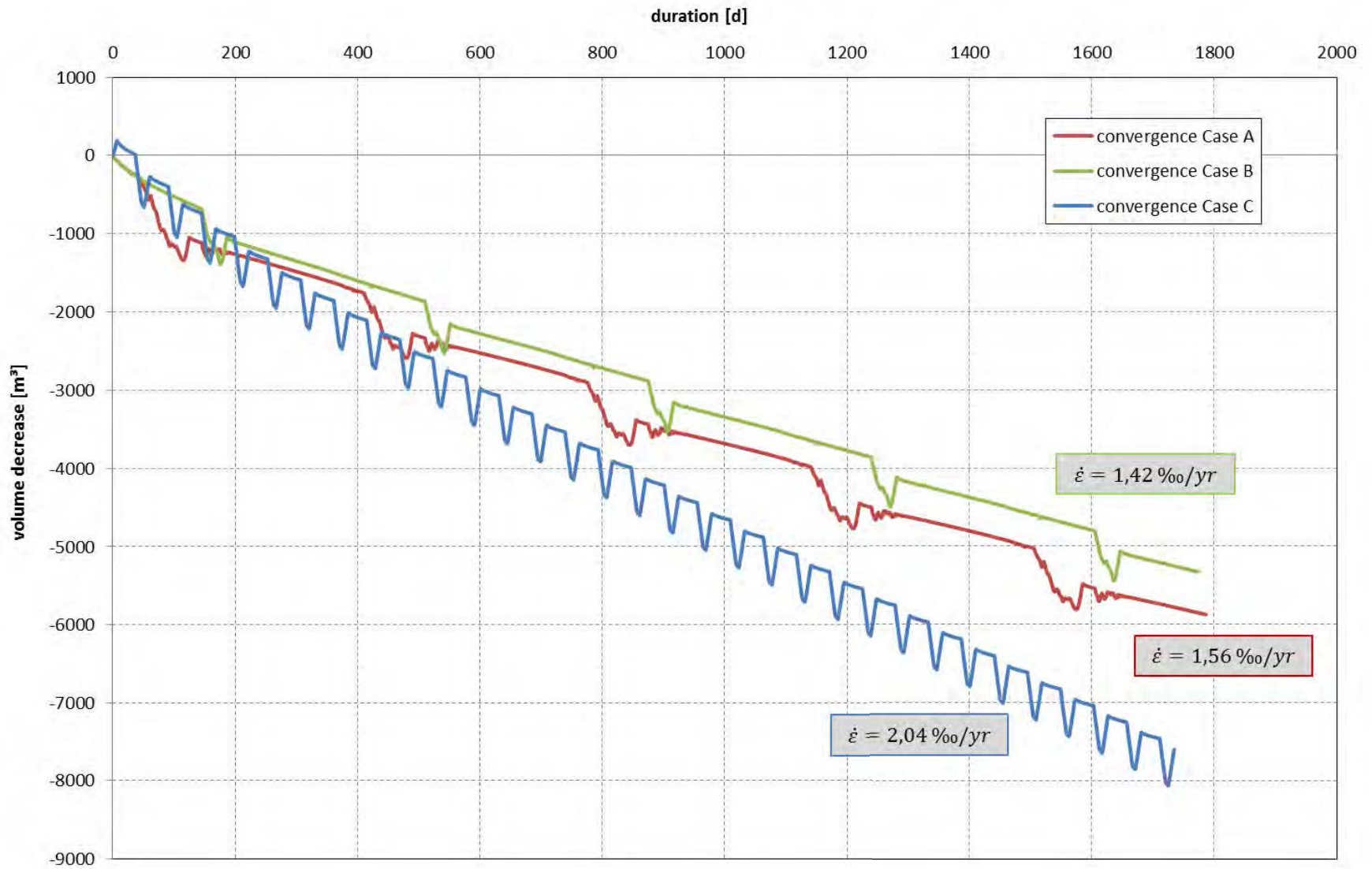
$$\varepsilon^P(MAX) = 0\%$$

Effective tensile stress

$$\sigma_{ten}^{eff} = 0$$

Concerning p_{MIN} the realized gas flow rates neither deformation infiltration of nitrogen arise at cavern contour





Tab: Permeabilitätuntersuchungen an Steinsalz



Permeabilitätsuntersuchungen an Steinsalz

Auftraggeber: DEEP. Underground Technologies GmbH
Bad Zwischenahn

Auftrag Nr. : Beauftragung mit Übergabe vom 03.03.2010

Projekt Nr. (IfG): IfG 30/2010

Bearbeiter: Dipl.-Phys. Dieter Brückner

Leipzig, 11/06/2010

Dr. - Ing. habil. Wolfgang Minkley
Geschäftsführer

Permeabilität und Nachweis der Gasdichtheit

Veranlassung

Im Rahmen des Gasspeicherprojektes Zuidwending sind am Institut für Gebirgsmechanik (IfG) in Leipzig Permeabilitätsteste an lokationsspezifischen Steinsalzproben durchgeführt worden. Zu Vergleichszwecken ist an einem der Proben bei der Bundesanstalt für Geowissenschaften und Rohstoffe (BGR) in Hannover ein Permeabilitätstest durchgeführt worden.

Da die von den beiden Instituten gemessenen Permeabilitätswerte sich stark voneinander unterschieden, ist die bei der BGR gemessene Probe nochmals beim IfG in Leipzig untersucht worden. Zusätzlich wurde die Permeabilität der Probe untersucht, die bei der BGR zur Bestimmung des Relaxationsverhaltens im Triaxialversuch genutzt worden war.

In dem vorliegenden Kurzbericht wird der Aufbau und Ablauf dieser Wiederholungsmessung wiedergegeben, die Messergebnisse dargestellt und der Frage nachgegangen, warum bei Permeabilitätsuntersuchungen an Salzkernen relativ große Unterschiede in den Ergebnissen möglich sind.

Abschließend wird die Relevanz der unterschiedlichen Messergebnisse hinsichtlich der Dichtheit einer Gasspeicherkaverne im Salz bewertet.

Untersuchungsmethodik

Für die Untersuchung des Gastransportverhaltens von Gesteinen unter definierten Belastungsbedingungen steht im IfG Leipzig eine servohydraulische Prüfmaschine mit $F_{\max} = 2500 \text{ kN}$ (Hersteller: Schenk/Trebel) zur Verfügung (vgl. Abb. 1). In der vorhandenen Triaxialzelle können Druckaufbautests an großvolumigen Gesteinsproben ($\varnothing=100 \text{ mm}$, $l \leq 200 \text{ mm}$) unter den Bedingungen eines geschlossenen oder kontrolliert drainierten Systems entweder unter hydrostatischen ($\sigma_1 = \sigma_3$) oder deviatorischen Bedingungen ($\sigma_1 \neq \sigma_3$) durchgeführt werden. Für die Messung hydraulischer Eigenschaften bzw. zur Applikation des Porendrucks befinden sich in den Stempeln Durchführungen, wobei bei Verformungsversuchen zusätzlich Bohrungen in die Endflächen der Proben eingebracht werden.

Die Gaspermeation lässt sich unter reproduzierbaren Versuchsbedingungen, d.h., mit definiert vorkompaktierten oder vorgeschädigten Proben entweder über den Druckabfall eines über der Probe unter Druck abgesperrten Fluidvolumens bzw. den Druckanstieg im Sekundärvolumen („instationäres Messverfahren“) beobachten. Weiterhin kann auch unmittelbar die primärseitig injizierte bzw. sekundärseitig austretende Fluidmenge als Durchflussrate („stationäres Messverfahren“) quantitativ bestimmt werden.

Die Ermittlung der Permeabilität und der Nachweis der Gasdichtheit von Steinsalz erfolgt an Prüfkörpern aus verschiedenen Teufenlagen einer geplanten Gasspeicherkaverne, z.B. beginnend im Rohrschuhbereich der letzten zementierten Rohrtour, d. h. dem höchst gelegenen, technisch ungeschützten Horizont des Gasspeichers, über den Bereich maximaler Querschnitte im mittleren Teil der Kaverne bis hin zum unteren Kavernenteil, dem Übergang zum Kavernensumpf.

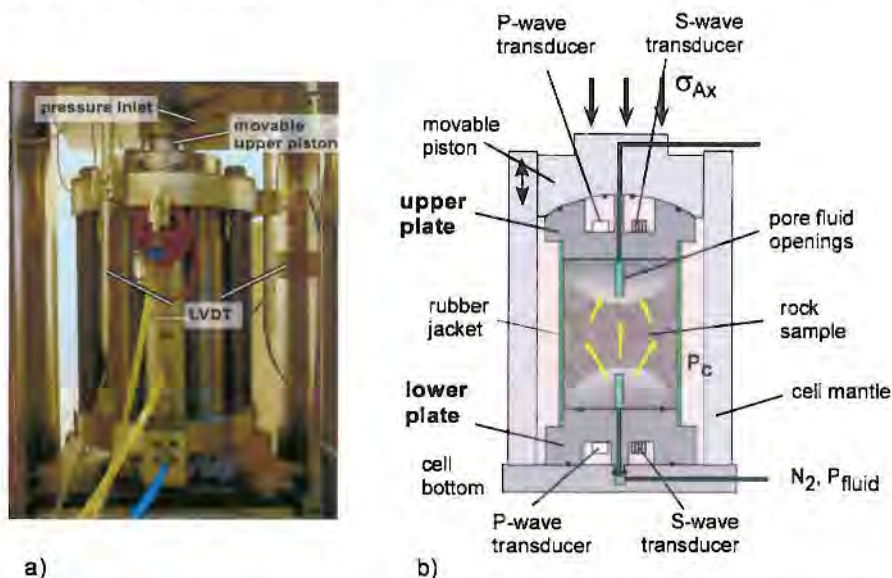


Abb. 1: Messaufbau zur Durchführung von Permeabilitätsuntersuchungen in der Triaxialzelle (a); schematische Versuchsanordnung für axiale Gasdurchströmung (b)

Zur Überprüfung der Gasdichtheit in vertikaler Richtung, d. h. in axialer Richtung durch einen Prüfkörper, wird zentrisch in der Achse des Prüfkörpers und ausgehend von den Stirnflächen jeweils ein Bohrloch von 4 mm Durchmesser und 40 mm Tiefe gebohrt. Diese Bohrlöcher dienen zur Hochdruckbeaufschlagung des Salzes bzw. zur Sammlung des durchströmenden Gases auf der gasdruckfreien Seite. Der Abstand dieser Bohrungen zueinander beträgt zwischen den Bohrlochenden ca. 100 mm.

Versuchsbeschreibung

Für die im Auftrag von DEEP. durchgeführten speziellen Wiederholungsuntersuchungen wurden 2 zylindrische Prüfkörper (PK) von der BGR zurückgeben:

1. PK A2A-02/007/018/01 (IfG-Bezeichnung 424/1) hatte eine Höhe von 180,30 mm und einen Durchmesser von 90,13 mm. Als Dichte wurde bestimmt $\rho = 2,221 \text{ g/cm}^3$. Die Ultraschalluntersuchung ergaben eine Longitudinalwellengeschwindigkeit von 4,2 km/s in axialer Richtung bzw. 4,5 km/s in radialer Richtung. Für den Durchgang der Transversalwelle in axialer Richtung wurden 2,59 km/s ermittelt. Diese Probe trug bei BGR die Bezeichnung 07006 und wurde dort für die Untersuchung des Relaxationsverhaltens genutzt.
2. PK A4A 06/008/044/02 (IfG-Bezeichnung 424/2) hatte eine Höhe von 192,46 mm und einen Durchmesser von 95,63mm. Als Dichte wurde bestimmt $\rho = 2,208 \text{ g/cm}^3$. Die Ultraschalluntersuchung ergaben eine Longitudinalwellengeschwindigkeit von 4,4 km/s in axialer Richtung bzw. 4,5 km/s in radialer Richtung. Für den Durchgang der Transversalwelle in axialer Richtung wurden 2,54 km/s ermittelt. Diese Probe trug bei BGR die Bezeichnung 07016 und wurde dort für die Untersuchung der Permeabilität genutzt.

Die untersuchten Prüfkörper sind in der folgenden Abbildung als Auflichtbild dargestellt.



Abb. 2: Prüfkörper für Gasdurchströmungstests

Die Steinsalzprüfkörper wurden vor Beginn der Permeabilitätsmessung in der Triaxialzelle bei einem allseitig wirkenden hydrostatischen Druck von 600 bar konsolidiert (Abb. 3).

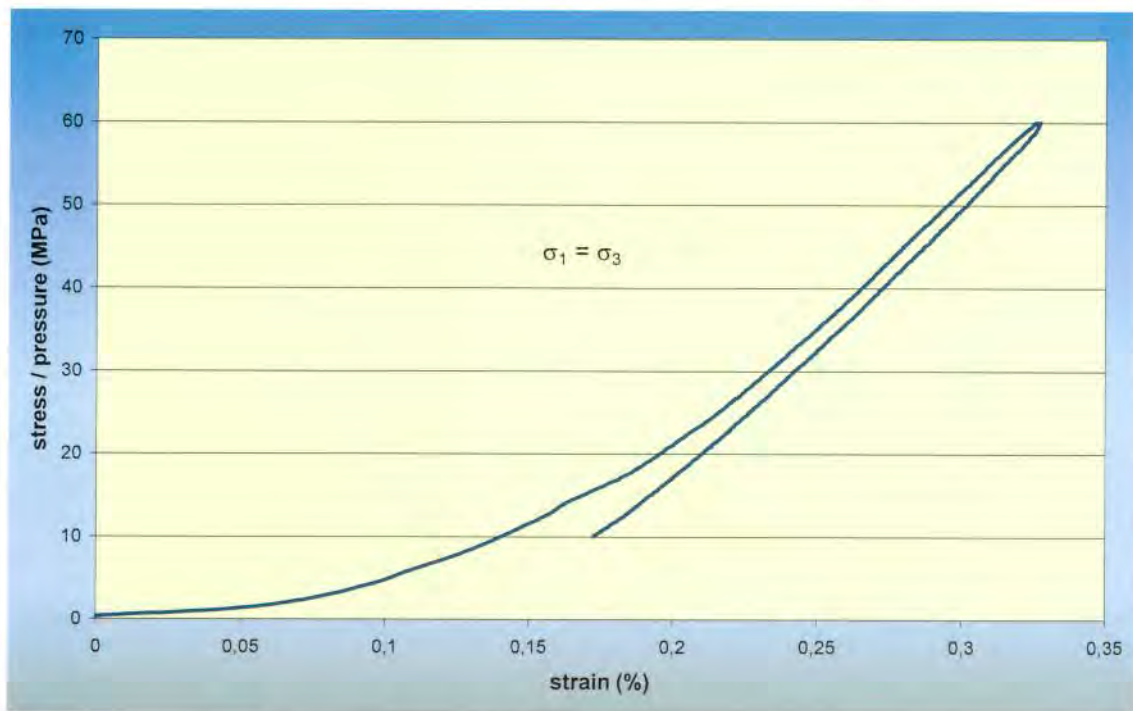


Abb. 3: Spannungs-Verformungs-Diagramm einer Konsolidierungsphase

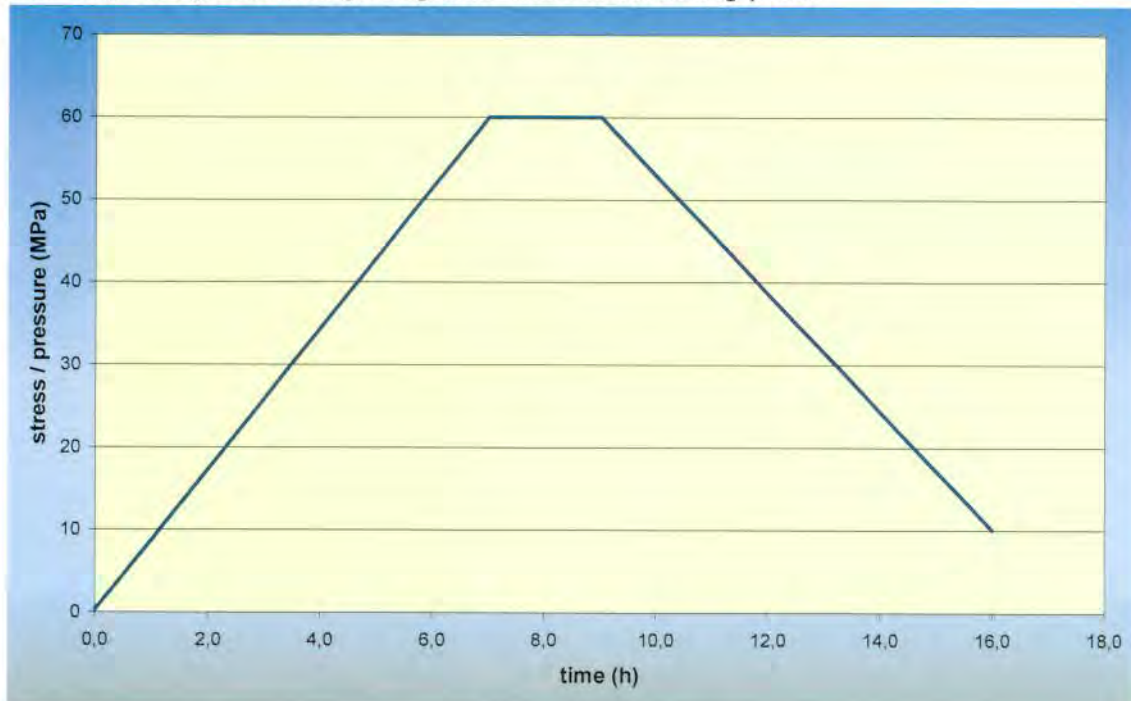


Abb. 4: Spannungs-Zeit-Diagramm einer Konsolidierungsphase

Wird zur Bestimmung des Kompressionsmoduls K die während der Entlastung im linear-elastischen Abschnitt aufgezeichnete axiale Verformung "strain %" genutzt, folgt unter der Annahme homogener Verformung K [MPa] ≈ 11 MPa. Dieser sehr geringe Wert weist auf erhebliche Auflockerung hin.

Vom Konsolidierungsdruck aus wurde in einer etwa 9-10 h dauernden Versuchsphase die hydrostatische Belastung auf den späteren im Permeationsversuch konstant gehaltenen Druck von 100 bar abgesenkt (vgl. Abb. 4).



Abb. 5.: Darstellung der Gasdruckbelastung im Permeationsversuch 424/1

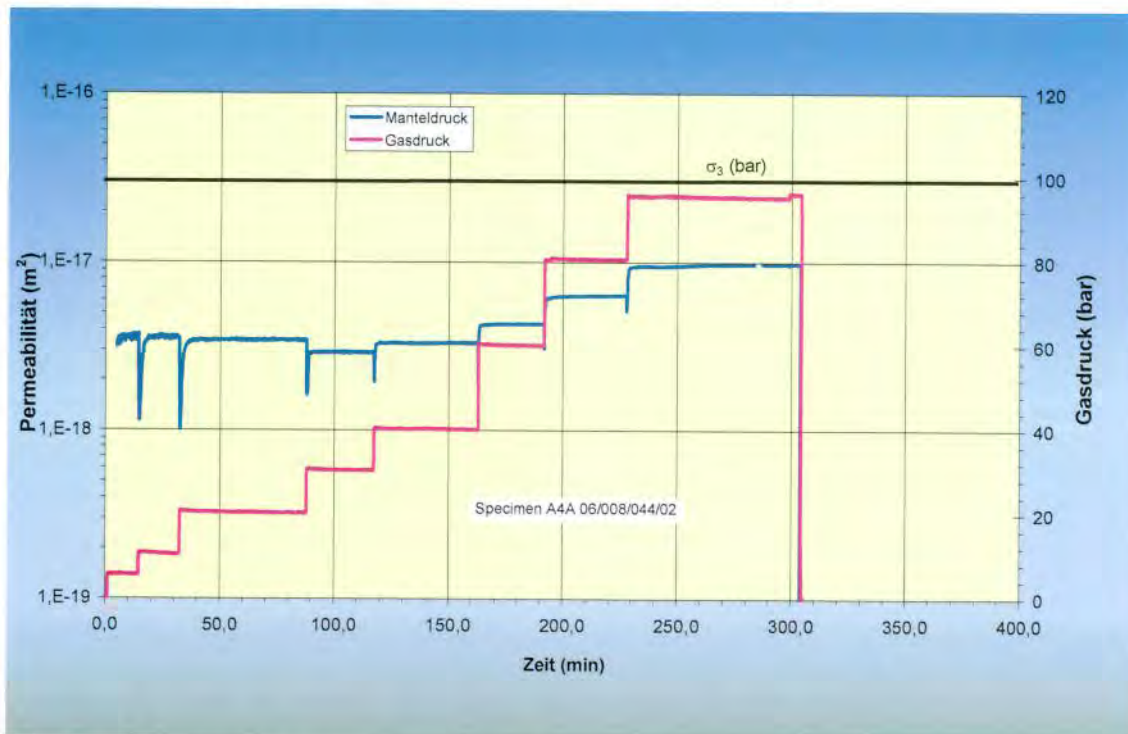


Abb. 6.: Darstellung der Gasdruckbelastung im Permeationsversuch 424/2

Primärseitig wurde der Gasdruck (Stickstoff) in der Prüfkörperbohrung stufenweise erhöht (vgl. Abb. 5), dabei wurde in der Bohrung auf der Niederdruckseite der Gasdurchtritt gemessen.

Untersuchungsergebnisse

Die Permeabilität wurde mittels der DARCY-Beziehung (s. Gl. 1) aus der gemessenen Durchflussmenge bestimmt.

$$\dot{V} = \frac{K}{\eta} \cdot A \cdot \frac{dp}{dr} \cdot \frac{p}{p_0} \quad (\text{Gleichung 1})$$

Dabei sind:

\dot{V}	durchströmende Gasmenge in Nm ³ /sec
K	Permeabilität
η	Viskosität des Gases (N ₂ : 1,75*10 ⁻⁵ Pa*sec)
A	durchströmter Querschnitt
dp/dr	Druckgefälle infolge des Durchströmwiderstandes
p	herrschender Gasdruck – hochdruckseitig
p ₀	10 ⁵ Pa.

Für den Fall der axialen Durchströmung leitet sich der in Gleichung 2 beschriebene Zusammenhang ab.

$$\dot{V} = \frac{K}{\eta} \cdot \frac{A}{l} \cdot \frac{p^2 - p_0^2}{2p_0} \quad (\text{Gleichung 2})$$

Dabei steht der Parameter *l* für den Abstand zwischen der primären Gashochdruckbohrung zu Gasdruckbeaufschlagung und der sekundären Gasaustrittsbohrung in der Probe, wodurch die Mächtigkeit der durchströmten Gesteinsschicht in der Probe charakterisiert wird.

Aus den Versuchsergebnissen konnten Permeabilitätswerte zwischen 4*10⁻¹⁸ und 5*10⁻¹⁷ m² im Versuch 424/1 und 2*10⁻¹⁹ und 1*10⁻¹⁷ m² für den Prüfkörper 424/2 in Abhängigkeit der primären Gasdruckbeaufschlagung ermittelt werden. Diese von IfG ermittelten Permeabilitäten liegen zumeist unterhalb der von der BGR angegebenen Werte zwischen 1 bis 5 *10⁻¹⁷ m².

Nach Beendigung der Versuche wurde eine Markierung der potentiellen Fließwege mit einem Farbtracer vorgenommen. Auf diese Weise ist z.B. in Abb. 7 und 8 deutlich zu erkennen, dass die (offenen) Korngrenzen einen wesentlichen Beitrag zum Fluidtransport geleistet haben.

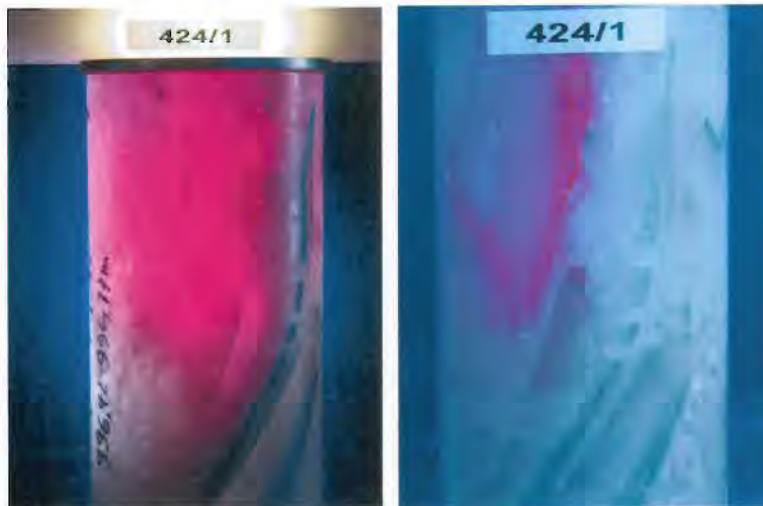


Abb. 7: Markierte Fließwege entlang der Korngrenzen im hochdruckseitigen Prüfkörperbereich



Abb. 8: Markierte Fließwege entlang der Korngrenzen im hochdruckseitigen Prüfkörperbereich

Auch in den bereits zuvor beim IfG durchgeführten Permeabilitätsuntersuchungen an Salzkernen aus der Lokation Zuidwending konnte gezeigt werden, dass im grobkristallinen Steinsalz die Korngrenzen als mögliche Fließwege in Frage kommen. Daher kommt dem Grad der möglichen Rekompaktion der Auflockerung des Materials infolge der Entspannung des Materials durch die Kernbohrung eine entscheidende Bedeutung zu. Bei Proben wie im vorliegenden mit relativ großen Kristallen können eingetragene Auflockerungen (Öffnungen

an den Korngrenzen) in laborüblichen Zeiträumen nicht konsolidiert werden, auch nicht unter Aufbringung hoher triaxialer Einspannungen.

Daraus kann für Permeabilitätsuntersuchungen der Schluss gezogen werden, dass ein besonderes Augenmerk auf die Auswahl der Prüfkörper zu legen ist und dabei solche Kernabschnitte zu bevorzugt werden sollten, in denen überwiegend mittel- bis feinkristallines Salz vorkommt. Die an grobkristallinen Kernabschnitten bestimmten relativ hohen Permeabilitäten sind in Bezug auf die Gasdichtheit des Speichers nicht relevant, da angenommen werden kann, dass die Bohrkernproben durch die Kerngewinnung stärker geschädigt sind und nicht den Zustand in situ repräsentieren. Aufgrund der Korngröße im Vergleich zur Probengröße führt eine relativ kurzzeitige hydrostatische Re-Kompaktion im Labor nicht zu einem Zustand, wie er sich langfristig in situ herausgebildet hat. Darüber hinaus ist zu berücksichtigen, dass i. a. die grobkristallinen Strukturen großräumig von feinkristallinen Strukturen umschlossen werden. Daraus folgt, dass die unterschiedlichen Untersuchungsergebnisse von BGR und IfG hinsichtlich der Permeabilität des Salzes der Lokation Zuidwending nicht im Widerspruch stehen und die grundsätzliche abdichtende Eigenschaft des Salzes der Lokation gegenüber dem in den Kavernen gespeicherten Gas nicht in Frage gestellt wird.

Weitere Untersuchungen zum Permeationsverhalten von Steinsalz der Lokation Zuidwending werden unter Berücksichtigung dieser Erkenntnisse im Rahmen von Indexversuchen an Bohrkernen aus den in der 2. Ausbaustufe des Kavernenspeichers Zuidwending abgeteufte Bohrungen durchgeführt.

Tab: Mapping Winschoten Saltdome

TNO-report
NITG 00-178-C

Mapping of the Winschoten Salt Dome

Confidential

Date

September 2000

Author(s)

M.C. Geluk
E.J.T. Duin

Terrein University College Utrecht
Kriekenpitplein 18 and 25
P.O.Box 80015
3508 TA Utrecht
The Netherlands

Project number

005.70114/01.03

Principal

Akzo Nobel Salt bv

All rights reserved.

No part of this publication may be reproduced and/or published by print, photoprint, microfilm of any other means without the previous written consent of TNO.

Approved

Project manager

In case this report was drafted on instructions, the rights and obligations of contracting parties are subject to either the Standard Conditions for Research Instructions given to TNO, or the relevant agreement concluded between the contracting parties. Submitting the report for inspection to parties who have a direct interest is permitted.

© 2000 TNO

Summary

A geological mapping of the Winschoten salt dome has been carried out by TNO-NITG. This mapping was based upon a conventional 35 km² fully migrated 3D seismic survey. The mapping was focussed upon the upper parts of the Winschoten salt dome, where Akzo Nobel Salt bv exploits the rock salt.

The mapping resulted in a set of new geological maps of the salt dome and its immediate surroundings. A study of the internal structure suggested that the major part of the salt dome Winschoten is composed of the Z2 (Stassfurt) Salt. Younger Zechstein salts only occur at the margins of the dome.

Contents

Summary	ii
List of figures	iv
List of maps.....	v
1 Introduction.....	1
2 Seismic Interpretation	2
2.1 Data base.....	2
2.2 Seismic interpretation	2
2.3 Time-depth conversion	4
3 Maps; discussion and uncertainties.....	5
4 Structure of the salt dome Winschoten	8
5 Conclusions.....	10
Appendix A Overview of well data base	

List of figures

- Figure 1. Example of an E-W seismic line from the Blijham-Groningen 3D survey. Three wells are projected on this line. The data hiatuses in the uppermost part of the section are due to data acquisition problems. The top of the dome is imaged by the dark green line and, at the top, by the bright green line. The red arrow indicates the position of an anhydrite floater or a caprock relict.3
- Figure 2. 3D perspective view of the base Tertiary. The horizon is situated on top of the dome close to the top caprock. Hence, the picture shows the shape of the top of the dome. The yellow lines represent the well trajectories above the base Tertiary. Obvious are the faulted areas, caused by salt dissolution, at the top and next to the dome.7
- Figure 3. Development of fault patters in the overburden as a result of salt movement. Note the relation between the simple normal fault below the salt, which triggered its movement, and the complex fault patters in the overburden as a result of extension (modified after RGD 1993, Explanation to Map Sheet III).9

List of maps

- Map 1. Depth of the top caprock
- Map 2. Depth of the top salt
- Map 3. Depth of the base of the Miocene (Upper North Sea Group)
- Map 4. Depth of the base of the Tertiary (North Sea Supergroup)
- Map 5. Depth of the base of the Upper Cretaceous (Chalk Group)
- Map 6. Isopach map of the Upper Cretaceous (Chalk Group)
- Map 7. Detailed depth map of the top caprock
- Map 8. Detailed depth map of the top salt
- Map 9. Structural profiles
- Map 10. Internal structure of the Winschoten salt dome at 500 m depth
- Map 11. Internal structure of the Winschoten salt dome at 1000 m depth
- Map 12. Internal structure of the Winschoten salt dome at 1500 m depth

1 Introduction

A geological mapping of the Winschoten salt dome has been carried out by TNO-NITG on behalf of Akzo Nobel Salt bv (letter 51/047913, March 22nd 2000). This mapping aimed at the update of old geological maps (vintage around 1970) of the concession, which were still in use within Akzo Nobel Salt bv.

A common interest has been defined between NAM and Akzo Nobel Salt bv in the mapping of the top salt of the Winschoten salt dome. This interest resulted in the support of NAM for this project, and allowed an exchange of data between NAM and Akzo Nobel Salt bv.

This project forms the third phase of the mapping of the Adolph van Nassau and Uitbreiding Adolph van Nassau concession areas. For the project description reference is made to the proposal NITG 98-10.390 (August 1998). In the first phase of this project, a quality check of the seismic surveys has been performed by TNO-NITG. Further, all geological data were gathered. In the second phase, the Zuidwending salt dome was mapped (NITG 99-209-c).

The third phase of the project started on May 15th 2000. A kick-off meeting took place in Utrecht at June 14th. The preliminary maps were handed over to Akzo Nobel Salt bv on July 15th 2000. The final results have been presented in September 2000 in Hengelo.

2 Seismic Interpretation

2.1 Data base

The data used for the seismic interpretation of the salt dome Winschoten consisted of the following items:

- 40 km² fully migrated 3D seismic survey Blijham-Groningen Central 4 3D; inlines 8880-9300, crosslines 7420-7800. Interval 0-2000 ms TWT.
- stratigraphical interpretations of the Akzo Nobel Salt wells Winschoten 1-14 and the NAM well Heiligerlee-1.

2.2 Seismic interpretation

In the seismic survey Blijham-Groningen the following horizons were interpreted (see also figure 1):

base Triassic (dark green),
base Upper Cretaceous (light green),
base Tertiary (yellow),
mid Miocene unconformity (black).

Due to erosion the Triassic and the Lower Cretaceous both are absent above the salt dome.

The top caprock horizon has been constructed from the horizons listed above; on the flanks of the dome this horizon is presented by the base Triassic, elsewhere by the base Upper Cretaceous. Locally, where the Upper Cretaceous has been eroded (i.e. in the vicinity of the wells Winschoten-13 and -14, and south of Winschoten-1) top caprock coincides with the base Tertiary.

Owing to acquisition problems, a number of hiatuses in the upper part of the seismic data appear (fig. 1). In those areas the mid-Miocene unconformity could not be interpreted on top of the salt dome. In these areas, the horizon has been interpolated. In view of the relative flat character of the horizon, no major uncertainties will have been introduced by this method.

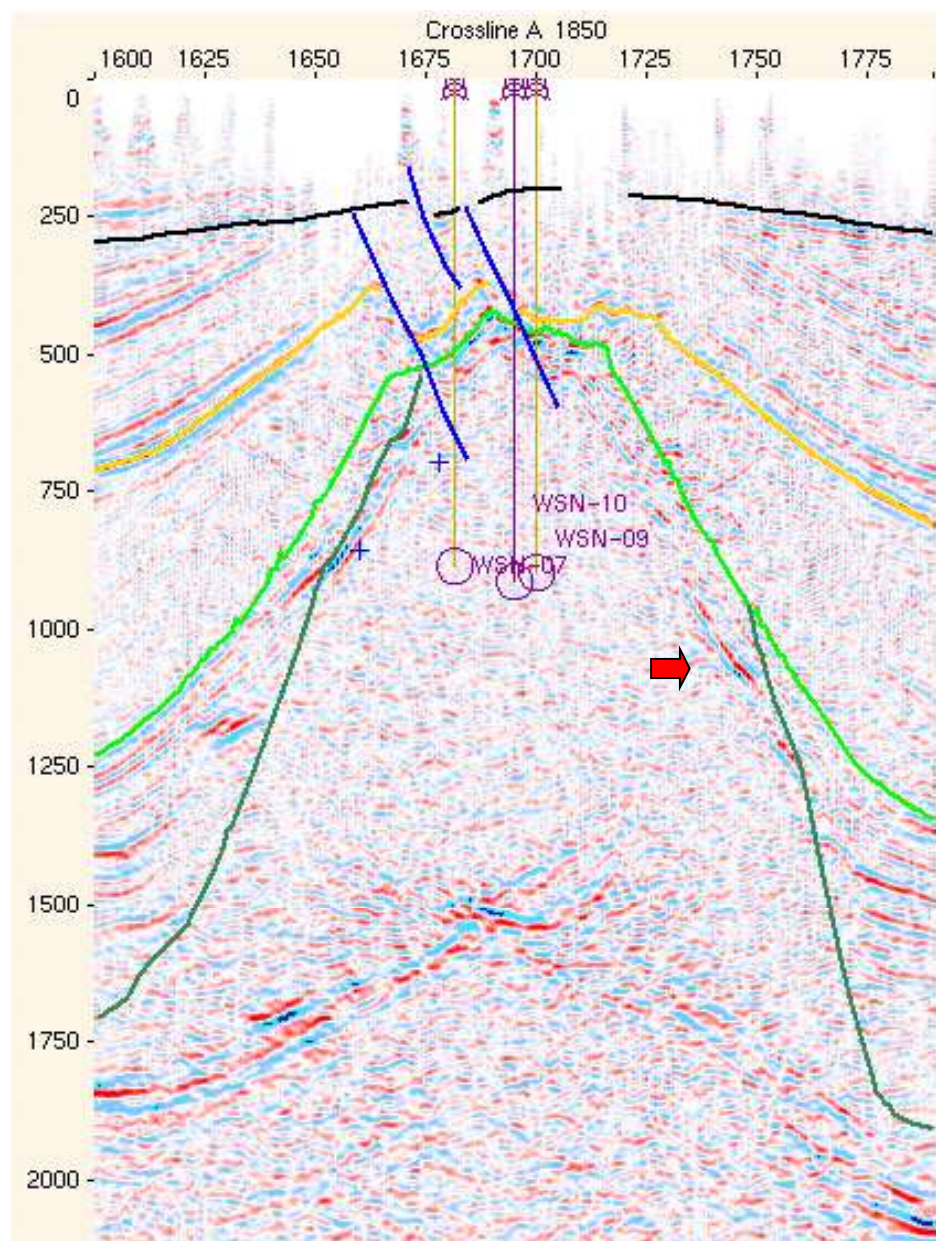


Figure 1. Example of an E-W seismic line from the Blijham-Groningen 3D survey. Three wells are projected on this line. The data hiatuses in the uppermost part of the section are due to data acquisition problems. The top of the dome is imaged by the dark green line and, at the top, by the bright green line. The red arrow indicates the position of an anhydrite floater or a caprock relict.

2.3 Time-depth conversion

The time to depth conversion of the interpreted seismic data has been done in a layer-cake approach. A velocity function has been determined for each interpreted formation. The parameters are given in table 1. The constant velocity of the Upper North Sea Group and the Tertiary was determined using the formation depths in the wells and the times from the seismic data. The calculated average constant velocity was also used to convert the interpretation of the mid-Miocene. For the other formations a linear function of the type $V_z = V_0 + kZ$ was used. V_0 and k are constants.

Table 1 Velocity parameters used for the time-depth conversion

Formation	V_0 (m/s)	K (1/s)
Miocene	1895	0
Tertiary	1895	0
Upper Cretaceous	2092	1.08
Lower Cretaceous	2046	0.53
Triassic	2350	0.69

3 Maps; discussion and uncertainties

This chapter will briefly discuss the content and uncertainties of the maps.

Map 1. Depth of the top caprock (1:25,000)

The map has been created by merging different depth maps. At the top of the dome, the Triassic and shallower formations have been eroded, and the top of the caprock coincides with the base of the Upper Cretaceous or locally with the base of the Tertiary. Because the caprock is only present at the top of the dome, the map is bounded by the 1000 m depth contour of the top caprock. This depth of 1000 m is based upon the occurrence of a 25 m thick anhydrite bed in the Heiligerlee-1 well, assumed to represent a caprock. Present-day formation of caprock will be, however, a slow process regarding the depth of the structure.

After the depth conversion, the depth errors at the Winschoten well locations ranged from -9 to +7 m. An error grid was created and added to the depth map to compensate for these differences in depth.

Map 2. Depth of the top salt (1:25,000)

The map was created by adding a difference grid, created by subtracting the well depths from the map depths at the well location, to the top caprock depth map.

Away from the dome, the top salt is identical with the base Triassic.

The salt dome Winschoten is an irregular, elongated salt dome with a N-S orientation. The top is situated at depths below 400 m in the vicinity of the Winschoten-1 well; this part has not been drilled. With depth, the shape of the salt dome becomes more irregular, with an interference of a N-S trend and NW-SE trend. These trends are linked to faults at shallower levels. The salt dome is characterised by overall steep flanks, but not vertical or overhanging as is the case in Zuidwending.

Map 3. Depth of the base of the Miocene (base Upper North Sea Group) (1:25,000)

The Miocene marker shows a clear doming above the Winschoten salt structure.

Here, it is situated at depths above 200 m, whereas away from the dome it deepens up to almost 300 m. Base Miocene is offset along several faults at the western margin of the dome. One of these faults is situated close to the production wells Winschoten-4, 5, 6, 7 and 11. The depth of the Miocene marker is indicative of the relative movements of the dome during the last 20 MA; these amount roughly up to 100 m.

Map 4. Depth of the base of the Tertiary (North Sea Supergroup) (1:25,000)

The blank areas represent a fault plane where the base of the supergroup is offset.

Figure 2 shows a 3D view of this horizon in time. The base of the Tertiary displays a strong variation in depth. A number of faults can be observed at the northern margin of the dome, due west and north of the production wells. The blank area

marks an important fault gap. The base of the Tertiary is indicative for the relative upwards movements of the salt dome, which amounts up to 300-400 m during the last 60 mA.

Map 5. Depth of the base of the Upper Cretaceous (Chalk Group) (1:25,000)

The Upper Cretaceous is present on top of most of the salt dome. It is missing on the crest, south of the Winschoten-1 well, and locally in the vicinity of the wells Winschoten-13 and -14. On the top of the dome, the base of the Upper Cretaceous can be found at depths below 400 m, while off the dome this base is found at depths of over 1600 m. Locally, i.e. in the case of the Winschoten-1 and -2 wells, this unit may include thin deposits of Early Cretaceous (Albian) age. These could not be mapped in view of the limited thickness.

Map 6. Isopach map of the Upper Cretaceous (Chalk Group) (1:25,000)

The Upper Cretaceous Chalk Group rests on most of the crest of the dome directly upon the caprock. It is missing locally on top of the dome (blank areas on the map). The thickness on top of the dome varies between 0 and 50 m, and increases away from the dome up to 650 m.

Map 7. Detailed depth map of the top caprock (1:10.000)

A detailed depth map of Map 1, the top caprock. The map outline represents the 1000 m depth contour of the top caprock.

Map 8. Detailed depth map of the top salt (1:10.000)

This map was created by adding a caprock thickness map, based on the well data, to the top caprock map.

Map 9. Structural profiles

A fence like diagram showing the structure of the salt dome.

Map 10. Internal structure of the Winschoten salt dome at 500 m depth

The map has been constructed from a time-slice at 540 ms.

It shows the most shallow part of the salt dome. In the vicinity of the wells, especially to the east of well Winschoten-10, several high-amplitude events occur. In vertical sections, these events have a more or less horizontal orientation. Since the internal structure observed in cores is that of steeply dipping salt, the reflections are assumed to be generated by the caprock.

Map 15. Internal structure of the Winschoten salt dome at 1000 m depth

The map has been constructed from a time-slice at 720 ms. The margin of the salt dome is characterised by strong reflections, especially at the northern margins. For the remaining part, only west of the Winschoten-2 and -14 wells strong reflections can be noted.

Based upon the interpretation of the well sections, all wells encountered steeply dipping (up to 75°) Z2 (Stassfurt) Salt at this depth. We assume that these stronger

reflections at the margin indicate either the presence of younger the Main Anhydrite and younger Zechstein Salts (Z3 (Leine) and Z4 (Aller) Formation), or a caprock; the latter interpretation is supported by the well results of Heiligerlee-1. Most part of the dome is, however, is assumed to be composed of Z2 (Stassfurt) halites.

Map 16. Internal structure of the Winschoten salt dome at 1500 m depth

The map has been constructed from a time-slice at 940 ms.

The map shows the increase of the outline of dome with depth. All wells reaching this depth (i.e. Winschoten-4-14; Heiligerlee-1) indicate the presence of Z2 (Stassfurt) halite here. Strong amplitudes can be observed east of the Winschoten wells at the margin and south of the Heiligerlee-1 well. These are interpreted as reflections generated by the younger Zechstein, the Z3 Main Anhydrite or the Z3 (Leine) and Z4 (Aller) Salt, or a caprock. A floating anhydrite bed can be observed also in the cross section of figure 1. Based upon these maps we expect that the major part of the dome at this depth will be composed of Z2 (Stassfurt) Salt.

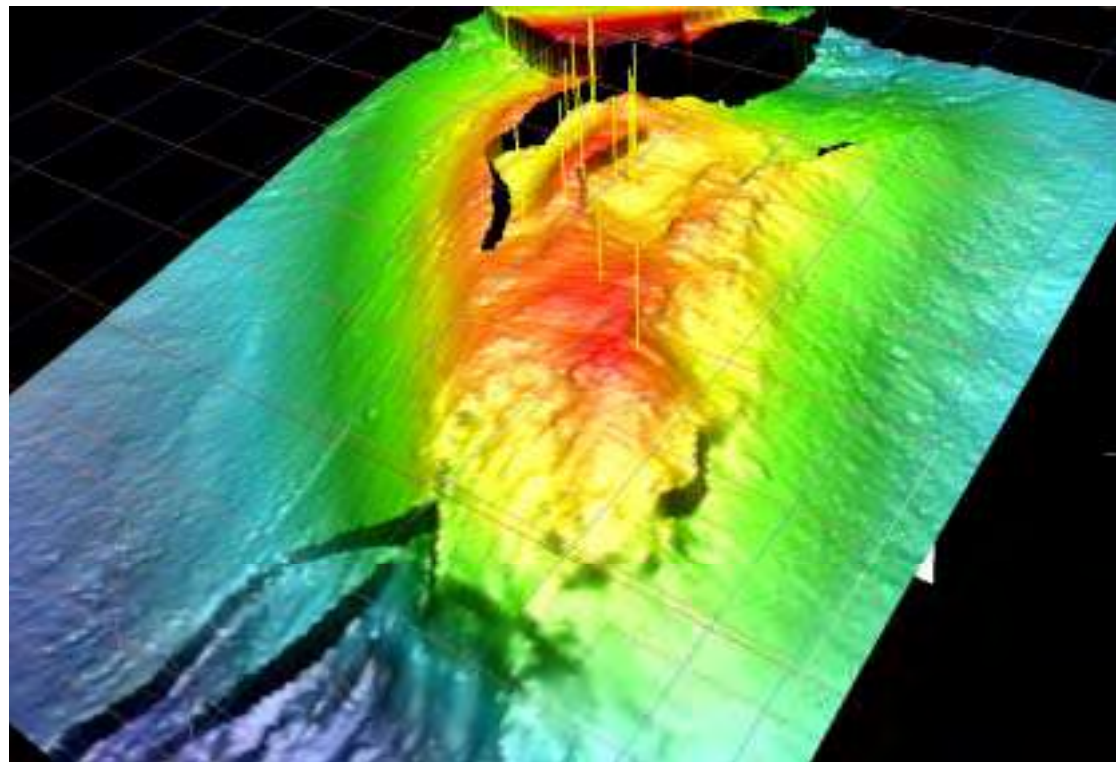


Figure 2. 3D perspective view of the base Tertiary. The horizon is situated on top of the dome close to the top caprock. Hence, the picture shows the shape of the top of the dome. The yellow lines represent the well trajectories above the base Tertiary. Obvious are the faulted areas, caused by salt dissolution, at the top and next to the dome.

4 Structure of the salt dome Winschoten

The mapping of the salt dome Winschoten has resulted in several new insights. First of all, a much more detailed series of maps of the salt dome is available now. Compared to the maps which were used up to recently (based upon the interpretation by Harsveldt and Akzo Nobel), these show that the outline of the dome is much better defined than previously.

The internal structure of the dome has been studied in wells and on the 3D seismics. On 3D seismics, reflections of thick anhydrite floaters were visible at the margins of the dome (Map 16; figure 1). Vertically dipping beds, however, will not reflect the signal upwards; these will be invisible. On three selected time slices, representing the depths of approximately 500, 1000 and 1500 m, the internal structure was studied. Dipping beds of up to 75° have been observed in cores from the Z2 (Stassfurt) Salt. Our conclusion is, that at the depths of 500, 1000 and 1500 m most of the dome is composed of Z2 (Stassfurt) Salt; only at the margins we find some indications for the Z3 Main Anhydrite or a caprock.

Following the interpretation of the caprock, the salt dome Winschoten was already a prominent structure previously to the Cretaceous. During the Cretaceous, strong upward movement of the dome took place. The movements decreased during the Tertiary; the base Miocene (Upper North Sea Group) is only mildly affected by the salt movement. Faulting in the overlying horizons is attributed to extension in the overburden as a result of salt movement, which caused the collapse structures (fig. 3). These faults have not been observed in the caprock reflector, and will not continue into the salt dome except the upper part.

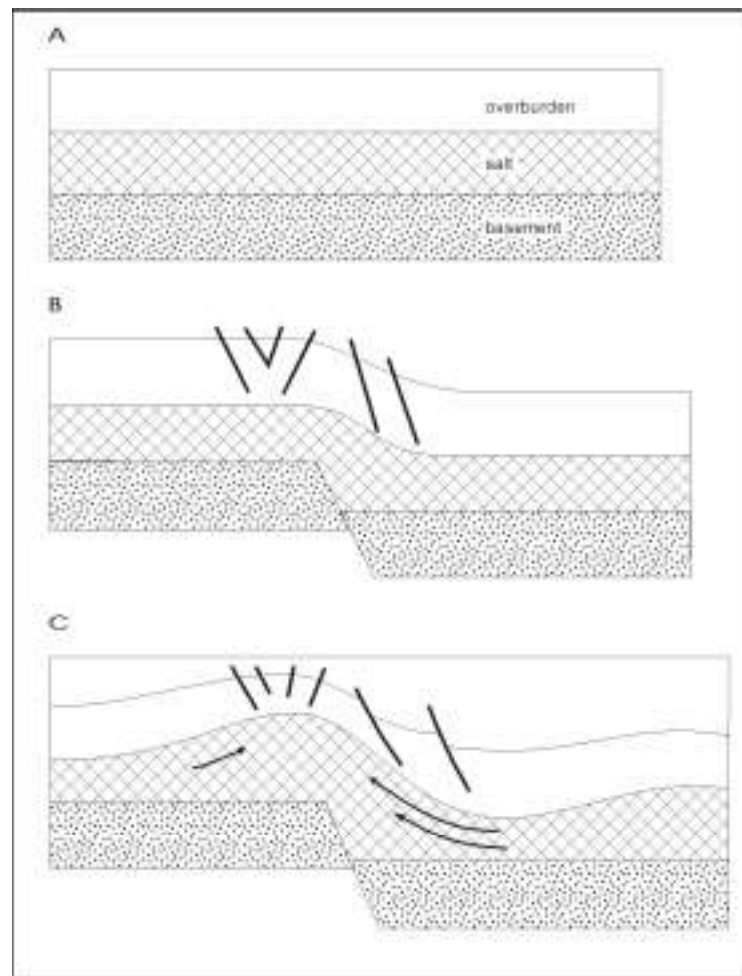


Figure 3. Development of fault patterns in the overburden as a result of salt movement. Note the relation between the simple normal fault below the salt, which triggered its movement, and the complex fault patterns in the overburden as a result of extension (modified after RGD 1993, Explanation to Map Sheet III).

5 Conclusions

The main conclusions from the mapping of the Winschoten salt dome are:

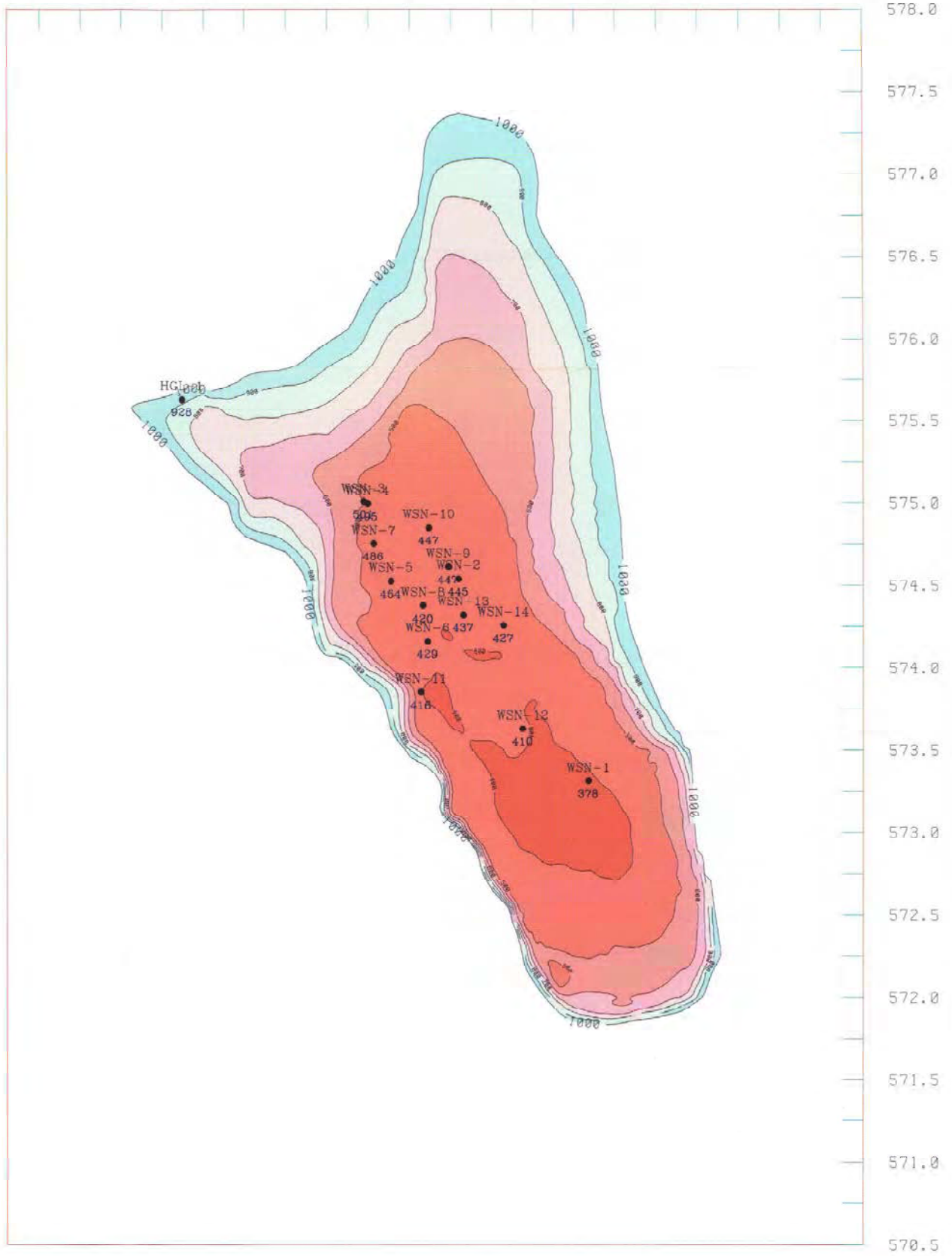
- The size of the Winschoten dome is much better defined than previously.
- The salt dome has a more complex structure than previously thought. This applies to the overburden, which is faulted at the western and northern flanks.
- The salt dome is characterised by steep flanks, but no overhangs have been detected.
- Most of the internal part of the dome at 500, 1000 and 1500 m is assumed to be composed of Z2 (Stassfurt) Salt.
- The salt in the dome itself is not affected by the faulting in the overburden, except for the uppermost tens of meters in the most shallow part of the dome.

Appendix A List of wells used

Winschoten-1	salt exploration well
Winschoten-2	salt exploration well
Winschoten-3	salt exploration well
Winschoten-4	Heiligerlee-A (HL-A)
Winschoten-5	Heiligerlee-B (HL-B)
Winschoten-6	Heiligerlee-C (HL-C)
Winschoten-7	Heiligerlee-D (HL-D)
Winschoten-8	Heiligerlee-E (HL-E)
Winschoten-9	Heiligerlee-F (HL-F)
Winschoten-10	Heiligerlee-G (HL-G)
Winschoten-11	Heiligerlee-H (HL-H)
Winschoten-12	Heiligerlee-J (HL-I)
Winschoten-13	Heiligerlee-K (HL-K)
Winschoten-14	Heiligerlee-L (HL-L)
Heiligerlee-1	NAM well

Mapping of the Winschoten Salt Dome

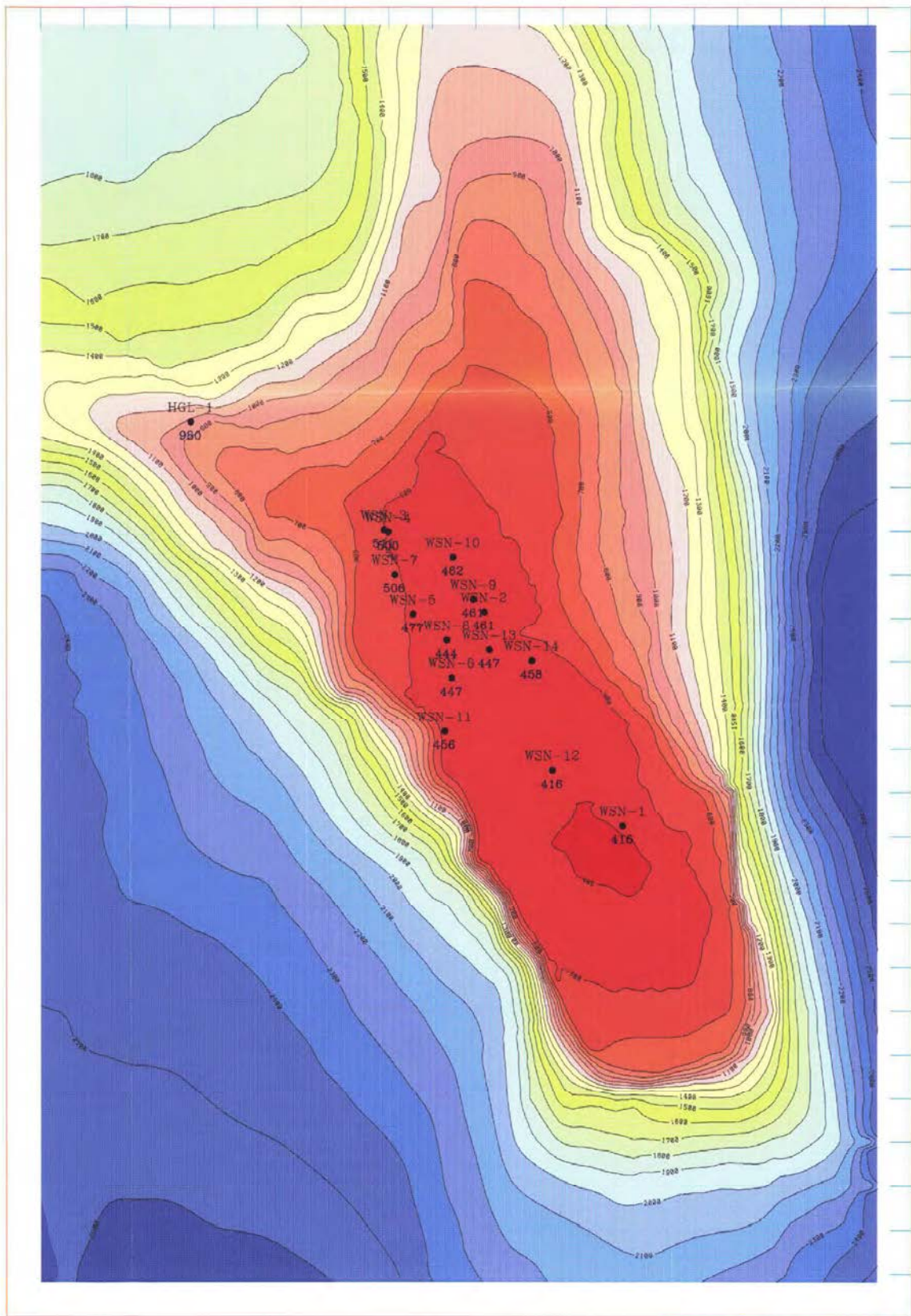
261.0 261.5 262.0 262.5 263.0 263.5 264.0 264.5 265.0 265.5 266.0



1:25000
 km 0 1 2 km

TNO-NITG, Dept. of Geo-Energy Akzo Nobel Salt bv Hengelo		
salt dome Winschoten top caprock depth (m below NAP)		
SCALE 1:25,000	DATE Map 1	DATE 12-JUL-08
CADASTR		

261.0 261.5 262.0 262.5 263.0 263.5 264.0 264.5 265.0 265.5 266.0



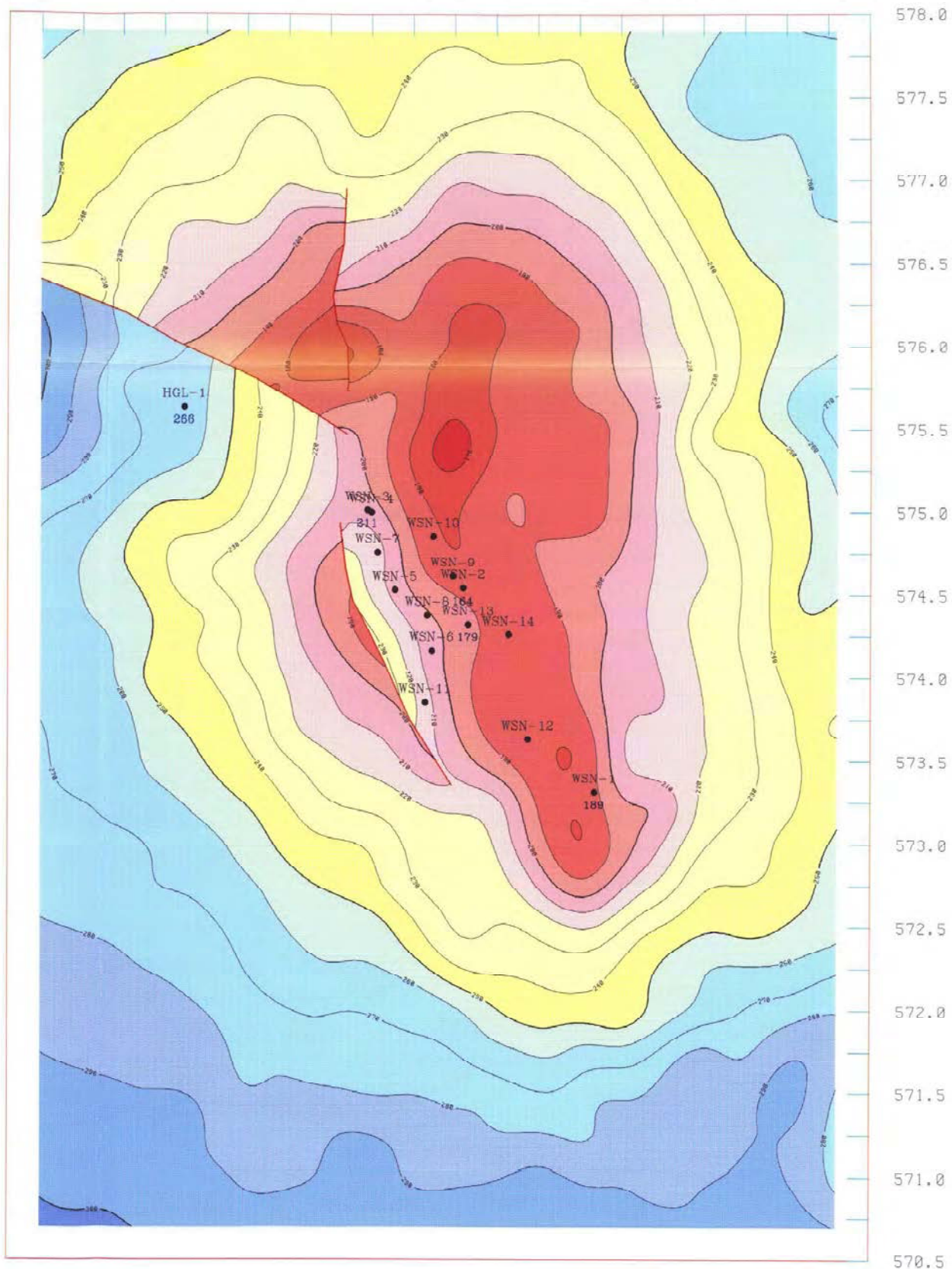
1:25000
km 0 1 2 km

TNO-NITG, Dept. of Geo-Energy
Akzo Nobel Salt bv Hengelo

salt dome Winschoten
top salt
depth (m below NAP)

SCALE 1:25,000	MAP 2	DATE 22-JUN-08
DATE		

261.0 261.5 262.0 262.5 263.0 263.5 264.0 264.5 265.0 265.5 266.0



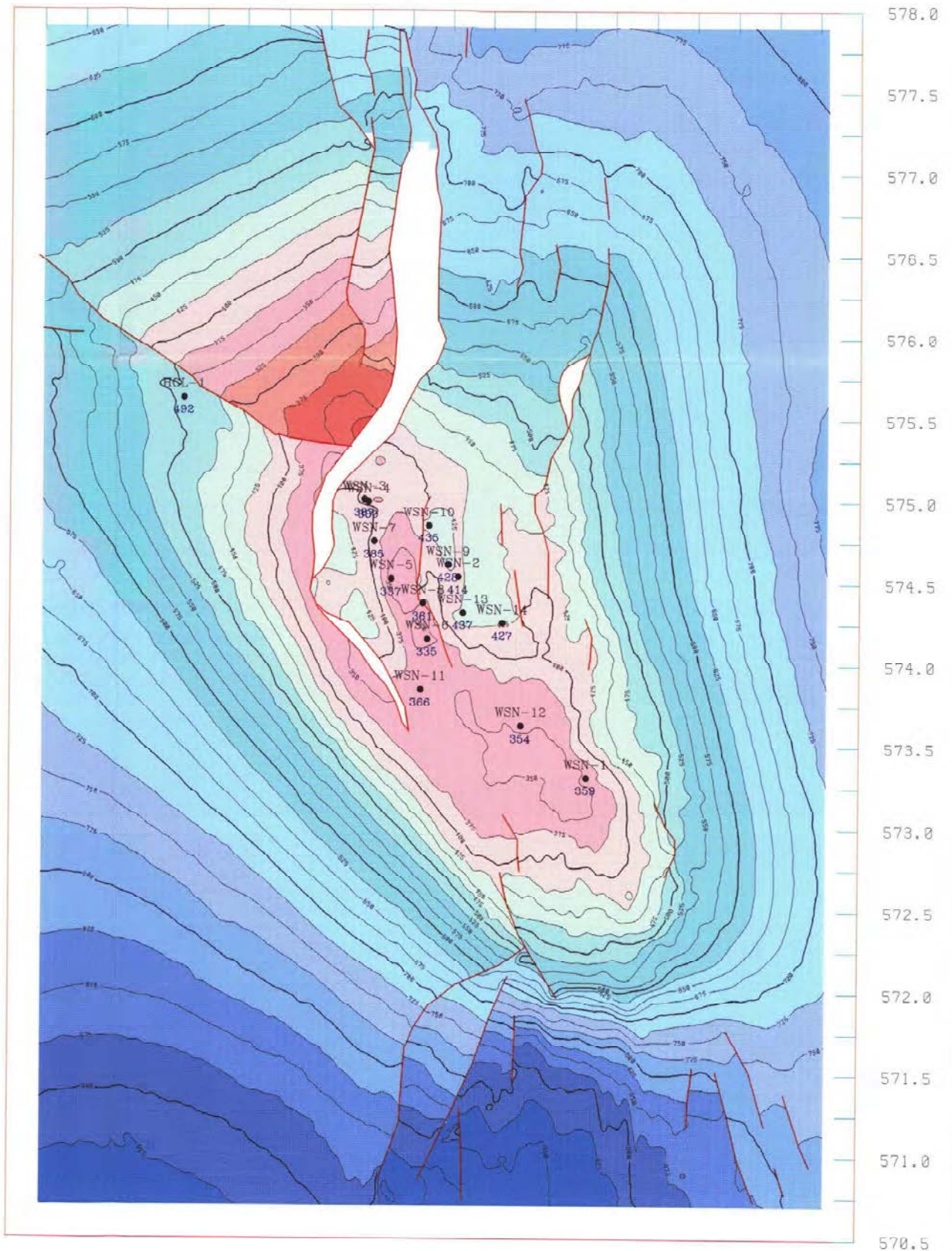
1:25000
km 0 2 km

TNO-NITG, Dept. of Geo-Energy
Akzo Nobel Salt bv Hengelo

salt dome Winschoten
base Miocene
depth (m below NAP)

SCALE 1:25,000 SHEET Map 3 DATE 22 JUN 88

261.0 261.5 262.0 262.5 263.0 263.5 264.0 264.5 265.0 265.5 266.0



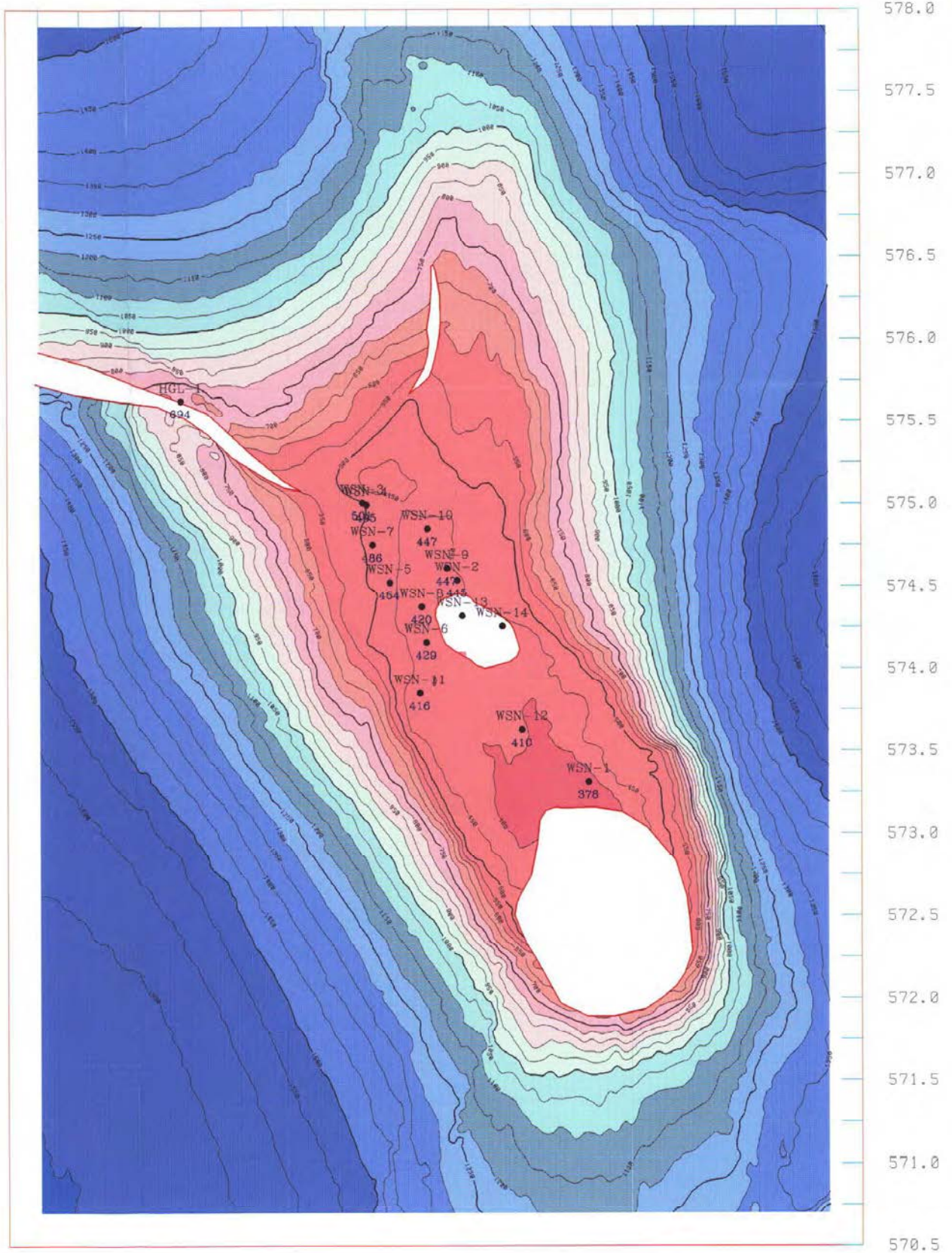
1:25000
km 0 1 2 km

TNO-NITG, Dept. of Geo-Energy
Akzo Nobel Salt bv Hengelo

salt dome Winschoten
base Tertiary
depth (m below NAP)

Scale 1:25,000 Map 4 Date 27-11-00

261.0 261.5 262.0 262.5 263.0 263.5 264.0 264.5 265.0 265.5 266.0



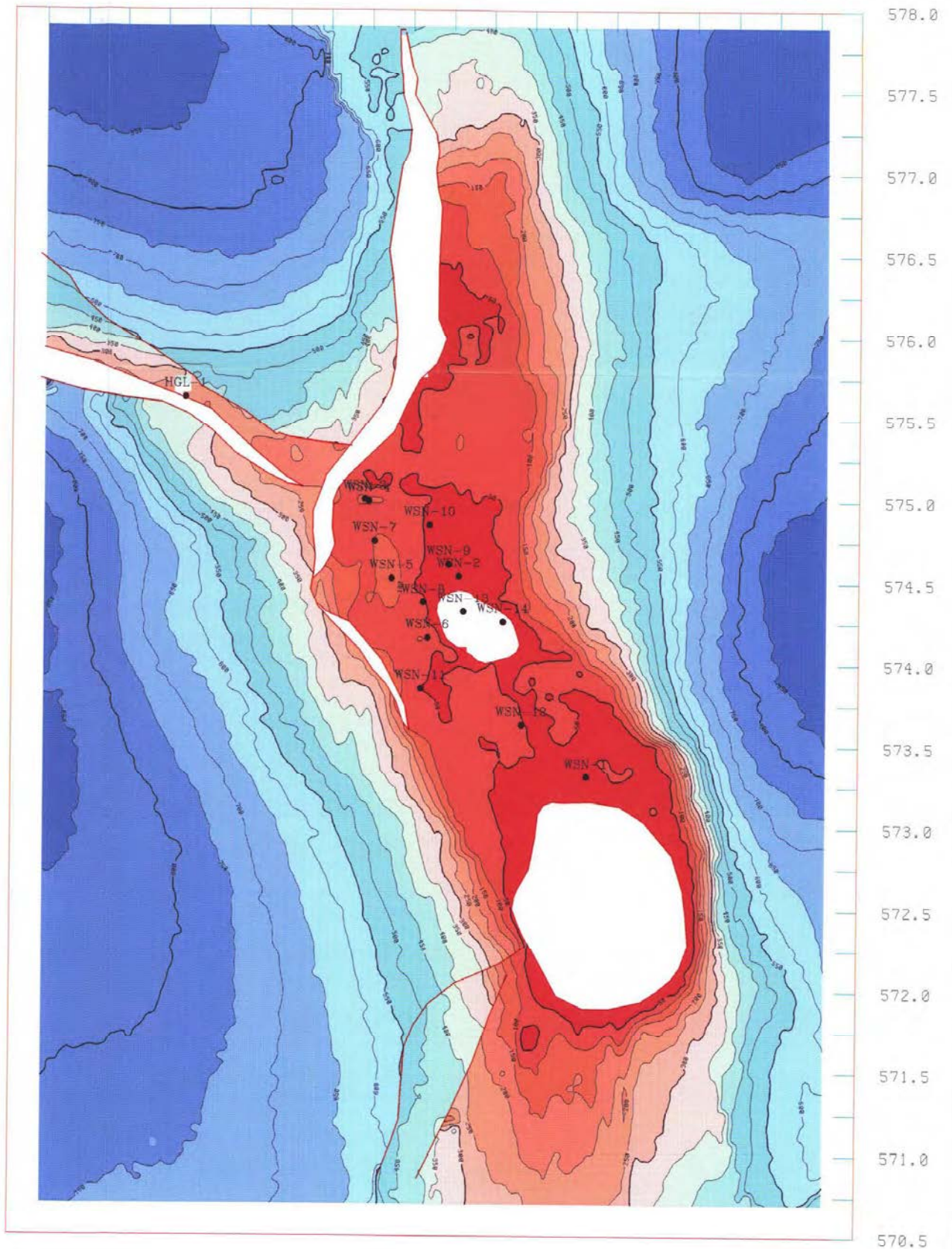
1:25000
 km 0 1 2 km

TNO-NITG, Dept. of Geo-Energy
 Akzo Nobel Salt by Hengelo

salt dome Winschoten
 base Upper Cretaceous
 depth (m below NAP)

Scale 1:25,000 Sheet Map 5 Date 29-JUN-00

261.0 261.5 262.0 262.5 263.0 263.5 264.0 264.5 265.0 265.5 266.0

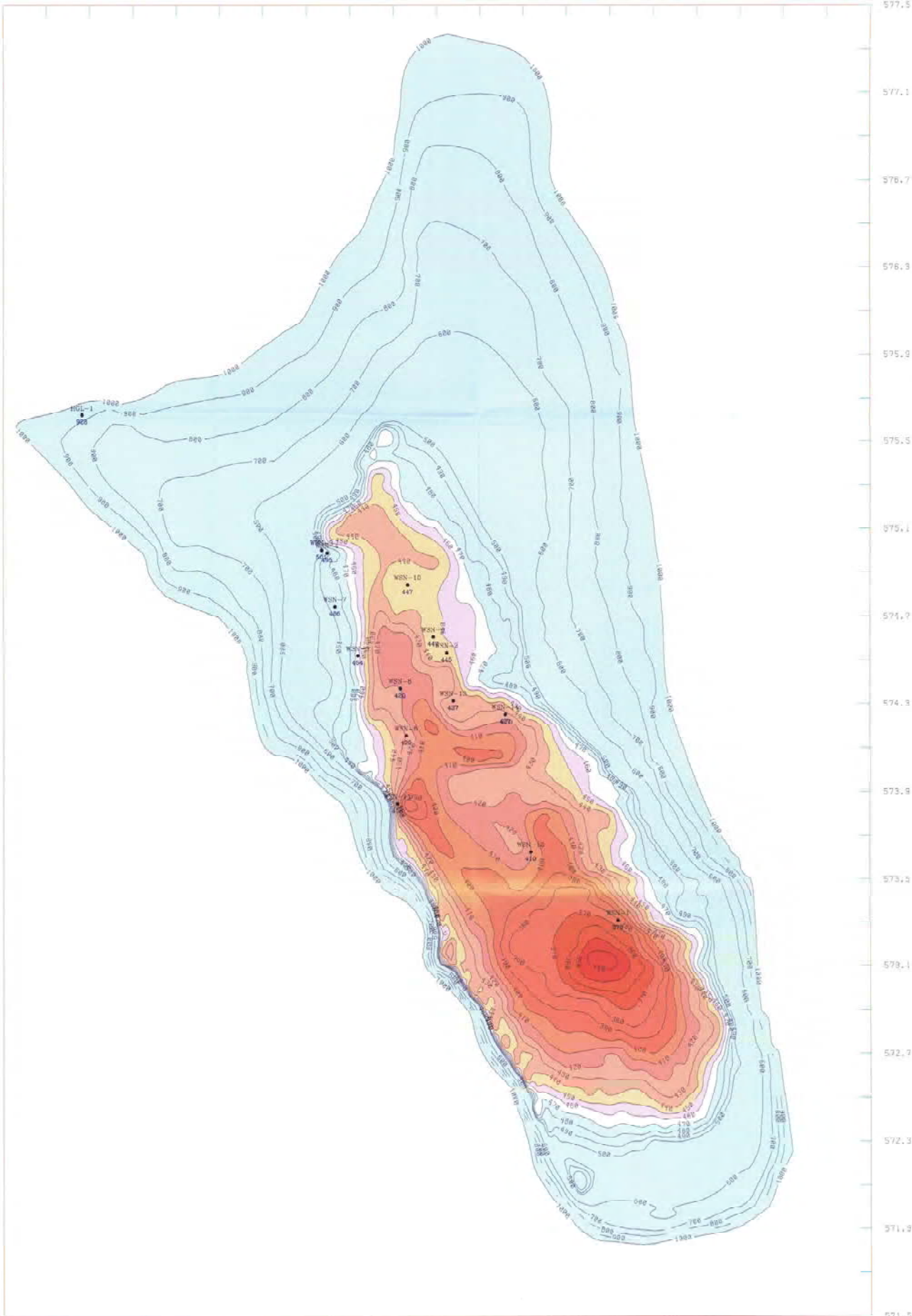


1:25000
km 0 1 2 km

TNO-NITG, Dept. of Geo-Energy
Akzo Nobel Salt bv Hengelo

salt dome Winschoten
Upper Cretaceous
thickness (m)

SCALE 1:25,000	DATE Map 6	DATE 22-JUN-88
----------------	------------	----------------



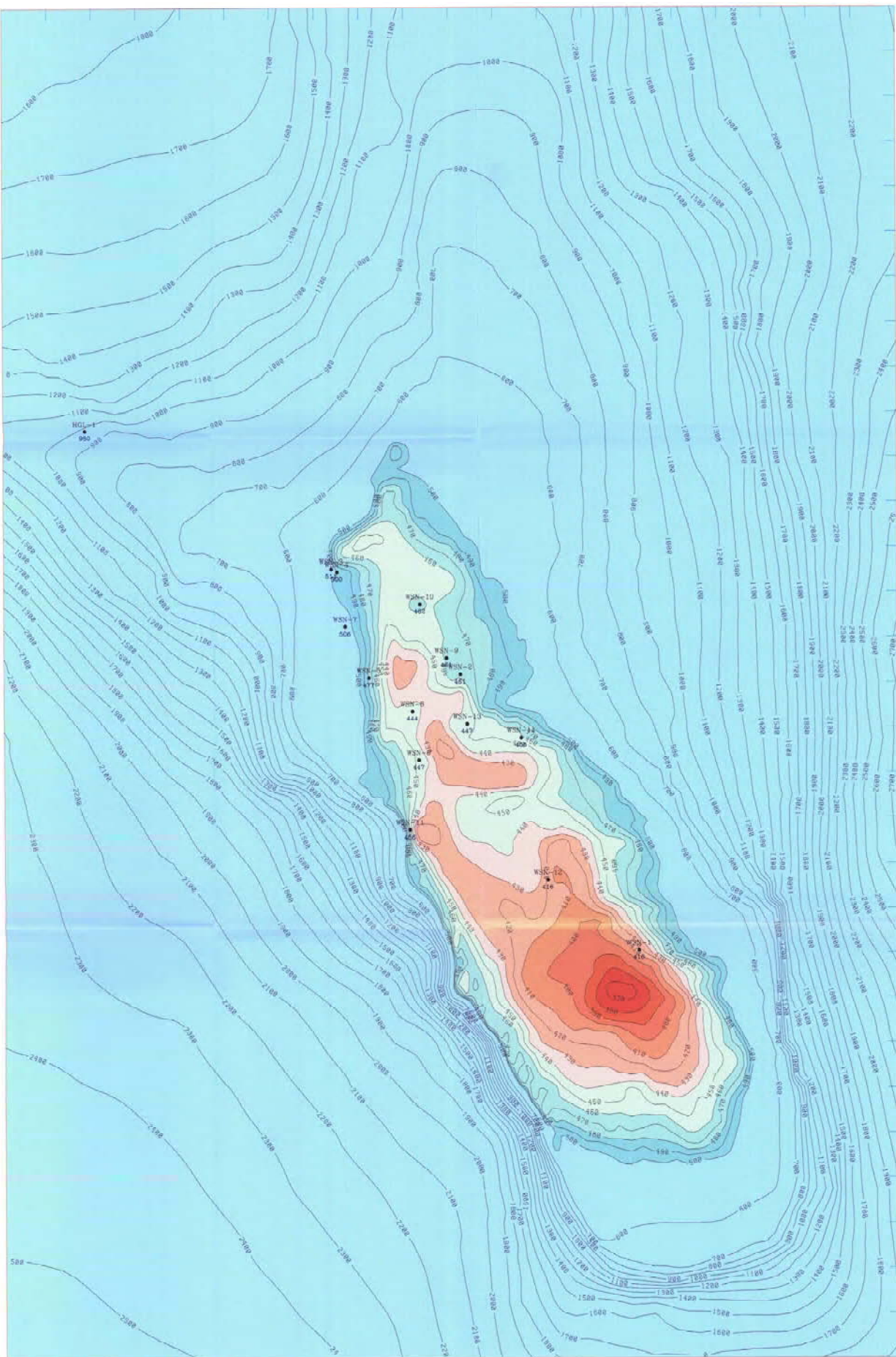
577.5
577.1
576.7
576.3
575.9
575.5
575.1
574.7
574.3
573.9
573.5
573.1
572.7
572.3
571.9
571.5



TNO-NITG, Dept. of Geo-Energy
Akzo Nobel Salt by Hengelo

salt dome Winschoten
top caprock
depth (m below NAP)

Scale 1:10,000 Map 7 Date 21-SEP-88



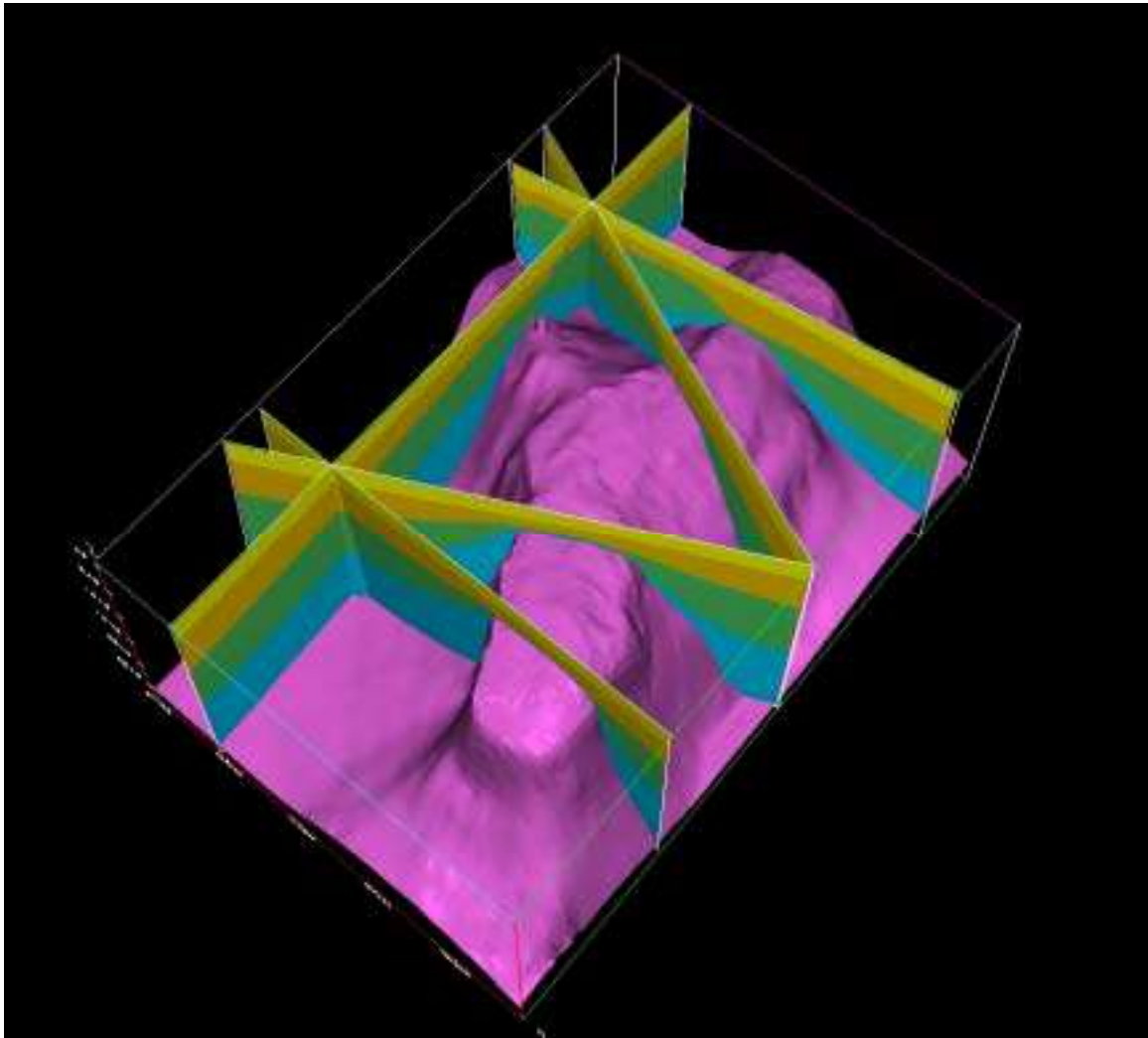
577.5
577.1
576.7
576.3
575.9
575.5
575.1
574.7
574.3
573.9
573.5
573.1
572.7
572.3
571.9
571.5



TNO-NITG, Dept. of Geo-Energy
Akzo Nobel Salt bv Hengelo

salt dome Winschoten
top salt
depth (m below NAP)

1:100,000 Map 8 21-SEP-00

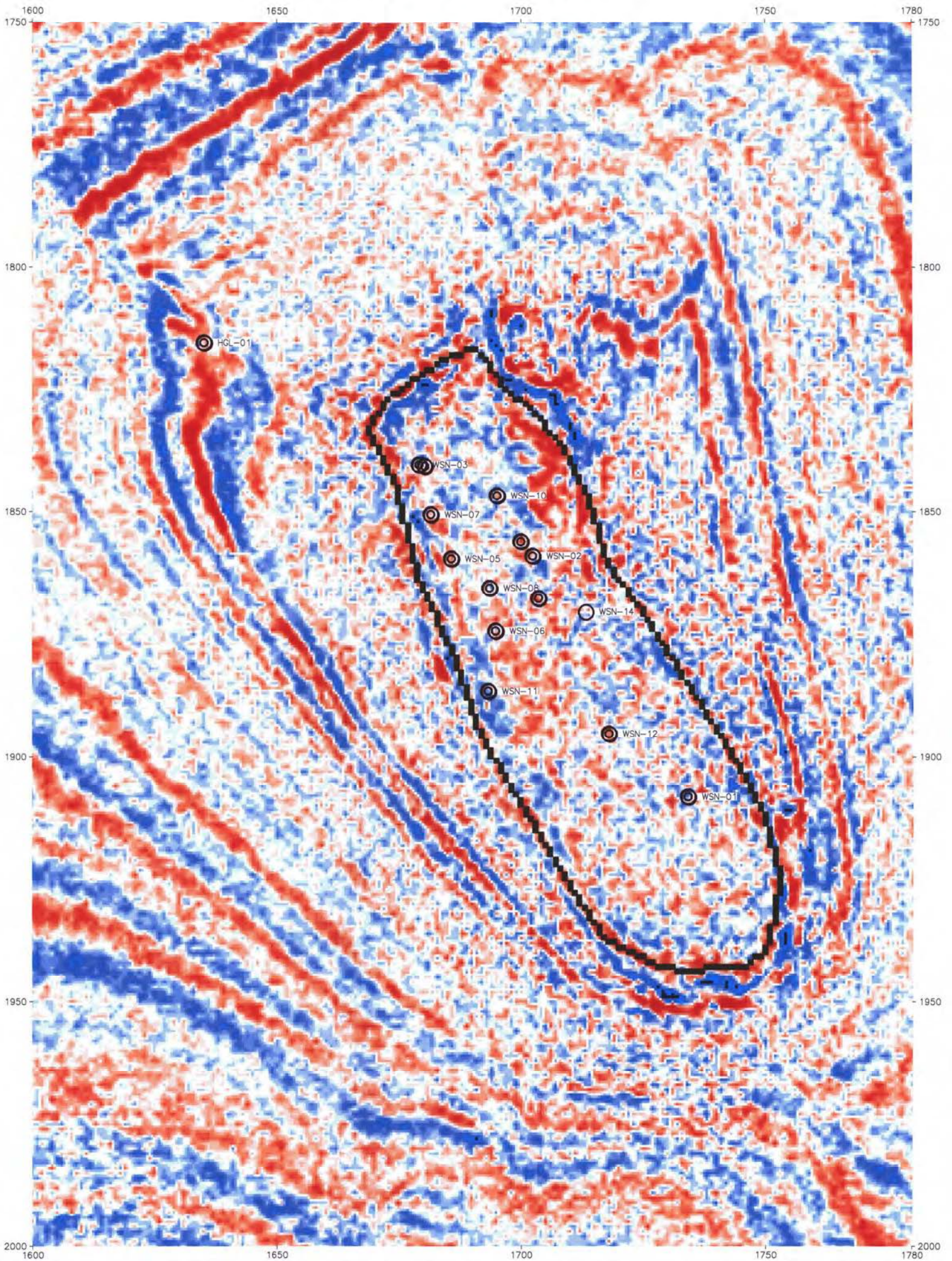


Map 9 Structural sections

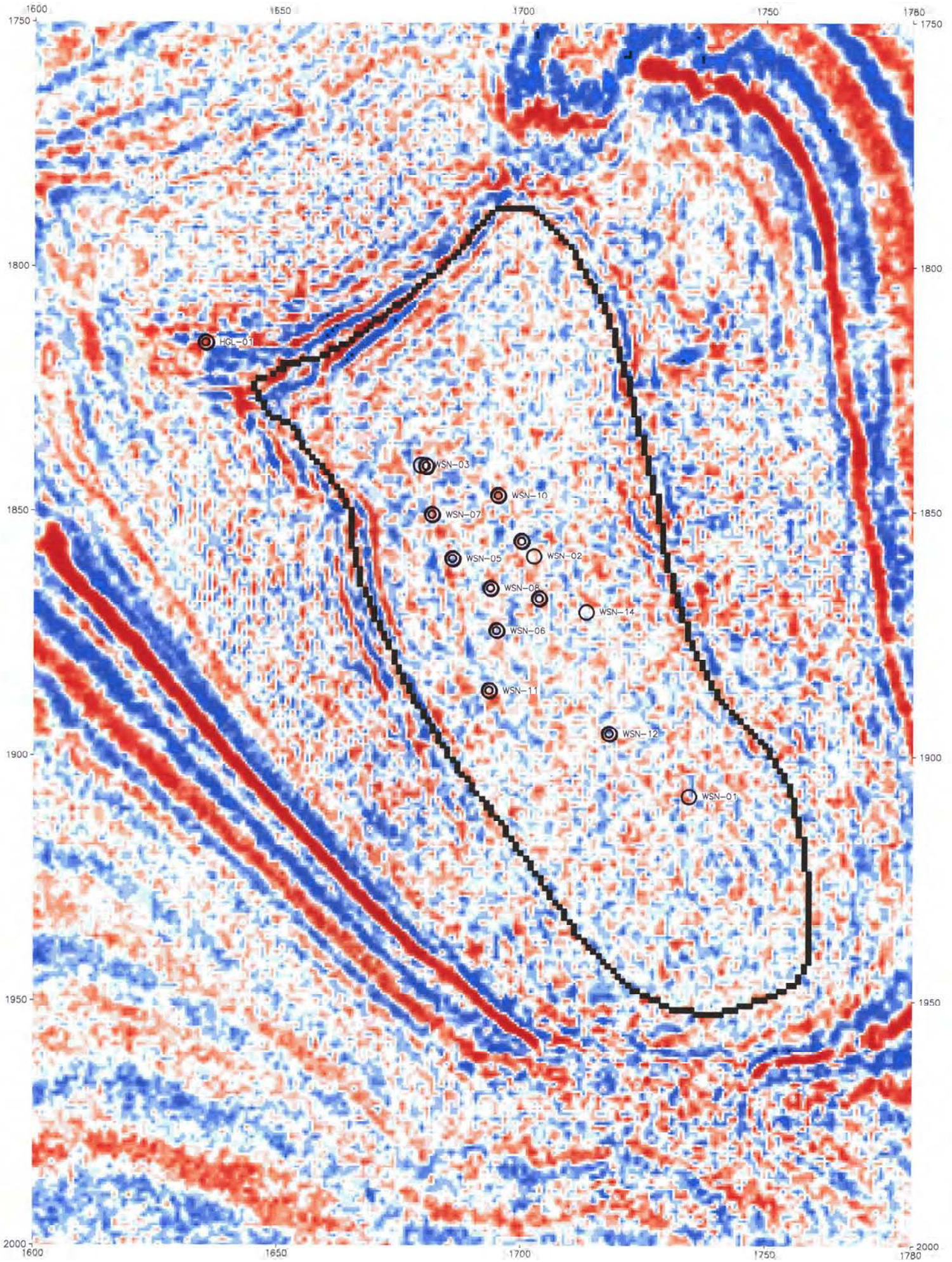
Upper Tertiary: yellow
Lower and Middle Tertiary: orange
Chalk Group: dark green
Lower Cretaceous + Triassic: blue
Top salt: purple

Timeslice 540

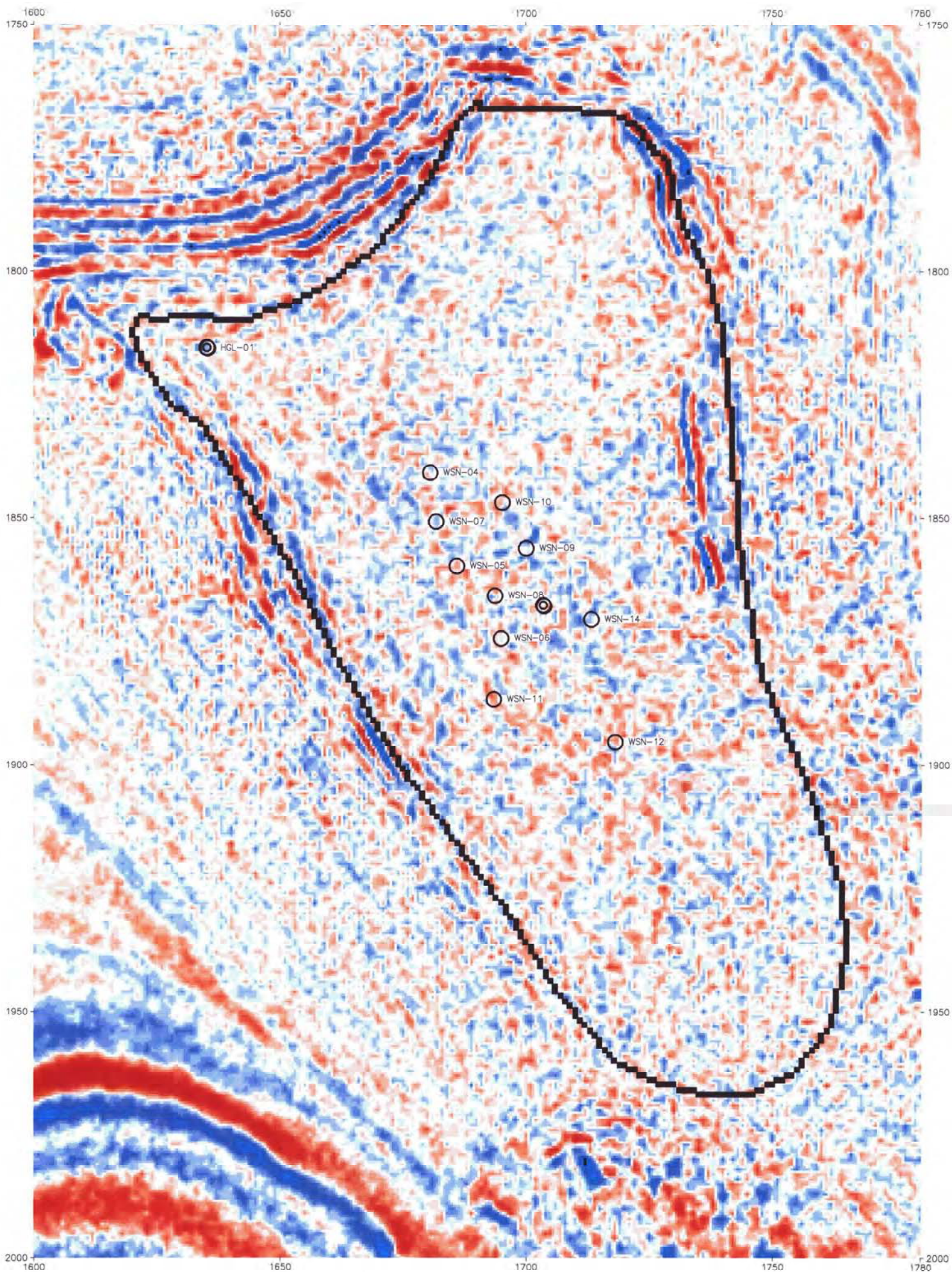
Map 10

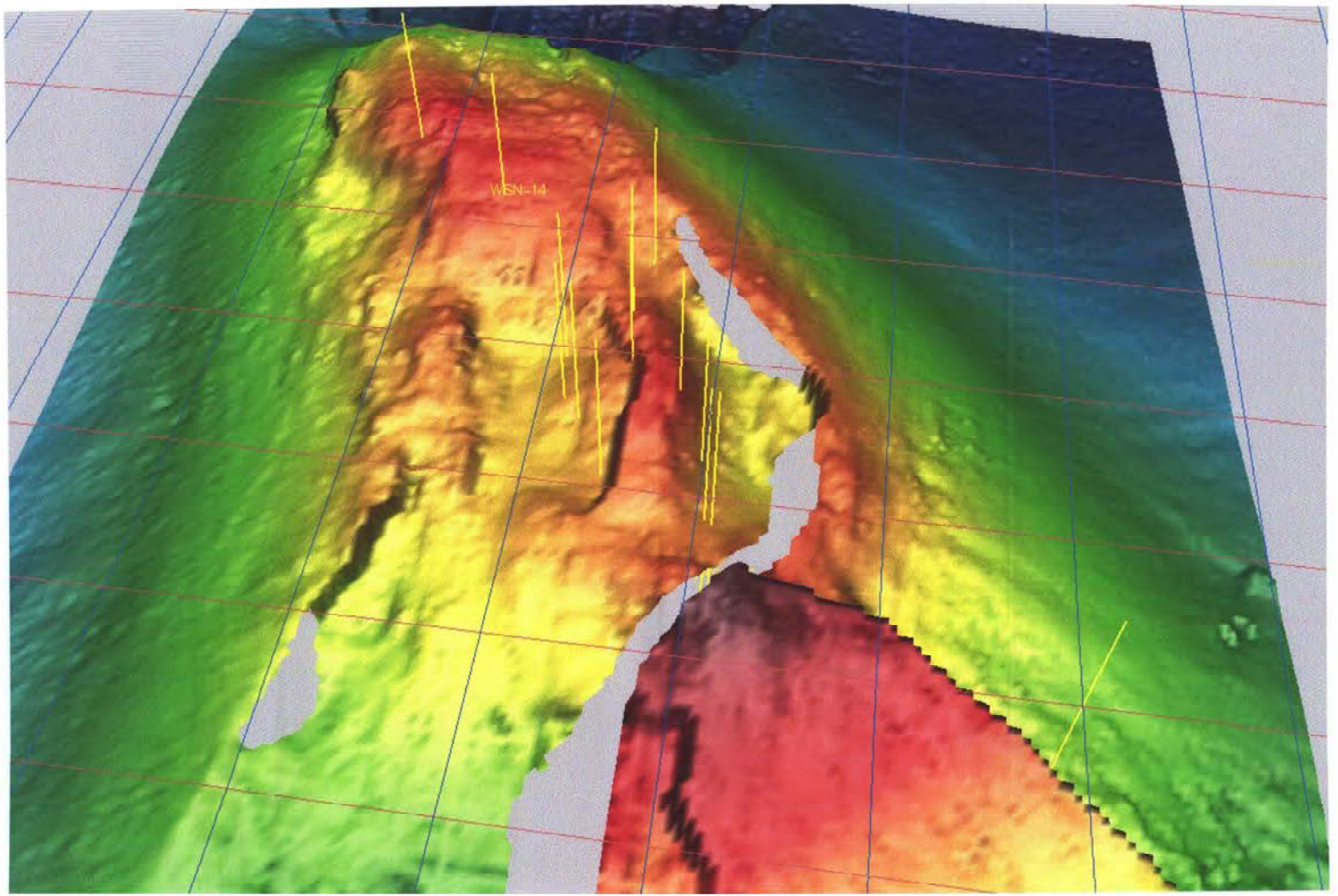


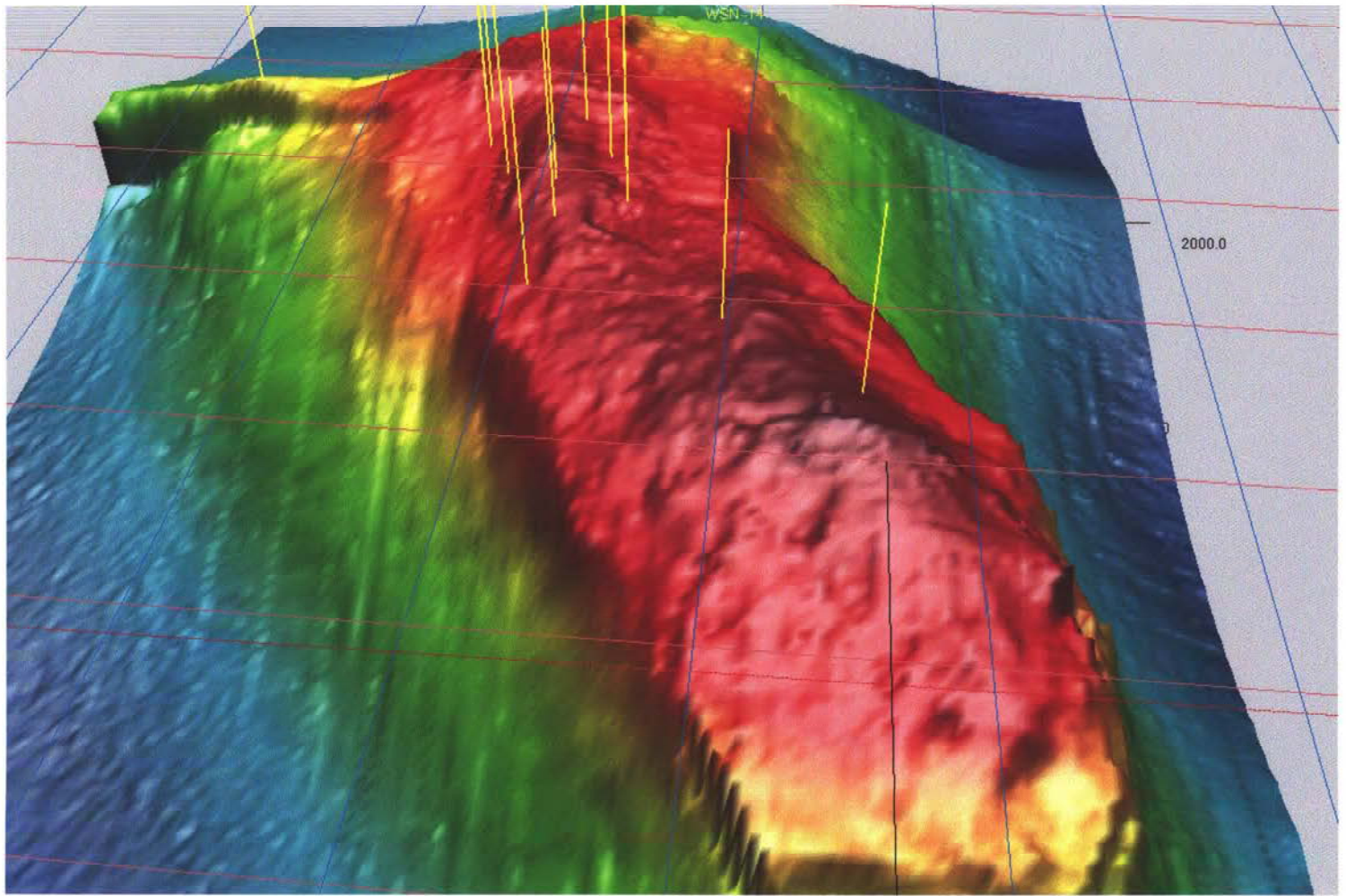
Timeslice 720

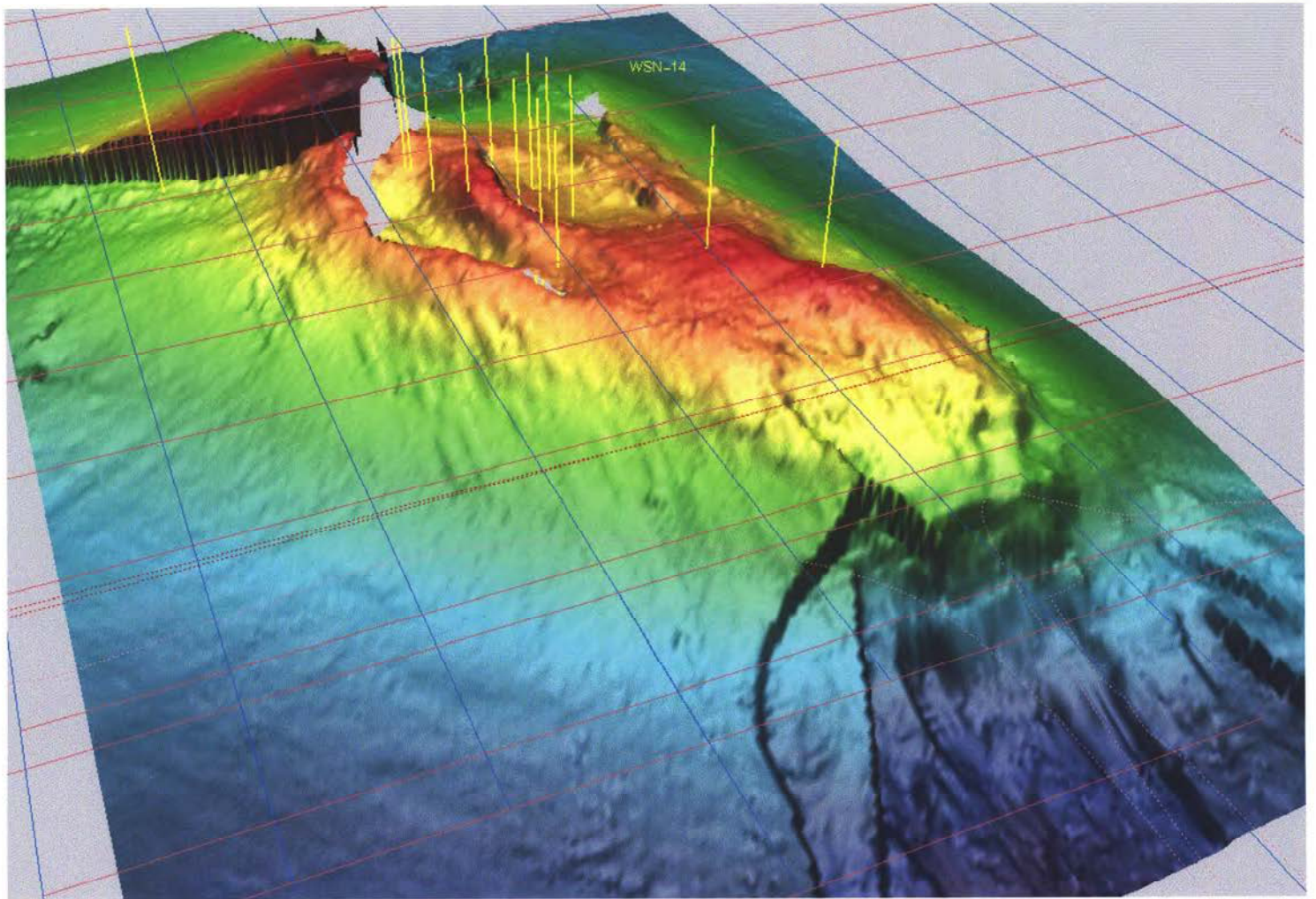


Timeslice 940









Tab: Actualisering bestaande geologische kaarten

Princetonlaan 6
Postbus 80015
3508 TA Utrecht

www.tno.nl

T 030 2564600
F 030 2564605
info@nitg.tno.nl

TNO-rapport

NITG 02-194-C

**Actualisering van de bestaande geologische
kaarten van de concessie Adolf van Nassau en van
de concessies Twenthe-Rijn, Buurse en
Uitbreiding Twenthe-Rijn**

Datum	18 december 2002
Auteur(s)	Hans Doornenbal Ed Duin Harald de Haan
Exemplaarnummer	
Oplage	4
Aantal pagina's	14
Aantal bijlagen	13
Opdrachtgever	Akzo Nobel Chemicals b.v. Postbus 25 7550 GC Hengelo
Projectnaam	Akzo Kaarten
Projectnummer	005.72021

Alle rechten voorbehouden.

Niets uit deze uitgave mag worden vermenigvuldigd en/of openbaar gemaakt door middel van druk, foto-kopie, microfilm of op welke andere wijze dan ook, zonder voorafgaande toestemming van TNO.

Indien dit rapport in opdracht werd uitgebracht, wordt voor de rechten en verplichtingen van opdrachtgever en opdrachtnemer verwezen naar de Algemene Voorwaarden voor onderzoeksovereenkomsten aan TNO, dan wel de betreffende terzake tussen de partijen gesloten overeenkomst.

Het ter inzage geven van het TNO-rapport aan direct belang-hebbenden is toegestaan.

Samenvatting

In opdracht van Akzo Nobel Chemicals b.v. te Hengelo zijn er fouten berekend in de dieptekaarten, die door TNO-NITG in 1997 geproduceerd werden, van de top van het zout van twee zoutdomees in de concessie Adolf van Nassau. De fout neemt over een afstand van 250 m vanaf de putlocatie lineair toe tot 8.5 m voor de Winschoten zoutdome en tot 6.0 m voor de Zuidwending zoutdome.

Ook zijn in deze studie de dieptekaarten van de door TNO-NITG in 1999-2000 gekarteerde horizons in de concessies Twenthe-Rijn, Buurse en uitbreiding Twenthe-Rijn geactualiseerd met de gegevens van 37 nieuwe boringen. Deze actualisering heeft geresulteerd in 4 nieuwe 1: 25.000 en 8 nieuwe 1: 10.000 dieptekaarten van basis Tertiair, basis Muschelkalk, top Röt zout, basis Röt-zout en de toppen en bases van de A-, B-, C- en D-zoutlaagpakketten van het Röt-zout.

Tevens is er nu een “fouten-kaart” geproduceerd, die een indruk geeft van de betrouwbaarheid van deze dieptekaarten op een willekeurige locatie in dit gebied. Deze “fouten-kaart” is met een speciale techniek (“kriging”) gecreëerd, welke met veel vertrouwen in dit gebied toegepast kon worden, vanwege het grote aantal boringen (503).

Aan Oranjewoud b.v. zijn (geactualiseerde) bestanden geleverd, die als input moet dienen voor het creëren van 3D modellen van geologische lagen in de Akzo Nobel concessies.

De voornaamste aanbevelingen die naar aanleiding van deze studie naar voren komen zijn, dat ook in de toekomst de diepte- en diktekaarten van de geologische lagen in de Akzo Nobel concessies regelmatig geactualiseerd dienen te worden met behulp van nieuw vergaarde basisgegevens en dat het ook erg belangrijk is om meerdere geavanceerdere technieken te testen, die toegepast kunnen worden bij het onderzoeken van de betrouwbaarheid van geproduceerde dieptekaarten.

Inhoudsopgave

1	Inleiding — 4
2	Activiteiten concessie Adolf van Nassau — 5
2.1	Betrouwbaarheid kaarten — 5
2.1.1	Winschoten zoutdome — 5
2.1.2	Zuidwending zoutdome — 5
2.2	Levering van ArcInfo gridfiles — 5
3	Activiteiten Concessies Twenthe-Rijn, Buurse en uitbreiding Twenthe-Rijn — 6
3.1	Updaten van bestanden — 6
3.2	1:10.000 kaarten — 7
3.2.1	Kriging methode — 7
3.2.2	Experimentele variogrammen en model variogrammen — 7
3.2.3	Geproduceerde kaarten — 9
3.2.4	Betrouwbaarheid kaarten — 10
3.3	1:25.000 kaarten — 11
3.4	Levering van ArcInfo gridfiles — 11
4	Resultaten — 12
5	Aanbevelingen — 13
6	Referenties — 14

1 Inleiding

In 1999-2000 zijn door TNO-NITG kaarten geproduceerd van de in de concessie Adolf van Nassau gelegen Winschoten zoutdome en Zuidwending zoutdome (zie rapporten TNO-NITG, 1999 en TNO-NITG, 2000)

In 1997 zijn in opdracht van Akzo Nobel Chemicals b.v. te Hengelo door TNO-NITG met behulp van nieuw beschikbare basisgegevens (boringen en seismiek) de oude geologische kaarten uit de zeventiger en begin tachtiger jaren geactualiseerd voor de concessies Twenthe-Rijn, Buurse en uitbreiding Twenthe-Rijn (zie rapport NITG-TNO, 1997). Deze kartering resulteerde in een aantal diepte- en diktekaarten. Om de zoutwinning zo efficiënt mogelijk te maken werd in bovengenoemd rapport aanbevolen de onzekerheden in diepte en dikte van de zoutlaagpakketten van het Röt Zout te reduceren door o.a. het vergaren van meer basisgegevens. Sinds 1997 heeft Akzo in dit gebied 37 nieuwe boringen verzameld.

Met dit project heeft Akzo Nobel Chemicals b.v. aangegeven het volgende te willen bereiken (zie ook inkoopopdrachtnummer/printdatum: 51/088089/28.05.2002):

- 1) Het actualiseren van door TNO-NITG geproduceerde kaarten met nieuw verkregen basisdata (boringen en seismiek).
- 2) Het verkrijgen van een beter inzicht in de onnauwkeurigheid van de dieptewaarden van de kaarten.
- 3) Input voor 3D-modellen. Akzo Nobel Chemicals bv is in samenwerking met Oranjewoud b.v. bezig om 3D-modellen van geologische lagen te creëren in de genoemde Akzo Nobel concessies.

2 Activiteiten concessie Adolf van Nassau

2.1 Betrouwbaarheid kaarten

Met een zelfontwikkeld programma foutdiep wordt de fout in de diepte tot een horizon in de ondergrond berekend. De fout wordt voornamelijk veroorzaakt door onzekerheden in het voor de tijd-diepte conversie van de seismische interpretatie gebruikte snelheidsmodel. Ook de onzekerheid in het interpreteren (het “picken”) van een horizon in een seismische sectie wordt door foutdiep meegewogen. De aldus berekende waarde is meer een indicatie voor de fout dan een exact weergave. Aangenomen kan worden dat de kans ongeveer 66% is, dat de werkelijke diepte van een horizon binnen de door foutdiep bepaalde foutenmarge valt. Omdat het uit de tijd-diepte conversie van de seismische interpretaties bepaalde dieptegrid van de top van de domes gecorrigeerd is voor de putwaarden, is op en in de nabijheid van de putlocaties de fout kleiner dan de met foutdiep bepaalde waarde. Aangenomen wordt dat vanuit de putlocatie de waarde van de fout over een afstand van ongeveer 250 m lineair toeneemt naar de met foutdiep bepaalde waarde. Omdat de kartering van de Winschoten en de Zuidwending zoutdome in de Adolf van Nassau concessie gebaseerd is op een seismische interpretatie, is deze methode daar toegepast.

2.1.1 Winschoten zoutdome

Voor de Winschoten zoutdome is met *foutdiep* een waarde voor de fout van 8.50 m bepaald. Het gecorrigeerde dieptegrid geeft op de locatie van de putten een gemiddelde afwijking van ongeveer 1.00 m. Aangenomen wordt dat de fout over een afstand van 250 m vanaf de putlocatie lineair toeneemt van 1.00 m naar 8.50 m.

2.1.2 Zuidwending zoutdome

Voor de Zuidwending zoutdome is met *foutdiep* een waarde voor de fout van 6.00 m bepaald. Het gecorrigeerde dieptegrid geeft op de locatie van de putten een gemiddelde afwijking van ongeveer 0.05(!) m. Aangenomen wordt dat de fout over een afstand van 250 m vanaf de putlocatie lineair toeneemt van 0.05 m naar 6.00 m.

2.2 Levering van ArcInfo gridfiles

Door TNO-NITG zijn ArcInfo ASCII-bestanden gemaakt door conversie van de Zycor ASCII-bestanden, die het resultaat waren van de seismische kartering in 1999-2000 (zie rapporten TNO-NITG, 1999 en TNO-NITG, 2000). De volgende bestanden zijn naar Oranjewoud gestuurd :

Winschoten zoutdome:

23 april 2002: top-caprock_WSN.asc, basis_trias_WSN.asc,
basis_bovenkrijt_WSN.asc, basis_tertiair_WSN.asc, basis_mioceen_WSN.asc
16 oktober 2002: WSN_topzout.asc

Zuidwending zoutdome:

23 april 2002: top_zout_ZW.asc, basis_trias_ZW.asc, basis_onderkrijt_ZW.asc
basis_bovenkrijt_ZW.asc, basis_tertiair_ZW.asc, basis_mioceen_ZW.asc
16 oktober 2002: ZW_topcaprock.asc

3 Activiteiten Concessies Twenthe-Rijn, Buurse en uitbreiding Twenthe-Rijn

3.1 Updaten van bestanden

De database van boringen is in juni-augustus 2002 door TNO-NITG en Akzo Nobel gecontroleerd door middel van het vergelijken van de database die door TNO-NITG in 1997 werd opgebouwd en de database die Akzo Nobel in zijn bezit had. Hierbij werden verschillen in coördinaten, TD en maaiveldhoogte maar ook in diepten van de verschillende horizons geconstateerd. Deze verschillen zijn door Akzo Nobel nader onderzocht en daarna verbeterd. Ook in een later stadium (oktober 2002) zijn er door Akzo Nobel nog van een aantal boringen de dieptewaarden van een aantal zoutlagen gecontroleerd, nadat uit de kartering van de desbetreffende horizon door TNO-NITG mogelijke anomale waarden waren geconstateerd. Ook werd de database uitgebreid met de data van 37 nieuwe boringen die sinds eind 1996 werden verzameld. Uiteindelijk heeft dit geresulteerd in een consistente database, die bij TNO-NITG en Akzo identieke waarden bevat. In totaal bevat deze database nu 503 boringen (zie bijlage 1).

3.2 1:10.000 kaarten

3.2.1 Kriging methode

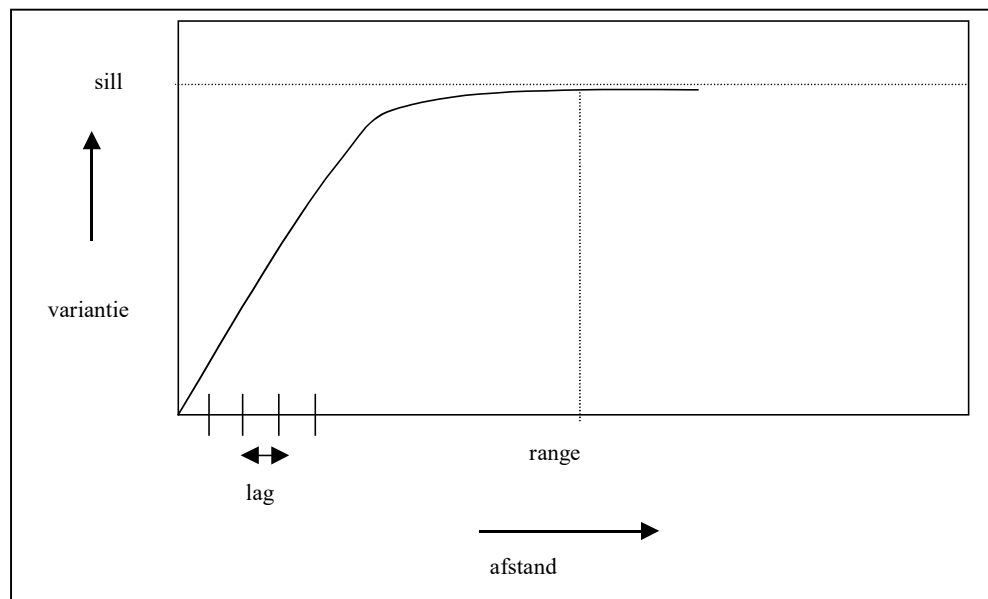
De dataset in de Twenthe-Rijn concessie bevat zeer veel datapunten van 503 boringen in een relatief klein gebied. Hierdoor is het een dataset die zich zeer goed leent om m.b.v. “kriging” te interpoleren.

Kriging is een interpolatiemethode waarbij de afhankelijkheid van datapunten als functie van de afstand bepalend is voor het gewicht van de punten die in het kriging proces worden gebruikt. Deze afhankelijkheid wordt weergegeven in een zogenaamd variogram. Het voordeel van de kriging methode t.o.v. andere interpolatiemethodes (zoals b.v. inverse distance gridding) is dat de weging van de datapunten niet bij voorbaat vaststaat maar wordt vastgesteld op basis van de data zelf. Een nadeel van de methode is dat er voldoende datapunten dienen te zijn om een betrouwbaar variogram vast te kunnen stellen. Voor de kriging is gebruik gemaakt van het geostatistische pakket Isatis van de firma Geovariances

Voor 8 horizons is de kriging uitgevoerd, Top zout-A t/m Top zout-D en Basis zout-A t/m Basis zout-D. Van de 503 boringen zijn 490 boringen gebruikt, waarin de dieptes van deze horizons zijn gedefinieerd.

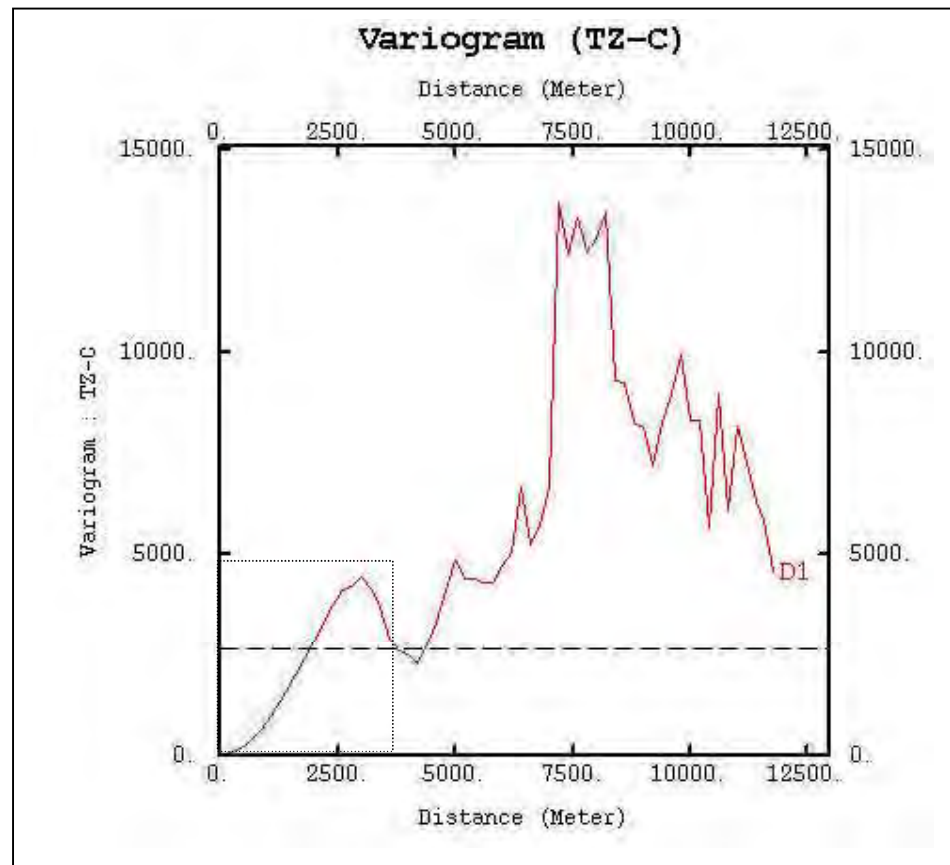
3.2.2 Experimentele variogrammen en model variogrammen

Een variogram wordt gekarakteriseerd door drie variabelen: de lag, de range en de sill (zie figuur 1). Allereerst worden de datapunten ingedeeld in afstandsklassen (lags). Binnen deze lags wordt bepaald wat de variantie van de punten binnen de betreffende lag is. De twee overige parameters, range en sill, leggen de vorm van het variogram vast. De range is de afstand waarbij het variogram vlak gaat lopen. Bij afstanden tussen datapunten groter dan de range worden punten als onafhankelijk van elkaar beschouwd. De sill geeft de grootte van de variantie aan bij afstanden groter dan de range.



Figuur 1 Karakteristieke parameters van een variogram

De experimentele variogrammen van de dieptewaarden van de verschillende horizons in de putten laten alle 8 een soortgelijk patroon zien. In figuur 2 is het experimentele variogram van Top zout-C afgebeeld. De variantie neemt toe tot ongeveer 3000 m en fluctueert daarna. Het gedrag van het experimentele variogram in de eerste 3000 m is erg glad en lijkt mede door het grote aantal datapunten dat hieraan ten grondslag ligt erg betrouwbaar.



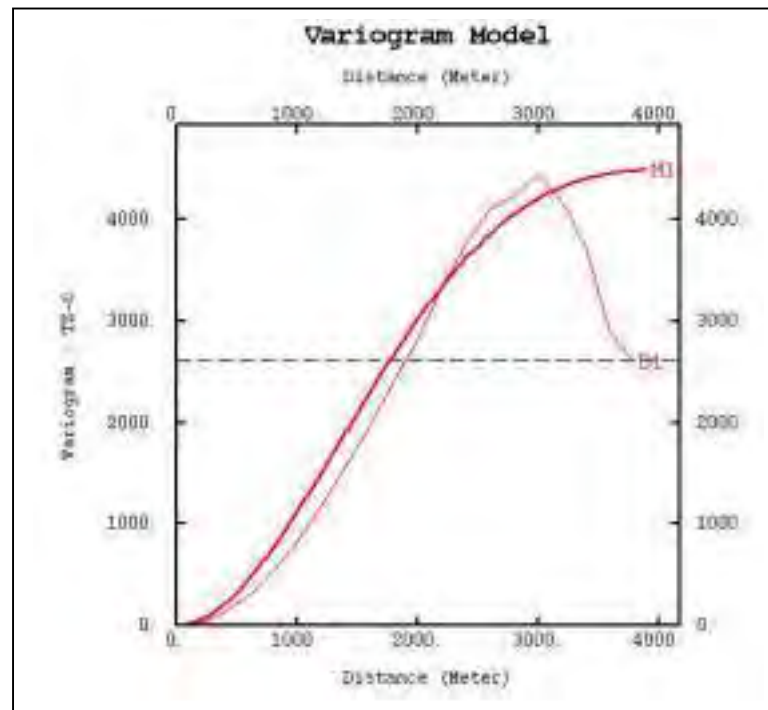
Figuur 2 Experimenteel variogram van Top zout-C (Tz-C). De gestippelde rechthoek geeft aan welk deel gebruikt is voor het bepalen van het Model variogram

Het feit dat het experimentele variogram niet naar een stabiel plateau gaat heeft twee redenen. Ten eerste veroorzaakt de structuur een spatiele afhankelijkheid die in het variogram naar voren komt. De afstanden in de grootste lags zijn afstanden langs de as van de structuur, waardoor ondanks de grote afstand de dieptewaarden van de datapunten niet veel verschillen. Ten tweede is in de grootste lags het aantal datapunten sterk verminderd, waardoor de variantie veel minder betrouwbaar is.

Figuur 3 geeft het experimentele en het modelvariogram voor Top zout-C. De model variogrammen die een beste fit gaven in de eerste 3000 à 4000 m staan in Tabel 1.

Horizon	type model	range	Sill
Top zout-D	Cubic	4500	3800
Basis zout-D	Cubic	4400	3800
Top zout-C	Cubic	4500	4500
Basis zout-C	Cubic	4500	4500
Top zout-B	Cubic	4500	4600
Basis zout-B	Cubic	4500	4500
Top zout-A	Cubic	4400	4500
Basis zout-A	Cubic	4500	5700

Tabel 1: De resulterende waarden voor de range en de sill van de modelvariogrammen van de horizons Top zout-D t/m Basis zout-A.



Figuur 3 Experimenteel variogram (D1) en Model variogram (M1)

3.2.3 Geproduceerde kaarten

De grids die berekend zijn met de kriging methode honoreren alle putdata exact. Doordat de dikte van de lagen in het model ten opzichte van de dieptewaarde erg klein is kan het voorkomen dat de resulterende gekrigde grids elkaar lokaal doorsnijden (dikte van laag < 0!). Daarom is er voor gekozen om alleen het gekrigde Top zout-C grid te gebruiken en op basis hiervan de Basis zout-C en de tops en bases van de andere zoutlagen te construeren. Daartoe zijn uit de putwaarden de diktes t.o.v. de Top zout-C berekend en vervolgens met een “least-squares methode” gegrid. Hierbij is net als voor

het Top zout-C grid een gridincrement van 50 m gebruikt. Vervolgens zijn diktegrids van de Top en de Basis zout-A, de Top en Basis zout-B en de Basis zout-C opgeteld bij en de Top en Basis zout-D diktegrid afgetrokken van het Top zout-C dieptegrid. Van de aldus verkregen dieptegrids zijn de contourkaarten gemaakt (zie bijlagen 5 t/m 12)

3.2.4 *Betrouwbaarheid kaarten*

Bij het krigen wordt behalve de waarden van de te berekenen punten ook een standaarddeviatie voor het punt worden berekend. Dit gebeurt voor elk punt op basis van het modelvariogram en de afstand van het te berekenen punt tot aan datapunten.

Voor het Top zout-C niveau is een standaarddeviatie grid berekend. De standaarddeviatie voor Top zout-C is erg klein in de omgeving van de putten (slechts enkele meters). Door uit de dataset willekeurig putten weg te laten en hiermee opnieuw te gaan krigen kan de berekende standaarddeviatie op haar validiteit getest worden. De voorspelde waarde op de plaats van de weggelaten put geeft dan een indicatie voor de betrouwbaarheid van de voorspelling. Na 20 putten te hebben weggelaten bleken 14 van de weggelaten putten een voorspelling te hebben die minder dan 1 m afweek van de werkelijke waarde. 5 putten hadden een afwijking tussen de 1 en 2 m en 1 put een afwijking tussen de 2 en 3 m. Deze resultaten zijn in lijn met het berekende standaarddeviatie grid.

De meeste putten zijn echter in clusters van meestal 3 putten geboord. Indien slechts 1 van de putten van een cluster wordt weggelaten dan geven de andere putten uit dat cluster een goede voorspelling van het weggelaten punt. Een heel ander resultaat levert het selectief weglaten van hele clusters. Om dit te testen zijn er een aantal clusters willekeurig verdeeld over het gebied weggelaten bij het krigen (totaal 60 putten) De verschillen tussen voorspelde dieptewaarden van de weggelaten putten en de werkelijke dieptewaarden liepen nu op tot 18 m. Het resultante standaarddeviatie grid liet ook grotere standaarddeviaties zien op de plaats van de weggelaten clusters maar qua grootte niet overeenkomstig met de aangetroffen verschillen in de test. Indien 3x de standaarddeviatie werd genomen bleek ongeveer 90% van de geobserveerde afwijkingen uit de test binnen deze 3x standaarddeviatie marge te liggen. Dit 3x standaarddeviatie grid is dan ook door TNO-NITG gebruikt om de onzekerheden te voorspellen. In Bijlage 13 is het 3x-standaarddeviatiegrid afgebeeld als gemiddelde foutenkaart. Voor een willekeurig gridpunt op de kaart kan de voorspelde dieptewaarde worden afgelezen op de Top zout-C dieptekaart (bijlage 7) en de onzekerheid op dit gridpunt op de 3x- standaarddeviatiekaart. Op het betreffende gridpunt geldt dan dat TNO-NITG de kans 90% schat dat de werkelijke dieptewaarde binnen de voorspelde waarde plus of min 3x standaarddeviatie ligt.

3.3 1:25.000 kaarten

Voor het updaten van de 1:25.000 kaarten zijn de bestaande dieptegrids, die het resultaat waren van de kartering in 1997 (zie rapport NITG-TNO, 1997), gecorrigeerd met de verkregen diepte waarden van de 37 nieuwe boringen. Hiertoe zijn de dieptecontouren daar waar nodig enigszins bijgesteld en is het grid vervolgens aangepast. Op de nieuwe kaarten staan de nieuw verkregen putten met een blauw vierkant symbool aangegeven (zie bijlagen 1 t/m 4).

3.4 Levering van ArcInfo gridfiles

Door TNO-NITG zijn ArcInfo ASCII-bestanden gemaakt door conversie van de geactualiseerde Zycor ASCII-bestanden.

De volgende bestanden zijn op 15 november 2002 naar Oranjewoud gestuurd :

- 1: 10.000 kaartbestanden

top_zoutlaagD.asc, basis_zoutlaagD.asc, top_zoutlaagC.asc, basis_zoutlaagC.asc,
top_zoutlaagB.asc, basis_zoutlaagB.asc, top_zoutlaagA.asc, basis_zoutlaagA.asc

- 1: 25.000 kaart-bestanden

basis_Tert.asc, basis_Musch.asc, top_zout.asc, basis_zout.asc

4 Resultaten

De volgende kaarten zijn geproduceerd:

Titel	Schaal	Bijlage
Diepte basis Tertiair	25000	1
Diepte basis Muschelkalk	25000	2
Diepte top Rot zout (=top D-zout of top C-zout)	25000	3
Diepte basis Rot zout	25000	4
Diepte top D-zout	10000	5
Diepte basis D-zout	10000	6
Diepte top C-zout	10000	7
Diepte basis C-zout	10000	8
Diepte top B-zout	10000	9
Diepte basis B-zout	10000	10
Diepte top A-zout	10000	11
Diepte basis A-zout	10000	12
Gemiddelde 90% fout	10000	13

5 Aanbevelingen

Uit deze studie komen de volgende aanbevelingen naar voren teneinde de geologische risico's voor Akzo Nobel te beperken:

- 1 *Kriging in twee richtingen.* Als in twee richtingen variogrammen worden gemaakt dan blijkt dat de dataset sterk anisotroop is. De afhankelijkheid van de datapunten loodrecht op de structuur is veel kleiner dan die parallel aan de structuur. Idealiter zou een kriging met deze twee hoofdrichtingen ideaal zijn. Een risico is dat is dat mogelijk geen stabiel model te construeren is dat de variogrammen in beide richtingen honoreert.
- 2 *Co-kriging van meerdere lagen.* Het effect dat gekrigde lagen elkaar kruisen kan wellicht voorkomen worden door co-kriging van de data te testen. Een probleem is dat het co-krigen van 8 lagen tegelijkertijd geen stabiele procedure is in Isatis. Wellicht zou eerst het co-krigen van enkele horizons getest moeten worden. Een andere mogelijkheid is om het lagenmodel in een ander pakket nl. Isatoil in te voeren. In Isatoil bestaat wel de mogelijkheid om het lagenmodel op te bouwen door de diktes van de afzonderlijke lagen gelijktijdig te co-krigen. TNO-NITG bezit momenteel echter geen licentie van Isatoil dus de software zou hiervoor geleased moeten worden. In Isatoil kunnen simulaties gerund worden van het lagenmodel, wat inzicht geeft over de onzekerheden binnen het lagenmodel. Bovendien kan het model ook met eigenschappen gevuld worden, waarmee volumetrie berekeningen verricht kunnen worden (deterministisch en stochastisch).
3. *Actualisering van bestaande kaarten.* Het verdient aanbeveling om de in deze studie geactualiseerde kaarten ook in de toekomst regelmatig te actualiseren met behulp van nieuwe basisgegevens.

6 Referenties

NITG-TNO (1997), *Kartering Twenthe-Rijn, Uitbreiding Twenthe-Rijn en Buurse Concessie*, drs. M.C. Geluk, drs. E.J.T. Duin, april 1997, Rapport no. NITG 97-69-C, Project nummer 147377611

TNO-NITG (1999), *Mapping of the Zuidwending Salt Dome*, M.C. Geluk, E.J.T. Duin, R.J. Arts, J.D. van Wees, December 1999, Rapport no. NITG 99-209-C, Project nummer 005.70114/01.02

TNO-NITG (2000), *Mapping of the Winschoten Salt Dome*, M.C. Geluk, E.J.T. Duin, September 2000, Rapport no. NITG 00-178-C, Project nummer 005.70114/01.03

No	Well	X	Y	MV	TD	Date_end	T.Te	B.Te	T.Mu	B.Mu	T.Z-D	B.Z-D	T.Z-C	B.Z-C	T.Z-B	B.Z-B	T.Z-A	B.Z-A
1	1	251438,9	473923,4	19,6	354,8	25-2-1935	-3,6	107,1					296,2	312,8	318,1	319,2	319,8	349,8
2	2	251341,8	473917,0	19,3	352,4	11-5-1935	5,0	109,6					300,0	316,5	317,9	322,7	323,4	347,6
3	3	251250,3	473916,4	18,8	369,1	31-7-1935	7,7	111,8	111,8				304,5	322,2	323,4	327,7	328,6	364,9
4	4	251161,2	473928,9	20,0	365,9	14-10-1935	6,5	113,3	113,3				310,1	324,6	326,3	330,0	330,8	360,3
5	5	251028,0	473950,5	20,1	364,3	23-12-1935	8,9	114,3	114,3	129,9			313,3	330,6	331,8	336,5	337,2	359,4
6	6	250893,7	473971,6	19,4	369,9	16-3-1936	7,9	115,9	115,9	120,2			317,3	336,1	336,7	340,9	341,8	364,9
7	7	251018,7	473844,9	19,2	365,3	18-7-1939	7,0	113,2	113,2	0,0			319,5	336,6	337,9	342,9	343,2	360,4
8	8	251024,8	473724,9	19,6	363,7	5-10-1939	5,5	109,7	109,7	0,0			326,9	342,8			343,9	360,5
9	9	250944,8	473672,7	19,5	369,3	29-5-1940	8,1	111,9	111,9	123,5			331,4	349,0	351,1	354,7	355,5	366,9
10	10	250852,7	473695,9	19,5	380,5	31-8-1940	10,3	112,7	112,7	125,5			335,3	353,1	354,5	358,0	359,4	375,6
11	11	250761,6	473722,1	19,9	384,2	21-3-1941	10,4	114,0	114,0	158,2			337,3	355,4	355,9	360,0	360,7	379,6
12	12	251547,1	473940,9	21,1	338,6	13-11-1947	5,9	106,7	0,0	0,0			286,4	304,1	305,4	310,6	311,4	333,9
13	13	251632,3	473873,0	21,1	332,5	23-2-1948	9,4	104,9	104,9	0,0			288,2	305,5	306,4	309,6	311,2	325,1
14	14	250892,0	473833,1	20,1	379,9	16-6-1948	6,9	107,4	107,4	0,0			322,1	340,6	342,7	347,7	348,8	371,8
15	15	250764,6	473847,1	19,6	387,3	25-9-1948	6,9	115,2	115,2	0,0			326,1	345,1	346,4	351,1	351,8	381,0
16	16	251204,5	473805,9	19,8	357,5	20-1-1949	8,5	112,0	112,0	0,0			315,5	321,7	323,2	324,7	332,7	347,1
17	17	251252,0	473695,1	19,8	356,3	3-5-1949	4,8	108,0	108,0	112,3			317,7	330,1	331,3	334,3	336,0	352,3
18	18	251266,1	473573,2	20,3	370,2	5-8-1949	14,2	106,2	106,2	122,5			316,7	334,1	335,6	340,0	340,7	361,0
19	19	251286,6	473454,0	20,4	377,1	14-11-1949	4,7	105,2	105,2	120,7			327,6	346,1	351,0	351,7	352,5	372,6
20	20	251315,1	473464,2	20,4	378,2	16-1-1950	4,6	108,2	108,2	121,6			325,4	344,2	345,9	348,8	350,6	376,5
21	21	251146,0	473620,8	19,7	361,8	25-5-1950	7,6	107,3	107,3	116,5			325,5	341,1	343,5	345,9	348,4	361,8
22	22	251147,3	473487,3	20,1	367,9	13-9-1950	5,2	106,3	106,3	114,8			333,4	350,1	351,1	355,6	358,1	374,1
23	23	251176,2	473365,5	20,6	383,8	25-11-1950	6,8	105,8	105,8	119,7			336,3	357,1	358,7	365,0	366,0	380,7
24	24	251263,6	473597,9	20,2	362,4	23-2-1951	10,3	106,5	106,5	122,1			314,8	331,3			332,5	359,3
25	25	251236,1	473230,5	20,5	392,8	1-6-1951	4,5	104,6	104,6	129,8			333,8	353,7	354,7	359,6	360,0	387,6
26	26	251248,2	473203,2	20,7	394,0	24-4-1952	5,6	104,3	104,3	127,4			333,3	352,8	353,8	358,7	359,5	384,5
27	27	250723,6	473586,1	20,0	390,4	9-8-1952	7,6	113,0	113,0	126,8			355,7	373,9			374,7	385,4
28	28	250725,9	473446,7	20,1	402,1	8-11-1952	7,6	111,0	111,0	137,7			363,1	376,7	376,7	380,6	380,6	393,5
29	29	250728,0	473306,7	20,6	409,1	24-2-1953	6,6	108,3	108,3	136,9			354,7	386,2			387,0	401,7
30	30	250730,8	473170,3	20,6	431,3	15-6-1953	6,4	109,5	109,5	131,6			363,4	383,5	384,4	389,5	390,2	423,7
31	31	250731,2	473140,3	20,7	426,2	16-10-1953	6,5	110,1	110,1	153,6			364,9	384,8	386,1	391,2	391,9	423,6
32	32	250874,1	473555,6	20,2	392,6	9-2-1954	9,4	110,8	110,8	134,3			351,1	367,3			368,0	381,0
33	33	250879,7	473396,0	20,8	398,2	3-6-1954	5,2	108,5	108,5	147,2			354,0	372,4			373,7	390,6
34	34	250881,2	473366,0	20,5	396,1	3-9-1954	6,9	108,2	108,2	148,0			351,5	373,0			374,8	390,8
35	35	250891,7	473217,5	20,3	419,4	6-12-1954	4,4	107,6	107,6	146,6			352,0	370,8	373,2	378,0	378,8	414,2
36	36	250899,6	473188,7	20,3	425,7	4-4-1955	2,9	107,6	107,6	147,9			353,2	372,7	375,6	379,0	381,7	420,9
37	37	250582,8	473788,1	19,5	400,2	4-7-1955	20,1	116,6	116,6	134,6			340,8	358,4	359,0	363,7	364,5	392,0

No	Well	X	Y	MV	TD	Date_end	T.Te	B.Te	T.Mu	B.Mu	T.Z-D	B.Z-D	T.Z-C	B.Z-C	T.Z-B	B.Z-B	T.Z-A	B.Z-A
38	38	250564,1	473662,7	19,4	396,3	5-10-1955	5,6	113,4	113,4	158,4			347,8	365,3	366,2	370,7	371,4	389,9
39	39	250552,1	473521,3	19,9	408,1	28-1-1956	6,9	112,4	112,4	151,9			363,5	377,8	378,8	381,2	382,6	397,7
40	40	250502,9	473349,0	20,0	416,2	29-3-1956	6,1	111,6	111,6	146,6			377,8	394,6	395,7	396,8	397,6	409,5
41	41	250495,7	473324,9	20,0	419,1	13-8-1956	7,1	111,6	111,6	165,1			378,4	395,6	396,8	399,5	400,1	411,1
42	42	251077,8	473187,3	20,8	407,6	22-11-1956	2,3	106,1	106,1	129,3	341,8	344,4	346,8	367,2	368,6	373,1	373,7	404,0
43	43	251084,9	473158,3	20,7	408,2	6-3-1957	6,3	105,7	105,7	129,3	343,5	346,7	347,5	368,8	370,0	374,0	374,8	405,1
44	44	251464,2	473712,0	20,9	348,9	31-5-1957	0,6	104,8	104,8	109,1			309,7	327,8	328,4	332,3	332,7	340,1
45	45	251496,1	473630,5	21,0	352,1	14-8-1957	6,0	103,8	103,8	107,0			315,6	333,3	334,5	338,5	339,0	346,3
46	46	251517,5	473545,8	21,0	359,1	31-10-1957	10,5	104,2	104,2	117,5			318,6	337,1	338,2	342,1	342,4	355,2
47	47	251538,9	473460,5	21,1	381,1	10-1-1958	11,5	104,0	104,0	122,5			317,2	330,3	331,7	336,9	337,6	372,1
48	48	251567,8	473377,7	21,0	373,5	23-4-1958	13,0	104,9	104,9	144,0			317,9	333,8	335,0	338,7	339,3	367,5
49	49	251599,3	473295,7	21,3	373,1	10-7-1958	8,7	106,0	106,0	118,5			322,2	340,0	341,6	345,1	345,7	365,6
50	50	251628,0	473221,9	21,4	359,4	29-9-1958	6,6	104,2	104,2	120,6			321,5	338,9	340,1	344,3	344,8	353,5
51	51	251428,0	473203,5	21,5	370,5	30-11-1958	6,0	103,7	103,7	117,2			327,0	348,1	349,4	354,1	354,8	367,7
52	52	251455,5	473121,2	21,2	372,6	21-1-1959	4,8	101,5	101,5	120,3			324,4	348,1	349,4	354,3	354,9	371,1
53	53	251480,0	473037,3	21,3	384,2	18-3-1959	5,7	100,1	100,1	130,6			329,8	350,5	351,5	356,5	357,1	378,5
54	54	251505,2	472953,4	21,1	386,0	2-5-1959	0,9	99,4	99,4	131,9			330,8	352,4	353,6	358,3	358,9	380,4
55	55	251522,8	472870,3	20,9	392,1	16-7-1959	-0,9	98,8	98,8	134,1			336,2	356,9	357,8	362,8	363,5	381,9
56	56	251548,4	472784,6	21,4	396,9	17-9-1959	-0,4	100,6	100,6	131,6			337,2	358,3	359,6	363,6	364,3	386,6
57	57	250831,6	472970,1	20,4	431,6	29-5-1959	22,8	106,9	106,9	148,7			365,4	385,6	386,7	391,1	391,6	422,3
58	58	250915,2	472945,6	21,0	422,3	23-6-1959	20,0	104,6	104,6	150,3			363,3	383,7	385,3	389,6	390,3	412,3
59	59	251002,0	472920,2	20,9	421,2	22-7-1959	14,6	105,5	105,5	163,1			359,6	381,0	382,1	387,1	387,6	408,8
60	60	251023,7	472647,3	21,3	433,1	13-8-1959	16,4	97,5	97,5	193,8			370,8	392,9	393,8	399,0	399,6	423,1
61	61	251109,0	472616,4	21,3	431,5	4-9-1959	16,2	102,7	102,7	149,7	363,8	364,9	369,0	389,8	391,3	396,3	397,0	421,5
62	62	251193,5	472584,4	21,8	430,2	6-11-1959	16,2	110,2	110,2	153,2	361,2	362,3	366,4	388,1	389,3	393,9	394,5	421,1
63	63	251781,9	473511,7	21,2	350,9	2-11-1960	36,8	102,1	102,1	140,1			302,4	317,2	317,9	322,9	323,5	345,0
64	64	251872,9	473563,3	21,7	346,0	31-3-1961	38,3	102,5	102,5	142,3			305,0	326,5	327,6	333,6	334,3	341,2
65	65	251965,0	473586,6	21,1	342,3	9-5-1961	39,0	102,0	102,0	119,0			299,1	318,9	320,3	324,1	325,0	338,3
66	66	251802,1	473361,8	21,7	372,3	2-3-1961	28,3	103,8	103,8	113,8			308,7	328,4	329,4	333,6	334,2	367,3
67	67	251798,8	473286,8	21,4	353,3	19-12-1960	37,6	102,8	102,8	128,7			310,4	328,5	329,4	333,8	334,5	346,6
68	68	251795,6	473212,8	21,3	354,5	31-1-1961	33,7	99,0	99,0	109,1			310,6	328,8	329,8	335,2	336,0	349,2
69	69	252258,0	473638,2	22,0	326,5	16-11-1961	-7,0	98,8	98,8	104,6	288,7	290,5	295,0	305,9	307,0	310,5	310,8	320,1
70	70	252340,1	473615,6	22,2	325,3	15-12-1961	-6,2	96,3	96,3				288,5	302,0	303,3	307,9	308,1	319,7
71	71	252420,9	473593,2	22,2	323,5	31-1-1962	-7,7	94,8	94,8				291,7	304,4	305,3	308,6	309,1	319,2
72	72	252180,8	473360,8	21,5	339,4	8-7-1961	41,5	100,0	100,0	104,5	285,1	286,7	289,7	312,0	313,8	318,0	318,6	335,6
73	73	252186,2	473276,6	22,0	333,5	28-8-1961	38,0	96,0	96,0	106,0	287,7	288,6	292,2	310,5	311,4	316,0	316,8	326,9
74	74	252191,2	473194,2	22,4	333,0	4-10-1961	27,6	92,6	92,6	101,9			293,8	316,1	317,4	319,1	319,8	330,0

No	Well	X	Y	MV	TD	Date end	T.Te	B.Te	T.Mu	B.Mu	T.Z-D	B.Z-D	T.Z-C	B.Z-C	T.Z-B	B.Z-B	T.Z-A	B.Z-A
75	75	252426,2	473324,0	22,2	327,8	2-5-1962	3,8	95,1	95,1	102,8			283,5	306,6	307,7	310,9	311,4	319,8
76	76	252522,1	473331,7	22,2	330,8	7-6-1962	3,8	94,8	94,8	99,8			278,9	293,0	294,2	300,7	301,4	323,5
77	77	252586,1	473395,8	23,0	328,0	5-7-1962	3,0	91,2	91,2	94,0			277,1	293,5	294,8	299,7	300,4	322,0
78	78	251704,2	472549,8	22,7	398,4	24-8-1962	7,3	95,1	95,1	117,3	337,6	338,5	345,1	362,6	363,8	369,5	370,6	396,8
79	79	251617,8	472546,6	22,5	402,0	29-11-1962	12,5	97,1	97,1	122,5	338,3	339,4	346,6	366,7	367,9	373,2	374,1	400,1
80	80	251532,9	472460,2	21,9	412,1	8-5-1963	13,1	98,1	98,1	172,1	347,2	348,2	356,0	378,3	379,5	384,4	384,9	411,4
81	81	251812,6	472930,3	22,5	372,5	12-8-1963	9,5	99,0	99,0	145,0			319,6	339,2	340,3	345,4	346,2	366,7
82	82	251811,7	472881,0	22,5	372,0	13-9-1963	9,5	99,0	99,0	139,0			320,8	337,5	338,7	342,9	343,5	369,1
83	83	251812,4	472830,9	22,9	376,6	21-10-1963	9,1	98,9	98,9	139,1			322,9	339,9	341,0	345,3	345,8	371,0
84	84	251948,7	472571,1	23,3	388,8	21-11-1963	11,2	94,7	94,7	133,7	330,3	332,4	334,4	354,1	355,3	360,0	360,9	384,9
85	85	251909,6	472575,8	23,1	394,4	19-12-1963	6,9	95,4	95,4	140,9	330,9	332,6	335,1	356,2	357,5	362,1	363,0	386,9
86	86	251371,3	472527,7	21,9	419,8	19-2-1964	12,2	97,7	97,7	168,2	351,7	352,8	360,5	382,4	383,5	388,1	388,7	414,3
87	87	251350,3	472490,8	22,0	419,8	24-3-1964	12,1	98,2	98,2	188,1	354,0	355,2	363,3	380,4	381,5	386,1	386,7	417,4
88	88	250834,9	472712,5	21,3	433,5	28-4-1964	13,7	106,2	106,2	152,2			376,1	397,4	398,5	405,5	406,1	426,1
89	89	250866,8	472700,8	21,4	430,1	2-6-1964	13,6	105,4	105,4	150,6			375,5	397,1	398,1	402,0	403,1	424,5
90	90	250730,3	472839,2	21,0	438,6	3-7-1964	12,5	106,5	106,5	143,0			373,7	392,7	393,9	397,5	398,1	430,7
91	91	250709,5	472856,7	20,8	435,4	18-8-1964	12,7	107,6	107,6	149,2			374,5	395,6	396,8	400,8	401,4	430,4
92	92	250563,6	473052,0	20,0	440,5	24-9-1964	12,1	112,1	112,1	170,1			373,7	398,1	399,3	403,2	403,8	434,3
93	93	250548,2	473027,3	20,1	435,5	28-10-1964	12,0	111,5	111,5	170,0			373,4	398,2	399,4	403,0	403,6	433,7
94	94	250436,0	473166,3	19,9	426,9	4-12-1964	14,2	112,1	112,1	180,2			381,4	397,3	398,5	403,8	404,4	424,2
95	95	250425,6	473134,2	20,2	431,2	6-1-1965	13,9	111,8	111,8	179,9			379,8	399,1	400,4	405,3	405,9	428,9
96	96	250377,4	472977,8	20,5	451,4	13-2-1965	12,5	112,2	112,2	189,5	371,5	374,5	377,5	403,0	404,5	409,1	409,7	445,0
97	97	250367,3	472945,5	20,9	454,3	17-3-1965	12,2	113,3	113,3	183,2	376,7	379,4	383,3	403,9	405,1	409,7	410,3	449,3
98	98	250508,8	472831,1	20,6	449,4	2-4-1965	12,4	109,4	109,4	194,4	380,2	383,0	386,8	406,6	407,7	412,3	412,9	443,4
99	99	250542,2	472820,6	20,9	449,6	16-4-1965	11,2	110,2	110,2	197,2	380,4	383,1	387,1	407,6	408,7	412,5	413,1	445,2
100	100	250736,0	472551,3	21,1	445,6	26-4-1965	10,9	104,2	104,2	200,9	382,2	386,0	389,5	411,5	412,8	417,2	417,8	439,6
101	101	250737,0	472511,3	21,2	444,5	31-5-1965	10,8	104,5	104,5	218,8	384,6	388,1	391,7	412,8	414,1	418,6	419,2	441,2
102	102	250739,5	472350,7	21,5	459,8	6-7-1965	12,5	102,8	102,8	233,5	397,0	398,0	402,5	426,6	427,8	432,3	432,9	455,1
103	103	250740,2	472310,6	21,7	452,6	6-8-1965	11,4	103,4	103,4	234,4	398,2	401,2	404,6	427,3	428,6	432,9	433,6	453,9
104	104	250825,9	472166,6	21,6	469,9	13-5-1965	13,4	105,9	105,9	188,4	403,8	405,0	409,1	428,4	430,1	433,2	436,2	463,9
105	105	250865,3	472169,9	21,8	468,2	2-6-1965	13,3	105,8	105,8	195,3	402,1	403,8	407,9	426,7	428,4	431,6	434,6	462,2
106	106	251025,2	472183,9	22,4	459,7	23-6-1965		96,1		185,7	393,5	395,3	399,5	417,6	421,4	425,2	426,3	453,7
107	107	251064,5	472187,6	22,5	456,6	14-7-1965		97,5		187,1	391,3	392,2	396,4	416,4	418,4	422,2	423,2	450,6
108	108	251213,5	472200,1	22,5	449,1	8-7-1965		95,8		209,6	383,9	385,1	388,7	408,0	409,6	413,0	414,5	442,7
109	109	251249,0	472203,3	22,5	445,5	27-7-1965		95,7		185,0	381,7	383,4	386,1	405,2	406,8	410,3	411,8	439,8
110	110	251493,8	472206,2	22,5	428,9	7-9-1965		95,6		185,0	373,1	374,2	376,9	392,9	393,7	399,5	400,0	426,7
111	111	251454,8	472203,1	22,4	437,5	19-10-1965		98,6		188,1	369,3	370,1	374,7	392,5	395,1	402,7	404,4	430,1

No	Well	X	Y	MV	TD	Date end	T.Te	B.Te	T.Mu	B.Mu	T.Z-D	B.Z-D	T.Z-C	B.Z-C	T.Z-B	B.Z-B	T.Z-A	B.Z-A
112	112	251625,6	472291,3	22,5	412,3	17-5-1966		94,4	94,4	167,6	355,4	357,3	361,0	377,3	378,6	388,1	389,1	412,5
113	113	251628,8	472327,8	22,4	419,2	17-6-1966		93,7	93,7	167,7	354,3	354,6	358,4	380,7	382,1	387,2	388,0	414,4
114	114	251810,6	472303,5	24,1	402,4	14-7-1966		91,9		169,9	345,7	348,3	352,3	368,7	369,6	379,8	380,8	399,7
115	115	251797,1	472339,2	23,5	398,5	11-8-1966		93,3		160,5	344,9	349,2	353,0	372,8	374,4	378,1	379,8	399,3
116	116	251663,0	472097,2	23,0	431,2	14-9-1966		92,9		197,0	365,9	367,5	371,6	393,9	395,4	398,9	400,2	427,5
117	117	251645,7	472133,6	22,9	424,1	11-10-1966		92,9		197,1	364,6	366,6	369,7	392,1	393,6	396,4	398,5	424,6
118	118	251590,3	471900,8	23,2	445,7	9-11-1966		96,9	96,9	206,9	379,2	381,8	385,7	404,2	405,0	413,2	414,1	441,9
119	119	251613,7	471931,7	22,8	439,7	7-12-1966	-12,8	94,2	94,2	201,2	376,2	378,7	381,2	401,2	402,6	409,0	411,0	438,8
120	120	251478,8	471755,8	22,5	463,8	3-3-1967	-12,5	95,1	95,1	207,6	393,9	395,8	400,1	421,2	422,2	427,1	427,9	456,0
121	121	251499,3	471782,9	22,5	458,0	7-4-1967	-12,5	94,5	94,5	207,5	389,5	393,0	396,6	418,6	421,0	423,6	426,3	454,0
122	122	250812,5	471923,4	22,5	486,2	12-5-1967	-2,5	97,5	97,5	237,5	419,7	420,9	423,9	445,1	446,6	451,6	452,4	480,9
123	123	250851,6	471928,4	22,6	478,5	6-6-1967	-2,6	96,0	96,0	227,5	416,5	418,0	420,5	444,1	445,7	449,4	450,3	478,0
124	124	251010,4	471948,9	22,4	471,0	6-7-1967	-2,4	97,0	97,0	197,6	408,6	410,0	414,3	434,5	435,9	440,3	441,1	469,9
125	125	251049,7	471954,0	22,7	466,3	2-8-1967	7,3	87,3	87,3	187,3	404,7	406,4	410,8	431,0	432,7	437,2	438,2	466,8
126	126	251230,7	471977,2	22,5	460,1	28-8-1967	17,6	86,6	86,6	197,6	394,4	395,9	400,0	420,9	422,2	426,4	427,0	455,9
127	127	251269,9	471982,0	22,4	452,1	20-9-1967	17,6	92,6	92,6	195,6	392,1	394,2	397,0	418,1	419,2	424,3	425,0	452,1
128	128	251434,5	472003,2	22,4	444,7	12-10-1967	17,7	97,7	97,7	207,7	381,3	383,3	388,0	410,5	411,3	415,2	416,2	443,5
129	129	251473,7	472008,1	22,3	443,4	2-11-1967	12,7	95,7	95,7	187,7	375,8	377,2	381,4	404,1	405,5	411,9	412,9	440,6
130	130	251966,3	472300,4	23,5	400,5	27-11-1967	26,5	93,0	93,0	126,5	341,0	343,5	345,1	369,0	371,0	374,1	375,5	400,3
131	131	251999,5	472289,2	23,7	402,3	19-12-1967	26,3	92,0	92,0	128,3	340,3	344,3	346,3	369,2	370,1	374,3	375,6	400,2
132	132	250321,3	472793,7	20,5	459,9	28-3-1968	29,5	110,5	110,5	209,5	384,1	385,8	394,0	410,9	412,1	418,4	419,4	459,7
133	133	250310,6	472759,8	20,4	460,0	6-4-1968	22,1	110,7	110,7	209,6	389,1	390,6	397,9	413,9	415,1	421,0	421,6	459,6
134	134	250262,0	472606,5	20,7	459,2	25-9-1967	29,3	111,3	111,3	209,3	401,1	403,0	406,8	427,8	429,0	433,9	434,6	451,3
135	135	250251,7	472573,6	20,8	453,5	6-10-1967	32,7	108,2	108,2	204,2	400,4	402,5	408,3	427,6	428,8	436,2	436,8	453,5
136	136	250227,1	472380,8	21,1	470,0	17-10-1967	39,0	108,0	108,0	231,0	415,1	416,2	420,1	441,0	442,2	446,6	447,3	466,5
137	137	250263,5	472365,0	21,1	466,4	27-10-1967	25,9	108,4	108,4	228,9	414,9	416,4	420,2	440,8	442,1	446,4	447,1	465,9
138	138	250411,7	472307,4	22,0	474,0	17-11-1967	25,0	108,0	108,0	236,0	414,4	414,8	418,4	439,2	440,9	444,9	445,8	469,8
139	139	250447,4	472291,1	21,7	470,7	30-11-1967	8,3	106,8	106,8	230,8	413,8	415,3	419,4	439,5	441,2	445,2	446,3	470,7
140	140	250593,8	472226,4	21,3	472,0	5-2-1968	8,7	107,2	107,2	198,7	411,2	413,2	416,7	433,7	434,3	441,5	442,7	469,8
141	141	250630,0	472210,3	21,5	469,1	29-2-1968	18,5	104,0	104,0	238,5	410,5	412,5	416,5	433,2	433,9	440,7	442,5	468,1
142	142	250222,5	472923,4	20,6	454,4	16-10-1968	9,4	113,4	113,4	187,4	378,9	380,9	383,9	404,4	405,9	410,4	411,4	451,4
143	143	250259,9	472911,1	20,6	455,5	6-11-1968	16,4	106,4	106,4	216,4	380,9	382,4	385,9	405,9	406,9	411,9	412,4	453,3
144	144	250063,2	472952,0	20,2	443,2	28-11-1968	15,8	115,8	115,8	204,8	377,1	378,1	381,9	402,4	403,7	410,7	411,3	441,0
145	145	250025,3	472963,9	20,6	440,9	20-12-1968	19,4	115,4	115,4	199,4	379,9	381,7	384,7	403,8	405,2	411,7	412,6	440,0
146	146	250458,6	472554,0	21,6	450,7	9-5-1968	18,4	105,9	105,9	203,4			400,4	424,5	425,8	431,3	432,2	448,9
147	147	250423,0	472571,1	21,6	449,8	24-5-1968	18,4	107,4	107,4	203,4			401,8	426,5	427,9	431,9	432,8	448,3
148	148	250063,3	472451,9	20,8	465,9	19-6-1968	14,3	104,3	104,3	234,3	416,2	417,9	421,7	441,1	442,3	448,7	449,5	461,8

No	Well	X	Y	MV	TD	Date_end	T.Te	B.Te	T.Mu	B.Mu	T.Z-D	B.Z-D	T.Z-C	B.Z-C	T.Z-B	B.Z-B	T.Z-A	B.Z-A
149	149	249912,2	472490,1	20,4	458,2	9-7-1968	14,6	105,6	105,6	244,6	414,8	418,3	422,0	441,0	442,2	446,2	446,8	456,6
150	150	249879,8	472485,8	20,4	460,0	30-7-1968	14,7	107,7	107,7	234,7	416,2	418,8	422,3	441,3	442,5	446,3	447,0	458,1
151	151	249727,5	472436,3	19,9	479,1	27-8-1968	15,1	106,1	106,1	235,1	418,0	421,1	425,9	444,6	445,7	451,4	452,2	476,8
152	152	249689,8	472424,0	19,9	479,6	17-9-1968	5,1	106,1	106,1	235,1	417,6	419,8	426,0	445,3	446,3	450,8	451,6	477,4
153	153	249445,6	472457,2	20,2	465,3	29-1-1969	4,8	120,8	120,8	234,8	417,4	417,4	421,2	440,7	441,8	446,6	447,2	462,4
154	154	249476,1	472442,9	20,2	465,2	13-2-1969	4,8	120,8	120,8	249,8	416,9	417,5	421,3	440,3	441,4	447,0	447,9	463,1
155	155	249506,8	472428,6	20,2	461,7	10-3-1969	4,8	114,8	114,8	249,8	415,8	418,3	420,8	436,9	442,0	443,5	444,1	459,2
156	156	249818,5	472769,8	19,9	511,7	24-7-1969	5,1	117,1	117,1	246,1	404,2	405,1	408,4	430,0	431,0	435,9	436,7	509,1
157	156A	249781,5	472778,2	19,9	491,9	30-6-1975	5,1	117,1	117,1	225,1	405,3	405,7	409,4	429,0	429,7	433,5	434,3	489,7
158	157	249856,4	472782,8	19,9	483,4	3-9-1969	30,1	117,1	117,1	245,1	406,6	406,8	408,6	428,5	431,6	433,2	434,2	479,9
159	158	249892,7	472799,3	20,1	480,5	1-10-1969	39,9	116,4	116,4	219,9	401,3	402,0	404,8	423,5	424,6	429,0	430,0	477,2
160	159	250083,3	472778,7	20,4	489,7	8-4-1969	19,6	113,6	113,6	209,6	396,4	397,4	401,6	421,2	422,3	426,3	427,3	485,6
161	159A	250049,6	472786,3	20,2	487,1	13-9-1975	20,4	114,4	114,4	205,9	397,7	398,5	402,1	421,6	424,0	427,3	428,1	484,9
162	160	250121,9	472770,1	20,2	482,8	29-5-1969	29,8	114,8	114,8	206,8	396,4	397,4	401,3	420,5	421,7	425,7	426,6	479,7
163	161	250161,1	472761,3	20,3	475,2	25-6-1969	29,7	114,7	114,7	203,7	396,4	397,3	401,1	420,6	421,7	425,6	426,5	473,2
164	162	249335,5	472660,4	20,1	485,9	23-10-1969	-3,1	114,9	114,9	244,9	412,9	414,4	417,4	436,9	437,9	442,4	443,4	483,0
165	163	249336,1	472620,8	20,2	482,9	10-11-1969	-3,2	119,8	119,8	239,8	414,9	415,0	418,7	438,2	439,5	443,9	444,7	480,0
166	164	249336,5	472581,1	20,2	481,4	10-12-1969	-3,2	119,8	119,8	239,8	416,1	416,2	420,5	439,4	440,3	444,6	445,5	480,3
167	165	249295,5	472862,3	19,8	466,4	25-11-1969	0,2	116,2	116,2	265,2	412,0	412,0	415,1	445,0	445,9	447,3	447,5	452,8
168	166	249266,8	472880,8	19,9	456,5	4-12-1969	0,1	114,1	114,1	265,1	419,5	419,9	422,9	441,8	444,0	446,5	446,7	452,5
169	167	249517,8	472797,8	19,9	486,3	16-1-1970	5,1	105,1	105,1	250,1	396,6	397,4	400,5	418,8	419,5	424,3	426,0	483,9
170	168	249552,6	472801,2	20,0	484,5	16-2-1970	25,1	107,1	107,1	285,1	399,0	399,5	403,4	419,3	421,7	427,9	430,0	481,7
171	169	249592,3	472804,0	20,0	482,6	11-3-1970	-5,0	110,1	110,1	260,1	397,7	400,4	403,0	421,4	422,8	426,0	427,0	479,9
172	170	250728,6	471700,5	22,5	502,1	18-8-1969	2,5	94,5	94,5	252,5	435,2	436,2	440,0	460,6	462,4	466,6	467,4	499,1
173	171	250728,1	471740,7	22,5	498,3	3-9-1969	2,5	97,5	97,5	249,5	432,5	433,5	437,5	458,9	461,0	464,8	465,5	496,7
174	172	250727,5	471781,3	22,4	496,0	12-9-1969	2,6	95,6	95,6	242,6	431,2	431,9	435,4	456,0	457,7	461,9	462,6	493,6
175	173	250123,6	472123,8	21,2	494,5	3-6-1970	33,8	98,8	98,8	258,8	431,3	431,6	435,7	455,6	456,7	461,4	462,0	492,0
176	174	250116,4	472154,2	21,0	491,3	26-6-1970	41,0	98,0	98,0	254,0	429,7	430,0	433,6	450,1	452,6	458,2	458,9	489,6
177	175	250109,2	472193,9	20,9	489,6	22-7-1970	39,1	109,1	109,1	239,1	427,7	428,1	431,9	451,3	452,4	458,1	458,9	487,3
178	176	250239,7	471953,0	21,3	499,4	24-9-1969	18,7	101,7	101,7	248,7	439,5	440,1	444,4	463,4	466,5	469,8	471,7	498,5
179	177	250279,6	471959,4	21,2	500,7	2-10-1969	13,8	103,8	103,8	238,8	437,4	438,4	441,9	462,0	463,1	467,9	468,7	499,5
180	178	250439,3	471980,0	21,4	496,6	14-10-1969	13,6	98,6	98,6	233,6	431,0	431,1	434,8	454,8	456,0	461,8	462,8	492,9
181	179	250478,1	471986,8	21,9	491,9	23-10-1969	14,1	98,1	98,1	243,1	428,9	429,2	433,0	453,0	455,1	459,8	460,7	490,5
182	180	250639,8	472015,5	22,2	484,4	4-11-1969	17,9	101,9	101,9	227,9	420,2	423,3	427,3	447,1	448,2	453,1	453,8	482,2
183	181	250678,6	472022,5	22,0	482,5	11-11-1969	15,0	101,0	101,0	233,0	415,9	419,0	425,5	446,0	448,0	449,1	449,9	479,7
184	182	250731,0	471486,0	23,0	513,8	23-7-1969	2,0	92,0	92,0	257,0	443,0	444,5	448,5	470,0	471,5	476,3	477,2	513,3
185	183	250730,3	471526,2	23,1	511,8	5-8-1969	1,9	91,9	91,9	256,9	441,1	441,6	445,3	466,9	468,1	473,0	474,0	511,4

No	Well	X	Y	MV	TD	Date_end	T.Te	B.Te	T.Mu	B.Mu	T.Z-D	B.Z-D	T.Z-C	B.Z-C	T.Z-B	B.Z-B	T.Z-A	B.Z-A
186	184	250574,8	471556,3	22,3	518,1	28-7-1970	12,7	96,7	96,7	262,7	447,5	447,9	452,0	472,5	473,7	479,7	480,6	516,0
187	185	250540,0	471575,4	21,9	518,8	17-7-1970	13,1	98,1	98,1	263,1	447,9	448,3	449,7	474,1	475,3	480,4	481,3	516,9
188	186	250504,9	471595,2	20,7	519,2	3-7-1970	14,3	101,3	101,3	263,3	447,7	448,2	452,6	475,4	476,6	483,7	484,6	517,2
189	187	250364,3	471670,7	21,8	517,8	23-6-1970	13,2	96,2	96,2	263,2	449,6	452,2	453,6	473,9	475,6	480,0	480,9	516,0
190	188	250329,3	471689,8	21,6	517,4	11-6-1970	13,4	96,4	96,4	266,4	448,2	451,4	454,4	473,2	474,9	479,3	480,2	515,4
191	189	250293,8	471709,0	21,4	519,6	27-5-1970	13,6	96,6	96,6	270,6	448,5	451,8	453,2	473,8	475,5	480,0	480,9	517,3
192	190	250025,0	471876,1	21,1	511,5	10-8-1970	33,9	100,9	100,9	260,9	447,6	449,6	452,8	473,6	474,7	478,8	479,6	509,8
193	191	250019,5	471918,3	21,2	508,0	25-8-1970	33,8	98,8	98,8	257,8	445,8	446,5	449,8	470,3	471,4	475,5	476,2	505,7
194	192	249873,2	473014,3	20,3	434,9	3-4-1970	19,7	106,7	106,7	224,7							418,8	430,1
195	193	249836,2	473028,5	20,2	432,9	24-4-1970	19,8	109,8	109,8	224,8							423,9	430,4
196	194	250141,9	471699,1	21,0	524,1	3-9-1970	34,0	102,0	102,0	274,0	457,2	458,1	462,0	481,4	482,5	486,8	487,5	521,9
197	195	250110,1	471676,7	21,0	526,5	16-9-1970	34,0	103,0	103,0	279,0	459,2	460,1	464,0	483,4	484,5	488,8	489,5	524,2
198	196	250048,9	471498,9	21,3	532,3	26-9-1970	33,7	104,7	104,7	298,7	468,7	472,2	475,2	496,2	497,7	501,5	502,4	540,7
199	197	250033,0	471455,1	21,4	548,3	9-10-1970	33,6	105,6	105,6	303,6	472,5	475,1	477,6	498,7	500,1	504,2	505,3	546,3
200	198	250759,6	471336,7	22,8	525,7	14-8-1970	16,2	92,2	92,2	262,2	443,2	445,2	449,2	471,2	472,7	478,2	479,0	521,8
201	199	250760,7	471300,5	23,0	525,7	11-9-1970	17,1	93,1	93,1	263,1	444,4	445,0	449,6	471,7	472,8	477,6	478,4	523,5
202	200	250760,8	471263,8	23,0	529,5	5-10-1970	19,0	93,0	93,0	267,0	445,0	446,0	451,0	472,0	473,5	479,0	480,0	526,0
203	201	251328,8	471562,5	22,9	477,4	26-10-1970	12,1	89,1	89,1	222,1	408,7	410,4	414,5	435,8	437,0	442,9	444,0	474,0
204	202	251352,6	471594,7	22,6	475,3	30-11-1970	12,4	85,4	85,4	214,4	406,3	408,0	412,1	433,1	434,7	440,1	441,2	470,7
205	203	251377,3	471626,6	22,7	471,6	30-12-1970	12,4	83,4	83,4	210,4	404,3	406,0	410,2	432,1	433,1	437,8	438,8	468,2
206	204	252150,6	473025,8	22,8	349,9	20-4-1971	11,2	92,2	92,2	114,2	292,8	294,8	299,8	318,6	319,8	325,2	326,1	348,1
207	205	252133,6	472990,1	22,8	353,2	26-3-1971	13,2	92,2	92,2	112,2	297,6	299,4	303,4	323,9	325,1	330,5	331,3	351,1
208	206	252116,4	472953,8	22,9	360,9	19-1-1971	11,1	92,1	92,1	115,1	300,5	301,2	304,1	326,0	327,3	332,0	332,9	355,4
209	207	252326,0	472904,3	24,1	355,2	3-6-1971	10,9	88,9	88,9	111,9	294,2	294,9	299,4	320,1	321,4	326,3	327,3	353,8
210	208	252366,3	472903,4	24,2	355,9	13-5-1971	10,8	90,8	90,8	112,8	293,0	293,7	298,2	319,5	320,8	325,6	326,6	355,3
211	209	252242,6	472616,4	24,1	372,9	17-4-1971	10,9	90,9	90,9	125,9	313,4	315,9	319,5	339,8	341,3	345,8	346,6	369,6
212	210	252265,2	472579,2	24,5	372,5	28-4-1971	10,5	90,5	90,5	117,5	314,6	314,7	318,4	340,4	341,9	346,4	347,0	370,0
213	211	252359,0	472455,9	25,1	382,8	12-5-1971	10,0	90,0	90,0	132,0	318,7	319,0	323,0	345,2	346,4	351,3	352,1	376,5
214	212	252381,7	472421,4	24,4	379,6	22-5-1971	10,6	90,6	90,6	134,6	319,6	321,6	323,6	345,6	346,8	349,2	350,0	376,4
215	213	252217,3	472303,2	24,2	393,2	26-7-1971	10,8	90,3	90,3	132,8	330,3	333,4	336,8	356,5	358,0	364,4	365,3	390,7
216	214	252177,5	472290,3	24,0	394,7	15-7-1971	11,0	91,5	91,5	135,0	335,1	336,1	340,8	360,2	361,7	366,4	367,1	392,4
217	215	252447,6	472287,1	24,6	385,5	4-6-1971	10,4	87,4	87,4	143,4	326,0	326,2	330,1	351,5	352,7	357,7	358,5	383,4
218	216	252464,7	472252,8	24,4	386,3	14-6-1971	10,6	85,6	85,6	134,6	327,9	328,2	332,2	353,6	354,6	359,2	360,0	384,3
219	217	252481,8	472218,2	23,8	388,6	23-6-1971	11,2	84,2	84,2	136,2	329,7	330,2	334,2	355,5	356,6	361,3	362,0	386,6
220	218	252303,8	471994,7	24,1	408,3	4-9-1971	5,9	80,9	80,9	140,9	347,1	348,6	352,5	373,5	374,7	379,2	379,9	405,2
221	219	252301,5	471955,2	24,2	406,9	12-8-1971	5,8	85,8	85,8	150,8	348,4	350,0	353,8	374,7	375,9	380,3	381,1	405,8
222	220	252034,0	472073,3	24,6	413,3	27-9-1971	10,4	72,4	72,4	150,4	351,3	352,9	357,1	377,8	379,1	383,5	384,4	410,7

No	Well	X	Y	MV	TD	Date_end	T.Te	B.Te	T.Mu	B.Mu	T.Z-D	B.Z-D	T.Z-C	B.Z-C	T.Z-B	B.Z-B	T.Z-A	B.Z-A
223	221	251999,4	472052,6	24,3	416,2	4-10-1971	10,7	72,7	72,7	160,7	354,3	355,9	359,6	380,3	381,5	385,9	386,7	413,2
224	222	251963,8	472031,6	24,4	418,3	2-11-1971	10,6	72,6	72,6	170,6	355,4	358,0	362,1	383,0	384,3	388,6	389,4	416,4
225	223	251773,1	471940,9	23,8	432,8	11-4-1972	11,3	71,3	71,3	183,8	368,8	370,5	375,1	395,1	396,5	401,3	402,3	430,6
226	224	251795,6	471905,3	24,1	432,0	25-5-1972	10,9	69,9	69,9	179,4	370,4	371,4	376,0	396,5	397,9	402,6	403,5	431,2
227	225	251844,9	471749,3	24,8	441,1	20-3-1972	10,2	70,2	70,2	177,7	375,8	377,4	381,6	401,2	402,6	407,2	408,2	436,8
228	226	251794,6	471721,3	24,2	442,7	14-2-1972	10,8	70,8	70,8	183,3	379,1	380,6	384,8	405,0	406,3	410,7	411,7	440,6
229	227	251749,0	471696,0	23,9	446,4	8-12-1971	11,1	76,1	76,1	189,1	383,3	384,8	389,0	409,7	411,1	415,5	416,4	444,9
230	228	252642,6	471980,8	23,8	397,3	5-7-1971	11,2	79,2	79,2	139,2	337,9	338,8	342,9	363,2	364,3	369,8	370,6	395,7
231	229	252668,7	471950,6	24,0	398,0	22-6-1971	11,0	76,0	76,0	141,0	338,2	338,9	342,7	363,6	364,8	369,8	370,6	395,6
232	230	252695,5	471921,6	24,2	399,3	9-7-1971	10,8	71,8	71,8	145,8	339,4	340,0	343,4	364,3	365,4	370,6	371,4	397,0
233	231	252871,8	471836,7	25,5	398,3	27-9-1972	-0,5	70,5	70,5	147,5	338,8	339,8	344,0	366,0	367,4	371,3	372,2	396,8
234	232	252912,9	471830,6	25,7	397,7	22-11-1972	-1,7	69,3	69,3	149,3	340,1	341,0	345,2	365,8	366,9	371,2	372,1	396,4
235	233	252955,3	471831,5	25,8	399,2	9-1-1973	-1,8	68,8	68,8	150,3	339,2	340,2	344,4	365,2	366,7	370,2	371,1	395,8
236	234	253122,2	471764,4	25,5	398,1	28-8-1973	-3,5	67,0	67,0	150,5	332,5	334,7	337,5	358,3	359,1	364,3	365,7	396,7
237	235	253157,5	471740,7	25,6	400,3	24-9-1973	-3,6	66,4	66,4	151,4	335,9	336,9	340,9	361,9	364,2	369,0	369,9	397,3
238	236	253191,5	471719,4	25,7	400,7	24-10-1973	-4,7	65,9	65,9	151,4	336,7	338,6	344,8	365,0	366,1	370,9	371,8	399,0
239	237	253333,0	471640,8	26,2	407,7	26-11-1973	-5,7	63,8	63,8	156,3	340,4	342,9	347,2	367,6	368,8	373,4	374,1	401,3
240	238	253369,8	471620,8	26,1	405,4	3-1-1974	-5,6	62,9	62,9	166,4	340,1	343,9	347,1	367,6	368,9	373,8	374,8	402,4
241	239	253707,3	471414,8	27,0	417,7	12-3-1974	-6,0	54,0	54,0	167,0	351,0	352,2	356,3	377,3	378,5	384,0	384,9	415,5
242	240	253736,0	471396,9	27,3	416,5	18-4-1974	-7,3	52,7	52,7	166,7	350,9	352,2	356,6	377,5	378,7	384,1	385,0	415,5
243	241	253765,2	471379,3	27,4	417,7	30-5-1974	-7,4	52,6	52,6	168,1	352,8	354,2	358,6	380,1	380,9	385,2	386,1	415,7
244	242	253853,7	471260,5	27,5	424,7	3-10-1974	-7,5	51,5	51,5	168,5	358,8	359,9	364,0	385,4	386,3	391,9	392,8	423,8
245	243	253867,9	471228,6	28,3	427,6	2-9-1974	-8,3	50,8	50,8	165,8	359,8	361,8	365,3	386,8	388,3	392,3	393,8	425,5
246	244	253881,5	471195,3	27,3	429,4	9-7-1974	-7,3	51,2	51,2	167,7	361,7	363,2	367,2	389,8	390,7	395,5	396,4	427,7
247	245	253939,7	471025,2	27,4	441,5	29-5-1973	-7,4	50,6	50,6	150,6	369,9	371,1	375,3	396,9	398,2	403,3	404,1	437,0
248	246	253954,1	470988,1	27,5	439,5	25-4-1973	-7,5	50,0	50,0	183,5	371,8	373,1	377,4	399,1	400,7	405,0	405,8	438,8
249	247	253966,5	470949,1	27,5	442,2	20-3-1973	-7,5	55,5	55,5	185,0	372,7	373,8	377,9	400,1	401,5	406,2	407,0	440,4
250	248	253557,1	471508,7	26,6	410,2	25-1-1977	3,9	58,4	58,4	164,9	344,7	347,8	352,2	373,0	374,3	379,1	380,0	409,5
251	249	253539,2	471550,0	26,6	407,6	22-12-1976	2,4	58,4	58,4	165,4	342,4	345,8	349,6	371,8	373,4	377,3	378,2	407,6
252	250	253531,7	471594,4	26,8	404,6	12-11-1976	3,2	59,2	59,2	160,2	340,0	344,6	348,3	369,0	370,3	375,4	376,4	403,6
253	251	253499,1	471764,7	26,3	394,4	16-8-1976	2,7	60,7	60,7	151,7	331,2	333,1	337,3	358,4	359,7	365,0	365,9	392,3
254	252	253543,4	471768,3	26,0	394,8	29-9-1976	2,0	60,0	60,0	151,0	330,8	332,8	337,0	358,4	359,8	363,5	364,9	393,0
255	253	252444,4	472605,9	24,8	365,0	13-11-1974	9,2	87,2	87,2	116,2	307,6	307,9	311,9	333,3	334,6	339,7	340,4	362,4
256	254	252488,2	472610,4	24,5	368,3	7-1-1975	9,0	84,5	84,5	111,5	305,9	306,3	310,6	330,0	331,4	336,5	337,3	360,9
257	255	252525,9	472604,6	24,9	366,0	30-1-1975	8,6	81,1	81,1	108,1	306,8	307,3	310,8	330,3	331,5	336,6	337,4	359,7
258	256	252540,1	472432,9	23,6	373,1	13-5-1975	9,9	81,4	81,4	115,4	313,6	314,7	319,2	340,9	342,2	346,9	347,8	370,2
259	257	252580,5	472436,7	23,7	371,7	10-4-1975	10,3	80,8	80,8	113,8	313,3	314,1	318,2	340,0	341,3	345,7	346,5	369,2

No	Well	X	Y	MV	TD	Date end	T.Te	B.Te	T.Mu	B.Mu	T.Z-D	B.Z-D	T.Z-C	B.Z-C	T.Z-B	B.Z-B	T.Z-A	B.Z-A
260	258	252618,1	472422,7	23,8	368,5	12-3-1975	10,2	80,2	80,2	114,2	312,8	313,5	317,0	338,8	340,1	345,7	346,5	368,2
261	259	252449,1	473114,3	23,9	334,3	24-12-1975	5,1	84,6	84,6	103,1	286,8	287,2	290,8	312,3	313,3	317,8	318,6	332,6
262	260	252463,4	473075,5	24,2	336,1	2-12-1975	6,8	85,8	85,8	106,8	289,0	289,5	292,9	314,1	315,2	319,7	320,5	335,5
263	261	252486,2	473044,2	24,1	340,9	30-10-1975	3,9	83,4	83,4	109,9	290,1	290,7	294,0	314,6	315,7	320,7	321,6	336,3
264	262	252540,9	472888,8	25,0	353,2	13-4-1976	6,6	85,1	85,1	109,1	294,9	295,4	299,1	320,1	321,5	326,5	327,3	350,7
265	263	252579,9	472875,1	24,9	350,2	11-5-1976	7,6	84,6	84,6	109,1	292,8	293,4	297,4	317,9	319,1	324,6	325,4	348,8
266	264	252619,7	472861,3	24,2	349,2	15-6-1976	9,8	83,8	83,8	102,3	292,9	293,5	296,0	316,4	317,9	323,3	324,1	348,2
267	265	253298,3	471477,0	25,9	414,1	10-3-1977	14,1	67,1	67,1	169,6	349,1	349,9	353,7	375,3	376,7	382,2	383,3	413,1
268	266	253272,4	471446,5	25,9	418,7	18-4-1977	14,1	70,1	70,1	172,6	350,0	351,6	355,5	376,2	377,9	382,7	383,7	413,7
269	267	253245,9	471416,5	25,9	418,6	17-5-1977	12,6	71,6	71,6	174,1	350,1	350,9	355,3	376,4	378,3	382,9	383,9	416,4
270	268	253151,6	471287,8	26,0	423,5	23-6-1977	21,5	73,0	73,0	185,0	361,8	365,4	369,4	389,7	391,0	395,8	396,9	423,4
271	269	253185,7	471260,8	26,2	428,0	29-7-1977	24,3	70,8	70,8	186,3	362,7	365,7	369,6	389,6	391,6	395,3	396,4	424,2
272	270	253534,2	471365,4	26,9	419,4	6-10-1977	13,6	68,6	68,6	177,1	354,4	356,5	360,1	380,4	382,4	386,8	387,7	417,7
273	271	253569,9	471346,7	27,0	427,1	7-9-1977	13,1	68,6	68,6	178,1	353,1	357,3	362,0	381,1	383,2	387,9	388,5	418,5
274	272	253477,4	471177,8	26,4	429,3	16-1-1979	5,6	60,6	60,6	184,1	362,7	364,6	368,9	389,6	391,4	395,7	396,7	427,9
275	273	253447,5	471204,3	26,3	428,4	14-11-1978	7,2	62,2	62,2	183,2	362,2	362,9	366,3	388,5	390,0	395,3	396,4	426,0
276	274	253417,8	471230,8	26,2	429,3	4-10-1978	6,8	63,8	63,8	182,8	361,1	362,7	366,6	387,8	390,1	394,1	395,1	425,4
277	275	253491,1	471017,3	26,8	435,5	28-6-1979	15,2	47,7	47,7	191,7	368,7	370,1	373,3	396,3	397,8	401,8	403,0	434,9
278	276	253493,1	470982,5	26,7	439,4	4-5-1979	13,3	48,3	48,3	192,8	371,5	372,1	375,8	396,9	399,8	402,8	403,7	436,1
279	277	253498,7	470948,3	26,8	439,2	8-3-1979	13,7	47,7	47,7	193,7	370,4	373,6	377,4	398,4	399,9	404,3	405,3	437,7
280	278	253587,3	470801,1	26,7	447,0	16-4-1980	11,8	47,3	47,3	198,3	375,8	377,2	380,9	403,0	404,8	408,7	409,5	444,7
281	279	253593,2	470761,7	26,7	449,9	12-3-1980	15,3	52,8	52,8	199,8	376,2	379,3	382,9	404,3	406,1	410,2	411,4	444,8
282	280	253599,0	470722,5	26,6	450,6	7-2-1980	11,4	52,4	52,4	200,9	377,9	380,9	384,6	405,8	407,3	411,6	412,6	443,7
283	281	254113,7	470886,7	28,4	445,9	26-5-1978	3,2	45,2	45,2	194,7	375,1	376,8	379,8	402,3	403,6	408,8	409,7	444,4
284	282	254152,5	470895,8	28,5	445,2	27-4-1978	2,0	45,0	45,0	194,0	373,2	377,2	380,5	402,2	403,4	408,5	409,3	444,2
285	283	254310,5	470927,6	28,6	443,2	29-3-1978	0,9	41,4	41,4	190,9	371,2	374,2	377,9	399,9	400,9	405,9	406,8	442,0
286	284	254349,6	470936,2	28,7	446,5	17-2-1978	-0,7	40,8	40,8	189,8	370,7	373,8	377,3	399,5	400,9	405,7	406,7	441,4
287	285	254507,4	470970,0	28,8	442,9	5-1-1978	-4,3	38,2	38,2	186,7	368,9	371,2	374,2	397,9	398,5	403,2	404,0	439,8
288	286	254546,1	470978,2	29,0	445,4	24-11-1977	-4,5	38,0	38,0	186,5	367,8	368,9	372,7	395,5	397,4	401,8	402,9	438,8
289	287	253811,5	470912,2	27,4	444,7	11-9-1979	16,1	50,1	50,1	195,6	373,6	376,9	381,2	402,2	403,5	408,0	409,0	442,1
290	288	253772,6	470921,9	27,3	443,3	25-10-1979	5,2	49,7	49,7	196,2	374,0	376,9	380,5	400,7	402,2	407,4	408,5	441,3
291	289	253731,1	470929,5	27,0	442,4	6-12-1979	15,0	53,0	53,0	195,5	372,5	375,0	379,2	399,8	400,9	405,6	406,2	439,4
292	290	253345,0	470869,4	26,5	440,0	20-5-1981	-1,5	73,5	73,5	200,5	373,5	375,7	378,0	399,0	400,5	406,0	406,8	440,1
293	291	253305,0	470864,3	26,4	442,1	1-7-1981	-1,4	73,6	73,6	200,6	374,1	376,2	379,3	401,0	402,1	407,2	407,3	439,8
294	292	253265,4	470858,8	26,4	439,4	1-9-1981	-1,4	73,7	73,7	200,7	374,0	375,7	379,6	401,1	401,2	405,3	406,9	437,8
295	293	253106,8	470837,7	26,2	440,7	2-4-1981	-1,2	73,8	73,8	199,3	375,9	378,0	381,4	401,7	403,2	408,1	408,9	439,5
296	294	253067,2	470832,1	26,3	439,2	6-3-1981	-1,3	73,8	73,8	200,8	377,0	378,5	382,1	403,0	404,2	409,4	410,2	438,9

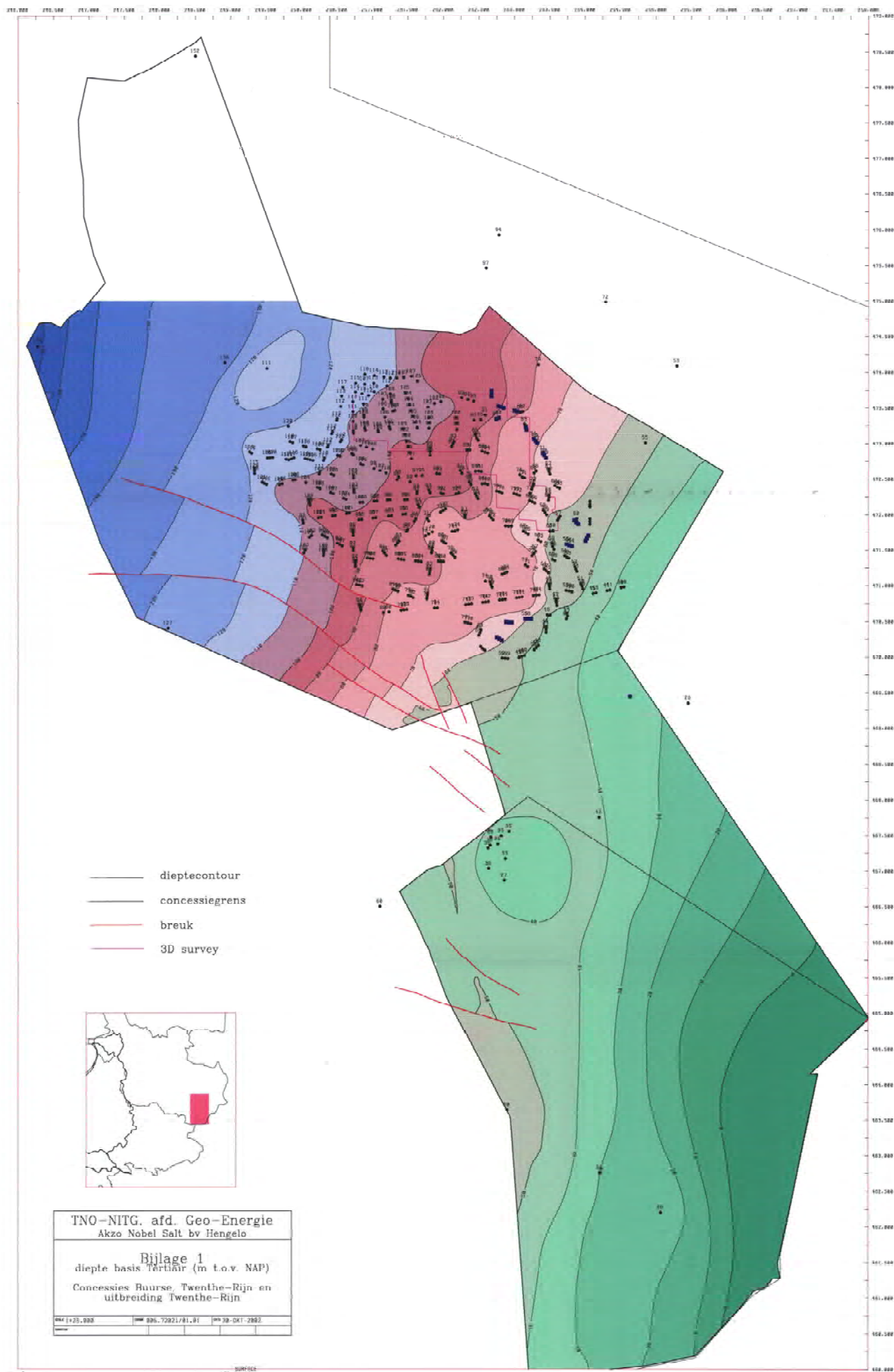
No	Well	X	Y	MV	TD	Date_end	T.Te	B.Te	T.Mu	B.Mu	T.Z-D	B.Z-D	T.Z-C	B.Z-C	T.Z-B	B.Z-B	T.Z-A	B.Z-A
297	295	253027,9	470826,6	26,3	441,9	10-2-1981	-1,3	73,8	73,8	202,3	377,7	379,7	383,7	403,9	405,9	410,3	411,4	441,1
298	296	252869,3	470805,6	26,0	440,9	29-12-1980	-1,0	74,1	74,1	203,1	379,2	380,5	383,0	401,4	402,9	406,9	407,6	440,1
299	297	252829,6	470800,0	26,1	441,9	22-10-1980	-1,1	73,9	73,9	203,9			379,6	399,5	400,7	405,6	407,6	440,5
300	298	252789,8	470794,7	26,2	442,4	23-9-1980	-1,2	73,8	73,8	204,2			381,6	401,5	403,8	408,3	410,3	440,8
301	299	252631,3	470773,4	25,9	444,9	9-6-1982	13,1	72,1	72,1	209,1	381,9	382,9	387,4	407,8	409,0	414,2	415,0	444,0
302	300	252591,5	470768,5	25,9	448,7	14-5-1982	13,1	74,1	74,1	209,1	382,3	383,9	388,7	407,6	409,1	414,1	415,3	445,0
303	301	252552,2	470763,0	25,8	446,4	23-4-1982	14,2	74,2	74,2	209,2	384,2	386,2	389,2	409,2	410,4	415,0	415,8	445,3
304	302	252393,9	470742,1	25,4	451,2	26-3-1982	-2,9	75,1	75,1	217,6	387,6	392,1	395,6	415,2	416,6	421,4	422,3	450,8
305	303	252354,2	470736,8	25,2	454,8	24-11-1981	-0,7	75,3	75,3	217,2	389,3	391,5	395,0	416,1	417,5	421,8	422,8	451,8
306	304	252315,1	470731,6	25,2	454,2	8-10-1981	-2,7	73,9	73,9	218,4	392,2	393,3	396,7	418,2	419,3	424,2	425,3	454,4
307	305	251196,9	471419,0	23,4	493,6	14-8-1980	13,6	90,6	90,6	234,6	417,7	421,0	425,2	447,4	448,8	452,9	454,2	490,4
308	306	251171,3	471450,0	23,2	494,1	1-7-1980	13,8	90,3	90,3	234,8	421,3	424,8	430,3	453,8	455,3	458,8	459,8	491,3
309	307	251145,6	471480,9	23,0	493,6	10-6-1980	14,0	91,0	91,0	235,0	420,7	425,7	430,5	451,5	453,0	458,0	458,8	490,8
310	308	251365,5	471369,0	23,5	484,8	6-9-1983	21,5	86,5	86,5	243,0	414,5	416,5	419,6	440,8	442,1	446,8	447,3	484,0
311	309	251404,7	471364,3	23,4	482,6	16-6-1983	23,1	86,6	86,6	242,6	411,5	414,3	417,6	439,8	441,4	445,8	447,0	482,1
312	310	251444,4	471359,7	23,3	483,6	20-4-1983	21,7	84,7	84,7	241,7	409,9	412,2	416,1	437,2	438,1	443,2	444,4	479,5
313	311	251608,9	471341,0	23,5	470,7	31-1-1983	21,0	85,5	85,5	234,0	404,3	406,2	410,0	431,3	433,0	437,1	438,3	470,0
314	312	251648,1	471336,4	23,8	469,4	2-12-1982	20,2	87,2	87,2	231,2	401,4	403,9	408,3	429,5	430,7	435,8	436,9	469,3
315	313	251687,5	471331,9	23,9	467,0	27-9-1982	20,1	84,1	84,1	228,1	400,5	402,2	405,9	427,7	428,9	434,0	435,3	466,7
316	314	251846,1	471532,8	24,1	448,4	23-2-1984	0,9	79,9	79,9	209,9	382,9	386,8	390,7	411,7	413,6	417,6	419,0	446,9
317	315	251839,8	471493,2	23,9	452,9	17-1-1984	0,9	80,1	80,1	214,6	388,5	390,1	393,9	415,1	416,0	421,3	422,0	449,8
318	316	251833,7	471453,6	24,2	453,3	24-11-1983	1,2	80,8	80,8	206,3	391,0	392,8	396,9	417,2	418,8	423,5	424,2	453,0
319	317	251814,7	471228,9	23,9	463,9	14-5-1984	1,0	82,7	82,7	216,9	397,6	398,6	402,7	423,2	424,4	429,7	430,7	463,2
320	318	251808,5	471189,3	24,1	465,7	27-6-1984	1,5	85,0	85,0	222,5	398,0	402,8	407,1	426,5	427,9	432,5	433,8	465,5
321	319	251802,4	471149,9	24,3	468,0	24-9-1984	2,0	87,5	87,5	229,7	400,6	403,6	408,0	427,7	428,9	433,9	434,8	467,5
322	320	251775,5	470888,1	24,4	475,4	13-11-1984	6,1	76,9	76,9	239,4	408,8	411,9	415,6	435,3	435,7	441,1	441,9	475,2
323	321	251771,0	470849,0	24,3	477,9	18-12-1984	3,8	75,8	75,8	240,5	409,7	411,7	416,0	435,6	436,6	441,4	442,4	477,2
324	322	251766,3	470809,3	24,4	478,9	13-2-1985	0,6	75,6	75,6	235,6	412,8	415,6	419,4	438,5	439,9	443,8	444,9	478,1
325	323	251875,6	470685,6	25,0	473,2	22-5-1985	8,0	75,6	75,6	242,5	408,7	412,6	416,4	435,0	436,2	440,5	441,8	473,0
326	324	251915,4	470688,6	25,5	471,7	12-4-1985	4,8	73,6	73,6	238,9	406,8	408,5	411,7	432,7	434,5	438,5	440,0	470,9
327	325	251931,6	471336,4	24,2	452,9	28-8-1985	10,3	82,5	82,5	217,7	388,1	391,4	394,7	416,1	417,2	422,3	423,1	452,5
328	326	251966,6	471334,7	24,3	452,0	3-10-1985	8,2	80,8	80,8	215,3	388,5	390,3	394,0	414,7	415,9	420,7	421,5	451,5
329	327	252001,7	471333,2	24,5	450,3	26-11-1985	9,4	80,2	80,2	214,6	387,6	389,0	392,7	414,0	415,1	420,1	421,0	450,1
330	328	252163,0	471392,6	25,0	441,0	21-8-1986	8,1	80,0	80,0	204,0	376,8	381,0	384,5	405,2	407,2	411,2	412,4	439,0
331	329	252135,8	471422,0	24,9	440,4	10-10-1986	8,7	79,1	79,1	203,3	377,4	381,4	385,1	404,4	406,1	411,2	411,6	440,0
332	330	252108,8	471451,4	24,9	440,8	7-11-1986	9,6	79,2	79,2	202,5	377,7	380,4	383,8	404,5	406,1	410,4	411,4	440,7
333	331	252034,7	471591,3	24,2	437,1	24-3-1987	10,9	67,3	67,3	199,8	372,8	375,5	378,3	400,4	401,4	406,2	406,8	436,3

No	Well	X	Y	MV	TD	Date_end	T.Te	B.Te	T.Mu	B.Mu	T.Z-D	B.Z-D	T.Z-C	B.Z-C	T.Z-B	B.Z-B	T.Z-A	B.Z-A
334	332	252006,1	471610,7	24,3	437,1	4-2-1987	10,8	77,7	77,7	201,1	372,3	374,7	378,3	400,8	401,5	406,8	407,5	436,9
335	333	251977,1	471630,2	24,1	437,5	16-12-1986	10,4	65,6	65,6	202,9	376,7	377,7	382,8	403,1	405,0	409,1	410,1	437,1
336	334	252124,0	471758,6	24,3	427,0	13-7-1987	5,7	73,7	73,7	185,7	363,2	367,2	370,7	391,1	392,6	397,3	398,5	424,5
337	335	252163,6	471763,5	24,2	423,6	16-6-1987	12,9	73,8	73,8	185,8	362,5	363,6	366,9	389,1	391,0	395,0	396,2	423,5
338	336	252202,9	471781,2	24,3	420,2	11-5-1987	5,7	73,7	73,7	185,7	359,4	361,1	364,9	387,1	388,5	392,5	393,5	420,0
339	337	251289,8	470946,9	23,8	507,4	19-4-1988	12,8	81,2	81,2	262,1	429,8	434,0	437,1	457,5	459,0	463,4	464,6	507,2
340	338	251324,9	470932,5	23,9	505,6	14-3-1988	14,1	79,0	79,0	262,2	429,6	433,7	437,4	456,2	457,9	462,3	463,5	506,5
341	339	251360,0	470918,0	24,0	503,9	4-2-1988	14,1	78,9	78,9	263,6	427,6	429,5	433,5	452,5	454,6	460,5	461,4	503,5
342	340	251507,8	470862,1	24,2	495,6	11-12-1987	6,9	77,4	77,4	256,9	423,2	426,7	430,8	449,8	450,7	455,1	456,3	495,0
343	341	251543,0	470847,8	24,4	494,1	5-11-1987	13,7	78,8	78,8	255,0	423,9	425,7	429,6	448,5	449,6	453,9	454,9	492,2
344	342	251575,0	470827,6	24,4	491,5	24-9-1987	13,1	82,1	82,1	254,2	422,4	423,7	426,9	447,2	448,6	452,1	453,0	490,6
345	343	251485,0	470663,3	24,7	499,0	1-8-1988	4,9	78,7	78,7	284,5	438,3	439,5	442,9	462,5	464,3	467,0	467,8	498,3
346	344	251445,3	470657,8	24,5	503,8	4-7-1988	6,1	78,6	78,6	285,5	445,7	449,3	452,3	469,5	470,3	472,6	473,5	503,5
347	345	251405,8	470652,4	24,6	508,4	7-6-1988	6,0	78,4	78,4	287,4	453,6	455,6	459,9	472,3	474,6	476,2	477,2	505,6
348	346	251234,5	470629,3	24,2	520,3	8-2-1990	9,8	89,8	89,8	287,8							497,8	517,2
349	347	250777,1	471008,3	22,9	541,6	12-10-1990	10,0	82,1	82,1	288,9	448,6	451,1	456,7	477,2	478,6	484,0	485,2	540,5
350	347A	250816,2	470999,9	22,8	539,1	11-9-1990	7,8	82,3	82,3	290,0	448,9	450,2	454,6	476,5	477,5	484,6	486,7	537,2
351	347B	250855,3	470991,5	22,8	535,9	18-7-1990	7,8	82,2	82,2	289,4	449,1	451,5	455,8	477,1	478,5	483,3	484,1	535,5
352	348	251155,4	470618,7	24,2	534,3	21-12-1989	9,8	79,8	79,8	279,8							512,6	524,3
353	349	250839,4	470652,6	23,1	548,8	18-6-1990	8,9	85,9	85,9	331,9	481,4	483,6	486,9	496,6	497,3	504,4	506,9	548,6
354	350	250831,2	470692,2	23,2	550,3	8-5-1990	11,2	82,8	82,8	331,9	478,4	480,5	484,8	497,9	498,8	502,5	505,0	546,7
355	351	250822,9	470731,4	23,2	552,0	16-3-1990	8,8	81,8	81,8	332,8	470,5	472,8	476,3	496,2	498,3	499,2	500,3	548,8
356	352	250928,6	471380,1	22,8	509,7	22-11-1988	10,2	85,2	85,2	269,4	434,8	436,3	440,2	462,2	463,3	469,1	470,2	508,7
357	353	250968,1	471375,1	22,9	507,9	28-10-1988	10,1	80,1	80,1	267,6	432,1	434,1	437,5	460,2	461,6	466,9	467,5	506,4
358	354	251007,9	471370,5	22,8	507,7	30-9-1988	10,2	80,2	80,2	265,4	428,2	428,9	437,6	459,2	460,4	465,9	466,7	505,9
359	355	250316,3	471492,9	21,4	532,5	11-1-1989	10,6	105,6	105,6	298,5	458,4	461,7	465,4	484,6	485,8	490,4	491,1	531,8
360	356	250314,1	471456,3	21,5	535,6	8-2-1989	10,5	105,5	105,5	301,0	458,7	461,0	464,3	485,3	486,1	491,6	493,5	534,8
361	357	250311,6	471419,6	22,1	537,5	17-3-1989	9,9	104,9	104,9	303,6	460,3	461,6	465,2	486,5	487,9	491,9	492,7	537,2
362	358	252683,0	470970,3	25,5	438,2	13-11-1989	4,5	70,5	70,5	203,9	378,7	379,7	383,8	404,5	405,7	410,0	411,0	437,8
363	359	252669,0	471007,7	25,9	438,5	17-10-1989	4,1	70,1	70,1	203,1	377,2	380,1	383,9	403,5	405,3	408,9	409,8	438,1
364	360	252655,3	471045,2	26,0	437,5	14-9-1989	4,0	70,0	70,0	201,8	376,8	378,4	382,2	402,2	403,9	408,0	409,3	437,0
365	361	252824,2	471154,1	26,4	433,3	19-6-1989	3,6	69,0	69,0	190,6	368,4	369,7	373,4	394,4	396,0	400,3	401,6	431,6
366	362	252858,9	471168,2	26,3	431,5	25-5-1989	3,7	68,4	68,4	191,7	367,2	371,5	375,2	394,8	397,0	400,9	401,9	430,7
367	363	252892,9	471183,2	26,0	428,5	18-4-1989	4,0	64,0	64,0	187,3	364,3	368,6	372,4	392,2	393,8	398,2	399,4	428,1
368	364	253738,3	470609,2	27,3	453,7	30-1-1991	2,7	48,7	48,7	203,3	381,9	383,4	387,5	408,4	410,8	414,5	415,7	450,4
369	365	253749,5	470571,2	27,6	454,9	25-2-1991	2,4	47,4	47,4	203,8	382,4	384,9	388,7	408,9	410,5	414,6	415,6	451,8
370	366	253734,0	470532,2	27,8	452,7	21-3-1991	2,2	47,2	47,2	205,2	383,5	386,3	390,0	410,6	412,3	416,4	417,2	452,6

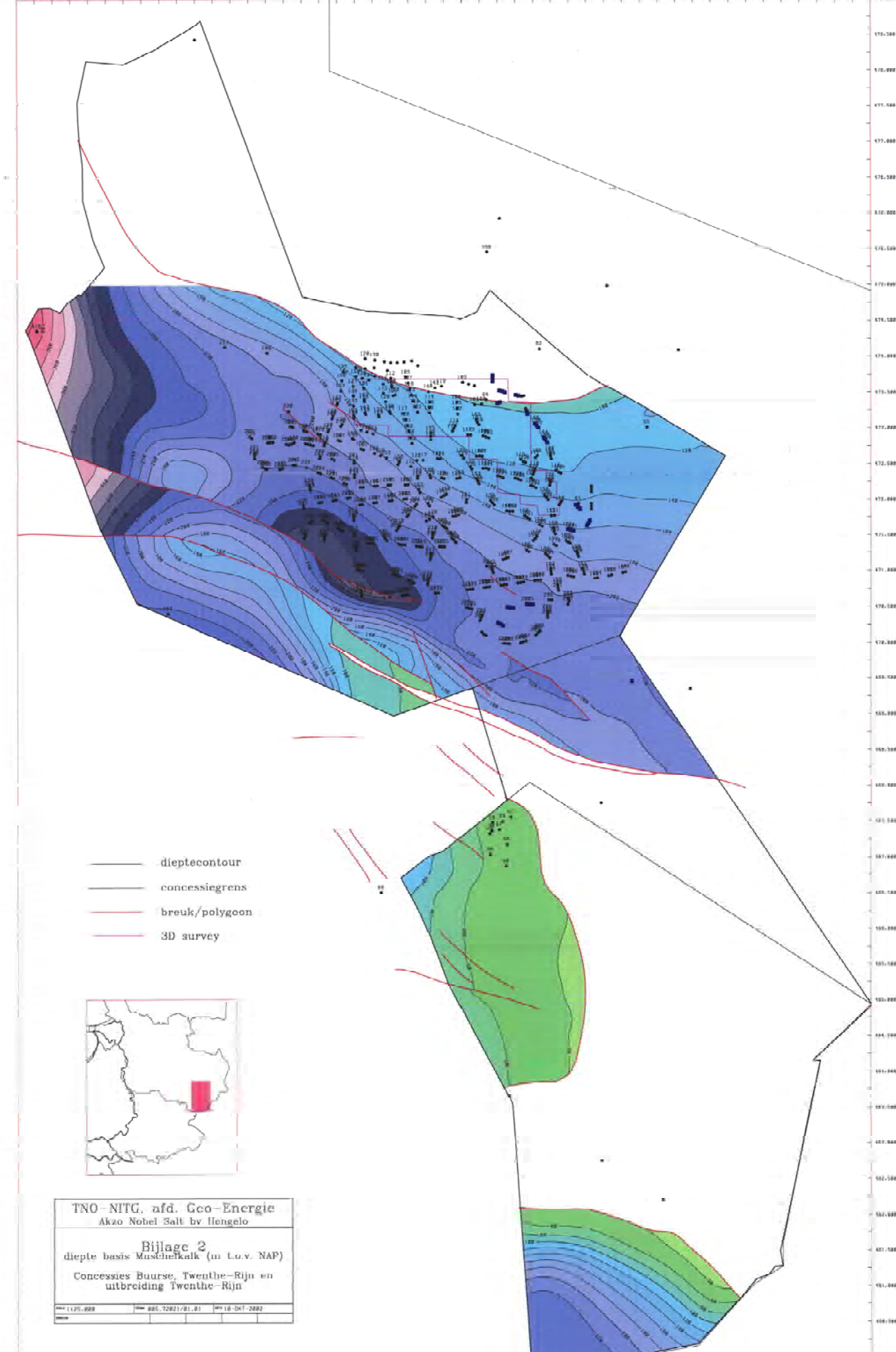
No	Well	X	Y	MV	TD	Date_end	T.Te	B.Te	T.Mu	B.Mu	T.Z-D	B.Z-D	T.Z-C	B.Z-C	T.Z-B	B.Z-B	T.Z-A	B.Z-A
371	367	253504,0	470588,7	27,5	449,2	16-12-1991	2,5				381,9	383,3	388,4	408,2	409,6	414,4	415,1	449,5
372	368	253464,1	470590,1	27,4	449,9	21-11-1991	-6,4	45,6	45,6	206,1	380,9	383,2	387,4	407,2	408,5	413,5	414,5	449,9
373	369	253445,5	470424,2	27,5	450,5	1-11-1990	-6,5	43,5	43,5	208,0	384,3	387,2	391,3	411,4	412,6	416,9	417,7	449,7
374	370	253445,9	470384,1	27,4	450,8	26-11-1990	-2,4	46,6	46,6	208,2	384,5	387,2	391,2	411,6	413,1	416,7	417,6	449,8
375	371	253446,2	470344,1	27,5	451,4	17-12-1990	-2,5	46,5	46,5	208,5	384,7	386,5	390,4	411,0	412,8	416,4	417,5	450,5
376	372	253337,4	470157,7	27,9	448,4	7-12-1992	-2,9	48,1	48,1	203,1	380,6	383,6	387,8	408,4	409,9	414,4	415,8	448,4
377	373	253308,1	470130,5	27,9	449,4	18-1-1993	2,1	49,1	49,1	202,1	379,4	382,9	387,7	407,3	409,0	413,4	414,3	448,8
378	374	253278,8	470103,3	27,8	449,1	12-2-1993	2,2	50,2	50,2	201,2	378,1	380,7	384,7	406,0	407,4	412,0	413,0	447,8
379	375	253141,2	470020,3	27,2	444,8	4-3-1993	2,8	48,8	48,8	202,3	373,5	375,8	379,1	397,5	399,2	402,5	403,9	444,6
380	376	253103,4	470007,3	27,1	443,5	31-3-1993	2,9	48,9	48,9	203,2	376,5	379,5	385,2	403,0	404,6	408,2	409,4	443,4
381	377	253065,6	469994,4	27,1	443,6	21-4-1993	2,9	48,9	48,9	203,9	377,9	382,7	385,8	403,5	404,9	408,7	409,9	443,5
382	378	252907,0	469976,5	26,1	442,8	28-5-1993	4,9	58,9	58,9	208,9	378,3	382,6	386,4	403,3	405,0	409,6	410,7	442,0
383	379	252867,1	469980,0	26,0	443,0	28-6-1993	5,0	57,0	57,0	209,0	378,6	382,7	386,8	404,7	405,9	410,1	411,3	441,7
384	380	252827,3	469983,3	26,0	443,0	23-7-1993	5,0	59,0	59,0	210,2	379,2	383,1	387,2	405,5	406,5	411,5	412,8	442,3
385	381	252581,7	470095,9	26,1	446,6	4-5-1998					395,7	397,3	401,9	414,9	420,0	422,1	423,5	445,7
386	382	252548,2	470115,5	26,2	447,6	10-6-1998					395,7	399,1	403,3	418,9	421,4	423,9	424,9	446,2
387	383	252521,0	470143,4	26,1	448,4	7-7-1998					395,3	400,3	403,3	420,0	421,9	423,8	424,8	447,5
388	384	252495,5	470300,9	25,9	450,1	17-2-1992	9,1	64,1	64,1	204,1			395,9	416,1	417,4	421,5	422,5	449,9
389	385	252510,8	470338,2	25,9	450,2	10-3-1992	9,1	66,1	66,1	204,1	389,3	390,5	394,3	415,3	416,7	421,4	422,5	449,9
390	386	252525,7	470375,2	25,6	449,6	13-4-1992	9,4	64,4	64,4	204,4	388,3	392,4	395,6	415,5	416,6	421,7	422,8	449,4
391	387	252380,8	470464,8	25,8	454,5	23-7-1992	6,2	70,2	70,2	225,2	392,9	395,1	399,0	418,8	420,5	424,1	425,2	454,2
392	388	252343,2	470475,5	25,8	457,5	2-7-1992	6,2	71,2	71,2	226,2	395,7	396,5	400,5	419,9	421,0	424,9	425,7	454,0
393	389	252304,9	470486,1	25,7	456,0	11-6-1992	6,3	72,3	72,3	227,3	396,5	400,1	403,3	423,1	424,1	428,1	429,1	456,1
394	390	252746,7	472329,2	24,7	370,1	21-10-1991	2,3	79,3	79,3	134,3	315,6	317,5	320,8	341,5	343,1	347,5	348,4	370,3
395	391	252784,7	472317,5	24,9	370,2	11-7-1991	2,1	77,1	77,1	133,1	314,1	316,6	320,0	341,1	342,5	346,9	347,6	369,8
396	392	252821,3	472301,9	24,9	370,7	27-6-1991	2,1	78,1	78,1	134,1	315,2	317,1	319,8	340,1	341,7	346,0	347,2	370,3
397	393	252990,4	472293,4	24,4	366,2	23-4-1991	-0,4	73,6	73,6	130,6	311,2	312,4	316,0	332,3	334,1	338,4	339,5	366,3
398	394	253029,6	472282,9	24,6	364,6	21-5-1991	-0,6	73,4	73,4	130,4	311,0	311,8	316,0	334,9	336,3	340,8	341,8	364,4
399	395	253067,2	472267,3	24,6	366,9	11-6-1991	-0,6	72,4	72,4	130,4	310,9	316,6	320,8	338,7	340,4	344,6	345,8	366,9
400	396	253208,7	472192,2	26,0	368,0	29-10-1992	1,0	66,0	66,0	130,0			315,9	336,7	338,0	343,8	344,7	368,0
401	397	253245,5	472176,9	25,9	367,9	7-1-1992	1,1	66,1	66,1	131,6	308,1	312,0	315,7	337,4	339,0	343,6	344,6	367,0
402	398	253281,0	472158,3	25,7	369,0	16-9-1992	1,3	66,3	66,3	132,3			316,5	338,8	340,7	344,8	345,5	368,5
403	399	253401,5	472056,6	26,7	373,8	16-3-1994	5,3	59,3	59,3	138,3	315,3	319,7	322,6	344,1	345,5	350,0	351,3	373,5
404	400	253428,3	472025,7	26,8	376,7	14-4-1994	5,2	59,2	59,2	138,2	315,4	320,7	324,2	344,2	346,2	350,7	352,2	375,6
405	401	253452,0	471992,8	26,8	378,2	25-5-1994	6,2	59,2	59,2	138,2	321,8	322,7	326,2	346,0	347,6	352,2	353,7	377,7
406	402	253241,7	472351,5	25,6	362,5	17-1-1995	8,4	70,4	70,4	122,4	303,4	305,0	308,7	329,7	331,2	336,0	337,0	361,9
407	403	253256,9	472388,6	26,2	359,5	2-2-1995	8,3	69,8	69,8	120,1	302,2	302,9	306,1	328,1	329,9	334,9	335,7	358,6

No	Well	X	Y	MV	TD	Date end	T.Te	B.Te	T.Mu	B.Mu	T.Z-D	B.Z-D	T.Z-C	B.Z-C	T.Z-B	B.Z-B	T.Z-A	B.Z-A
408	404	253268,5	472426,6	26,2	356,4	27-2-1995	7,3	69,8	69,8	118,0	300,5	301,5	304,9	326,2	327,5	332,6	333,4	356,0
409	405	253135,6	472515,8	25,1	353,8	6-4-1995	-2,1	71,4	71,4	116,2	296,7	297,9	302,1	322,1	323,3	328,7	329,5	353,0
410	406	253104,5	472527,0	25,0	351,6	11-5-1995	-8,0	73,3	73,3	116,1	294,9	297,9	301,7	322,9	324,5	329,2	329,9	350,9
411	407	253069,7	472559,6	24,8	352,9	15-6-1995	2,3	73,5	73,5	115,3	297,1	297,4	302,3	322,6	323,8	330,1	330,5	352,6
412	408	253476,5	472197,3	25,4	367,2	30-6-1994	8,6	64,6	64,6	127,6			313,6	335,2	336,1	342,4	343,1	366,6
413	409	253485,1	472233,4	25,6	367,6	21-7-1994	8,4	65,4	65,4	125,9			312,4	333,8	334,9	340,2	341,4	364,7
414	410	253484,7	472270,1	25,8	362,6	10-11-1994	7,2	66,2	66,2	125,7	306,8	308,7	311,6	334,2	335,1	339,6	340,6	362,0
415	411	253605,5	471914,8	27,1	381,8	9-2-1994	4,9				322,7	324,7	327,9	349,2	350,7	355,4	356,7	381,2
416	412	253623,5	471944,7	26,9	380,3	16-12-1993	5,1	57,1	57,1	140,1	319,1	323,3	326,0	347,6	349,4	353,6	354,9	379,1
417	413	253642,0	471974,6	26,7	377,7	12-11-1993	5,3				317,0	320,9	323,9	345,6	347,1	352,1	353,3	376,8
418	414	253273,4	472584,9	26,2	347,8	10-10-1995		65,8		110,8	292,8	293,5	296,8	317,3	318,5	323,7	324,5	347,0
419	415	253302,7	472612,0	26,6	345,4	7-11-1995		66,3		108,4			294,4	316,0	317,4	322,3	322,9	345,3
420	416	253485,0	472644,1	25,6	345,7	14-3-1996		67,4		104,4			292,2	312,0	313,4	317,8	319,2	345,4
421	417	253484,8	472605,8	25,6	341,6	25-4-1996		67,4		106,4			295,0	313,3	314,8	319,4	321,1	341,3
422	418	253497,3	472568,6	25,6	343,6	23-5-1996		66,6		108,8	291,9	292,4	295,9	316,0	317,3	322,3	323,4	342,8
423	419	253567,1	472403,5	26,6	352,3	4-7-1996		63,4		116,4	297,8	299,6	302,8	323,8	325,2	329,6	330,5	352,3
424	420	253603,5	472380,6	25,8	353,7	4-9-1996		63,8		118,3			305,6	325,5	326,6	331,6	332,3	353,3
425	421	253635,1	472367,1	26,2	353,8	14-10-1996		62,6		116,8			304,8	324,6	326,0	330,9	331,8	353,1
426	430	253140,2	473267,9	24,4	314,8	6-11-1996		64,6					268,6	287,4	288,8	293,8	294,8	314,0
427	457	254066,2	471859,0	27,4	436,8						321,6	322,6	326,6	347,5	349,6	354,3	355,1	380,6
428	458	254066,2	471898,7	27,3	434,4						319,9	320,5	324,9	345,9	347,9	352,6	353,9	378,5
429	459	254066,4	471938,4	27,5	432,1						316,7	318,8	323,1	343,8	345,0	350,2	351,3	375,6
430	460	254066,4	472102,5	27,7	420,3								311,9	333,8	334,9	339,7	340,8	363,8
431	461	254066,4	472142,7	27,3	416,9						304,0	305,1	308,8	330,6	332,1	336,0	337,6	359,6
432	462	254066,3	472182,7	27,3	414,0						301,6	303,2	307,0	327,6	329,5	333,2	334,6	358,0
433	422	253442,5	472799,4	25,4	331,2	15-10-1997	-1,4	69,1		149,6			283,5	304,4	305,7	310,4	311,2	330,8
434	423	253419,4	472832,3	25,2	330,1	16-9-1997	7,8	69,3		147,8	277,8	278,8	282,3	303,8	305,2	310,0	310,6	329,8
435	424	253398,3	472862,0	25,3	328,7	29-5-1997	7,1	70,8		144,5	276,6	277,5	280,7	303,1	305,8	308,9	309,8	328,3
436	425	253318,7	472999,1	25,3	321,4	8-4-1997	6,7	72,2		141,7	276,1	276,1	296,5	297,5	302,9	303,9	303,9	320,9
437	426	253295,3	473032,8	25,3	321,7	5-3-1997	0,9	69,3		138,2	270,5	271,7	275,9	295,1	296,3	301,9	302,9	321,3
438	427	253269,8	473064,5	25,3	321,0	5-2-1997	11,7	73,5		139,5			274,4	294,2	295,4	300,7	302,1	320,5
439	428	253165,7	473189,9	24,5	316,6	14-10-1996							271,1	290,5	292,0	297,3	298,4	316,6
440	429	253156,4	473231,1	24,2	340,2	25-11-1996							269,6	288,1	289,6	294,8	295,7	315,1
441	432	253037,7	473449,0	23,7	318,3	3-3-1999							273,0	288,6	290,4	295,2	296,0	317,2
442	433	252999,2	473459,6	23,7	322,4	28-1-1999							273,2	290,7	292,6	297,4	299,2	321,0
443	434	252845,2	473501,9	23,5	330,7	9-6-1999							281,9	299,9	301,6	313,9	315,0	329,6
444	435	252806,8	473512,7	23,6	325,2	5-5-1999							283,5	301,2	304,6	309,3	310,3	323,4

No	Well	X	Y	MV	TD	Date_end	T.Te	B.Te	T.Mu	B.Mu	T.Z-D	B.Z-D	T.Z-C	B.Z-C	T.Z-B	B.Z-B	T.Z-A	B.Z-A
445	436	252768,2	473523,0	23,3	317,9	26-3-1999							286,2	304,2	305,9	311,7	313,3	315,3
446	437	252674,8	473657,2	23,3	319,9	19-11-1999							280,4	294,7	296,3	300,8	301,7	318,6
447	438	252675,2	473694,7	23,3	318,7	2-11-1999							276,2	293,0	294,1	299,3	300,3	317,4
448	439	252675,5	473734,6	23,2	315,2	14-7-1999							274,4	288,8	290,3	295,0	296,0	313,6
449	443	252742,0	473341,2	23,8	316,3	20-1-2000	6,1	81,1					271,3	291,3	292,3	297,2	298,2	315,3
450	444	252779,7	473354,2	23,8	314,7	16-12-1999	6,2	80,2					270,9	289,5	290,9	295,8	296,8	313,3
451	448	253733,7	471578,4	26,9	405,6	6-3-2000	0,6	55,1		160,9	340,7	343,1	346,9	368,1	369,8	373,7	374,8	404,1
452	449	253771,9	471566,6	27,4	406,1	31-3-2000	0,6	54,6		160,1	341,2	344,3	348,2	366,6	371,1	374,4	375,4	405,0
453	450	253810,0	471555,0	27,6	406,5	16-5-2000	-1,1	54,4		160,9	342,1	344,4	348,4	368,4	370,4	374,9	376,0	405,4
454	451	254004,5	471628,1	28,3	399,3	22-6-2001					335,7	339,4	343,4	363,4	364,7	369,8	371,0	397,8
455	452	254023,3	471663,3	28,6	396,3	29-5-2001					334,6	335,8	339,9	360,7	362,5	366,7	367,8	395,3
456	453	254042,1	471698,5	28,8	393,5	1-5-2001					331,4	332,9	336,4	358,6	359,9	364,6	365,8	392,4
457	454	253901,6	471860,2	27,9	385,0	19-9-2001					323,7	325,6	329,7	351,0	352,5	357,6	358,9	382,8
458	455	253872,1	471887,7	28,0	382,8	11-10-2001					322,6	324,8	328,4	350,6	351,9	356,6	357,6	381,4
459	456	253844,2	471916,8	27,8	380,4	7-11-2001					320,7	322,0	325,8	347,9	349,1	353,9	355,0	378,0
460	469	253232,3	470527,3	27,0	445,9	29-1-1998					379,2	380,7	384,7	406,2	407,8	411,9	412,8	444,8
461	470	253192,5	470530,6	27,0	445,6	18-12-1997	3,0	57,5		205,0	380,4	382,2	386,4	407,3	409,0	413,0	414,0	444,8
462	471	253152,7	470533,9	27,0	452,9	20-11-1997	1,3	59,1		204,1			385,2	407,1	408,7	413,2	414,3	444,7
463	472	252961,3	470483,7	26,8	443,7	3-12-1998					381,5	381,9	388,1	408,7	410,5	414,8	416,2	442,9
464	473	252921,7	470487,0	26,6	446,0	28-10-1998					382,7	383,1	386,8	408,3	409,8	414,1	415,1	444,3
465	474	252882,0	470490,2	26,5	446,1	30-9-1998					382,7	383,2	387,5	409,3	411,4	415,0	416,0	444,7
466	475	252749,3	470272,6	26,2	445,9	10-1-2001					381,6	382,4	386,4	409,4	411,2	416,2	417,0	444,6
467	476	252783,9	470252,4	26,4	445,3	27-3-2001					381,2	382,1	385,9	408,8	410,5	415,3	416,2	444,4
468	477	252818,4	470232,3	26,5	445,5	21-2-2001					380,3	382,7	386,9	408,9	410,4	415,1	416,0	444,3
469	515	254633,7	469440,1	31,7	434,5	10-7-2000					367,3	370,9	374,9	396,1	397,9	402,0	403,1	434,1
470	BKM-01	248117,0	470404,0	21,5	482,4		-19,0	126,7		242,5	459,1	460,9						
471	BOR-01	248502,0	478441,0	17,5	544,0		4,5	151,5					322,5					345,5
472	BSL-01	252900,0	463640,0	31,2	370,0		-23,2	60,4									291,5	303,4
473	BUS-01	254210,0	462750,0	33,0	917,8		-27,0	30,1					237,1		237,1	238,3	242,5	263,0
474	Pb.L	255070,0	462200,0	32,0	176,0		-23,0	26,0										
475	BUU-01	252629,0	467313,0	27,9	403,0		-20,2	36,1		58,4	297,1	300,0	304,6	326,1	327,5	330,6	332,0	372,5
476	BUU-02	252670,0	467469,0	27,6	396,1		-20,9	37,6		50,5	290,3	294,0	297,9	318,5	320,2	323,0	324,4	364,4
477	BUU-03	252859,0	466863,0	29,2	390,7		-20,2	26,6		49,8	286,7	291,8	296,2	318,2	319,6	323,0	325,3	355,3
478	BUU-04	252637,0	467025,0	28,0	398,6		-19,6	36,1		58,0	294,8	298,0	302,7	325,1	327,2	330,1	333,9	369,1
479	BUU-05	252873,0	467166,0	28,2	386,7		-20,7	33,2		46,3	280,7	284,3	285,6	308,7	310,6	313,1	313,6	358,0
480	BUU-06	252925,0	467550,0	27,9	385,9		-20,7	34,7		47,3	263,1	267,1	269,8	291,3	292,9	297,9	300,3	356,1
481	BUU-07	252767,0	467373,0	27,7	389,5		-20,8	35,1		47,1	285,2	288,8	292,9	314,6	316,1	319,4	320,6	359,9



246.000 248.000 250.000 252.000 254.000 256.000 258.000 260.000 262.000 264.000 266.000 268.000 270.000 272.000 274.000 276.000 278.000 280.000

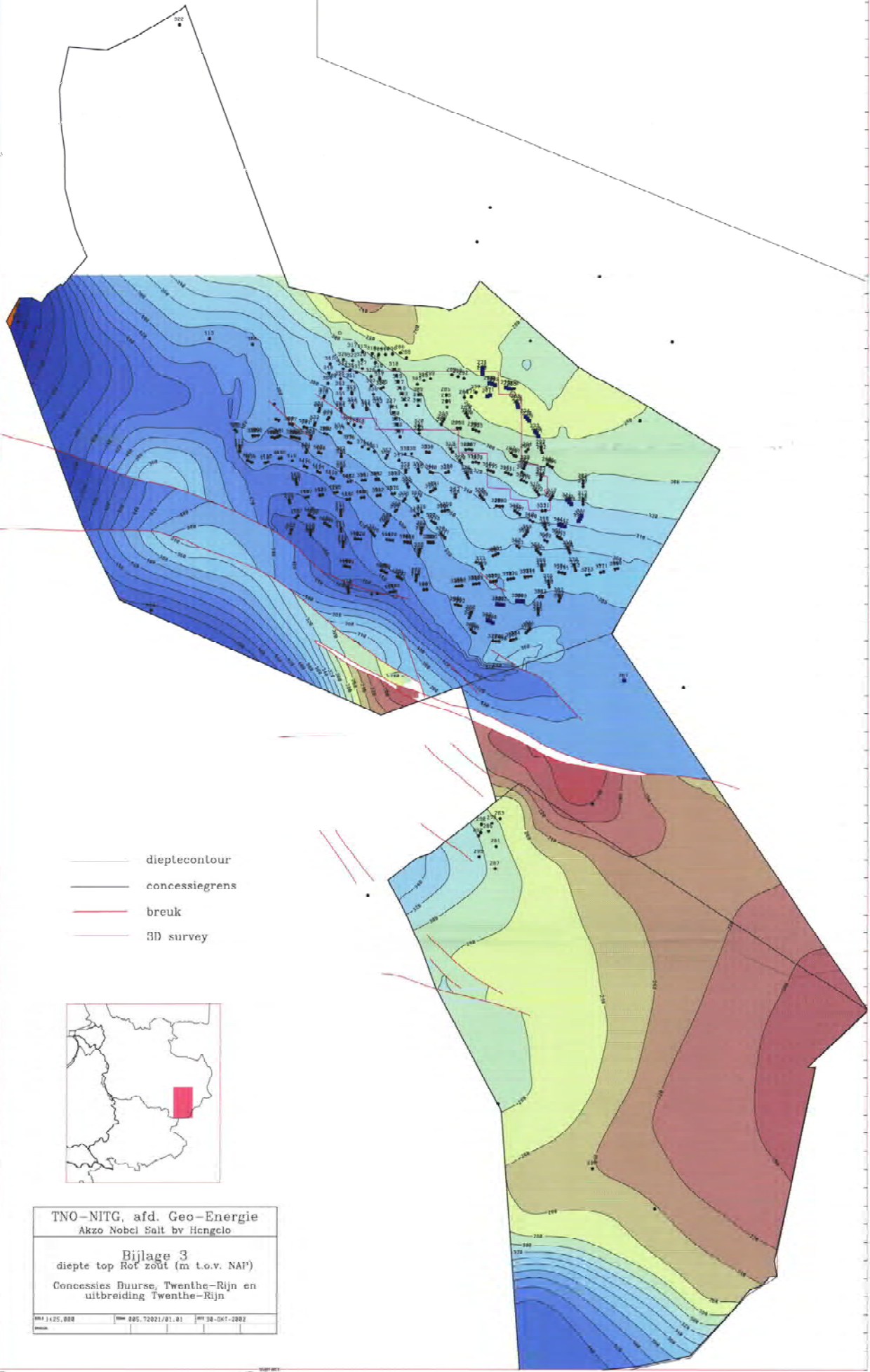


PMUSC05082801 2ycor S-Dec-2002 08:29

PMUSC05082801 2ycor S-Dec-2002 08:29

216.000 216.100 216.200 216.300 216.400 216.500 216.600 216.700 216.800 216.900 217.000 217.100 217.200 217.300 217.400 217.500 217.600 217.700 217.800 217.900 218.000

579.000
578.500
578.000
577.500
577.000
576.500
576.000
575.500
575.000
574.500
574.000
573.500
573.000
572.500
572.000
571.500
571.000
570.500
570.000
569.500
569.000
568.500
568.000
567.500
567.000
566.500
566.000
565.500
565.000
564.500
564.000
563.500
563.000
562.500
562.000
561.500
561.000
560.500
560.000



- dieptecontour
- concessiegrens
- breuk
- 3D survey

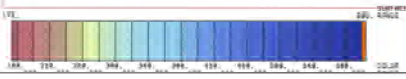


TNO-NITG, afd. Geo-Energie
Akzo Nobel Salt bv Hengelo

Bijlage 3
diepte top Rof zout (m t.o.v. NAP)

Concessies Bourse, Twenthe-Rijn en
uitbreiding Twenthe-Rijn

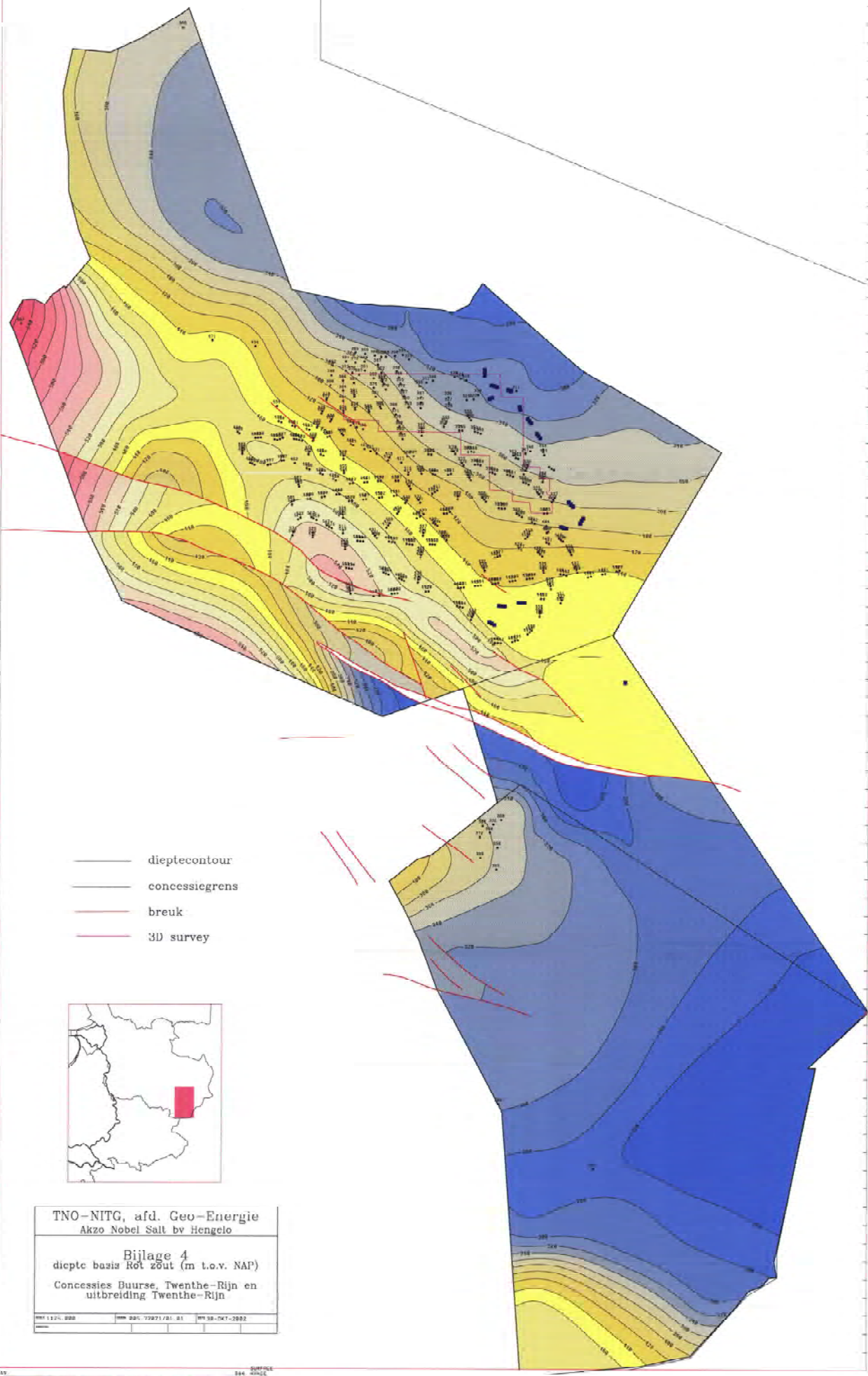
1:125,000 895.72021/01.01 30-OKT-2002



1:25000 2 km

246.000 246.500 247.000 247.500 248.000 248.500 249.000 249.500 250.000 250.500 251.000 251.500 252.000 252.500 253.000 253.500 254.000 254.500 255.000 255.500 256.000 256.500 257.000 257.500 258.000

176.000
175.000
174.000
173.000
172.000
171.000
170.000
169.000
168.000
167.000
166.000
165.000
164.000
163.000
162.000
161.000
160.000
159.000
158.000
157.000
156.000
155.000
154.000
153.000
152.000
151.000
150.000
149.000
148.000
147.000
146.000
145.000
144.000
143.000
142.000
141.000
140.000
139.000
138.000
137.000
136.000
135.000
134.000
133.000
132.000
131.000
130.000
129.000
128.000
127.000
126.000
125.000
124.000
123.000
122.000
121.000
120.000
119.000
118.000
117.000
116.000
115.000
114.000
113.000
112.000
111.000
110.000
109.000
108.000
107.000
106.000
105.000
104.000
103.000
102.000
101.000
100.000

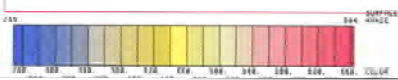


TNO-NITG, afd. Geo-Energie
Akzo Nobel Salt bv Hengelo

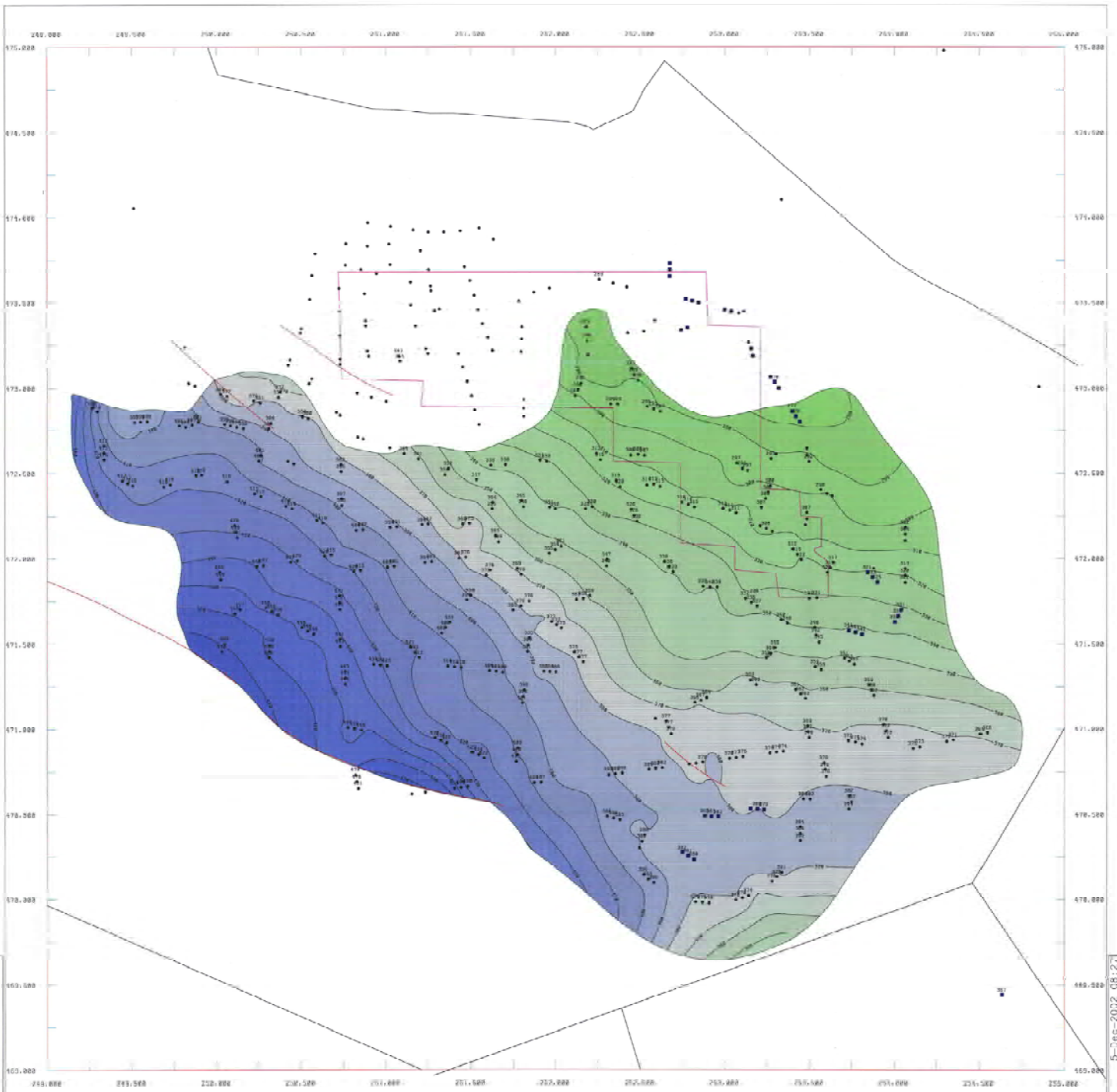
Bijlage 4
diepte basis Rol zout (m t.o.v. NAP)

Concessies Buurse, Twente-Rijn en
uitbreiding Twente-Rijn

1125-000	000-22071/01-01	000-0000-0000
----------	-----------------	---------------

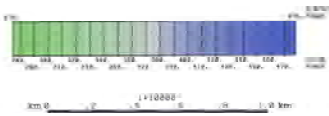


1:25000
0 2 km



5-Dec-2002 08:27

5-Dec-2002 08:27



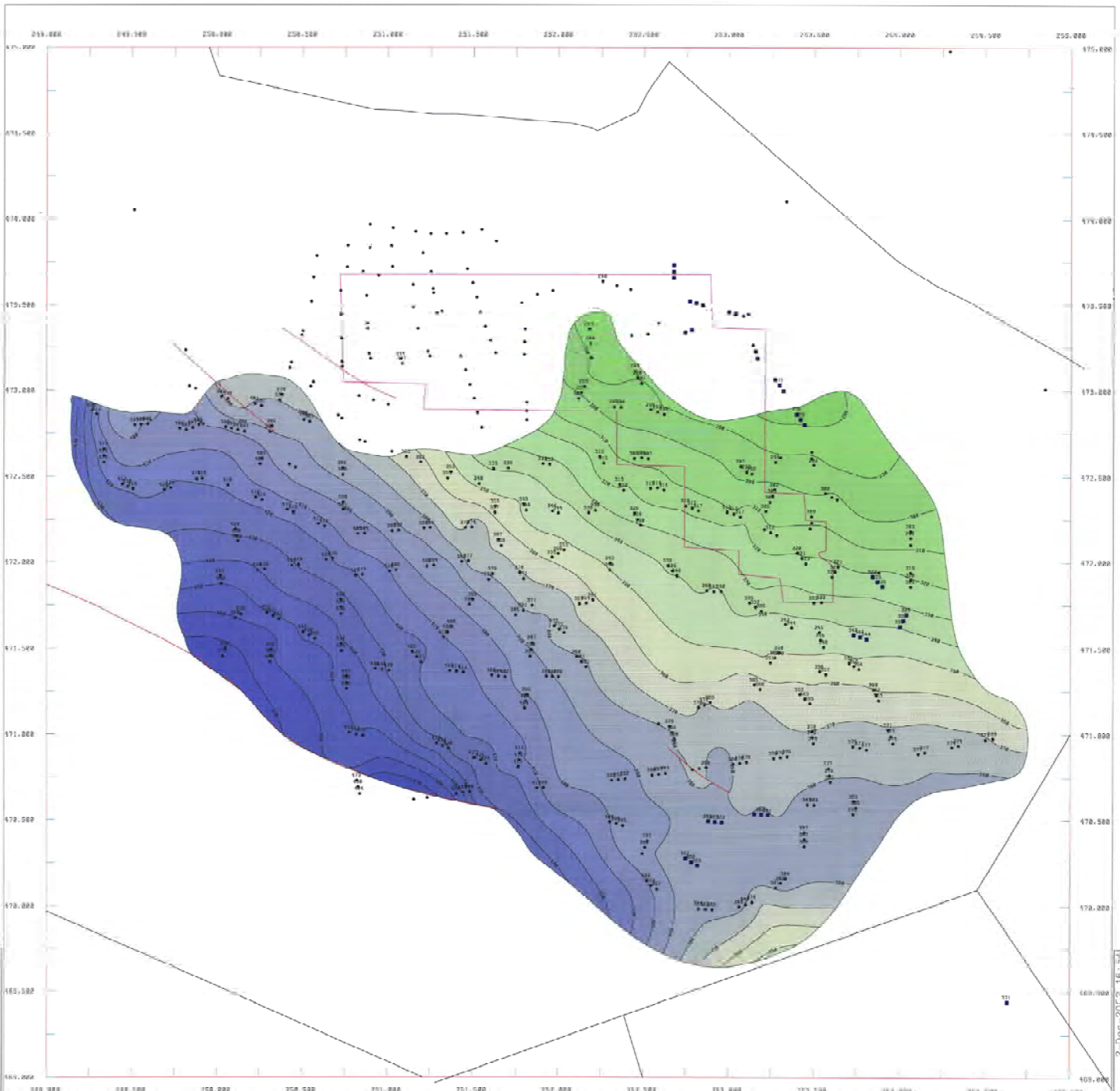
- deplecontour
- concessiegrens
- break
- 3D survey
- polygon

TNO-NITG, afd. Geo-Energie
 Akzo Nobel Salt bv Hengelo

bijlage 5
 diepte top D-zout (m t.o.v. NAP)

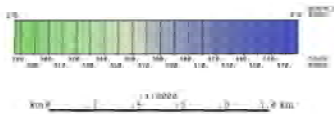
Concessies Buurse, Twente-Rijn en
 uitbreiding Twente-Rijn

175.000 170.000 165.000
 250.000 255.000 260.000



2-Dec-2002 16:34

2-Dec-2002 16:34



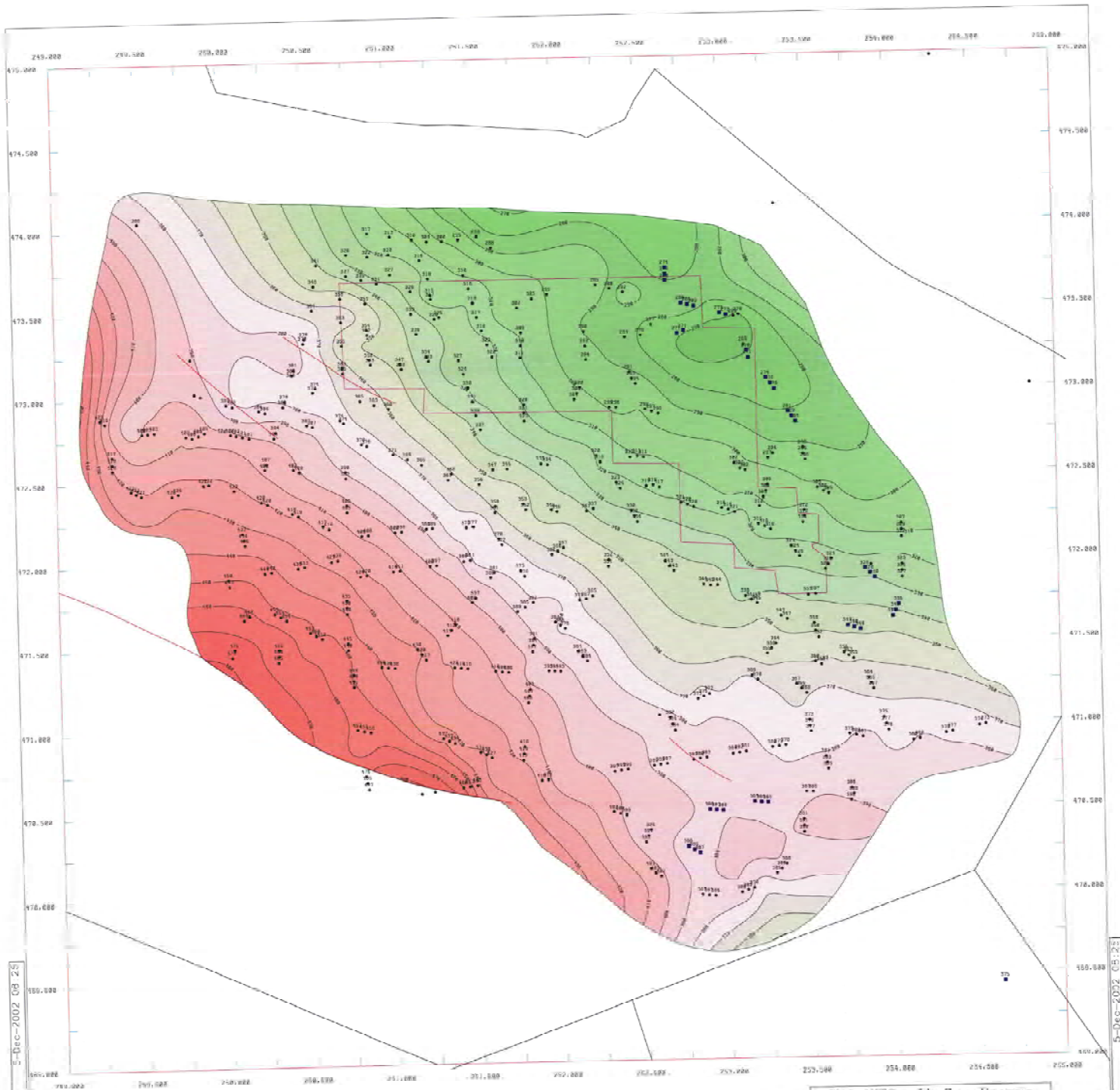
- dieptecontour
- concessiegrens
- breuk
- 3D survey
- polygon

TNO-NITG nfd Geo-Energie
Akzo Nobel Salt by Hengelo

bijlage 6
 diepte basis D-zout (m t.o.v. NAP)

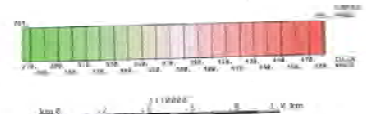
Concessies Buurse, Twente-Rijn en
 uitbreiding Twente-Rijn

1:10,000 1000 0 1000 2000 3000 4000 5000 6000 7000 8000 9000 10000
 2000 4000 6000 8000 10000
 2000 4000 6000 8000 10000



5-Dec-2002 09:23

5-Dec-2002 09:23



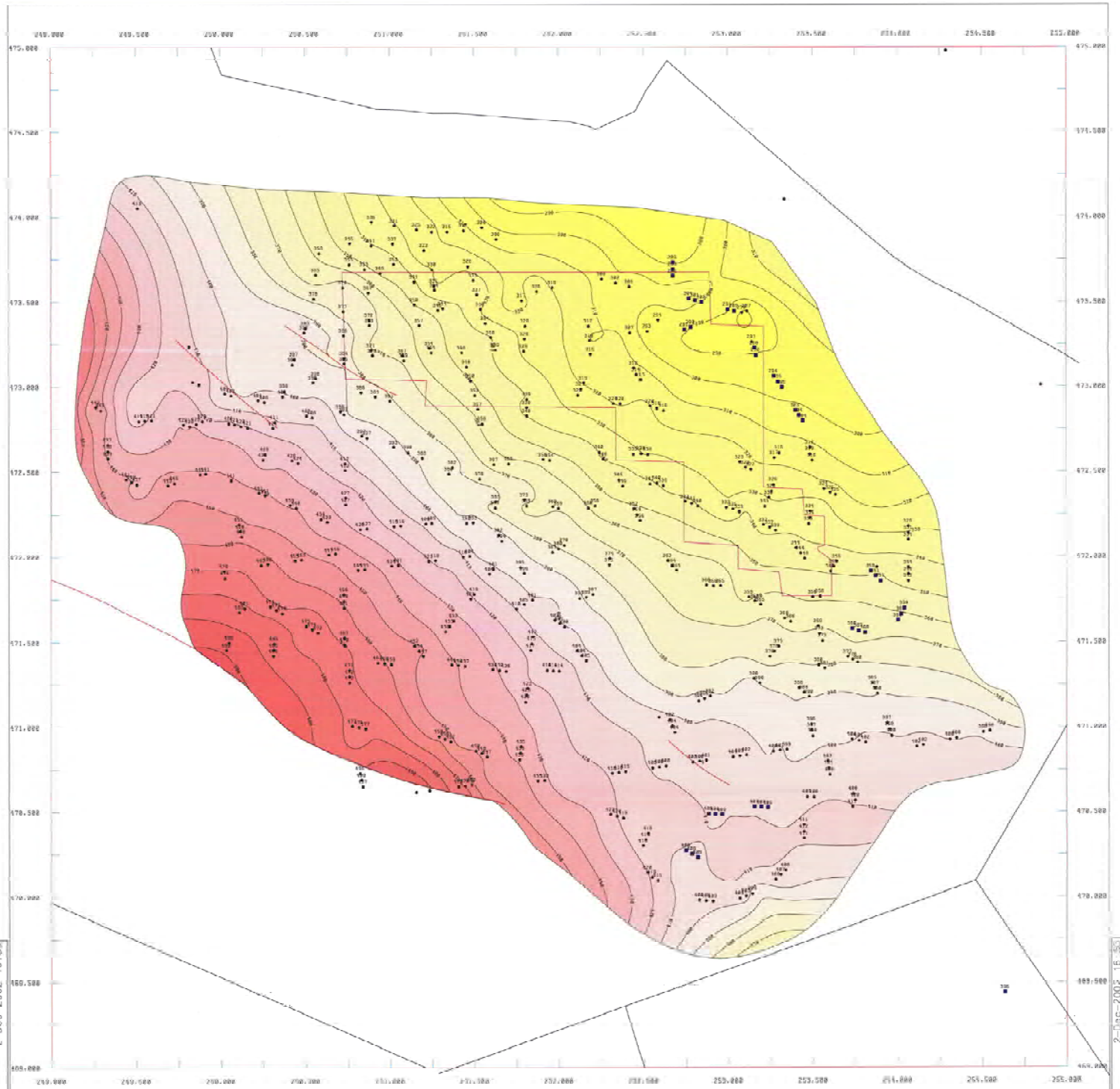
- dieptecontour
- concessiegrens
- breuk
- 3D survey
- polygon

TNO-NITG, afd. Geo-Energie
 Akzo Nobel Salt by Hengelo

bijlage 7
 diepte top C-zout (m t.o.v. NAP)

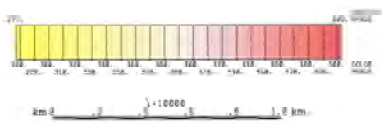
Concessie Bourse, Twente-Rijn en
 uitbreiding Twente-Rijn

1118.000 1000.000 1000.000 1000.000 1000.000



2-Dec-2002 16:53

2-Dec-2002 16:53



- dieptecontour
- concessiegrone
- breuk
- 3D survey
- polygoon

TNO-NITG, afd. Geo-Energie
 Akzo Nobel Salt by Itenselo

bijlage B
 diepte basis C-zout (m t.o.v. NAP)

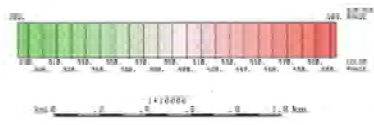
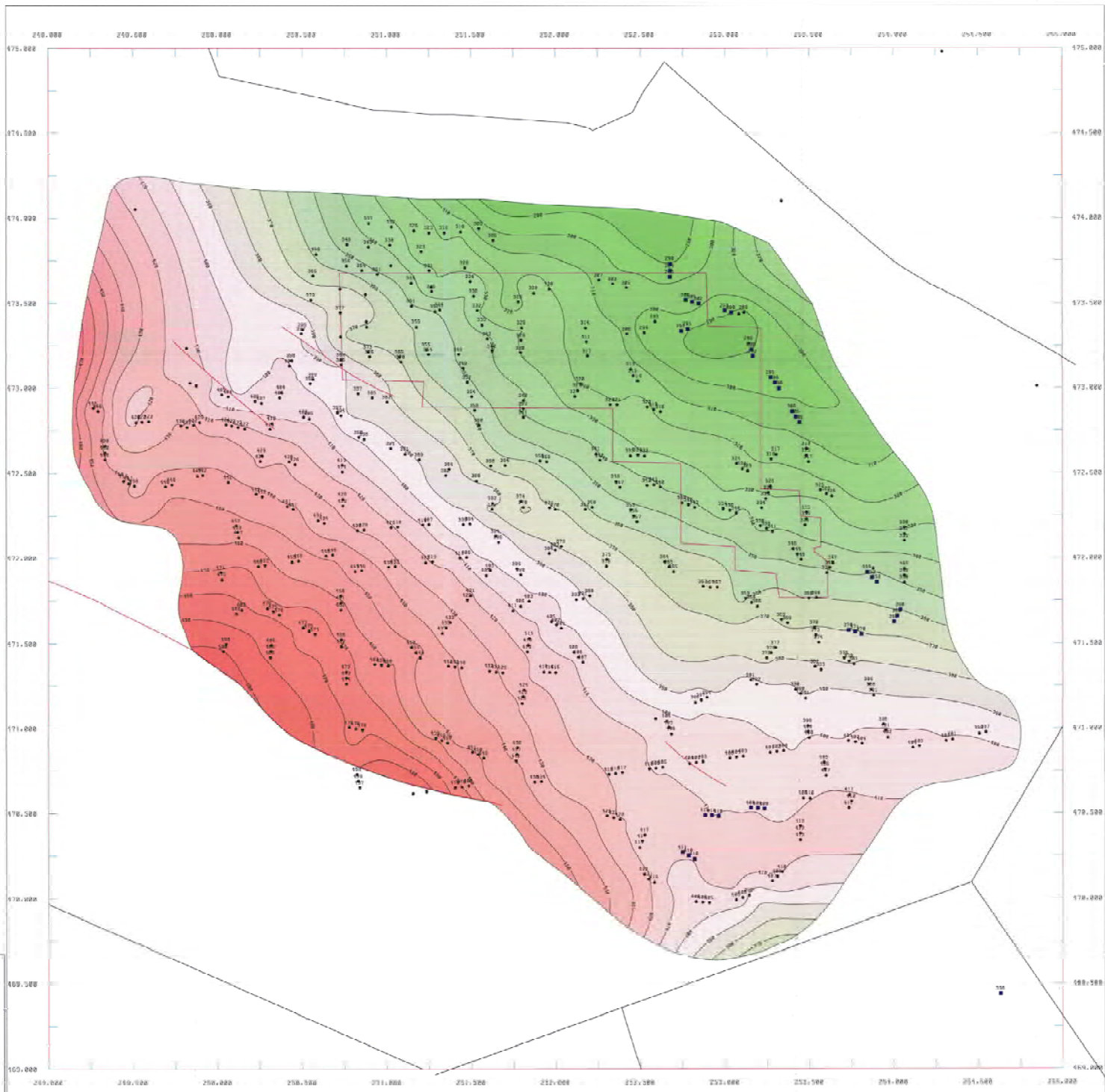
Concessies Buurse, Twente-Rijn en
 uitbreiding Twente-Rijn

1118.888 882.7482/81.81 88-083-88

bas 2002 165307 27500

tc02111713 mesdag 27-Mar-2003 13:20

tc02111713 mesdag 27-Mar-2003 13:20



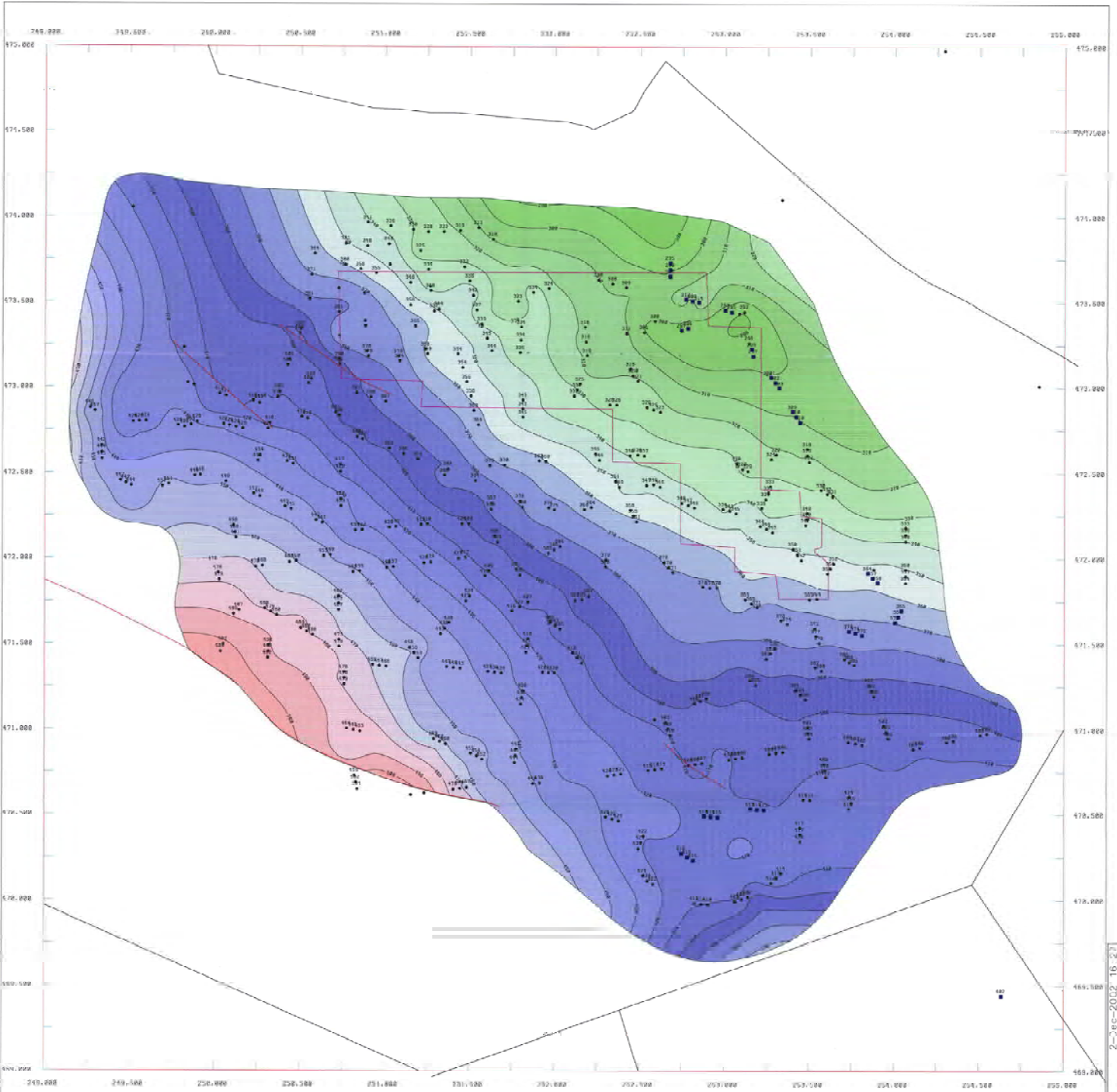
- dieptecontour
- concessiegrens
- breuk
- 3D survey
- polygon

TNO-NITG, afd. Geo-Energie
 Akzo Nobel Salt by Hengelo

bijlage 9
 diepte top B-zout (m t.o.v. NAP)

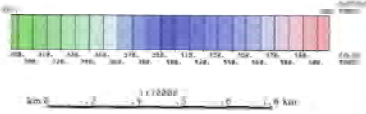
Concessies Buurse, Twente-Rijn en
 uitbreiding Twente-Rijn

1:10,000 0 100 200 300 400 500 600 700 800 900 1000



Eos 158-2-152 (4.5 km) 2-Dec-2002 16:27

Eos 158-2-152 (4.5 km) 2-Dec-2002 16:27



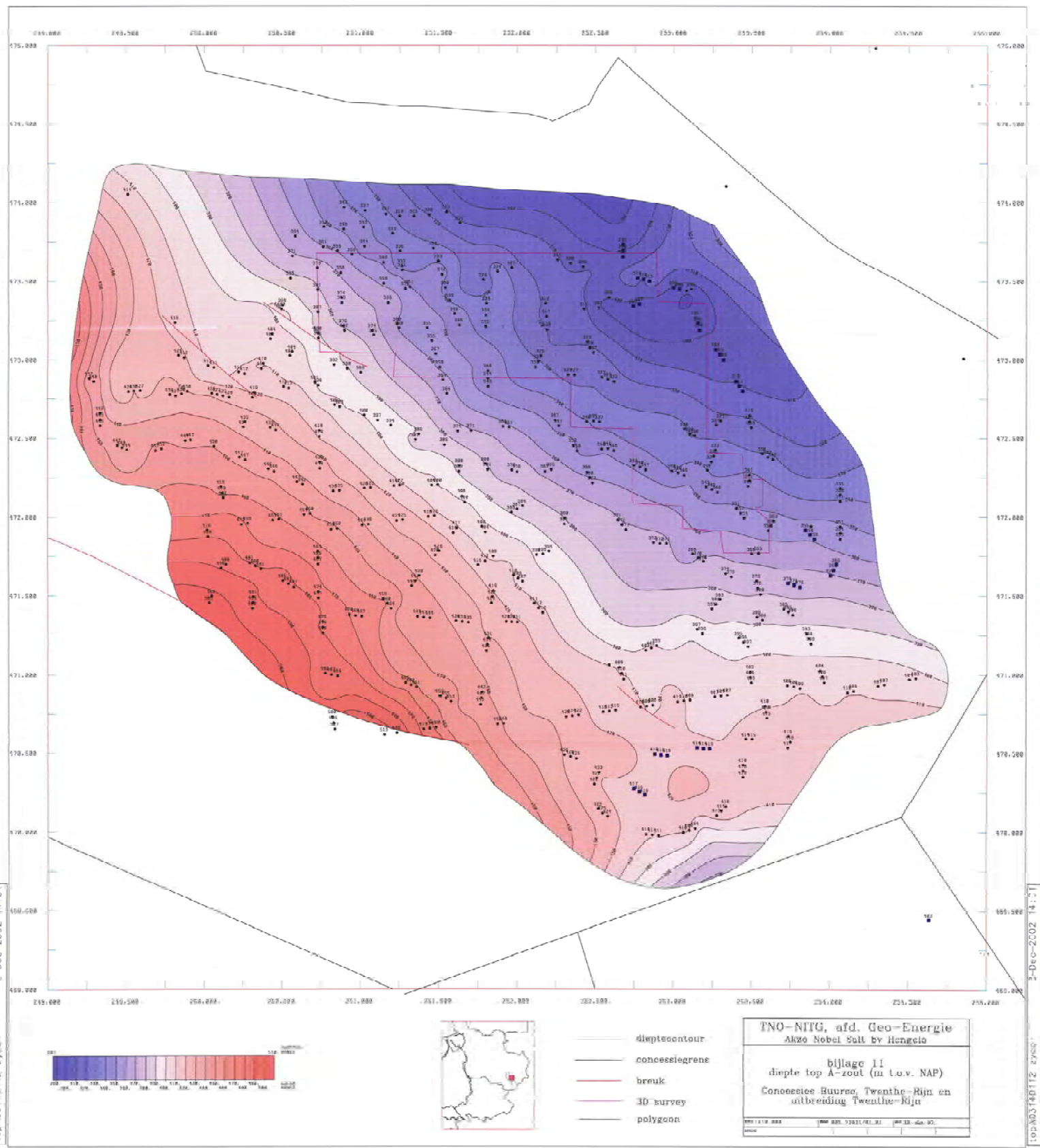
- dieptecontour
- concessiegrens
- breuk
- 3D survey
- polygoon

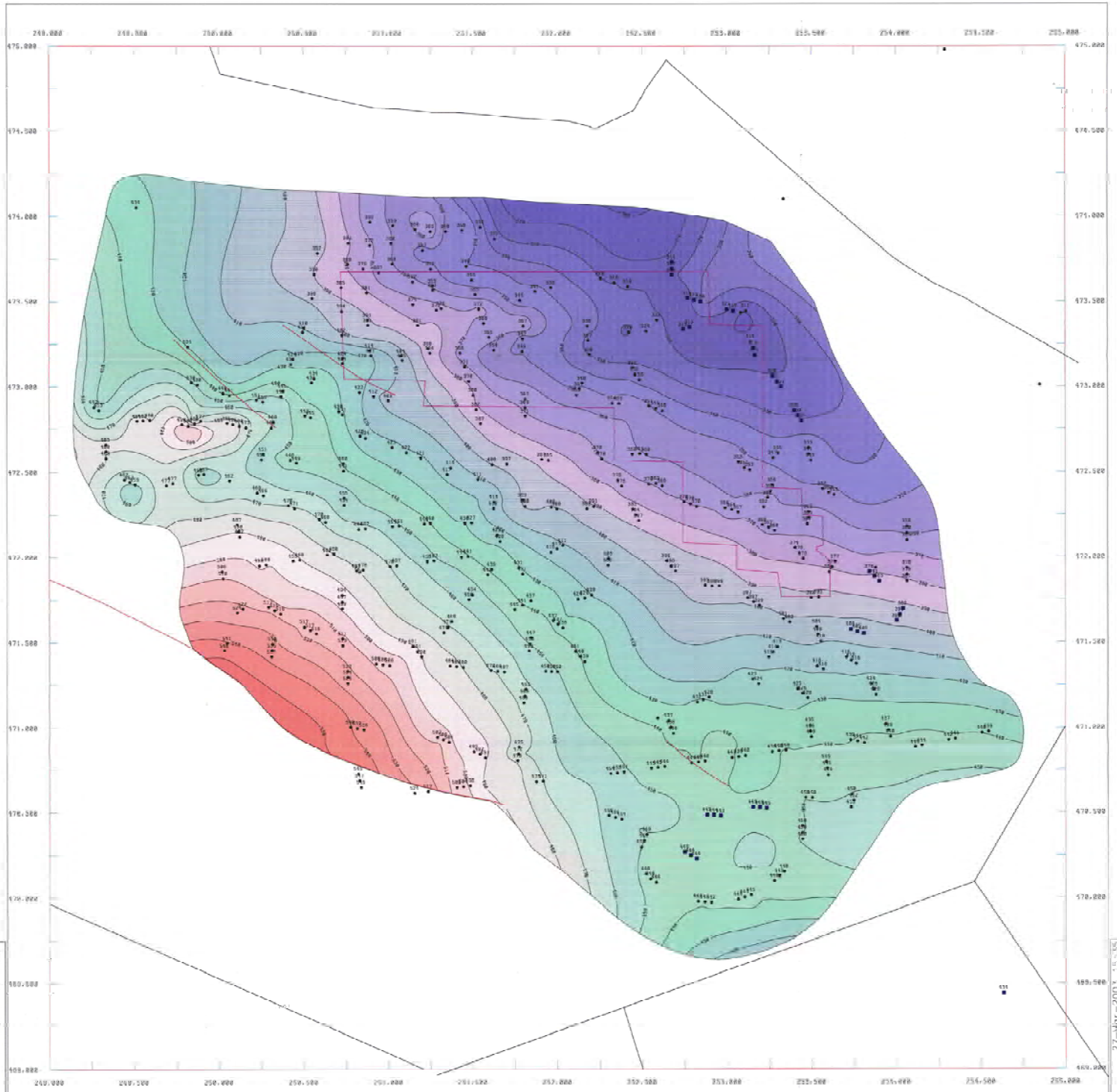
TNO-NITG, afd. Geo-Energie
 Akzo Nobel Salt by Hengelo

bijlage 10
 diepte basis B-zout (m t.o.v. NAP)

Concessies Buurse, Twente-Rijn en
 uitbreiding Twente-Rijn

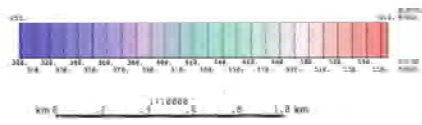
UTM: 118.000 122.170 127.300
 470.000 474.170 479.300





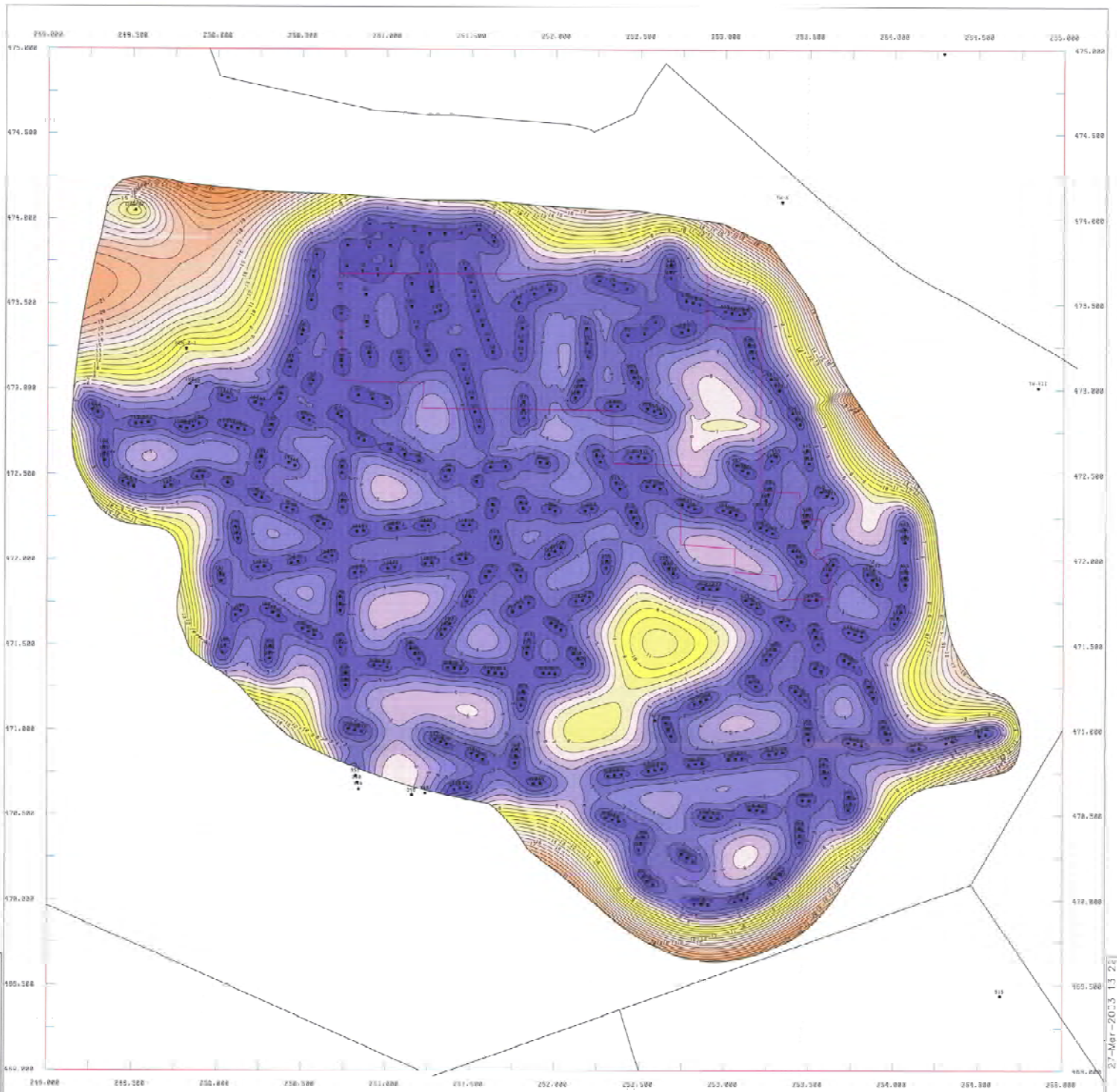
27-Mar-2003 15:35
bas1627153511.mxd

27-Mar-2003 15:35
bas1627153511.mxd



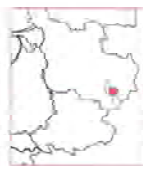
- dieptecontour
- concessiegrens
- breuk
- 3D survey
- polygoon

TNO-NITG, afd. Geo-Energie Akzo Nobel Salt by Hengelo	
bijlage 12 diepte basis A-zout (m t.o.v. NAP)	
Concessies Baurec. Twentse-Rijn en uitbreiding Twentse Rijn	
1:10,000	2003-12-22 11:41:51



13.22 27-Mar-2003 13:22

13.22 27-Mar-2003 13:22



- diktecontour
- concessiegrens
- breuk
- 3D survey
- polygoon

TNO-NITG, nfd. Geo-Energie
 akzo Nobel Salt by Hengelo

bijlage 13
 gemiddelde 90%fout (m)

Concessies Bourse, Twente-Rijn en
 uitbreiding Twente-Rijn

118.000 991.72921/91.91 18-08-97

Tab: History matching of surface subsidence due to solution mining

***History matching of surface
subsidence due to solution mining
operations in the Zuidwending and
Heiligerlee brinefields***

C.E. Oldenziel, Minerals Department,
Hengelo, The Netherlands
November 5, 1999
Document : 9911501.doc
Project No. :

Table of Contents

1.	Summary	3
2.	Introduction	4
3.	Surface subsidence based on levelling measurements	5
	3.1 Zuidwending	5
	3.2 Heiligerlee	6
4.	Convergence rate calculation	8
	4.1 Zuidwending	8
	4.2 Heiligerlee	9
	4.3 Convergence rates given by Wassmann	9
5.	Calculated surface subsidence	11
	5.1 Zuidwending	11
	5.2 Heiligerlee	12
6.	Conclusions and recommendations	13
7.	References	14
8.	Appendices	15
	8.1 NAM subsidence until 1998 (based on H-model)	15
	8.2 Volume development of Zuidwending caverns	16
	Volume development of Heiligerlee caverns	16
	8.4 Zuidwending subsidence	17
	8.4.1 Constructed subsidence bowl	17
	8.4.2 Calculated subsidence bowl	18
	8.4.3 Comparison constructed and calculated subsidence bowl	19
	8.5 Heiligerlee subsidence	20
	8.5.1 Constructed subsidence bowl (no water correction)	20
	8.5.2 Calculated subsidence bowl (due to salt production only)	21
	8.5.3 Comparison constructed and calculated subsidence bowl	22

1. Summary

In order to get a better understanding of surface subsidence caused by salt solution mining a history analysis was performed. The following subjects were covered:

- Construction of net surface subsidence
- Determination of convergence rate per cavern / field
- Calculation of theoretical surface subsidence

Construction of net surface subsidence was based on levelling measurements. A correction for both gas production and natural compaction was performed. Ultimately this led to a maximum surface subsidence of 29.9 mm in the Zuidwending field and 70 mm in the Heiligerlee field. However, as water production also took place in the Heiligerlee area a further correction was necessary. Due to a lack of data this water correction could not be identified and therefore fell outside the scope of this analysis.

In order to calculate the theoretical surface subsidence a convergence rate per cavern / field had to be determined. As no individual information for the brine wells was available a calculation was performed, based on representative caverns, to identify the convergence rate for each cavern field. Ultimately this led to a convergence rate of 0.08 %/a for the Zuidwending field and 0.03 %/a for the Heiligerlee field.

The theoretical surface subsidence was based on both the convergence rate per cavern field and sonar surveys of individual caverns to identify the cavern volume development over time.

For the Zuidwending field this resulted in a calculated surface subsidence of 84 mm over the period 1969-1998, a factor 2.8 higher as observed in the field. Questionable is whether the calculated convergence rate is too high, other studies will have to acknowledge that.

In the Heiligerlee brinefield a surface subsidence of 42 mm was observed. This subsidence is less than constructed from surface levelling measurements, which can be expected as water production also causes surface subsidence.

Although history matching was hampered by lack of sufficient and consistent data, concluding it can be stated that:

- No evidence has been found to affirm a different behaviour of the two salt domes.
- Convergence rates are found to be of the same order of magnitude (0.03–0.08 %/a).
- Observed surface subsidence does not support a levelling frequency every two years.
- A decision regarding diameter enlargement in the Heiligerlee field cannot solely be based on the results of this report.

Further investigation of the rock mechanical parameters of the Heiligerlee salt structure and comparing them to the known parameters of the Zuidwending salt structure is recommended.

2. Introduction

In order to get a better understanding of the surface subsidence caused by salt solution mining in the concession “Adolf van Nassau” and extension in the northern part of The Netherlands a history analysis was performed.

Goals of the project were:

- evaluation of cumulative subsidence over total production life of the Heiligerlee and Zuidwending brinefields
- determination of possible differences between the Heiligerlee and Zuidwending brinefields in terms of convergence rate and surface subsidence
- determination of an optimum period between two surface levelling measurements
- development of rock mechanical evidence supporting future development of both brinefields

To achieve these goals, the history analysis consisted of two independent subsidence evaluations for each brinefield:

- construction of net surface subsidence
- calculation of surface subsidence

The net surface subsidence by salt solution mining is based on levelling measurements and corrected for subsidence due to gas production, groundwater production and natural compaction.

In order to calculate surface subsidence the convergence rate for each individual cavern field had to be determined. This is done based on the method described in the IUB¹ expertise report for the Hvornum brinefield, Mariager, Denmark of 1998.

Chapter 3 will discuss the construction of the net surface subsidence for the Heiligerlee and Zuidwending brinefields, based on levelling measurements.

The following chapter discusses the calculation of the convergence rate for both brinefields.

In Chapter 5 the surface subsidence is theoretically calculated, using the previous calculated convergence rate.

Finally, conclusions and recommendations are drawn in chapter 6.

¹ Institut für Unterirdisches Bauen (IUB), Universität Hannover, Germany

3. Surface subsidence based on levelling measurements

Both the brinefields of Heiligerlee and Zuidwending are influenced by the gas production from the Slochteren gas field. Gas production, as well as salt production, causes surface subsidence. Therefore a correction has to be made in order to determine the net surface subsidence caused by salt production.

Natural compaction of the ground also results in a minor subsidence factor of about 0.33 mm/a [1]. During the period-evaluated, 1969-1998, total surface subsidence due to natural compaction is considered to be equal to 10 mm.

For the Heiligerlee brinefield another, more complex factor influences the total surface subsidence. Groundwater production, required for the leaching process has attributed to the total surface subsidence until 1996 at which point in time a switch to surface water was made.

In the following paragraphs surface subsidence in both brinefields is discussed separately.

3.1 Zuidwending

As already discussed, the total surface subsidence in the Zuidwending area consists of three parts:

- Gas production induced subsidence
- Salt production induced subsidence
- Natural compaction

First an evaluation of the total surface subsidence was made on the basis of 30 years of levelling data. This resulted in a total of 20 points that were measured during the whole period (table 1).

Afterwards a correction was made for subsidence due to gas production. An evaluation² of the NAM³, Assen, see Appendix 8.1, was used in order to determine the surface subsidence due to gas production in those 20 levelling points (table 1). Furthermore the natural compaction, 10 mm over the total period, was subtracted resulting in the net surface subsidence due to salt production (table 1).

Concluding, it can be stated that a maximum surface subsidence, due to salt production, of 29.9 mm in the deepest point of the trough can be observed. This equals to an average subsidence rate of 1 mm/a over the total production period. A graphical representation of the Zuidwending subsidence bowl, based on levelling measurements, can be found in Appendix 8.4.1.

² Based on NAM's surface subsidence H-model

³ Nederlandse Aardolie Maatschappij b.v.

Table 1: Levelling points measured 1969-1998 (ZW field)

Levelling point	Total measured subsidence (mm)	Modelled subsidence due to gas production (mm)	Subsidence due to natural causes (mm)	Net surface subsidence due to salt production (mm)
012F0021	- 61.1	- 32.3	- 10	- 18.8
012F0027	- 62.7	- 38.5	- 10	- 14.2
012F0033	- 72.5	- 48.1	- 10	- 14.4
012F0034	- 67.0	- 46.3	- 10	- 10.7
012F0037	- 62.1	- 45.3	- 10	- 6.8
012F3100	- 61.6	- 39.3	- 10	- 12.3
012F3210	- 70.5	- 37.4	- 10	- 23.1
012F3400	- 64.9	- 35.3	- 10	- 19.6
012F3500	- 70.2	- 36.7	- 10	- 23.5
012F3600	- 77.8	- 37.9	- 10	- 29.9
012F3700	- 69.2	- 37.4	- 10	- 21.8
012F5012	- 61.9	- 43.6	- 10	- 8.3
012F5013	- 74.9	- 42.5	- 10	- 22.4
012F5016	- 52.9	- 30.8	- 10	- 12.1
012F5017	- 35.2	- 27.8	- 10	+ 2.6
012F5101	- 61.4	- 47.4	- 10	- 4.0
012F5102	- 50.1	- 47.1	- 10	+ 7.0
013A0037	- 32.3	- 27.4	- 10	+ 5.1
013A0046	- 42.0	- 28.8	- 10	- 3.2
013A5011	- 34.0	- 32.9	- 10	+ 8.9

3.2 Heiligerlee

Total surface subsidence consists of four parts:

- Gas production induced subsidence
- Salt production induced subsidence
- Groundwater production induced subsidence
- Natural compaction

Especially the subsidence caused by groundwater production is difficult to evaluate, as it is totally dependent on the local hydrological situation.. A theoretical model describing the surface subsidence caused by water production is not at hand. Only the net surface subsidence due to salt and groundwater production could be calculated corresponding to the above-described method.

After ceasing groundwater production in 1996 no surface subsidence has been measured during the 1998 levelling survey. On the contrary, a small uplift of the surface was identified. The contribution of groundwater production to the total surface subsidence will be evaluated in a pending study of Oranjewoud⁴.

⁴ The results of the study "Determination of the leveling frequency by means of dynamic geodetic modeling" will be available Q1 2000.

Evaluation of all the levelling points resulted in a total of 16 points, see table 2, that are measured during the whole period evaluated (1969-1998). Total subsidence due to salt and groundwater production is found to be equal to 70.4 mm⁵ in the deepest point of the trough, see Appendix 8.5.1.

Table 2: Levelling points measured 1969-1998 (HL field)

Levelling point	Total measured subsidence (mm)	Modelled subsidence due to gas production (mm)	Subsidence due to natural causes (mm)	Subsidence due to salt <u>and</u> groundwater production (mm)
008C0001	- 117.7	- 74.8	-10.0	- 32.9
008C0137	- 100.0	- 74.8	-10.0	- 15.2
013A0097	- 96.8	- 70.0	-10.0	- 16.8
013A0113	- 149.1	- 61.3	-10.0	- 77.8
013A0114	- 100.0	- 62.3	-10.0	- 27.7
013A123	- 123.3	- 70.0	-10.0	- 43.3
013A0124	- 112.8	- 71.9	- 10.0	- 40.9
013A0125	- 139.7	- 65.5	- 10.0	- 64.2
013A0130	- 140.1	- 65.6	- 10.0	- 64.5
013A1300	- 132.3	- 65.2	- 10.0	- 57.1
013A1400	- 146.8	- 71.0	- 10.0	- 65.8
013A1500	- 146.2	- 66.4	- 10.0	- 69.8
013A1600	- 144.7	- 67.2	- 10.0	- 67.5
013A1700	- 148.9	- 68.5	- 10.0	- 70.4
013A1800	- 96.7	- 63.1	- 10.0	- 23.6
013A5105	- 73.3	- 59.1	- 10.0	- 4.2

⁵ Levelling point 013A0113 is considered not representative. Subsidence is too high compared to neighbouring points.

4. Convergence rate calculation

Surface subsidence is caused by convergence of the underground cavern volume, due to the ability of salt to creep. Due to creep, a cavern will converge resulting in a decrease of cavern volume. This decrease of cavern volume is assumed to be equal to the surface subsidence volume. So, in order to determine the theoretical surface subsidence caused by solution mining the convergence rate had to be determined.

For both brinefields the following study was executed:

Using production data: water injection, brine production, brine density and NaCl-content of the brine, a difference between actual salt production and theoretical possible salt production can be determined [2].

The difference between the actual and theoretical salt production is caused by the volume convergence of the cavern. Ultimately the convergence rate of each individual cavern or of a total cavern field can be calculated.

Sonar measurements are used for comparison. Comparing the difference between the calculated cavern volume and the measured cavern volume over the same time period, results in an accuracy control.

In the following paragraphs the convergence rate for both the brinefields will be presented.

4.1 Zuidwending

The use of the calculation method developed by IUB for the Hvornum brinefield resulted in the figures presented in table 3.

The convergence rates per cavern vary greatly, which is caused by insufficient data, as only the average brine quality of the total brinefield is reported. Although this doesn't represent the actual situation, it was presumed to be equal for all caverns in the same field. Water injection volumes were used to calculate the total theoretically extractable amount of salt.

After evaluation of the results, it was decided that only the caverns ZW-1, 3, 5, 7 and ZW-9 are representative for the total brinefield. For these caverns, mismatch in calculated volume increase and measured volume increase is up to 2.5 %. ZW-2 is not considered representative, as no control sonar measurement is available. ZW-4 and ZW-6 are not thought to be representative as mismatches are too large. Calculation of the field convergence rate, using the representative caverns only, resulted in an average convergence rate of 0.08 %/a.

The above calculated convergence rate (0.08 %/a) is used for the calculations of the theoretical surface subsidence in chapter 5.

Table 3: Cavern convergence in the Zuidwending brinefield

Well	Convergence rate (%/a)	Calculated volume difference (m ³)	Measured volume difference (m ³)	Mismatch in volume increase (%)
ZW-1	0.09	808,819	826,580	2.20
ZW-2	0.01	275,665	No measurement	
ZW-3	0.13	1,009,890	1,018,758	0.88
ZW-4	- 0.29	1,039,155	893,460	- 14.02 ⁶
ZW-5	0.16	813,953	822,108	1.00
ZW-6	0.12	1,003,509	910,748	- 9.24
ZW-7	0.06	831,054	852,230	2.55
ZW-9	0.11	271,359	272,235	0.32

4.2 Heiligerlee

The same study as for the Zuidwending brinefield was carried out for the Heiligerlee field. The individual cavern convergence rates can be found in table 4. Only three caverns, HL-D, E and I, are considered representative for the whole cavern field. Calculation of the field convergence rate, using the representative caverns only, resulted in an average convergence rate of 0.03 %/a.

4.3 Convergence rates given by Wassmann

For the Zuidwending brinefield a 5-month test period was used to determine a convergence rate of 0.04 %/a. As no data is currently available it is not possible to check the accuracy of the test. It is therefore considered that a calculated convergence rate of 0.08 %/a is likely to be correct.

For the Heiligerlee brinefield, Wassmann concluded from combined pressure and brine flux tests in two (?) wells⁷ that the convergence rate was 0.15-0.22 %/yr. This convergence rate was calculated by releasing the pressure of shut-in caverns and measuring the produced volume of brine (m³). However, this brine flux is also influenced by:

- Temperature increase in the cavern
- Atmospheric pressure

Due to temperature increase the brine will expand, thus resulting in a higher brine flux than would be encountered by convergence only. Total temperature increase of the brine inside the cavern was not determined exactly, only the temperature of the produced brine was measured, so no real effect can be calculated.

Pressure relief during periods of lower atmospheric pressure will result in a higher brine flux than during high atmospheric pressure. This phenomenon is also encountered during workovers when a drop in atmospheric pressure results in a brine flux at the surface. Although this effect is limited to some m³ per event it could make a difference in the calculated convergence rate as measured brine volumes are relatively small (700 - 1,000 m³ per event).

⁶ Negative value is caused by a higher convergence rate as calculated !

⁷ Only the data of the HL-I study are currently known

Convergence rates of 0.15 %/a resp. 0.22 %/a will lead to a theoretical maximum subsidence in the deepest point of the trough of 211 mm resp. 310 mm in 1998⁸. These values are not observed in the field and are not considered realistic. Although Wassmann [3] spoke of a convergence rate of 0.15-0.22 %/yr the currently calculated convergence rate is considered more accurate. Therefore an average convergence rate of 0.03 %/a will be used for the calculation of the theoretical surface subsidence in chapter 5.

Currently BGR is performing a theoretical pressure calculation⁹. This calculation is based on the data of the pressure test of HL-I. Goal of this calculation is to verify the results of Wassmann.

Tabel 4: Calculated cavern convergence in the Heiligerlee brinefield

Well ¹⁰	Convergence rate (%/yr)	Calculated volume difference (m ³)	Measured volume difference (m ³)	Mismatch in volume increase (%)
HL-A	0.04	581,603	472,389	-18.78 ¹¹
HL-B	-0.01	336,284	279,106	-17.00
HL-C	0.03	350,967	No measurement	
HL-D	0.05	335,820	333,899	-0.57
HL-E	0.06	478,601	489,666	2.31
HL-F	0.07	458,571	379,205	-17.31
HL-G	0.01	516,002	461,391	-10.58
HL-H	-0.04	485,210	514,330	6.00
HL-I	0.02	309,690	307,590	-0.68

⁸ The presented values are calculated, using the method of chapter 5.

⁹ The calculation is part of a general sensitivity study on optimal cavern field development. Delivery is expected Q1 2000.

¹⁰ Caverns HL-K and HL-L are not presented as no echolog measurement has been carried out

¹¹ Negative value is caused by a higher convergence rate as calculated !

5. Calculated surface subsidence

Calculation of the theoretical surface subsidence requires some specific data:

- Convergence rate
- Volume development of caverns
- Influence function

The convergence rate was determined in Chapter 3 and is considered to be 0.08 %/a for the Zuidwending and 0.03 %/a for the Heiligerlee field.

Development of the cavern volume was solely based on sonar measurements. The influence function (1) was taken from a paper published in Kali u. Steinsalz [4]. The function calculates the subsidence caused by convergence of a single cavern. Addition of the individual surface subsidences caused by each individual cavern led to the total subsidence of each cavern field.

$$(1) \quad dS = a * \frac{(\tan \beta)^2}{z^2} * \exp\left\{-\pi * (\tan \beta)^2 * \frac{d^2}{z^2}\right\} * dV$$

in which:

- dS = surface subsidence due to convergence
- a = factor (subsidence = convergence volume) = 1
- β = angle of draw = 45° [5]
- z = depth of cavern (total depth of drilled hole)
- d = distance to well (centre point, wellhead)
- dV = convergence volume

Especially the factor “a” will allow for a certain curve-fitting. It is however chosen to use the factor a = 1 in order to calculate a conservative subsidence. Actual subsidence will be lower due to a so-called “time effect”. It takes a certain time period before the total converged volume arrives at surface.

5.1 Zuidwending

In order to calculate the convergence volume per cavern, first the cavern volume development had to be determined. Sonar surveys were used to determine the development of the caverns over the period observed. In Appendix 8.2 the development of the Zuidwending caverns can be seen.

In 1989 a partial sonar measurement was run in well ZW-2, this resulted in a too low cavern volume. It was therefore decided to set the cavern volume of ZW-2 at 2,500,000 m³ for 1989, this is in line with past development.

Using a convergence rate of 0.08 %/a a maximum subsidence of 83.6 mm in the deepest part of the subsidence trough was calculated. The calculated surface subsidence is found to be a factor 2.8 higher as the values observed in the field.

This could be caused by:

- A too high convergence rate
 - Incorrect construction of the net subsidence
-

- Inadequate value for “a”

More detailed information will follow from the studies performed by Oranjewoud and BGR.

In Appendix 8.4.2 the calculated subsidence bowl is given. A comparison between the calculated and constructed subsidence bowl, based on levelling measurements, can be found in Appendix 8.4.3.

5.2 Heiligerlee

In order to calculate the convergence volume per cavern, first the cavern volume development had to be determined. Sonar surveys were used to determine the development of the caverns over the period observed. In Appendix 8.3 the results for the Heiligerlee caverns can be found.

Using a convergence rate of 0.03 %/a, a maximum subsidence of 42.2 mm in the deepest part of the subsidence trough was calculated, see Appendix 8.5.2. This subsidence is smaller as the observed subsidence due to water and salt production, as could be expected.

In Appendix 8.5.3 a comparison is made between the constructed surface subsidence (water correction incl.) and the calculated surface subsidence.

6. Conclusions and recommendations

In the Zuidwending brinefield observed surface subsidence is limited to 30 mm in the period 1969-1998. The convergence rate calculated for the Zuidwending field is 0.08 %/a, resulting in a calculated theoretical surface subsidence of 84 mm during the period 1969-1998. A difference of 280 % is found between the calculated and constructed surface subsidence figures.

In the Heiligerlee brinefield both water and salt production cause surface subsidence. The total surface subsidence caused by salt solution mining and groundwater production is found to be 70 mm over the whole period observed. A convergence rate of 0.03 %/a was found for the Heiligerlee field, resulting in a calculated surface subsidence of 43 mm in the period 1969-1998. This would mean that surface subsidence due to water production is around 27 mm in the same period. The present study undertaken by Oranjewoud will have to acknowledge that.

Concluding it can be stated that:

- No evidence has been found to affirm a different behaviour of the two salt domes.
- Convergence rates are found to be of the same order of magnitude (0.03–0.08 %/a).
- Observed surface subsidence does not support a levelling frequency every two years.

Further investigation of the rock mechanical parameters of the Heiligerlee salt structure and comparing them to the known parameters of the Zuidwending salt structure is recommended.

At this moment three studies are performed:

- BGR: Optimisation of the cavern field layout (ZW and HL)
- BGR: Laboratory tests on HL-L core material
- Oranjewoud: Modelling of surface subsidence

The results of the above mentioned studies are expected Q1 2000. The results of these studies will provide a basis for decisions regarding future exploitation of the brine fields.

7. References

- [1] ir. J.J.E. Pöttgens Bodemdaling zoutwinning concessie “Adolf van Nassau”. (Vertrouwelijk rapport)
Heerlen, 14 februari 1973, Staatstoezicht op de Mijnen

 - [2] Prof. Dr. R.B. Rokahr Expertise on Dimensioning and Convergence of the Brine filled Caverns of the Hvornum Brine Field at Mariager.
1998, Ronnenberg, Germany.

 - [3] Th. Hans Wassmann Mining subsidence above cavities created by solution mining of rocksalt.
Seventh Symposium on Salt, 1993, Tokyo

 - [4] Dr.-Ing. Anton Sroka,
Dipl.-Geophys. K. Schrober Die Berechnung der maximalen bodenbewegungen über kavernenartigen Hohlräumen unter Berücksichtigung der Hohlraumgeometrie.
Institut für Markscheidewesen der TU Clausthal, Aug. 1982.

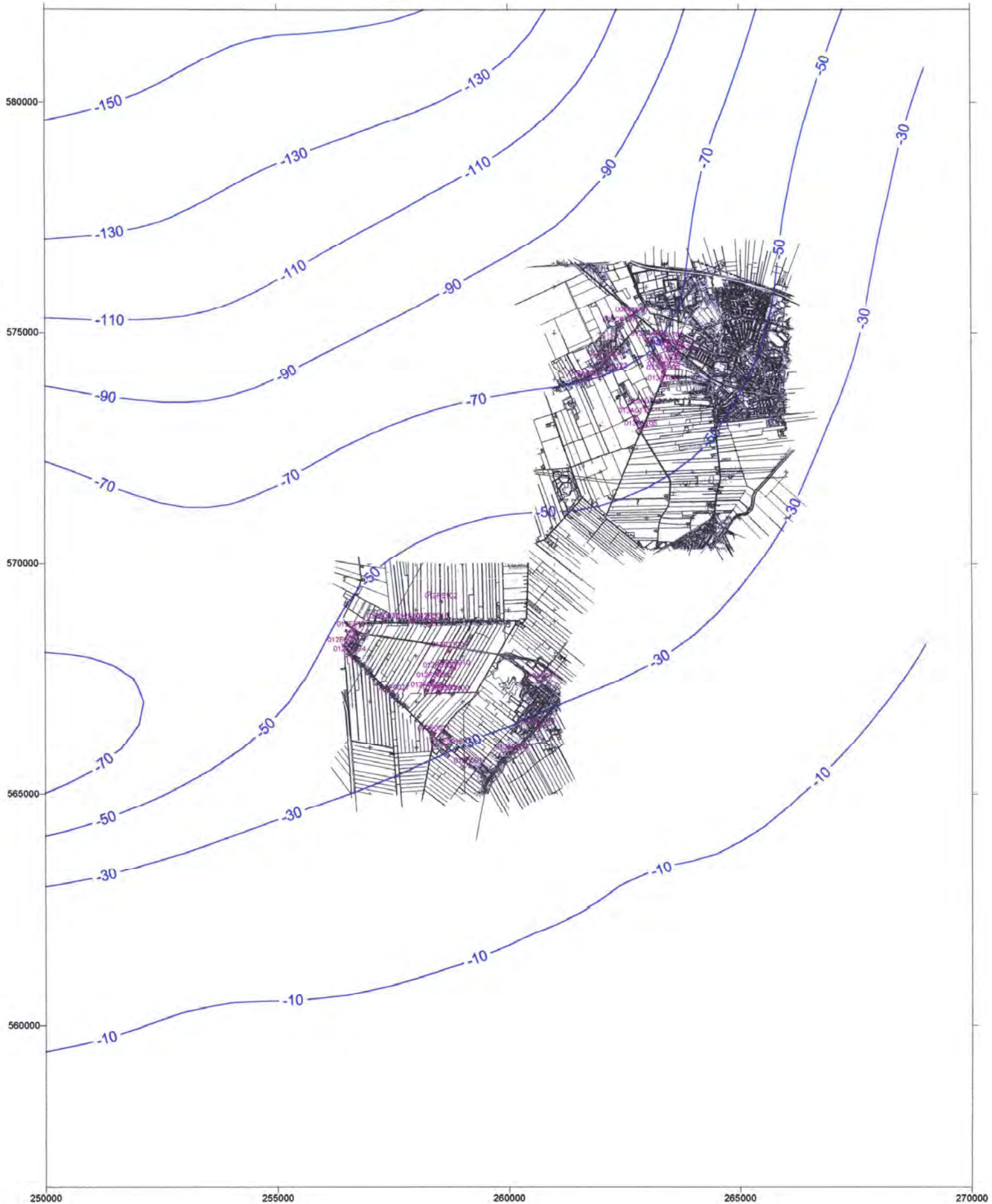
 - [5] A.J. Reitze, H. von Tryller Subsidence above cavities in salt domes – Theoretical principles and practical experience.
SMRI Fall meeting 1996, Cleveland, Ohio USA
-

8. Appendices

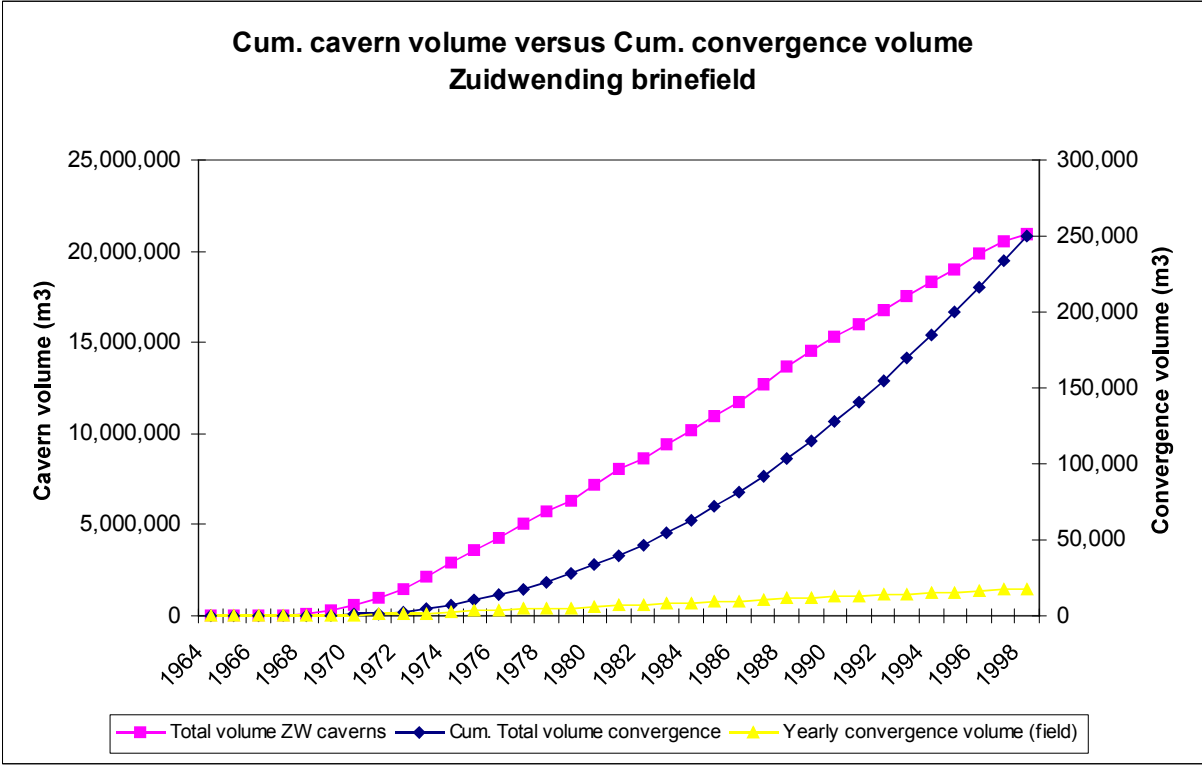
8.1 NAM subsidence until 1998 (based on H-model)

Surface subsidence Groningen 1998 (Akzo Nobel)

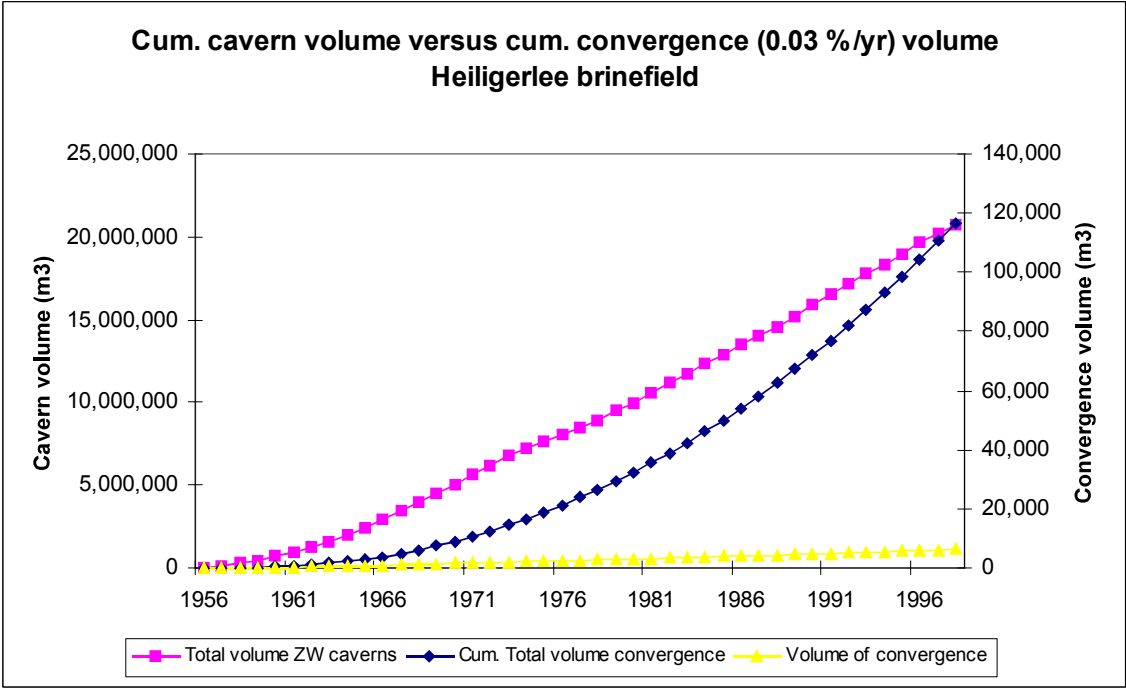
Blue: Hmodel98+residuals (using scandefo)



8.2 Volume development of Zuidwending caverns





8.3 Volume development of Heiligerlee caverns



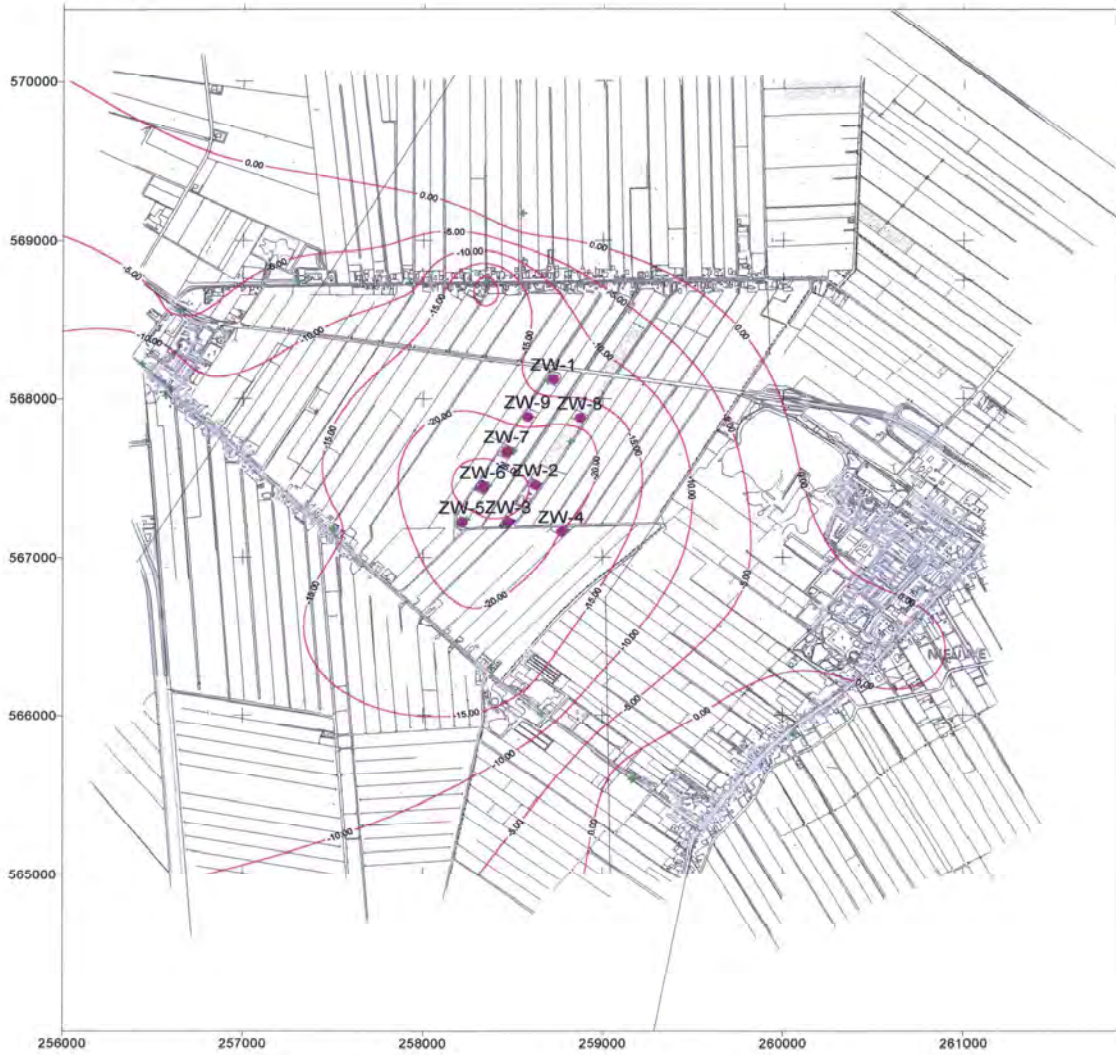
8.4 Zuidwending subsidence

8.4.1 Constructed subsidence bowl

Legend:  Levelling points


 Brine well

ZW-field: Surface subsidence based on corrected levelling measurements (1969-1998)
Filename: ZWfieldconstr.srf



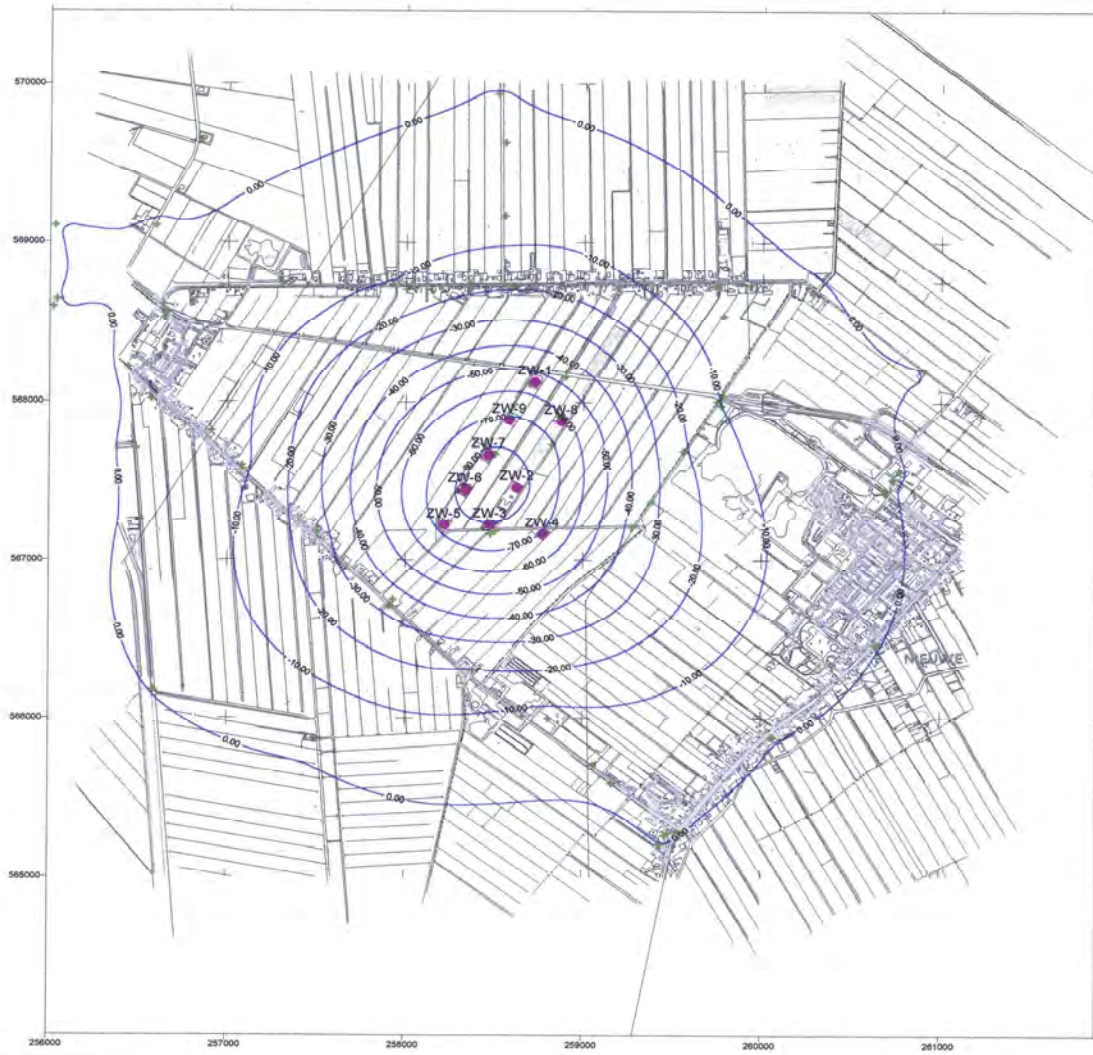
8.4.2 Calculated subsidence bowl

Legend:  Calculated points

 Brine well



ZWfield: Surface subsidence based on calculated values (1969-1998).
Filename: ZWfieldcalc.srf

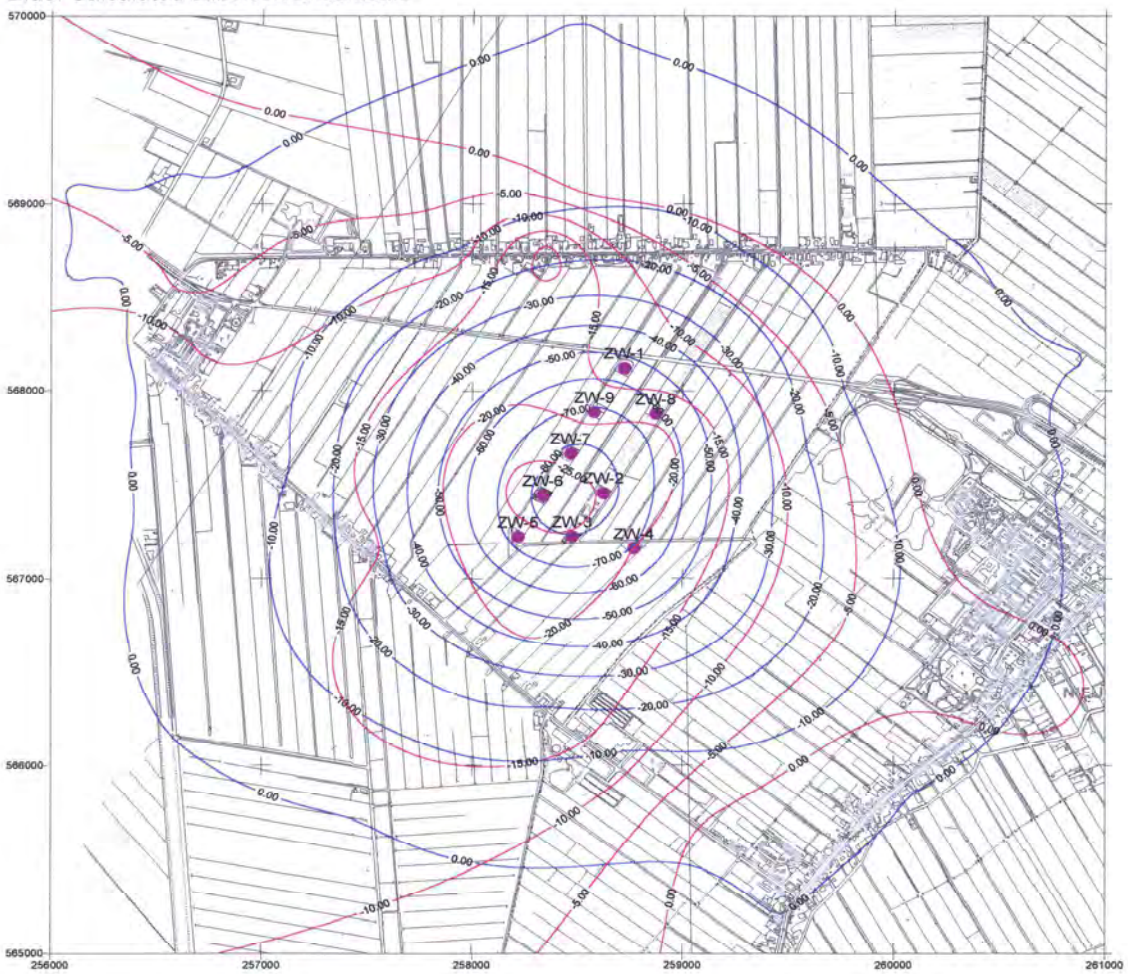


8.4.3 Comparison constructed and calculated subsidence bowl




ZWfield: Surface subsidence comparison (1969-1998).
Filename: ZWfield.srf

Red: Constructed from levelling measurements
Blue: Calculated subsidence contours




8.5 Heiligerlee subsidence

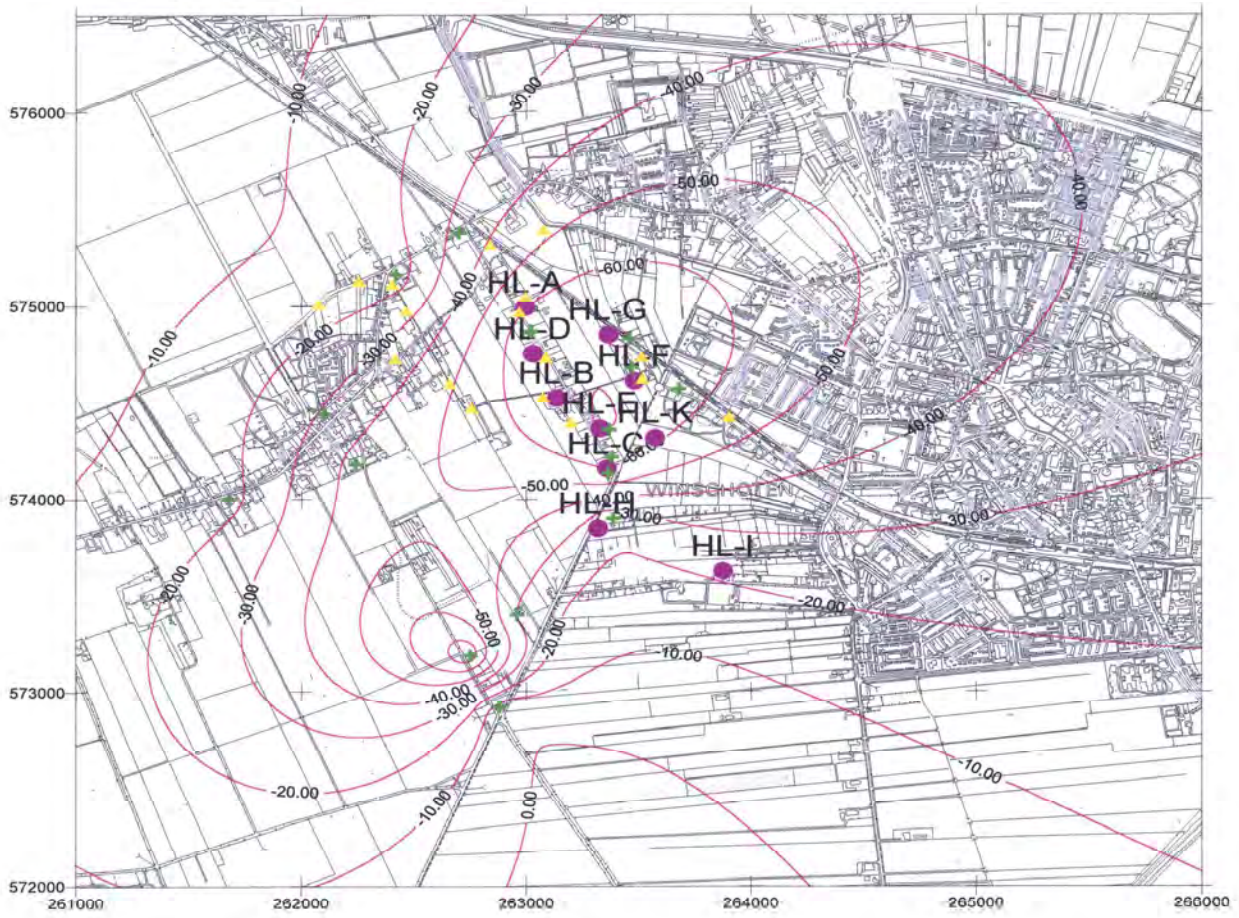
8.5.1 Constructed subsidence bowl (no water correction)

Legend:  Levelling points

 Brine well


 Water production well


HL-field: Surface subsidence based on corrected levelling measurements
(no water correction taken into account), period 1909-1998
Filename:HLfieldconstr1.srf



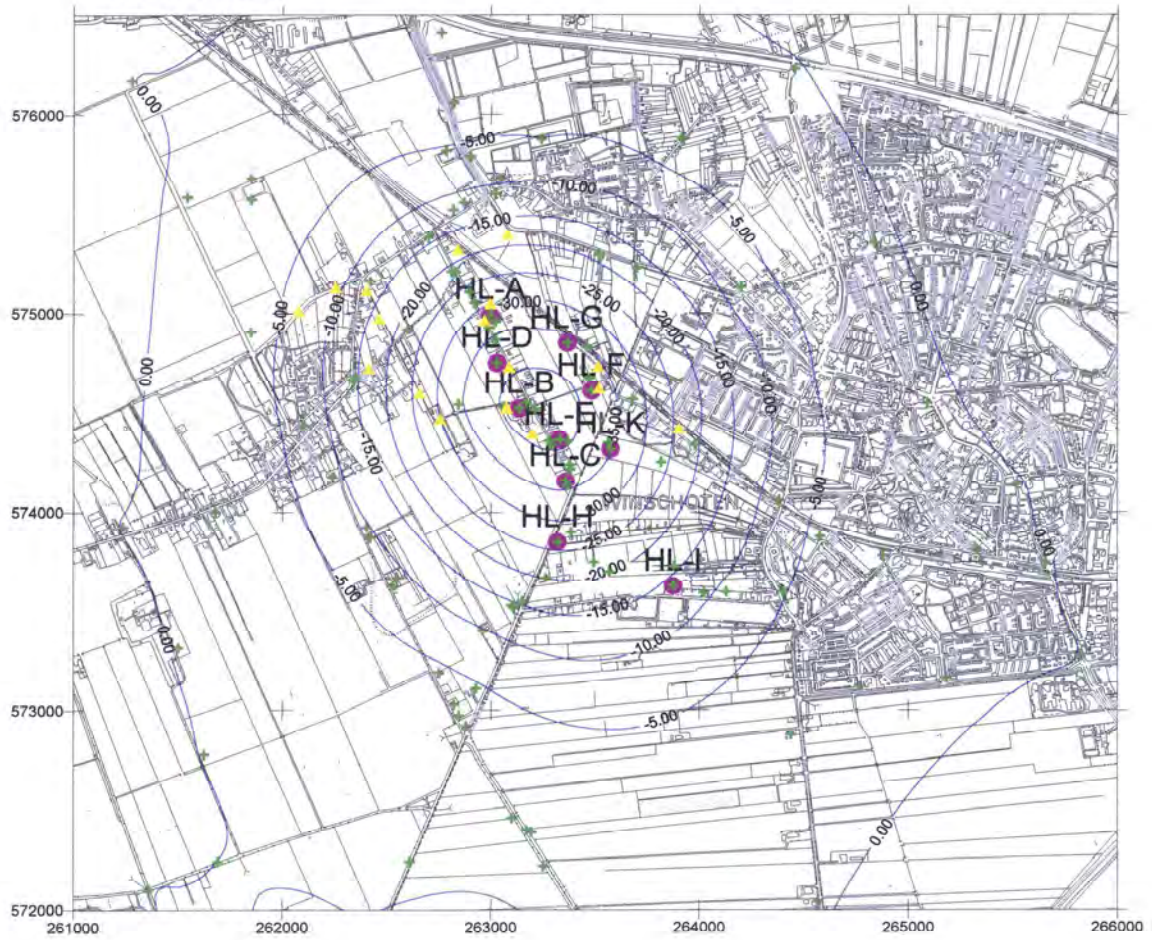
8.5.2 Calculated subsidence bowl (due to salt production only)

Legend:  Calculated points

 Brine well

 Water production well

HL-field: Calculated surface subsidence, period 1969-1998
Filename: HLfieldcalc.srf

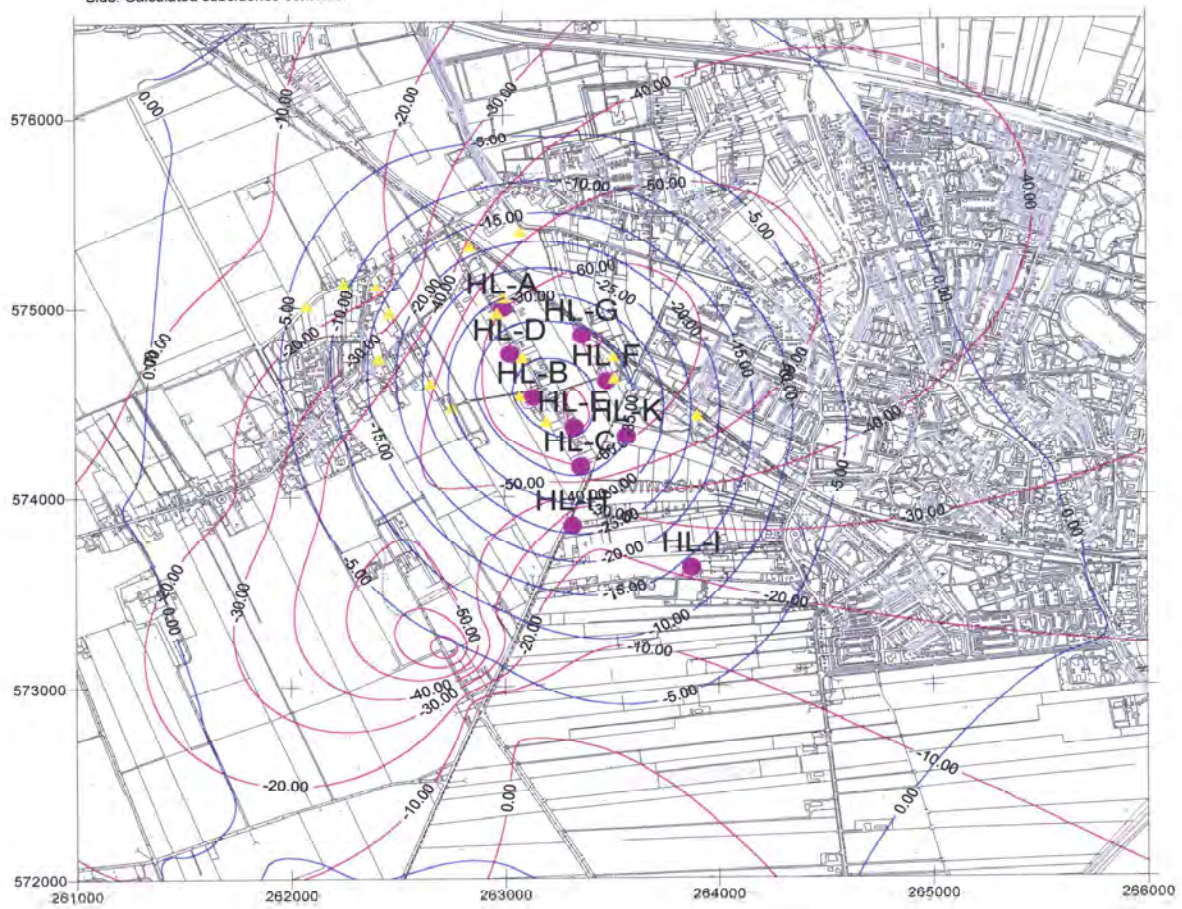


8.5.3 Comparison constructed and calculated subsidence bowl



HL-field: Surface subsidence comparison, period 1969-1998
Filename:HLfield.srf

Red: Constructed from levelling measurements
Blue: Calculated subsidence contours.



Tab: HL WP1 Report Subsidence Documentation

Prediction of Subsidence above Caverns at Heiligerlee, The Netherlands

Report on WP1: Review of Documentation

For

ANIC

Akzo Nobel Industrial Chemicals Delftzijl

Osterborn 4, Central Warehouse

9936 HD Delftzijl

THE NETHERLANDS

Client PO No.: 4570130812

Client Project No.:

KBB UT Project No.: 5240-881094

Author(s): Dr.-Ing. Dirk Zander-Schiebenhöfer, KBB UT

B. SC. Birgit Horváth, KBB UT

Dipl.-Geol. Raphael Schäfer, DEEP.

Checked: BB

Approved: DZ

Date: 31.03.2015

Revision: 00



Table of Contents

1 Introduction	3
2 Scope of Work – WP1	4
3 Compilation of Key Findings from Selected Documentation	5
3.1 Levelling campaigns	5
3.2 Subsidence prediction studies	6
3.3 Comment on Prediction 2007 vs. Levelling Data 2010	7
4 Conclusions	8



List of Tables

Table 3.1	Compilation of interpreted values for maximum subsidence and subsidence rates due to levelling campaign 1998, 2005 and 2010 with reference to 1969 (see ORANJEWOUD (2005) and HOENTJEN and DAM (2011)	6
Table 3.2	Predicted increase of subsidence and subsidence rate according BGR (2007) [4], [5] with reference to 1969.....	6

1 Introduction

Since 1956 Akzo Nobel Industrial Chemicals Delftzijl (AkzoNobel), The Netherlands, is leaching salt caverns at Heiligerlee, The Netherlands. Currently 11 caverns (HL-A to HL-J and HL-L to HL-M) are in operation for brine production and one cavern (HL-K) has been converted into a nitrogen storage cavern which is operated by Energystock, Groningen, The Netherlands, which is a Gasunie, Groningen, The Netherlands, company. Well HL-N is drilled and remains as a reserve.

Salt caverns, either for gas storage or brine production, show volume losses (convergence) over time due to creep of the surrounding salt rock mass. These volume losses are transferred via the overburden layers to the surface, where they form a subsidence bowl. Keeping cavern convergence and therefore subsidence as small as possible is of vital importance for the operator as well as for the public. It is therefore mandatory to measure subsidence after specified periods of time. Furthermore, the authorities in the Netherlands demand for subsidence prediction in advance of every levelling campaign.

At Heiligerlee, different sources – gas production, salt production, gas storage, ground compaction, and erosion – contribute to surface subsidence. Therefore, theoretical modelling is required in order to differentiate the individual contributions to surface subsidence. Thus, the involved operators can document their shares.

KBB Underground Technologies GmbH, Hannover, Germany, was appointed by AkzoNobel to develop a model that is capable of matching the so far history of subsidence and enables reliable predictions of the surface subsidence that will be caused due to brine production and nitrogen storage in the caverns at Heiligerlee in the future.

Prior to subsidence modelling the existing documentation on surface subsidence measurement, evaluation and modelling had to be compiled according to **Work Package 1 (WP1) – Review of Documentation**. This information provides basic knowledge about the field development and subsidence observations, which will be used for confidence building and validating of the newly set-up applied subsidence model.

The present report summarizes findings and conclusions of the work according to WP1.

2 Scope of Work – WP1

The new subsidence model has to show that the continuity of the existing studies and observations is considered. This refers to modelling assumptions in principle and to measurement results. Finally it aims at a reliable history matching of modelled versus observed values of surface subsidence.

Provided documentation, studies and measurement reports have been screened with focus on information about cavern field and subsidence development. Evaluations, which were carried out to determine the individual contribution of the salt caverns to surface subsidence, were searched for. The essential results, observations and findings, as presented in the documents, form the basis for building and setting-up of the new subsidence model. In this report these essential findings are summarized in short.

The present report focusses on the provided documentation about subsidence measurements, their interpretation and subsidence prediction. Besides this information a considerable documentation on cavern development was delivered by AkzoNobel and Gasunie. This set of data is essentially required for the set-up of the subsidence prediction model. These data were taken as facts without further interpretation. The integration of these data into the subsidence model is documented in the report on WP 2 where it is described how the subsidence model is built-up and validated.

3 Compilation of Key Findings from Selected Documentation

By screening the provided information a set of reports has been identified that contains key information about the development of surface subsidence above the Heiligerlee caverns. These reports are following:

- History Matching of subsidence
by OLDENZIEL, AKZONOBEL (1999) [1]
- Subsidence Prognosis study
by EICKEMEIER and HEUSERMANN, BGR (2007) [4] and [5]
- Evaluation of Levelling Data
by ORANJEWOUD (2006) [2]
- Evaluation of Levelling Data
by HOENTJEN and DAM, ORANJEWOUD (2011) [3]
- Comment on the results of the levelling campaign 2010
by PINKSE, AKZONOBEL (2014) [6]

The general findings and conclusions are discussed subsequently.

3.1 Levelling campaigns

Levelling campaigns were carried out almost every 5 years. Provided documentation describes, evaluates and partly comments/interprets the measurements of 1998, 2005 and 2010.

The report of OLDENZIEL (1999) makes use of the levelling data from 1998 for selected benchmarks. Individual contributions to subsidence by gas production were estimated by using global subsidence maps of 'Nederlandse Aardolie Maatschappij' (NAM), which show values of 59 to 75 mm of total subsidence above the Heiligerlee cavern area with reference to the beginning of 1969. By subtracting individual contributions due to gas production (between 59.1 and 74.8 mm) and due to natural causes (assumed with 10 mm across the whole area) and by an additional independently checking of the individual contributions of the brine production caverns (cavern HL-K was not filled with nitrogen at that point in time) a maximum subsidence of 77.8 mm is figured out. However, the influence of groundwater production that ceased in 1996 could not be determined. Therefore the amount of subsidence anticipated for the period from 1969 to 1998 contains shares from brine and groundwater production.

Further reports on levelling campaigns with interpretation of the measurement results were prepared by ORANJEWOUD for the campaign of 2005 [2] and of 2010 [3]. Therein the raw data were filtered in a sequence of

- stability analysis (correction through assessment of the reliability of the benchmarks),
- object point analysis (subtraction of contributions by ground compaction and gas production), and
- deformation analysis (checking of time dependent continuity of measurements for each benchmark).

Maximum values of subsidence as well as subsidence rates due to cavern convergence are compiled in Table 3.1.

Table 3.1 Compilation of interpreted values for maximum subsidence and subsidence rates due to levelling campaign 1998, 2005 and 2010 with reference to 1969 (see ORANJEWOUD (2005) and HOENTJEN and DAM (2011))

reference year	2000	2005	2011
maximum subsidence rate at the beginning of the reference year [mm/a]	3.52	3.47	3.38
maximum increase of subsidence between 1969 and the reference year [mm]	109	125	142

3.2 Subsidence prediction studies

EICKEMEIER and HEUSERMANN (2007) performed a subsidence prediction study based on the 2005 levelling campaign data. The applied subsidence model considers the brine production data and takes into account the individual convergence behaviour of the caverns by calculation of convergence rates from numerical cavern models. Calculated subsidence was compared to measured values at selected reliable benchmarks and matched by adjusting the creep behaviour of the salt. At the end of this history matching process a trustworthy basis was found in order to give predictions of the future subsidence development while assuming different scenarios with respect to production and cavern abandonment. Thereby, cavern HL-K was not taken into account as nitrogen storage cavern.

According to the investigated scenario for brine production with subsequent abandonment of the caverns (scenario HL01) the resulting increase in subsidence as well as related subsidence rates were calculated for different points in time as listed in Table 3.2.

Table 3.2 Predicted increase of subsidence and subsidence rate according BGR (2007) [4], [5] with reference to 1969

reference year	1990	2000	2018	2050
maximum subsidence rate at the beginning of the reference year [mm/a]	2.97	2.65	3.91	3.61
maximum increase of subsidence between 1969 and the reference year [mm]	27.3	50.3	100.8	210.9

3.3 Comment on Prediction 2007 vs. Levelling Data 2010

PINKSE (2014) compared the subsidence prediction of EICKEMEIER and HEUSERMANN (2007) for the year 2018 with the interpreted results of the levelling campaign of 2010 (HOENTJEN and DAM (2011)). A comparison of predicted versus observed values by using rough calculations indicates that observed subsidence is greater by 49 mm than the predicted for 2018 by EICKEMEIER and HEUSERMANN (2007).

4 Conclusions

The existing documents provide a reliable data base for setting up the subsidence model that will be applied for an update of predictions. When comparing observed subsidence values with formerly predicted, the following can be highlighted:

- A quick comparison of the latest predictions and measurements show that observed subsidence develops faster than predicted. This may be due to the fact that the actually extracted volume of salt differs from the assumptions made for the prediction.
- Subsidence due to gas production from the Slochteren field can only be estimated from large scale maps.

References

- [1] OLDENZIEL, C.:
'History matching of surface subsidence due to solution mining operations in the Zuidwending and Heiligerlee brinefields',
AkzoNobel, Minerals Department, 1999.
- [2] ORANJEWOUD:
'Rapport Frequentiemodellering deformatiemetingen 2005 Winningvergunningen Adolf van Nassau en Adolf van Nassau Uitbreiding',
projectnr. 15575-61467-16, revisie 00, oranjewoud, 28 juni 2006.
- [3] HOENTJEN, K. H., DAM, J.:
'Rapport Geodetische analyse deformatiemeting 2010; Bepaling van de zoutwinning veroorzaakte bedemdaling, Winningvergunningen Uitbreiding Adolf van Nassau II en III Opslagvergunning Zuidwending, Winningvergunningen Adolf van Nassau II en III Opslagvergunning Winschoten II en III',
projectnr. 242314, revisie 02, oranjewoud, 31 oktober 2011.
- [4] EICKEMEIER, R., HEUSERMANN, S.:
'Kavernenfelder Winschoten / Heiligerlee und Zuidwending Senkungsprognosen für die Kavernenfelder Winschoten / Heiligerlee und Zuidwending (Datenbasis 2005)
Abschlussbericht – Textband, Bundesanstalt für Geowissenschaften und Rohstoffe (BGR), Hannover, Juni 2007
- [5] EICKEMEIER, R., HEUSERMANN, S.:
'Kavernenfelder Winschoten / Heiligerlee und Zuidwending Senkungsprognosen für die Kavernenfelder Winschoten / Heiligerlee und Zuidwending (Datenbasis 2005)
Abschlussbericht – Anlagenband, Bundesanstalt für Geowissenschaften und Rohstoffe (BGR), Hannover, Juni 2007.
- [6] PINKSE, T.:
'Bodemdaling door zoutwinning in de boorterreinen Heiligerlee en Zuidwending'
Memorandum, AkzoNobel, 12 september, 2014.

Tab: HL WP2 Report Subsidence Modelling

Prediction of Subsidence above Caverns at Heiligerlee, The Netherlands Operation Phase Report on WP2: Applied Subsidence Model

for

ANIC

Akzo Nobel Industrial Chemicals Delftzijl

Osterborn 4, Central Warehouse

9936 HD Delfzijl

THE NETHERLANDS

Client Inquiry No.: 4570130812

Client Project No.:

KBB UT Project No.: 5240-881094

Author(s): Dr.-Ing. Dirk Zander-Schiebenhöfer, KBB UT

B. SC. Birgit Horváth, KBB UT

Dipl-Geol. Raphael Schäfer, DEEP.

Checked: Sf

Approved: DZ

Date: 31.08.2015

Revision: 01

Table of Contents

1	Introduction	3
2	Scope of Work – WP2.....	4
3	Basics of the Applied Subsidence Model	6
3.1	Principle Understanding of the Process.....	6
3.2	Assumptions for the Heiligerlee Subsidence Model.....	7
3.2.1	Shape of the Subsidence Bowl	7
3.2.2	Angle of Draw	7
3.2.3	Representative Depth.....	7
3.2.4	Bulking Factor	8
3.2.5	Creep Response	8
4	Implementation of the Subsidence Model.....	10
4.1	General Procedure.....	10
4.2	Cavern Field Setup	10
4.3	Consideration of Caverns	10
4.4	Assembly for Calculation of the Total Subsidence due to Cavern Operation.....	12
4.5	Consideration of Non-Cavern related Subsidence.....	12
5	Confidence Building and Validation	14
5.1	Subsurface.....	14
5.1.1	Confidence building at subsurface	14
5.1.2	Validation process at subsurface	15
5.2	Surface.....	16
5.2.1	Confidence building at surface	16
5.2.2	Validation process at surface	17
6	Proposed Procedure for Subsidence Prediction.....	20
6.1	Proposed Steps	20
6.2	Capabilities	20
6.3	Maps and Graphs	20
7	Summary and Conclusion	21
	References	22
	List of Enclosures.....	24
	Enclosures	26

List of Tables

Table 4.1	Compilation of values for subsidence above the Heiligerlee cavern area related to non-cavern sources with respect to levelling campaigns	12
Table 5.1	Compilation of values for maximum subsidence above the Heiligerlee cavern area due to interpretation of the levelling data	17
Table 5.2	Maximum subsidence or subsidence rates as predicted by EICKEMEIER ET AL. (2007).....	18

1 Introduction

Since 1956 Akzo Nobel Industrial Chemicals Delfzijl (AkzoNobel), The Netherlands, is leaching salt caverns at Heiligerlee. Currently 11 caverns (HL-A to HL-I and HL-L to HL-M) are in operation for brine production and one cavern (HL-K) has been converted into a nitrogen storage cavern which is operated by Energystock, Groningen, The Netherlands, which is a company of Gasunie, Groningen, The Netherlands. Well HL-N has been drilled and stays in reserve for future brine production.

Salt caverns, either for gas storage or brine production, show volume losses (convergence) over time due to creep of the surrounding salt rock mass. These volume losses are transferred through the overburden layers to the surface, where a subsidence bowl is created. Keeping cavern convergence and thereby subsidence as small as possible is of vital importance for the operator as well as for the public. Thus it is mandatory to periodically measure subsidence. Furthermore, the authorities in the Netherlands demand for the prediction of subsidence prior to each levelling campaign.

At Heiligerlee, different sources – gas production, brine production, gas storage, ground compaction, and erosion – contribute to surface subsidence. Therefore, theoretical subsidence models can help to differentiate the individual contributions to surface subsidence and relate them to the involved operators.

KBB Underground Technologies GmbH, Hannover, Germany, was appointed by AkzoNobel to develop a model that is capable of matching the so far history of subsidence and enables reliable predictions of the surface subsidence that will be caused due to brine production and nitrogen storage in the caverns at Heiligerlee in the future.

After screening and summarizing the relevant documentation on subsidence due to brine production and gas storage at Heiligerlee (see report '**Work Package 1 (WP1) – Screening of Documentation**') the simulation model can be established based on this information. The present report on '**Work Package 2 (WP2) Establishing the Simulation Model**' describes the principal steps of this set-up procedure. In the subsequent **Work Package 3 (WP3)** this model will be applied for the prediction of subsidence.

The fine-tuning of the simulation model will be carried out within the scope of WP3, which aims at subsidence prediction related to salt caverns operation. This prediction has to be presented to the authorities prior to the next levelling campaign at Heiligerlee, which is scheduled for the end of 2015.

2 Scope of Work – WP2

The applied subsidence model has to represent continuity with the existing studies and observations. This refers to the modelling assumptions and to measurements and observations as well.

By history matching of the model with the observed surface subsidence in principle, confidence in the applied model can be build up. By comparing produced subsidence values with observations the model can be validated. If confidence building and validation processes have been successfully passed, the subsidence model can be used for predictions.

Essential results, observations and findings as contained in the existing documents have been summarized in the report on WP1. This information forms the basis for the setup of the subsidence model. The present report describes how the subsidence model is organized and built-up, and also documents the confidence building and validation process.

A main approach of the subsidence model for Heiligerlee is to provide a possibility to distinguish between individual contributions to the total subsidence, i.e. salt caverns, gas production, and ground compaction. Especially the individual shares of the caverns on the overall total subsidence have to be made accessible, because different operators are active in the cavern field. Therefore, the production history from brine production caverns as well as the operating history of the nitrogen storage cavern has to be taken into account. Consequently, individual cavern modules have been set up within the subsidence model. These cavern modules represent the specific volume growth and convergence behaviour of each cavern.

These individual cavern modules have to be synchronized with respect to time. Thereby their contributions to surface subsidence can be superimposed, in order to obtain values for the total subsidence above the cavern field, which is generated by the caverns (brine production and nitrogen storage). As the observed total subsidence at Heiligerlee contains portions caused by gas production from the Slochteren field and by ground compaction, these contributions have to be considered in the history matching process as well.

Confidence building and validation of the subsidence model have been carried out in two steps: (1) at subsurface and (2) on surface:

- At subsurface, calculated cavern volumes over time have been compared with sonar measurements for each cavern in order to check the applied creep model. The creep model represents the in-situ behaviour of the salt rock mass surrounding the individual cavern and directly influences the convergence volume.

- At surface level the overall confidence building and validation process has been carried out by history matching of the observed subsidence:
 - A qualitative proof (confidence building) can be given by showing that the growth of the subsidence bowl with time represents the assumed deformation mechanism.
 - A quantitative proof can be achieved by matching the observed subsidence history at selected (reliable) benchmarks above the cavern field represents. History matching has been focused on the interpreted results from levelling campaigns in 1998, 2005 and 2011.

Having passed the confidence building and validation process successfully, the subsidence model can be considered as ready for use for subsidence predictions. These predictions will be performed within the scope of WP3 and summarized in a separate report.

3 Basics of the Applied Subsidence Model

3.1 Principle Understanding of the Process

The general understanding of surface subsidence modelling is that volume losses caused by mining activities at subsurface lead to surface subsidence.

As part of surface subsidence predictions an assumption has to be made on the deformation mechanism, i.e. how the volume losses are transferred via the involved geological formations from subsurface to surface. Finally this leads to a description of the shape and the extension of the subsidence bowl at surface that will be created and gives information on how far it will be laterally extended. Due to the time dependent behaviour of the rock salt mass, which contains the caverns, the bowl will also grow over time. This means that the development of the subsidence bowl over time has to be considered as a consequence of salt creep behaviour. The creep behaviour is responsible for the volume losses of the caverns over time, because cavern pressures during normal operation will always be below lithostatic stress.

A generally well accepted model for subsidence that is caused by caverns in rock salt has been developed by SROKA and SCHOBBER (1982) and generalized by EICKE-MEIER (2005). The main ideas of this model, which are applied in this study, are briefly presented in the following.

The principal assumptions of the SROKA/SCHOBBER subsidence model can be summarized as follows:

- A normalized Gaussian type shape function represents the subsidence bowl (or trough) which is influenced by some specific parameters. Among these parameters the angle of draw β , the bulking factor a of the overlying rocks and the convergence itself are of major importance for the subsidence transformation process. The subsidence process starts with rock mass deformation due to cavern convergence and finally appears on surface as subsidence. Thereby the convergence rate $V_C(t)/dt$ is the driving mechanism.
- The angle of draw β together with representative cavern depth z determines the rock mass volume from subsurface to surface that is involved in the subsidence process due to the volume losses $V_C(t)$. The angle of draw is measured against the horizontal and referenced to a representative cavern depth z .
- The bulking factor a describes the ratio of convergence volume produced at subsurface compared to the subsidence volume showing at surface.
- The convergence rate $V_C(t)/dt$ describes the loss of cavern volume over time due to rock mass deformation.

3.2 Assumptions for the Heiligerlee Subsidence Model

3.2.1 Shape of the Subsidence Bowl

The shape of the subsidence bowl is assumed by the Gaussian functions as described by SCHOBBER ET AL. (1987). The mathematical description according to EICKEMEIER (2005) follows Equation 3.1.

$$f(r) = \frac{1}{R^2} \cdot e^{\left(-\pi\left(\frac{r}{R}\right)^2\right)}$$

Equation 3.1

with: $f(r)$ shape function related to the distance from the cavern axis
 R maximum radial extent of the subsidence bowl
 r point of interest at radial and lateral distance from cavern axis

3.2.2 Angle of Draw

The angle of draw differs from location to location. With regard to long-term subsidence observations above salt caverns, this value can be assumed in a range of about 25° and 45°. Over long periods it is likely that the angle of draw will become smaller due to the overall creep behaviour of the salt deposit and the extension of the salt structure (see GAULKE et al. (2007) and ZANDER-SCHIEBENHÖFER (2007)). Within the scope of the confidence building and history matching process the angle of draw is considered as a matching parameter. However, it has to stay within limits of known values from other cavern sites. In principle an assumed lower value of the angle of draw leads to the prediction of smaller subsidence values while the involved surface area of the subsidence bowl will be larger.

3.2.3 Representative Depth

Together with the angle of draw the representative depth determines the extension of the subsidence bowl on surface. Different alternatives have been proposed in the past. SCHOBBER ET AL. (1987) recommended the reference point to be calculated according to Equation 3.2

$$R = \frac{\sqrt{z_{sump} \cdot z_{roof}}}{\tan \beta}$$

Equation 3.2

with: z_{sump} depth of the cavern sump
 z_{roof} depth of the cavern roof

With respect to caverns of varying partial volumes versus depth, different depth ranges can be specified, as it is done for the calculation of the convergence in the studies of EICKEMEIER et al. (2007).

Within the scope of the present study a different approach is used: The reference depth for subsidence modelling as well as for convergence modelling is assumed by the depth of the midpoint of the geometrical volume, which is determined from the sonar measurements. Thereby the representative depth can change over time. This represents the leaching process that starts from the bottom and volume increase is then developed upwards. Additionally a correction factor can be applied in order to adapt creep response to specific cavern shapes.

3.2.4 Bulking Factor

The bulking factor α is assumed to be 1. This means that the convergence volume and the surface subsidence volume are of the same value. This assumption can be considered as conservative with regard to the prediction of subsidence at surface.

3.2.5 Creep Response

The ability of the rock salt mass to creep continuously leads to volume losses of the caverns (convergence). The driving force of the creep process is the difference between the pressure in the cavern and the far field stress state in the surrounding rock mass. As the creep process is an on-going mechanism (as long as the driving forces are not equal to the supporting forces, i.e. cavern pressures are lower than the lithostatic stress), subsidence increases over time. Furthermore, salt creep is highly non-linear with respect to the level of stressing and temperature.

The creep model, which is applied in the subsidence model, considers the following:

- the non-linear increase of the creep response with depth of the cavern caused by an increasing difference between the internal cavern pressure and the lithostatic stress,
- the non-linear increase of the creep response with depth of the cavern due to the increase of the rock mass temperature.

Creep response within the scope of this study is calculated using an analytical formula as given by VAN SAMBEEK (1993). This formula (see Equation 3.3) represents the long-term creep response of a cylindrical cavern based on the material law of NORTON-HOFF. This material law is also used in the subsidence model of EICKEMEIER et al. (2007).

$$\frac{\dot{V}}{V} = -\sqrt{3} \cdot \left[\frac{\sqrt{3}}{n} \cdot (P_{\infty} - P_i) \right]^n \cdot A \cdot e^{\left(-\frac{Q}{RT} \right)}$$

Equation 3.3

with:	\dot{V}	volume change rate
	V	volume of the brine-filled borehole section
	P_{∞}	far field formation pressure (lithostatic stress)
	P_i	internal well pressure
	n	stress exponent
	A	structural parameter
	Q	activation energy
	R	gas constant
	T	rock mass temperature

With regard to tall cylindrical caverns the stress profile as well as the temperature profile with depth has to be taken into account. As already stated above (see 3.2.3) the volumetric midpoint of the cavern has been selected as reference depth of the caverns, but a correction factor has been introduced in order to take into account that creep behaviour is non-linear with depth.

Furthermore, the creep response of an individual cavern depends on the status and the history of the cavern field development. For a single cavern in a salt deposit the creep response is smaller than for the same cavern located in the middle of a field of several neighbouring caverns, because the available pillar surrounding a single cavern is only limited by geological boundaries. This effect is considered by an empirical factor according to Equation 3.4.

$$\text{correction factor of } \dot{C} = 2.6 \cdot \left(\frac{\text{pillar}}{\text{diameter}} \right)^{(-1/0.6)} + 1.28$$

Equation 3.4

with:	\dot{C}	convergence rate
	<i>pillar</i>	average salt pillar to cavern neighbours
	<i>diameter</i>	maximum cavern diameter

Finally, as creep is influenced by the cavern pressure, the individual pressure history has to be considered in the subsidence model. As this is the case especially for the nitrogen storage cavern, the creep response is calculated on a daily basis within the history matching process for this cavern.

4 Implementation of the Subsidence Model

4.1 General Procedure

The implementation of the applied subsidence model has been organized by interconnected modules of Microsoft Excel Spreadsheets, which obey a hierarchy of different levels. In the base level the general setup of the cavern field is organized. The second level represents the individual cavern modules. Calculation and superimposing of the subsidence contributions by all caverns is carried out on the third level. Comparison of the simulation results with measurements is possible on the fourth level. At this level also contributions to surface subsidence that are not caused by caverns are considered.

Via interfaces special graphical representations such as subsidence maps can be generated. For this purpose the QGIS software under the GNU public license (see www.qgis.org/de/site) is used.

4.2 Cavern Field Setup

The geographically setup of the cavern field is compiled from the following data:

- coordinates of the cavern wellheads,
- coordinated of the last cemented casing shoe,
- depth of cavern roof and sump,
- sonar measurements.

4.3 Consideration of Caverns

The cavern modules have to fulfil the objective of combining cavern operation history and convergence development. In this regard they represent the operation history of the caverns, apply the creep model. Finally the cumulated convergence volume over time is calculated in these modules.

The cavern volume development during brine production has been calculated from the production data, which have been provided by AkzoNobel in terms of produced tons of salt on surface over time. By applying a mass balance concept (see OLDENZIEL ET AL. (2000)) and further assuming an average content of insolubles of 3% and an initially estimated convergence rate of 0.08% per year, the created cavern volume at subsurface could be calculated from these data. Resulting values of dissolved tons of salt at subsurface and of back-calculated cavern volumes are presented in Enclosure 1 and Enclosure 2 respectively.

Comparing the cavern volume development, which has been derived from the production data, with the sonar survey results provides the first possibility to check the volume development versus time. However, sonar surveys often represent only a partial volume, which then has to be corrected for reasons of comparison. On the

other hand, if data from production are missing, this can possibly be corrected by the sonar measurements.

Creep response is initially calculated with the same creep ability for the rock mass surrounding all caverns. From cavern to cavern there may be differences in the local creep behaviour of the surrounding the rock salt mass. However, in the initial setup phase of the subsidence model the creep response is assumed to be equal all over the Heiligerlee salt dome. For future fine tuning this possible variation in local creep behaviour may be taken into account.

Besides, the general creep behaviour of the salt, the specific creep response with respect to the specific cavern, as well as the specific point in time within the operating history depends on the stress difference between the lithostatic stress and the cavern pressure state, as well as the temperature of the rock (see Equation 3.3). Thus, creep response has been calculated under consideration of

- the lithostatic pressure based on the density profile,
- the temperature based on a temperature profile
- the internal cavern pressure by taking into account the brine column plus wellhead pressure of 20 bars (assumed value) for caverns in leaching mode, or
- the statically determined gas pressure plus wellhead pressure for caverns in gas storage mode. Whenever possible it has been made use of daily average values for the wellhead pressure.

As creep response is depth dependent, the depth at volume mid-point has been taken into account as representative depth for the calculation of creep response. Especially, for the brine production caverns this provides the possibility to take into account the leaching of preferred depth ranges. Finally, creep response has been combined with the volume development in order to determine the convergence volume with respect to time.

The assumed general creep response for the Heiligerlee salt is demonstrated in Enclosure 3 where the steady state creep rate is shown versus the equivalent stress. The equivalent stress represents the stressing of the rock mass that causes creep deformation. In comparison to the well-known creep characteristic of BGRa the so far assumed creep ability for Heiligerlee rock salt is lower. Site specific creep tests of rock salt from Heiligerlee were not available.

Convergence volume with time has been calculated based on the *theoretically existing cavern volume*, which has been produced by the application of the creep model. The theoretically existing cavern volume is derived from the production data by ignoring that insolubles have settled in the sump. Superposition of the three volume shares of convergence volume, theoretically created cavern volume and the sump volume results in the *theoretically calculated observable cavern volume*. This volume can be compared with the volume measured by sonar survey.

Calculated and corrected individual curves for cavern volumes versus time are represented by Enclosure 4 to Enclosure 15 for each cavern respectively. Therein sonar surveys are displayed by symbols representing the measured value (red

squares) as well as the corrected (green squares). The convergence volume, which results from creep calculations, is also displayed versus time but with regard to the right hand side ordinate.

4.4 Assembly for Calculation of the Total Subsidence due to Cavern Operation

In order to obtain the resulting subsidence from calculated convergence volumes the subsidence model as described in Chapter 3.2 has been applied.

In the first step the subsidence bowl parameters for each cavern have been compiled. Thereby their individual lifetime has been taken into account. It has been assumed that the angle of draw changes individually with time from steeper to more flat angles for each cavern according to their individual time of operation.

In the second step all individual subsidence bowls have been superimposed while considering the specific geographical location of each cavern. The resulting overall subsidence bowl for a selected calendar date has been obtained by superposition of the individual subsidence contributions of every cavern at that point in time.

4.5 Consideration of Non-Cavern related Subsidence

As mentioned before the observed subsidence above the Heiligerlee cavern area contains also portions from gas production, and ground compaction (non-cavern sources).

These values have been estimated according to the information as given in the subsidence interpretation reports following the levelling campaigns. Typical values are compiled in Table 4.1.

Table 4.1 Compilation of values for subsidence above the Heiligerlee cavern area related to non-cavern sources with respect to levelling campaigns

	1998	2005	2010/2011
gas production [mm]	59 to 75	51 to 102 ^{*1)}	68 to 113 ^{*1)}
ground compaction [mm]	10	34 to 175 ^{*2)}	58 to 206 ^{*2)}

*1) according to object point analysis of ORANJEWOUD (2006) or HOENTJEN (2011)

*2) according to deformation analysis of ORANJEWOUD (2006) or HOENTJEN (2011)

Values for subsidence due to gas production have been deduced from isokatabases maps, which were provided by the Nederlandse Aardolie Maatschappij (NAM). According to these maps subsidence due to gas production is not uniform. Values are increasing from south-east to north-west above the Heiligerlee cavern area. Values compiled in Table 4.1 have been taken from the reports of OLDENZIEL (1999), ORANJEWOUD (2006), and HOENTJEN (2011). A possible later refinement of the assumptions/interpretation may be discussed.

Ground compaction has so far been assumed by OLDENZIEL (1999) by a constant value of 10 mm and has been implicitly considered in the evaluation procedure of ORANJEWOUUD (2006), and HOENTJEN (2011). As the validation process for the subsidence prediction model is based on the comparison of calculated results with observations at specified benchmarks, interpreted values from the levelling campaigns have been directly included in this process.

5 Confidence Building and Validation

The confidence building process has been focused on the demonstration that the principal mechanisms of subsidence can be simulated by the model (qualitative proof), whereas validation means proving that the model represents the observed subsidence accurately over time also by value (quantitative proof).

Both processes have been applied to the subsurface and the surface part of the simulation model.

5.1 Subsurface

5.1.1 Confidence building at subsurface

Confidence building of the subsurface part means that the model has to show

- (A) an increasing cavern volume over time with on-going brine production or leaching as long as the convergence is not faster than volume creation,
- (B) an on-going cavern convergence, which increases with production,
- (C) a higher convergence volume with growing depth location and/or volume of the cavern as well as lower internal cavern pressure.

Calculated convergence volumes versus time are shown in Enclosure 4 to Enclosure 15 by the light blue graph.

As can be seen from these graphs the convergence volume increases over time and during leaching time as well as during gas storage operations (Criterion A).

Cavern volumes of cavern HL-K to HI-M (see Enclosure 13 to Enclosure 15) are much smaller than those of caverns HL-A to HL-I (see Enclosure 4 to Enclosure 12). Thus the calculated convergence volumes of the smaller caverns reveals as smaller than for the bigger caverns (Criterion A).

Especially for the bigger brine production caverns, e.g. for caverns HL-A to HL-F (see Enclosure 4 to Enclosure 9) there is an accelerated increase of convergence volume with continuation of the leaching process (Criterion B), because the absolute cavern volume has been increased.

Up to the development of a cavern volume of two million cubic meters cavern HL-B shows a smaller convergence volume than cavern HL-G (compare Enclosure 5 and Enclosure 10), because the depth location of the reference point for creep calculations is deeper for cavern HL-G (Criterion C).

In summary the confidence building process can be regarded as successfully completed.

5.1.2 Validation process at subsurface

The validation process has been performed by selecting the observable cavern volume versus time as the assessment parameter. Observed cavern volumes are obtained as results of the sonar surveys. Theoretically observable cavern volumes are calculated by the subsidence simulation model by applying a mass balancing method based on the production data (see OLDENZIEL ET AL. (2000)) and taking into account the creep of the salt (in order to determine the convergence volume). In the validation process all influencing factors (such as creep of the salt, insoluble content, etc.) are evaluated in total.

Successful validation in this context means that the simulation model has to match the observed cavern volumes from measurement to measurement. Starting from the measured cavern volume at the beginning of each period between two sonar measurements, the cavern volume development has been calculated up to the end of this period by application of the creep model. When the calculated cavern volume at the end of the examined period matches the sonar measurement, this indicates a perfect agreement of the theoretical subsurface model and therefore a successful validation.

Difficulties originated from various aspects. First of all sonar surveys are sometimes representing only partial measurements. These values have been corrected by employing the production data. Where cavern volumes have been corrected by taking into account the production data, red squares representing the sonar measurement and green squares representing the corrected value distinguish from each other. Partial sonars exist for example for cavern HL-B (see Enclosure 5), HL-C (see Enclosure 6), HL-I (see Enclosure 12) or HL-K (see Enclosure 13). In some instances cavern volumes derived from production data have been considered as more reliable (e.g. cavern HL-A, see Enclosure 4, or cavern HL-H, see Enclosure 7).

A principal difference in convergence behaviour exists between brine production caverns on the one hand side and gas storage caverns as well as brine production caverns at standstill on the other hand. Whereas brine production caverns in operation show a permanent increase in volume that mostly is greater than the volume loss by convergence, the creep response is masked behind the volume versus time curves. With gas storage caverns or brine production caverns at standstill, cavern volumes decrease over time. This decline can be directly related to creep of the surrounding rock salt mass. With regard to Heiligerlee caverns this effect can currently not be evaluated, because for brine production caverns at standstill (caverns HL-E, HL-G and HL-K) no follow-up measurement has been performed in the standstill period. The nitrogen storage cavern HL-K has been measured three times since the end of leaching, but only partial surveys have been carried out. However, the trend of the measured partial volumes of cavern HL-K follows the development as calculated by the creep model (see Enclosure 13).

For all caverns the applied simulation model shows quite good agreement with the sonar measurements. As represented for caverns HL-A to HL-M in Enclosure 4 to Enclosure 15, the theoretically observable cavern volume matches with the sonar measurements. Fitting parameters used during history matching were insoluble content, bulking factor and creep ability of the salt rock mass. The *theoretically observ-*

able cavern volume (as described in Chapter 4.3) over time takes into account that parts of the cavern sump are filled with insolubles that have settled in the sump by showing a kind of bulking effect. It can be assumed that with regard to the long-term leaching process of brine production caverns this bulking effect must certainly be smaller than due to the faster leaching process of the gas storage cavern HL-K. As a consequence the bulking factor for brine production caverns may be assumed with a smaller value than that for the gas storage cavern. However, the leaching process for cavern HL-K has not been principally different from the brine production caverns, because initially cavern HL-K was also planned as a brine production cavern. Therefore, for all caverns the same behaviour for the settling of the insolubles in the sump has been assumed. A value of 3% for the insoluble content has been assumed, because no information has been found in the documentation.

The results of the history matching process with respect to cavern volume can be checked by comparing the blue curves, which represent the theoretically observable cavern volume, with the green squares, which mark the corrected sonar measurements. It can be seen from Enclosure 4 to Enclosure 15 that the curves of the calculated cavern volumes finally match very well the observed (and corrected) cavern volumes. For each individual cavern there appears hardly any difference between the calculated volume (blue line) at the end of each interval between two sonar surveys and the green squares, which represent the corrected measurement value.

Thus, the subsurface part of validation can be considered as successfully passed.

5.2 Surface

5.2.1 Confidence building at surface

Confidence building at surface level has been referred to the following criteria:

- (A) Subsidence due to cavern operation has to increase over time and the subsidence bowl has to show an increasing horizontal spread.
- (B) Maximum subsidence exclusively due to cavern operation has to be located above the centre of the caverns, which are currently in operation.

As can be shown by comparison of the subsidence (isokatabase) maps for the following points in time end of September 1998, end of September 2005, and end of January 2011 (see Enclosure 20, Enclosure 23, and Enclosure 26) the horizontal spread of the subsidence bowl extends over time while at the same time showing an increasing maximum value with respect to each specific location (Criterion A). The centre of the subsidence bowl is created above the cavern HL-C, HL-E and HL-K and gradually moves over time towards the south-east due to the start of leaching of caverns HL-K to HL-M (compare Enclosure 20 and Enclosure 26) (Criterion B).

The confidence building process at surface can be assumed as successfully passed.

5.2.2 Validation process at surface

Validation of the subsidence model is demonstrated according to the interpreted results of the levelling campaigns 1998, 2005, and 2011 by applying the following criteria:

- (A) Theoretically calculated subsidence as displayed in isokatabases maps have to match the maximum observed subsidence.
- (B) Calculated subsidence curves over time at benchmarks have to match the observed values.
- (C) Subsidence rates calculated by the model are compared with selected benchmarks.

Principally the observed values have to be reduced by the contributions from gas production and ground compaction before they can be compared with the values produced by the simulation model. In order to validate the subsidence model the interpreted subsidence values as determined in the evaluation reports on the levelling campaigns in 1998, 2005 and 2011 by OLDENZIEL (1999), ORANJEWOUT (2006) and HOENTJEN ET AL. (2011) have been used. Modelled subsidence rates have been compared with predicted values according to the studies of EICKEMEIER ET AL. (2007). Applied reference values for subsidence and subsidence rates as given in the mentioned studies are compiled in Table 5.1 and Table 5.2.

Table 5.1 Compilation of values for maximum subsidence above the Heiligerlee cavern area due to interpretation of the levelling data

Levelling campaign	Interpreted maximum subsidence due salt caverns [mm]	Reference
1998	70 to 78	OLDENZIEL (1999)
2005	102 to 125	ORANJEWOUT (2005)
2011	119 to 142	HOENTJEN ET AL. (2011)

Table 5.2 Maximum subsidence or subsidence rates as predicted by EICKEMEIER ET AL. (2007)

Year	Maximum subsidence since 1969 [mm]	Maximum subsidence rate at the beginning of the reference year [mm/a]
1990	27.3	2.97
2000	50.3	2.65
2018	108.8	3.91
2050	210.9 ^{*1)} (288.8 ^{*2)})	3.61 ^{*1)} (6.79 ^{*2)})

*1) according to BGR Scenario HL01 considering brine production and cavern abandonment

*2) according to BGR Scenerio HL02 considering brine production and non-abandoned caverns after production

Subsidence maps are presented for the following points in time end of September 1998, end of September 2005, and end of January 2011 in Enclosure 20, Enclosure 23, and Enclosure 26. Cross sectional views are additionally presented for the W-E as well as S-N direction. They are representing the vertical cross-section approximately at the centre above the cavern area (see Enclosure 18 and Enclosure 19 for 1998, Enclosure 21 and Enclosure 22 for 2005, Enclosure 24 and Enclosure 25 for 2011).

It can be deduced from these representations that the calculated maximum values of subsidence in the centre above the caverns match quite well with values presented in the above mentioned studies as compiled in Table 5.1. Although maximum values as given by the previous studies cannot be reproduced by value, subsidence values as calculated by the new subsidence simulation model are within the given range. Especially for 2005 and 2011 maximum values as calculated by the applied new model differ from values given in previous studies by about 20 mm. When data are analysed in greater detail however, the maximum values as figured out in the studies of ORANJEWOUD (2005) and HOENTJEN ET AL. (2011) at benchmark 13A1250 can be interpreted as an isolated occurrence, because this benchmark is not located in the centre of the bowl as predicted by the simulation model. It is anticipated that a local effect is responsible for this spot.

For selected benchmarks located above the caverns curves of calculated subsidence versus time are compared with directly measured as well as interpreted values as shown in Enclosure 27 to Enclosure 36. In these diagrams calculated subsidence due to salt cavern operation is represented by the dark blue line. Whereas, the dark green line stands for subsidence due to brine production caverns (HL-A to HL-I and HL-L to HI-M) and the light green line represents the nitrogen storage cavern (HL-K). In order to be able to compare the simulation results with those from the interpretation of the measurements, the grey line is additionally shown. This line represents the modelled results (dark blue line) when relating them to the zero measurement of

the selected benchmark. The light blue line shows the subsidence rate, which has theoretically been calculated from the convergence of all salt caverns. Total subsidence calculated from the original measurement results at the specific benchmark are shown by red diamonds. The interpreted measurements results, representing only contributions from the salt caverns, are marked by green diamonds. Subsidence rates deduced from the measurements are represented by the beige squares.

Representations for the selected benchmarks above the caverns show a quite good agreement with interpreted measurement results (see Enclosure 27 to Enclosure 32). Only for the benchmark 013A1700 above cavern HL-G (see Enclosure 32) and benchmarks 013A0131 and 013A1250 above cavern HL-B (see Enclosure 33 and Enclosure 34) the model underestimates the interpreted subsidence. Interpreted values at benchmark 013A1250 have already been discussed above and are considered as isolated occurrences. With respect to the increase of subsidence between 1969 and 2000 as given by EICKEMEIER ET AL. (2007) the applied simulation model produces higher values. As pointed out by PINKSE (2014) subsidence in the centre of the bowl as predicted by EICKEMEIER ET AL. (2007) for 2010 turned out to be too small, when compared with the results from the follow-up measurement in 2011. Thus, the here applied subsidence model reflects this most recent observation. Therefore, it is comprehensible that also subsidence rates as calculated by the applied simulation model are higher than those predicted by EICKEMEIER ET AL. (2007). Calculated maximum rates are in the range of 4 to 5 mm per year when most recent data are considered.

Enclosure 36 is shown in order to demonstrate that the subsidence bowl calculated by the model also fits quite well with measurements that have been taken at locations that are located more distant from the centre of the subsidence bowl.

It can be concluded that the model is very well suited for the prediction of subsidence, which will be caused by the salt caverns in the future – brine production caverns and nitrogen storage cavern, because the subsidence history can be reproduced not only for maximum subsidence values but also for selected benchmarks in the field. Thereby, it has to be considered that a perfect match by 100% could not be expected, because measurements had to be interpreted in terms of non-cavern related contributions and also benchmarks may be influenced by local effects.

In conclusion the validation process for the subsidence model is regarded as successfully passed.

6 Proposed Procedure for Subsidence Prediction

6.1 Proposed Steps

Having successfully passed the confidence building and validation process the subsidence prediction model can be considered as suitable and ready for application for subsidence prognosis due to operation of salt caverns at Heiligerlee.

Subsidence predictions have to be shown to the Staatstoezicht op de Mijnen (SodM) in advance to every mandatory scheduled levelling campaign as well as for the date of measurement and for the intended end of operations.

As the future operating history can only be estimated, two different scenarios for prediction are suggested: a conservative and a progressive case with respect to subsidence development. Progressive in this sense and with regard to the gas storage means that on average cavern pressures are low. The conservative scenario will represent the opposite case. Conservative or progressive operations of brine production caverns can be related to volume development or intended brine production/produced salt mass. AkzoNobel and Gasunie together will provide input data in order to compile these two cases of future operations. Scenarios in terms of well-head pressures and production data versus operation time until 2050 are required.

6.2 Capabilities

The predictions will show the total subsidence from all caverns as well as only for the nitrogen storage cavern in order to be able to check and differentiate their partial contributions.

Total subsidence including also ground compaction as well as gas production might be considered in the maps and graphs, if required and if reliable data are available. Input data are then needed in terms of expected subsidence by gas production (by NAM) and due to compaction effects of the ground.

6.3 Maps and Graphs

The results of the predictions will be presented by subsidence maps (plots of isokatabases) as well as by diagrams showing predicted subsidence versus time (at selected benchmark locations). Maps for subsidence rates will also be created.

Presentations of further parameters such as horizontal displacements, tilts, curvature and strains may be selected on request provided that non-cavern related contributions to subsidence can be determined reliable. Otherwise these maps remain merely theoretical.

7 Summary and Conclusion

The present report describes the establishment of the subsidence prediction model that will be used for the prediction of cavern related subsidence in the Heiligerlee area.

The principal assumptions and applied mechanisms are demonstrated. The focus of the model is set to the representation of the individual contributions of each cavern, because subsidence created by the nitrogen storage cavern shall be differentiated from subsidence caused by the brine production caverns. In this regard the model takes into account cavern pressures of the nitrogen storage cavern on a daily base as well as salt production data for brine production caverns.

The built-up subsidence model is in good agreement with the applied confidence building criteria with respect to the subsurface and surface part of the model. This especially means that the main processes at subsurface as cavern convergence and creep are represented in a reliable way, and that at surface the development of the subsidence bowl follows the expected behaviour, which means deepening and widening of the bowl over time.

With respect to validation further subsidence contributions, e.g. due to ground compaction and gas production from the Slochteren field, have to be considered. Estimates for these contributions have been taken from third party reports, which provide interpretations of the results from former levelling campaigns (see OLDENZIEL (1999), ORANJEWOUDE (2006), and HOENTJEN (2011)). According to the postulated validation criteria for the surface part of the model – (1) representation of maximum observed subsidence value, and (2) matching of the subsidence history at selected (reliable) benchmarks – it can be stated that the validation process has been successfully passed.

Subsidence predictions with this model are planned to be carried out for two different operation scenarios:

- a scenario that can be considered as more conservative with regard to brine production, and
- a scenario that can be considered as more progressive.

Scenarios will be compiled together with Gasunie and AkzoNobel according to their business perspective.

The first step and milestone of the subsidence prediction will be the presentation of a subsidence prognosis prior to the next levelling campaign, which is scheduled for the end of 2015.

References

- [1] SROKA, A., SCHOBBER, F. (AUGUST 1982):
'Die Berechnung der maximalen Bodenbewegung über kavernenartigen Hohlräumen unter Berücksichtigung der Hohlraumgeometrie',
Kali und Steinsalz.
- [2] SCHOBBER, F., SROKA, A., HARTMANN, A. (1987):
'Ein Konzept zur Senkungsberechnung über Kavernenfeldern' ,
Kali und Steinsalz, Bd. 9, Heft 11, 1987.
- [3] EICKEMEIER, R. (2005): Senkungsprognosen über Kavernenfeldern - Ein neues Modell, Tagungsbeitrag zum 34. Geomechanik-Kolloquium, Leipzig.
- [4] NEUHAUS, W. (1976):
'Die Berechnungsgrundlagen der bergschadenkundlichen Einwirkungsnetze und ihre Möglichkeiten und Grenzen',
Mitteilungen aus dem Markscheidewesen, 83, Heft 2, Deutscher Markscheider-Verein e.V., Essen.
- [5] GAULKE, K., ROKAHR, R., STAUDTMEISTER, K., ZANDER-SCHIEBENHÖFER, D. (2007):
'Re-assessment of the Creep Behaviour of the Rüstringen Salt Dome for Optimization and Future Development of the Crude Oil Cavern Storage Facility',
SMRI Technical Paper, Fall Conference 2007.
- [6] ZANDER-SCHIEBENHÖFER, D. (2007):
'Kriechverhalten von Salzgestein in der Umgebung von Kavernenfeldern',
Forschungsergebnisse aus dem Tunnel- und Kavernenbau Gottfried Wilhelm Leibniz Universität Hannover, Heft 23, Hannover.
- [7] VAN SAMBEEK, L. L. (1993):
'Evaluating Cavern Tests and Surface Subsidence Using Simple Numerical Models',
Seventh Symposium on Salt, Vol. I, p. 433-439.
- [8] OLDENZIEL, C. (1999):
'History matching of surface subsidence due to solution mining operations in the Heiligerlee and Heiligerlee brinefields',
AkzoNobel, Minerals Department.
- [9] OLDENZIEL, C., ZANDER-SCHIEBENHÖFER, D.: (2000):
'Confidence Building in Relation of the Optimization and extension of the Hvornum Brine Filed in Mariager, Denmark',
8th World salt symposium, 2000.
- [10] ORANJEWOUDE (2006):
'Rapport Frequentiemodellering deformatiemetingen 2005 Winningvergunningen Adolf van Nassau en Adolf van Nassau Uitbreiding',
projectnr. 15575-61467-16, revisie 00, oranjewoud, 28 juni 2006.
- [11] HOENTJEN, K. H., DAM, J. (2011): :
'Rapport Geodetische analyse deformatiemeting 2010; Bepaling van de

zoutwinning veroorzaakte bedemdaling, Winningvergunningen Uitbreiding Adolf van Nassau II en III Opslagvergunning Heiligerlee, Winningvergunningen Adolf van Nassau II en III Opslagvergunning Winschoten II en III', projectnr. 242314, revisie 02, oranjewoud, 31 oktober 2011.

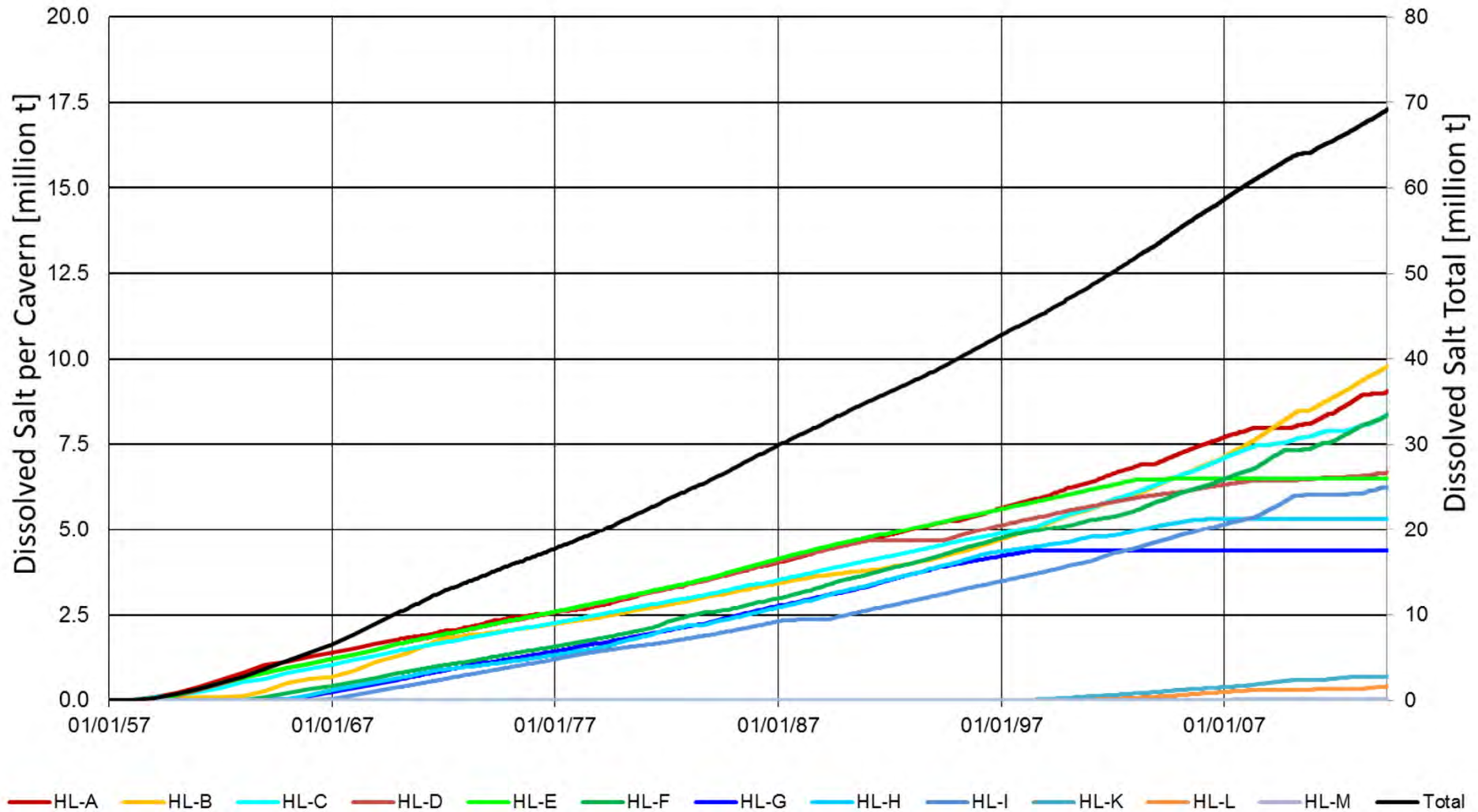
- [12] EICKEMEIER, R., HEUSERMANN, S. (2007):
'Kavernenfelder Winschoten / Heiligerlee und Heiligerlee Senkungsprognosen für die Kavernenfelder Winschoten / Heiligerlee und Heiligerlee (Datenbasis 2005)
Abschlussbericht – Textband, Bundesanstalt für Geowissenschaften und Rohstoffe (BGR), Hannover.
- [13] EICKEMEIER, R., HEUSERMANN, S. (2007):
'Kavernenfelder Winschoten / Heiligerlee und Heiligerlee Senkungsprognosen für die Kavernenfelder Winschoten / Heiligerlee und Heiligerlee (Datenbasis 2005)
Abschlussbericht – Anlagenband, Bundesanstalt für Geowissenschaften und Rohstoffe (BGR), Hannover.
- [14] PINKSE, T. (2014):
'Bodemdaling door zoutwinning in de boorterreinen Heiligerlee en Heiligerlee'
Memorandum, AkzoNobel, 12 september, 2014.

List of Enclosures

- Enclosure 1 Dissolved tons of salt at subsurface – back-calculated from production data
- Enclosure 2 Cavern volumes – back-calculated from production data
- Enclosure 3 Assumed creep response compared to BGRa reference
- Enclosure 4 Cavern HL-A –
Calculated volume versus time compared to sonar measurements
- Enclosure 5 Cavern HL-B –
Calculated volume versus time compared to sonar measurements
- Enclosure 6 Cavern HL-C –
Calculated volume versus time compared to sonar measurements
- Enclosure 7 Cavern HL-D –
Calculated volume versus time compared to sonar measurements
- Enclosure 8 Cavern HL-E –
Calculated volume versus time compared to sonar measurements
- Enclosure 9 Cavern HL-F –
Calculated volume versus time compared to sonar measurements
- Enclosure 10 Cavern HL-G –
Calculated volume versus time compared to sonar measurements
- Enclosure 11 Cavern HL-H –
Calculated volume versus time compared to sonar measurements
- Enclosure 12 Cavern HL-I –
Calculated volume versus time compared to sonar measurements
- Enclosure 13 Cavern HL-K –
Calculated volume versus time compared to sonar measurements
- Enclosure 14 Cavern HL-L –
Calculated volume versus time compared to sonar measurements
- Enclosure 15 Cavern HL-M –
Calculated volume versus time compared to sonar measurements
- Enclosure 16 Heiligerlee – Calculated convergence volume versus time
- Enclosure 17 Heiligerlee – Map of cavern and benchmark locations
- Enclosure 18 Heiligerlee – Subsidence bowl at fixed Northing 574,500 – 30/09/1998
- Enclosure 19 Heiligerlee – Subsidence bowl at fixed Easting 263,400 – 30/09/1998
- Enclosure 20 Heiligerlee – Subsidence bowl – 30/09/1998
- Enclosure 21 Heiligerlee – Subsidence bowl at fixed Northing 574,500 – 30/09/2005
- Enclosure 22 Heiligerlee – Subsidence bowl at fixed Easting 263,400 – 30/09/2005
- Enclosure 23 Heiligerlee – Subsidence bowl – 30/09/2005
- Enclosure 24 Heiligerlee – Subsidence bowl at fixed Northing 574,500 – 31/01/2011
- Enclosure 25 Heiligerlee – Subsidence bowl at fixed Easting 263,400 – 31/01/2011
- Enclosure 26 Heiligerlee – Subsidence bowl – 31/01/2011

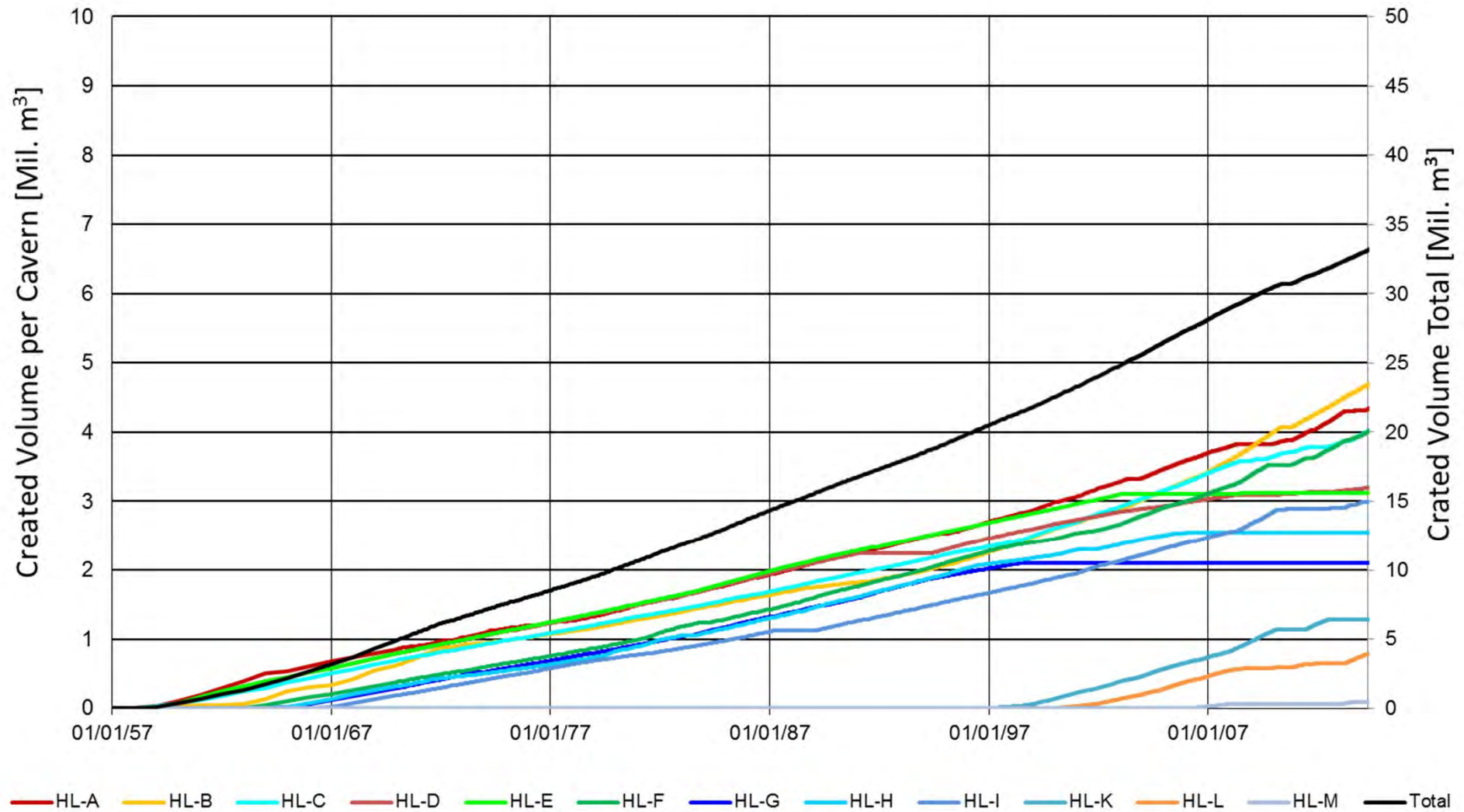
- Enclosure 27 Heiligerlee – Benchmark 013A1100 –
Comparison of observed subsidence with measured values
- Enclosure 28 Heiligerlee – Benchmark 013A1300 –
Comparison of observed subsidence with measured values
- Enclosure 29 Heiligerlee – Benchmark 013A1400 –
Comparison of observed subsidence with measured values
- Enclosure 30 Heiligerlee – Benchmark 013A1500 –
Comparison of observed subsidence with measured values
- Enclosure 31 Heiligerlee – Benchmark 013A1600 –
Comparison of observed subsidence with measured values
- Enclosure 32 Heiligerlee – Benchmark 013A1700 –
Comparison of observed subsidence with measured values
- Enclosure 33 Heiligerlee – Benchmark 013A0131 –
Comparison of observed subsidence with measured values
- Enclosure 34 Heiligerlee – Benchmark 013A1250 –
Comparison of observed subsidence with measured values
- Enclosure 35 Heiligerlee – Benchmark 013A5510 –
Comparison of observed subsidence with measured values
- Enclosure 36 Heiligerlee – Benchmark 013A5025 –
Comparison of observed subsidence with measured values

Enclosures



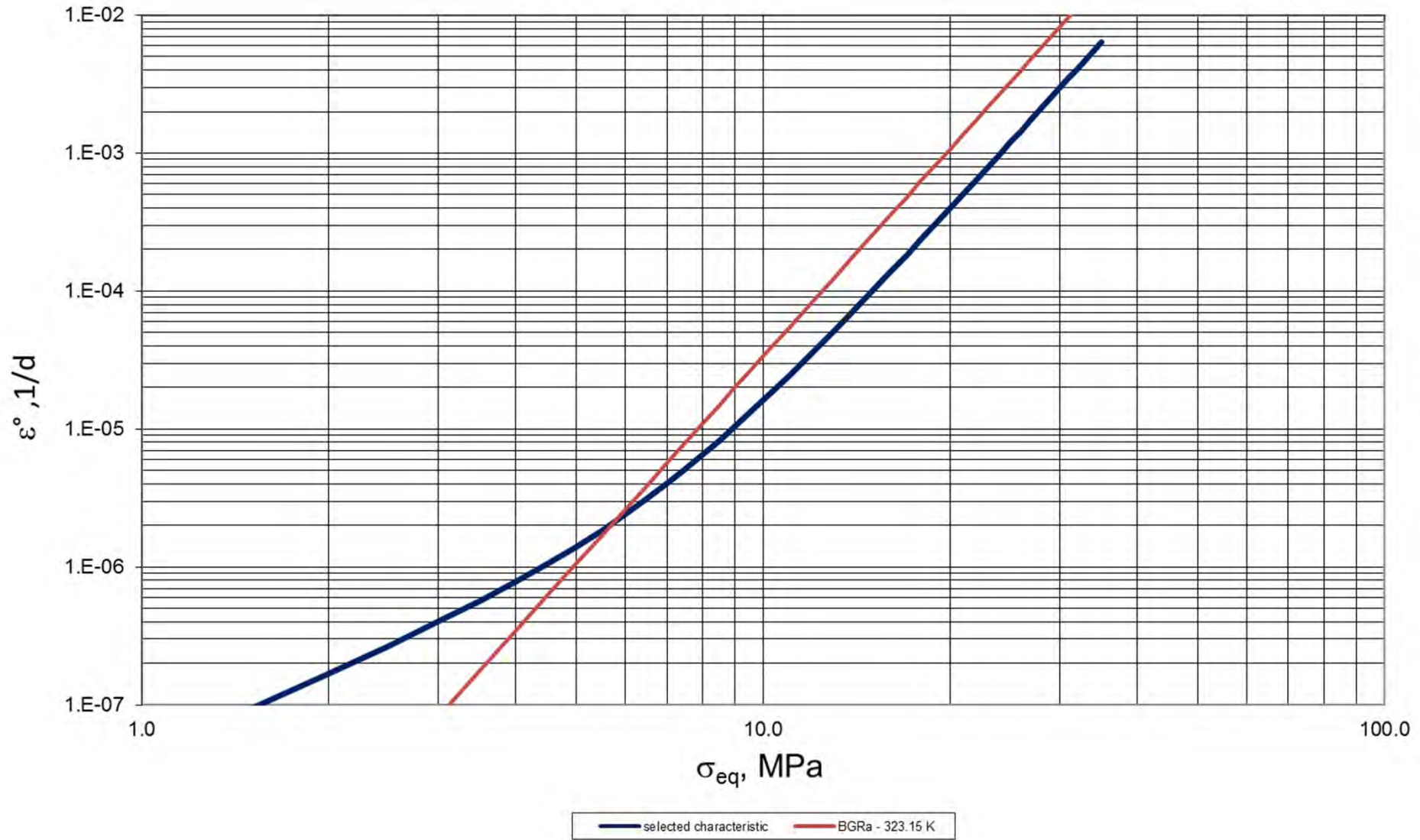
Enclosure 1

Dissolved tons of salt at subsurface – back-calculated from production data



Enclosure 2

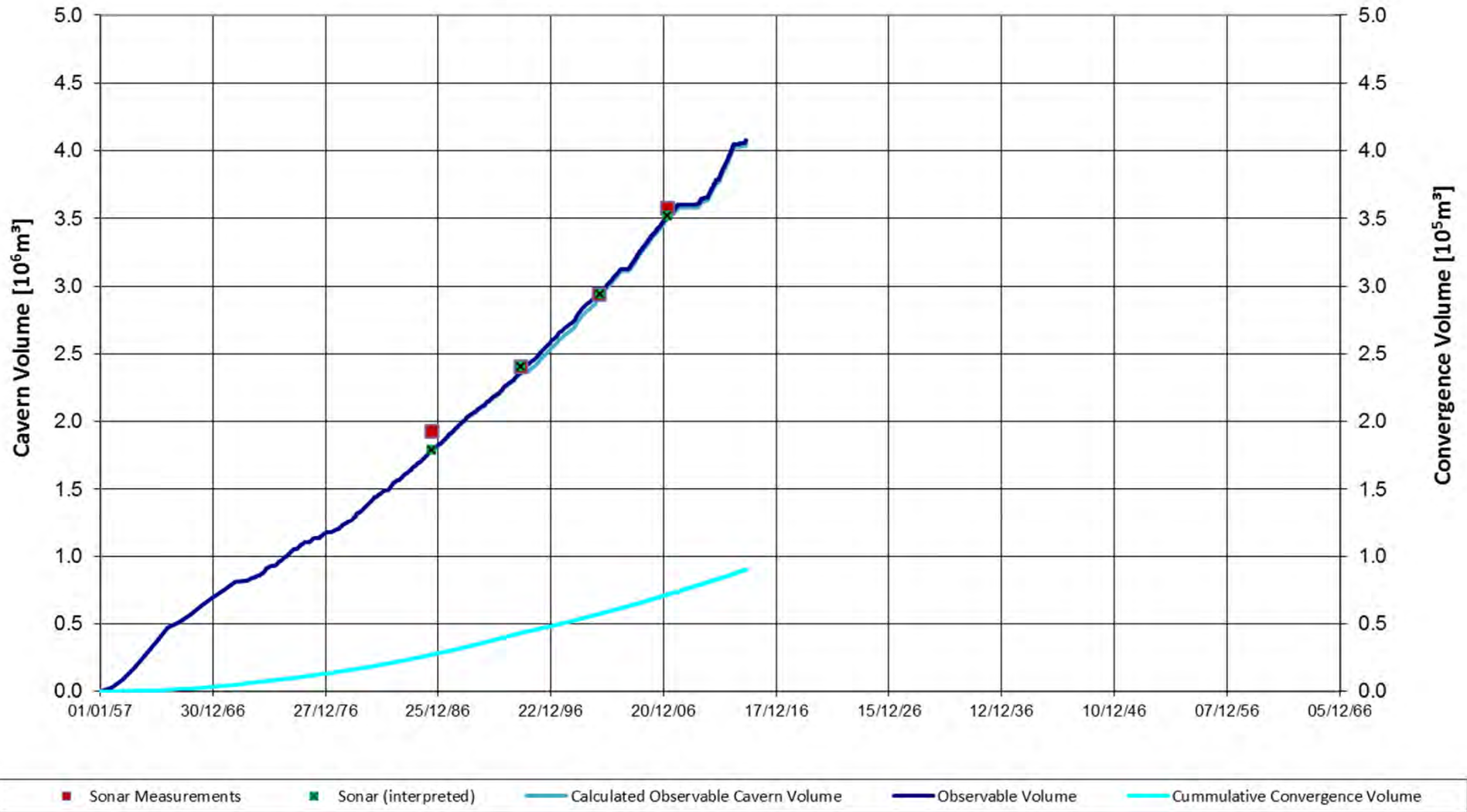
Cavern volumes – back-calculated from production data



Enclosure 3

Assumed creep response compared to Heiligerlee lab-test results

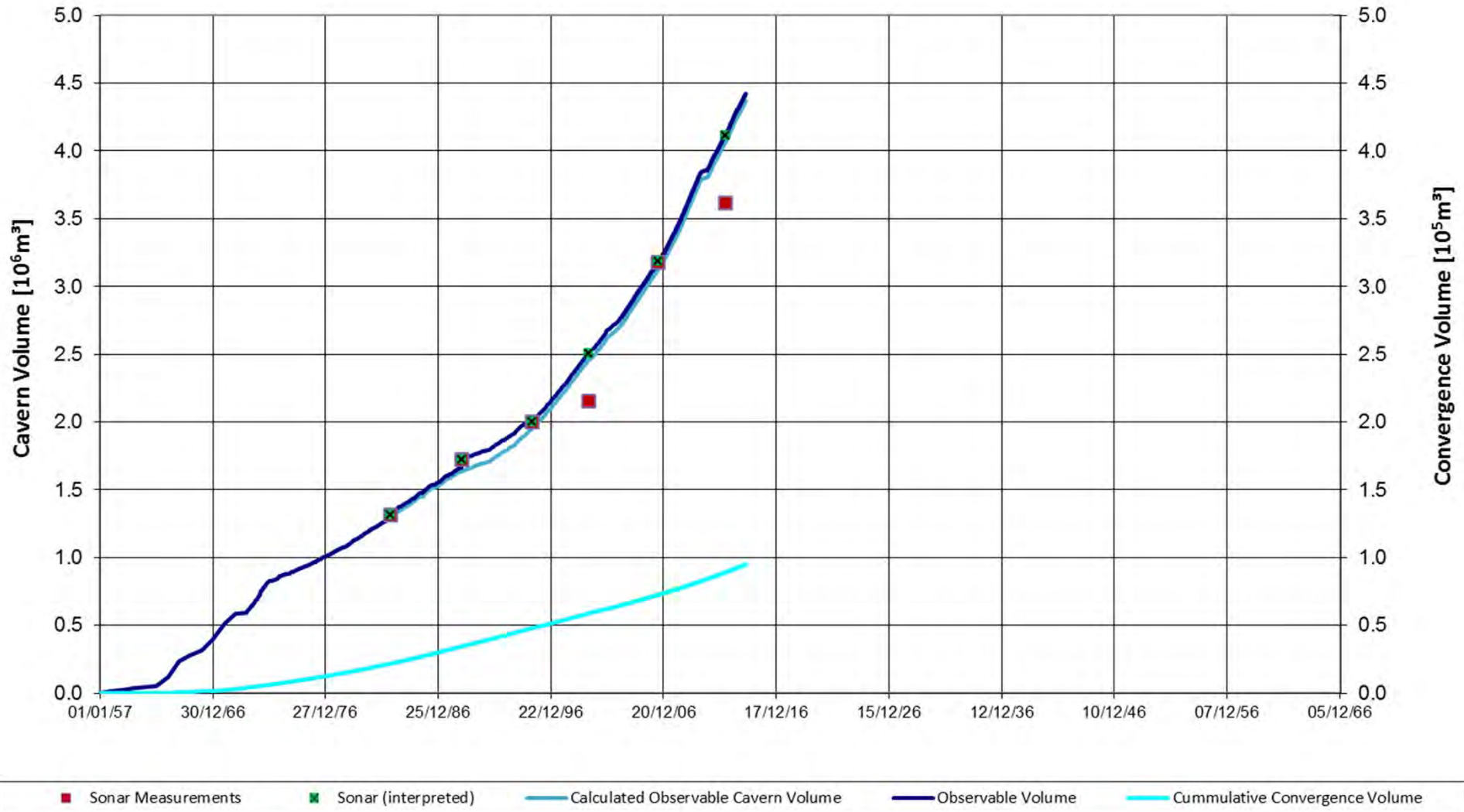
Cavern HL-A - Operation History - Cavern Volumes vs Time



Enclosure 4

Cavern HL-A – Calculated volume versus time compared to sonar measurements

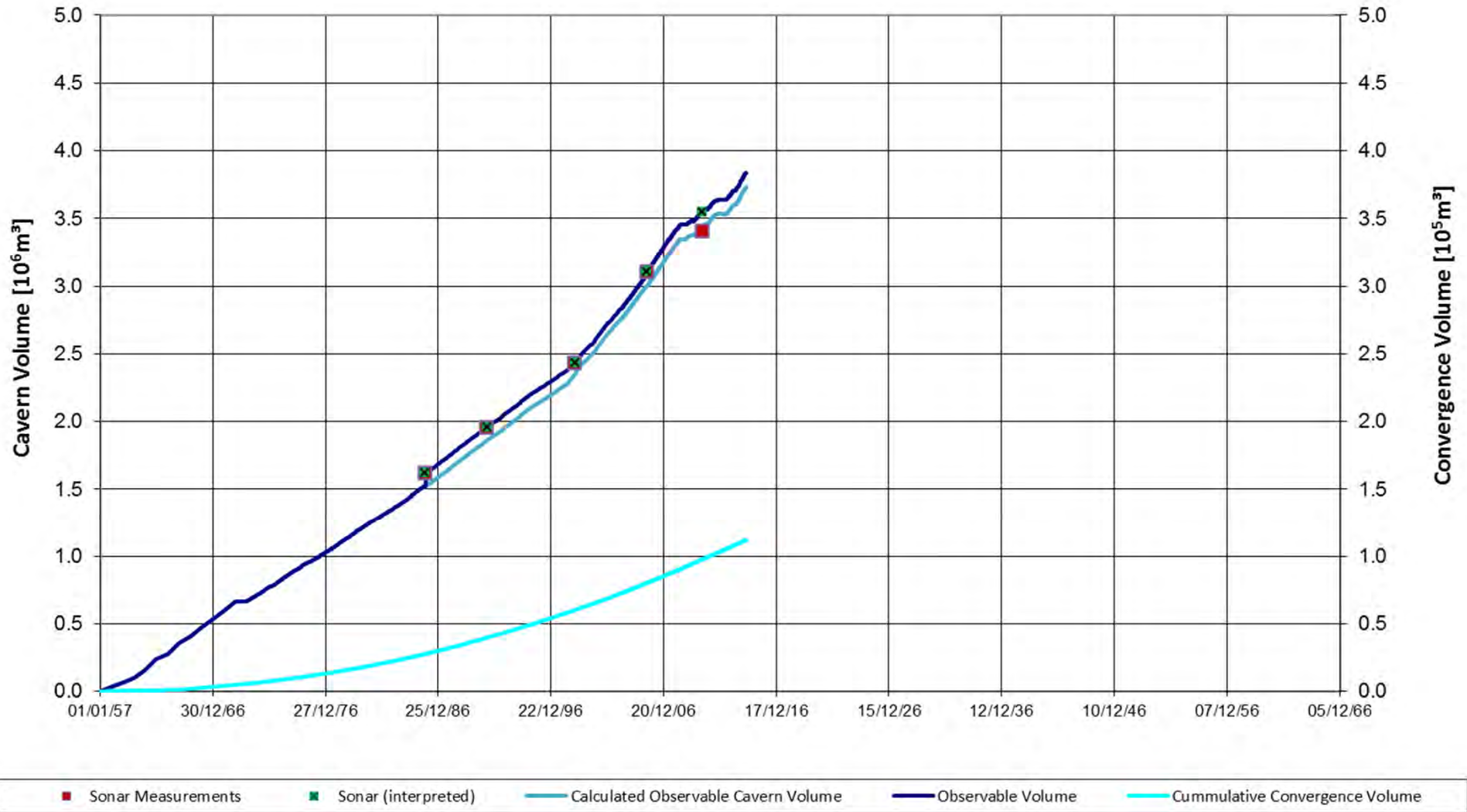
Cavern HL-B - Operation History - Cavern Volumes vs Time



Enclosure 5

Cavern HL-B – Calculated volume versus time compared to sonar measurements

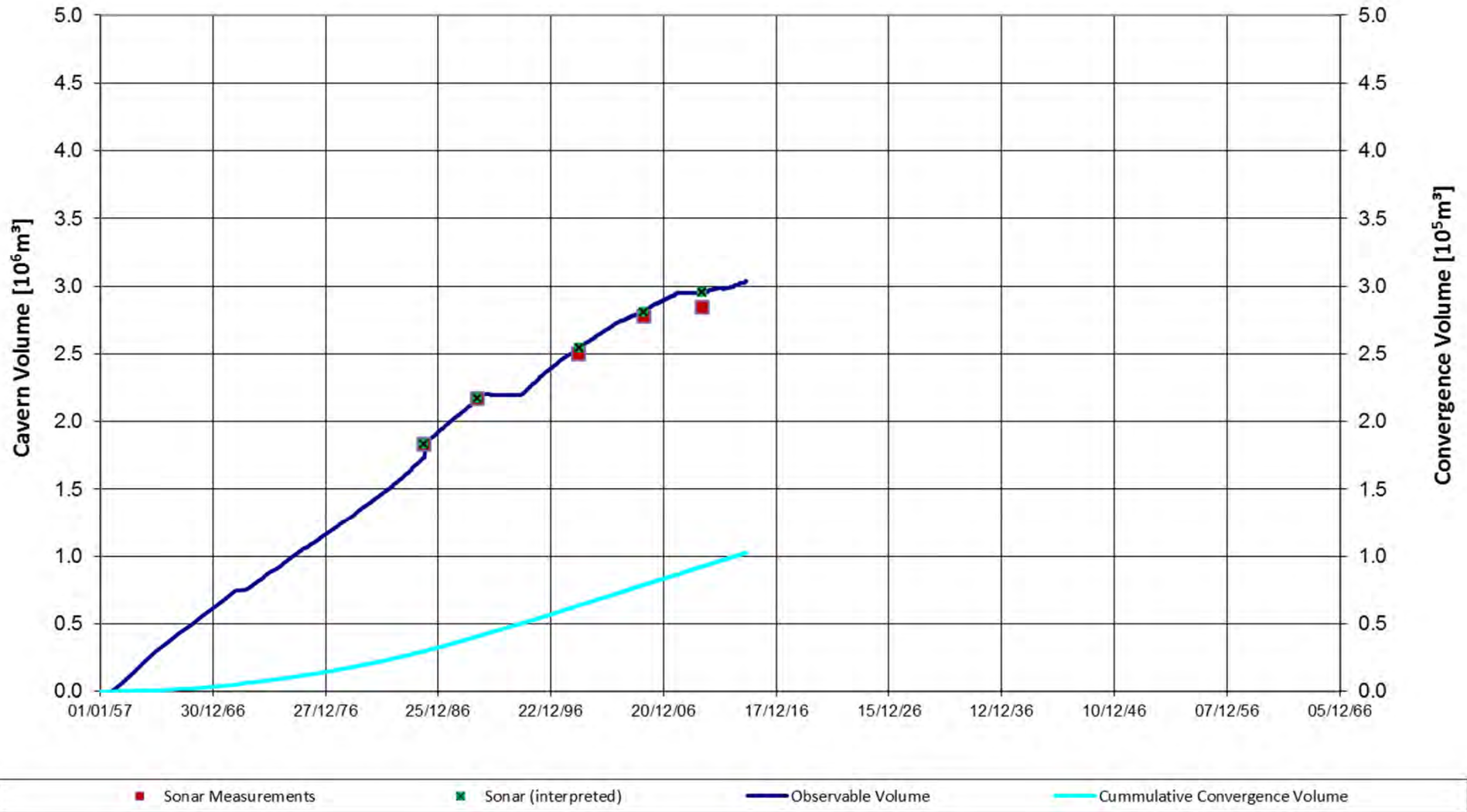
Cavern HL-C - Operation History - Cavern Volumes vs Time



Enclosure 6

Cavern HL-C – Calculated volume versus time compared to sonar measurements

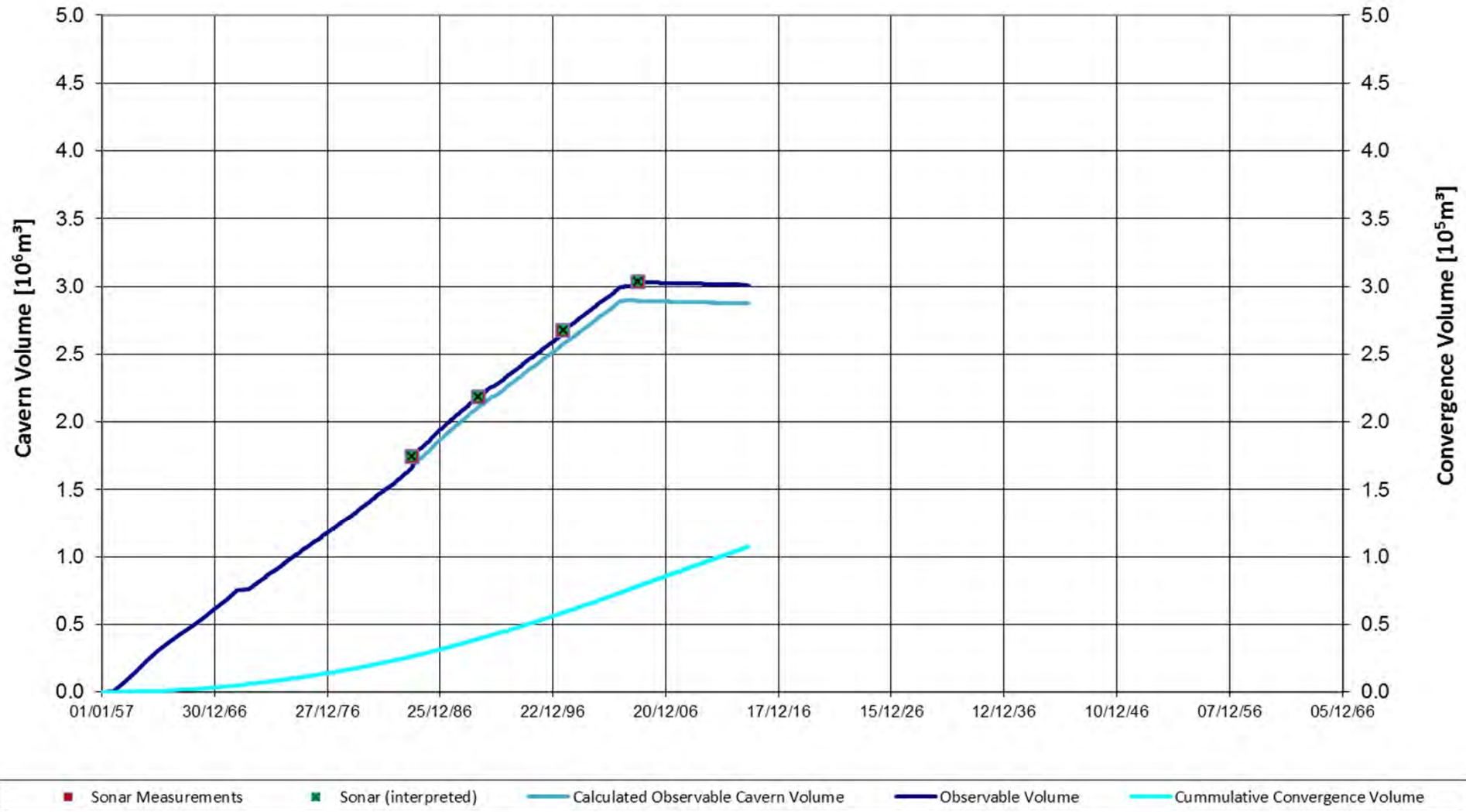
Cavern HL-D - Operation History - Cavern Volumes vs Time



Enclosure 7

Cavern HL-D – Calculated volume versus time compared to sonar measurements

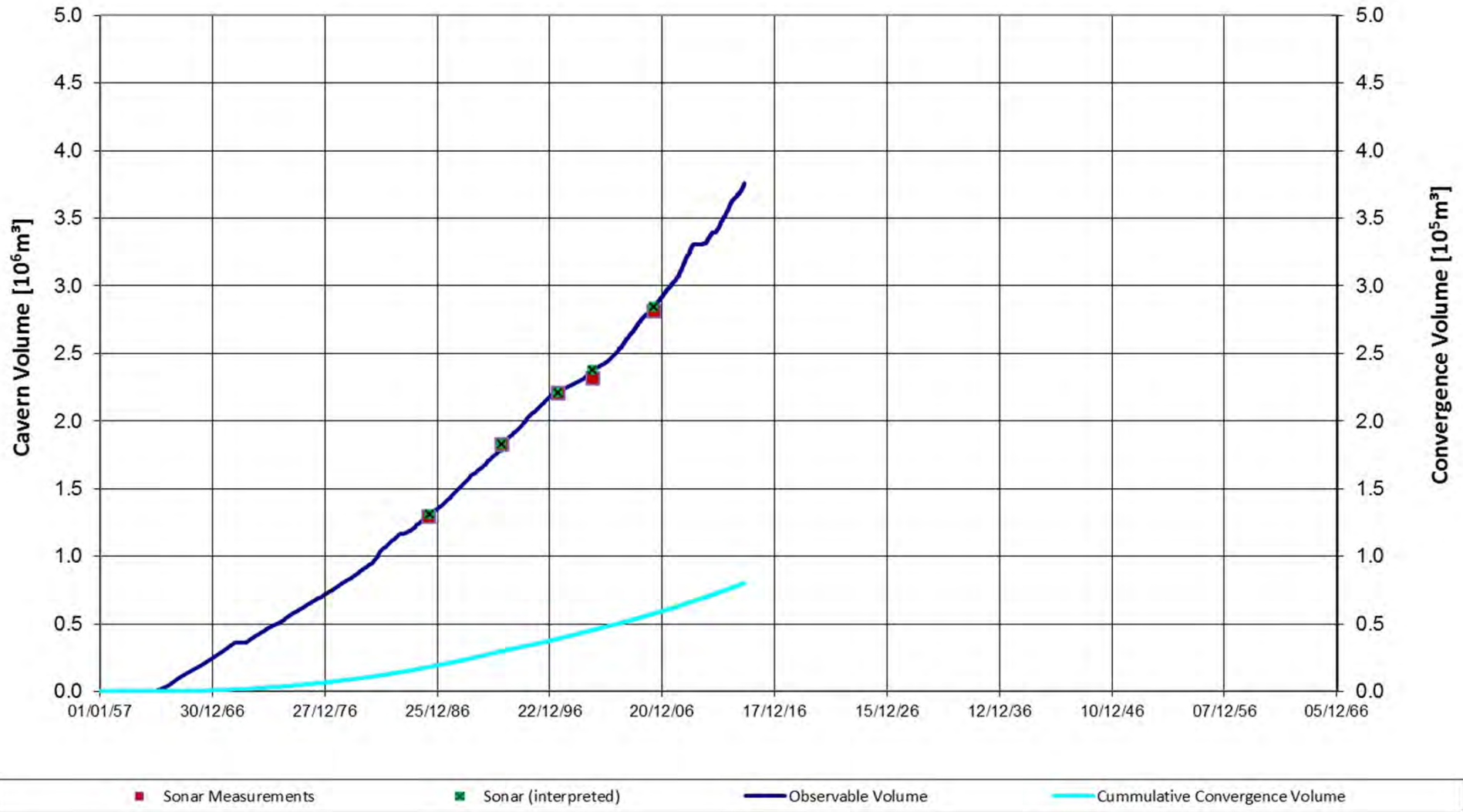
Cavern HL-E - Operation History - Cavern Volumes vs Time



Enclosure 8

Cavern HL-E – Calculated volume versus time compared to sonar measurements

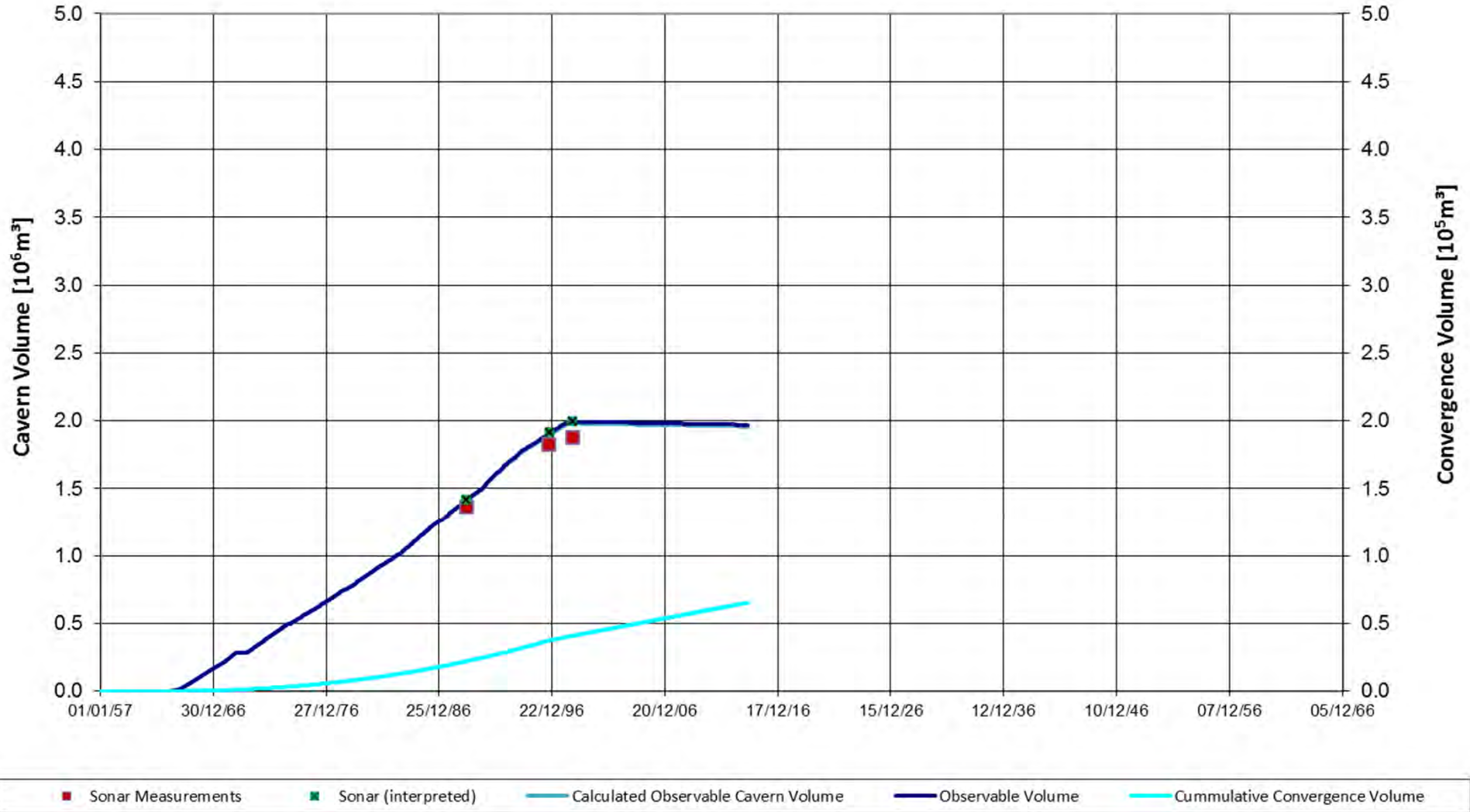
Cavern HL-F - Operation History - Cavern Volumes vs Time



Enclosure 9

Cavern HL-F – Calculated volume versus time compared to sonar measurements

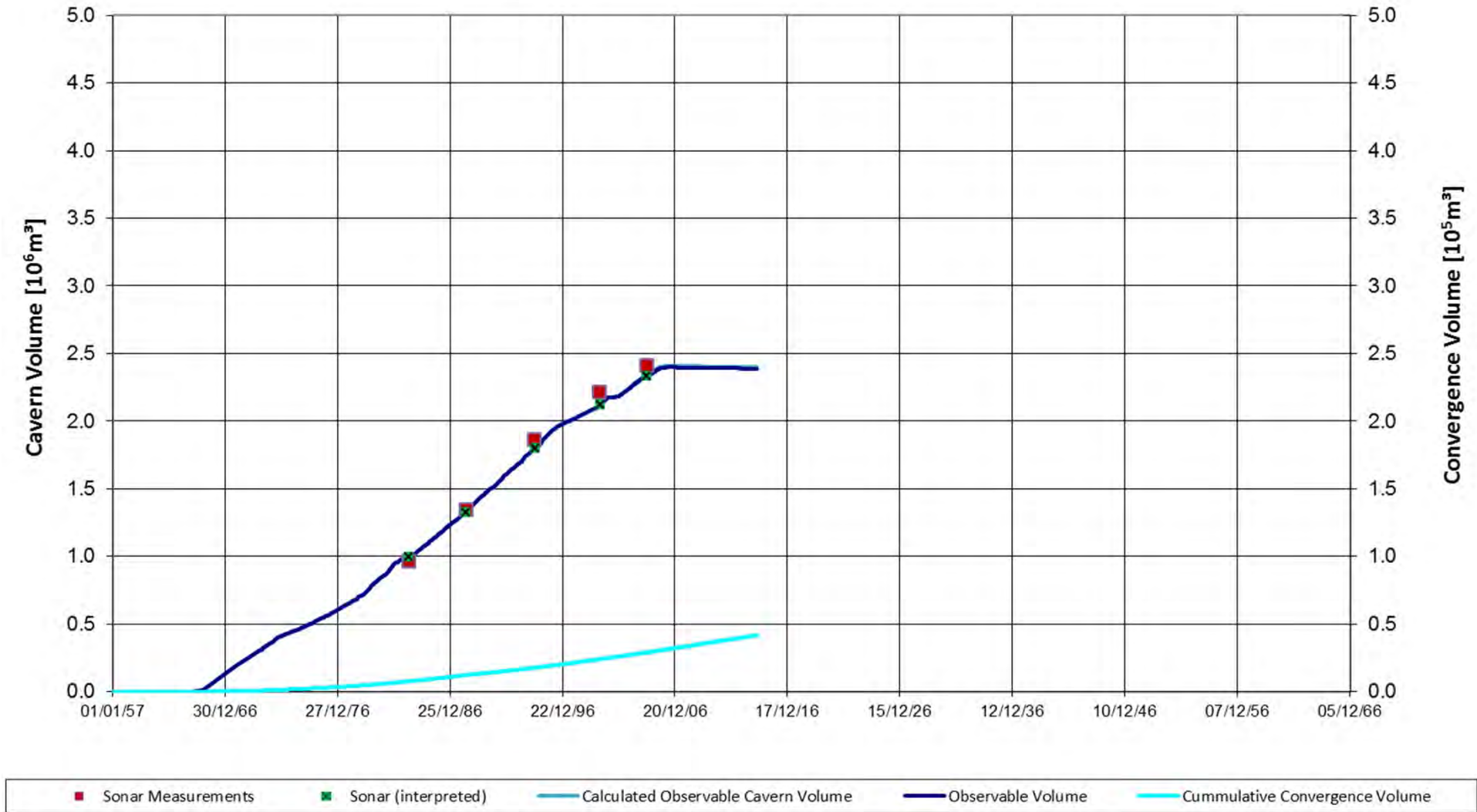
Cavern HL-G - Operation History - Cavern Volumes vs Time



Enclosure 10

Cavern HL-G – Calculated volume versus time compared to sonar measurements

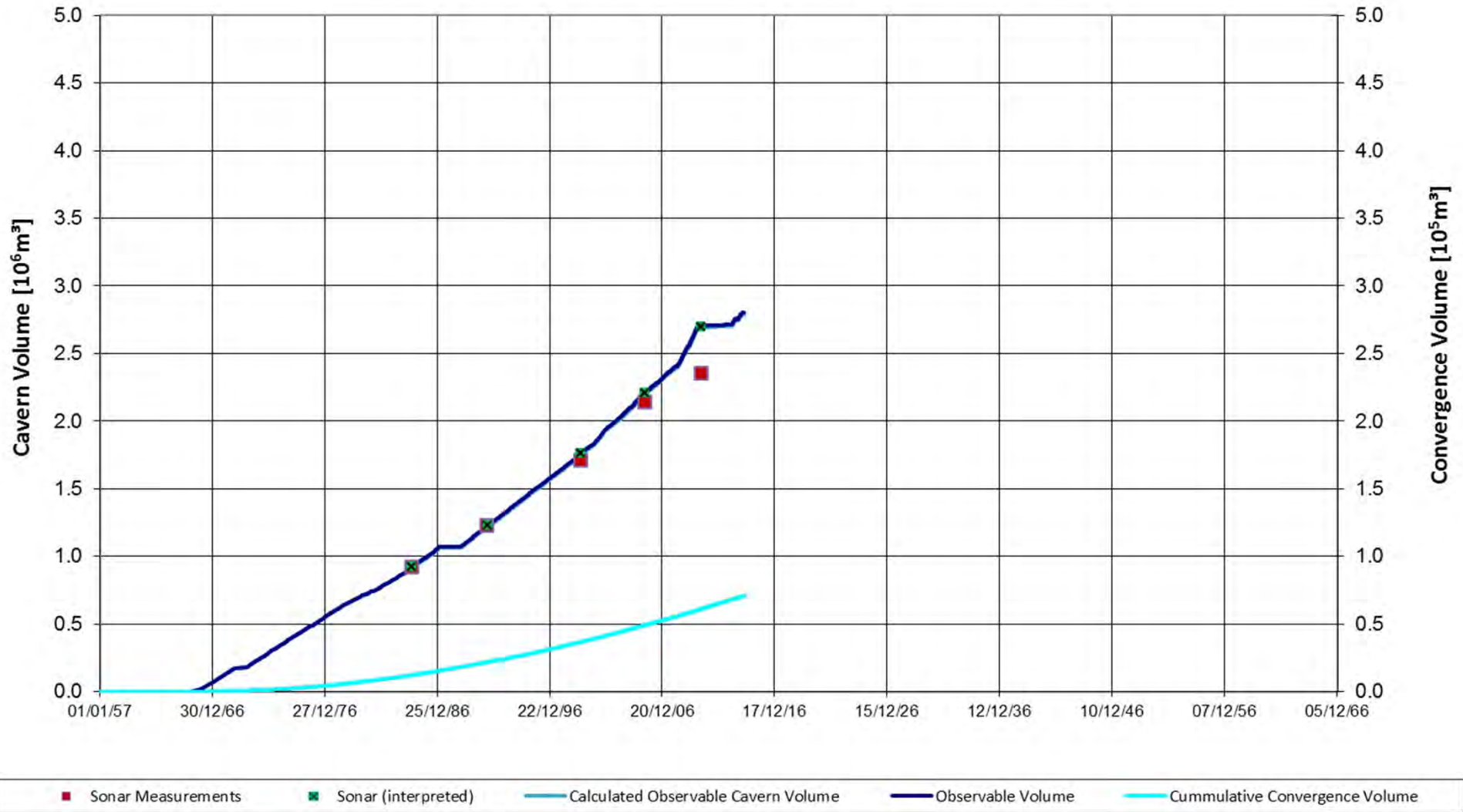
Cavern HL-H - Operation History - Cavern Volumes vs Time



Enclosure 11

Cavern HL-H – Calculated volume versus time compared to sonar measurements

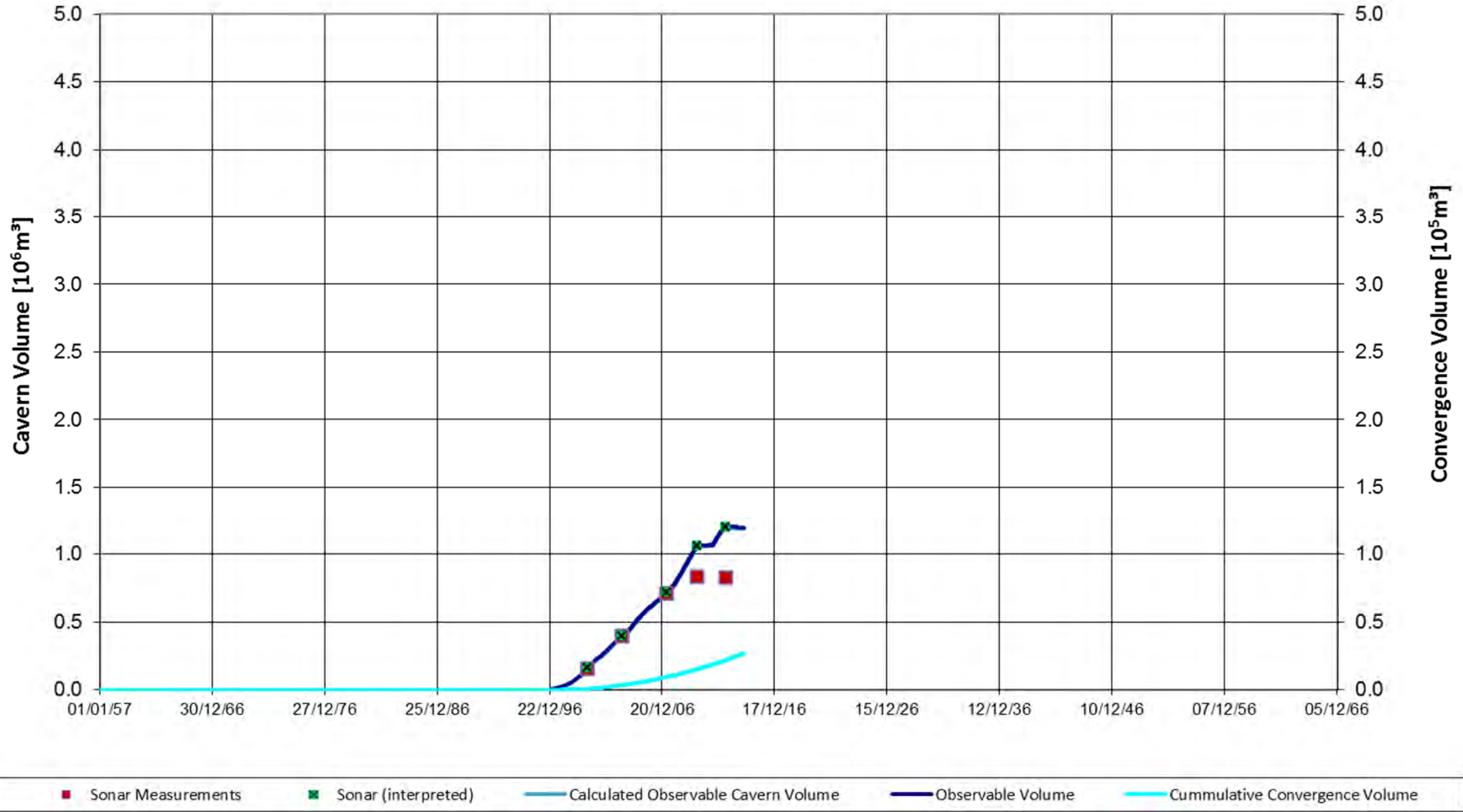
Cavern HL-I - Operation History - Cavern Volumes vs Time



Enclosure 12

Cavern HL-I – Calculated volume versus time compared to sonar measurements

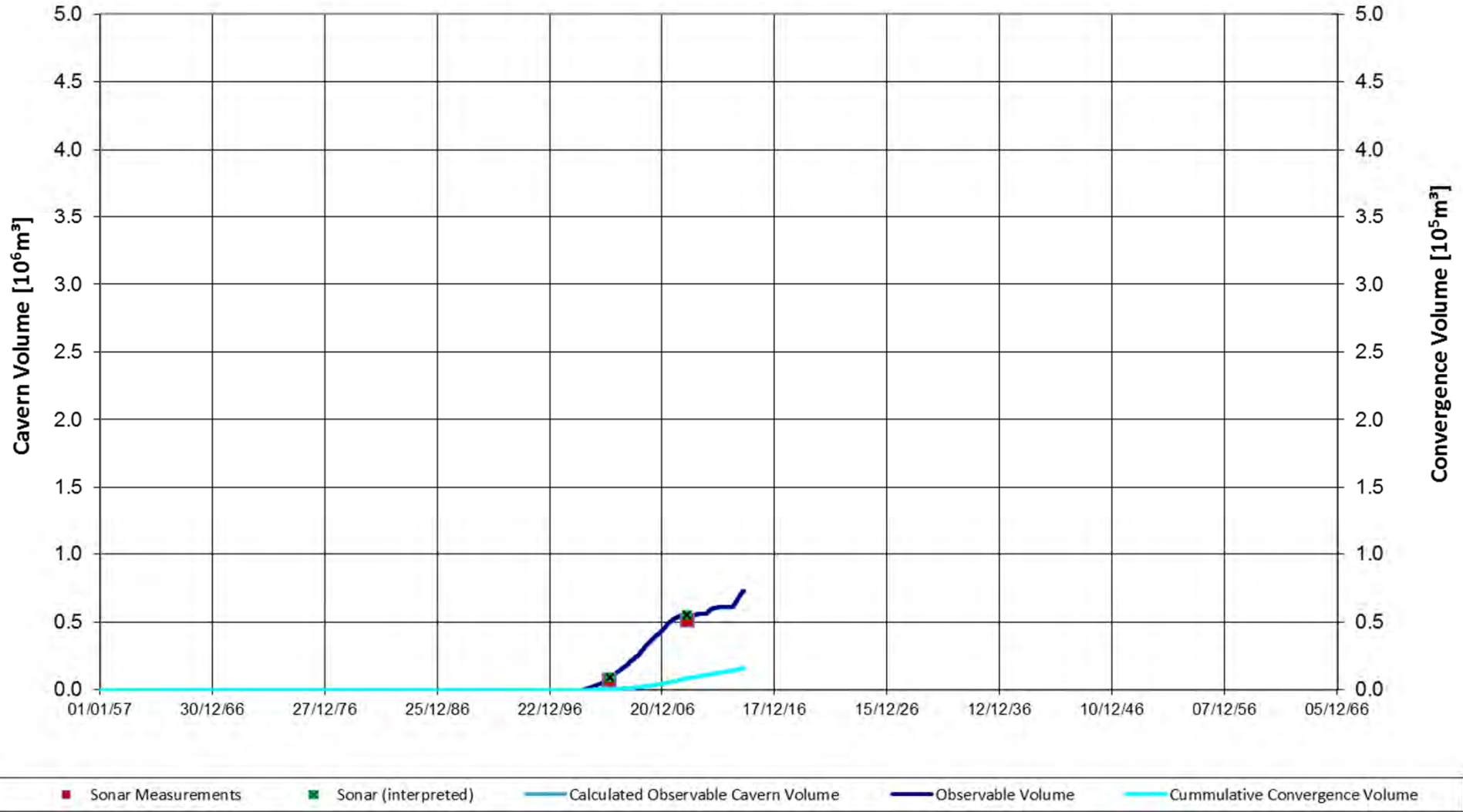
Cavern HL-K - Operation History - Cavern Volumes vs Time



Enclosure 13

Cavern HL-K – Calculated volume versus time compared to sonar measurements

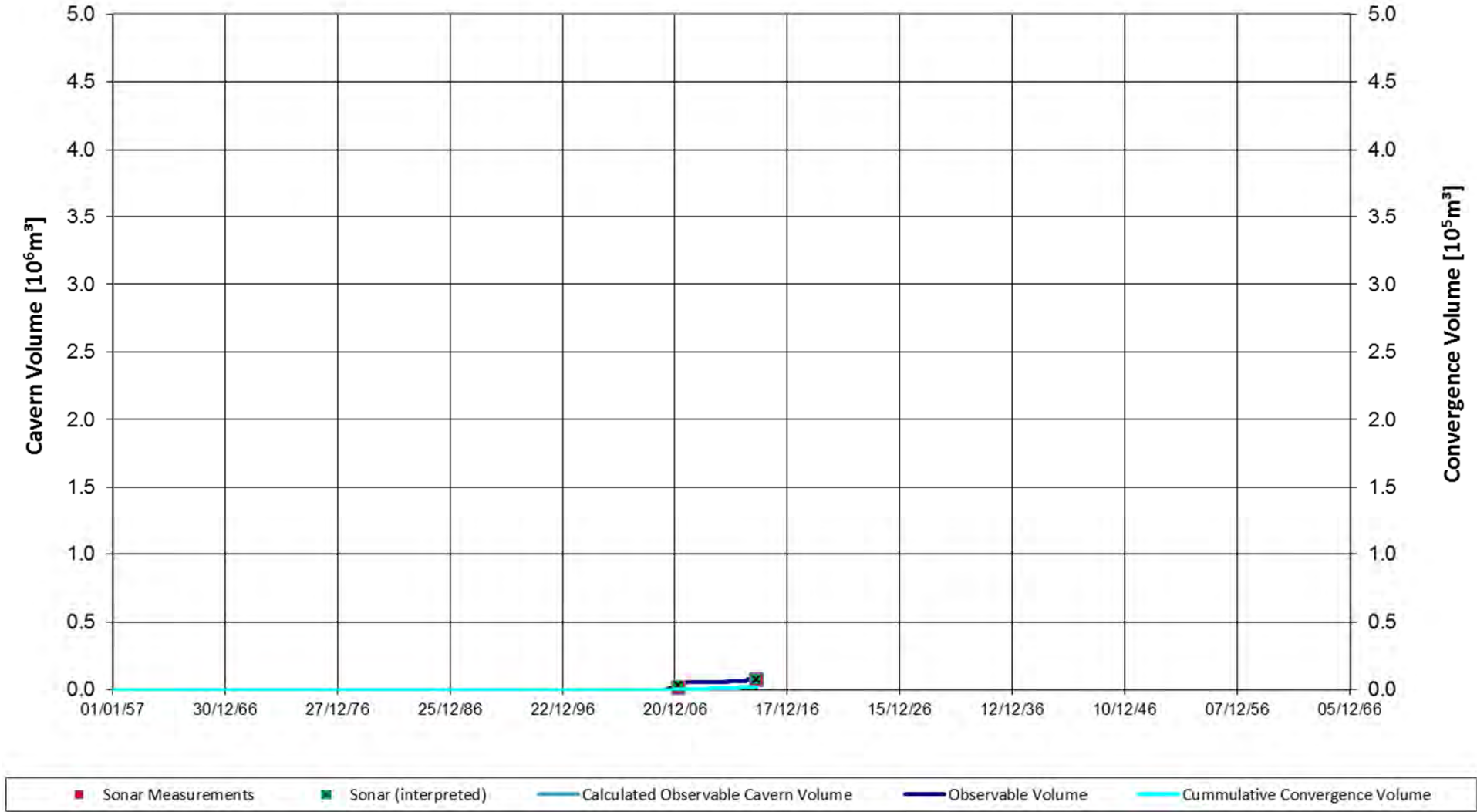
Cavern HL-L - Operation History - Cavern Volumes vs Time



Enclosure 14

Cavern HL-L – Calculated volume versus time compared to sonar measurements

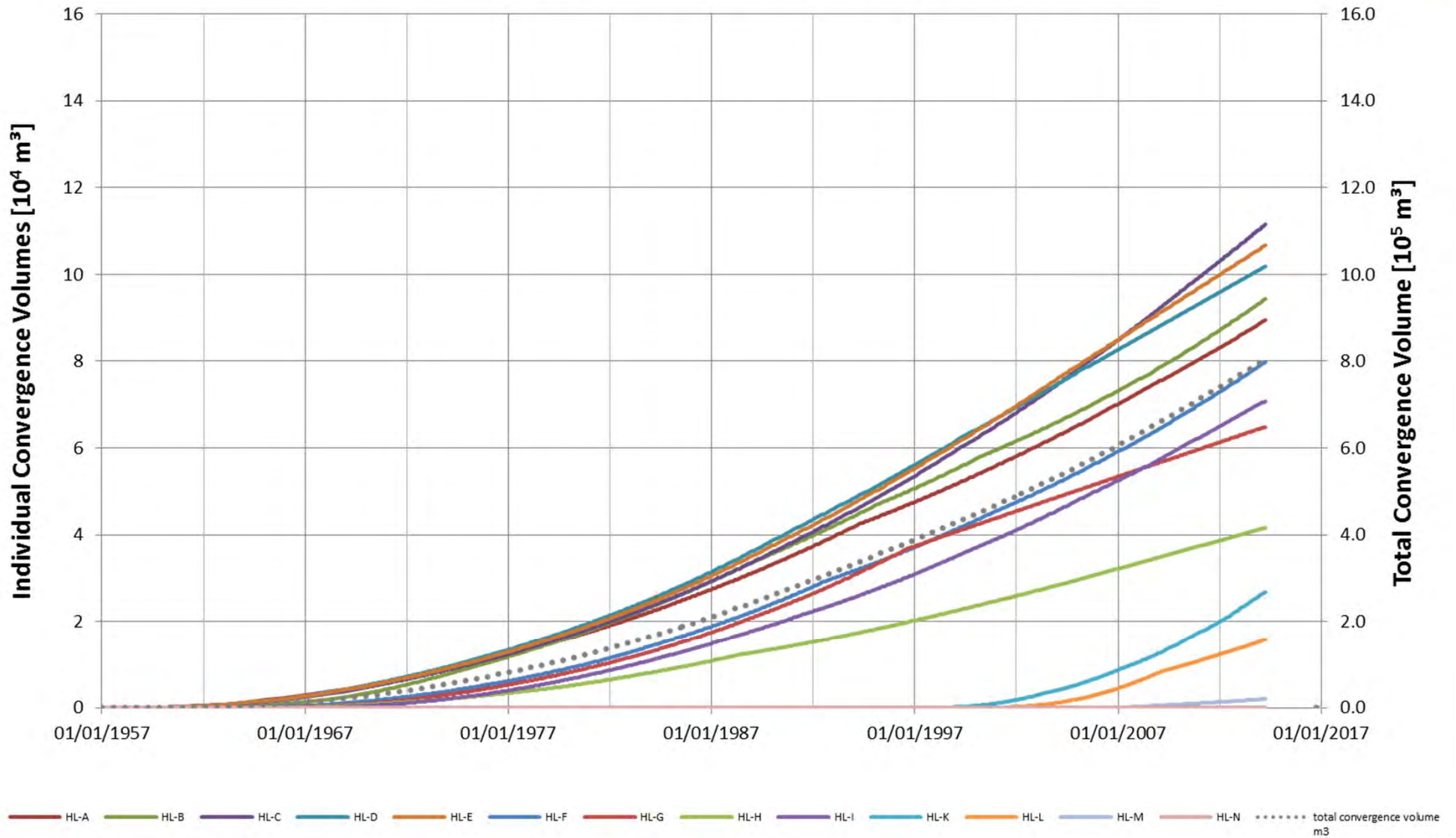
Cavern HL-M - Operation History - Cavern Volumes vs Time



Enclosure 15

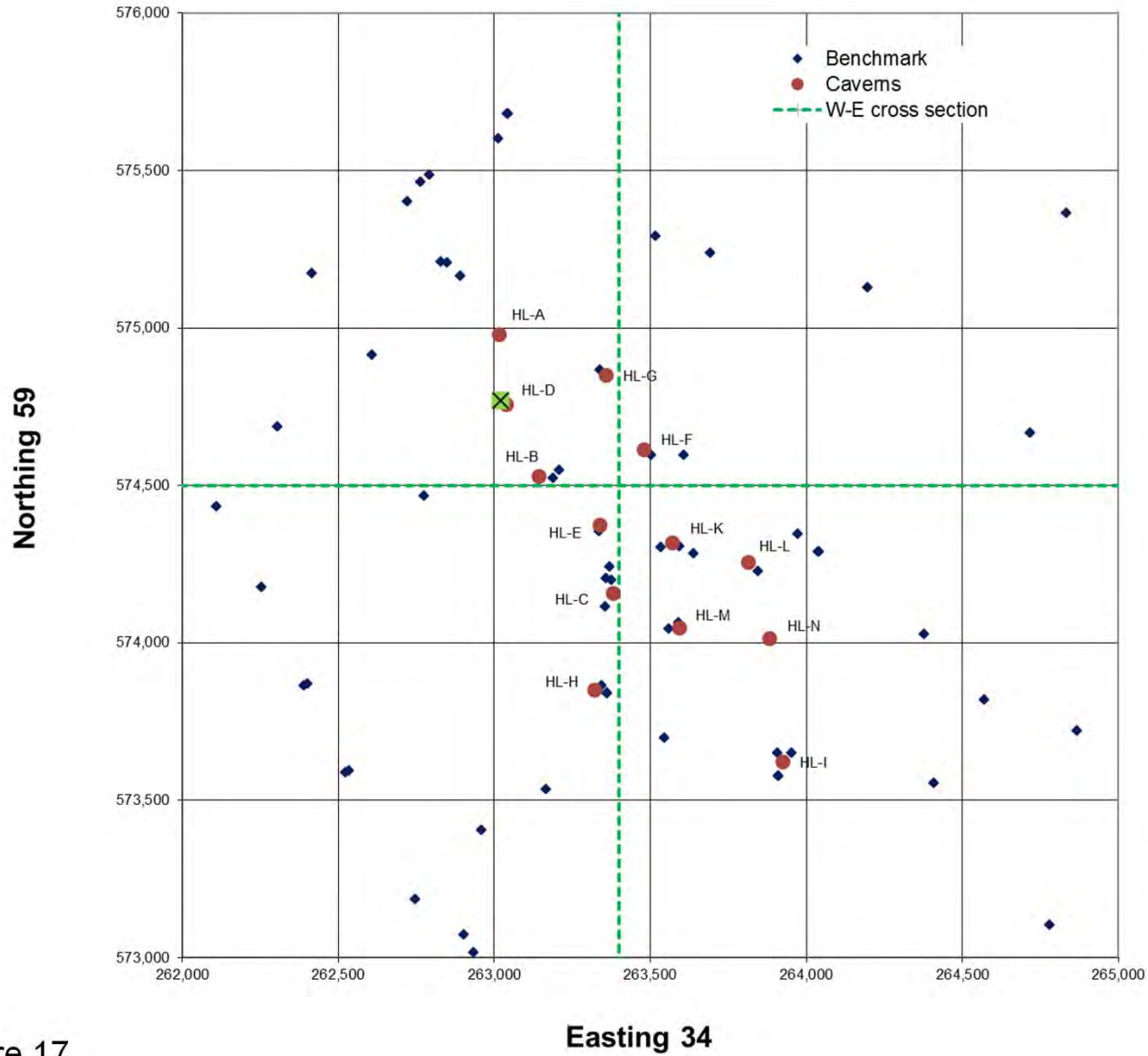
Cavern HL-M – Calculated volume versus time compared to sonar measurements

Akzo Nobel /Gasunie - Cumulated Convergence Volume



Enclosure 16

Heiligerlee – Calculated convergence volume versus time

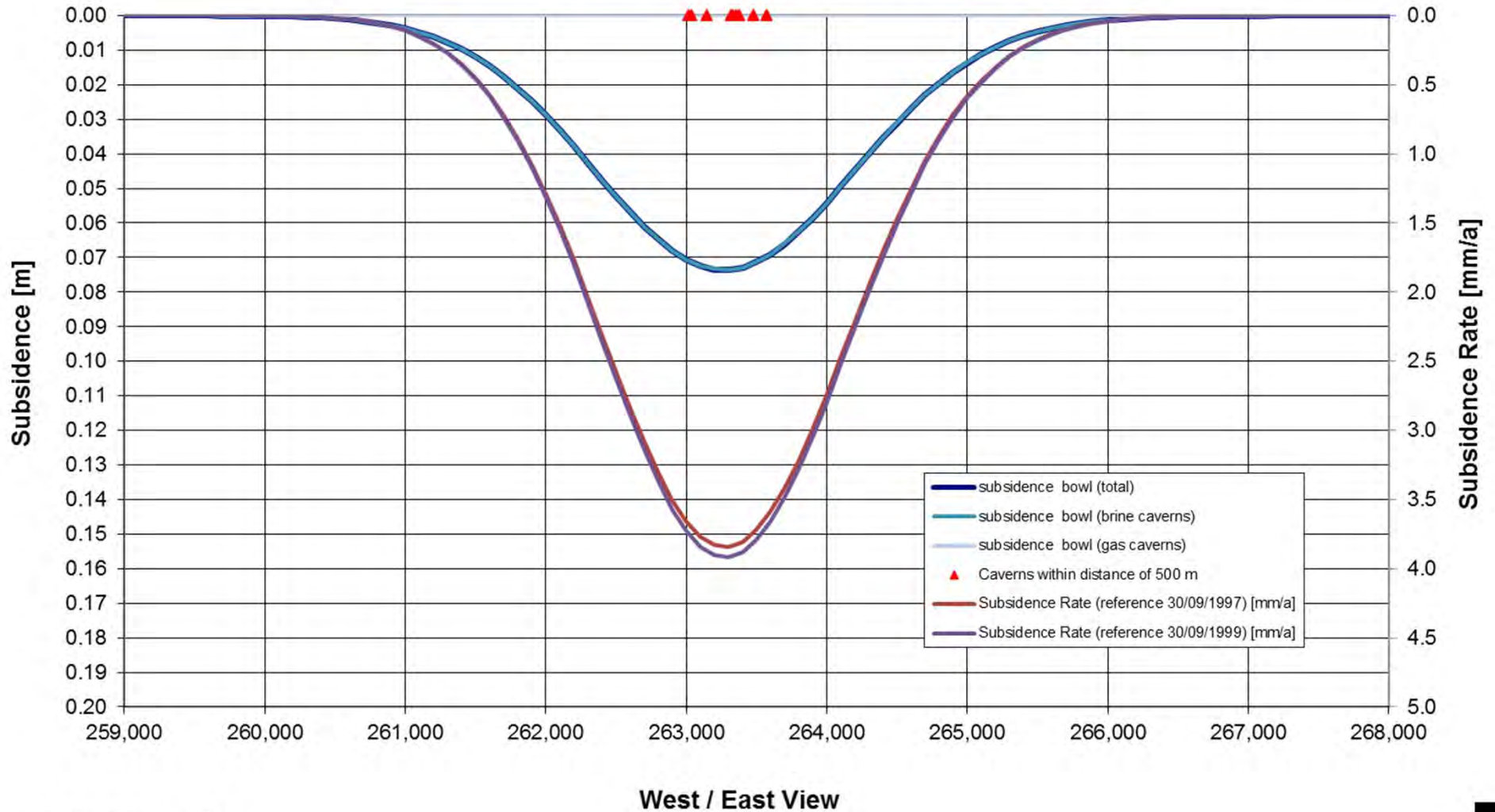


Enclosure 17
Heiligerlee – Map of cavern and benchmark locations

Subsidence Bowl at fixed Northing 574,500 (30/9/1998)

Heiligerlee - Superposition of all Caverns

Subsidence Modell 35-25-30-1-0.12-2-40-0.8-5-60



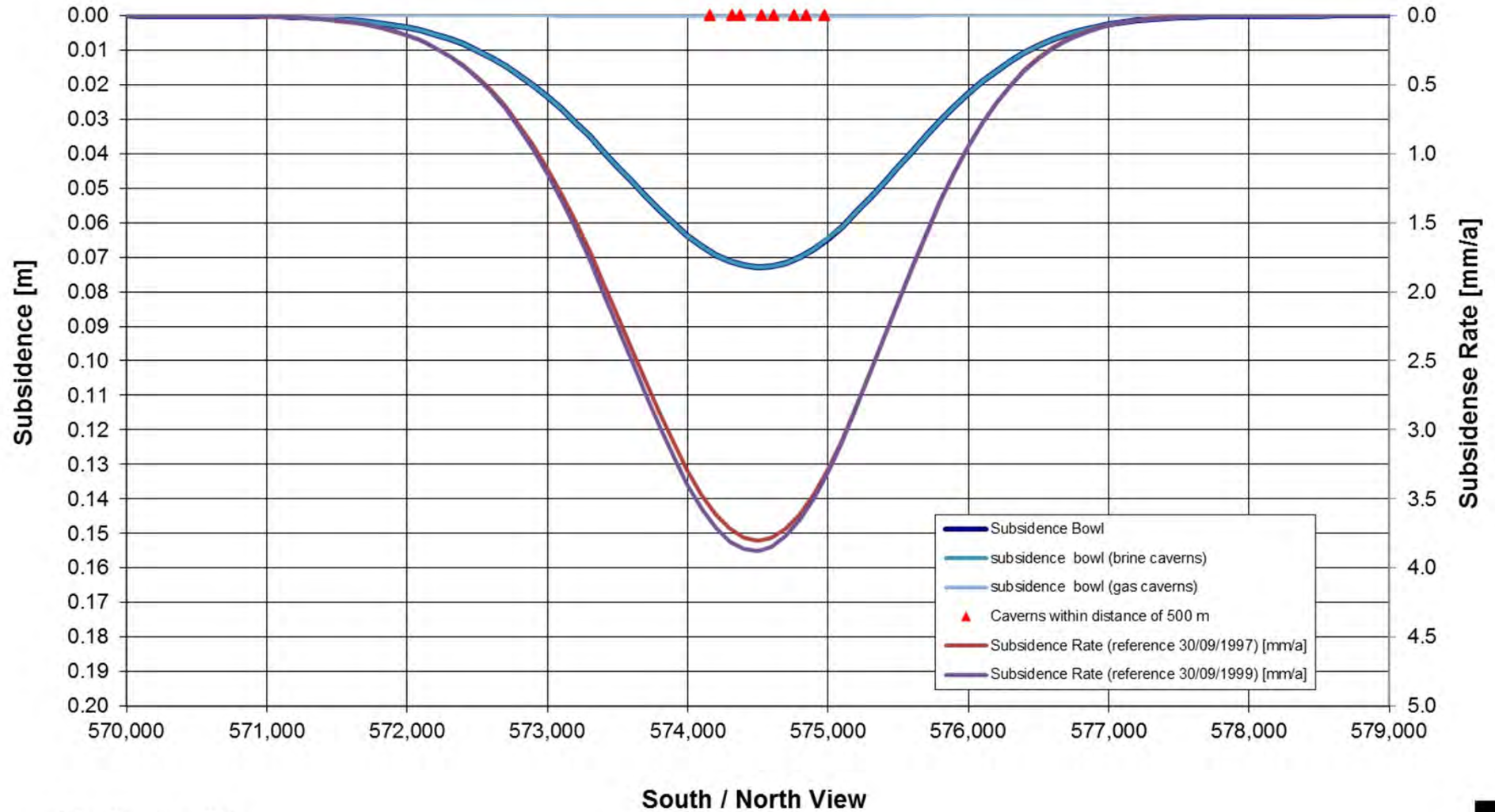
Enclosure 18

Heiligerlee – Subsidence bowl at fixed Northing 574,500 – 30/09/1998

Subsidence Bowl at fixed Easting 263,400 (30/9/1998)

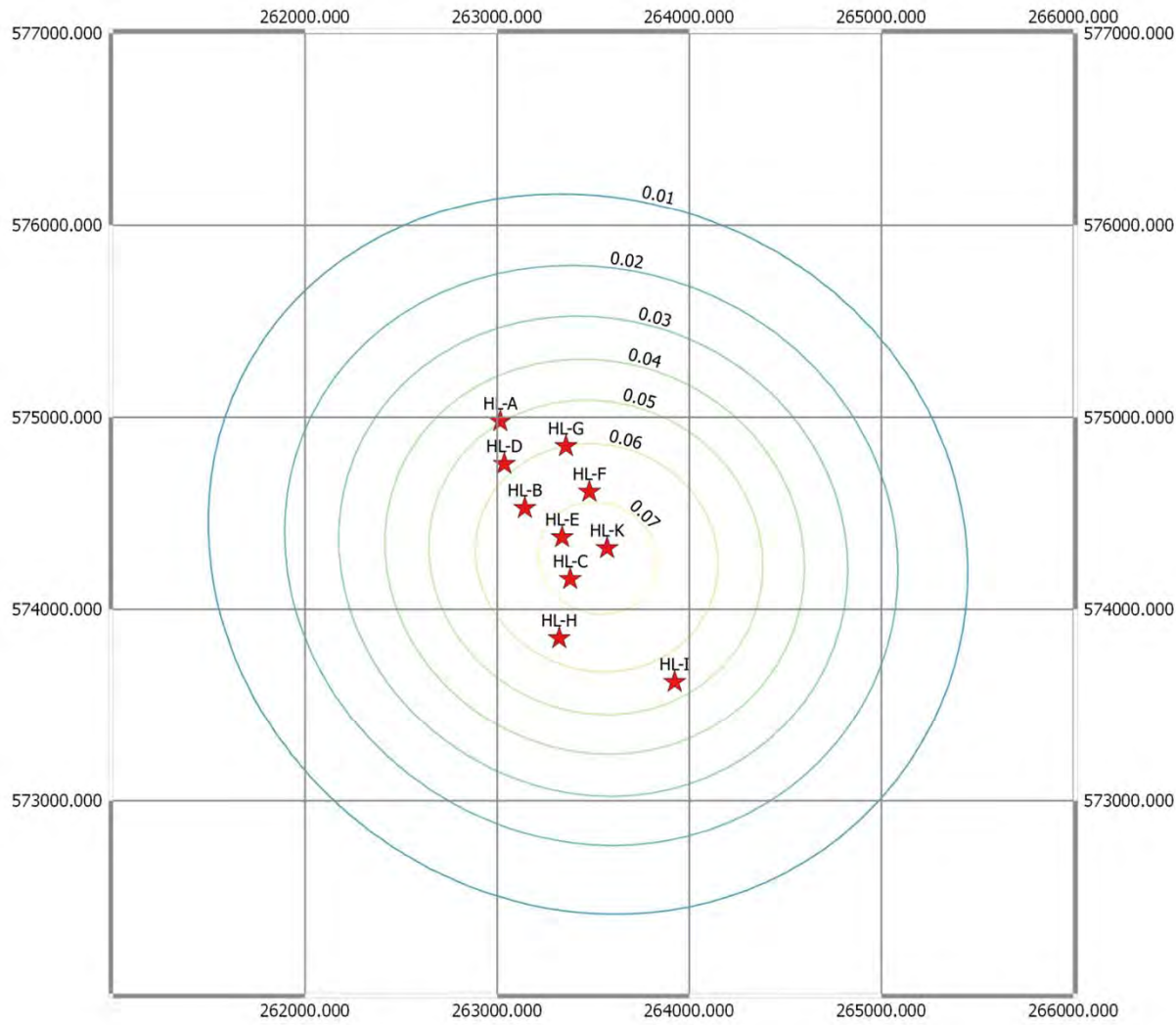
Heiligerlee - Superposition of all Caverns

Subsidence Modell 35-25-30-1-0.12-2-40-0.8-5-60



Enclosure 19

Heiligerlee – Subsidence bowl at fixed Easting 263,400 – 30/09/1998



Legende

1998 subsidence data_30/09/1998

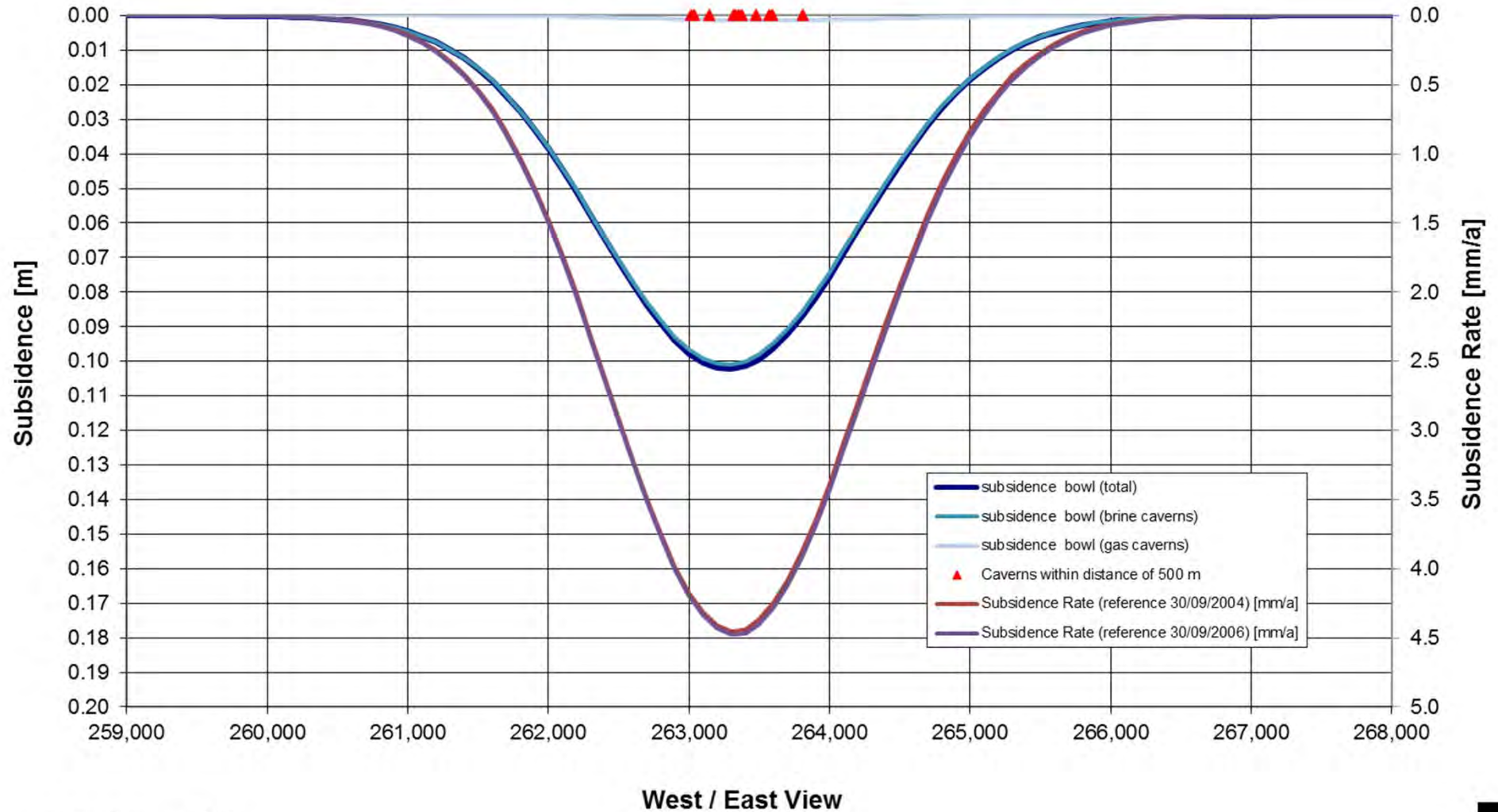
- 0
- 0.01
- 0.02
- 0.03
- 0.04
- 0.05
- 0.06
- 0.07
- 0.08
- 0.09
- 0.1
- 0.11
- 0.12
- 0.13
- 0.14
- 0.15
- 1998 subsidence data
- ★ 1998 cavern_data

Heiligerlee – Subsidence bowl – 31/10/1998

Subsidence Bowl at fixed Northing 574,500 (30/9/2005)

Heiligerlee - Superposition of all Caverns

Subsidence Modell 35-25-30-1-0.12-2-40-0.8-5-60



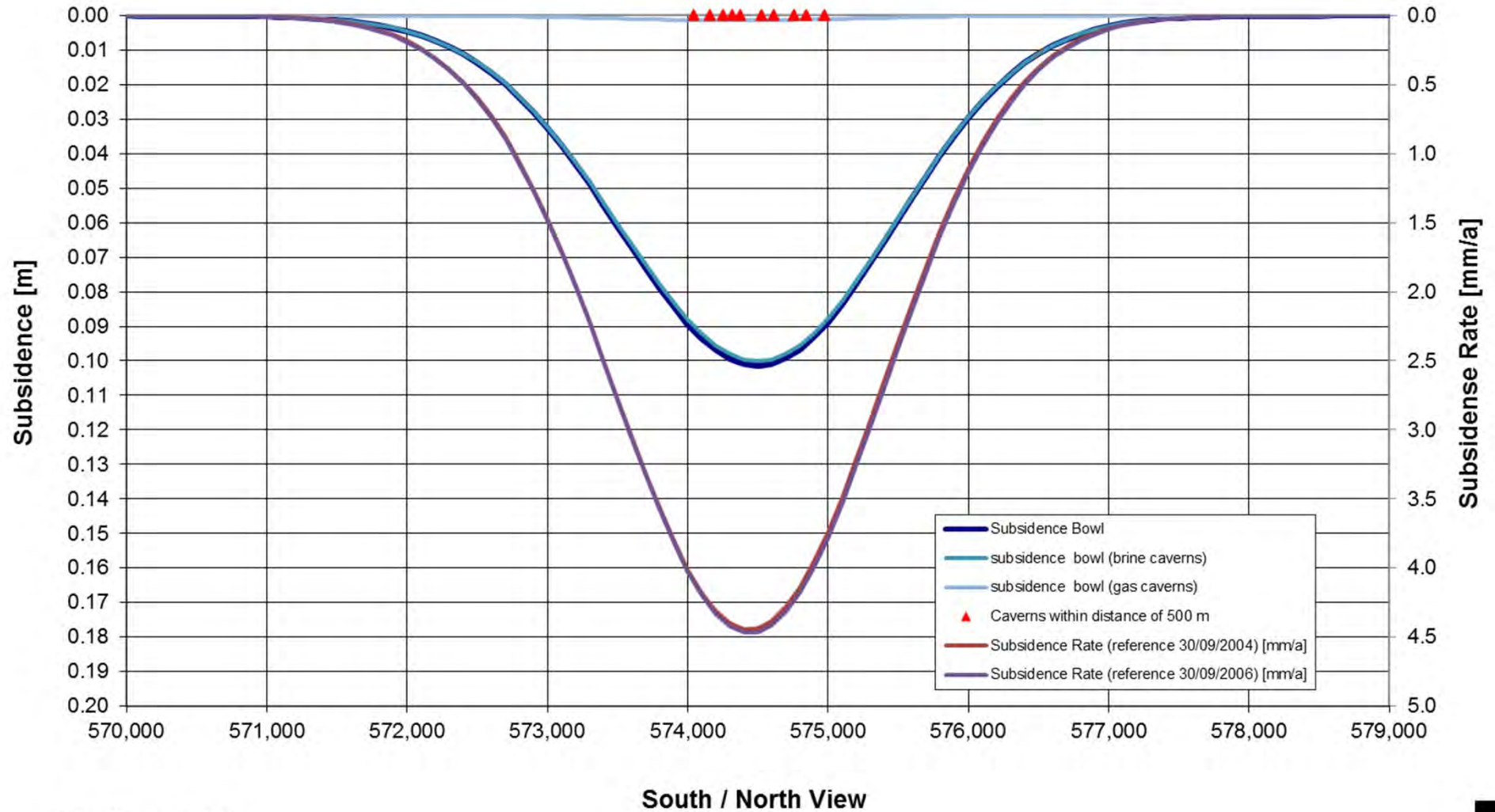
Enclosure 21

Heiligerlee – Subsidence bowl at fixed Northing 574,500 – 31/10/2005

Subsidence Bowl at fixed Easting 263,400 (30/9/2005)

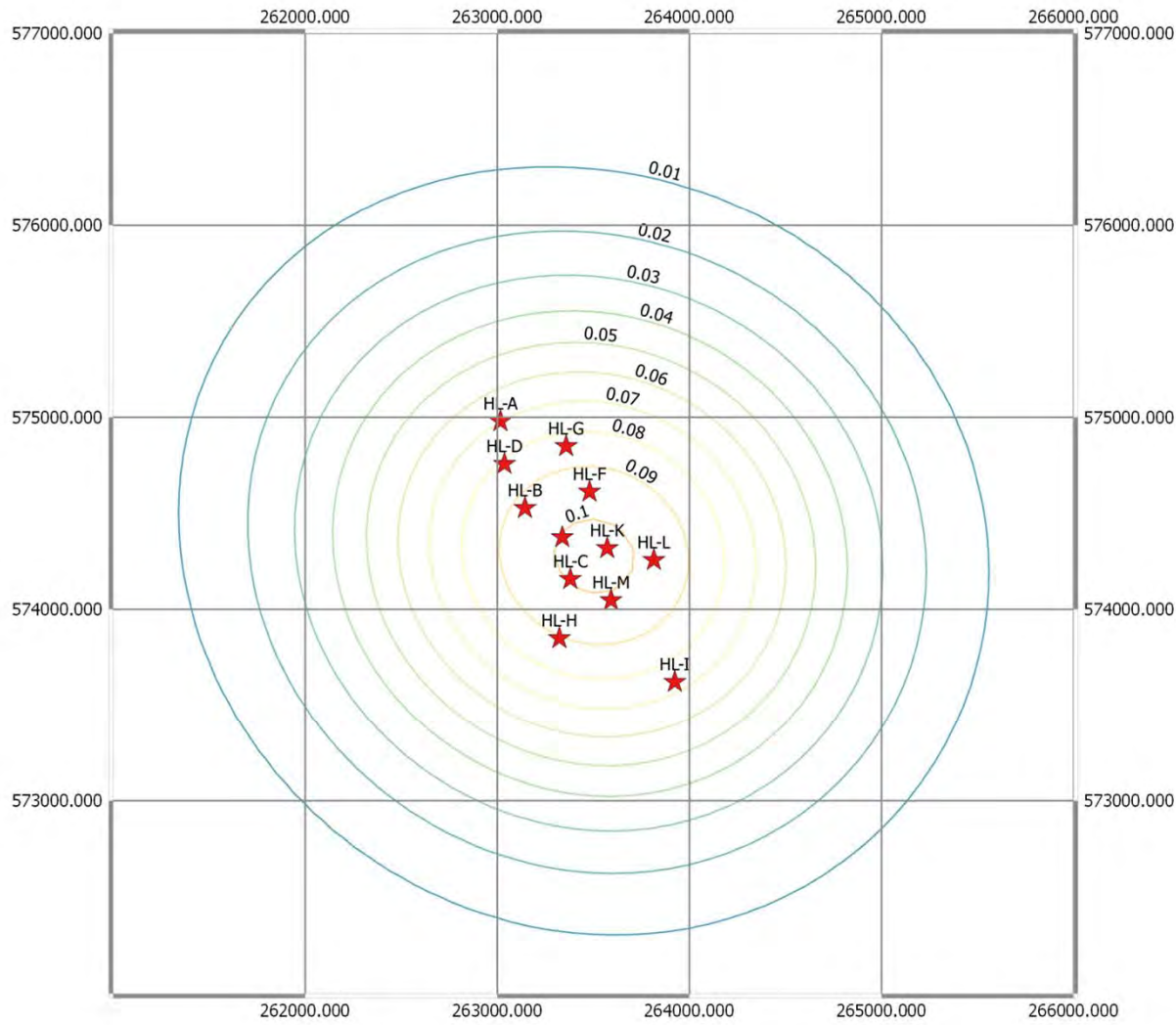
Heiligerlee - Superposition of all Caverns

Subsidence Modell 35-25-30-1-0.12-2-40-0.8-5-60



Enclosure 22

Heiligerlee – Subsidence bowl at fixed Easting 263,400 – 31/10/2005



Legende

2005 subsidence data_30/09/2005

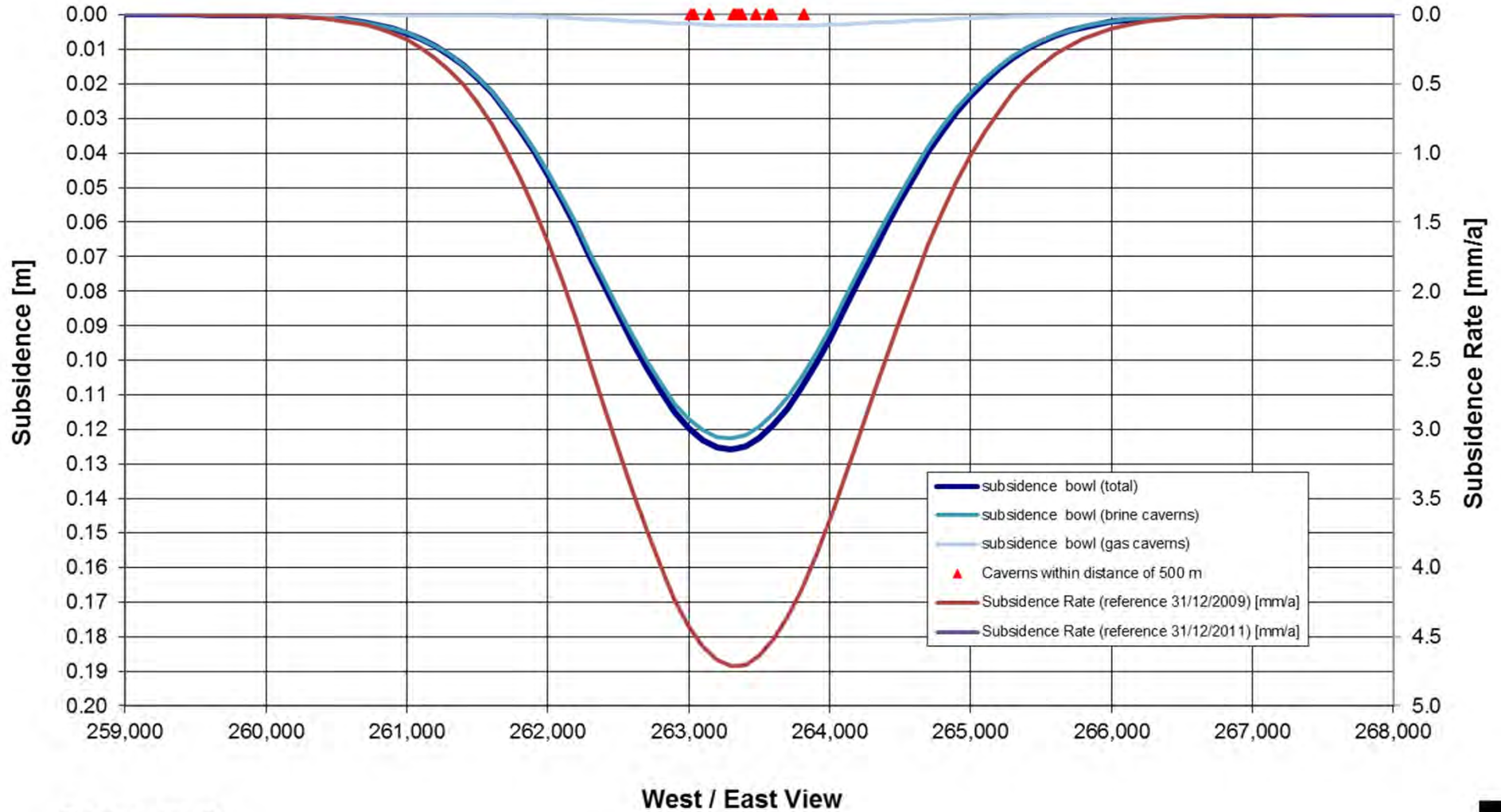
- 0
- 0.01
- 0.02
- 0.03
- 0.04
- 0.05
- 0.06
- 0.07
- 0.08
- 0.09
- 0.1
- 0.11
- 0.12
- 0.13
- 0.14
- 0.15
- 2005 subsidence data
- ★ 2005 cavern_data

Heiligerlee – Subsidence bowl – 31/10/2005

Subsidence Bowl at fixed Northing 574,500 (31/12/2010)

Heiligerlee - Superposition of all Caverns

Subsidence Modell 35-25-30-1-0.12-2-40-0.8-5-60



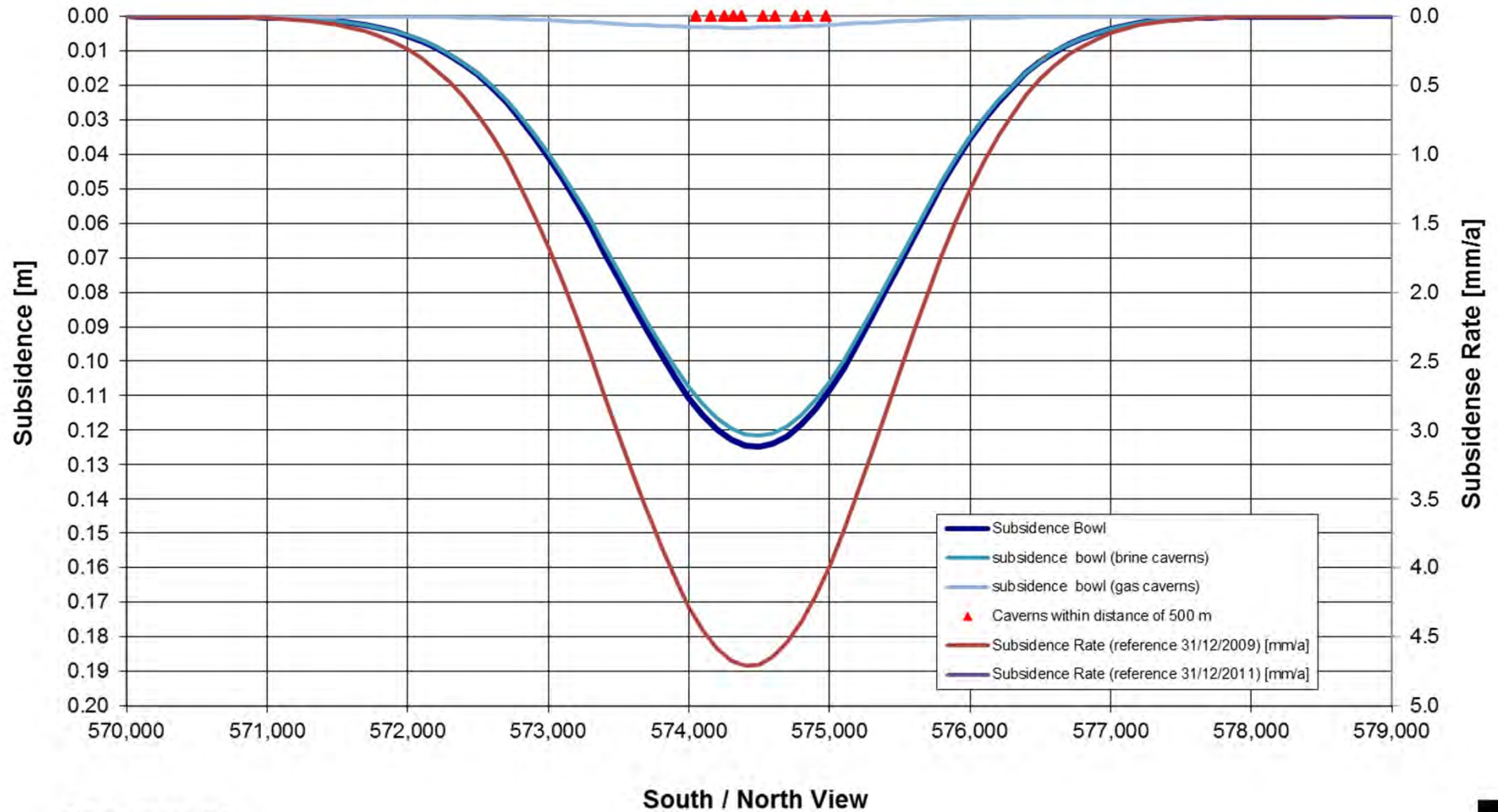
Enclosure 24

Heiligerlee – Subsidence bowl at fixed Northing 564,500 – 31/12/2010

Subsidence Bowl at fixed Easting 263,400 (31/12/2010)

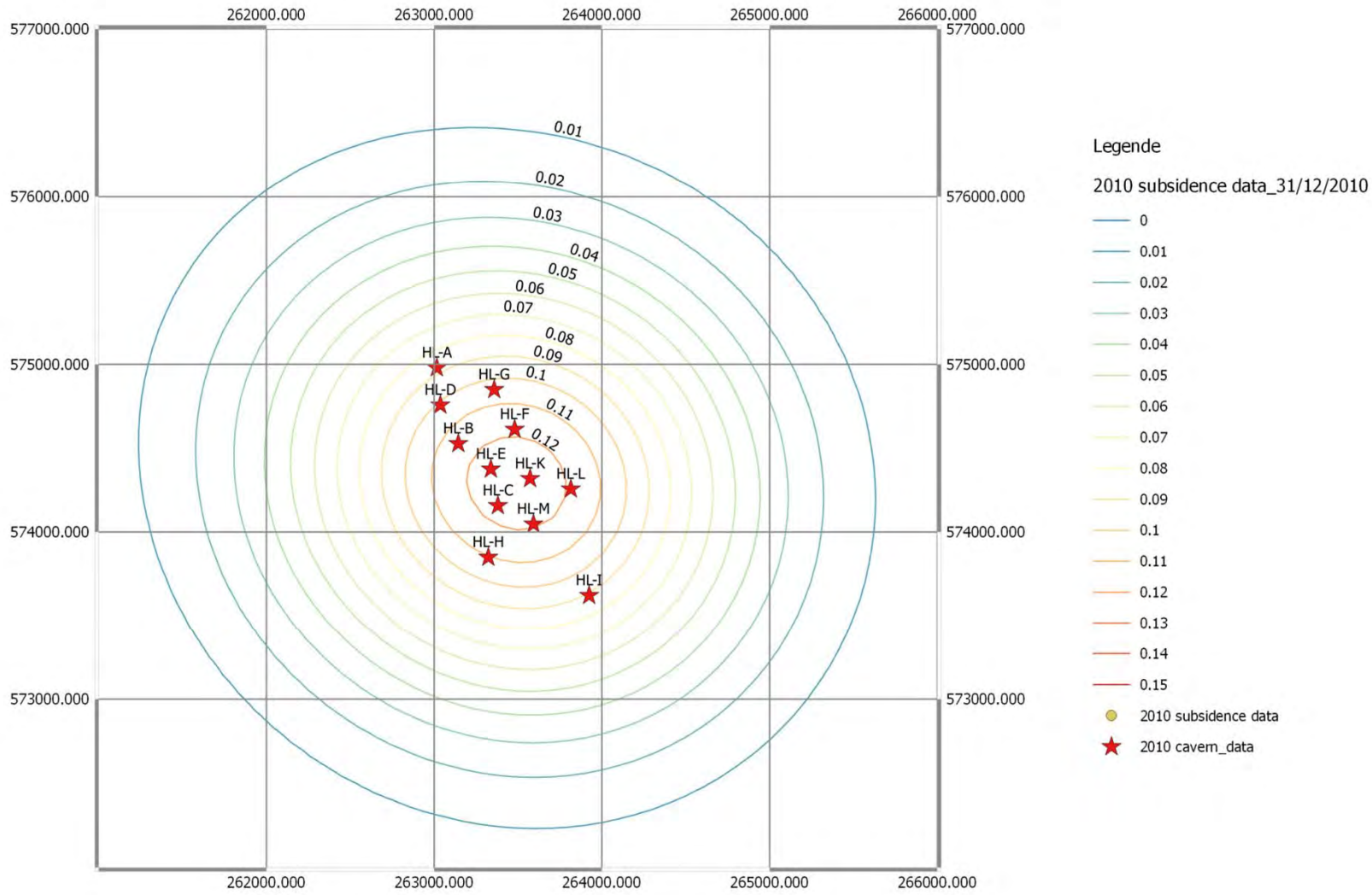
Heiligerlee - Superposition of all Caverns

Subsidence Modell 35-25-30-1-0.12-2-40-0.8-5-60



Enclosure 25

Heiligerlee – Subsidence bowl at fixed Easting 263,400 – 31/12/2010

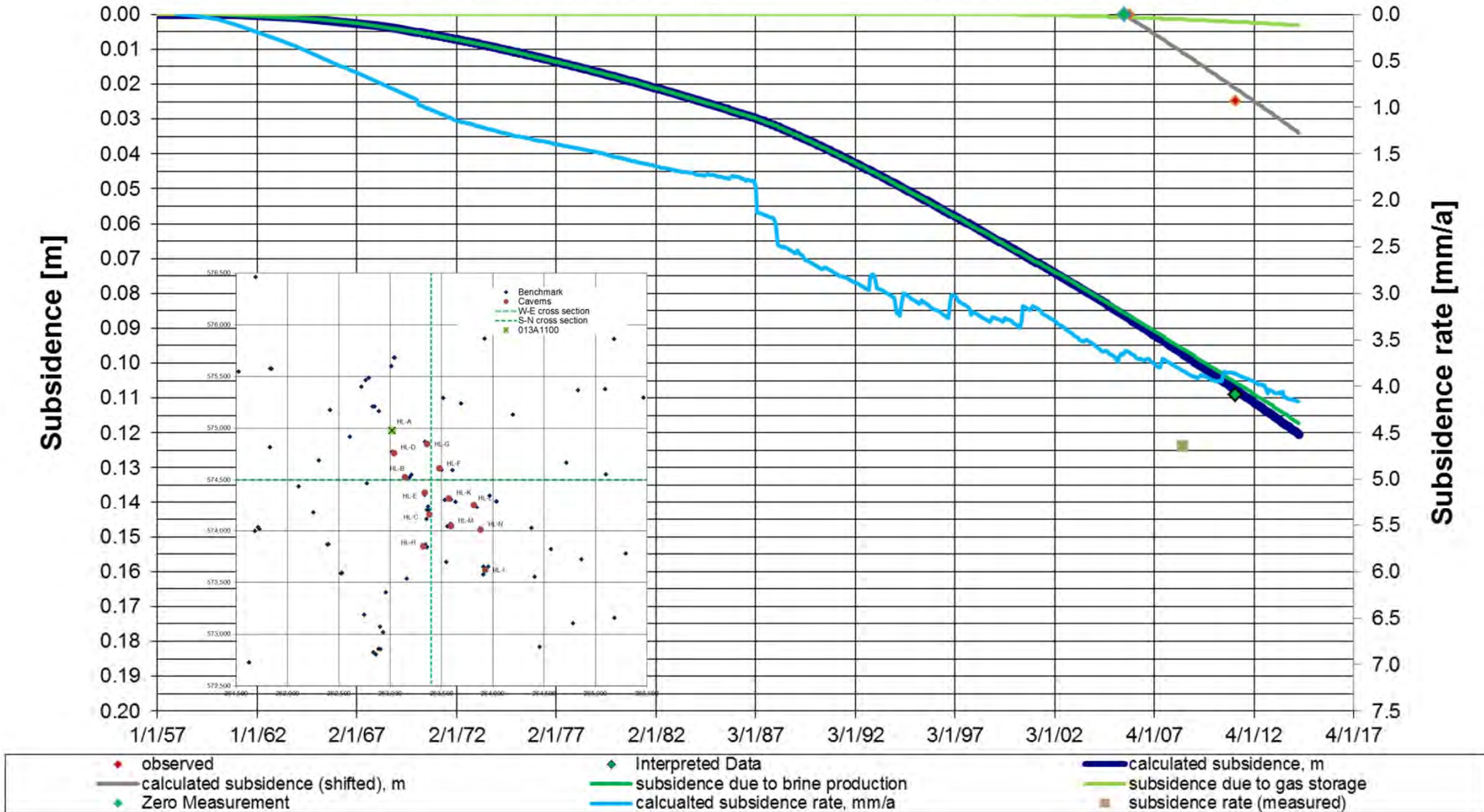


Heiligerlee – Subsidence bowl – 31/12/2010

AkzoNobel / Gasunie (Heiligerlee) - Subsidence Bowl (Gauss)

Benchmark 013A1100 (HL-A)

Subsidence Modell 35-25-30-1-0.12-2-40-0.8-5-60



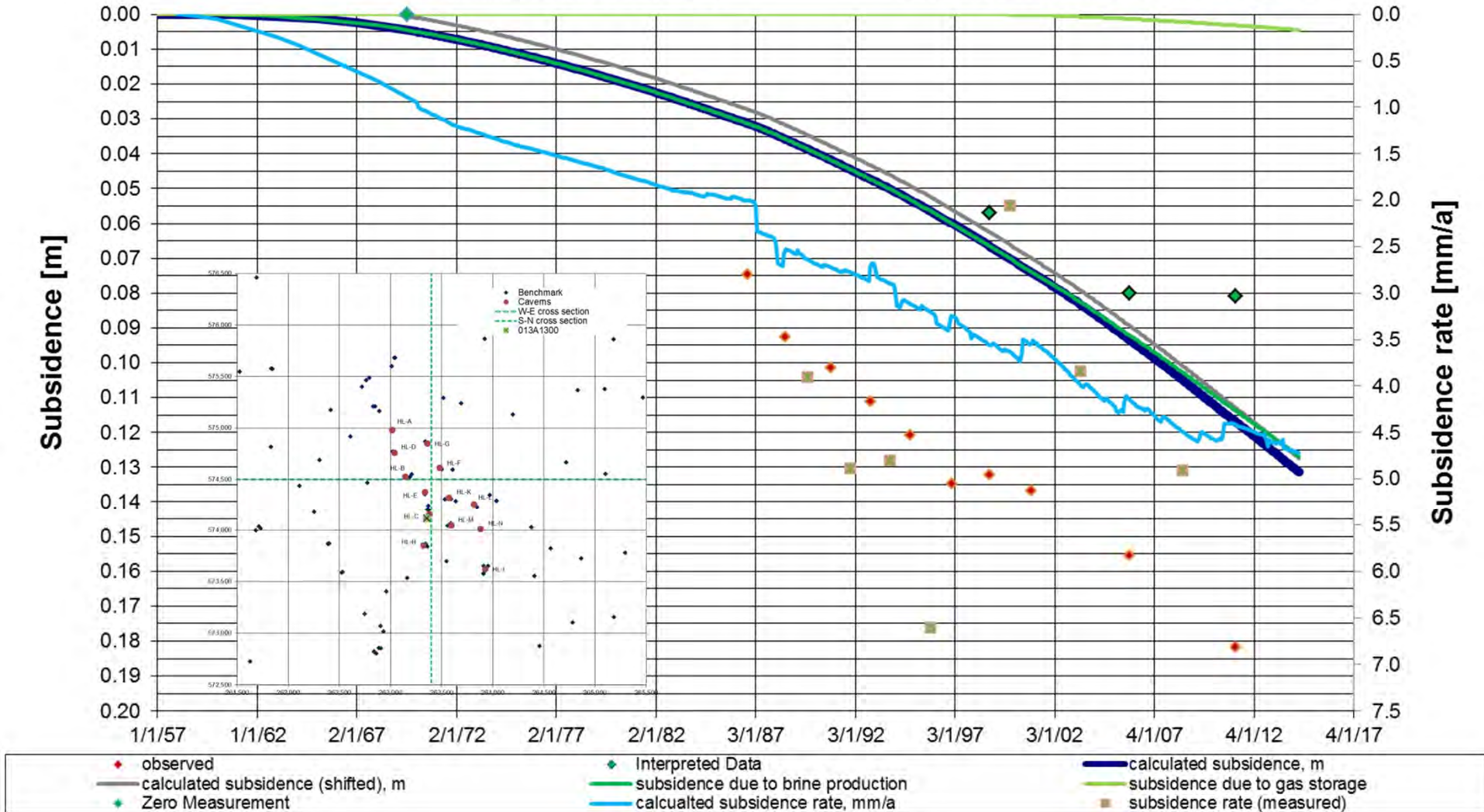
Enclosure 27

Heiligerlee – Benchmark 013A1100 – Comparison of observed subsidence with measured values

AkzoNobel / Gasunie (Heiligerlee) - Subsidence Bowl (Gauss)

Benchmark 013A1300 (HL-C)

Subsidence Modell 35-25-30-1-0.12-2-40-0.8-5-60



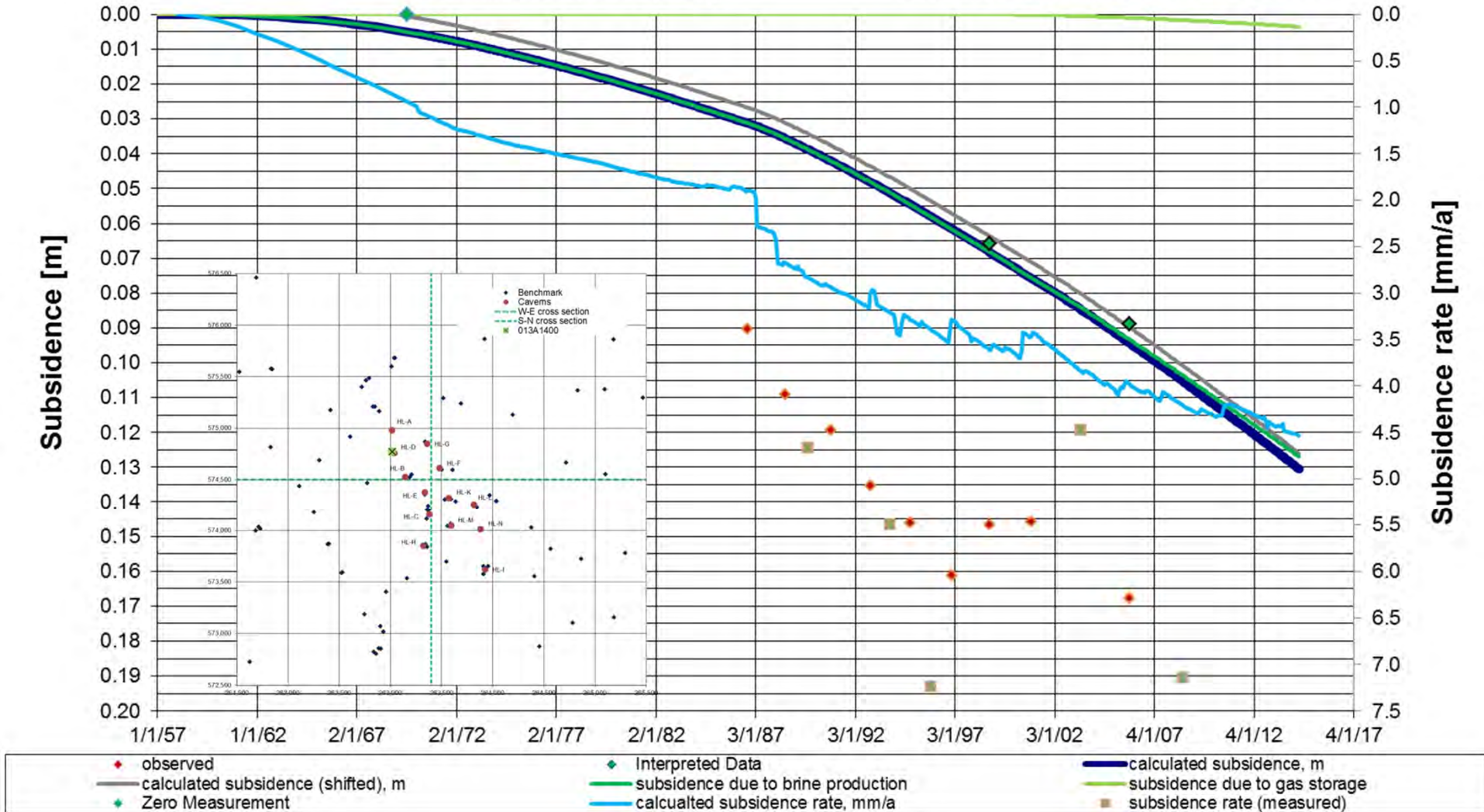
Enclosure 28

Heiligerlee – Benchmark 013A1300 – Comparison of observed subsidence with measured values

AkzoNobel / Gasunie (Heiligerlee) - Subsidence Bowl (Gauss)

Benchmark 013A1400 (HL-D)

Subsidence Modell 35-25-30-1-0.12-2-40-0.8-5-60



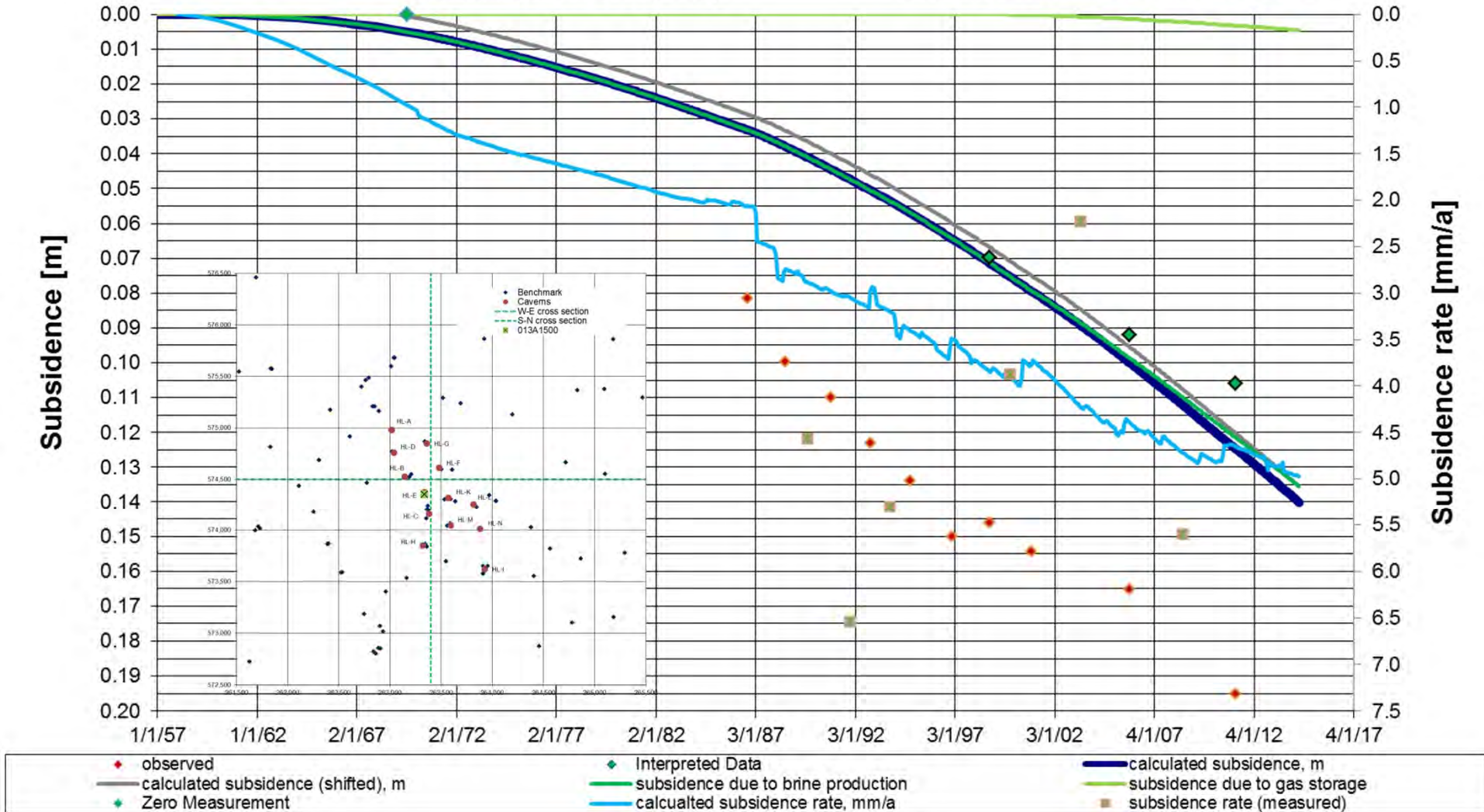
Enclosure 29

Heiligerlee – Benchmark 013A1400 – Comparison of observed subsidence with measured values

AkzoNobel / Gasunie (Heiligerlee) - Subsidence Bowl (Gauss)

Benchmark 013A1500 (HL-E)

Subsidence Modell 35-25-30-1-0.12-2-40-0.8-5-60



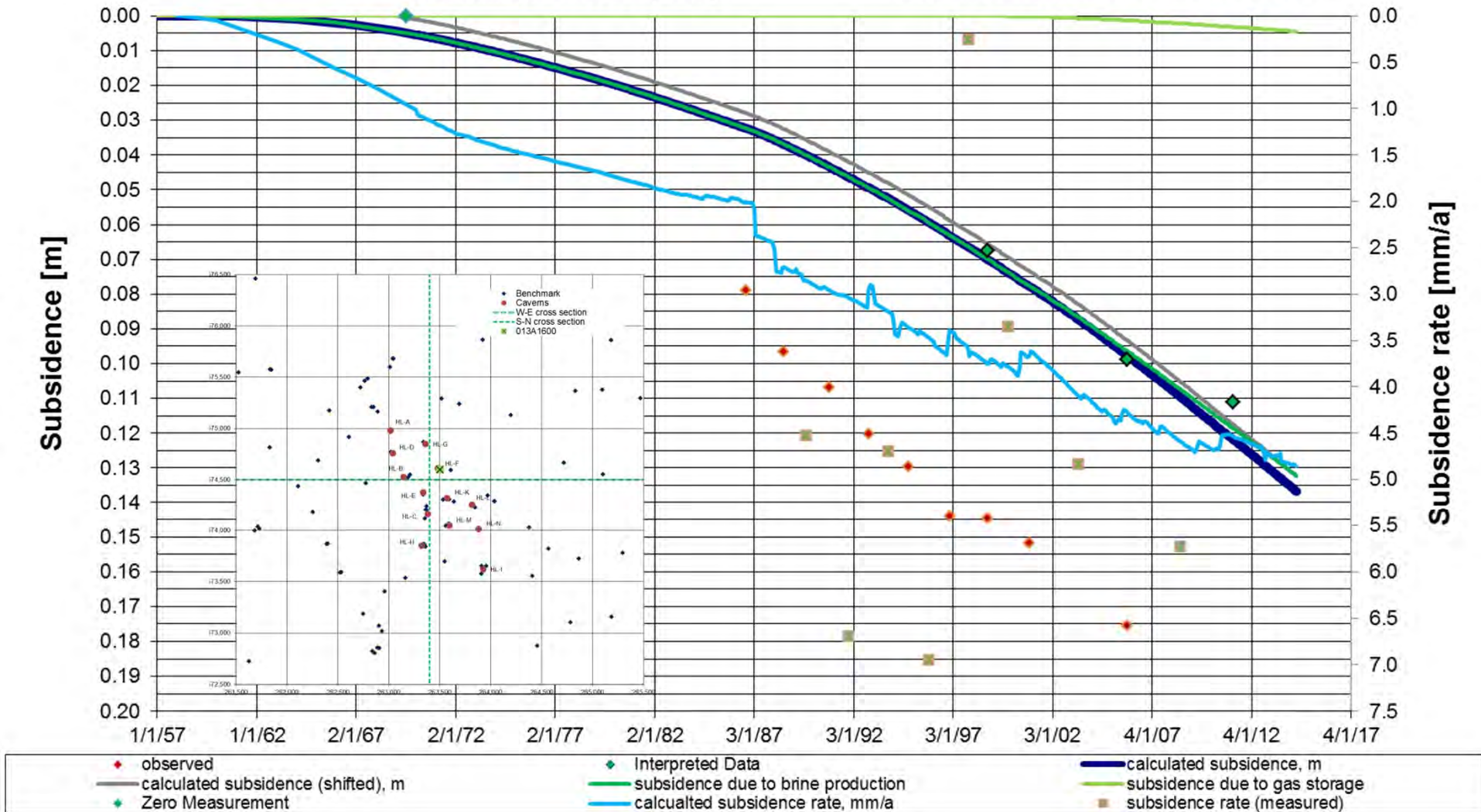
Enclosure 30

Heiligerlee – Benchmark 013A1500 – Comparison of observed subsidence with measured values

AkzoNobel / Gasunie (Heiligerlee) - Subsidence Bowl (Gauss)

Benchmark 013A1600 (HL-F)

Subsidence Modell 35-25-30-1-0.12-2-40-0.8-5-60



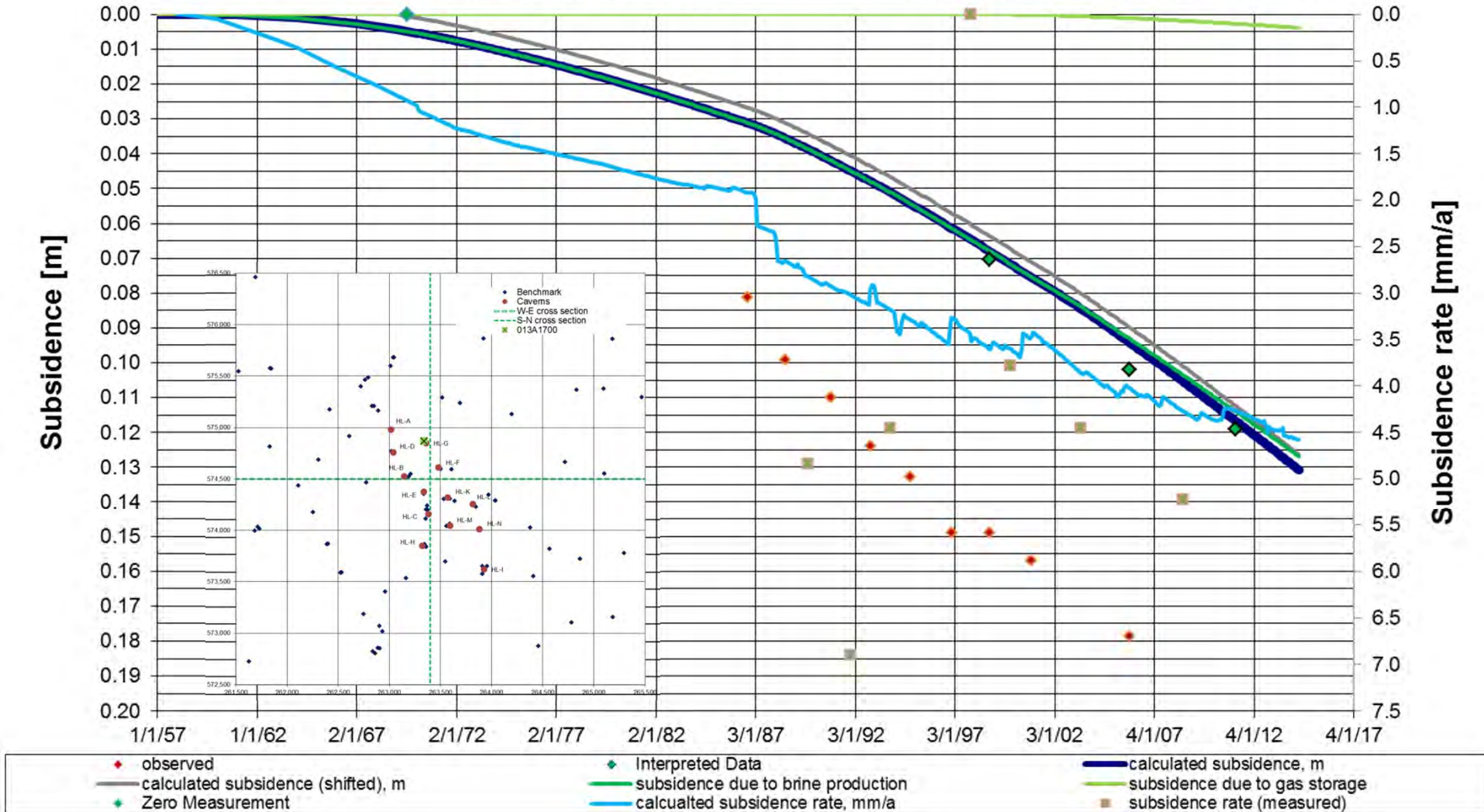
Enclosure 31

Heiligerlee – Benchmark 013A1600 – Comparison of observed subsidence with measured values

AkzoNobel / Gasunie (Heiligerlee) - Subsidence Bowl (Gauss)

Benchmark 013A1700 (HL-G)

Subsidence Modell 35-25-30-1-0.12-2-40-0.8-5-60



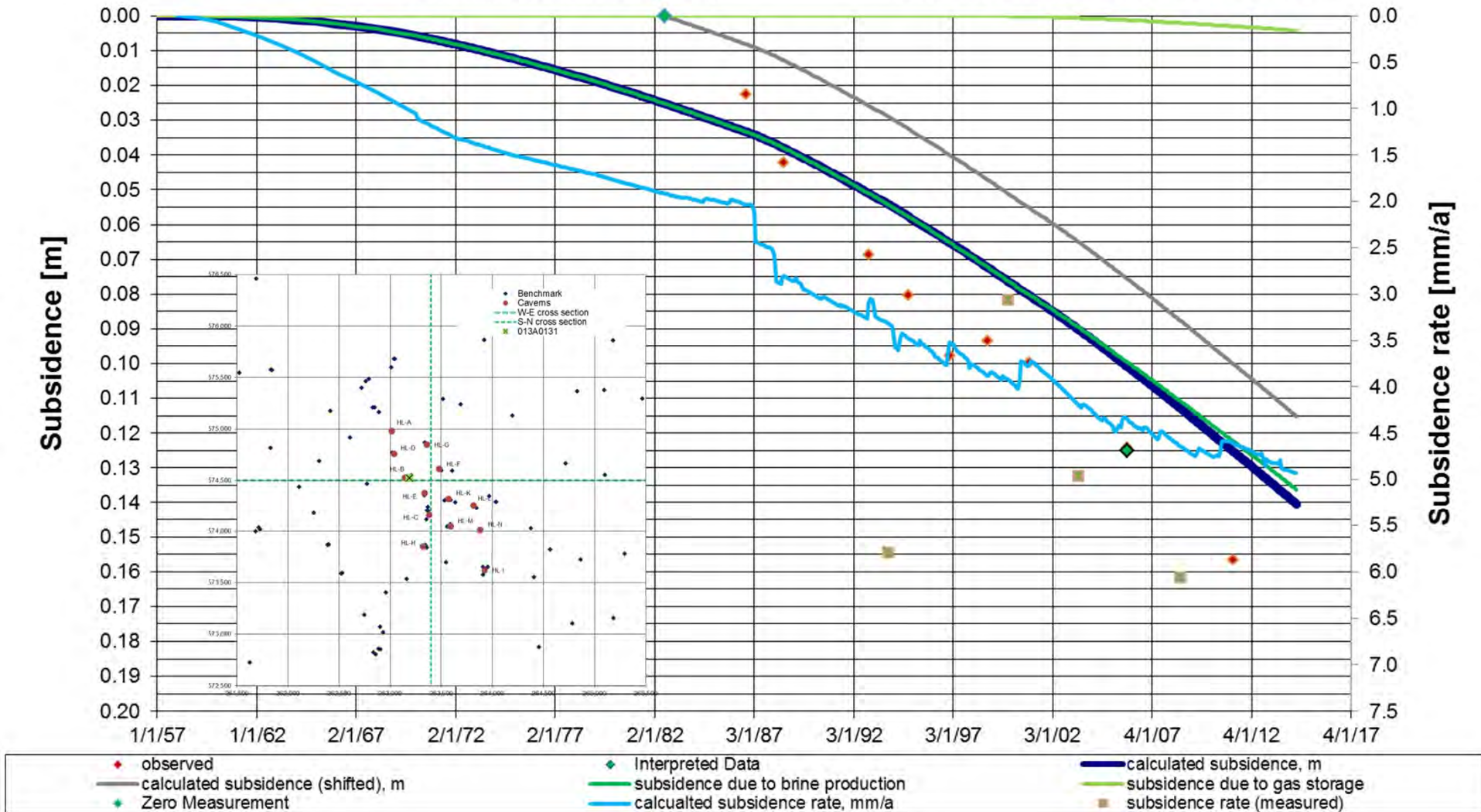
Enclosure 32

Heiligerlee – Benchmark 013A1700 – Comparison of observed subsidence with measured values

AkzoNobel / Gasunie (Heiligerlee) - Subsidence Bowl (Gauss)

Benchmark 013A0131 (HL-B)

Subsidence Modell 35-25-30-1-0.12-2-40-0.8-5-60



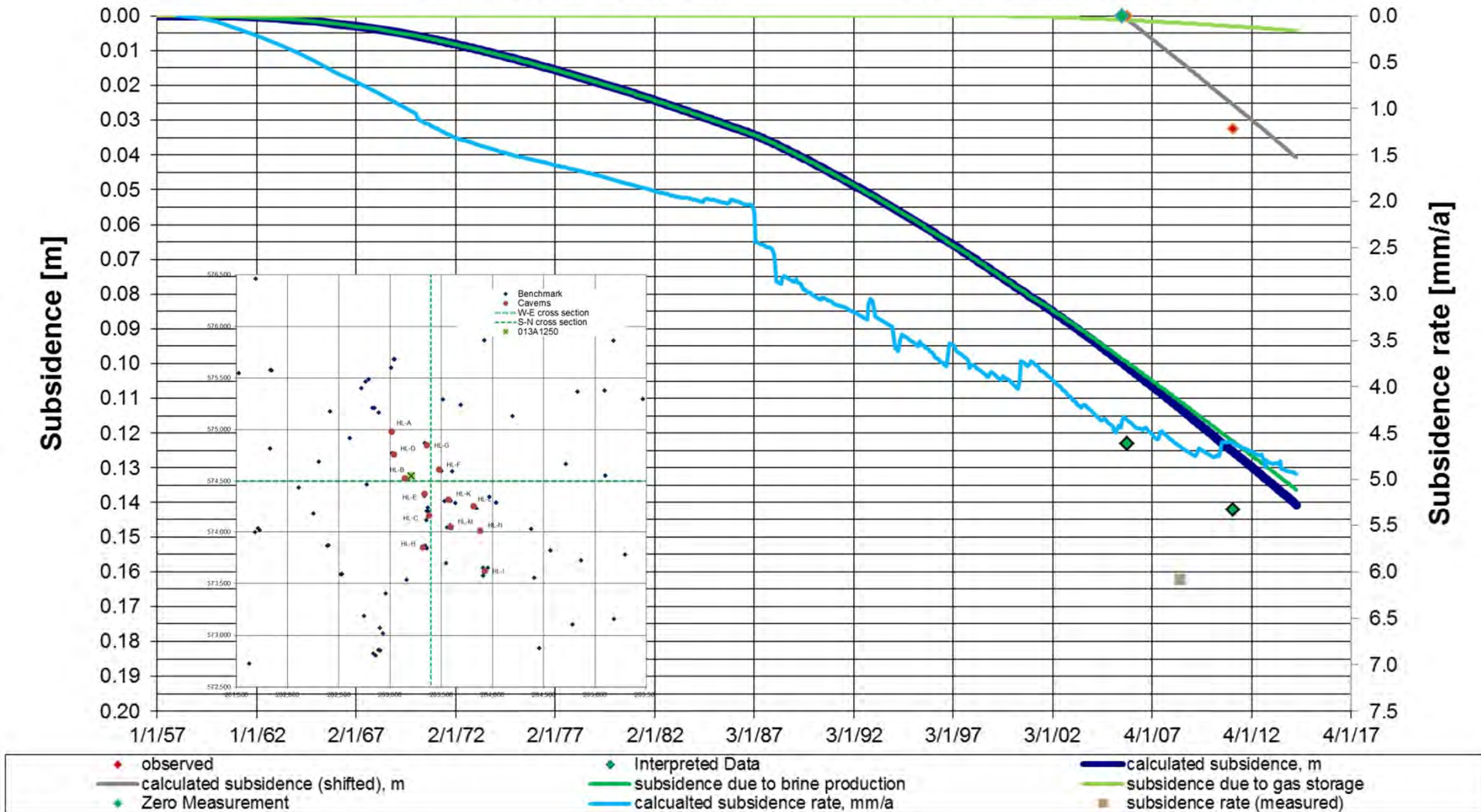
Enclosure 33

Heiligerlee – Benchmark 013A0131 – Comparison of observed subsidence with measured values

AkzoNobel / Gasunie (Heiligerlee) - Subsidence Bowl (Gauss)

Benchmark 013A1250 (HL-B)

Subsidence Modell 35-25-30-1-0.12-2-40-0.8-5-60



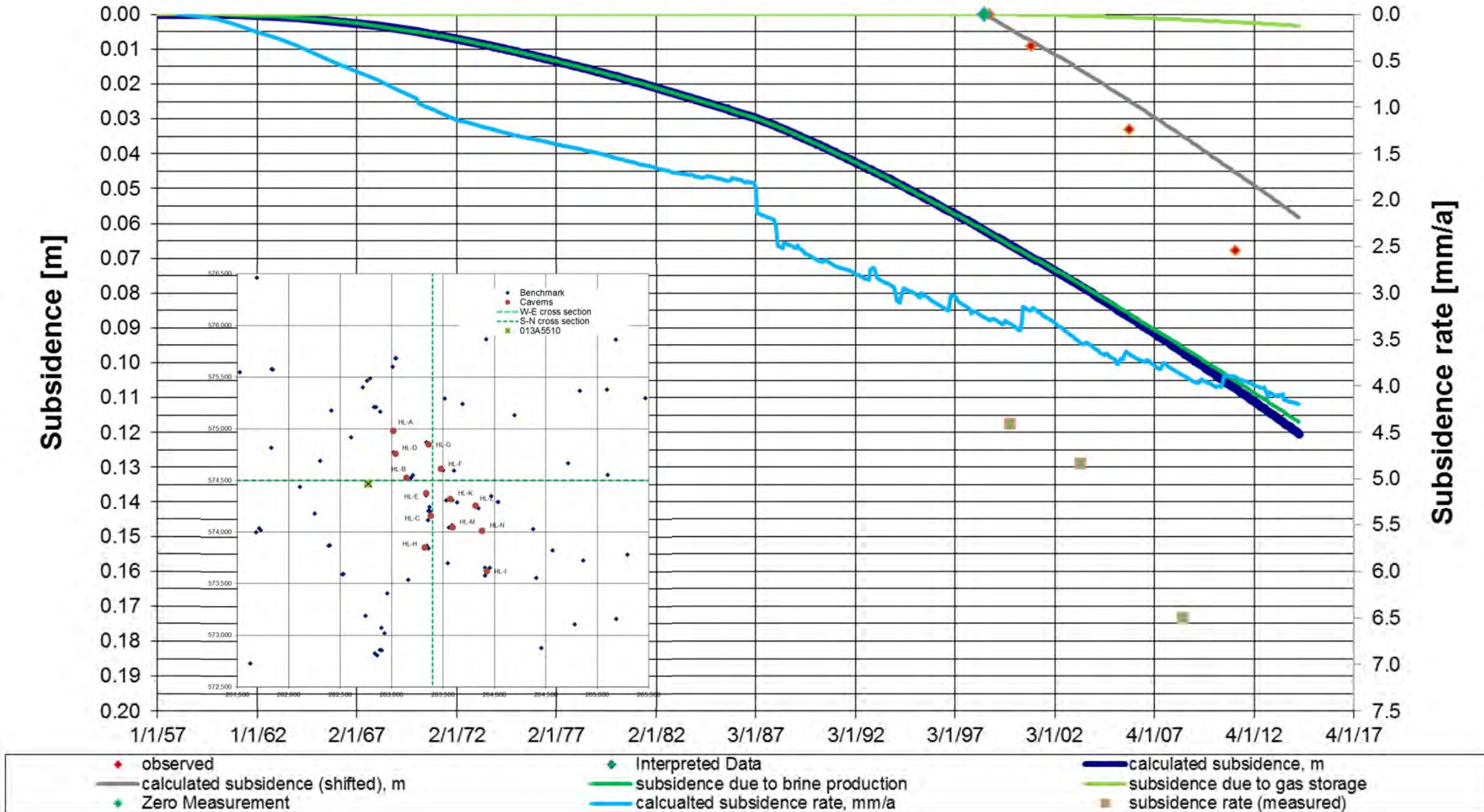
Enclosure 34

Heiligerlee – Benchmark 013A1250 – Comparison of observed subsidence with measured values

AkzoNobel / Gasunie (Heiligerlee) - Subsidence Bowl (Gauss)

Benchmark 013A5510 (HL-B)

Subsidence Modell 35-25-30-1-0.12-2-40-0.8-5-60



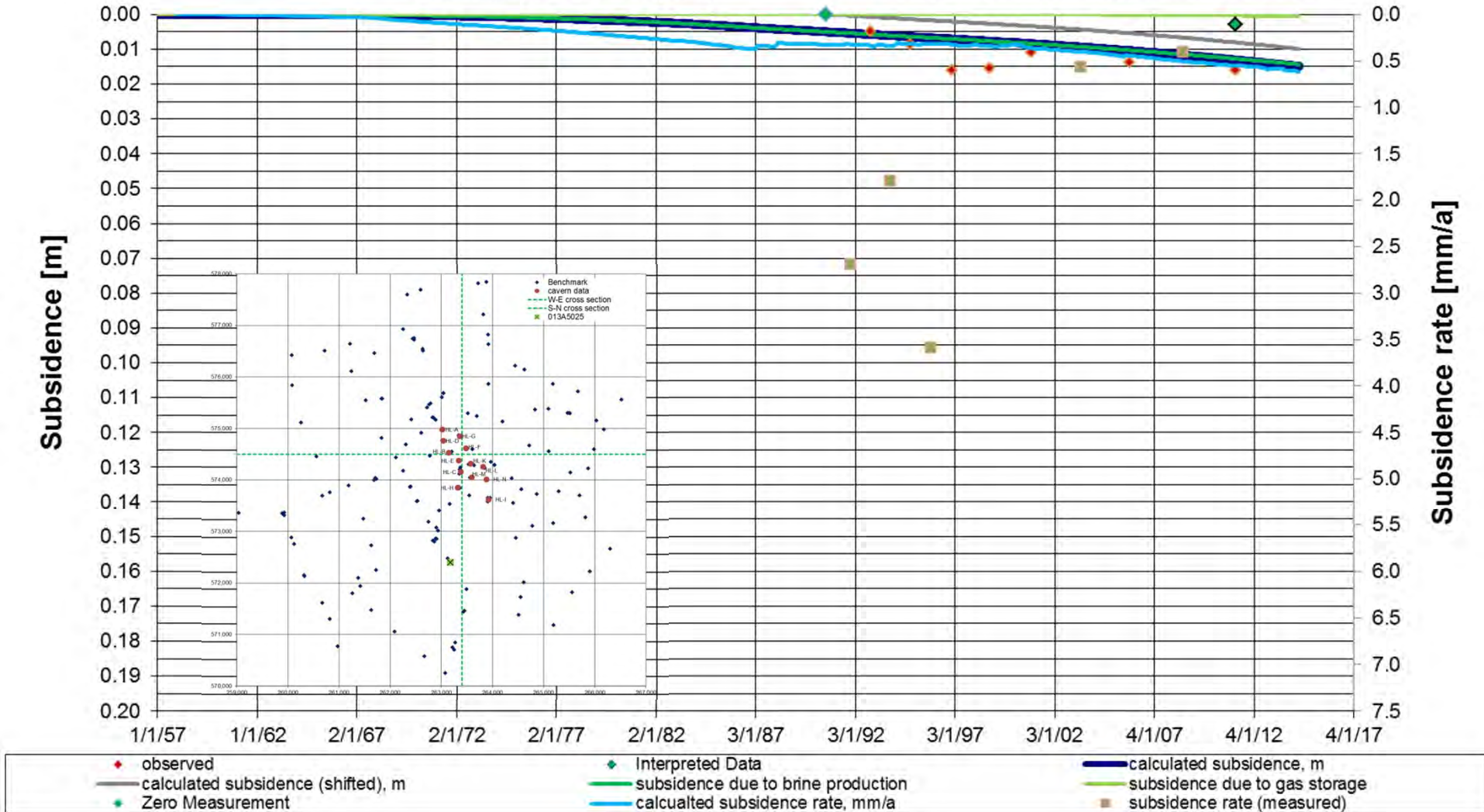
Enclosure 35

Heiligerlee – Benchmark 013A5510 – Comparison of observed subsidence with measured values

AkzoNobel / Gasunie (Heiligerlee) - Subsidence Bowl (Gauss)

Benchmark 013A5025 (HL-I)

Subsidence Modell 35-25-30-1-0.12-2-40-0.8-5-60



Enclosure 36

Heiligerlee – Benchmark 013A5025 – Comparison of observed subsidence with measured values

Tab: HL WP3 Report Subsidence Prediction

Prediction of Subsidence above Caverns at Heiligerlee, The Netherlands Operation Phase Report on WP3: Subsidence Prediction

for

ANIC

Akzo Nobel Industrial Chemicals Delftzijl

Osterborn 4, Central Warehouse

9936 HD Delfzijl

THE NETHERLANDS

Client Inquiry No.: 4570130812

Client Project No.:

KBB UT Project No.: 5240-881094

Author(s): Dr.-Ing. Dirk Zander-Schiebenhöfer, KBB UT

B. Sc. Birgit Horváth, KBB UT

Dipl.-Geol. Raphael Schäfer, DEEP.

Checked: Sf

Approved: DZ

Date: 13.04.2016

Revision: 00c

Table of Contents

1	Introduction	3
2	Scope of Work – WP3	4
3	Subsidence Prediction for End of October 2015	5
3.1	Procedure	5
3.2	Maps and Graphs	5
3.3	Discussion of the results	5
4	Subsidence Prediction until End of 2050	6
4.1	Procedure	6
4.2	Maps and Graphs	6
4.3	Discussion of the results	7
5	Summary and Conclusion	9
	References	10
	List of Enclosures.....	11
	Enclosures	13

List of Tables

Table 3.1	Selected representation of the subsidence prediction for October 31, 2015	5
Table 4.1	Selected representation of the subsidence predictions	7
Table 4.2	Predicted values of maximum subsidence due to cavern operation at Heiligerlee	8

1 Introduction

Since 1956 Akzo Nobel Industrial Chemicals Delfzijl (AkzoNobel), The Netherlands, is leaching salt caverns at Heiligerlee. Currently 11 caverns (HL-A to HL-I and HL-L to HL-M) are in operation for brine production and one cavern (HL-K) has been converted into a nitrogen storage cavern, which is owned by Gasunie Transport Services B.V. (subsidiary of N.V. Nederlandse Gasunie) and operated by N.V. Nederlandse Gasunie, The Netherlands. Well HL-N has not been drilled so far, only the location has been planned.

Salt caverns, either for gas storage or brine production, show volume losses (convergence) over time due to creep of the surrounding salt rock mass. These volume losses are transferred through the overburden layers to the surface, where a subsidence bowl develops. Keeping cavern convergence and thereby subsidence as small as possible is of great importance for the operator as well as for the public. Thus, it is mandatory to periodically measure subsidence by levelling measurements. Furthermore, the authorities in the Netherlands demand for the prediction of subsidence prior to each levelling campaign.

At Heiligerlee, different sources – gas production, brine production, gas storage, ground compaction and erosion – contribute to surface subsidence. Therefore, theoretical subsidence models are applied in order to differentiate the individual contributions to surface subsidence and relate them to the involved operators. Within the scope of the present study calculated and/or predicted subsidence or subsidence rates are only due to convergence and are *explicitly not given* due to other influencing factors like oxidation of special layers, compaction of the ground and change in ground water level.

KBB Underground Technologies GmbH, Hannover, Germany, has been appointed by AkzoNobel to develop a capable simulation model matching the so far history of subsidence. DEEP Underground Engineering (DEEP), Bad Zwischenahn, Germany, has been subcontracted in order to contribute to this study. The developed model shall reliably predict future surface subsidence caused only by brine production and nitrogen storage in the caverns at Heiligerlee.

After screening and summarizing the relevant documentation on subsidence due to brine production and gas storage at Heiligerlee (see report '**Work Package 1 (WP1) – Screening of Documentation**') the subsidence simulation model has been established according to the scope of '**Work Package 2 (WP2) Establishing the Simulation Model**'. The present report summarizes the results according to the scope of work of '**Work Package 3 (WP3)**'. The aim of WP3 is to predict cavern related subsidence at Heiligerlee until 2050 by applying the established, verified and validated subsidence.

During execution of the scope of work, it turned out that the authorities demand for an additional subsidence prediction in advance to the levelling campaign, which was scheduled for autumn, 2015. This prediction should be based on up-to-date operation data. Therefore, it has been decided to choose the end of October, 2015 as reference and present an additional prediction for this point in time. This prediction is also given in the present report.

2 Scope of Work – WP3

Two different kinds of predictions have to be delivered:

- Subsidence prediction up to the end of October, 2015
- Subsidence predictions for various points in time for the period up to the end of 2050

For these predictions, the model as established and validated by history matching for the period 1956 to 2010 during execution of the scope of work of WP2 has been applied. However, an extension of the model was necessary:

- With regard to the additionally required prediction for the end of October; 2015 the brine production data of AkzoNobel as well as the as the wellhead pressures for the nitrogen storage cavern HL-K had been added to the database.
- For predicting subsidence up to the end of 2050, the model had to be extended. As some the existing brine production caverns at Heiligerlee will attain their maximum extraction capacity within the mentioned timespan, these exploited caverns will have to be abandoned and new caverns will have to be created.

The database that could be used for the predictions contained production and operation data from start of operations in 1956 up to November 19th, 2015. Brine production plans until 2050 have been provided by AkzoNobel in terms of intended average hourly brine flow rates. These brine outflow rates have been applied for the calculation of the related cavern volume increase at subsurface over time.

The intended future operation pattern for cavern HL-K has been provided by Gasunie in terms of injection and withdrawal flow rates. Therefore, a thermodynamic simulation of cavern HL-K was necessary in order to receive wellhead pressures. This simulation has been carried by KBB UT.

Subsidence predictions had to be provided for end of 2020, 2030, 2040 and 2050.

3 Subsidence Prediction for End of October 2015

3.1 Procedure

Production and operation data as provided by AkzoNobel and Gasunie until end of October 2015 have been added to the database of the existing subsidence model. A prediction of the subsidence produced by the caverns has then been calculated by applying the existing subsidence model with the updated database.

3.2 Maps and Graphs

The results of the prediction for the end of October 2015 are presented by

- cross sectional views at either fixed northing or easting through the predicted subsidence bowl,
- the isokatabases map for October 31, 2015, and
- graphs showing the course of subsidence versus time at selected benchmarks.

Selected representations are listed in Table 3.1. The location of the selected cross sections with either fixed northing or easting is given in Enclosure 1.

Table 3.1 Selected representation of the subsidence prediction for October 31, 2015

Subsidence in West to East cross section at fixed Northing	Enclosure 2
Subsidence in South to North cross section at fixed Easting	Enclosure 3
Subsidence Contour Map	Enclosure 4
Subsidence versus time at benchmark 013A1100	Enclosure 5
Subsidence versus time at benchmark 013A1300	Enclosure 6
Subsidence versus time at benchmark 013A1600	Enclosure 7

3.3 Discussion of the results

For the time period starting at the beginning of cavern operations in 1956 up to the end of October 2015 a maximum subsidence of about 150 mm has been calculated above caverns HL-C, HL-E and HL-K. This maximum value can be identified in Enclosure 2, Enclosure 3, and Enclosure 4. The subsidence rates due to cavern operations, which are calculated as moving average values from the calculated subsidence calculation, stay at about 4.5 mm/a in this region (see Enclosure 6) and also in the region above cavern HL-F (see Enclosure 7). Whereas the calculated subsidence rate above cavern HL-A is lower at a value of about 4 mm/a (see Enclosure 5). From end of 2010 (last levelling campaign) until the beginning of 2013 calculated subsidence rates stay at almost the same value. Subsidence rates increase since the beginning of 2013, because brine production was raised to levels that had been maintained before November 2007.

4 Subsidence Prediction until End of 2050

4.1 Procedure

The existing subsidence model has been extended by adding five caverns for the purpose of salt mining. This expansion is required for matching AkzoNobel's future need of brine.

Up-to-date records about brine production and wellhead pressure were available up to November 19th, 2015. This point in time fixes the transition point from recorded data to assumed future operation data. Data about intended brine production from Heiligerlee caverns until the end of 2050 have been provided by AkzoNobel

All information and data about intended future expansion and salt production have been provided by AkzoNobel on a confidential basis. This information can be requested from AkzoNobel, when required.

Intended future operation of cavern HL-K in terms of wellhead pressure over time had to be calculated from given values for flow rates of injection or withdrawal for a typical annual storage cycle. The required wellhead pressures have been determined by applying a thermodynamic simulation model, which is based on the KBB UT thermal simulator PVT3. The results of the numerical simulation are presented in Enclosure 8.

Applying the subsurface part of the subsidence model provides the cavern volume losses. Individual convergence volumes versus time are given as well as the cumulative value of all caverns.

4.2 Maps and Graphs

The results of the subsidence predictions up to the end of 2050 are presented in subsidence maps (plots of isokatabases) as well as in diagrams showing graphs of predicted course of subsidence versus time at specific benchmarks. Selected representations are listed in Table 4.1 with their link to the respective enclosures.

Table 4.1 Selected representation of the subsidence predictions

Kind of Representation	2020	2030	2040	2050
Subsidence in West to East cross section at fixed Northing	Enclosure 9	Enclosure 12	Enclosure 15	Enclosure 18
Subsidence in South to North cross section at fixed Easting	Enclosure 10	Enclosure 13	Enclosure 16	Enclosure 19
Subsidence Contour Map	Enclosure 11	Enclosure 14	Enclosure 17	Enclosure 20
Subsidence versus time at benchmark 013A1100		Enclosure 21		
Subsidence versus time at benchmark 013A1300		Enclosure 22		
Subsidence versus time at benchmark 013A1400		Enclosure 23		
Subsidence versus time at benchmark 013A1500		Enclosure 24		
Subsidence versus time at benchmark 013A1600		Enclosure 25		
Subsidence versus time at benchmark 013A1700		Enclosure 26		
Subsidence versus time at benchmark 013A10131		Enclosure 27		
Subsidence versus time at benchmark 013A1250		Enclosure 28		
Subsidence versus time at benchmark 013A5510		Enclosure 29		
Subsidence versus time at benchmark 013A5301		Enclosure 30		
Subsidence versus time at benchmark 013A5025		Enclosure 31		
Subsidence versus time at benchmark 013A0112		Enclosure 32		

4.3 Discussion of the results

A gradual increase of subsidence is predicted over the coming years. By the help of Enclosure 9 to Enclosure 20 this is demonstrated as wells as for the centre of the bowl and for the overall spread of the subsidence trough. The centre of the bowl stays moves slightly from above caverns HL-B, HL-F and HL-E in the direction of above cavern HL-E. The newly created caverns in the southern part of the field already have a small influence on the location of the subsidence bowl in 2050. Predicted maximum values of subsidence are compiled in Table 4.2 with reference to the selected years of evaluation.

For the period 1956 up to the end of 2050 a maximum subsidence of 330 mm is predicted due to salt cavern operation

Values for maximum subsidence rates as given in Table 4.2 have been calculated from monthly periods, whereas graphs for subsidence rates versus time as shown in Enclosure 21 to Enclosure 32 are given as moving averages. Moving averages for presenting the course of subsidence rate versus time have been selected, because the subsidence simulation model produces a direct (with respect to time non-delayed) response at surface. It has been observed above salt caverns that the response to cavern convergence at surface can be detected after a relatively short period. But in this regard several weeks to months seem to be reasonable. For the subsidence rates versus time plots therefore the moving annual average has been chosen on order to show the long-term development.

Table 4.2 Predicted values of maximum subsidence due to cavern operation at Heiligerlee

point in time	predicted maximum value subsidence [mm]	predicted maximum subsidence rate [mm/a]	spread of the bowl (isokatabase 1 mm) [km]
31.12.2020	175	4.9	4.8
31.12.2030	220	4.6	5.1
31.12.2040	275	6.0	5.4
31.12.2050	330	6.3	5.7

Whenever a large cavern, which has reached its production limit, has been plugged and abandoned this is clearly shown by the graphs for the predicted subsidence versus time at benchmarks that are located in the area of influence of these caverns (see Enclosure 21 to Enclosure 32). The shorter the distance the more pronounced is the effect (compare for example benchmark 013A1500 above cavern HL-E (see Enclosure 24), which is located in the centre of the bowl, with benchmark 013A0112 (see Enclosure 32), which is situated in the south region of the field).

Estimated subsidence rates increase from 2020 to 2050 by almost 30%. Although caverns are partly abandoned they still have a big volume and a small convergence rate is still taken into account. At the same time, the field expansion continues by the creation of new caverns.

The extent of the subsidence bowl measured in between the 25 mm isokatabase increases by about 1 km from 2020 to 2050. The 25 mm interval has been chosen with regard to clear arrangement of the isokatabases.

5 Summary and Conclusion

Observed surface subsidence at Heiligerlee is being generated by various sources. In this regard gas production, brine production from salt cavern, gas storage in salt caverns, water management and ground compaction have to be mentioned. As AkzoNobel and Gasunie are obliged to report to the authorities about the amount of subsidence that has been caused by the salt caverns, this share has to be calculated and predicted.

The present report describes the prediction of subsidence development that can be related to the Heiligerlee salt caverns. In this regard the calculated and/or predicted subsidence or subsidence rates are given only due to convergence and are explicitly not given due to other influencing factors like oxidation of special layers, compaction of the ground and change in ground water level.

It is mandatory to show both, the prediction for the cavern subsidence prior to the planned next surface levelling campaign (Autumn 2015) and for the following decades of cavern operation until 2050.

For both periods, the subsidence prediction has been processed by the application of the model that has been developed and validated against historical data within the scope of the previous work package (WP2).

Subsidence prediction for October 31st, 2015 is based on data recorded during operations. The predictions until 2050 use a database that has been extended by the data indicating the intended future brine production or gas storage operation at Heiligerlee. For the nitrogen storage cavern HL-K a representative annual storage cycle has been deduced from the existing historical data.

The predictions show an increasing subsidence over time. The forecast for the maximum valued at the end of October 2015 is about 175 mm. Until the end of 2050, this value will increase to about 330 mm. During this period, the centre of the bowl stays more or less at the same location above the caverns, because the planned new caverns in the southern part of the field will be developed not earlier than 2046.

The estimated maximum subsidence rate increases from 4.9 mm/a in 2020 to 6.3 mm/a in 2050. Due to the planned abandonment of some caverns it could be expected that subsidence rates will be reduced due to a substantial decline of convergence rates of these abandoned caverns. However, these abandonments are planned close to the end of the considered period and in the meantime additional cavern volume is generated continuously due to brine production.

During the period from 2020 to 2050 the predicted maximum extent of the subsidence bowl with reference to the 25 mm isocatabase increases by about 1 km.

To minimize subsidence brine production, caverns should be plugged and abandoned shortly after production has halted from a particular cavern.

The optimization potential with regard to convergence for the nitrogen storage cavern can be assumed of second order influence, as it is only one cavern, the volume is not as big as those of brine production caverns and the considered annual cycle shows only limited periods at relatively low cavern pressures.

References

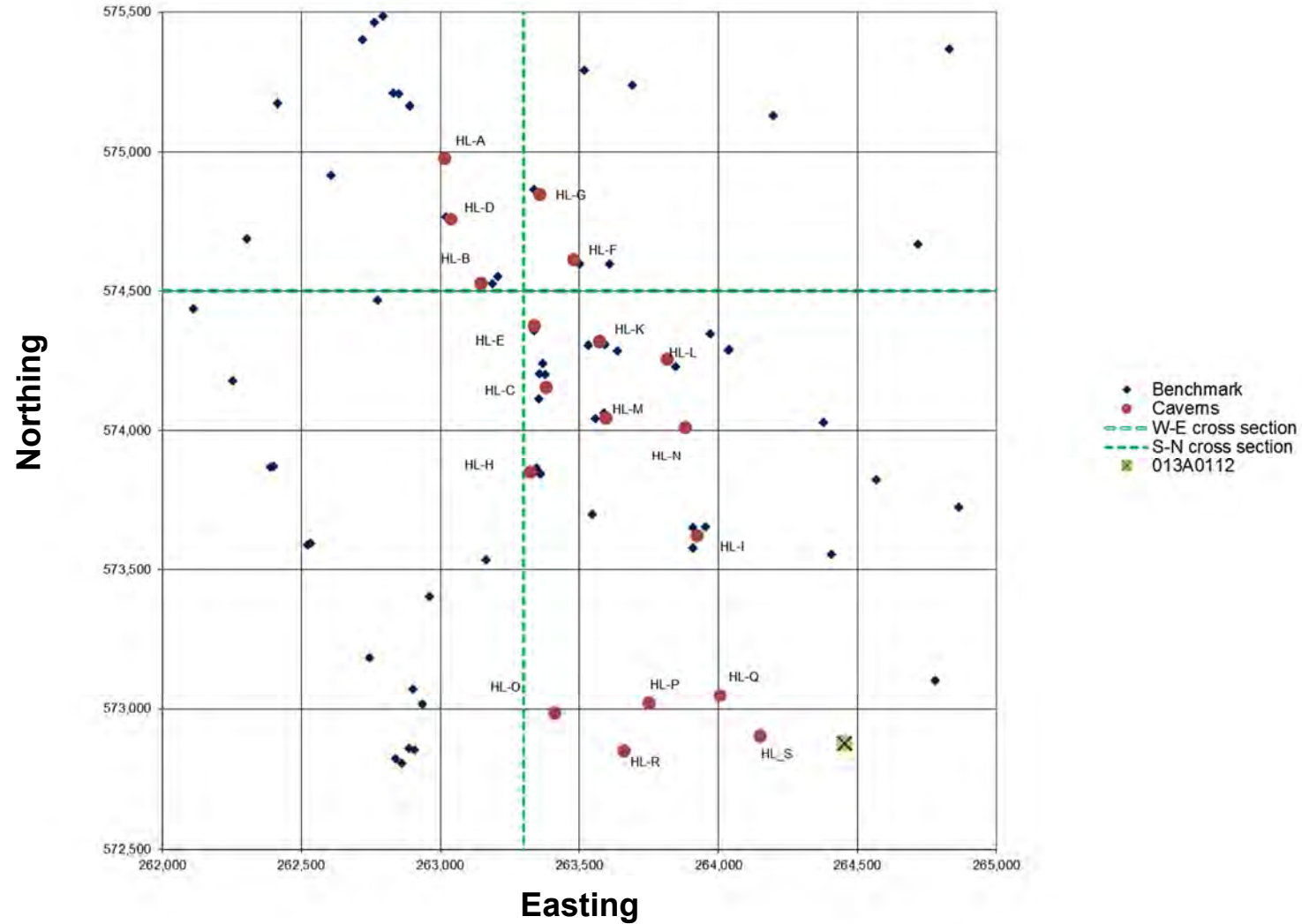
- [1] ZANDER-SCHIEBENHÖFER, D., HORVÁTH, B., SCHÄFER, R., (2015): 'Prediction of Subsidence above Caverns at Heiligerlee, The Netherlands, Operation Phase, Report on WP1: Review of Documentation', KBB UT project report for Akzo Nobel Industrial Chemicals Delftzijl, Hannover, 31.03.2015.
- [2] ZANDER-SCHIEBENHÖFER, D., HORVÁTH, B., SCHÄFER, R., (2015): 'Prediction of Subsidence above Caverns at Heiligerlee, The Netherlands, Operation Phase, Report on WP2: Applied Subsidence Model', KBB UT project report for Akzo Nobel Industrial Chemicals Delftzijl, revision 01, Hannover, 31.08.2015.

List of Enclosures

- Enclosure 1 Heiligerlee – Map of cavern and benchmark locations
- Enclosure 2 Heiligerlee – Subsidence bowl at fixed Northing 574,500 – 31/10/2015
- Enclosure 3 Heiligerlee – Subsidence bowl at fixed Easting 263,300 – 31/10/2015
- Enclosure 4 Heiligerlee – Subsidence bowl – 31/10/2015
- Enclosure 5 Heiligerlee – Benchmark 013A1100 – Comparison of observed subsidence with measured values
- Enclosure 6 Heiligerlee – Benchmark 013A1300 – Comparison of observed subsidence with measured values
- Enclosure 7 Heiligerlee – Benchmark 013A1600 – Comparison of observed subsidence with measured values
- Enclosure 8 Heiligerlee – Assumed annual pressure cycle for HL-K (wellhead, casing shoe and cavern pressures)
- Enclosure 9 Heiligerlee – Subsidence bowl at fixed Northing 574,500 – 31/12/2020
- Enclosure 10 Heiligerlee – Subsidence bowl at fixed Easting 263,400 – 31/12/2020
- Enclosure 11 Heiligerlee – Subsidence bowl – 31/12/2020
- Enclosure 12 Heiligerlee – Subsidence bowl at fixed Northing 574,500 – 31/12/2030
- Enclosure 13 Heiligerlee – Subsidence bowl at fixed Easting 263,400 – 31/12/2030
- Enclosure 14 Heiligerlee – Subsidence bowl – 31/12/2030
- Enclosure 15 Heiligerlee – Subsidence bowl at fixed Northing 574,500 – 31/12/2040
- Enclosure 16 Heiligerlee – Subsidence bowl at fixed Easting 263,400 – 31/12/2040
- Enclosure 17 Heiligerlee – Subsidence bowl – 31/12/2040
- Enclosure 18 Heiligerlee – Subsidence bowl at fixed Northing 574,500 – 31/12/2050
- Enclosure 19 Heiligerlee – Subsidence bowl at fixed Easting 263,400 – 31/12/2050
- Enclosure 20 Heiligerlee – Subsidence bowl – 31/12/2050
- Enclosure 21 Heiligerlee – Benchmark 013A1100 – Comparison of observed subsidence with measured values
- Enclosure 22 Heiligerlee – Benchmark 013A1300 – Comparison of observed subsidence with measured values
- Enclosure 23 Heiligerlee – Benchmark 013A1400 – Comparison of observed subsidence with measured values
- Enclosure 24 Heiligerlee – Benchmark 013A1500 – Comparison of observed subsidence with measured values
- Enclosure 25 Heiligerlee – Benchmark 013A1600 – Comparison of observed subsidence with measured values
- Enclosure 26 Heiligerlee – Benchmark 013A1700 – Comparison of observed subsidence with measured values

-
- Enclosure 27 Heiligerlee – Benchmark 013A0131 – Comparison of observed subsidence with measured values
- Enclosure 28 Heiligerlee – Benchmark 013A1250 – Comparison of observed subsidence with measured values
- Enclosure 29 Heiligerlee – Benchmark 013A5510 – Comparison of observed subsidence with measured values
- Enclosure 30 Heiligerlee – Benchmark 013A5301 – Comparison of observed subsidence with measured values
- Enclosure 31 Heiligerlee – Benchmark 013A5025 – Comparison of observed subsidence with measured values
- Enclosure 32 Heiligerlee – Benchmark 013A0112 – Comparison of observed subsidence with measured values

Enclosures

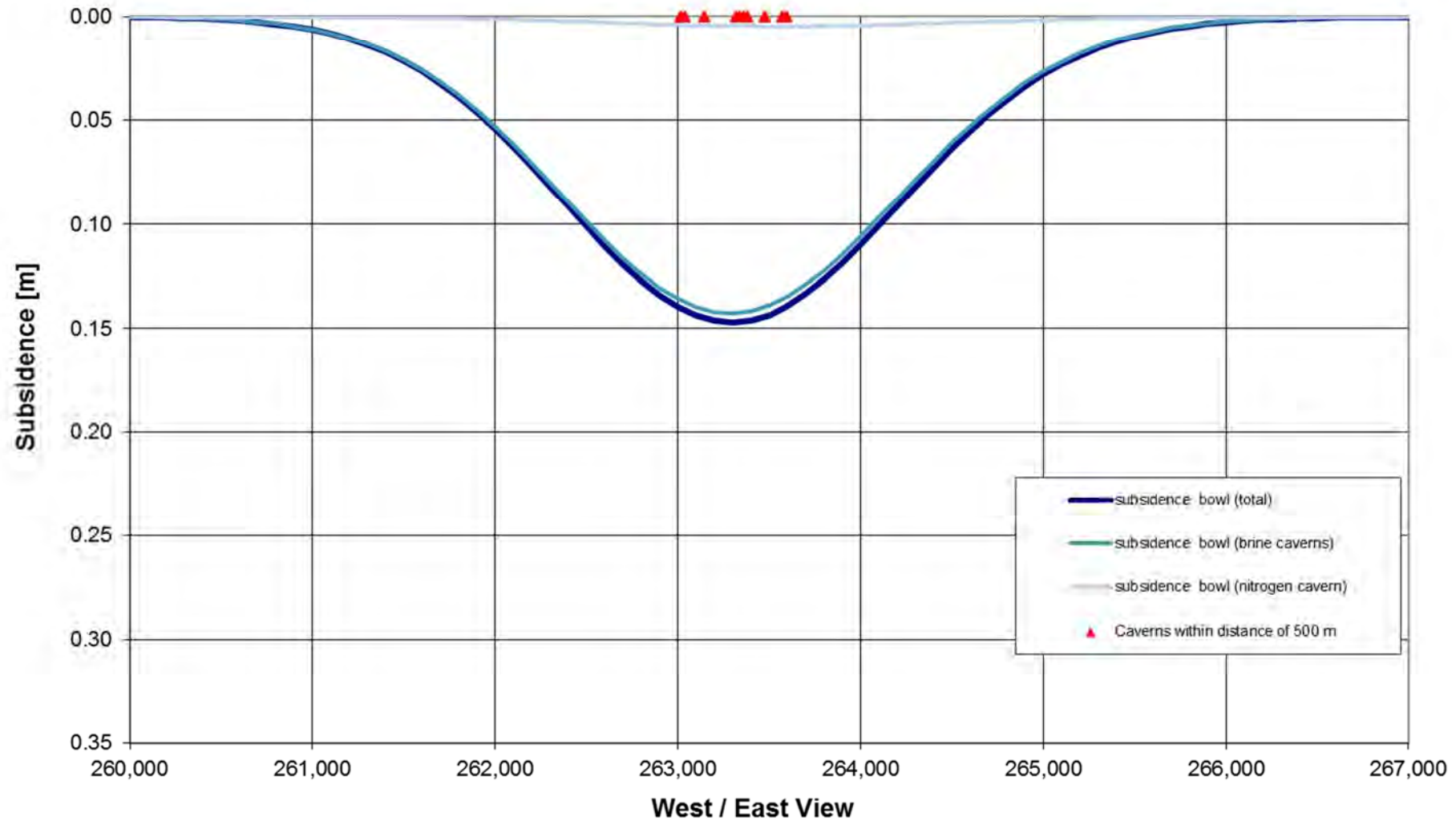


Enclosure 1
 Heiligerlee – Map of cavern and benchmark locations

Subsidence Bowl at fixed Northing 574,500 (31/10/2015)

Heiligerlee - Superposition of all Caverns

Subsidence Modell 35-25-30-1-0.12-2-40-0.8-5-60



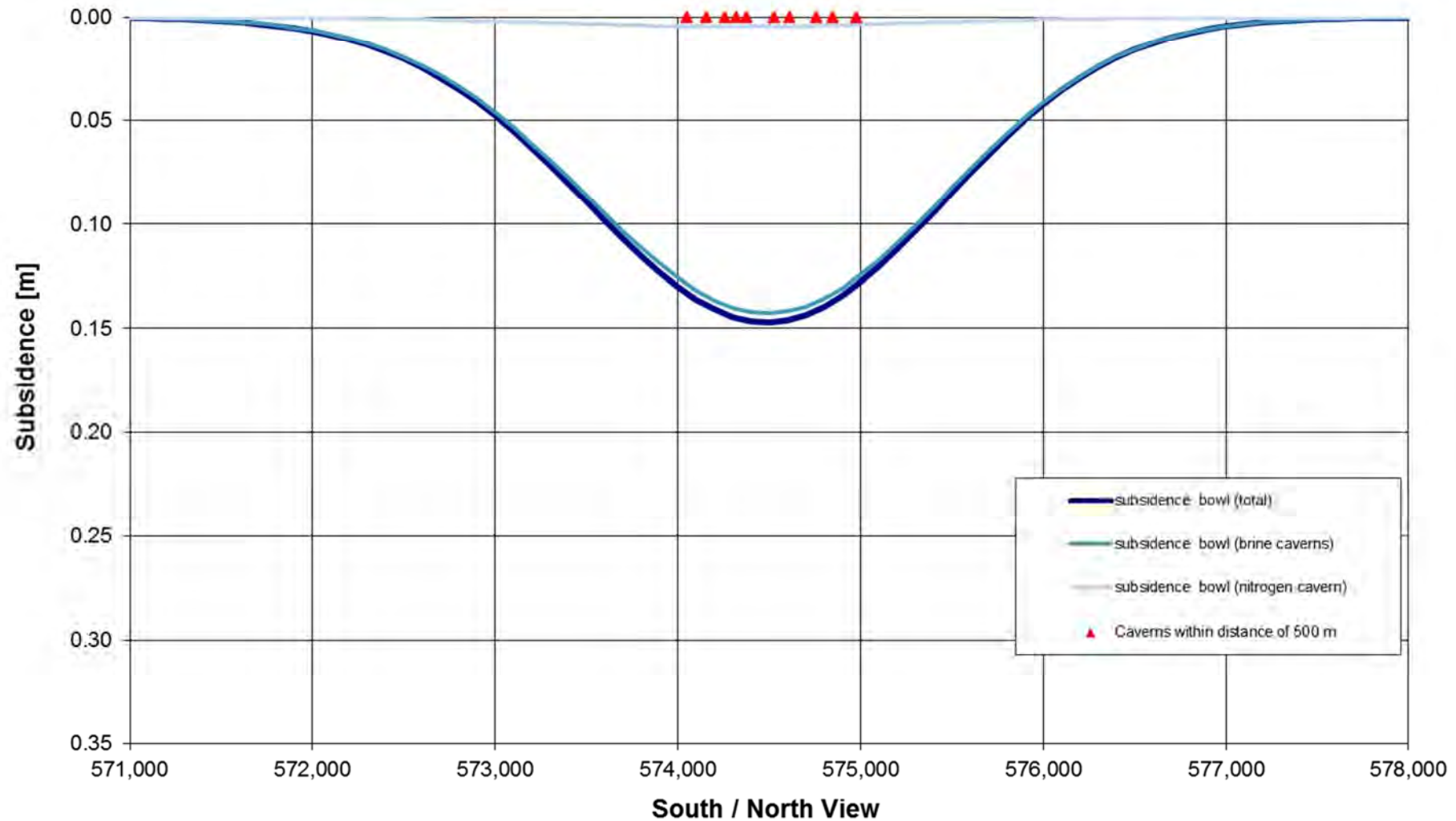
Enclosure 2

Heiligerlee – Subsidence bowl at fixed Northing 574,500 – 31/10/2015

Subsidence Bowl at fixed Easting 263,300 (31/10/2015)

Heiligerlee - Superposition of all Caverns

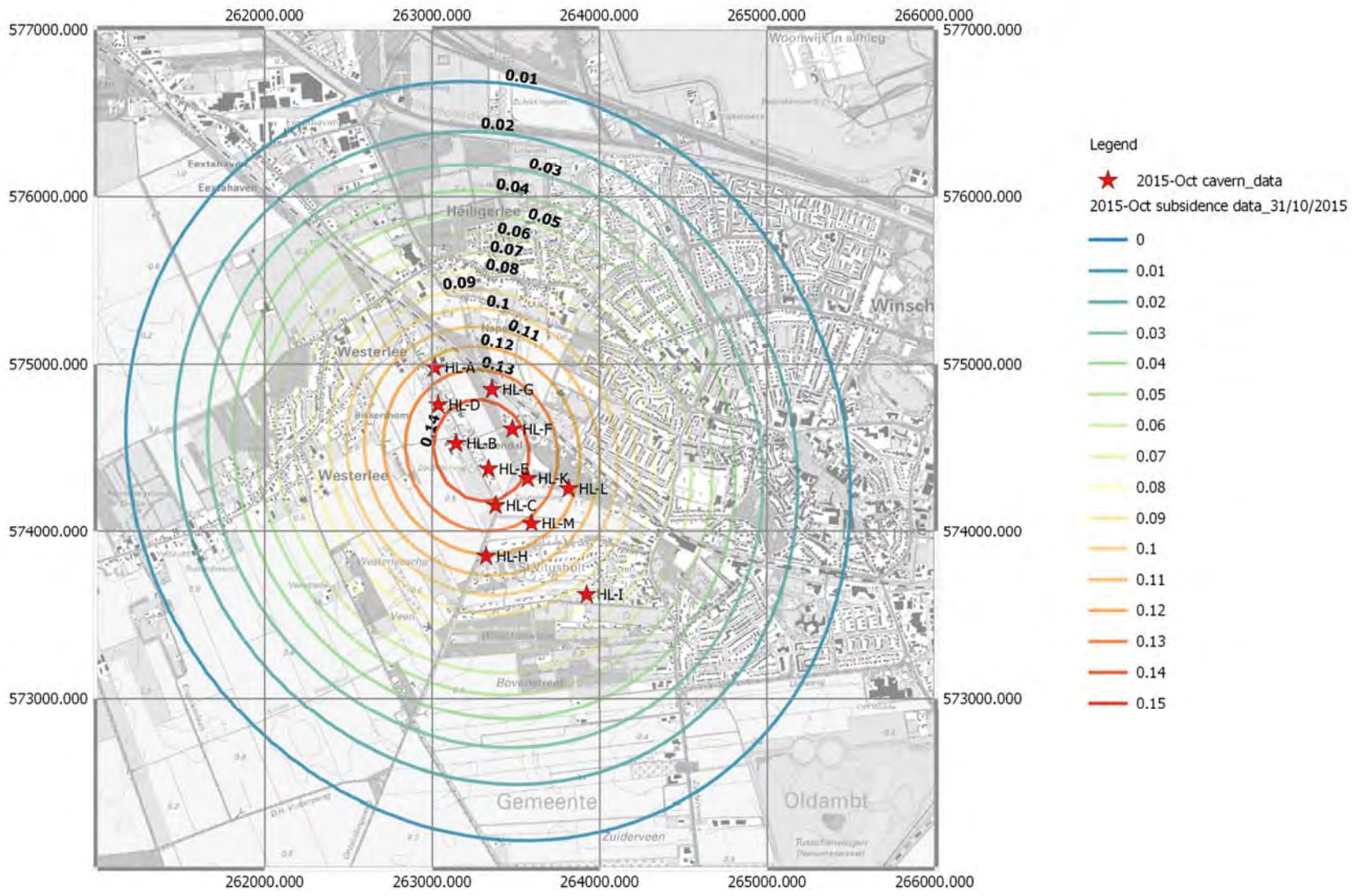
Subsidence Modell 35-25-30-1-0.12-2-40-0.8-5-60



Enclosure 3

Heiligerlee – Subsidence bowl at fixed Easting 263,300 – 31/10/2015

map produced with QGIS, see <http://www.qgis.org/de/site/>
 topographic map appears under the free license agreement, downloaded from
<https://www.pdok.nl/nl/producten/pdok-downloads/basis-registratie-topografie/topografie/toprafter/toprafter-actueel/top25rafter>



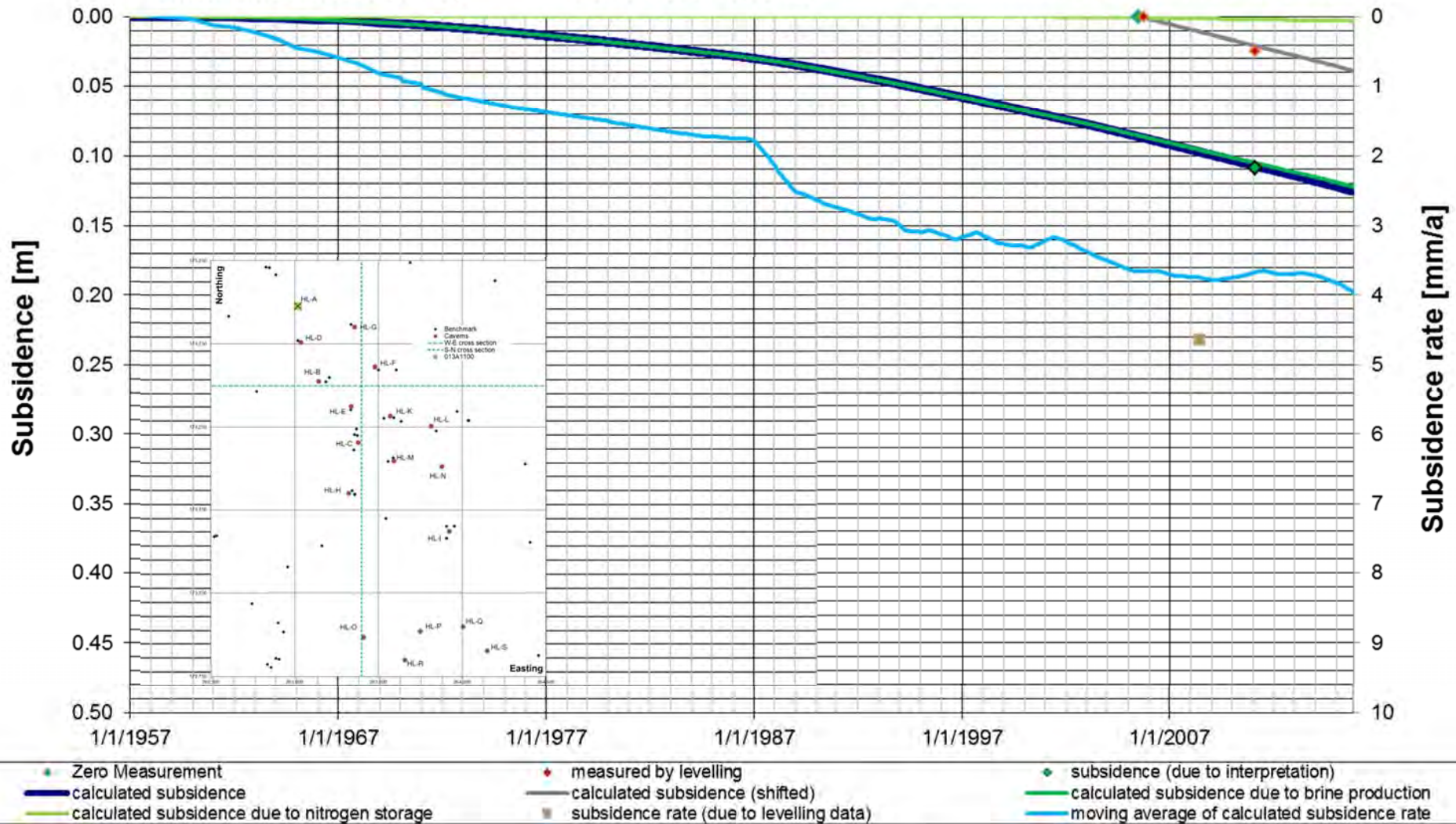
Enclosure 4
 Heiligerlee – Subsidence bowl – 31/10/2015

AkzoNobel / Gasunie (Heiligerlee) - Subsidence Bowl (Gauss)

Benchmark 013A1100 (HL-A)

Period (1957- 10/2015)

Subsidence Modell 35-25-30-1-0.12-2-40-0.8-5-60



Enclosure 5

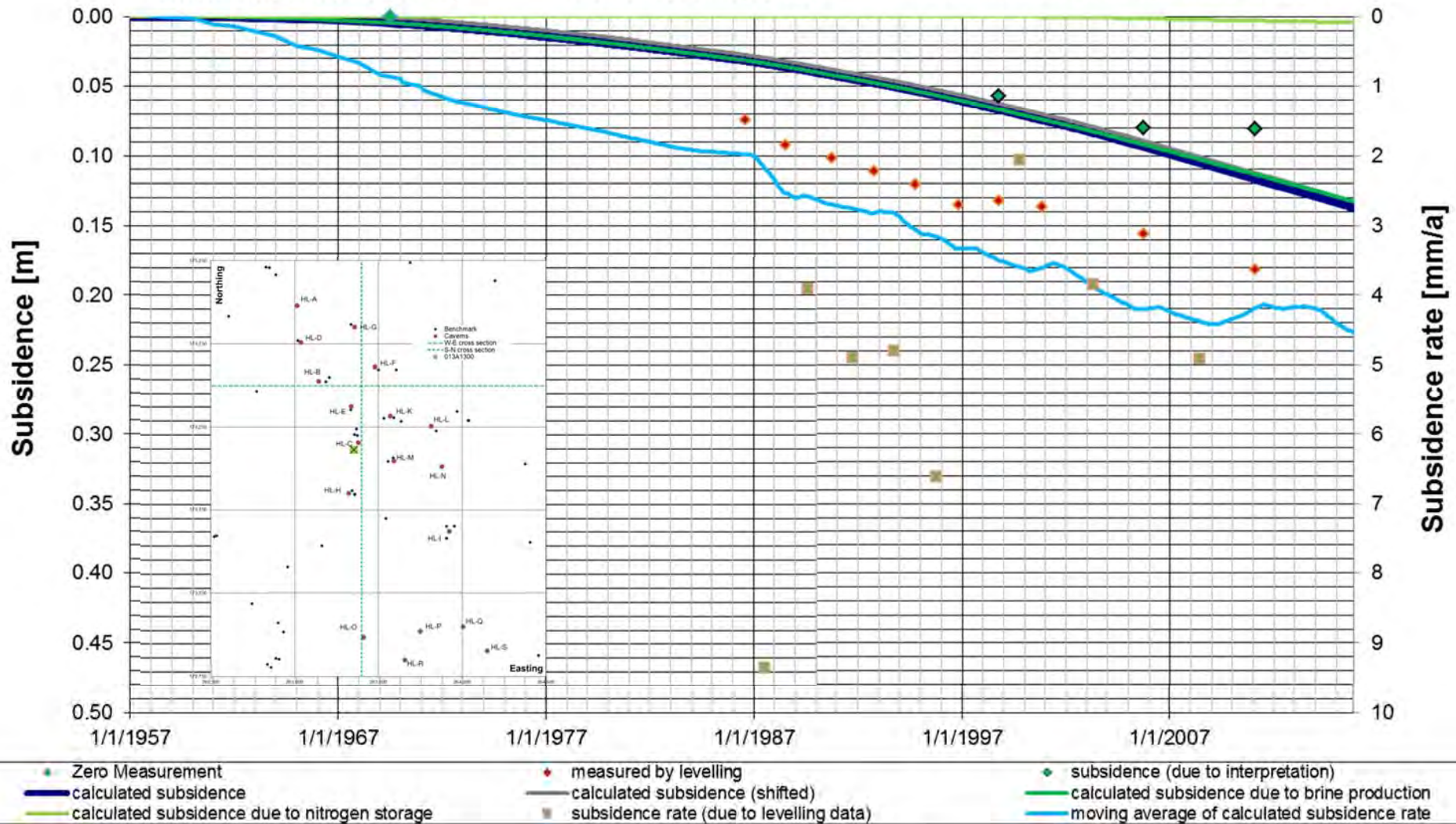
Heiligerlee – Benchmark 013A1100 – Comparison of observed subsidence with measured values

AkzoNobel / Gasunie (Heiligerlee) - Subsidence Bowl (Gauss)

Benchmark 013A1300 (HL-C)

Period (1957- 10/2015)

Subsidence Modell 35-25-30-1-0.12-2-40-0.8-5-60



Enclosure 6

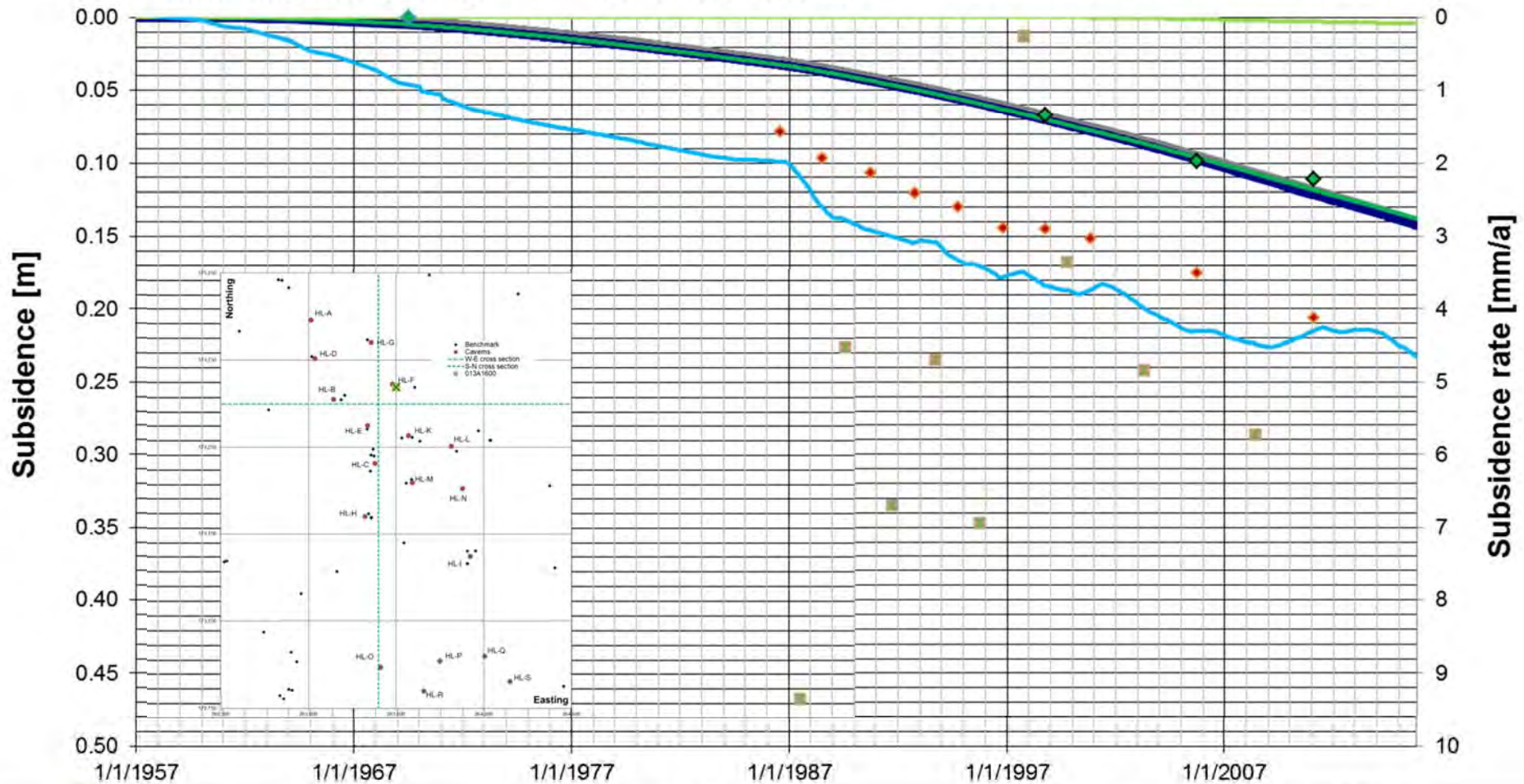
Heiligerlee – Benchmark 013A1300 – Comparison of observed subsidence with measured values

AkzoNobel / Gasunie (Heiligerlee) - Subsidence Bowl (Gauss)

Benchmark 013A1600 (HL-F)

Period (1957- 10/2015)

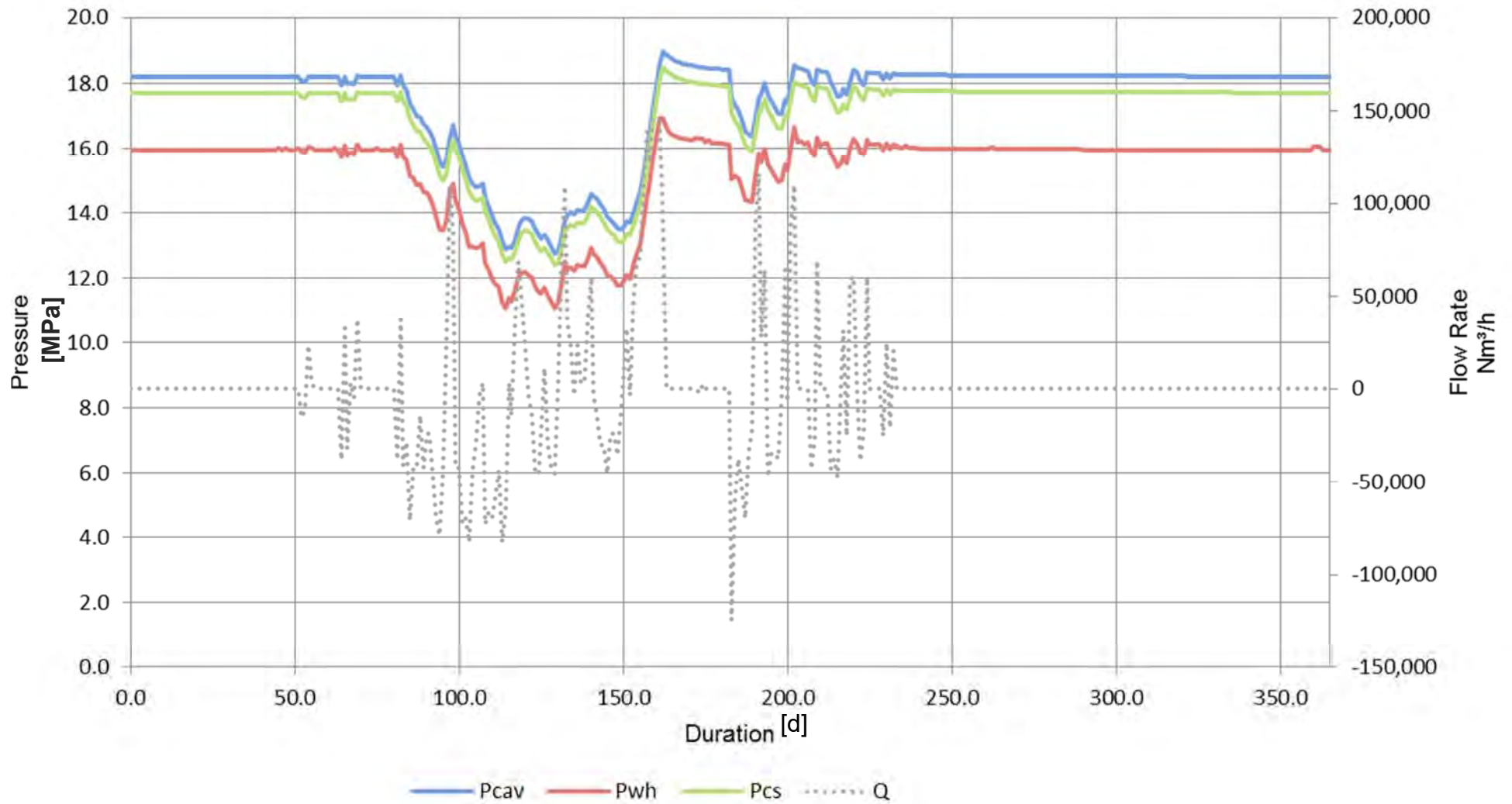
Subsidence Modell 35-25-30-1-0.12-2-40-0.8-5-60



Zero Measurement	measured by levelling	subsidence (due to interpretation)
calculated subsidence	calculated subsidence (shifted)	calculated subsidence due to brine production
calculated subsidence due to nitrogen storage	subsidence rate (due to levelling data)	moving average of calculated subsidence rate

Enclosure 7

Heiligerlee – Benchmark 013A1600 – Comparison of observed subsidence with measured values



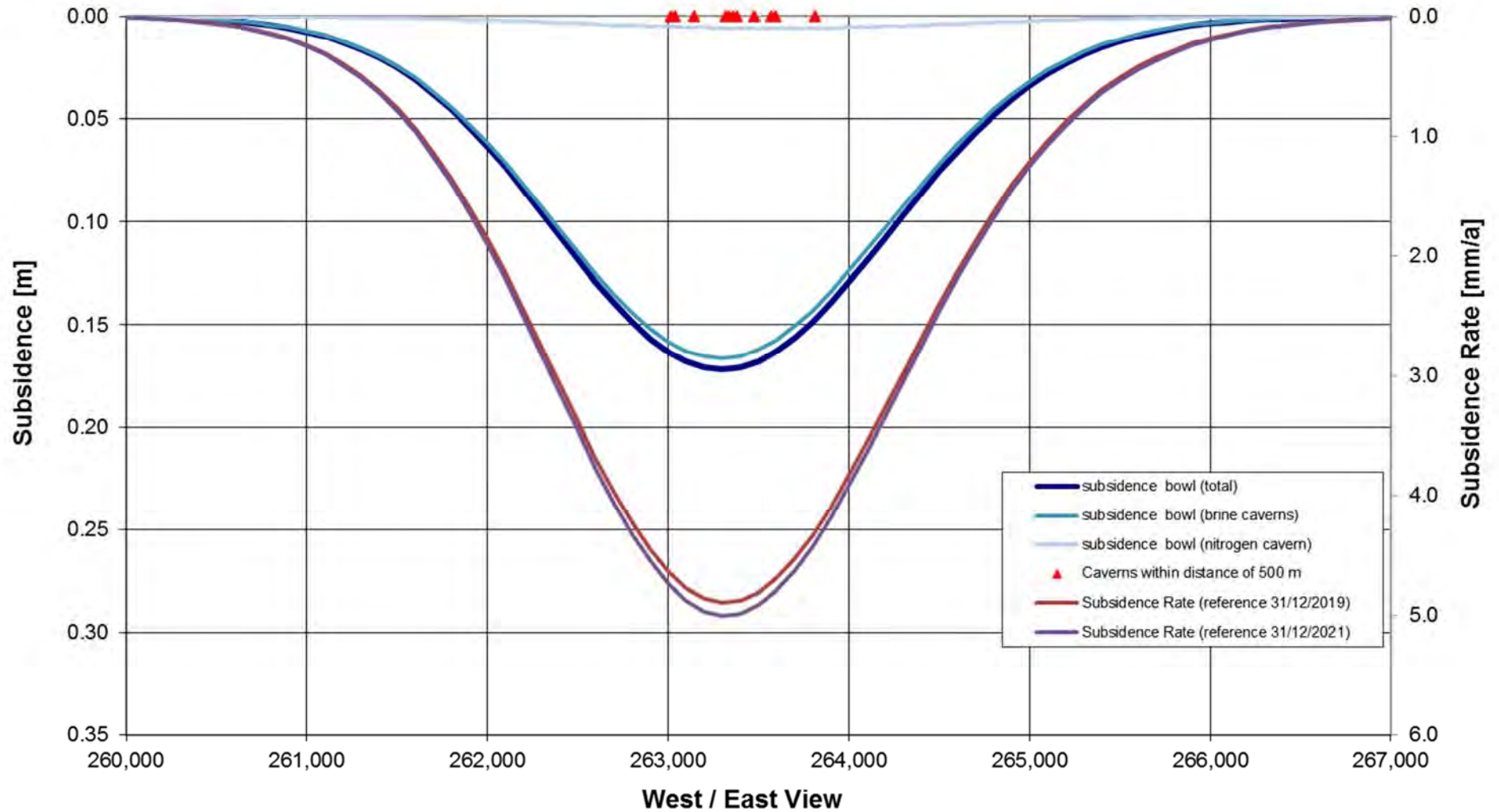
Enclosure 8

Heiligerlee – Assumed annual pressure cycle for HL-K (wellhead, casing shoe and cavern pressures)

Subsidence Bowl at fixed Northing 574,500 (31/12/2020)

Heiligerlee - Superposition of all Caverns

Subsidence Modell 35-25-30-1-0.12-2-40-0.8-5-60



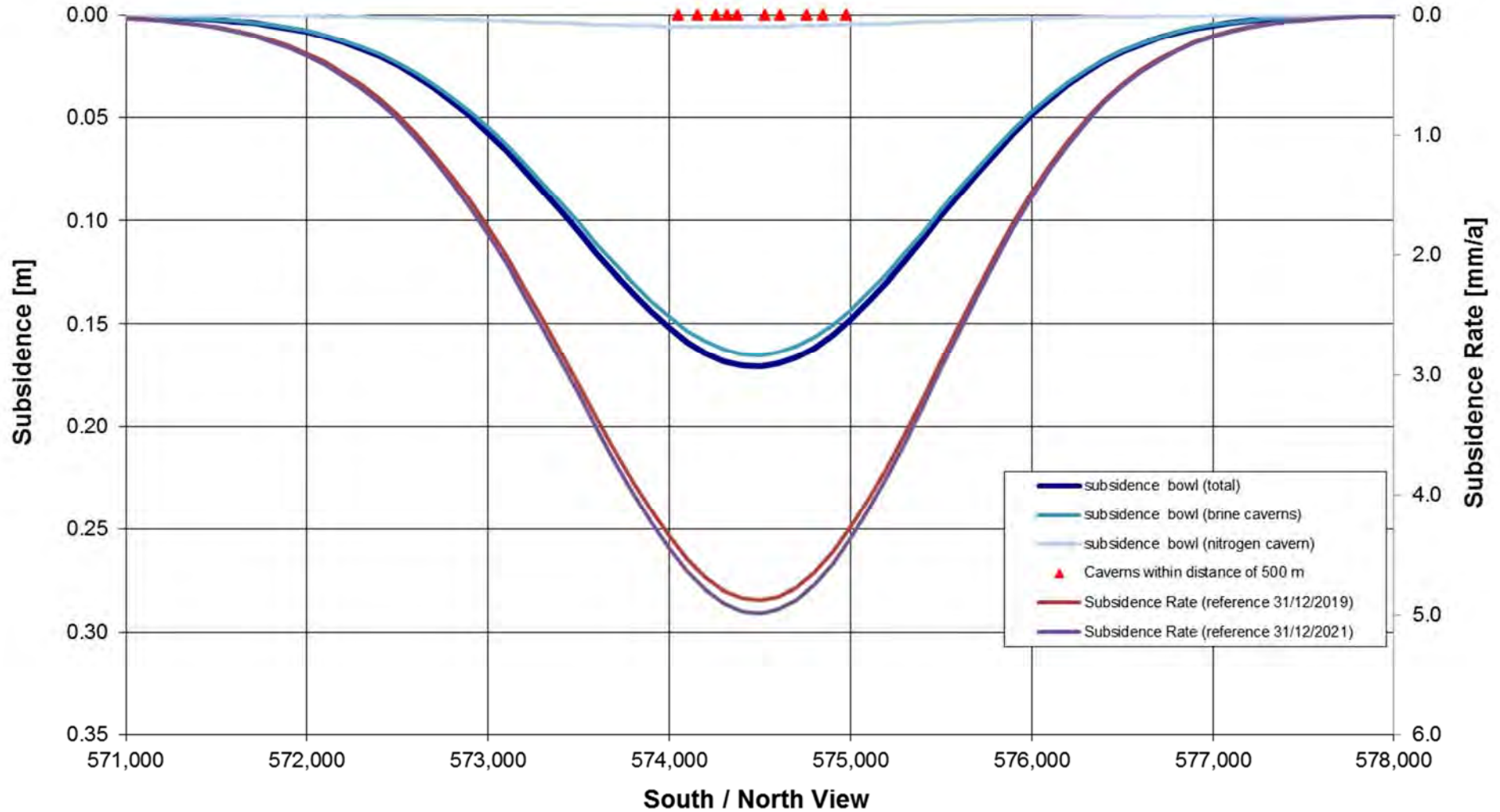
Enclosure 9

Heiligerlee – Subsidence bowl at fixed Northing 574,500 – 31/12/2020

Subsidence Bowl at fixed Easting 263,400 (31/12/2020)

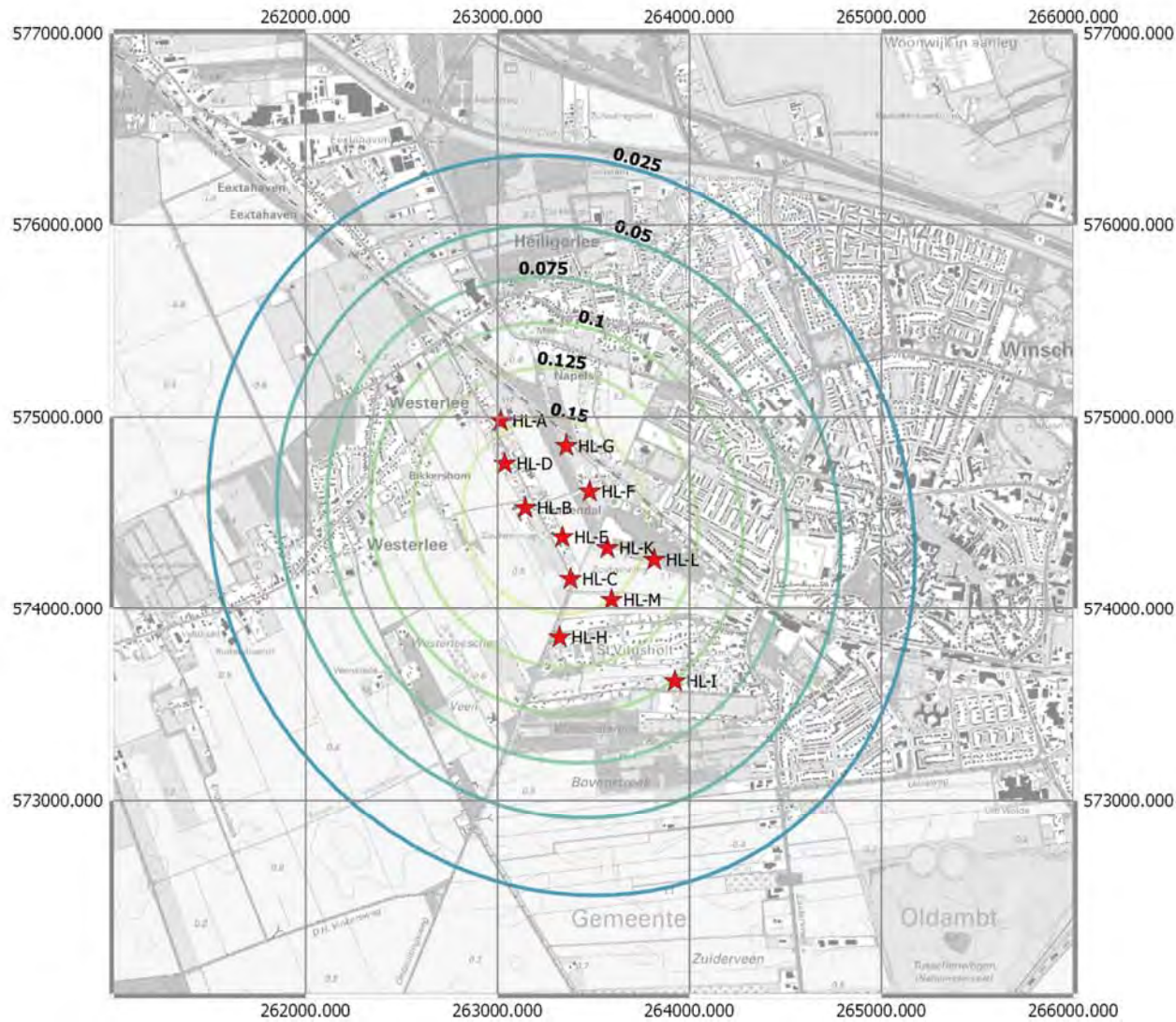
Heiligerlee - Superposition of all Caverns

Subsidence Modell 35-25-30-1-0.12-2-40-0.8-5-60



Enclosure 10

Heiligerlee – Subsidence bowl at fixed Easting 263,400 – 31/12/2020



Legend

- ★ 2020 cavern_data
- 2020 subsidence data_31/12/2020
- 0
- 0.025
- 0.05
- 0.075
- 0.1
- 0.125
- 0.15
- 0.175
- 0.2
- 0.225
- 0.25
- 0.275
- 0.3
- 0.325
- 0.35

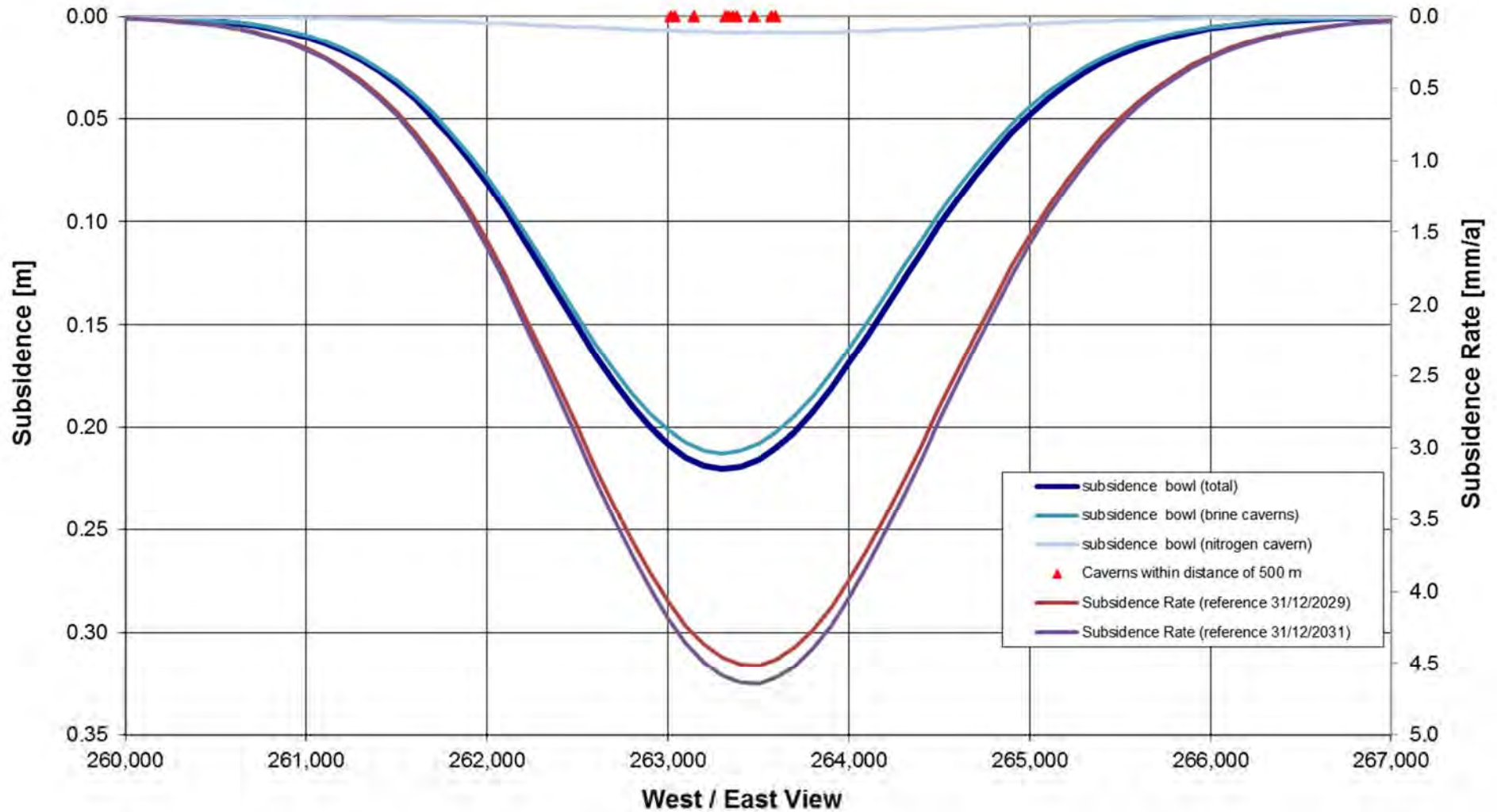
map produced with QGIS, see <http://www.qgis.org/de/site/>
topographic map appears under the free license agreement, downloaded from
<https://www.pdok.nl/nl/producten/pdok-downloads/basis-registratie-topografie/toprafter/toprafter-actueel/top25rafter>

Enclosure 11
Heiligerlee – Subsidence bowl – 31/12/2020

Subsidence Bowl at fixed Northing 574,500 (31/12/2030)

Heiligerlee - Superposition of all Caverns

Subsidence Modell 35-25-30-1-0.12-2-40-0.8-5-60



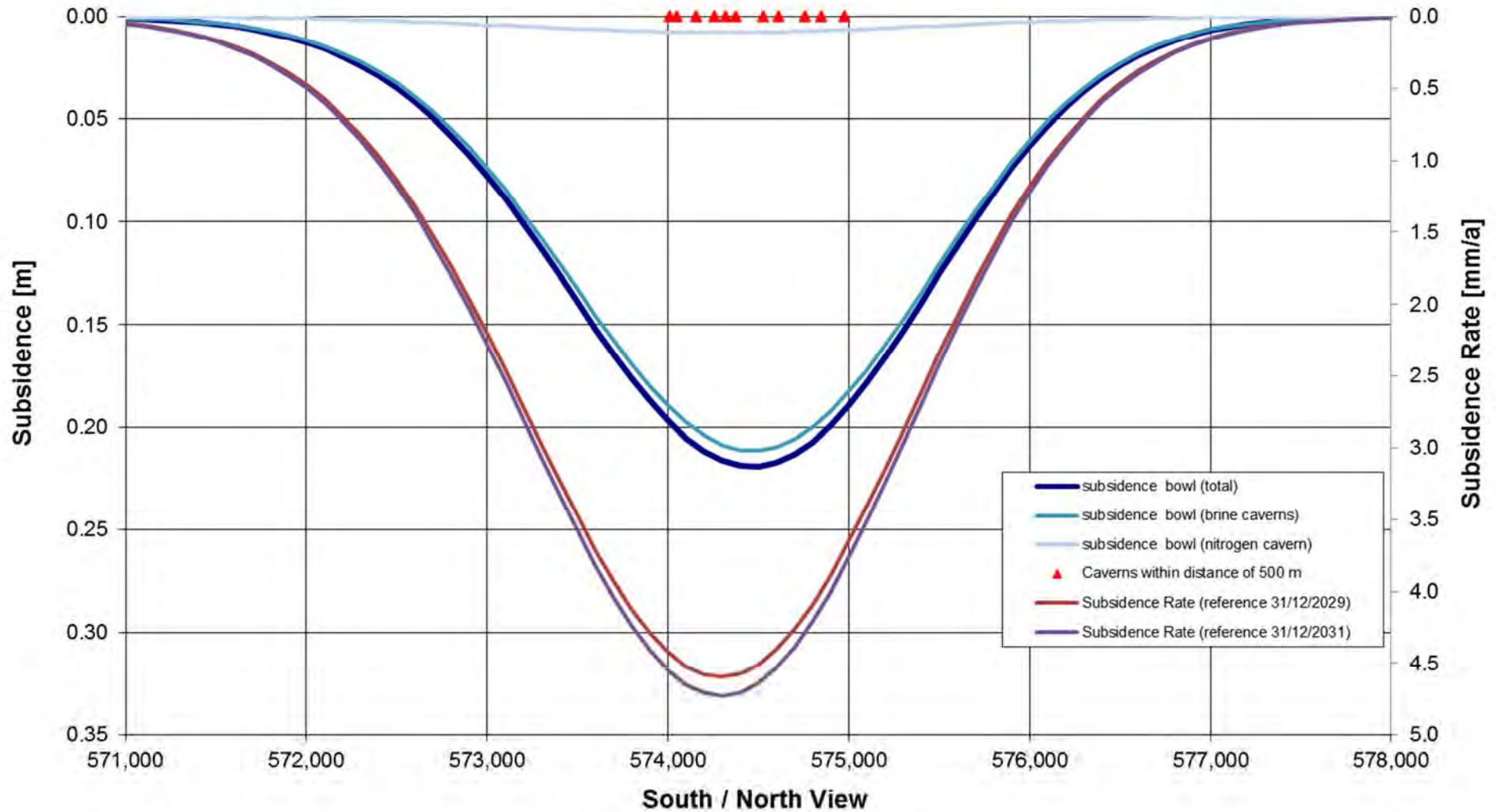
Enclosure 12

Heiligerlee – Subsidence bowl at fixed Northing 574,500 – 31/12/2030

Subsidence Bowl at fixed Easting 263,400 (31/12/2030)

Heiligerlee - Superposition of all Caverns

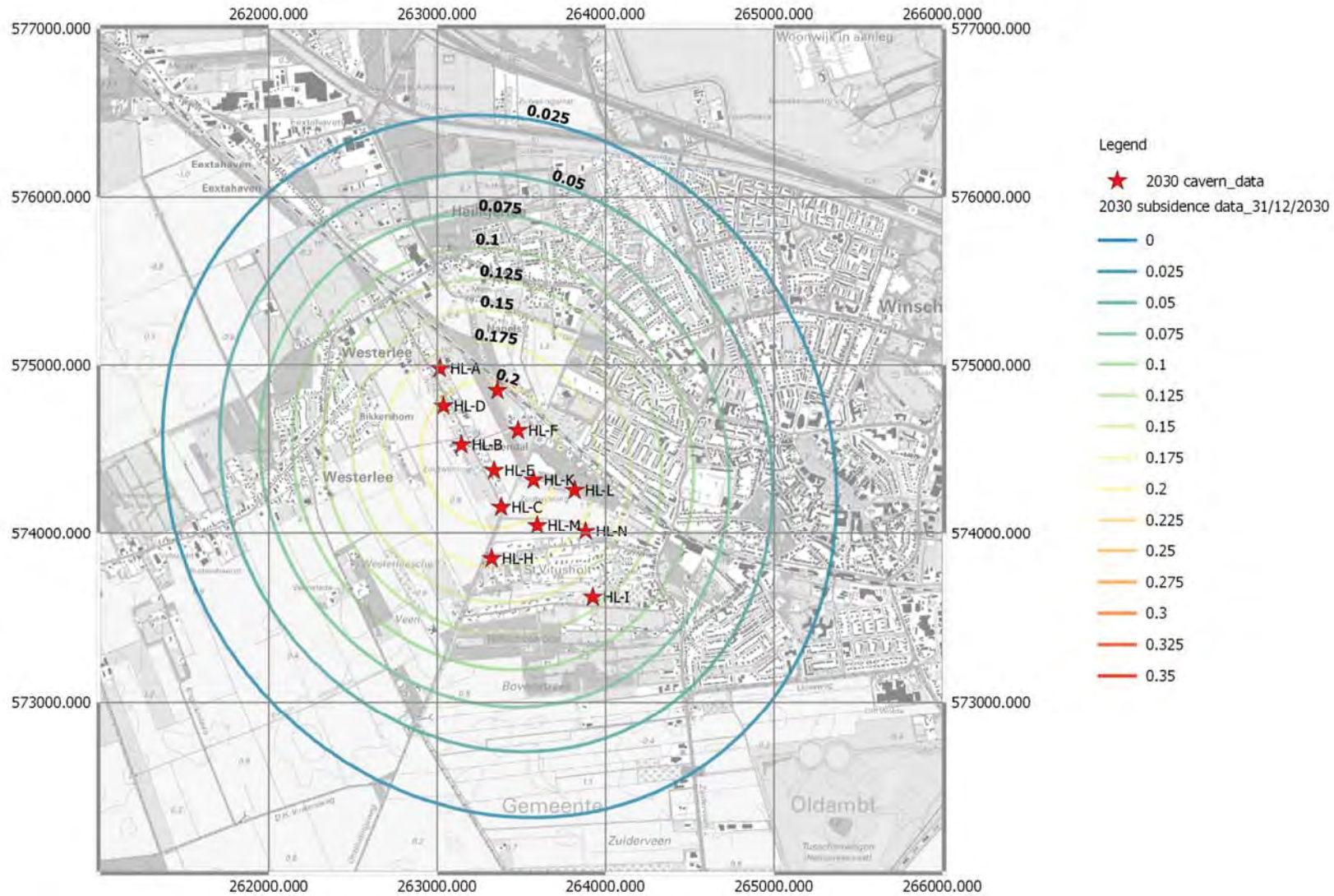
Subsidence Modell 35-25-30-1-0.12-2-40-0.8-5-60



Enclosure 13

Heiligerlee – Subsidence bowl at fixed Easting 263,400 – 31/12/2030

map produced with QGIS, see <http://www.qgis.org/de/site/topographic>
 map appears under the free license agreement, downloaded from <https://www.pdok.nl/nl/producten/pdok-downloads/basis-registratie-topografie/toprafter/toprafter-actueel/top25rafter>

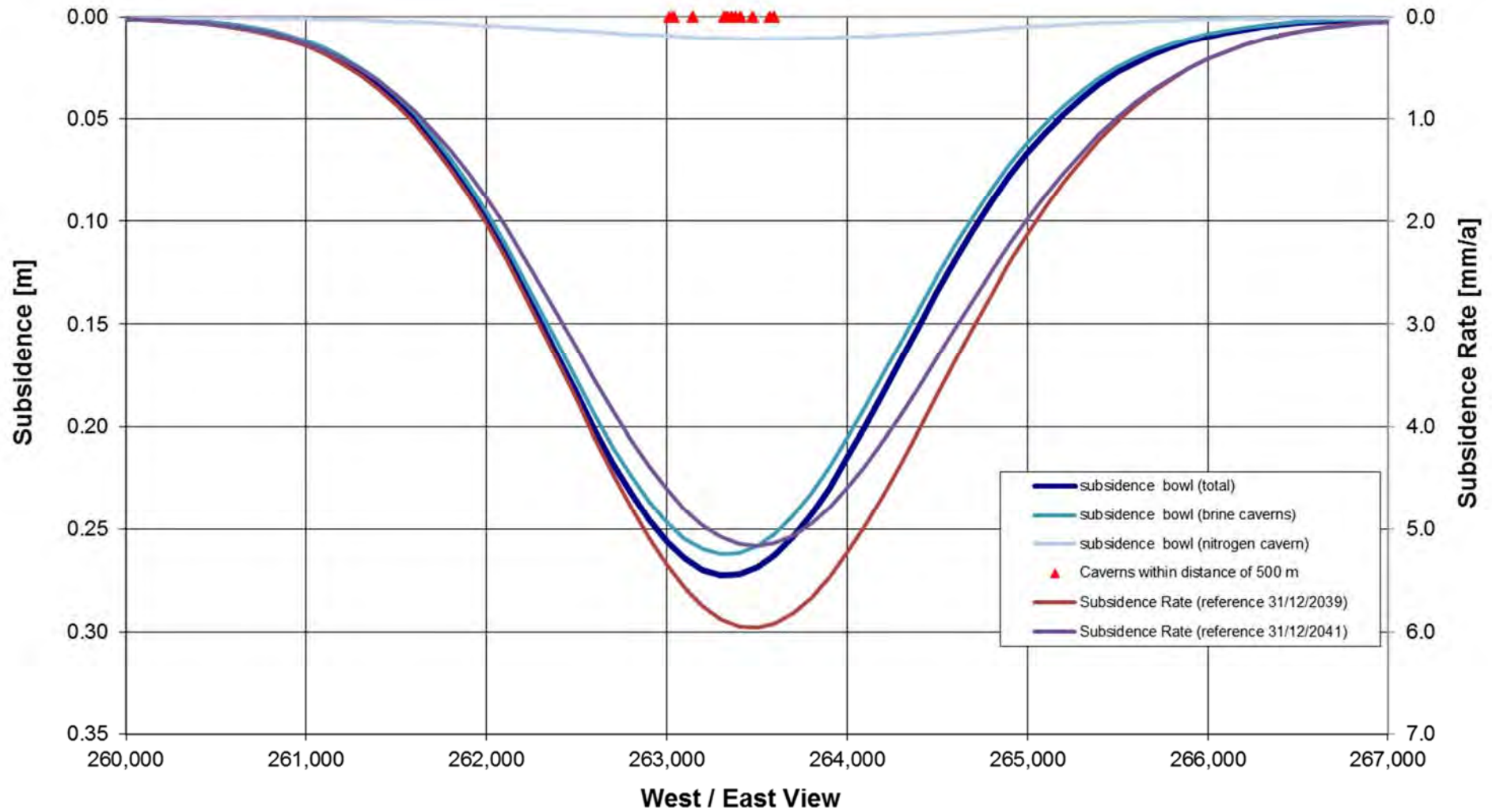


Enclosure 14
 Heiligerlee – Subsidence bowl – 31/12/2030

Subsidence Bowl at fixed Northing 574,500 (31/12/2040)

Heiligerlee - Superposition of all Caverns

Subsidence Modell 35-25-30-1-0.12-2-40-0.8-5-60



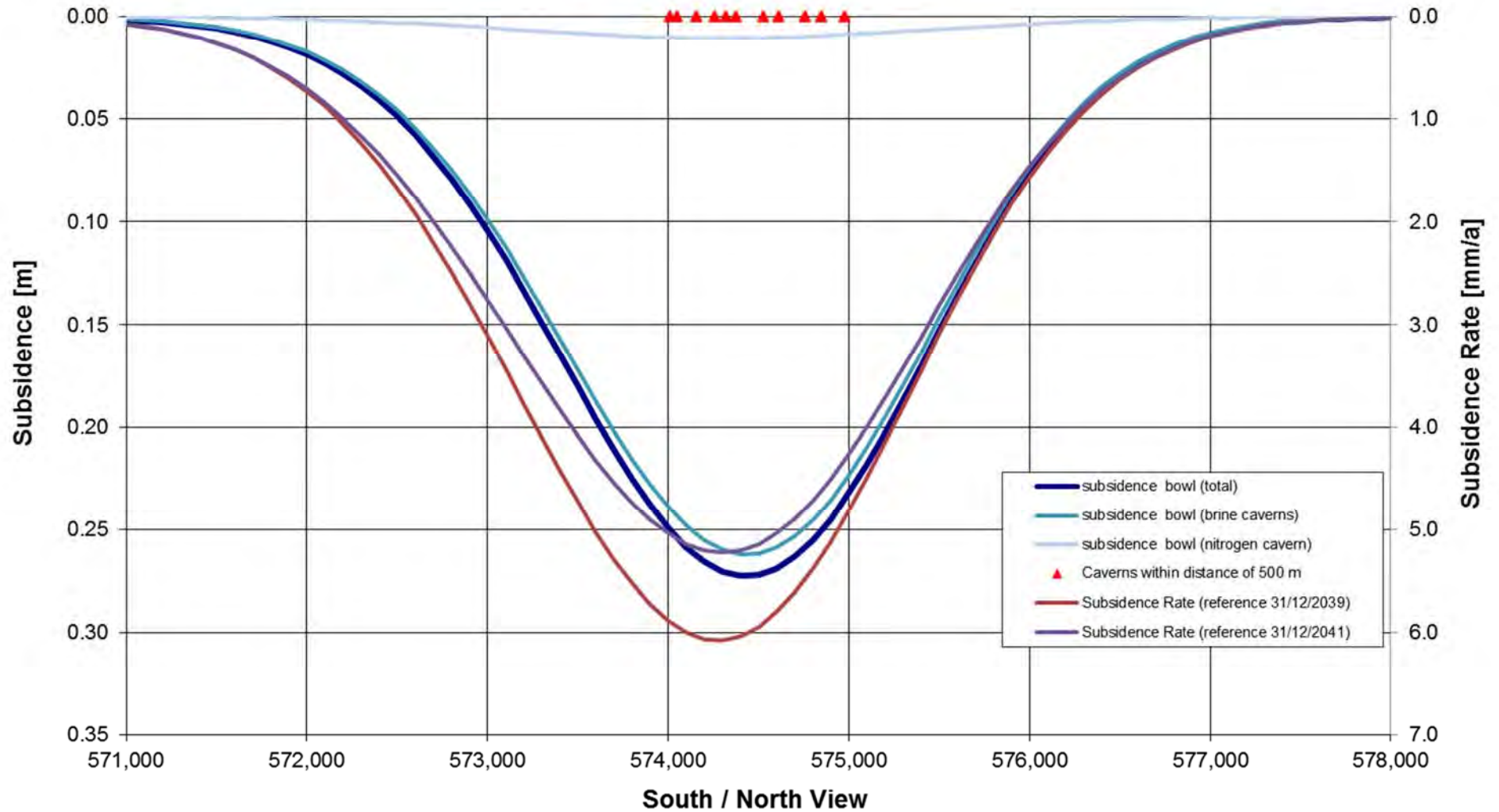
Enclosure 15

Heiligerlee – Subsidence bowl at fixed Northing 574,500 – 31/12/2040

Subsidence Bowl at fixed Easting 263,400 (31/12/2040)

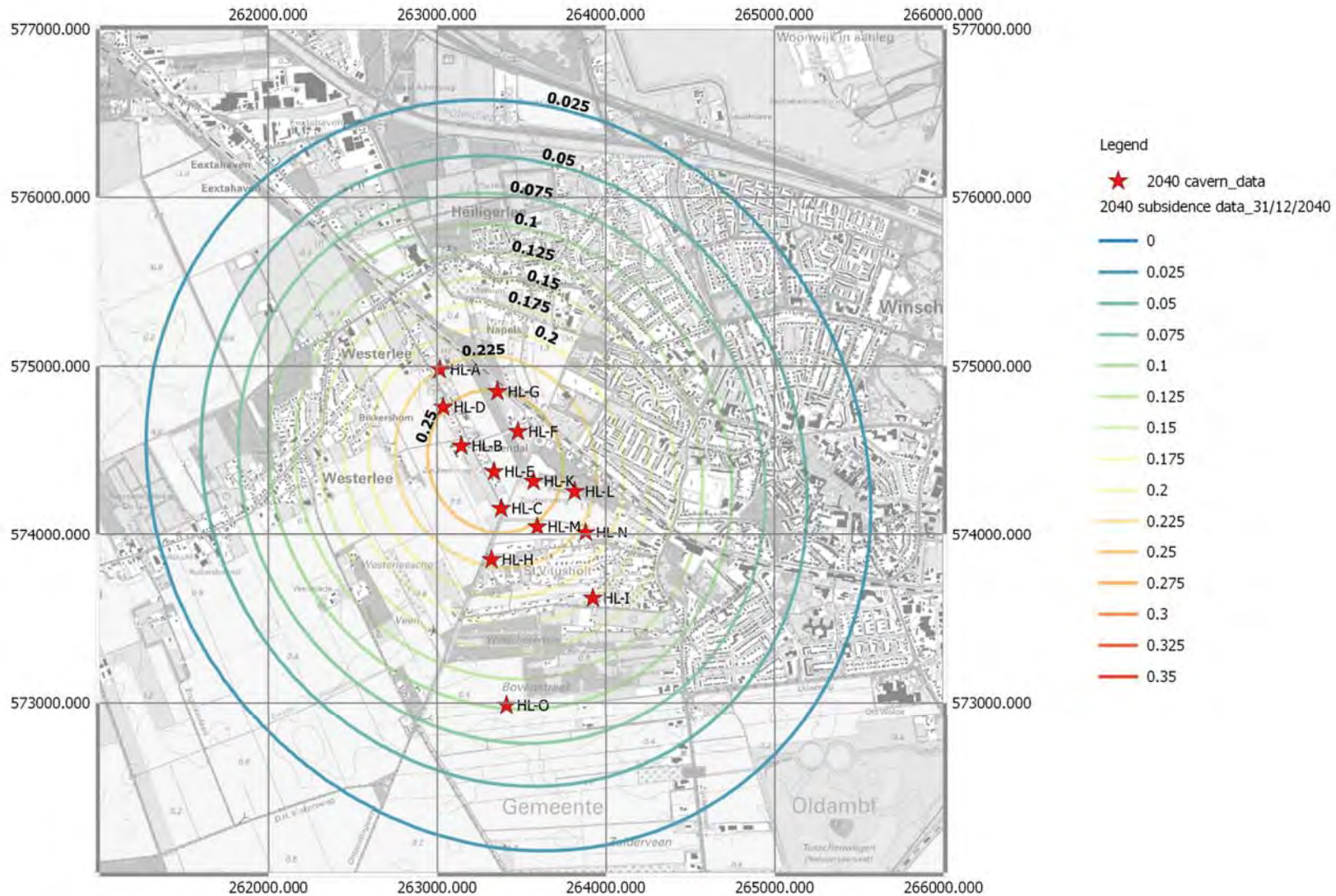
Heiligerlee - Superposition of all Caverns

Subsidence Modell 35-25-30-1-0.12-2-40-0.8-5-60



Enclosure 16

Heiligerlee – Subsidence bowl at fixed Easting 263,400 – 31/12/2040



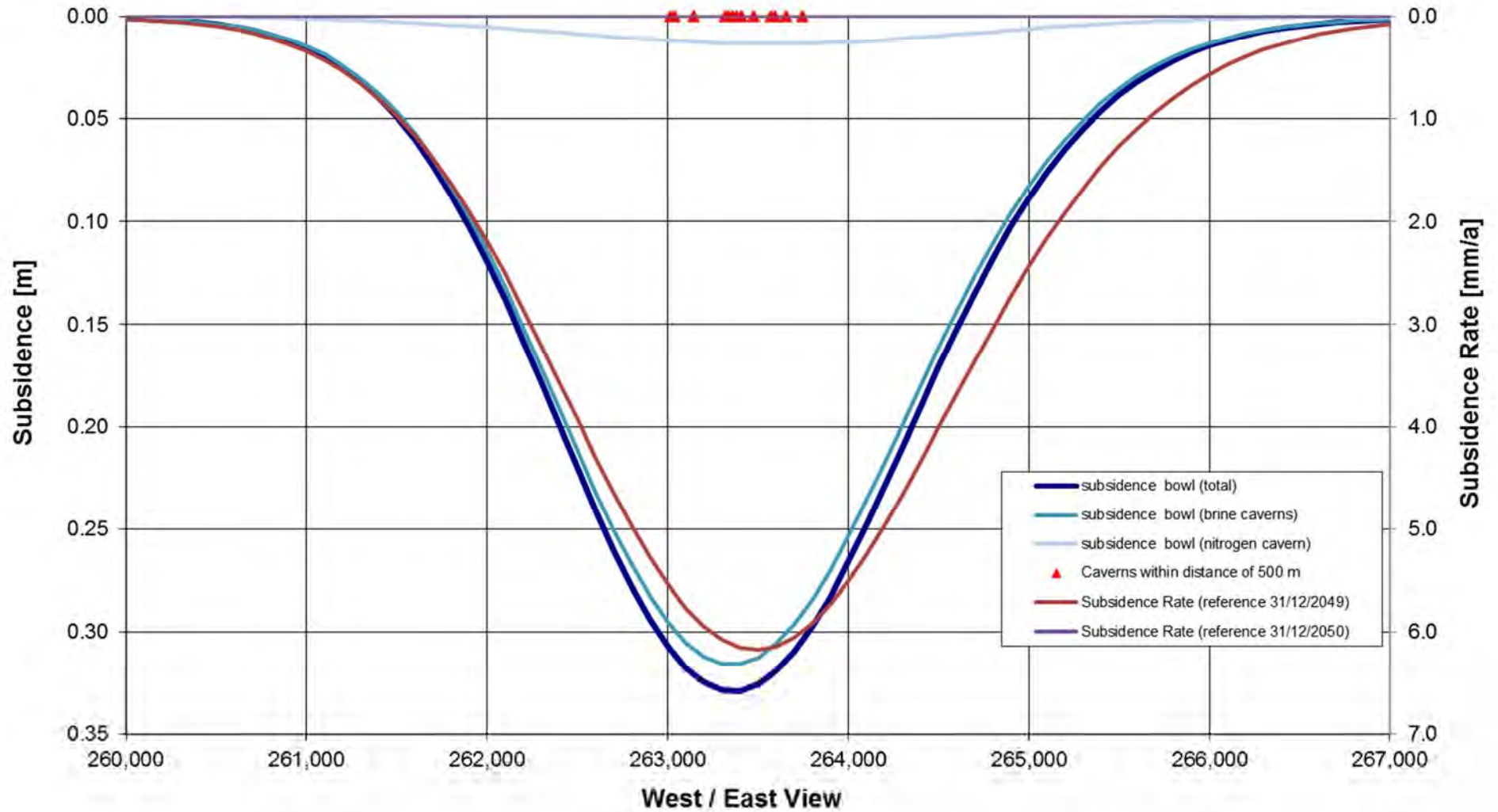
map produced with QGIS, see <http://www.qgis.org/de/site/>
topographic map appears under the free license agreement, downloaded from
<https://www.pdok.nl/nl/producten/pdok-downloads/basis-registratie-topografie/toprafter/toprafter-actueel/top25raster>

Enclosure 17 Heiligerlee – Subsidence bowl – 31/12/2040

Subsidence Bowl at fixed Northing 574,500 (31/12/2050)

Heiligerlee - Superposition of all Caverns

Subsidence Modell 35-25-30-1-0.12-2-40-0.8-5-60



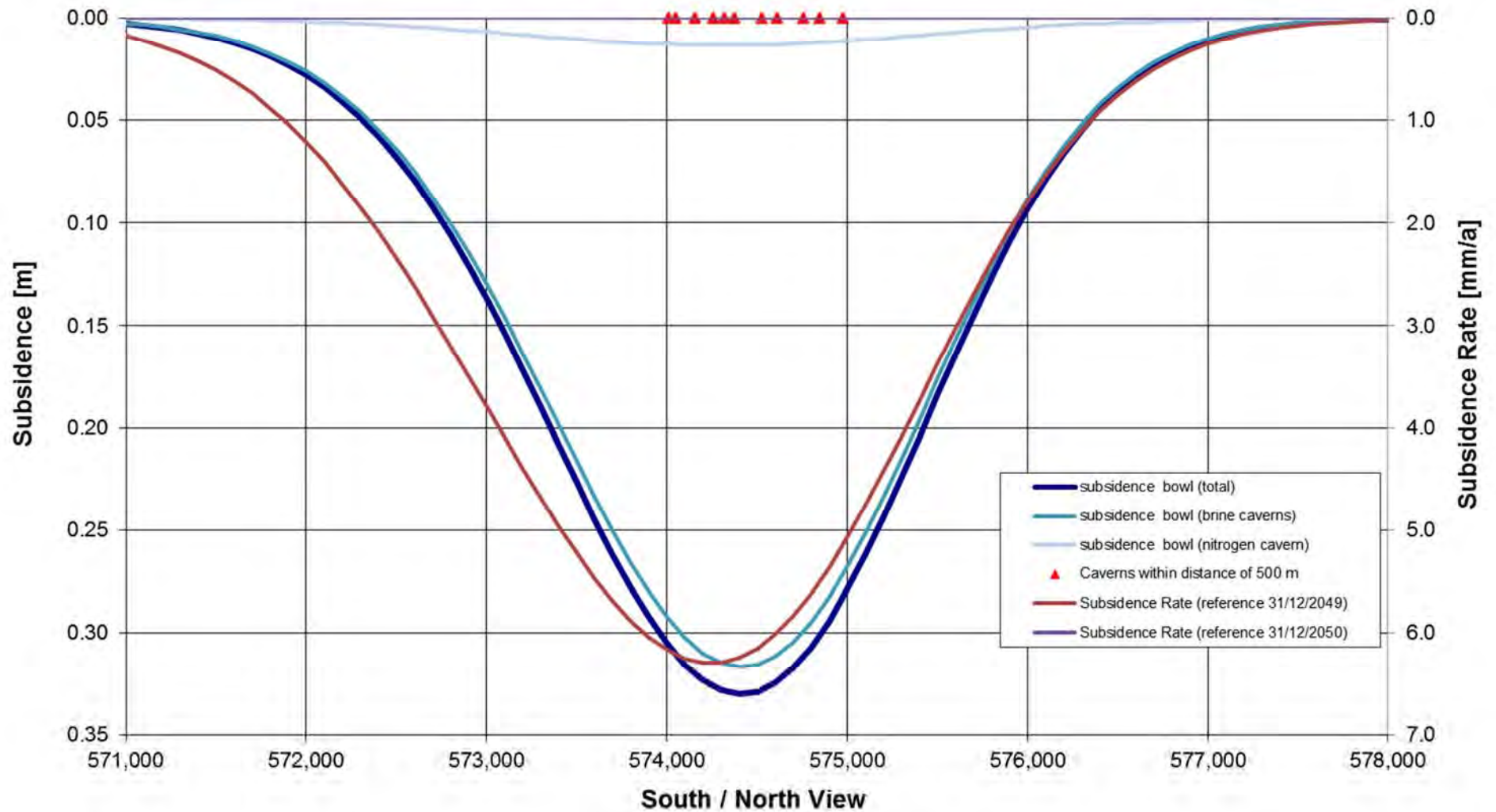
Enclosure 18

Heiligerlee – Subsidence bowl at fixed Northing 574,500 – 31/12/2050

Subsidence Bowl at fixed Easting 263,400 (31/12/2050)

Heiligerlee - Superposition of all Caverns

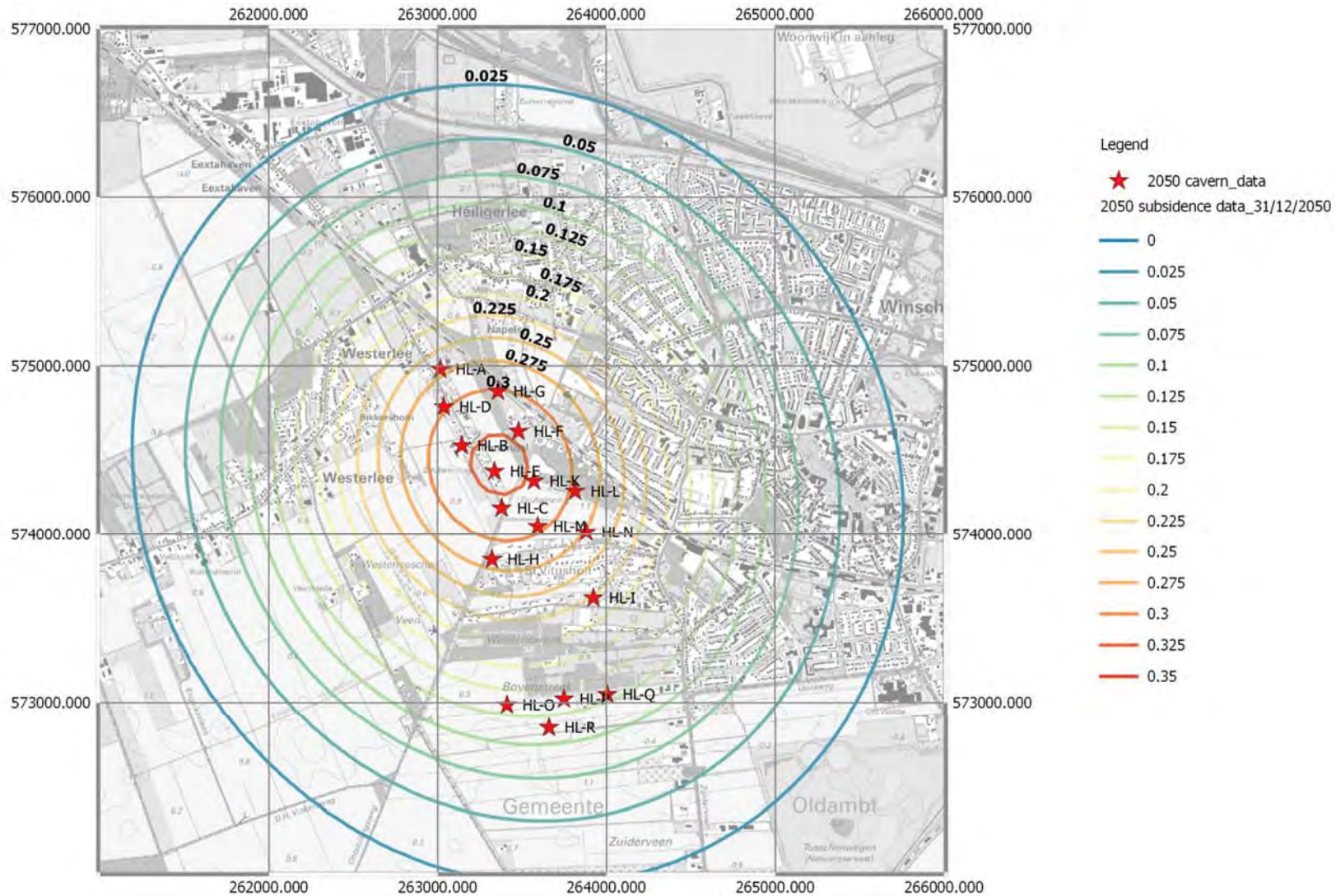
Subsidence Modell 35-25-30-1-0.12-2-40-0.8-5-60



Enclosure 19

Heiligerlee – Subsidence bowl at fixed Easting 263,400 – 31/12/2050

map produced with QGIS, see <http://www.qgis.org/de/site/>
 topographic map appears under the free license agreement, downloaded from
<https://www.pdok.nl/nl/producten/pdok-downloads/basis-registratie-topografie/toprafter/toprafter-actueel/top25rafter>



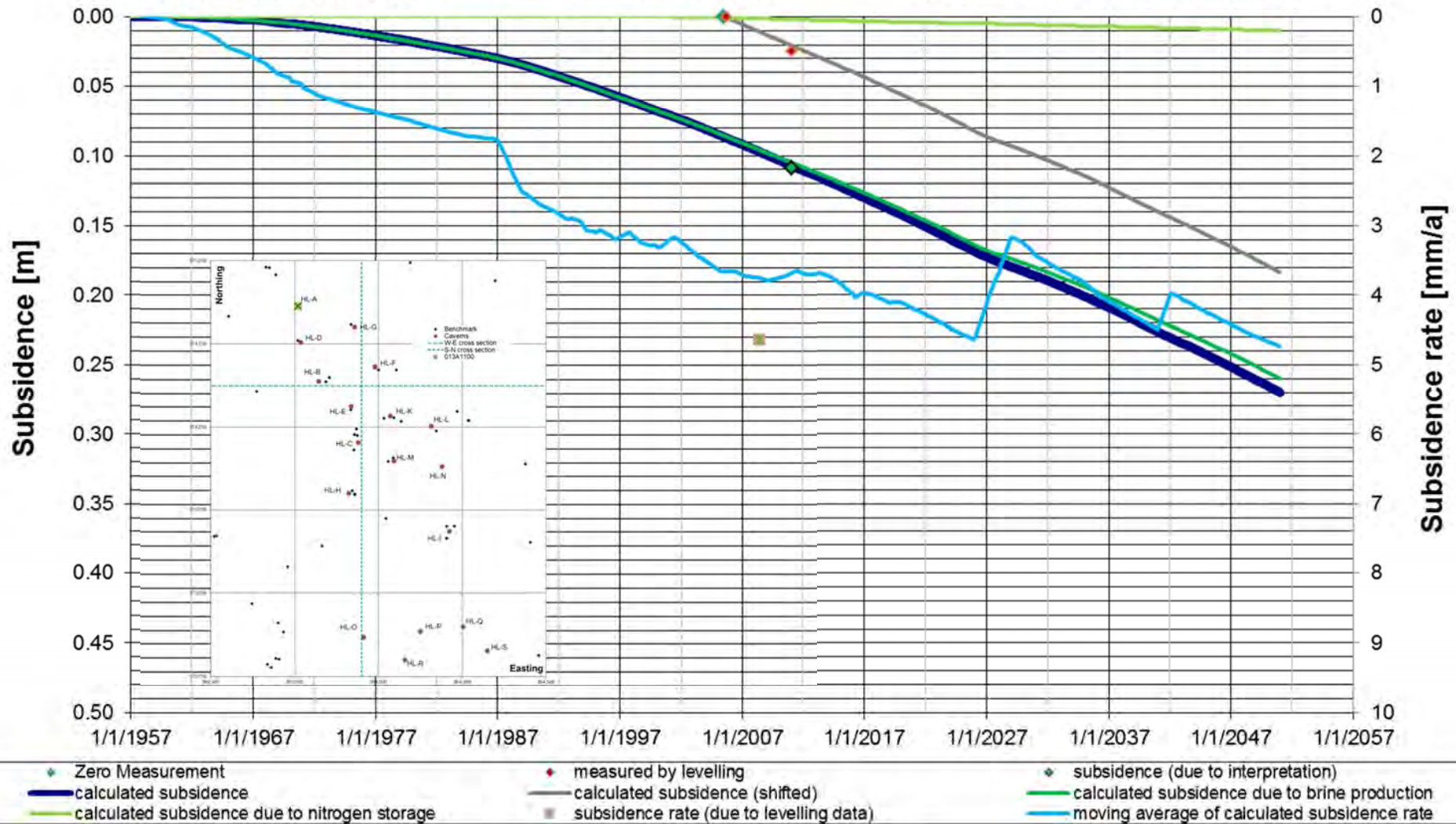
Enclosure 20
 Heiligerlee – Subsidence bowl – 31/12/2050

AkzoNobel / Gasunie (Heiligerlee) - Subsidence Bowl (Gauss)

Benchmark 013A1100 (HL-A)

Period (1957-2050)

Subsidence Modell 35-25-30-1-0.12-2-40-0.8-5-60



Enclosure 21

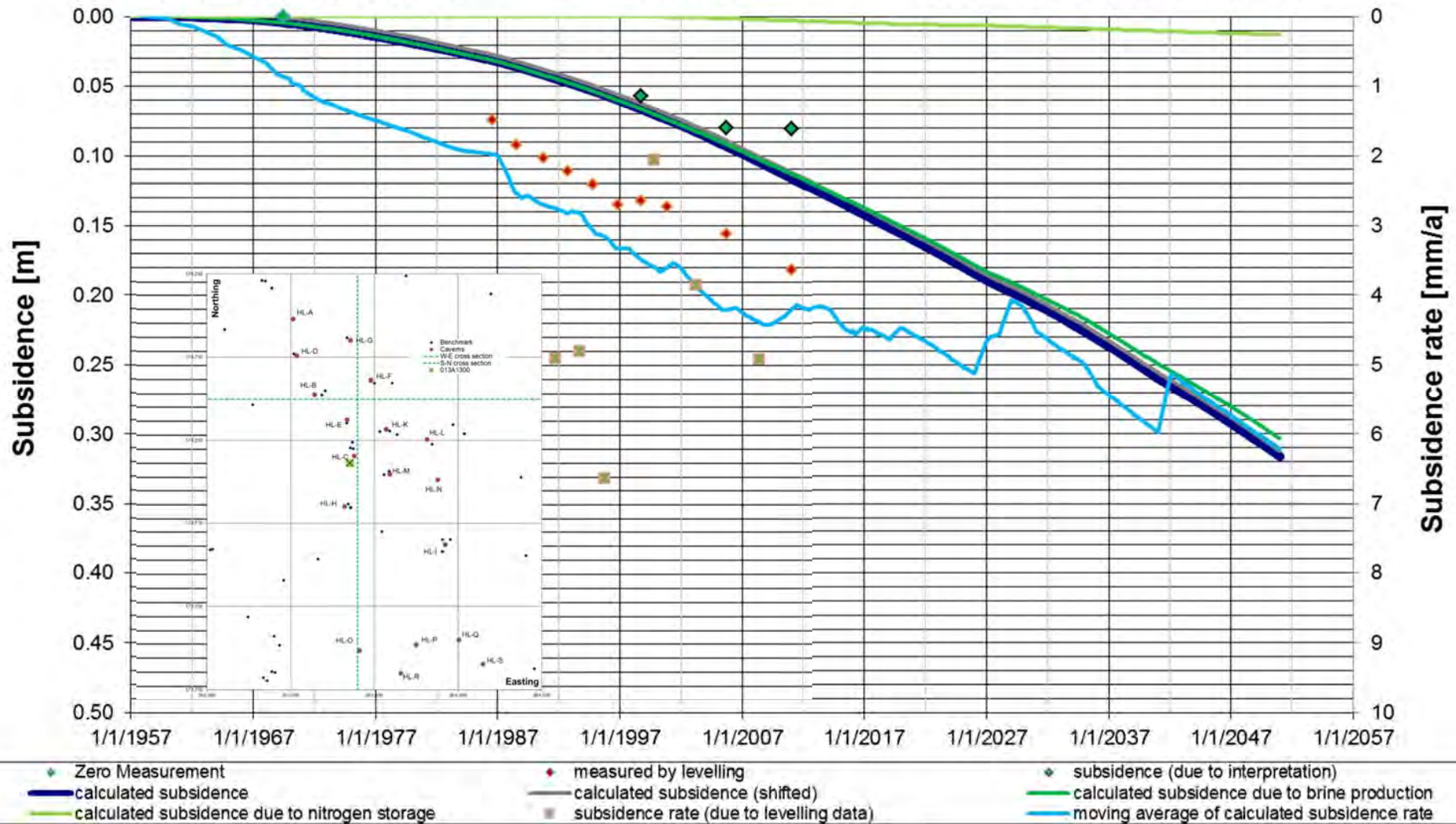
Heiligerlee – Benchmark 013A1100 – Comparison of observed subsidence with measured values

AkzoNobel / Gasunie (Heiligerlee) - Subsidence Bowl (Gauss)

Benchmark 013A1300 (HL-C)

Period (1957-2050)

Subsidence Modell 35-25-30-1-0.12-2-40-0.8-5-60



Enclosure 22

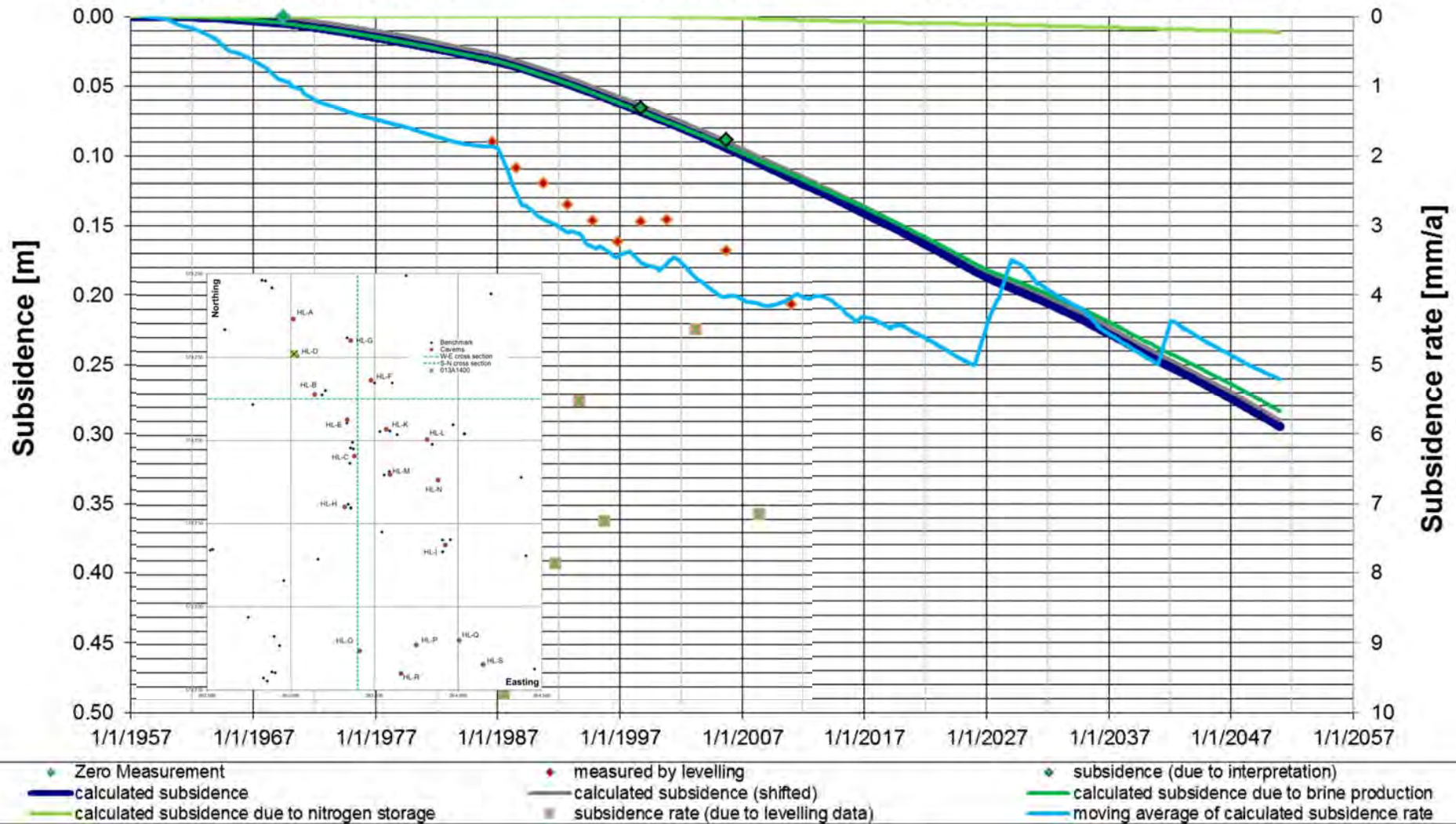
Heiligerlee – Benchmark 013A1300 – Comparison of observed subsidence with measured values

AkzoNobel / Gasunie (Heiligerlee) - Subsidence Bowl (Gauss)

Benchmark 013A1400 (HL-D)

Period (1957-2050)

Subsidence Modell 35-25-30-1-0.12-2-40-0.8-5-60



Enclosure 23

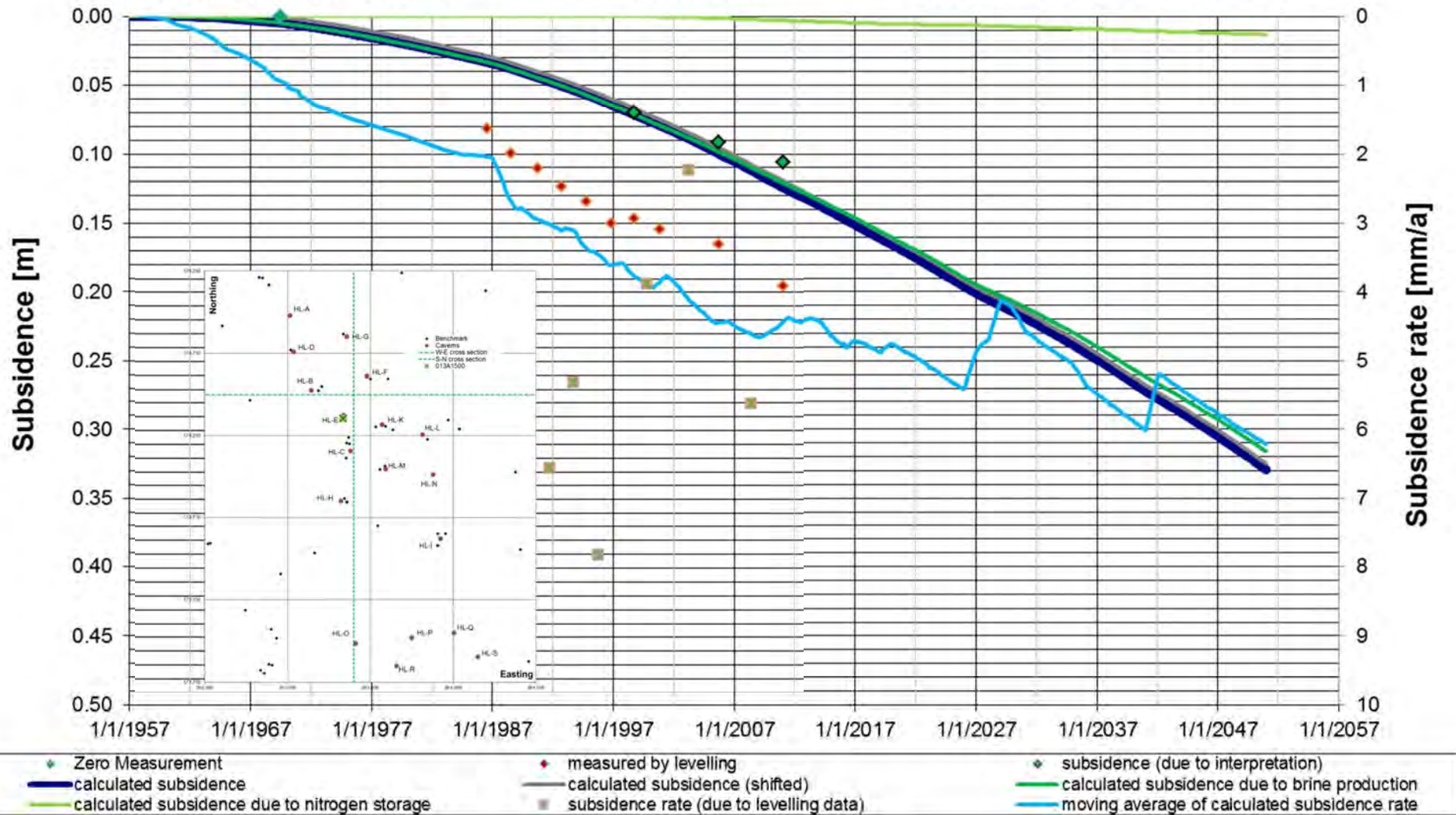
Heiligerlee – Benchmark 013A1400 – Comparison of observed subsidence with measured values

AkzoNobel / Gasunie (Heiligerlee) - Subsidence Bowl (Gauss)

Benchmark 013A1500 (HL-E)

Period (1957-2050)

Subsidence Modell 35-25-30-1-0.12-2-40-0.8-5-60



Enclosure 24

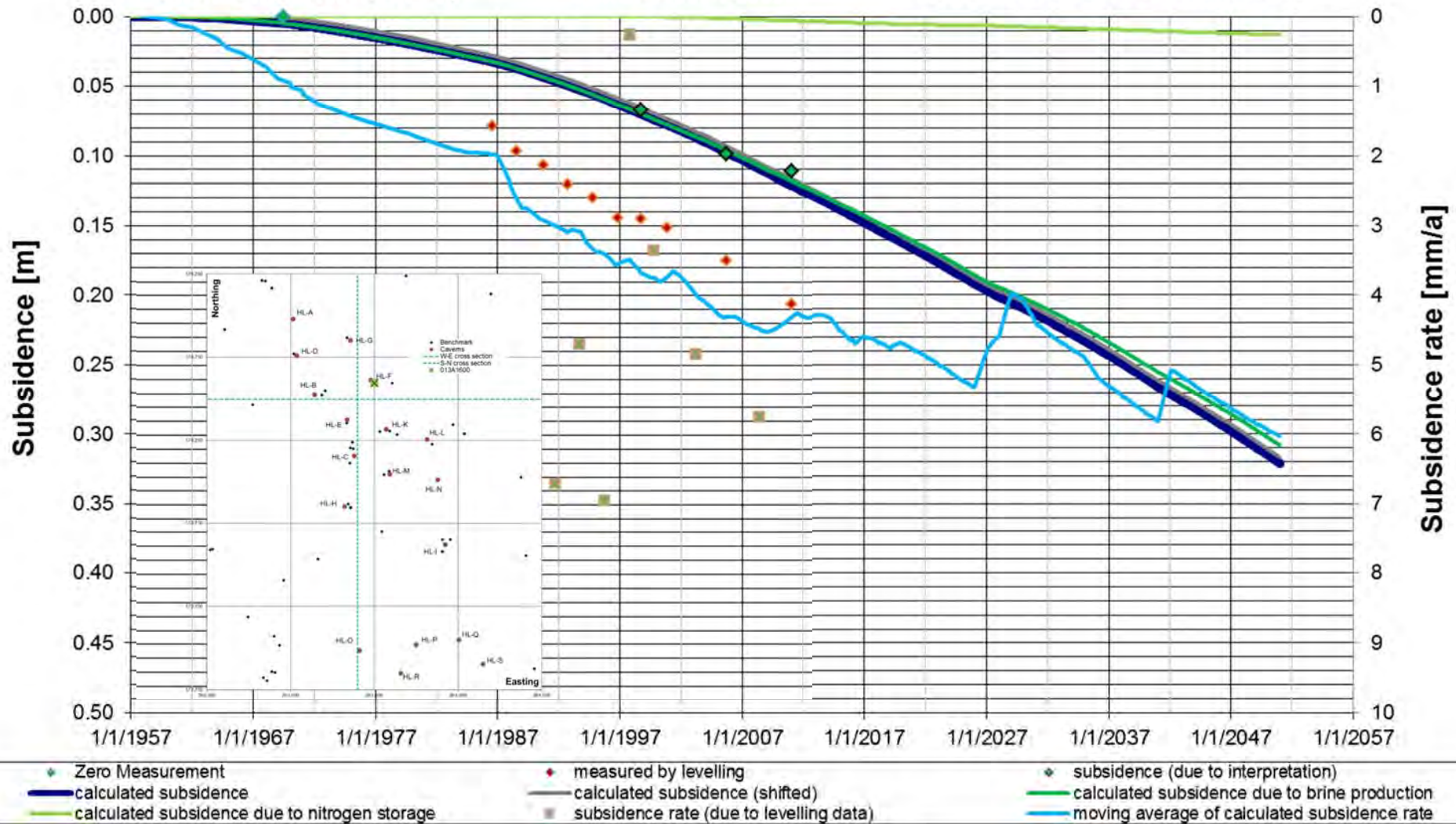
Heiligerlee – Benchmark 013A1500 – Comparison of observed subsidence with measured values

AkzoNobel / Gasunie (Heiligerlee) - Subsidence Bowl (Gauss)

Benchmark 013A1600 (HL-F)

Period (1957-2050)

Subsidence Modell 35-25-30-1-0.12-2-40-0.8-5-60



Enclosure 25

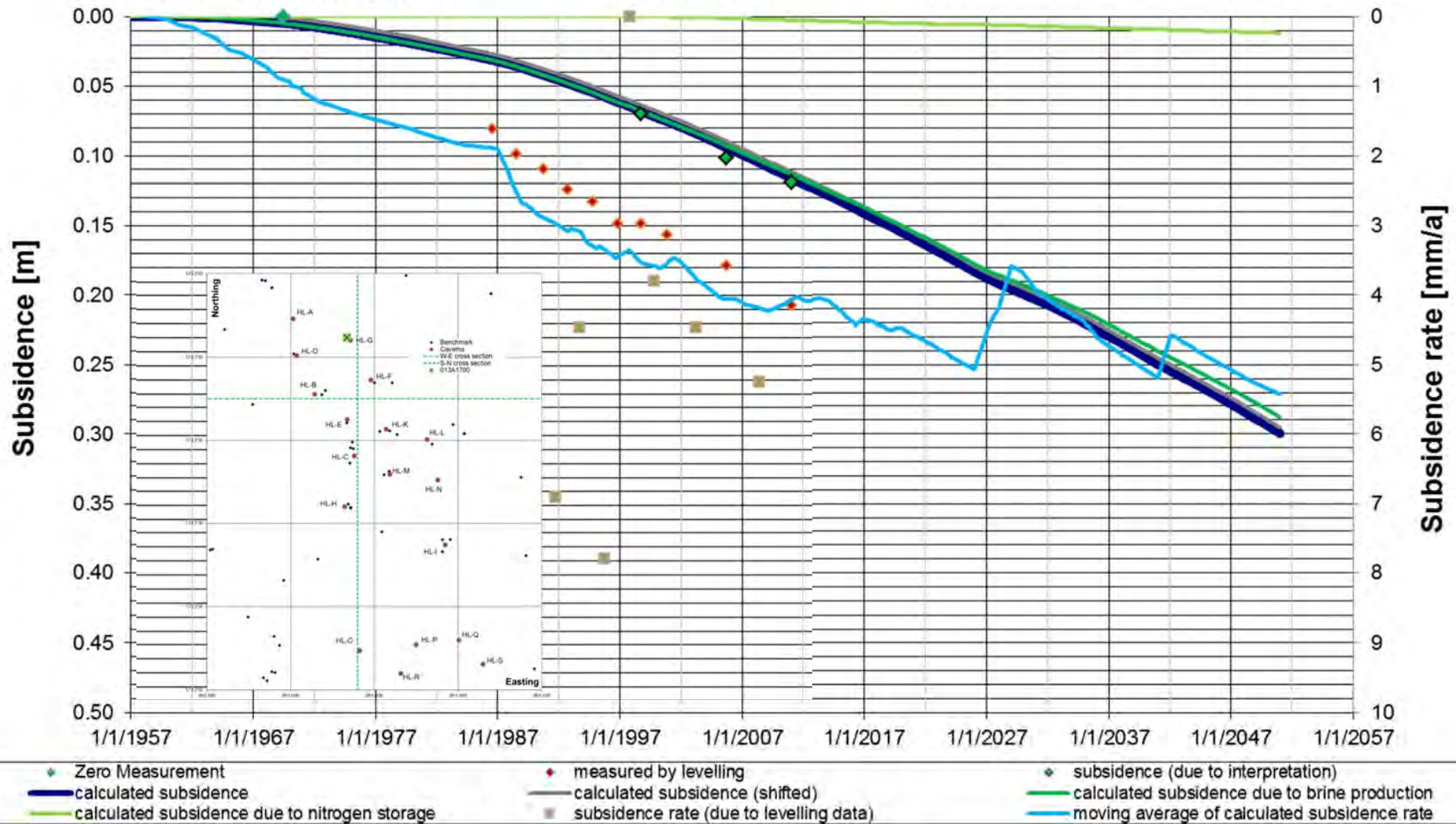
Heiligerlee – Benchmark 013A1600 – Comparison of observed subsidence with measured values

AkzoNobel / Gasunie (Heiligerlee) - Subsidence Bowl (Gauss)

Benchmark 013A1700 (HL-G)

Period (1957-2050)

Subsidence Modell 35-25-30-1-0.12-2-40-0.8-5-60



Enclosure 26

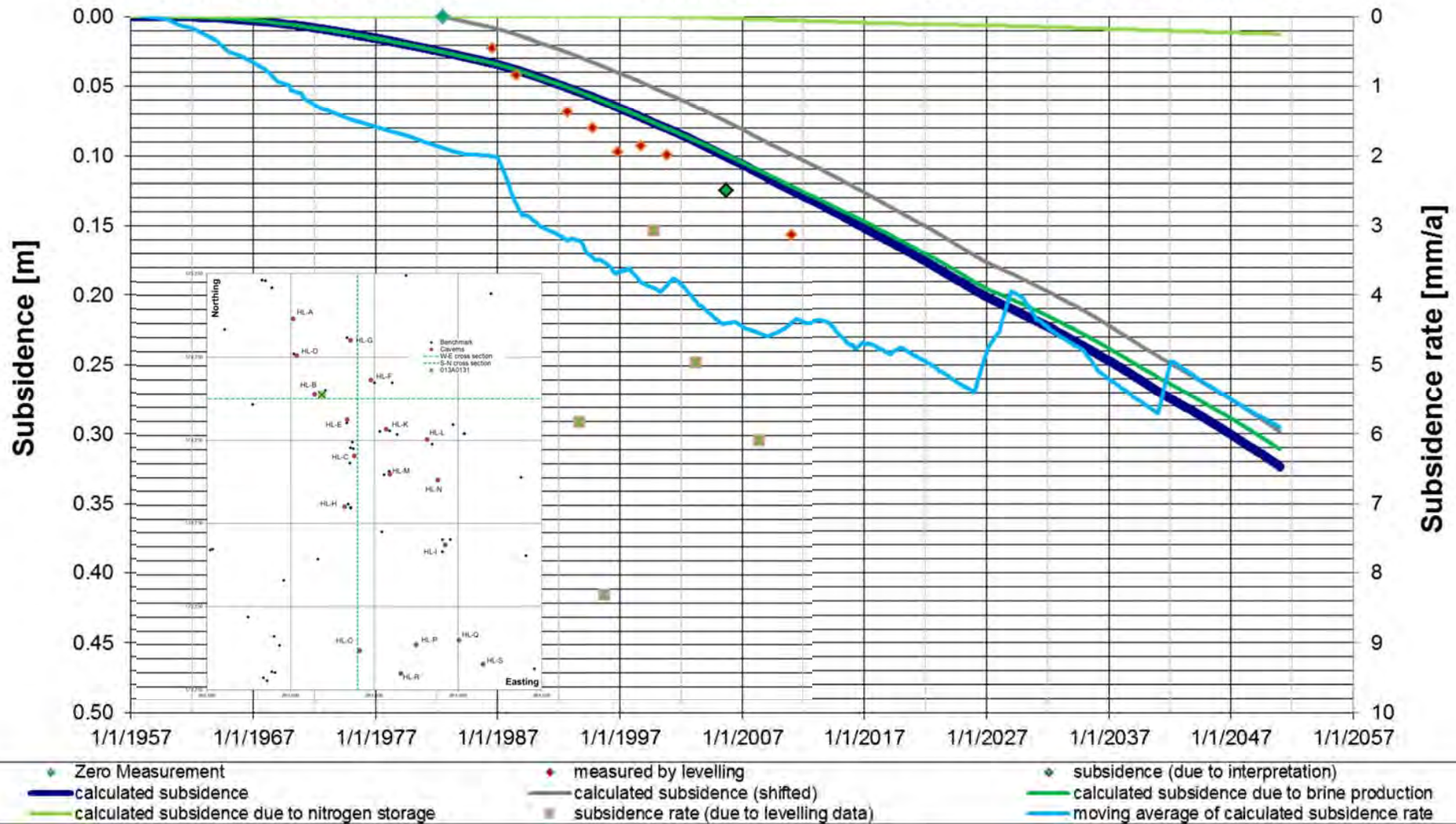
Heiligerlee – Benchmark 013A1700 – Comparison of observed subsidence with measured values

AkzoNobel / Gasunie (Heiligerlee) - Subsidence Bowl (Gauss)

Benchmark 013A0131 (HL-B)

Period (1957-2050)

Subsidence Modell 35-25-30-1-0.12-2-40-0.8-5-60



Enclosure 27

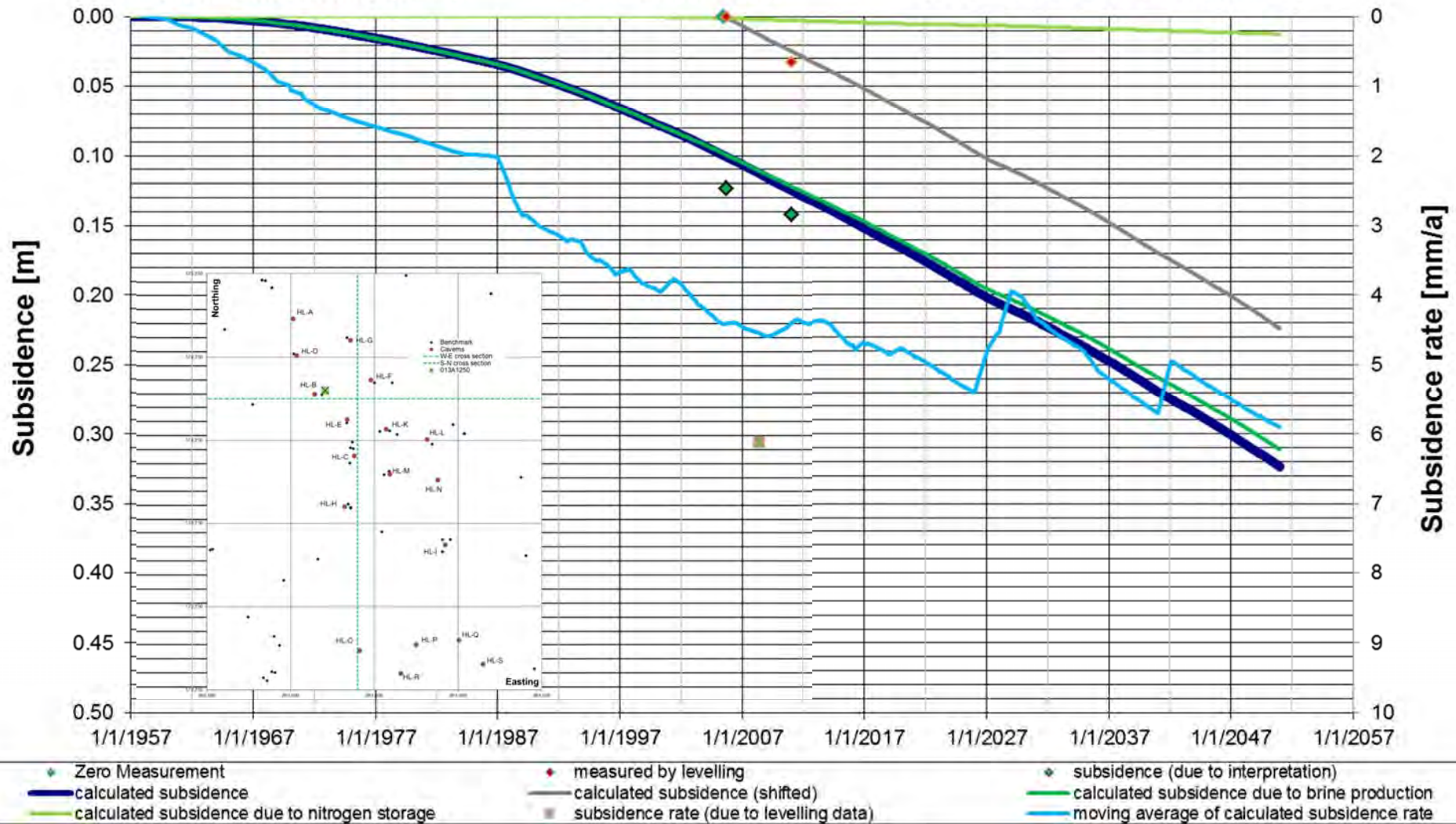
Heiligerlee – Benchmark 013A0131 – Comparison of observed subsidence with measured values

AkzoNobel / Gasunie (Heiligerlee) - Subsidence Bowl (Gauss)

Benchmark 013A1250 (HL-B)

Period (1957-2050)

Subsidence Modell 35-25-30-1-0.12-2-40-0.8-5-60



Enclosure 28

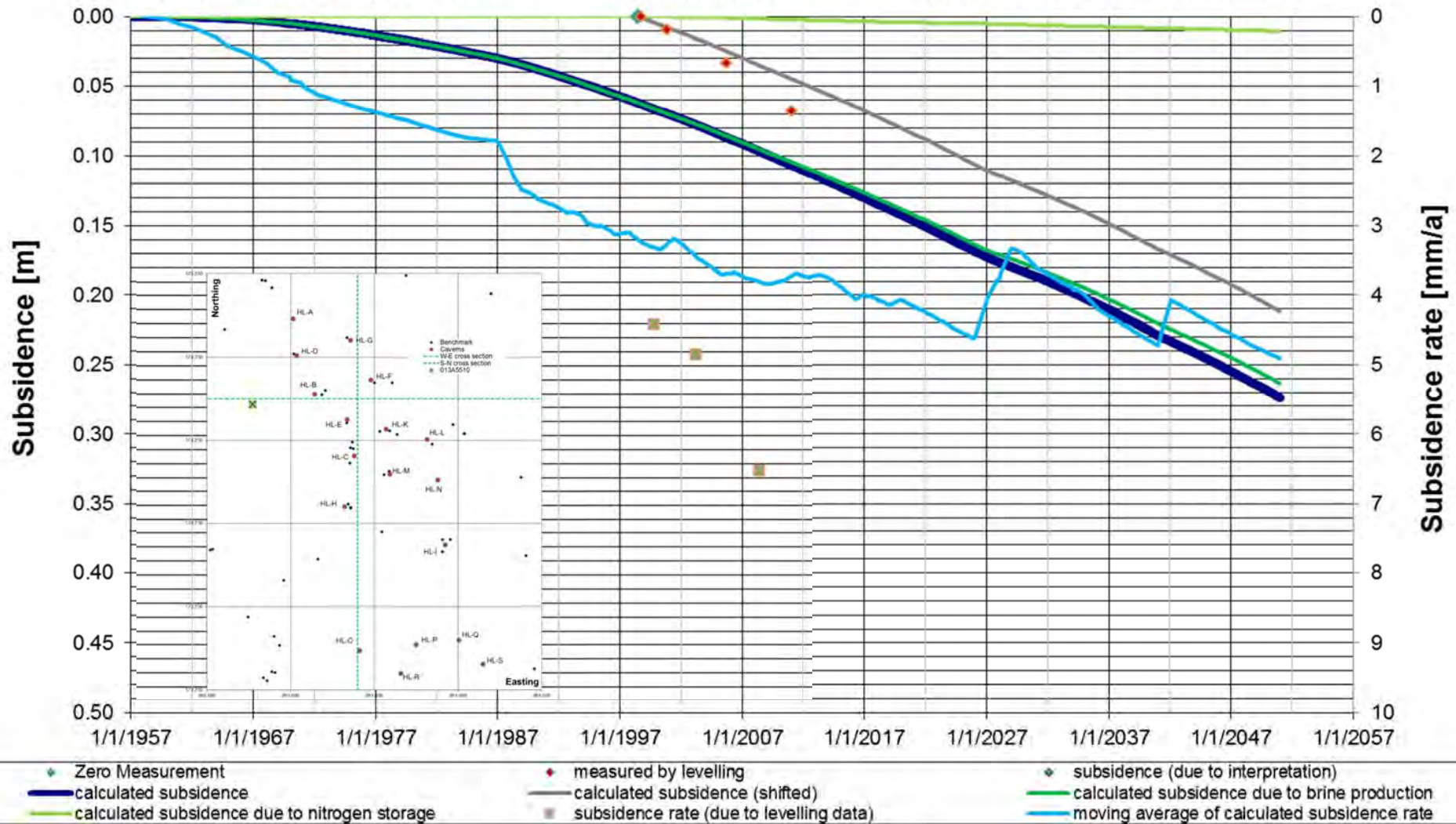
Heiligerlee – Benchmark 013A1250 – Comparison of observed subsidence with measured values

AkzoNobel / Gasunie (Heiligerlee) - Subsidence Bowl (Gauss)

Benchmark 013A5510 (HL-B)

Period (1957-2050)

Subsidence Modell 35-25-30-1-0.12-2-40-0.8-5-60



Enclosure 29

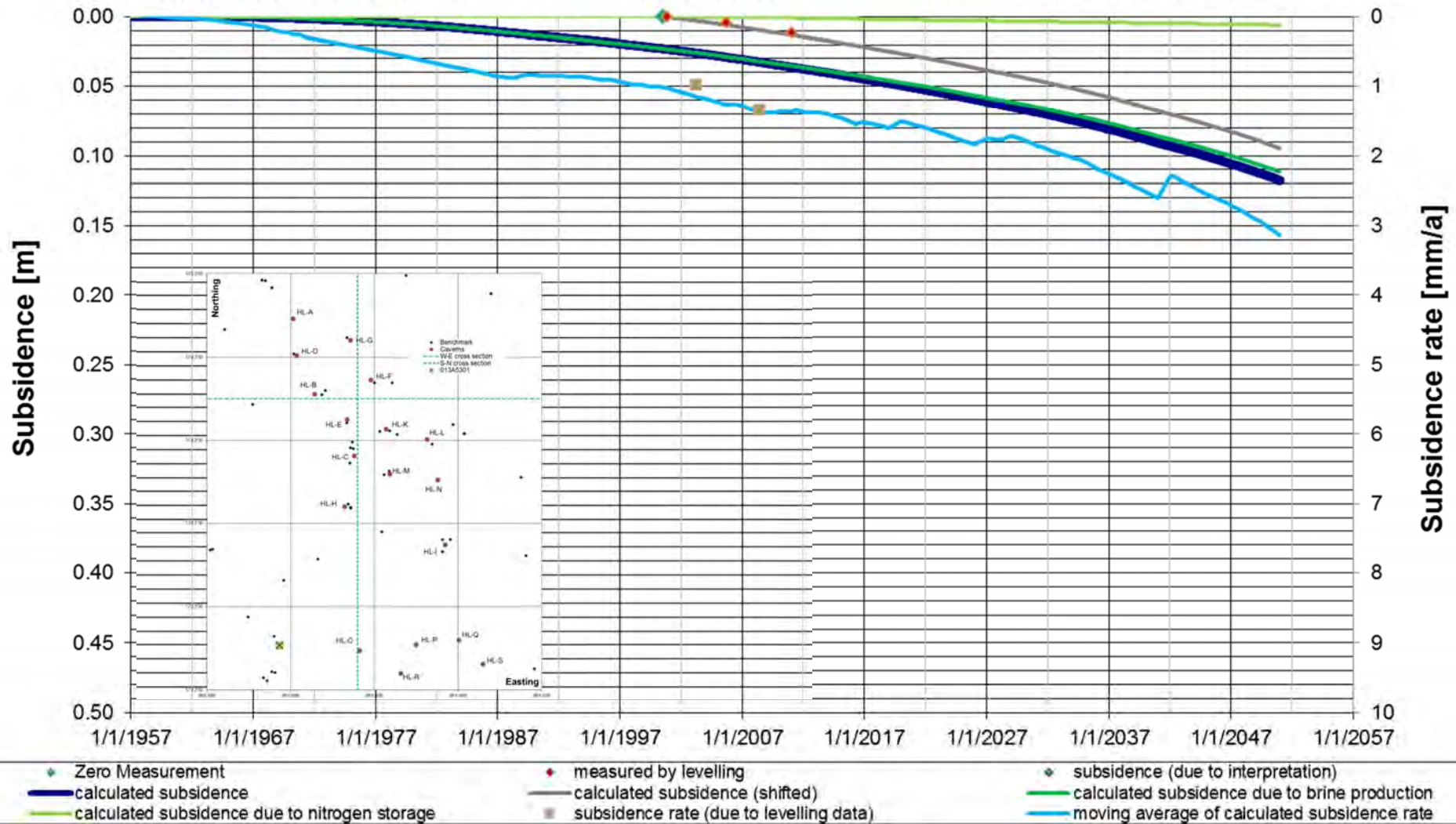
Heiligerlee – Benchmark 013A5510 – Comparison of observed subsidence with measured values

AkzoNobel / Gasunie (Heiligerlee) - Subsidence Bowl (Gauss)

Benchmark 013A5301 (HL-O)

Period (1957-2050)

Subsidence Modell 35-25-30-1-0.12-2-40-0.8-5-60



Enclosure 30

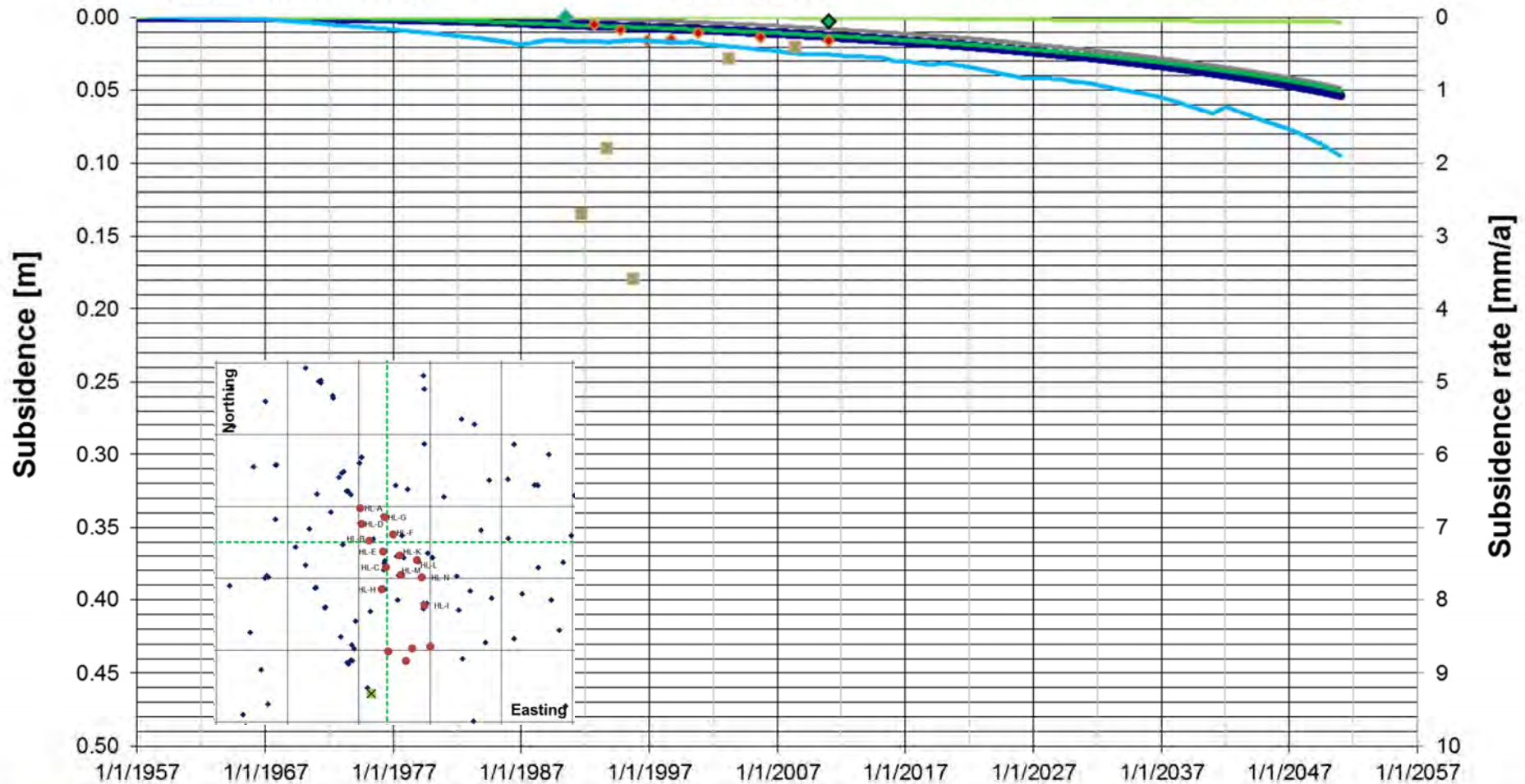
Heiligerlee – Benchmark 013A5301 – Comparison of observed subsidence with measured values

AkzoNobel / Gasunie (Heiligerlee) - Subsidence Bowl (Gauss)

Benchmark 013A5025 (HL-O)

Period (1957-2050)

Subsidence Modell 35-25-30-1-0.12-2-40-0.8-5-60



Enclosure 31

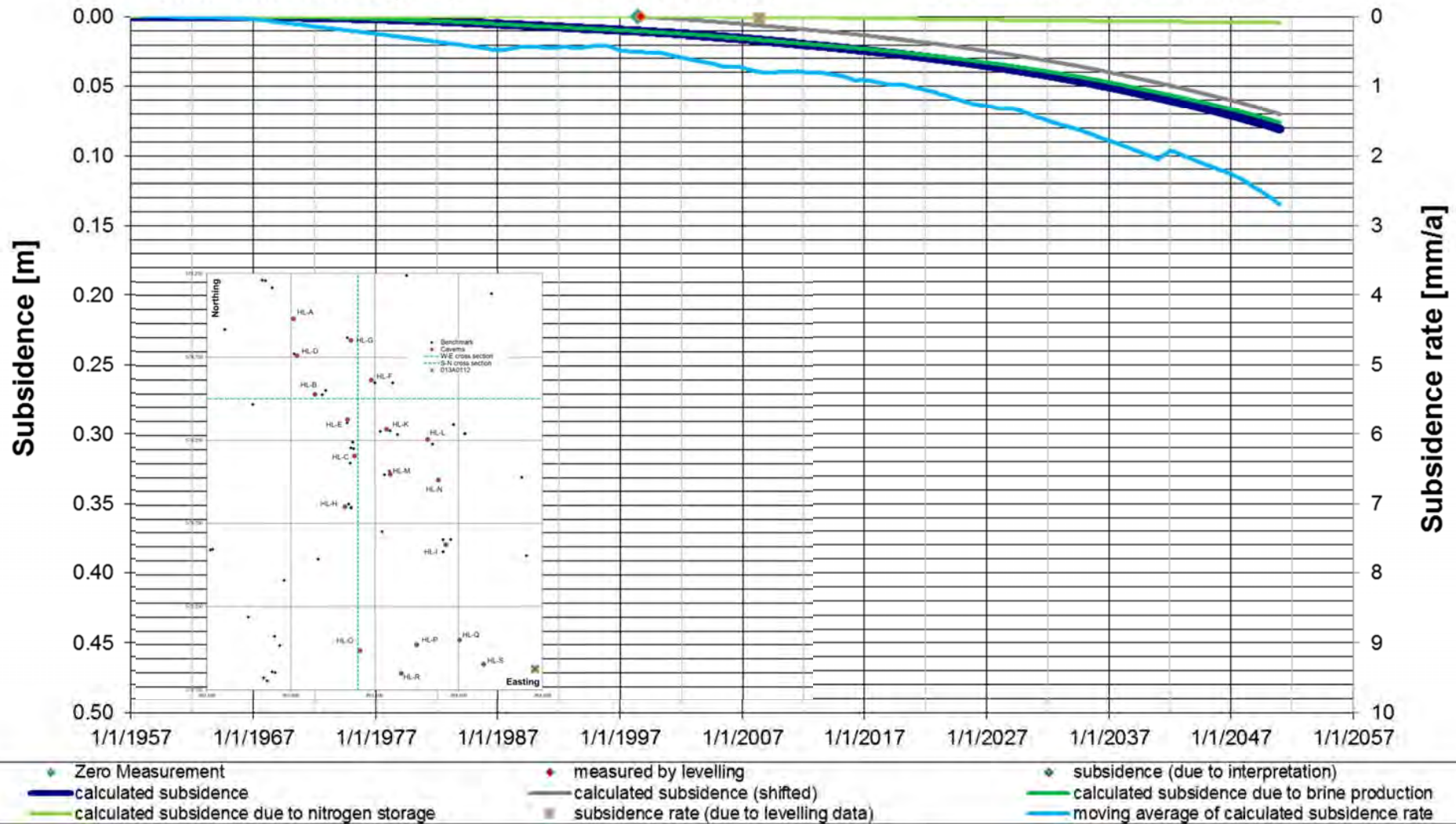
Heiligerlee – Benchmark 013A5025 – Comparison of observed subsidence with measured values

AkzoNobel / Gasunie (Heiligerlee) - Subsidence Bowl (Gauss)

Benchmark 013A0112 (HL-S)

Period (1957-2050)

Subsidence Modell 35-25-30-1-0.12-2-40-0.8-5-60



Enclosure 32

Heiligerlee – Benchmark 013A0112 – Comparison of observed subsidence with measured values

Tab: Seismic Network Specifications

13 Fitzroy Street
London
W1T 4BQ
United Kingdom
www.arup.com

t +44 20 7636 1531
d +44 20 7755 2569

Project title	Salt Mine Seismicity	Job number	260166-00
cc	Manuela Villani, Ziggy Lubkowski	File reference	60
Prepared by	Thomas Ader (London)	Date	20 March 2018
Subject	Seismic Monitoring Network Technical Specifications - RevB		

1 Introduction

This note aims to provide the technical performance specifications for the seismic monitoring network that shall be deployed at the salt caverns in Heiligerlee (HL) and Zuidwending (ZW). This seismic monitoring network shall be able to record relevant seismic activity at the salt caverns in order to assess any potential hazard due to operations. We propose a preliminary design for the monitoring network using already available locations.

2 Network Specifications

The monitoring network shall achieve the following performance requirements:

- The monitoring system shall be able to detect and locate all events down to at least a magnitude of -1.0 within an area extending 500m away from the salt caverns;
- The location accuracy (95% confidence intervals) shall be better than 50m horizontally and 150m vertically, in order to be able to distinguish which salt cavern the event has occurred in or next to;
- The maximum azimuthal gap in coverage should not exceed 90°, assuming a source at the centre of the network; and
- The monitoring instruments shall record a frequency content wide enough, from 1Hz to 250Hz, in order to record micro tremors as well as possible rock collapse in brine.

The network should incorporate sufficient redundancy so that data quality and analysis capability is not compromised in the event of a reasonable percentage of equipment failure.

3 Instrumentation and Measurements

Measurements and data interpretation shall need to provide reliable determination of microseismic source parameters, such as origin time, magnitude and 3D location (latitude, longitude and depth).

Technical Note

260166-00

20 March 2018

The sensors in the monitoring network should have sufficient sensitivity to reliably resolve ground motion for the smallest magnitude events of interest. The recorded data should have a minimum signal-to-noise ratio of three for an event of the minimum magnitude (-1.0) near the zone of interest, in order to provide reliable identification of seismic phases and corresponding location accuracy. We expect that a noise level and a sensitivity below 0.1 $\mu\text{m/s}$ (or equivalent for hydrophone) shall be required.

The sensors and the digital recording equipment shall have a high dynamic range.

The seismic sensors can be a combination of hydrophones and 3D geophones or accelerometers, in order to optimize the costs of the network, while providing enough information on the failure mechanism and wave propagation attributes, as well as providing data for required location accuracy.

In order to determine the actual ground motion at the sensor locations, the calibration information or instrument response of the sensors and recording equipment shall be provided.

The Contractor shall provide the technical specifications of the instruments that they intend to use in the microseismic monitoring network.

4 System Operation

Real-time data shall be required for the network, which should be fully integrated within the existing KNMI seismic monitoring network. The Contractor shall examine the best option to achieve real-time data coverage, between cable and 4G, which shall involve checking the reliability of the local 4G coverage.

A full and complete metadata shall be created and maintained. This shall include the location of each station and the serial numbers of all instrumentation present as well as the instrument response data, along with a history of any changes to that instrumentation due, for example, to failure.

Continuous data from all stations in the system shall be archived. The archived data shall contain not only the raw data but also the instrument response information. The recorded time series and metadata, both for individual events and the continuous recordings from each site shall be in an internationally recognised format for data exchange.

5 Data Interpretation

The data interpretation methodology should be sufficient to provide a three dimensional view of the events. Each event data point shall include, as a minimum, longitude, latitude, depth, magnitude, time at origin and type of movement.

6 Monitoring Strategy

6.1 Existing Instruments and Possible Locations

Several locations are available to install monitoring instruments either inside salt caverns or at the surface. Figure 1 shows the available surface locations (dark green areas) and available salt caverns.

Technical Note

260166-00

20 March 2018

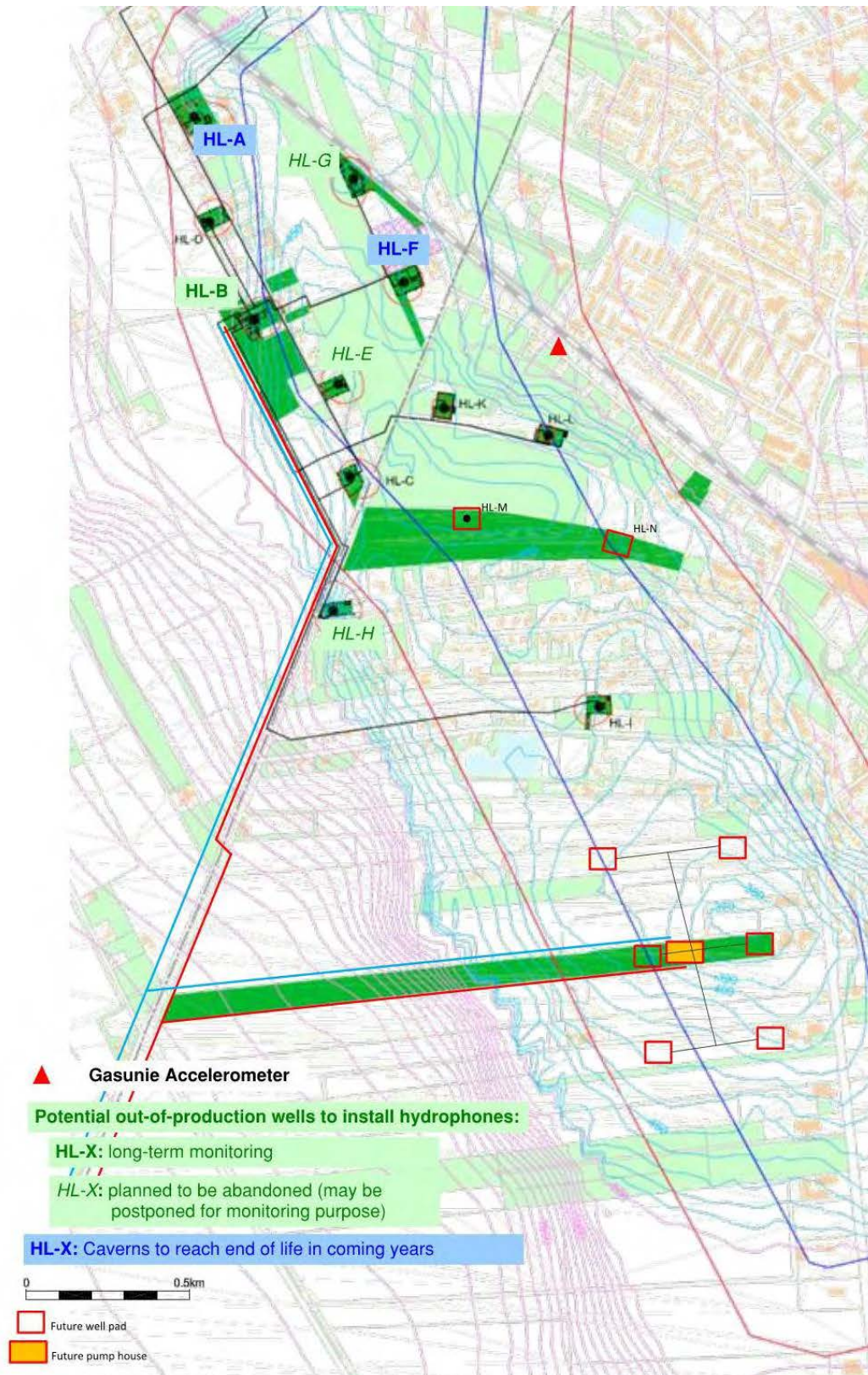


Figure 1: Locations of Gasunie accelerometer, of caverns that could potentially host a recording instrument, presently or in the future. The dark green areas are AzkoNobel property and could potentially be used for installation of surface monitoring equipment.

Technical Note

260166-00

20 March 2018

Gasunie already has an accelerometer in place in the vicinity of the salt caverns and its location is shown in Figure 1 (red triangle). From the recordings at this accelerometer, the noise level is about:

- $2 \times 10^{-5}g$ in the X direction;
- $5 \times 10^{-5}g$ in the Y direction; and
- $3 \times 10^{-5}g$ in the Z direction.

Performance of this accelerometer shall be specified and this accelerometer shall be included in the network design.

For the salt caverns:

- Four caverns are currently available to install monitoring equipment: HL-B, HL-E, HL-G and HL-H (in green in Figure 1);
- Three of these four caverns are planned to be abandoned: HL-E, HL-G and HL-H. However, the plan to abandon these caverns may be postponed for monitoring purposes; and
- Two salt caverns will reach end-of-life in the coming years: HL-A and HL-F (in blue in Figure 1). These caverns could therefore host monitoring instruments in the future, possibly from the caverns that will be abandoned.

6.2 Feasibility Study

The typical approach in designing a seismic network consists in first performing a feasibility study. The feasibility study shall provide different options for seismic network designs, with an estimate of the technical performances for each design. The feasibility study shall provide the following information:

- Number of stations necessary to achieve the required performance specifications;
- Location of the different stations (surface location and depth in the salt caverns); and
- Associated capex plan.

Typically, the feasibility study shall determine whether the performance specifications are achievable by using only the surface locations and caverns available. If it is achievable, the feasibility study shall provide:

- The minimum number of instruments required to achieve the required performance and the corresponding optimum configuration of the recording instruments; and
- The performance (magnitude sensitivity and location accuracy) achievable with a smaller network (with one and two fewer instruments) and the corresponding optimum configuration.

If the required performance is not achievable with the available locations for monitoring equipment, the feasibility study shall provide:

- The performance achieved by networks of four to twelve recording instruments, optimally distributed at the available locations;
- The requirements in terms of monitoring instruments outside of the available locations in order to achieve the required performance.

Technical Note

260166-00 20 March 2018

This information shall support the decision-making process in order to select a network design as fit for purpose as possible, which respecting budget and time constraints.

6.3 Network Design Strategy

Given the sense of urgency to deploy a seismic monitoring network, time needs to be optimised while reaching a compromise between the time taken to install the network, the cost of the network and the technical performance of the network.

When installing a seismic-monitoring network, a progressive approach is the preferred way to reduce the cost. Initially a limited network should be installed, which provides preliminary data on existing noise levels and refine estimates of achievable technical performance. This initial set of data shall then be used to expand the network, if necessary, to a final network. This shall be optimised in terms of technical performance and cost. Even if the initial network needs to be extended, the data from this initial network shall already be useful. This is a way to install a seismic network as quickly as possible. This shall depend on the conclusions of the feasibility study.

KNMI already has some stations in place, as shown in Figure 2, but most of these stations are too far from the salt caverns to provide the expected sensitivity and accuracy. Only G57 may be close enough to be integrated into the local seismic monitoring network.

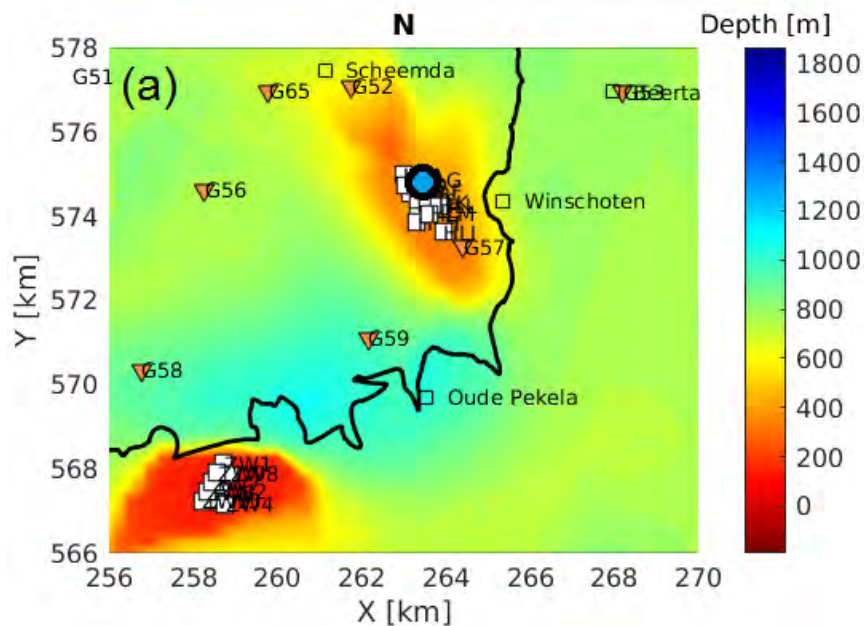


Figure 2: Location of the KNMI seismic stations (orange triangles) with respect to the salt caverns of Heiligerlee (HL) and Zuidwending (ZW). The map's background represents the depth of the North Sea group sediments so that the salt domes appear in red. The border of the Groningen gas field is indicated by the black line.

7 Preliminary Seismic Network Design

To facilitate the development of the network, a preliminary seismic network has been developed to monitor seismic activity within the HL salt dome. The Contractor shall provide a quote on the cost to build such a network and a realistic system commissioning date (date at which the system will be

Technical Note

260166-00

20 March 2018

able to start acquiring and providing data). Note that the system shall be in place as soon as possible and not later than 30 September 2018. The Contractor should suggest modifications to this layout, in order to maximise performance. These should be discussed and agreed during an inception meeting.

The preliminary design consists of six three-component (3C) geophones and four hydrophones. Three of the hydrophones are located within the wells of three salt caverns and one is positioned inside the fourth salt cavern, in order to be below the casing shoe in that cavern. The six 3C geophones are located within shallow 20m-deep boreholes (Figure 3). The ten instruments are therefore divided into:

- Four hydrophones, located below the casing shoe of the available caverns:
 - One hydrophone at a depth of 700m inside HL-B;
 - One hydrophone at a depth of 900m inside HL-E;
 - One hydrophone at a depth of 650m inside HL-G; and
 - One hydrophone at a depth of 700m inside HL-H.
- Six 3C 1Hz geophones divided as follows:
 - Four 3C 1Hz geophone located in shallow 20m-deep boreholes next to the boreholes of the salt caverns HL-B, HL-E, HL-G and HL-H; and
 - Two 3C 1Hz geophones located within shallow boreholes, at a depth of 20m, at locations indicated in Figure 3.

The use of the two additional shallow boreholes will provide a better azimuthal coverage of the network.

The depth of the shallow boreholes has been selected at 20m in order to minimize the amount of surface noise and attenuation from Holocene sediments. An analysis of the thickness of Holocene deposits from DINOloket (GeoTop v1.3 geological model) reveals that the thickness of Holocene deposits is less than 3.5m within 2km of the centre of the site (Figure 4) and that the depth of the bottom of the Boxtel (BX) layer is always less than 15m. The depth of 20m therefore ensures that the instruments are located within the Peel (PE) formation (Figure 4).

The use of 1Hz geophones will enable the monitoring network to capture low frequency signals, while the hydrophones will capture higher frequency content.

Figure 5 provides a cross section of the different caverns and the locations of the hydrophones and geophones in the wells of the selected caverns.

For future development, if the plan to abandon caverns HL-G, HL-E and/or HL-H is adopted, the option to embed 3C geophones in the seal of these caverns shall be considered. The hydrophones may be displaced to caverns HL-A and HL-F when operations in these caverns cease.

Technical Note

260166-00

20 March 2018

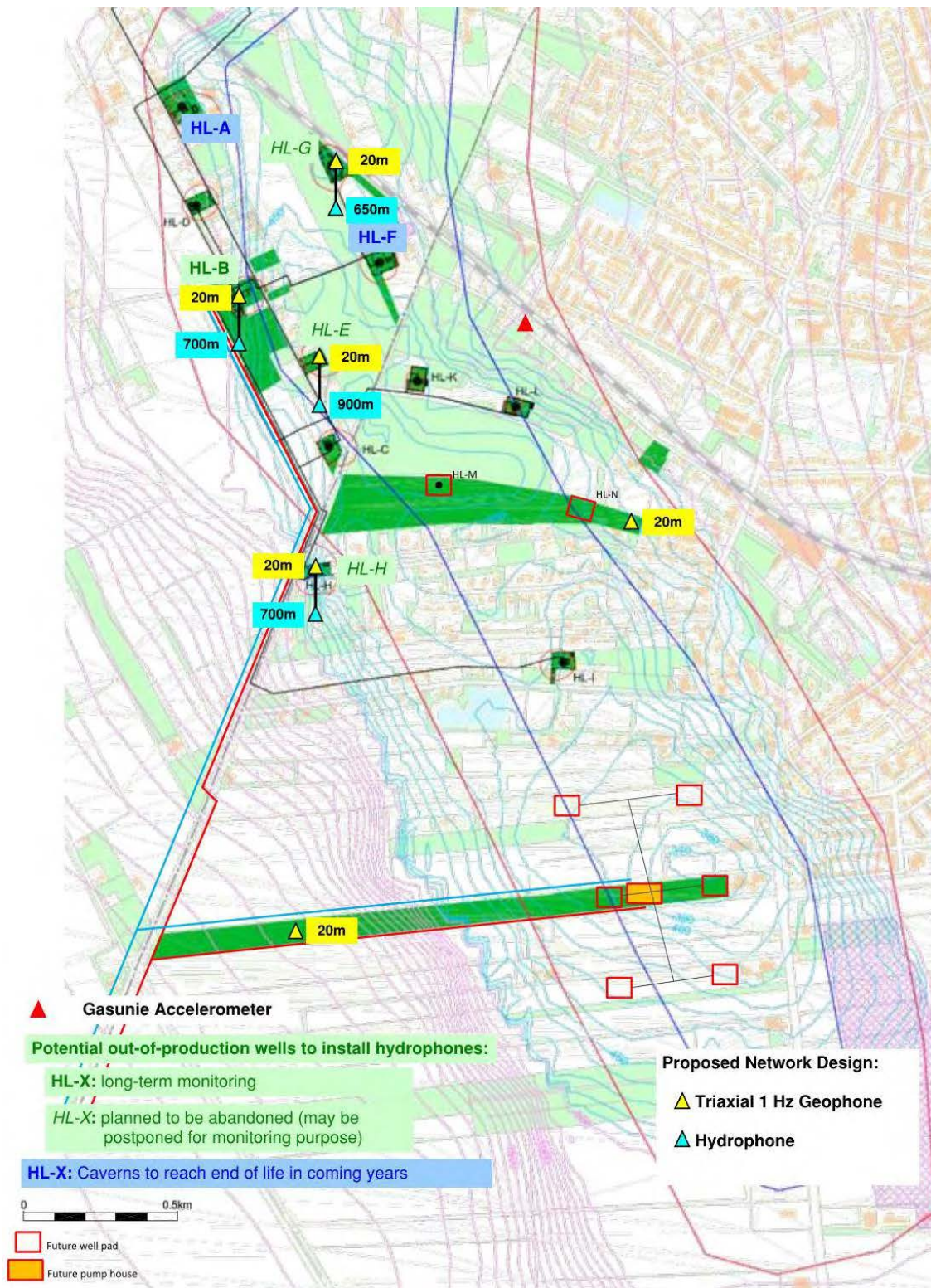


Figure 3: Map showing the location of the 10 instruments proposed in the design of the microseismic monitoring network in the HL salt dome. The depths of the different instruments are indicated in the Figure.

Technical Note

260166-00

20 March 2018

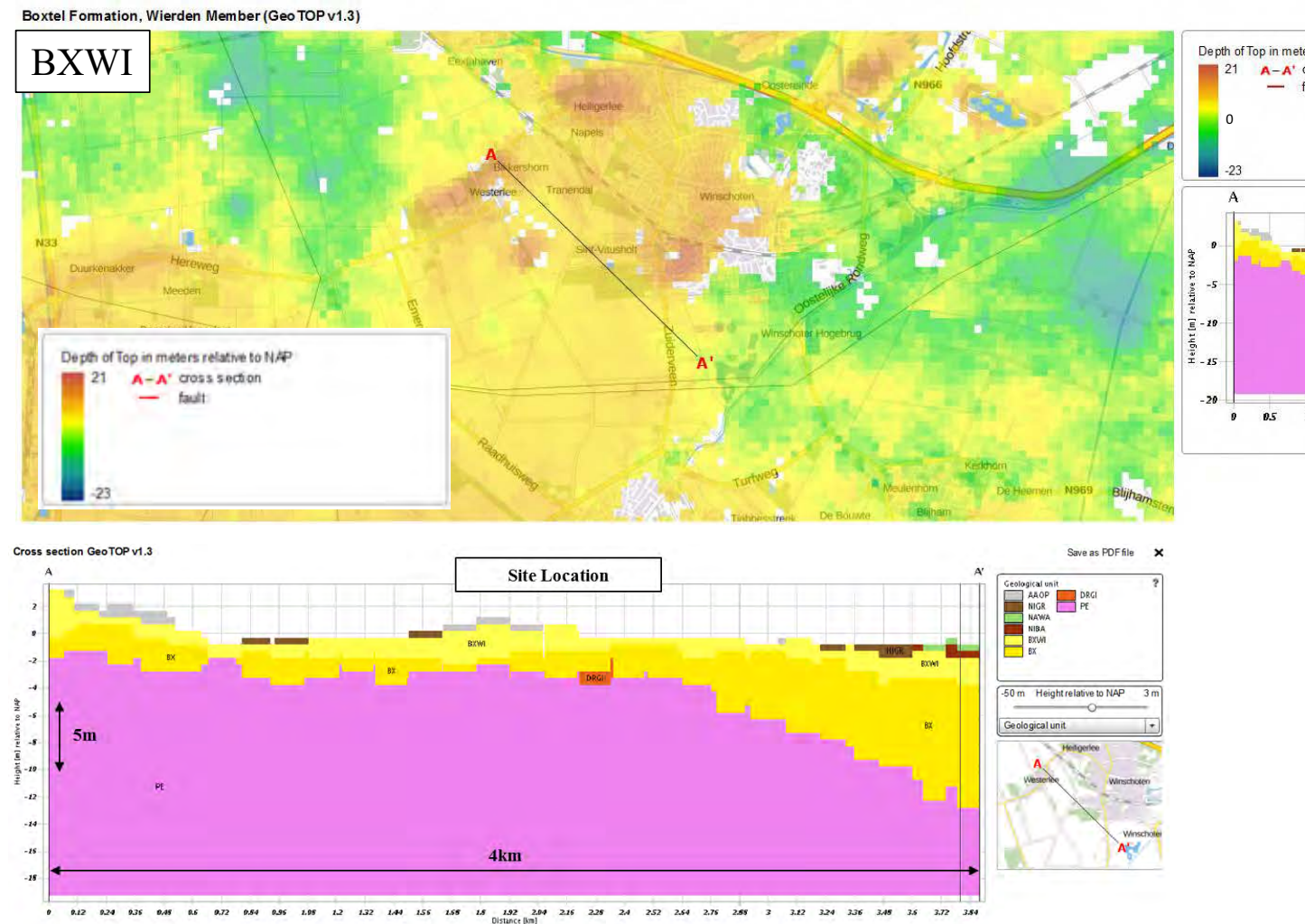


Figure 4: Depth of the top of the Pleistocene sediments (top) and cross-section along the AA' profile (bottom). Note that both BX and PE layers on the cross section are Pleistocene sediments.

Technical Note

260166-00

20 March 2018

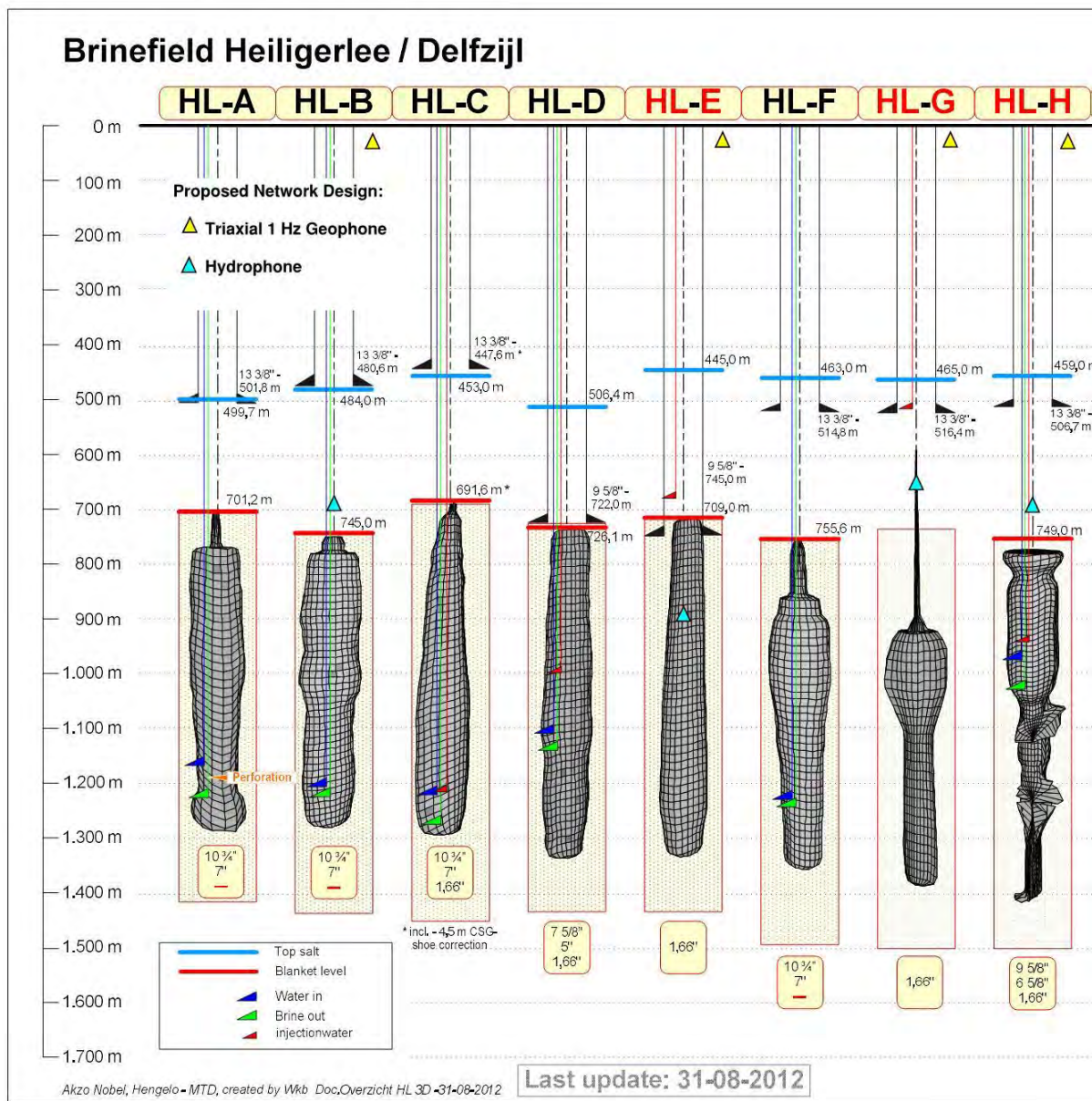


Figure 5: Cross section showing the depth of the instruments installed in or near the wells of the salt caverns.

DOCUMENT CHECKING (not mandatory for File Note)

	Prepared by	Checked by	Approved by
Name	Thomas Ader (London)	Manuela Villani	Ziggy Lubkowski
Signature			